DIELS–ALDER–INITIATED ORGANOCASCADES

EMPLOYING ACYLAMMONIUM CATALYSIS:

SCOPE, MECHANISM, AND APPLICATION

A Dissertation

by

MIKAIL EMINOVICH ABBASOV

Submitted to the Office of Graduate and Professional Studies of
Texas A&M University
in partial fulfillment of the requirements for the degree of

DOCTOR OF PHILOSOPHY

Chair of Committee,	Daniel Romo
Committee Members,	Daniel A. Singleton
	John A. Gladysz
	Jean–Philippe Pellois
Head of Department,	François P. Gabbaï

December 2015

Major Subject: Chemistry

ABSTRACT

Following the turn of the millennium, the role of asymmetric covalent organocatalysis has developed into a scalable, synthetic paradigm galvanizing the synthetic community toward utilization of these methods for more practical, metal–free syntheses of natural products. A myriad of reports on asymmetric organocatalytic modes of substrate activation relying on small, exclusively organic molecules are delineating what has now become the multifaceted field of organocatalysis paving the way to a vast array of reaction types.

α,β–Unsaturated acylammonium salts, generated *in situ* from commodity acid chlorides and a chiral isothiourea organocatalyst, comprise a new and versatile family of chiral dienophiles for the venerable Diels–Alder (DA) cycloaddition. Their reactivity is unveiled through a highly diastereo– and enantioselective Diels–Alder/lactonization organocascade that generates *cis*– and *trans*–fused bicyclic γ– and δ–lactones bearing up to five contiguous stereocenters. Moreover, the first examples of DA–initiated, stereodivergent organocascades are described delivering complex *oxa*–bridged *trans*–fused tricyclic γ–lactams found in bioactive compounds. An evaluation of various experimental and computational parameters was performed in order to derive a more detailed understanding of what renders this process selective. The utility of this methodology is showcased through a concise approach to the core structures of glaciolide, isatisine A and nonpeptidyl ghrelin–receptor inverse agonists, and formal syntheses of indoprofen, dihydrocompactin, fraxinellone, trisporic acids, and trisporols.

DEDICATION

This work is dedicated to my wife Amy, daughter Joplin, and sons Jude and Jax whose sacrifices, which were realized by our loss of precious time together, were for me the most painful and humbling of all.

ACKNOWLEDGEMENTS

I would like to thank all people who have helped and inspired me during my graduate study. Foremost, I wish to express my highest gratitude to my advisor, Professor Daniel Romo, without whom this work would have been impossible to accomplish. I greatly appreciate his support and guidance given to me throughout the course of my graduate studies and research. His motivation, enthusiasm, and immense knowledge have made him a constant oasis of ideas that inspired and enriched my growth as a student. I am deeply indebted to Professors Gene Carlisle and James Woodyard for their inspiring and invaluable guidance, for all the advice, encouragement, and help, and for everything that I learned from them. My sincere thanks are due to Professor Daniel Singleton for his kind interest in my work and his encouragement. I warmly acknowledge Professor John Gladysz for his help and constant support. I would also like to thank Professor Jean–Philippe Pellois for providing invaluable suggestions and comments for my dissertation. I wish to express my warm and sincere thanks to my friends and colleagues and the department faculty and staff for making my time at Texas A&M University a great experience.

I owe my loving thanks to my wife, Amy, my daughter Joplin, my sons Jude and Jax, my brother, Magerram, and my parents, Lyudmila and Emin. Without their love, support, understanding, and caring, I would not have survived. To them I dedicate this dissertation. Lastly and most importantly, thanks be to God for my life through all tests and to whom I owe my very existence.

TABLE OF CONTENTS

CHAPTER

LIST OF FIGURES

LIST OF TABLES

CHAPTER I

INTRODUCTION: THE EVER–EXPANDING ROLE OF ASYMMETRIC

COVALENT ORGANOCATALYSIS IN SCALABLE,

NATURAL PRODUCT SYNTHESIS*

1.1   A Brief Historical Perspective

"I will therefore call it the 'catalytic force' and I will call 'catalysis' the decomposition of bodies by this force, in the same way that we call by 'analysis' the decomposition of bodies by chemical affinity."

These famous observations by the Swedish chemist Jöns Jakob Berzelius of the University of Stockholm in 1835 sparked a new era of catalysis [1a]. The first organocatalytic transformation was reported in 1860 by Justus von Liebig in conversion of cyanogen to oxamide in the presence of aqueous acetaldehyde [1b]. The historic roots of the first asymmetric organocatalytic reaction date back to 1912, when two German chemists Bredig and Fiske reported that addition of hydrogen cyanide to benzaldehyde catalyzed by the cinchona alkaloids yields cyanohydrins in ~10% *ee* [1c]. The use of amino acids as catalysts for aldol and condensation reactions of acetaldehyde was first documented in 1931 by Fischer and Marschall [1d]. In 1936, Kuhn1e found that ammonium carboxylates of optically active amines effectively catalyze the aldol

reaction. The analogies in the catalytic action of enzymes and organic substances were recognized as early as 1928 by the German chemist Wolfgang Langenbeck [1f]. In 1949, Langenbeck revealed the conceptual difference between covalent and non–covalent catalysis, and coined the term "organic catalysis" [1g] Pracejus reported the first enantioselective synthesis of esters in 1960 from phenyl methyl ketene and methanol using 1 mol% *O*–acetylquinine as catalyst in a quite remarkable 93% yield and 74% *ee* [1h,i]. In 1971, the discovery of *L*–proline as catalyst for the intramolecular asymmetric aldol cyclodehydration was exemplified in the Hajos–Parrish–Eder–Sauer–Wiechert reaction [1j,k]. Surprisingly, the viability of small organic molecules as organocatalysts in asymmetric reactions remained subcritical and over the next few decades, the area of asymmetric organocatalysis was heavily overlooked with a paucity of isolated reports [2]. However in 2000, two pioneering reports by List, Lerner, Barbas [3] and MacMillan [4] reignited the modern age of organocatalysis triggering the "gold rush" in the last decade. MacMillan coined the term "organocatalysis" which is defined as the acceleration of a chemical transformation through addition of a substoichiometric amount of an organic compound which does not contain a metal atom [4]. The operational simplicity, robustness, low–cost, availability, chemical efficiency and non–toxicity render organocatalysis advantageous over metal and enzyme catalysis. Organocatalysis remains a vital pillar and popular strand of contemporary asymmetric catalysis research and is now well established in academia and industrial sectors. A myriad of excellent reviews have permeated the chemical community since 2010 in this highly topical field covering many discrete areas of organocatalysis [5]. Regrettably, it is

impossible to report every contribution to this rapidly growing field; therefore, a cross–section of the most recent developments in asymmetric covalent organocatalysis is described in this thesis to provide a flavour of the exciting advances in this area and specifically their growing impact in scalable natural product synthesis.

1.2   Classification of Asymmetric Modes of Activation in Organocatalysis

The classification of asymmetric modes of activation in organocatalytic reactions is challenging. A general distinction can be made between organocatalytic processes that form covalent intermediates between catalyst and substrate and processes that rely on non-covalent interactions (Figure 1.1).
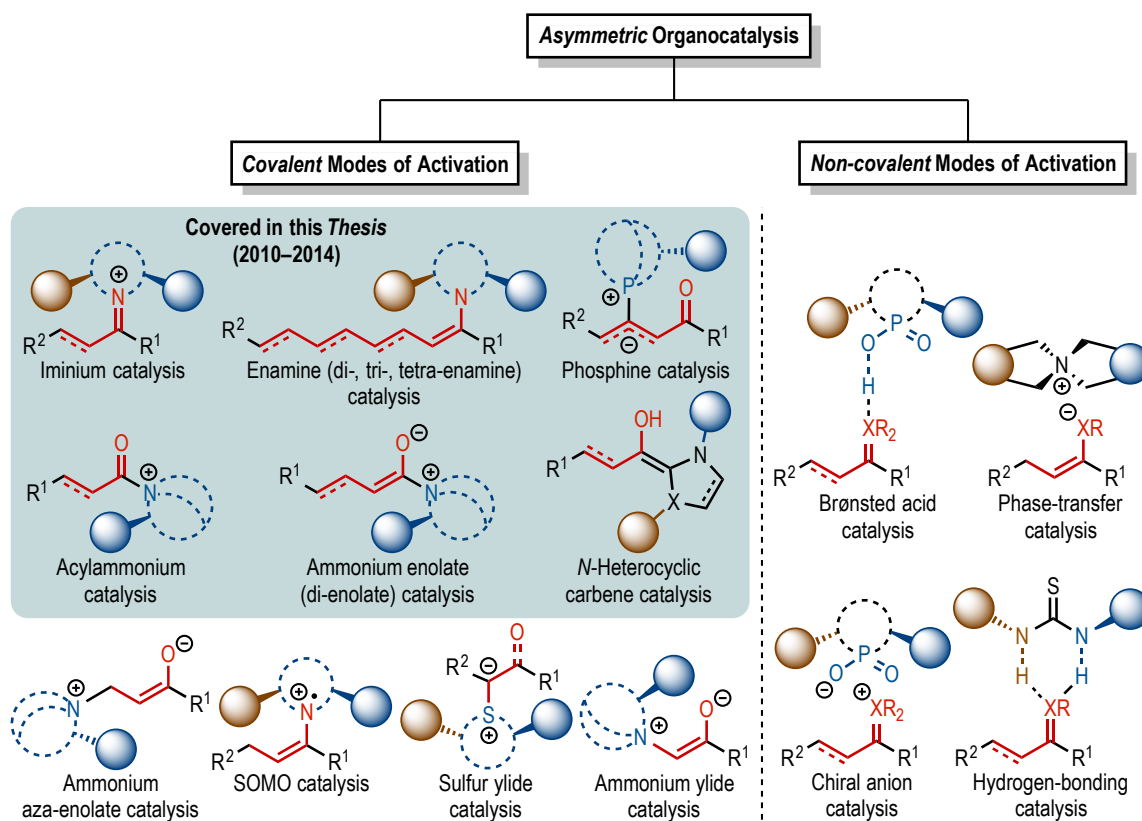
Figure 1.1 Classification of asymmetric modes of activation in organocatalysis [64].

Further differentiation within each category can be made on the basis of the mode of substrate activation: highest occupied molecular orbital (HOMO) activation (*e.g.*, enamine, *N*–heterocyclic carbene catalysis, etc.) or lowest unoccupied molecular orbital (LUMO) activation (*e.g.*, iminium, acylammonium, etc.). It should be noted that a single organocatalyst can promote reactions by several modes of activation and thus can be classified a multifunctional catalyst [6].

An *iminium* activation mode exploits the reversible condensation of a chiral secondary or primary amine catalyst (*e.g.*, *L*–proline, MacMillan's imidazolidinones, cinchona-derived primary amines, etc.) with an α,β–unsaturated aldehyde or ketone to form an iminium ion intermediate. This system effectively lowers the LUMO energy of the π–system and thus enhances its reactivity toward nucleophiles. This strategy has been successfully employed in various types of asymmetric transformations [7].

In the case of saturated carbonyl systems, the LUMO energy lowering induced by the formation of an iminium ion intermediate increases the acidity of the α–proton, enabling facile deprotonation and leads to the generation of the *enamine*. The resultant enolate, with an effectively elevated HOMO energy, augments its reactivity toward electrophiles. This activation mode has led to the development of a vast number of asymmetric α–functionalizations of aldehydes and ketones with carbon– and heteroatom–based electrophiles [8]. This concept has been extended to unsaturated carbonyl systems resulting in the discovery of dienamine [9], trienamine [10], and more recently tetraenamine [11] activation modes.

In *phosphine* catalysis, a conjugate addition to an activated carbon–carbon double or triple bond by a chiral tertiary phosphine organocatalyst forms a β–phosphonium enolate, β–phosphonium dienolate, or vinyl phosphonium ylide as reactive intermediates. These zwitterionic species react with a broad array of nucleophiles (LUMO activation mode) and electrophiles (HOMO activation mode) to generate diverse carbo– and heterocyclic molecular architectures [12].

Acylammonium catalysis is initiated by the nucleophilic attack of a chiral tertiary amine catalyst with an activated carboxylic acid derivative (*e.g.*, acid halide, anhydride) to form an acylammonium ion intermediate. This activation mode effectively lowers the LUMO energy of the carbonyl system thus enhancing its reactivity toward nucleophiles. Several acyl–transfer organocatalysts have been developed for asymmetric acylammonium–catalyzed transformations [13], including trans–esterifications, kinetic resolutions, desymmetrizations, and Steglich rearrangements. Organocatalysts utilized include Fu's chiral ferrocenyl PPY catalyst [14], Vedejs' TADMAP catalyst [15], Okamoto's annulated benzothiazolylidenamine catalysts [16] and Birman's dihydroimidazole CF_3–PIP [17] and isothiourea–based BTM [18] and HBTM [19] catalysts. Furthermore, this activation concept has recently been extended to unsaturated carbonyl systems prompting a diverse array of previously undisclosed complexity–generating organocascades [20].

In *ammonium enolate* catalysis, the nucleophilic enolate equivalent (HOMO activation mode) is generated either by addition of a chiral tertiary amine catalyst to a ketene or via direct α–deprotonation of an acylammonium species. This activation mode

has led to the development of numerous asymmetric α–functionalizations with carbon–and heteroatom–based electrophiles [21a] and prompted a spate of elegant, scalable syntheses [21b,c]. Further exploration of this activation concept unveiled yet another reactive intermediate, zwitterionic ammonium dienolate, generated *in situ* by a direct γ–deprotonation of unsaturated acylammonium ions enabling a variety of asymmetric annulations [22].

In *N–heterocyclic carbene* (NHC) catalysis, the nucleophilic attack of the carbene catalyst (*e.g.*, thiazolium, triazolium salts) on the carbonyl carbon (typically aldehydes) forms the initial adduct that leads to the Breslow intermediate through an external base deprotonation of the carbene–aldehyde adduct. This acyl anion equivalent can then react with different electrophiles, including another carbonyl compound as in the benzoin reaction, with Michael acceptors in the Stetter reaction, with activated or unactivated double and triple bonds without electron–withdrawing groups, or with alkyl halides. This unique mode of HOMO activation takes advantage of the inversion of classical reactivity (umpolung) and offers a broad range of unconventional transformations [23].

1.3   Recent Developments in the Iminium/Enamine Catalysis: Synopses of Examples Including Formal Syntheses

Jørgensen [9a] recently introduced a new dual activation mode of α,β–unsaturated aldehydes **1**, via dienamine formation, and activation of nitro–olefins **2**, via hydrogen–bonding, affording fully substituted cyclobutanes **4** by an organocatalytic

formal [2 + 2]–cycloaddition catalyzed by a computationally designed catalyst **3** (Figure

1.2a). In other work, Jørgensen [10c] utilized trienamine–activated dienes, generated *in*

situ from α,β,γ,δ–dienyl aldehydes **5** and chiral aminocatalyst **7**, in thio–Diels–Alder

reactions with thiocarbonyls **6** to access highly enantioenriched dihydrothiopyrans **8**

(Figure 1.2b).
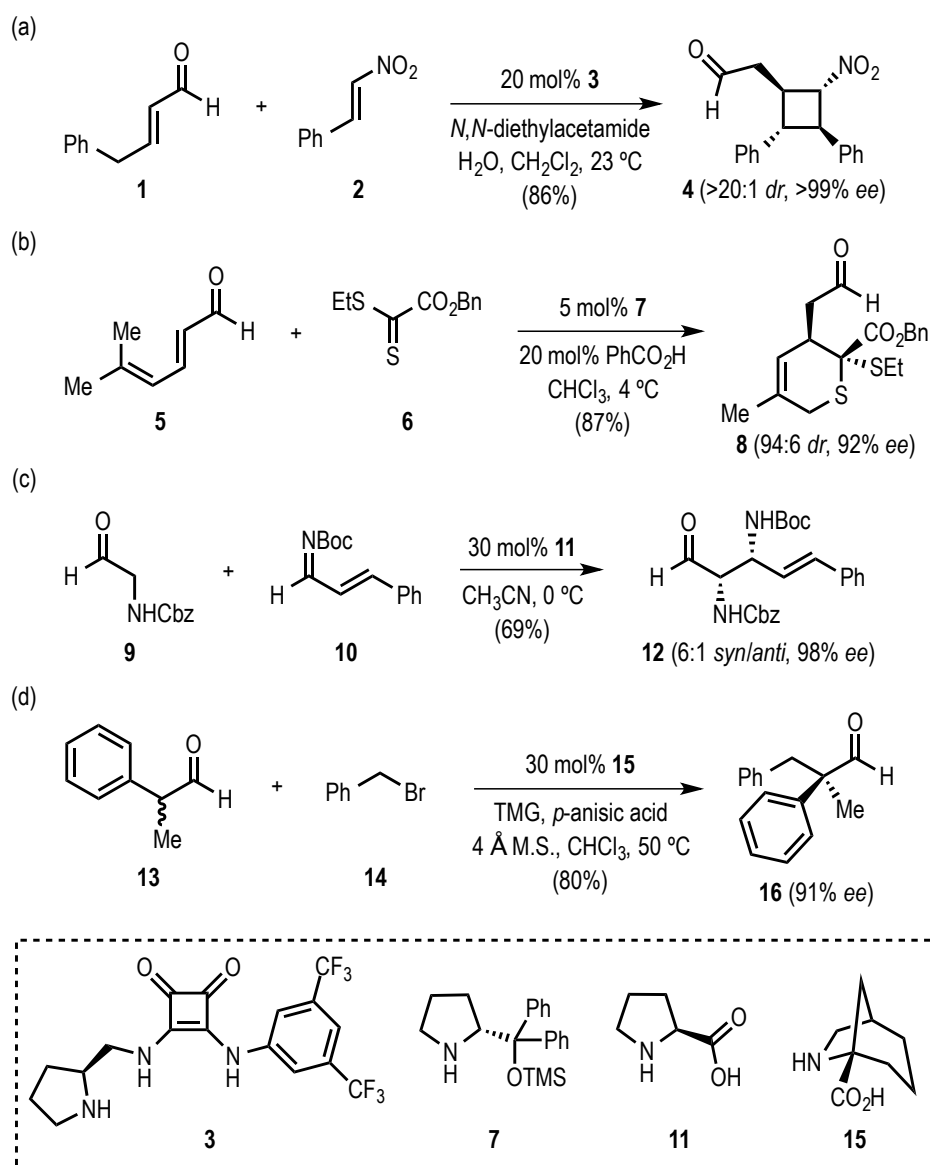
Figure 1.2 Recent examples of asymmetric iminium/enamine catalysis [64].

In 2012, Maruoka and co–workers [24] developed the first diastereo– and enantioselective direct Mannich reaction (Figure 1.2c) of *N*–protected α–aminoacetaldehydes **9** with *N*–protected imines **10** catalyzed by *L*–proline (**11**). This organocatalytic process delivers optically active vicinal diamines **12**, motifs present in a number of natural products and useful chiral catalysts. More recently, List [25] disclosed the first amino– catalyzed α–alkylation of racemic α–branched aldehydes **13** with benzyl bromide (**14**) as alkylating agent via enamine catalysis (Figure 1.2d). Using a sterically demanding proline–derived catalyst **15**, enantiomerically enriched α–alkylated aldehydes with quaternary stereogenic centers were obtained in good yields and high enantioselectivities.

Maruoka successfully demonstrated the synthetic utility of the developed Mannich reaction in the formal synthesis of (−)-agelastatin A, a potent antitumor marine alkaloid (Figure 1.3).
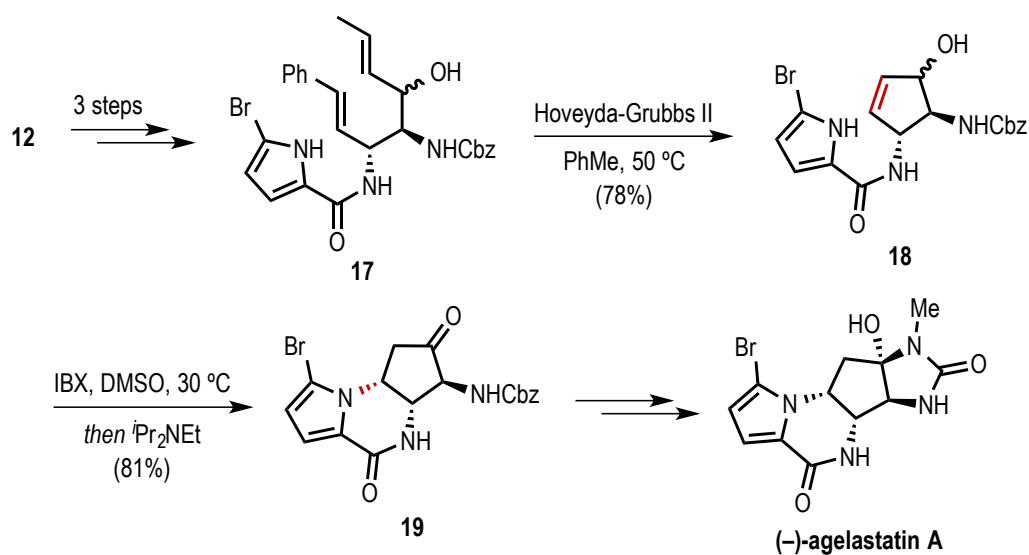
Figure 1.3 Application of diamine **12** towards the formal synthesis of (−)-agelastatin A [64].

8

Mannich product, diamine **12**, was converted to diene **17** in 3 steps. Treatment of **17** with Hoveyda–Grubbs second–generation catalyst afforded cyclopentene **18**, which was converted in one pot to cyclopentanone **19**, an intermediate previously used in the synthesis of (–)-agelastatin A.

1.4   MacMillan's Total Synthesis of (–)-Vincorine

In 2013, Horning and MacMillan [26a] reported a concise, enantioselective total synthesis of (–)-vincorine, an akuammiline alkaloid containing a tetracyclic cage–like core with a strained seven–membered azepanyl ring system. Various members of this alkaloid family are known to exhibit anti–cancer activity and glycine receptor antagonism. A prominent feature of the synthesis is a scalable, organocatalytic Diels–Alder/iminium cyclization cascade, the general synthetic strategy for representative polycyclic indole alkaloids [26b], initiated by a highly enantioselective *endo* Diels–Alder reaction between diene **20** and *in situ* generated α,β–unsaturated iminium dienophile **24** delivering cycloadduct **25** (Figure 1.4).
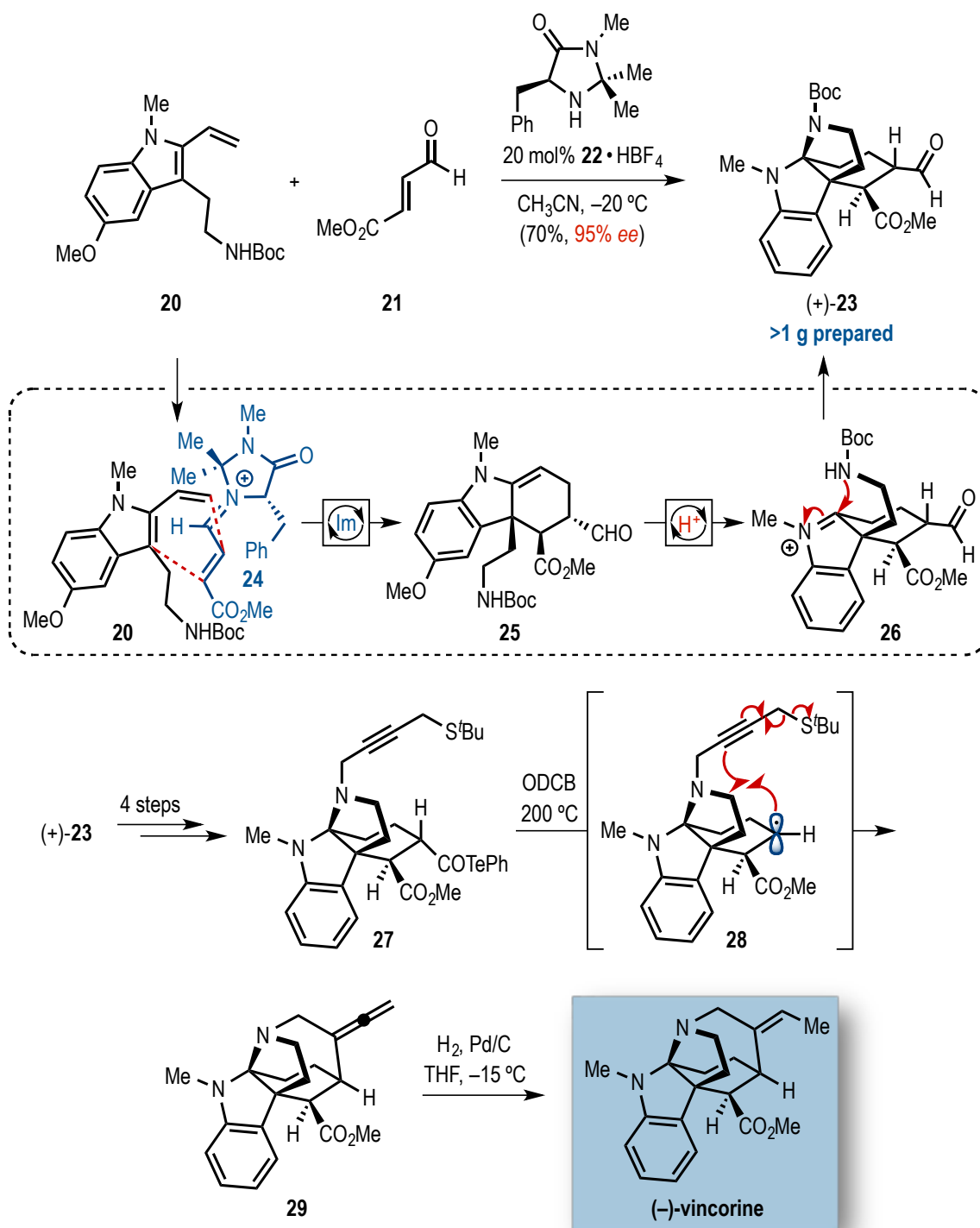
Figure 1.4 MacMillan's total synthesis of (–)-vincorine [64].

Subsequent, Brønsted acid–mediated conversion of **25** to iminium **26** prompted intramolecular 5–exo cyclization by the pendant carbamate group to generate the tetracyclic adduct **23**, on gram scale (>1 g), bearing three of four stereocenters found in vincorine including the all–carbon quaternary center. Final seven–membered azepanyl ring annulation was accomplished by 7–exo–dig radical cyclization initiated with an unusual acyl telluride precursor **27** under thermal conditions providing allene **29**. The authors postulate C–Te bond homolysis and loss of carbon monoxide to generate alkyl radical **28**. Selective terminal hydrogenation from the less hindered face of the allene functionality furnished (–)-vincorine as a single olefin isomer in nine total steps and 9% overall yield.

1.5   Recent Developments in *N*–Heterocyclic Carbene Catalysis: Synopses of Examples Including Formal Syntheses

In 2012, Bode [27a] disclosed a new class of NHC–catalyzed annulations of trisubstituted α,β–unsaturated aldehydes **30** and cyclic *N*–sulfonylimines **31** (Figure 1.5a) operating through the catalytic generation of α,β–unsaturated acyl azoliums in the presence of catalyst **32** and oxidant **33**. Scheidt and co–workers [27b] developed a highly selective synthesis of γ–butyrolactones through a formal [3 + 2] annulation (Figure 1.5b) of α,β–unsaturated aldehydes **35** and acyl phosphonates **36** catalyzed by a computationally designed, C1–symmetric biaryl-saturated imidazolium catalysts **37**. Rovis[27c] recently developed a novel chiral *N*–heterocyclic carbene catalyst **41** that favors a homoenolate pathway over the established acyl anion (Stetter) pathway.
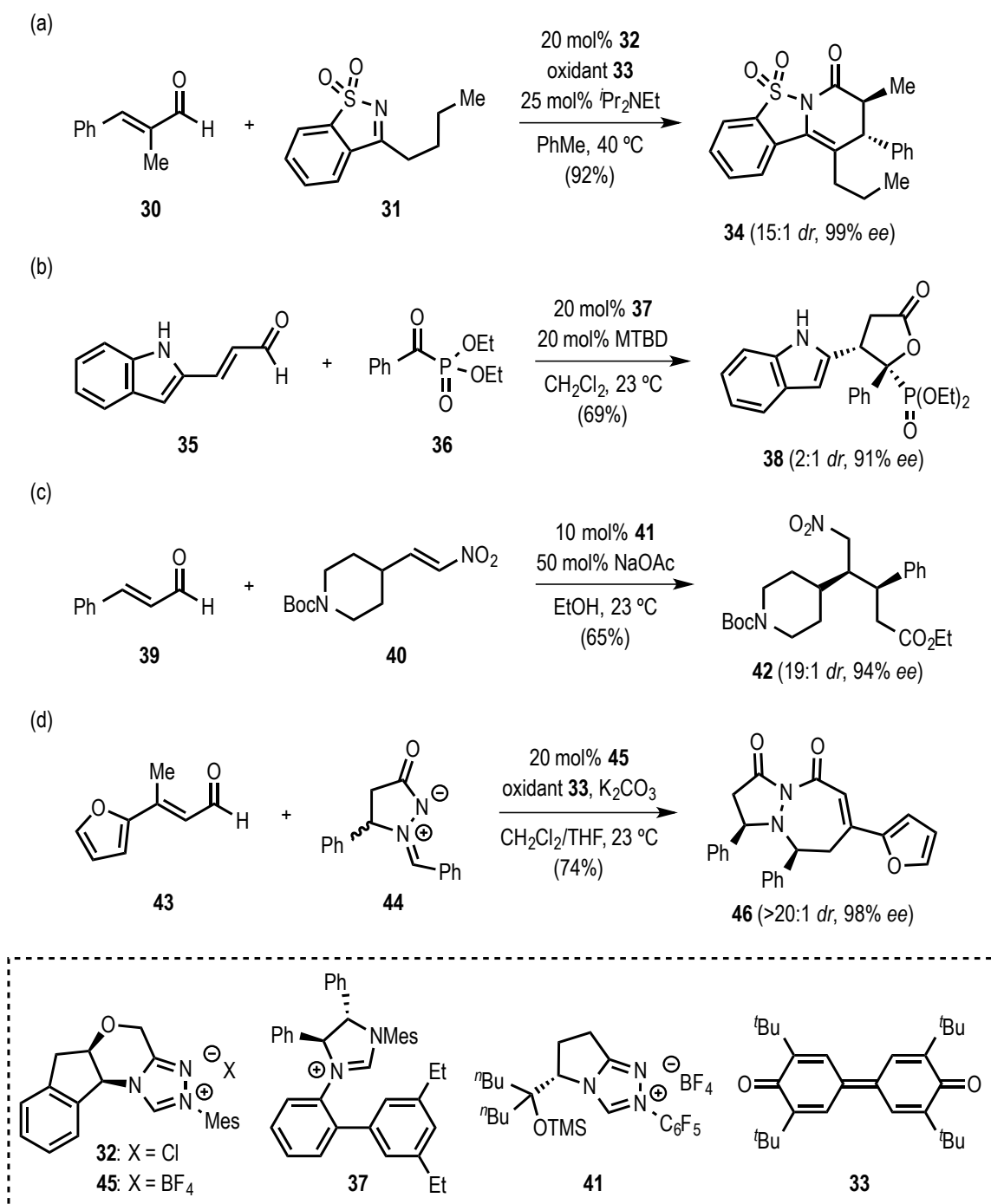
Figure 1.5 Recent examples of asymmetric *N*–heterocyclic carbene catalysis [64].

This enabled a novel coupling between α,β–unsaturated aldehydes **39** and nitroalkenes **40** to access a diverse array of *syn*–δ–nitroesters **42** (Figure 1.5c). More recently, Chi and co–workers [27d] disclosed the first *N*–heterocyclic carbene catalyzed [3 + 4] cycloaddition of α,β–unsaturated aldehydes **43** and azomethine imines **44** to generate dinitrogen–fused seven–membered heterocycles **46** (Figure 1.5d). In this process, NHC catalyst **45** also enables a highly effective kinetic resolution of racemic azomethine imines **44**.

Activation of the otherwise inert β–sp^3 carbon of saturated esters as nucleophiles has recently been achieved by Chi and co–workers [28] utilizing NHC catalyst **49**. This methodology delivers a diverse set of optically active substrates including cyclopentenes, γ–butyrolactones and γ–lactams (*e.g.*, **50**, Figure 1.6). Chi then established the utility of this methodology employing saturated ester **47** and hydrazone **48** to provide a concise, formal asymmetric synthesis of (*S*)–rolipram, a potent phosphodiesterase inhibitor (Figure 1.6). The synthesis of **51**, a key intermediate previously employed in the synthesis of (*S*)–rolipram, was achieved in 5 steps from γ–lactam **50**.
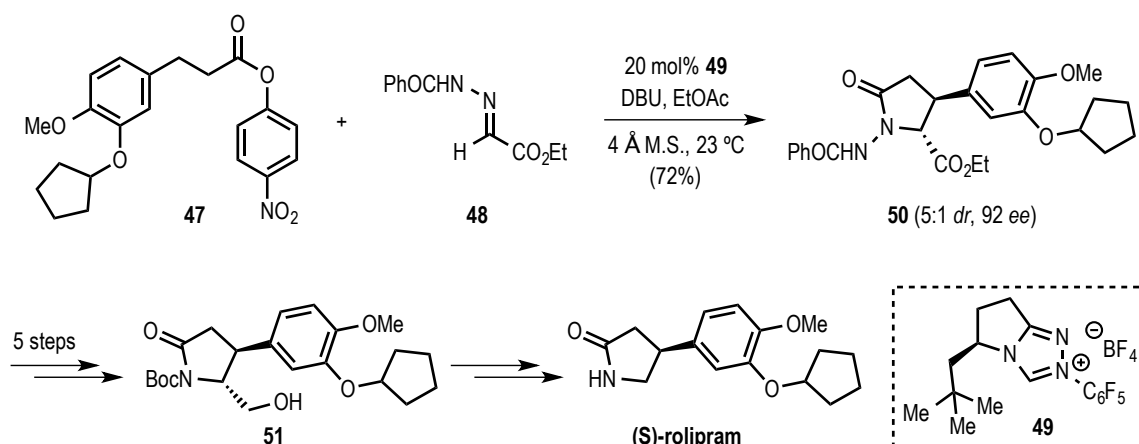
Figure 1.6 Application of γ–lactam **50** towards the formal synthesis of (*S*)–rolipram [64].

1.6   Scheidt's Total Syntheses of (–)-Bakkenolides I, J, and S

Scheidt has recently described the utility of the tricyclic β–lactone (+)-**54**, obtained by desymmetrization through an aldol–lactonization reaction of readily accessible 1,3–diketone **52** catalyzed by *N*–heterocyclic carbene **53**,[29a] as a key intermediate in the enantioselective total syntheses of (–)-bakkenolides I, J, and S (Figure 1.7) [29b]. The tricyclic β–lactone (+)-**54** was prepared on gram scale (>3 g) in 69% yield with 98% *ee* as a single diastereomer.
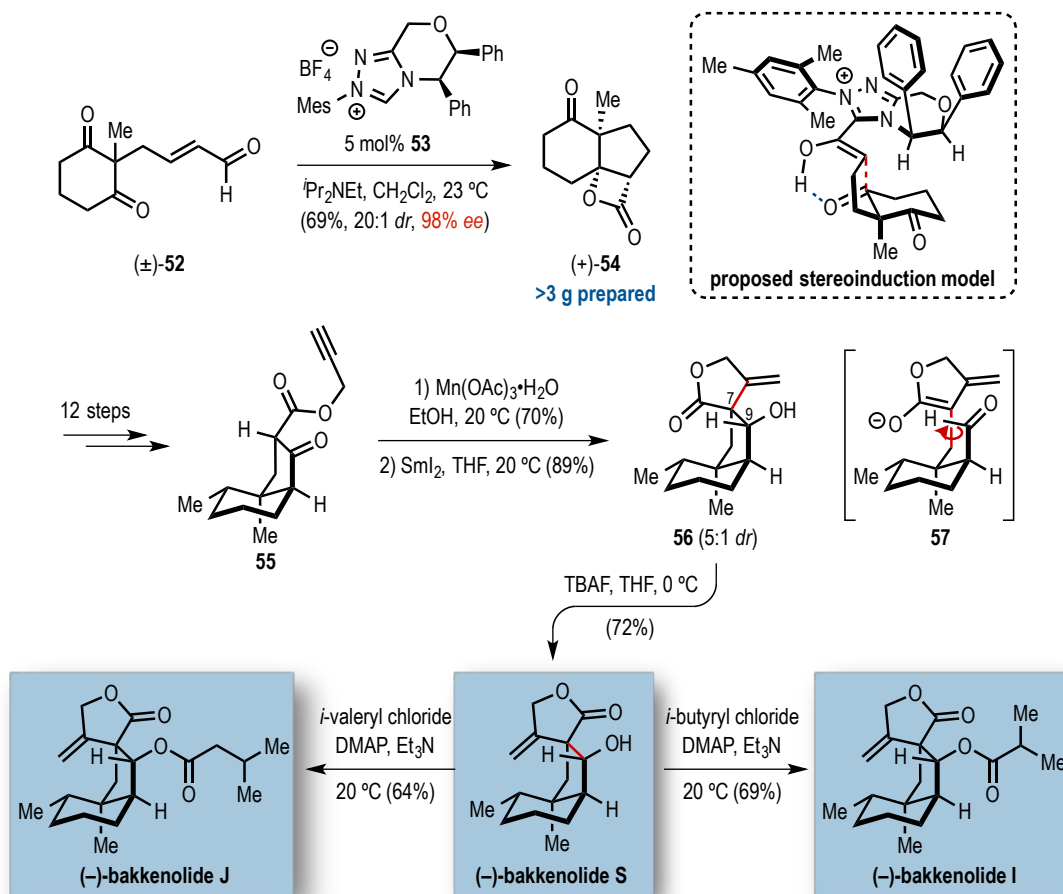
Figure 1.7 Scheidt's total syntheses of (–)-bakkenolides I, J, and S [64].

The stereochemical outcome of the reaction was rationalized through the transition state model depicted in Figure 1.7. A 12–step elaboration of the fused 6,5–bicyclic ring system (+)-**54**, led to the β–keto propargyl ester **55** and set the stage for the formation of the key γ–spirobutyrolactone. Thus, in the presence of Mn(OAc)₃, the β–keto propargyl ester **55** cyclized, forming the γ–spirobutyrolactone **56** as a 5:1 mixture of diastereomers, following reduction of the resulting ketone using SmI₂. However, this route produced the undesired epimer at the C7 position. Fortunately, exposure of **56** to TBAF promoted an

intriguing retro–aldol/aldol sequence (via formation of transient aldehyde **57**) to afford the desired diastereomer, (–)-bakkenolide S. The authors hypothesized that this thermodynamically favoured process is driven by hydrogen bonding between the C9 secondary alcohol and the γ–spirobutyrolactone carbonyl oxygen. Finally, conversion to (–)-bakkenolides I and J was accomplished by direct acylation of (–)-bakkenolide S with isobutyryl and isovaleryl chlorides, respectively. These natural products possess a wide spectrum of biological activity including antifeedant effects, platelet aggregation inhibition, and potent inhibitory activity against a variety of tumor cell lines.

1.7 Recent Developments in Phosphine Catalysis: Synopses of Examples Including Formal Syntheses

The Lu group [30a] broadened the potential of chiral peptide–based phosphines **60** for catalysis of allene–alkylimine [3 + 2] annulations (Figure 1.8a) leading to synthetically valuable optically pure five–membered *N*–heterocycles (*e.g.*, **61**). Recently, Barbas [30b] utilized C2–symmetric phospholane **64** to promote an expeditious assembly of complex polysubstituted spirocyclopentenebenzofuranones **65** (Figure 1.8b) consisting of three contiguous stereocenters, including an all–carbon quaternary carbon. In their recent studies, Fu and co–workers [30c] reported the first examples of intra– and intermolecular γ–umpolung additions of nitrogen nucleophiles to allenoates and alkynoates (Figure 1.8c) with spirophosphepine **67** found to be the optimal catalyst. More recently, Lu [30d] disclosed the first asymmetric phosphine–catalyzed Michael

addition (Figure 1.8d) mediated by a chiral phosphine **71** that was presumed to promote additional catalyst–substrate interactions through hydrogen bonding.
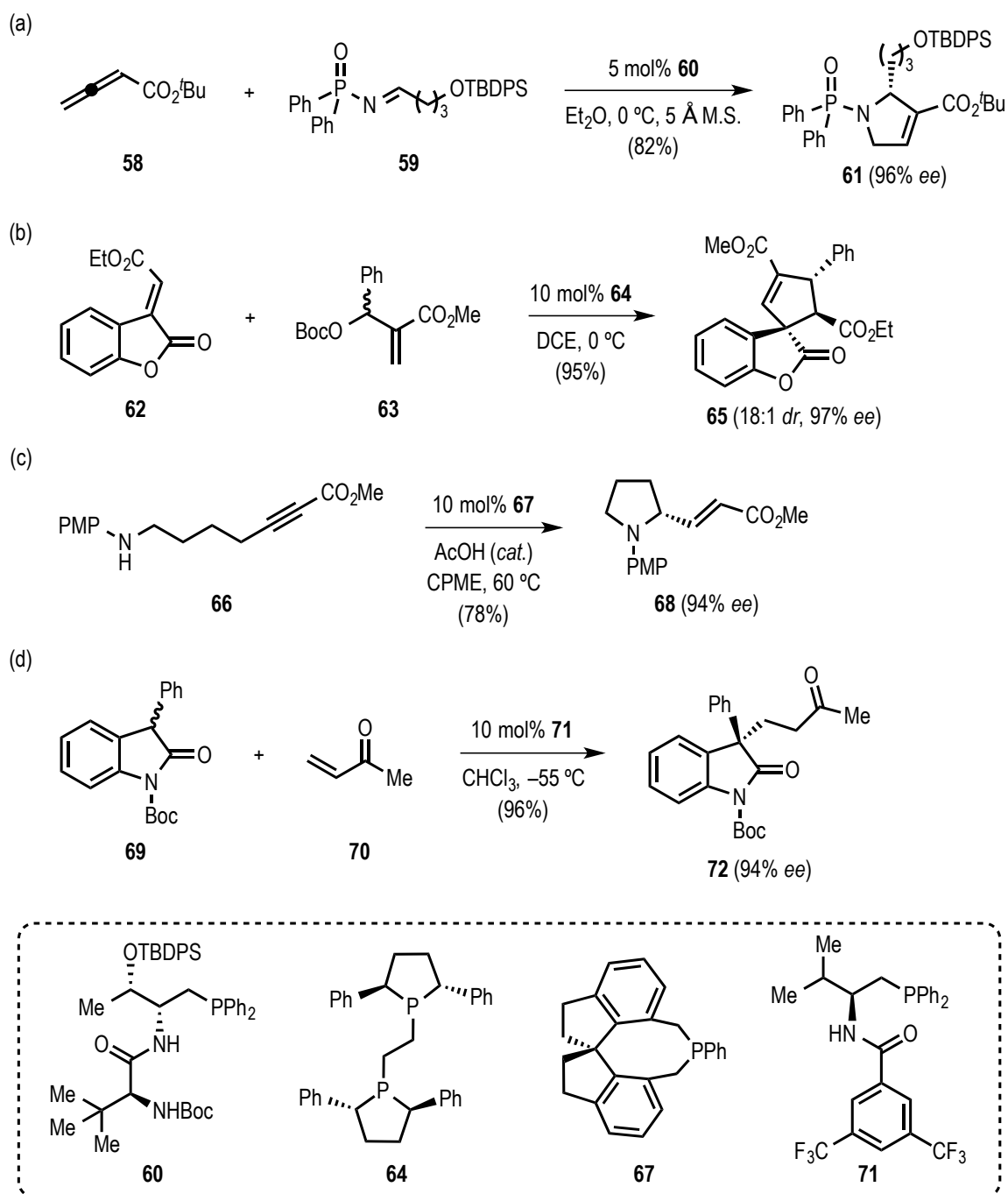
Figure 1.8 Recent examples of asymmetric phosphine catalysis [64].

Lu and co–workers demonstrated the utility of the asymmetric allene–alkylimine [3 + 2] methodology by a concise formal asymmetric synthesis of (+)-trachelanthamidine (Figure 1.9).
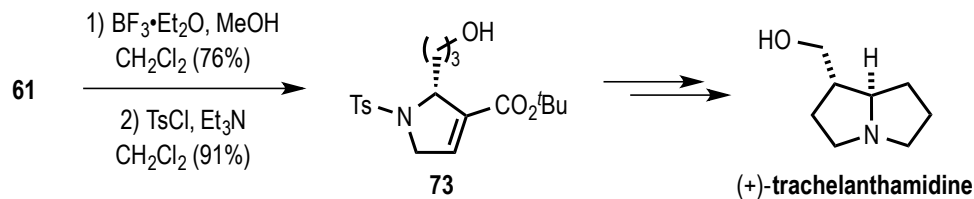
Figure 1.9 Application of dihydropyrroline **61** towards the formal synthesis of (+)-trachelanthamidine [64].

The synthesis of **73**, a key intermediate previously employed in the synthesis of (+)-trachelanthamidine, a pyrrolizidine alkaloid possessing a wide range of pharmacologically relevant activities, was secured from dihydropyrroline **61** following removal of protecting groups.

1.8   Kwon's Total Synthesis of (+)-Ibophyllidine

Recently, Andrews and Kwon reported the first example of asymmetric phosphine–catalyzed [3 + 2] annulation employed in the total synthesis of (+)-ibophyllidine [31] (Figure 1.10), a member of the terpene indole alkaloids possessing intriguing biological activities. The practical procedure allowed the preparation of the optically pure pyrroline (+)-**77** as a single *syn*–diastereomer on 30 g scale in excellent yield with high enantiocontrol employing the readily accessible allenoate **74** and imine **75** with the chiral [2.2.1] bicyclic phosphine catalyst **76**. Following a 7–step elaboration

of the pyrroline (+)-**77** to the cyclization precursor **78**, AgOTf–mediated intramolecular

spiroalkylation delivered the desired indolenine **79**.
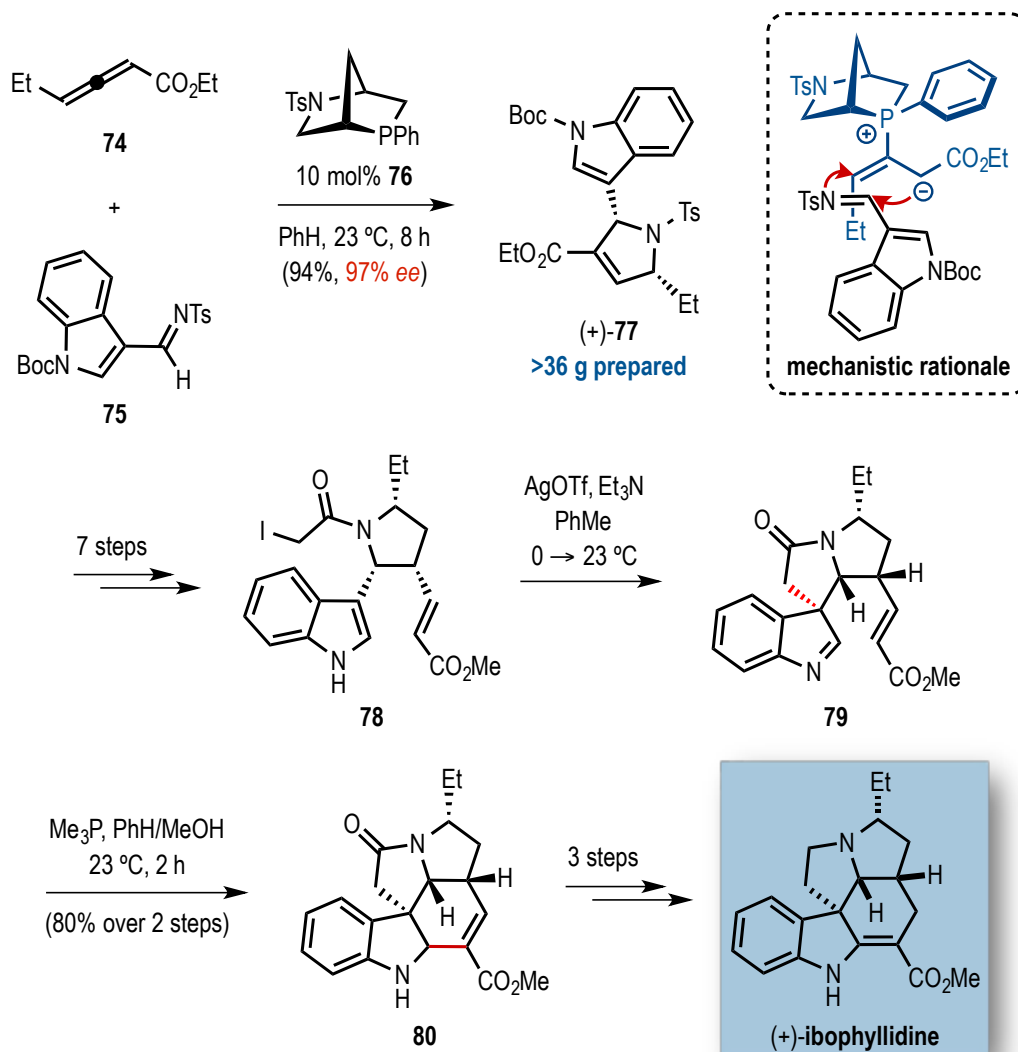
Figure 1.10 Kwon's total synthesis of (+)-ibophyllidine [64].

The final six–membered E–ring of (+)-ibophyllidine was formed via an intramolecular

aza–Morita–Baylis–Hillman reaction, again through phosphine catalysis, yielding the

desired pentacyclic framework **80** in 80% yield over two steps. Overall, the first enantioselective synthesis of (+)-ibophyllidine was accomplished in 15 steps and 13% overall yield through enantioselective phosphine-based catalysis.

1.9 Recent Developments in Acylammonium/Ammonium Enolate Catalysis: Synopses of Examples Including Formal Syntheses

The Smith [22b] group recently utilized *in situ* activated β,γ–unsaturated alkenoic acids **81** through mixed anhydride formation, as ammonium dienolate precursors in an enantioselective formal [2 + 2] cycloaddition with *N*–tosyl aldimines **82** promoted by a chiral isothiourea HBTM–2.1 (**83**) catalyst (Figure 1.11a). Building on early work by Fu, who demonstrated the potential of acid fluorides and unsaturated acylammonium catalysis for a tandem allylsilane/ene reaction [20a], Smith recently demonstrated the utility of mixed anhydrides and unsaturated acylammoniums for the enantioselective synthesis of enol lactones **87** (Figure 1.11b) [20b]. In our own studies in this area, the full potential of the latent, triply reactive, α,β–unsaturated acylammonium catalysis was realized employing acid chlorides (*e.g.*, **88**, **92**) and carboxylic acids in a rapid assembly of complex cyclopentanes [20d] **95** (Figure 1.11d) and in a further extension, *N*–heterocycles [20c] **91** (Figure 1.11c). Furthermore, we very recently demonstrated the utility of these chiral α,β–unsaturated acylammonium salts as competent chiral dienophiles in a Diels–Alder/lactonization (DAL) organocascade [20e] (Figure 1.11e).
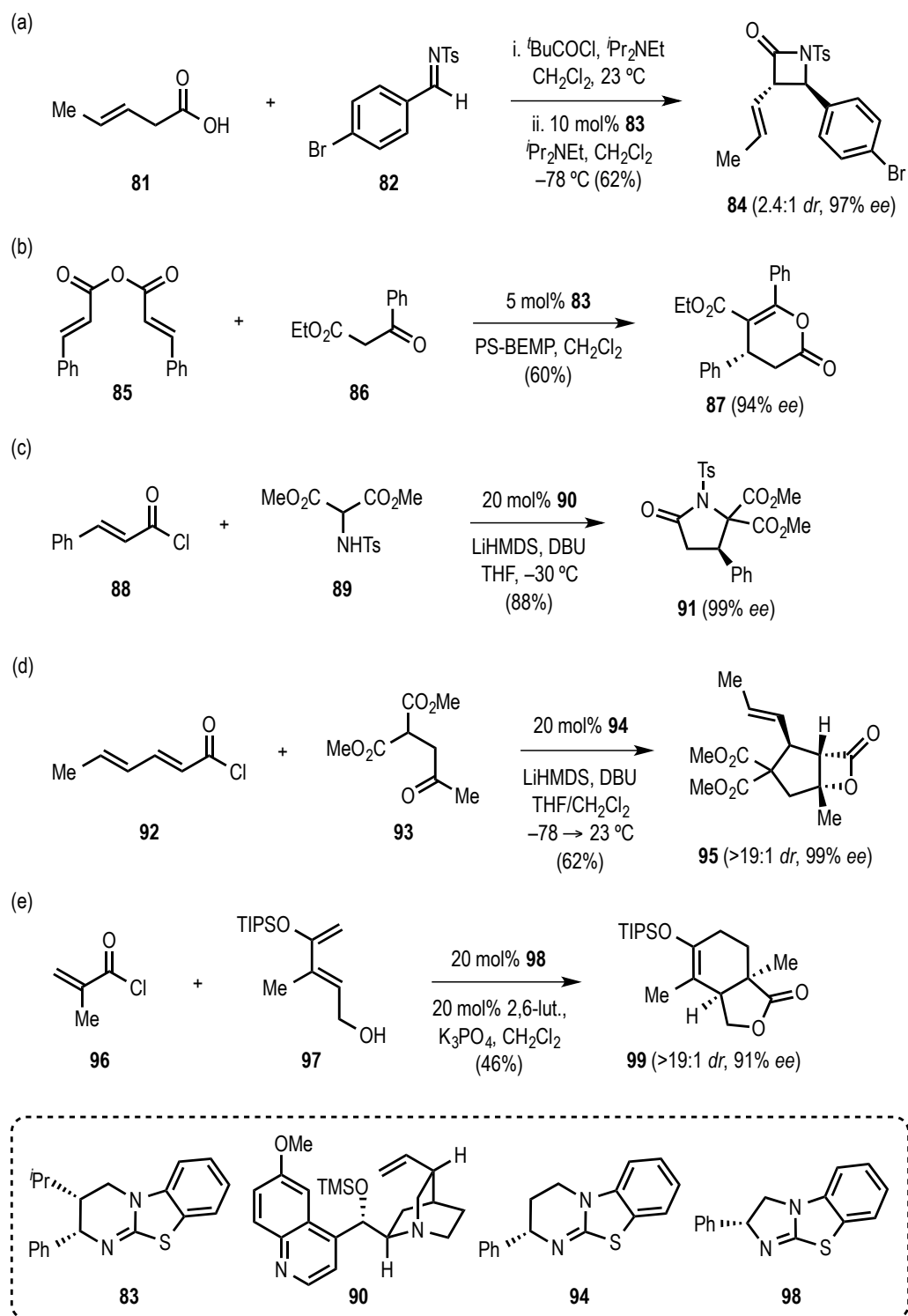
Figure 1.11 Recent examples of asymmetric acylammonium/ammonium enolate catalysis [64].

The utility of the DAL methodology was validated through a short, enantioselective synthesis of cyclohexenone (–)-**100** from cycloadduct **99**. Bicyclic lactone **100** was previously employed in racemic form for the synthesis of (±)-fraxinellonone, a degraded limonoid that displays moderate antifeedant and ichthyotoxicity activity, in addition to (±)-trisporic acid and (±)-trisporols, naturally occurring fungal pheromones derived from β–carotene (Figure 1.12).
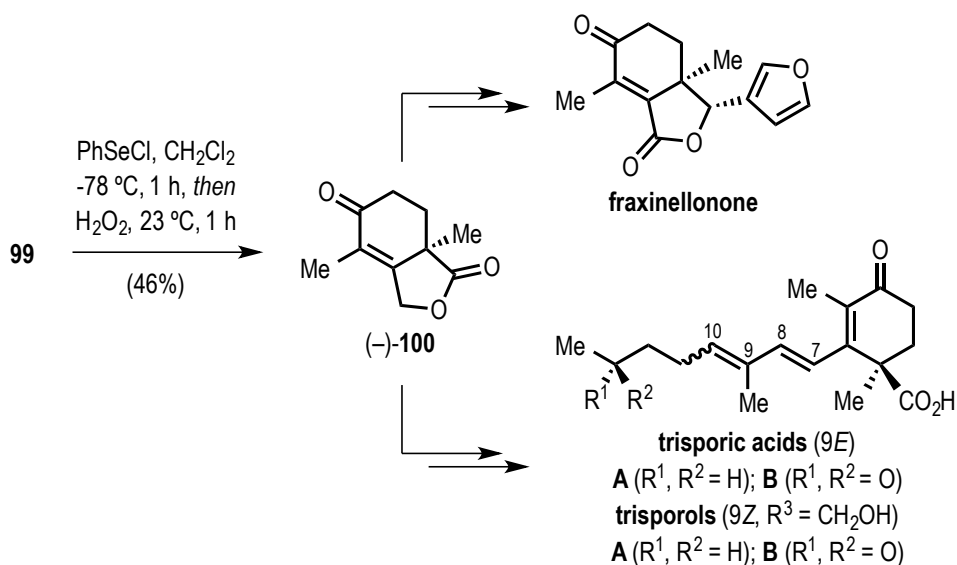
Figure 1.12 Application of bicyclic γ–lactone **99** towards the formal syntheses of fraxinellonone, trisporic acids, and trisporols [64].

1.10   Romo's Total Synthesis of (–)-Curcumanolide A and (–)-Curcumalactone

A recent example of scalable, ammonium enolate catalysis can be found in the asymmetric, divergent route to the spirocyclic sesquiterpene natural products (–)-curcumanolide A and (–)-curcumalactone from common spirocycle **105** (Figure 1.13) [32a].
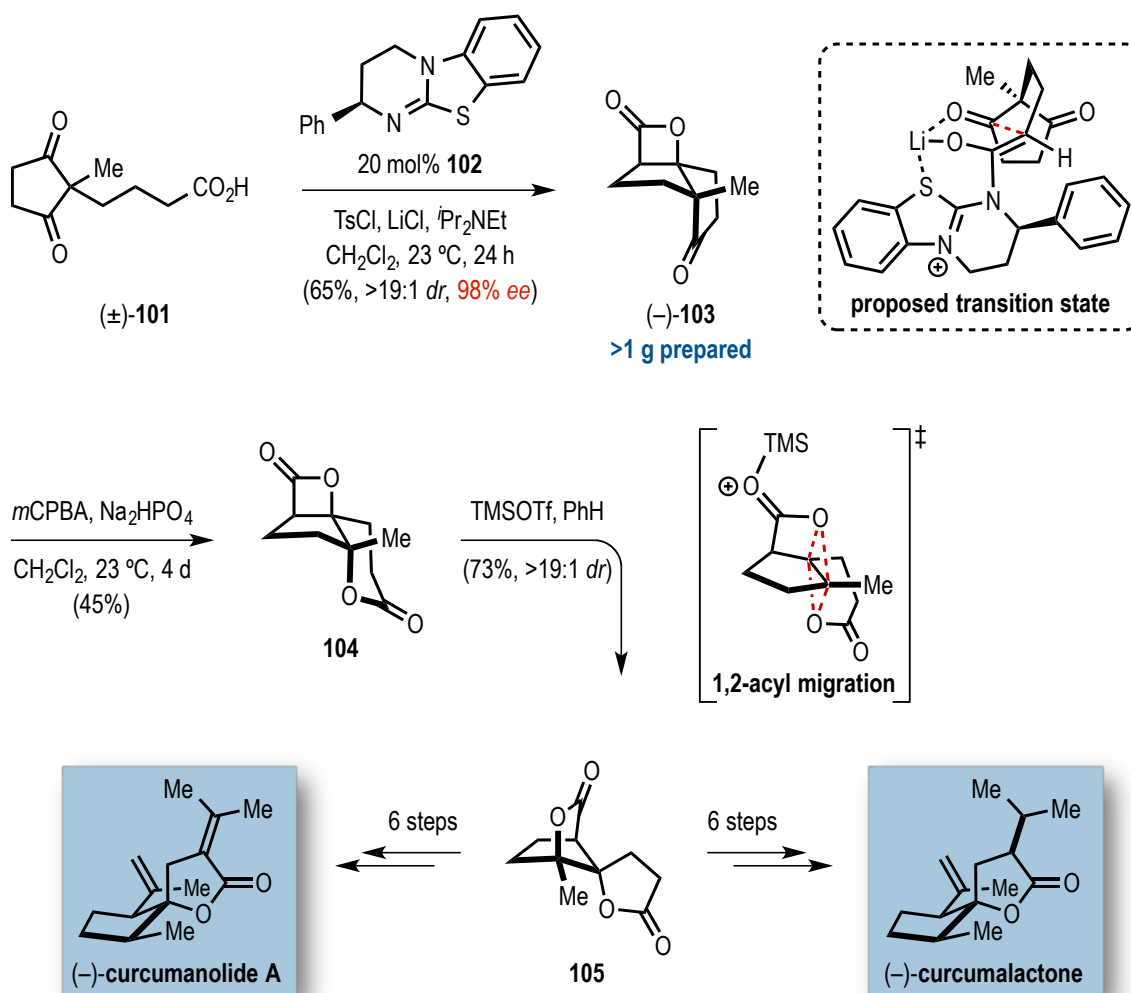
Figure 1.13 Romo's total synthesis of (–)-curcumanolide A and (–)-curcumalactone [64].

These spirolactone–containing sesquiterpenoids are present in the crude drug Zedoary, have been used as remedies for cervical cancer, and were reported to exhibit anti–inflammatory activity. The synthesis of these natural products demonstrated the gram-scale utility of the organocatalytic, asymmetric nucleophile–catalyzed aldol–lactonization (NCAL) desymmetrization process [32b] of dione acid (±)-**101** leading to a

tricyclic β–lactone (−)-**103** via a proposed bicyclic boat–like transition–state arrangement (as depicted in Figure 1.13). Furthermore, the ability to perform a Baeyer–Villiger oxidation in the presence of a β–lactone (−)-**103** led to the ring–expanded δ–lactone **104** and set the stage for a key dyotropic rearrangement. This rare dyotropic process, involving a fused bis–lactone **104** possessing both β– and δ–lactone moieties, enabled rapid access to the core structure **105** of curcumanolide A and curcumalactone. Our current mechanistic understanding of the transition state for this transformation, based on computational studies by the Tantillo group, involves a nearly concerted, stereospecific, "double S_N2" 1,2–bis–acyl migration process (as shown in Figure 1.13) delivering the bridged, spiro–γ–butyrolactone **105** [32c]. The described enantioselective total synthesis of curcumanolide A and curcumalactone was accomplished in 11 and 12 steps, respectively, and employed scalable, ammonium enolate organocatalysis.

Although racemic, a recent application of the NCAL methodology by Weinreb deserves mention given that it was performed on >2 g scale and utilized as a key step for constructing the *cis*–2–azadecalin found in the indole alkaloids, (±)-alstilobanine A and E, and (±)-angustilodine [33].

1.11 Conclusions and Perspective

In the past decade, the field of asymmetric covalent organocatalysis has seen tremendous progress. This thesis has briefly illustrated the power of these organocatalytic reactions, which have become a prevalent and highly efficient tool in organic chemistry. The discovery and implementation of new reactivities and

organocatalysts led to a considerable surge in reaction efficiency and selectivity. Indeed, the discovery of novel activation modes for substrates employing secondary amine catalysis, *N*–heterocyclic carbine catalysis, phosphine catalysis, and tertiary amine catalysis has enabled rapid construction of molecular complexity with excellent levels of stereocontrol and simple operational procedures employing non–heavy metal catalysts. These advances have led to many successful and imaginative applications of asymmetric covalent organocatalysis in the field of scalable natural product synthesis. Despite significant innovations in this highly topical area, there still remain many challenges and opportunities ahead. Certainly, the relatively high catalyst loading (*e.g.*, 10 and 20 mol%) in many cases leaves room for future improvement. Furthermore, the discovery of novel modes of substrate activation, especially of commodity chemicals, will drive further advances in the area of organocatalysis enabling unusual disconnections and more practical procedures. Based on the diversity of recently developed activation modes involving covalent organocatalysis, numerous organocascade sequences can be envisaged and will undoubtedly be applied to more ambitious synthetic targets. Given these advances, we further anticipate powerful strategies for the scalable synthesis of biologically relevant molecules including bioactive natural products and pharmaceuticals, providing invaluable tools for continued advances in biology. However, realizing these goals in earnest, necessitates not only the discovery but also invention of new modes of reactivity, that either exposes or amplifies both the innate and sometimes hidden reactivity of organic substrates, which in turn contributes to further

developments in chemical synthesis logic. This principle finds its full expression in the words of the epitome of the artist–scientist, Leonardo da Vinci:

"*Where nature finishes producing its own species, man begins, using natural things and with the help of this nature, to create an infinity of species.*"

CHAPTER II

ACYLAMMONIUM SALTS AS DIENOPHILES IN

DIELS–ALDER/LACTONIZATION ORGANOCASCADES*

2.1   Background and Significance

Transformations that rapidly generate complex and structurally diverse molecular architectures are essential components of modern organic chemistry [34]. In this regard, the Diels–Alder (DA) cycloaddition is arguably the most versatile and powerful transformation in chemical synthesis [35]. In particular, catalytic asymmetric DA reactions are unparalleled in their ability to rapidly and efficiently generate optically active, architecturally complex, and densely functionalized heterocycles and carbocycles from simple achiral substrates [36]. Furthermore, enantioselective organocatalytic DA variants have recently been established using iminium [37], enamine [38], bifunctional acid–base catalysis [39], and hydrogen–bonding catalysis [40]. MacMillan and co–workers employed both α,β–unsaturated aldehydes [37a] and ketones [37b] in cycloadditions through iminium–activated chiral dienophiles, whereas α,β–unsaturated aldehydes [40b] and indolinones [40c] were activated through hydrogen–bonding catalysis by Rawal and Barbas, respectively. Surprisingly, however, simple acid chlorides have yet to be successfully employed in organocatalyzed DA reactions. Herein,

we report the first enantioselective organocatalytic DA reactions with α,β–unsaturated acid chlorides activated *in situ* by a chiral isothiourea catalyst.

The potential of α,β–unsaturated acylammonium catalysis was first realized by Fu in asymmetric, net [3+2] annulations leading to diquinanes [41a]. Building on this early work, Smith recently employed mixed anhydrides as α,β–unsaturated acylammonium precursors for the direct synthesis of dihydropyranones and dihydropyridones [41b]. Furthermore, we demonstrated the full potential of chiral, triply reactive, α,β–unsaturated acylammonium salts for the rapid assembly of complex cyclopentanes [41c] and optically active γ–lactams and piperidones [41d]. Inspired by these studies, we sought to explore the reactivity of α,β–unsaturated acylammonium salts as dienophiles in DA reactions anticipating that these intermediates might emulate the electronic properties of activated dienophiles.

To test the reactivity of α,β–unsaturated acylammonium salts as dienophiles, we targeted the synthesis of *cis*– and *trans*–fused bicyclic γ– and δ–lactones which are ubiquitous structural motifs found in bioactive terpenoids and pharmaceuticals (Figure 2.1a). We envisioned that this bicyclic architecture could be constructed in a single operation by a Diels–Alder/lactonization (DAL) cascade between acylammonium salts, generated *in situ* from acid chlorides or carboxylic acids (activated *in situ*) **1**, a chiral tertiary amine organocatalyst, and rationally designed dienes **2** (Figure 2.1b). We recognized the potential for further stereochemical diversity if racemic dienes bearing a pendant carbinol, *e.g.*, ($\pm$)-**2** ($R^6 \neq R^7$), could participate in an unprecedented DA-initiated, stereodivergent [42] organocascade.
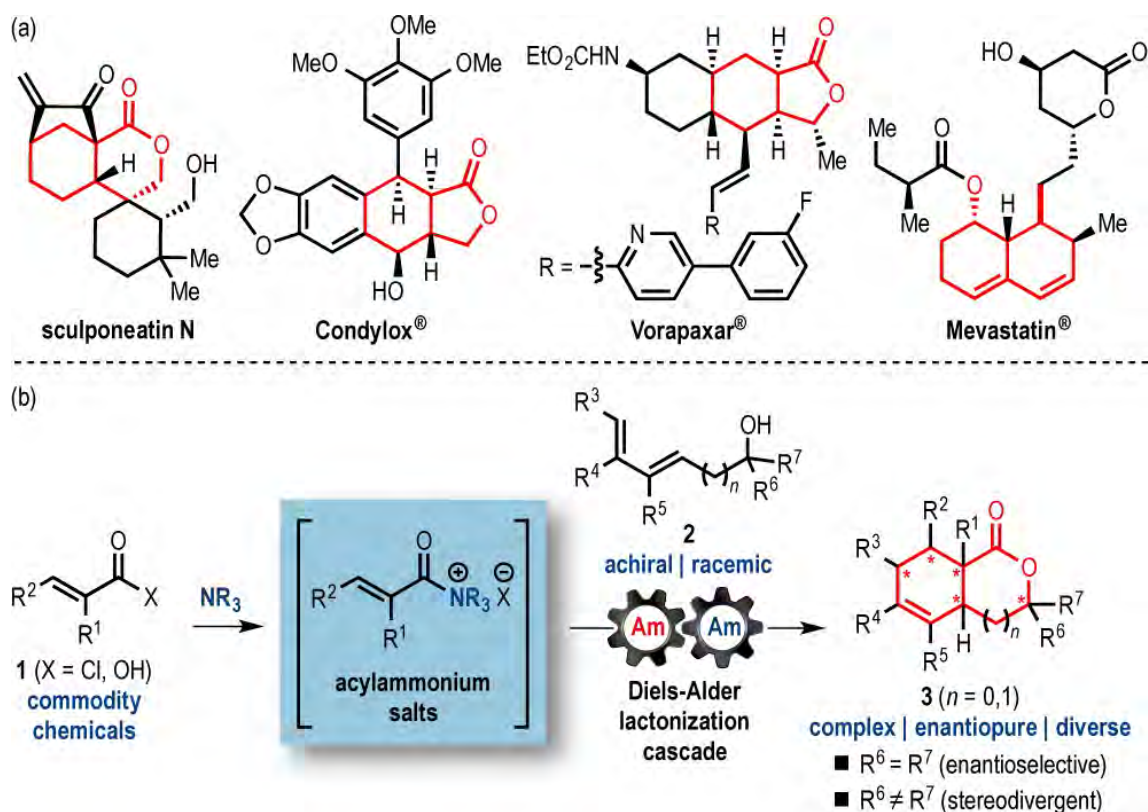
Figure 2.1 (a) Selected natural products and pharmaceuticals containing or derived from *cis*– or *trans*–fused bicyclic γ– or δ–lactones. (b) The described organocatalytic Diels–Alder/lactonization cascade sequence [65].

This process could proceed through catalyst control during the DA step, independent of the resident stereocenter, and the subsequent lactonization step would generate diastereomeric lactones **3** with distinct topologies that could facilitate chromatographic separation, a common challenge for stereodivergent processes.

2.2 Optimization Studies of the DAL

We initiated our studies of the DAL organocascade with a Danishefsky diene **2a** bearing a tethered tertiary alcohol to minimize competitive acylation while providing

greater reactivity and synthetic versatility [43]. In the absence of a nucleophilic promoter, a significant background DAL proceeds with ethyl fumaroyl chloride (**1a**) to afford an inseparable mixture of *endo/exo* diastereomers of bicyclic γ–lactones **3a** and **3a′** in 21% yield (Supporting Information (SI), Table S1).

Table 2.1 Selected Optimization Studies of the DAL[a]
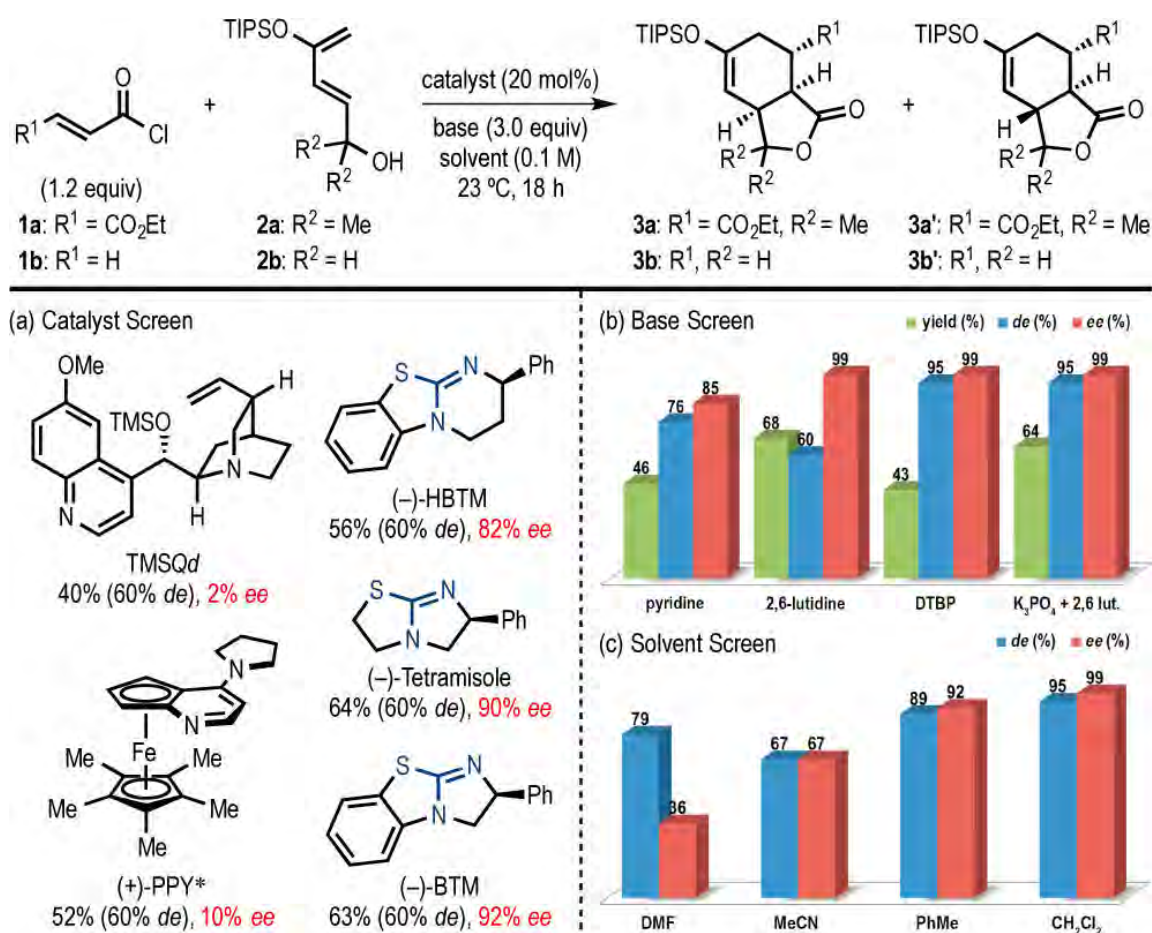
[a]Yields of isolated, purified products; *endo/exo* ratios determined by ^{1}H NMR analysis; *ee* determined by chiral–phase HPLC and only shown for *endo* diastereomer (see SI for details). Reaction conditions: (a) **1a**, **2a**, 2,6–lutidine, CH$_2$Cl$_2$; (b) **1b**, **2b**, (–)-BTM, CH$_2$Cl$_2$; (c) **1b**, **2b**, DTBP, (–)-BTM. DTBP = 2,6–di–*tert*–butylpyridine [65].

A catalyst screen revealed that chiral isothioureas [44] were superior (Table 2.1a) with best results obtained using benzotetramisole, (−)-BTM [44b]. Extending addition times of **1a** through syringe pump addition ensured high enantioselectivity (Table S1, entries 9, 11) presumably by enabling the asymmetric DAL to compete effectively with the racemic background pathway. Further optimization studies revealed that *endo*/*exo* selectivity was highly dependent on the Brønsted base and also that pendant primary alcohols were tolerated. Thus, we next screened various Brønsted bases with diene **2b**, acid chloride **1b**, and (−)-BTM as catalyst (Table 2.1b). Generally, pyridine bases afforded superior levels of enantioselectivity (Table S2, entries 6–15), while substantial steric bulk adjacent to the pyridine nitrogen suppressed formation of the *exo* diastereomer with concomitant reduction in yield (Table S2, entry 8). Use of a shuttle base [45] was successful and delivered **3b** in 64% yield (95% *de*, 99% *ee*). Finally, a solvent screen revealed that chlorinated solvents provided the highest levels of diastereo– and enantioselectivity (Table 2.1c; Table S3, entries 8–10).

Table 2.2 Scope of the Enantioselective DAL

The scope of the DAL was studied under optimized conditions with dienes **2b–f** and commercially available acid chlorides **1a–d** possessing varying electronic and steric properties. Diastereoselectivities were consistent (>19:1 *endo*/*exo*), while enantioselectivities ranged from 91 to 99% *ee* (Table 2.2).

Table 2.2 Enantioselective DAL Organocascade[a]

(−)-**3b**	(−)-**3c**	(−)-**3d**
62%, 94% *ee*	68% (40%[†]), 99% *ee*	84%, 99% *ee*
	[gram scale]	[gram scale]
(−)-**3e**	(−)-**3f** [(+)-**3f**][‡]	(−)-**3g**
92%, 99% *ee*	74% (71%[‡]), 98% *ee* (96% *ee*[‡])	55%, 95% *ee*
(−)-**3h**	(+)-**3i**	(+)-**3j**
46%, 91% *ee*	48% (37%[§]) 99% *ee*	54%, 92% *ee*
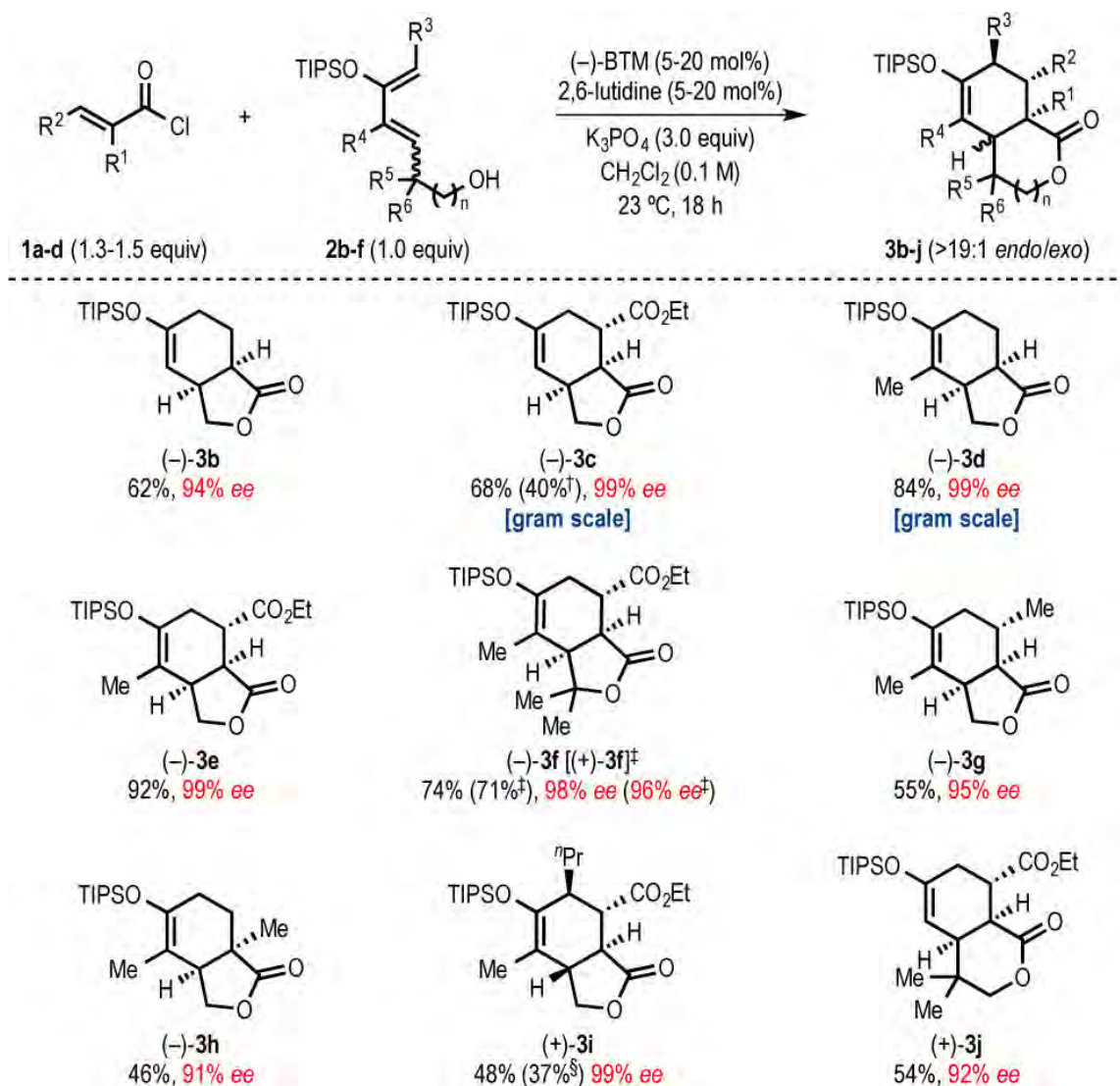
[a]Yields refer to isolated, purified products; *endo*/*exo* ratios determined by ^{1}H NMR analysis; *ee* determined by chiral–phase HPLC. [†](−)-BTM (10 mol%) was used. [‡](+)-BTM (20 mol%) was used. [§](−)-BTM (5 mol%) was used [65].

Cis–fused bicyclic γ–lactones **3b**–**h** were readily obtained from (*E*)-dienes with both α–

and β–substituted acid chlorides. Use of crotonoyl chloride (**1c**) and methacryloyl

chloride (**1d**) led to less reactive acylammonium dienophiles, as reflected in reduced

32

yields of cycloadducts (–)-**3g** and (–)-**3h**; however, enantioselectivity was maintained. Use of a (*Z,Z*)–configured diene **2e** produced the *trans*–fused bicyclic γ–lactone (+)-**3i** in 48% yield (99% *ee*) despite the unfavorable conformation that typically impedes effective cycloaddition [46]. Variation in tether length of the pendant alcohol as in diene **2f** (*n* = 1) afforded the bicyclic δ–lactone (+)-**3j** in 54% yield (92% *ee*). Use of the enantiomeric isothiourea catalyst, (+)-BTM, provided the enantiomeric lactone (+)-**3f** in 71% yield (96% *ee*). Lowered catalyst loadings of 10 and 5 mol% gave *cis*– and *trans*–fused bicyclic γ–lactones (–)-**3c** and (+)-**3i** with similar levels of enantioselectivity but diminished yields. In these cases, lower yields were due to decomposition of dienes and irreversible acylation of the tethered alcohol moiety leading to dienyl esters (*e.g.*, see SI, p S120). The preparative utility of the DAL was demonstrated by two gram–scale reactions affording 1.4 g of (–)-**3c** (68% yield) and 4.0 g of (–)-**3d** (84% yield).

2.4   Stereodivergent DAL Organocascade

Given the terminal lactonization step, we reasoned that a stereodivergent resolution of a racemic diene possessing a pendant stereogenic carbinol using the DAL strategy would be feasible. Indeed, reaction of racemic diene (±)-**2g** bearing a pendant, secondary alcohol delivered readily separable fused, tricyclic γ–lactones (–)-**3k** (50% yield, 99% *ee*) and (–)-**3k'** in (35% yield, 99% *ee*) which are useful intermediates toward compactin [47] and forskolin [48]. The stereochemistry of (–)-**3k** and (–)-**3k′** was assigned by X–ray analysis; in the latter case following cleavage with 4–bromobenzylamine (Table 2.3a, insets; Figures S1 and S2).

Table 2.3 Stereodivergent DAL Organocascades[a]
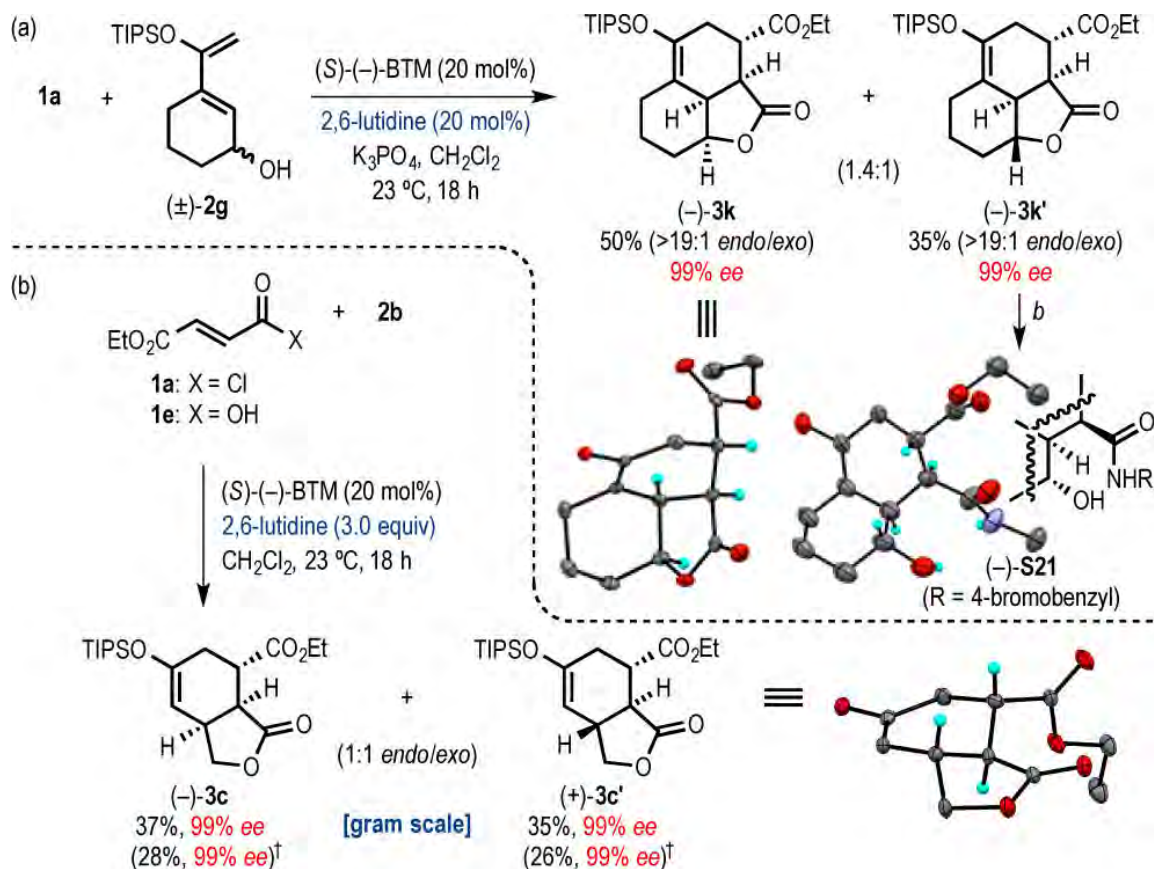
[a]Yields and ratios of isolated, purified products; *ee* determined by chiral–phase HPLC. Insets are single crystal X–ray structures in ORTEP format (50% probability; TIPS and 4–bromobenzyl groups are removed for clarity). Reaction conditions: 4–BrC$_6$H$_4$CH$_2$NH$_2$, THF, 23 °C, 36 h (73%). [†]Reaction performed with carboxylic acid **1e** activated *in situ* by TsCl (SI, p S134) [65].

During optimization studies, we noted the profound impact of the Brønsted base on *endo/exo* selectivities, and sought access to *trans*–fused bicyclic lactones through judicious combination of a Lewis and Brønsted base to enhance *exo* selectivity. Indeed, use of 2,6–lutidine (3.0 equiv) with (–)-BTM and diene **2b** altered the *endo/exo* selectivity to furnish readily separable *cis*– and *trans*–fused bicyclic γ–lactones (–)-**3c**

(37%, 99% *ee*) and (+)-**3c′** (35%, 99% *ee*) (Table 2.3b). We cannot speculate regarding the origins of this Brønsted base dependence at this time, however we are investigating this phenomena further through both experimentation and computation. We also studied *in situ* activated carboxylic acids in this context, to expand the substrate repertoire of the DAL, and found that activation of mono–ethyl fumarate (**1e**) with TsCl afforded (–)-**3c** and (+)-**3c′** with identical enantiopurity but slightly reduced yields. The absolute configuration of bicyclic γ–lactone (+)-**3c′** was determined by X–ray anomalous dispersion (Figure S3). These data, in conjunction with detailed 2D NMR analysis and both predicted and calculated (*vide infra*) lowest energy transition states, enabled assignment of relative and absolute configurations of cycloadducts **3b**–**j**.

2.5   Synthetic Utility

We next sought to demonstrate the utility of the enantioenriched lactones obtained through the DAL (Figure 2.2). Bicyclic γ–lactone (–)-**3d** was converted to α,α–dimethyl lactone (–)-**4** corresponding to the core of glaciolide [49a], a degraded and rearranged diterpenoid, *via* regioselective α–methylation. Direct α–selenylation of silyl enol ether (–)-**3h** followed by oxidative elimination delivered enone (–)-**5**, an intermediate previously employed as a racemate toward fraxinellonone [49b], and the fungal pheromones, trisporic acids and trisporols [49c].
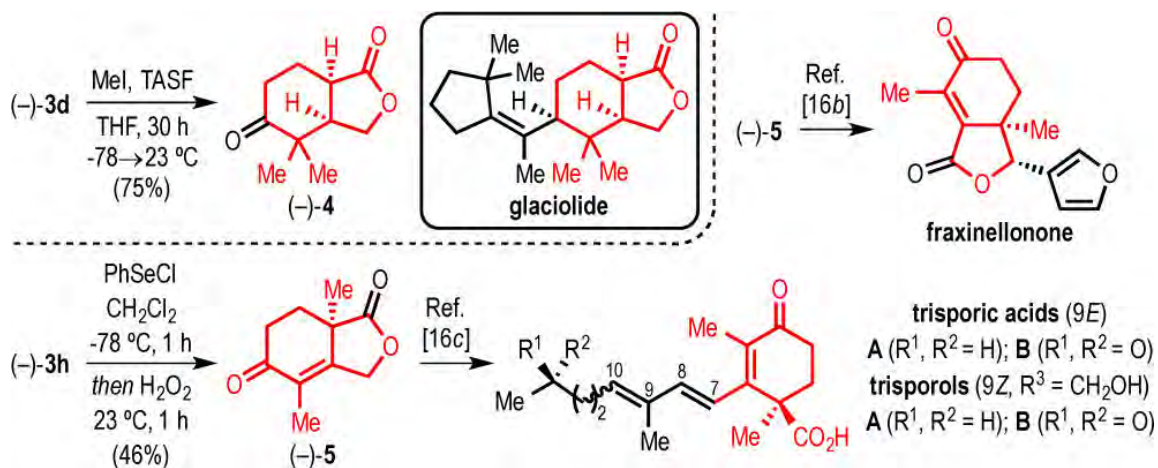
Figure 2.2 Synthetic utility of bicyclic γ–lactones [65].

2.6 Postulated Reaction Pathway for the DAL

To understand the origins of the enantio– and diastereoselectivity induced by (–)-BTM, all four possible transition state structures (TSSs) for the catalyzed DAL were compared to each other and to background DA cycloadditions proceeding directly with acid chloride. Analysis of the lowest energy conformations of each TSS indicates a kinetic preference (1–2 kcal/mol) for *endo* approach (Figure 2.3) and an even larger preference (>5 kcal/mol) for approach of diene from the bottom face of the dienophile opposite the phenyl substituent of (–)-BTM, leading to the observed major enantiomer.
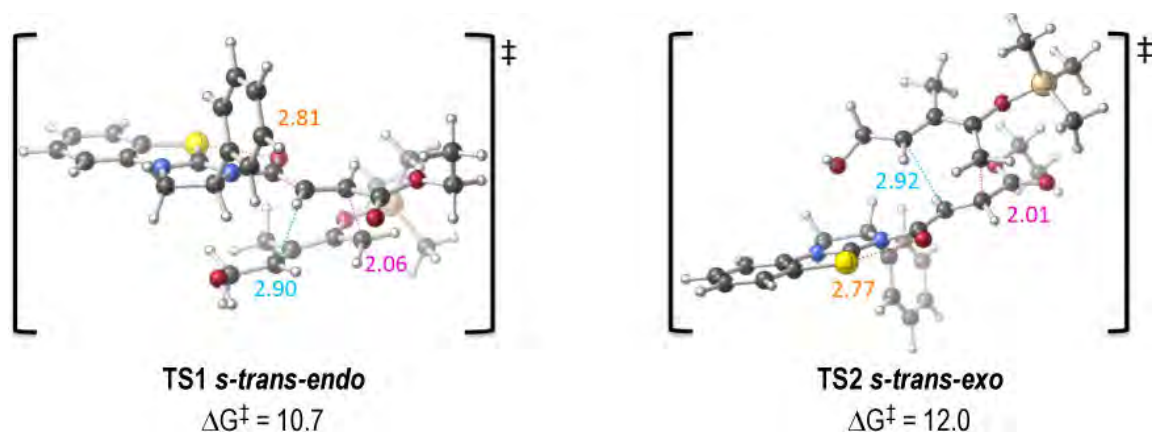
Figure 2.3 Calculated transition structures for the DA step of the DAL optimized at the M06–2X/6–31G(d) level with an implicit solvent model [SMD (dichloromethane)]. Gibbs free energies in kcal/mol shown are relative to the reactants. Selected bond distances are shown (Å) [65].

This selectivity model is predicated on a preference for a close contact between the carbonyl oxygen and sulfur atom of the catalyst restricting rotation about the C–N bond of the acylammonium salt (see inset, Figure 2.4). Such a preference is indeed found in isolation (2.81 Å) and in the TSSs (2.81 and 2.77 Å, *endo/exo*, respectively). The apparent S–O attraction for isothiourea catalysts [50] appears in this case to be driven by a combination of orbital interactions (probed with NBO), in particular, lone pair$_S$ ↔ $\sigma^*_{C–H}/\sigma_{C–H}$ interactions that disfavor the alternative conformation with a O–C–N–C dihedral angle of 180°. Furthermore, the catalyzed DA reaction is predicted to have a lower activation barrier than the background reaction.

A postulated reaction pathway is illustrated in Figure 2.4. Reaction of acid chloride **1a** with (–)-BTM forms acylammonium salt **6** that undergoes *endo*–selective intermolecular DA with diene **2b** to form an initial, catalyst–bound cycloadduct **7**. The

presumed tetrahedral intermediate **8** then enters a shuttle deprotonation cycle in which catalytic 2,6–lutidine relays its proton to stoichiometric K$_3$PO$_4$ and undergoes intramolecular lactonization to form **3e** and regenerate the catalyst.
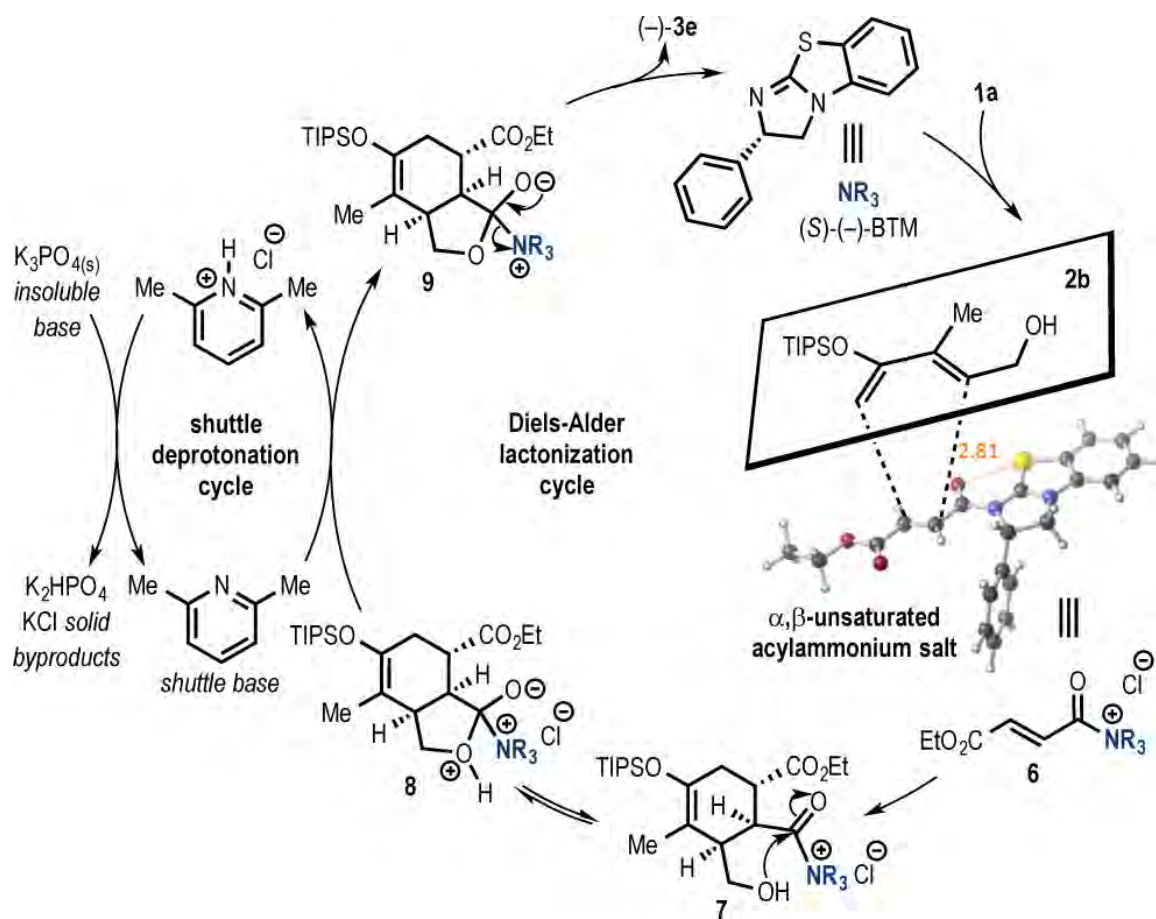
Figure 2.4 Postulated reaction pathway for the DAL [65].

2.7   Conclusions

In summary, we have unveiled a new and versatile family of chiral dienophiles, α,β–unsaturated acylammonium salts, that undergo enantioselective and stereodivergent DAL organocascades rapidly generating complex and stereochemically diverse scaffolds. This scalable process proceeds under mild conditions, provides excellent relative and absolute stereocontrol, and utilizes readily prepared dienes, commodity acid chlorides, and commercially available organocatalysts. A prominent feature of the described methodology is the use of a DA reaction to initiate an organocascade; a strategy with limited precedent [51]. The utility of the DAL was demonstrated by conversion of the derived bicyclic lactones to several core structures of natural products constituting formal syntheses in some cases. Computational results suggest kinetic preference for an *endo* TS with enantiocontrol ascribed to stereoelectronic and conformational preferences of the acylammonium salt dienophiles. Further applications and mechanistic investigations are underway to delineate the scope of this methodology.

CHAPTER III

STEREODIVERGENT, DIELS–ALDER–INITIATED ORGANOCASCADES

EMPLOYING ACYLAMMONIUM CATALYSIS

3.1   Background and Significance

The development of efficient transformations that provide expedient and selective access to the full stereochemical array of compounds with multiple stereocenters remains a notable challenge in chemical synthesis [52]. Such stereodivergent processes have particular impact beyond the realm of synthetic chemistry. The specificity of action and biological properties of an organic molecule correlate to its structural complexity and well–defined three–dimensional architecture and directly depend on its stereochemical configuration [53]. Essentially, the ability to access all stereoisomeric permutations of a natural product or lead candidate allows complete evaluation of stereochemical structure–activity relationships. Access to the complete set of stereoisomers of a given scaffold from the same substrate has been previously realized for conjugate addition [54], Mannich reaction [55], intramolecular allylic substitution [56], deracemization [57], sulfa–Michael addition [58], hydrohydroxyalkylation [59], and most recently an elegant example involving α–allylation of aldehydes was reported by Carreira [60]. Prospectively, the complex stereoselectivity issues inherent to DA cycloaddition provide an opportunity to address the most significant limitation of asymmetric catalytic variants of this venerable transformation: when applied towards generating complex chiral molecules with

multiple stereocenters in a single operation, chemists cannot selectively access the full matrix of stereoisomers using a single chiral organocatalyst. Enantiomeric pair of a chiral catalyst individually provides the mirror image products (complementary enantioselectivity); however, researchers are still unable to modulate the sense of diastereoselectivity (control over the relative stereochemistry) in DA cycloadditions using a single chiral catalyst.

Comparably, synthetic methods that efficiently transform racemic mixtures into complex enantioenriched products are important components of modern organic chemistry but remain scarce [61]. These include underutilized stereodivergent processes, which convert racemates to non–enantiomeric products [62]. Catalytic asymmetric variants of these reactions employing racemic substrates represent an unexploited strategy toward accessing a full complement of stereoisomers, wherein both optical antipodes of a starting material react with a catalytically activated intermediate to furnish non–enantiomeric products. Sarpong recently described an elegant example of a stereodivergent process applied to natural product synthesis [63], however majority of these reactions suffer from the crucial practical issue of inseparable, diastereomeric products [62].

We have recently reported a new concept for covalent [64] asymmetric, organocatalytic LUMO–lowering acylammonium activation of α,β–unsaturated acid chlorides and carboxylic acids as competent dienophiles and demonstrated its applicability in the Diels–Alder/lactonization organocascade [65]. The potential of α,β–unsaturated acylammonium catalysis (Figure 3.1) was first demonstrated by Fu employing α,β–

unsaturated acyl fluorides in a net [3 + 2] annulation promoted by a chiral 4-pyrrolidinopyridine catalyst [66].
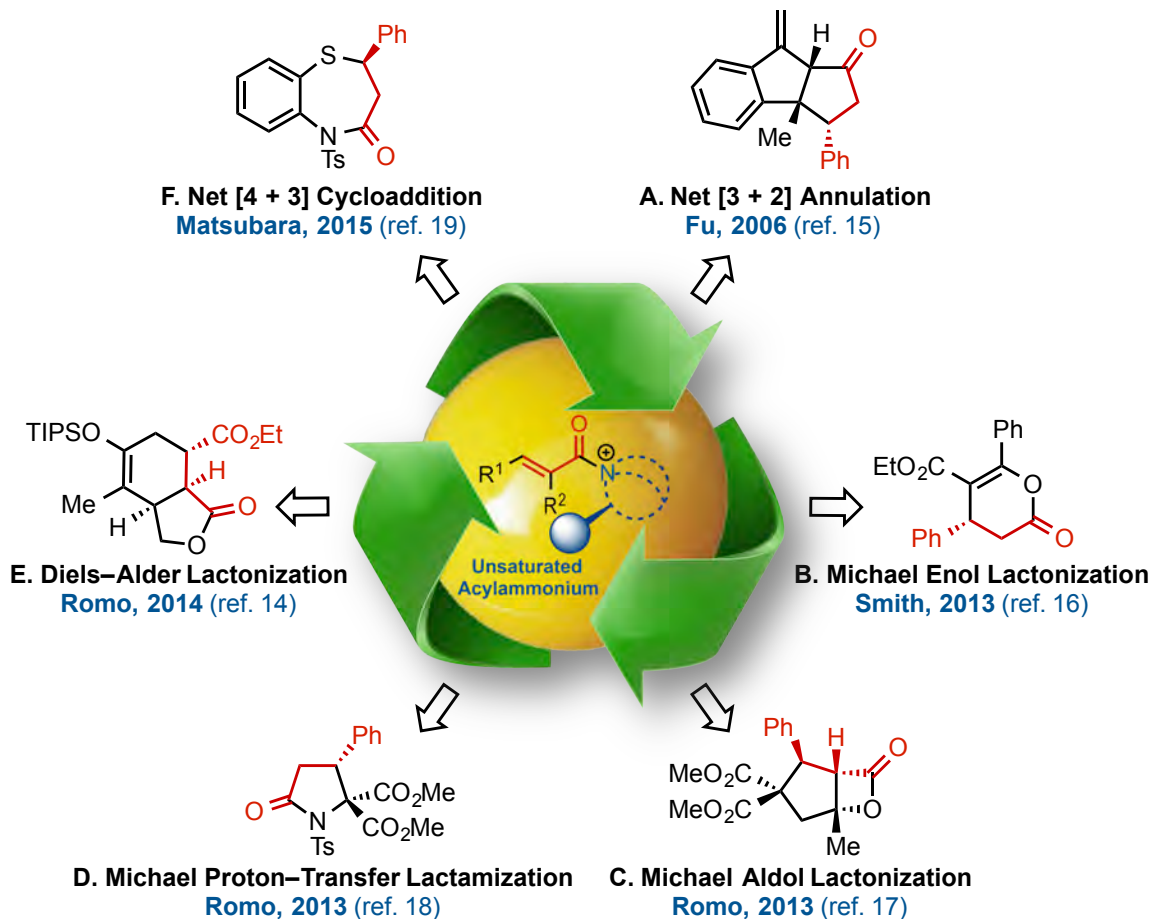
Figure 3.1 The ever–expanding potential of covalent α,β–unsaturated acylammonium organocascade catalysis.

Building on this early work, the Smith group [67] recently utilized α,β–unsaturated mixed anhydrides in an enantioselective tandem Michael–enol–lactonization. Furthermore, we demonstrated the full potential of chiral, triply reactive, α,β–unsaturated acylammonium salts derived from commodity acid chlorides for the rapid assembly of complex cyclopentanes through a nucleophile–catalyzed Michael–

aldol–β–lactonisation organocascade (NCMAL) [68]. Optically active γ–lactams and piperidones could also be rapidly synthesized through a Michael–proton transfer–lactamization (NCMPL) [69] process utilizing these intermediates. Most recently, Matsubara described the first example of a highly enantioselective net [4 + 3] cycloaddition to afford 1,5-benzothiazepines by utilizing α,β–unsaturated acylammonium intermediates generated by a chiral isothiourea catalyst [70].

Despite its rich history, utility [71], simplicity of operation, and continued evolution of strategies that broaden the scope and improve the stereoselectivity of the venerable Diels–Alder (DA) reaction, this cycloaddition arguably remains the most versatile and powerful transform in chemical synthesis [72]. In particular, catalytic asymmetric DA reactions are unparalleled in their ability to rapidly and efficiently generate optically active, architecturally complex, and densely functionalized heterocycles and carbocycles from simple achiral substrates. Furthermore, enantioselective organocatalytic DA variants have recently been established using iminium [73], enamine [74], bifunctional acid-base catalysis [75], and hydrogen–bonding catalysis [76]. MacMillan and coworkers employed both α,β–unsaturated aldehydes [73a] and ketones [73b] in cycloadditions through iminium–activated chiral dienophiles **2**, whereas unsaturated aldehydes [76a] and indolinones [76b] were activated through hydrogen–bonding catalysis **3** by Rawal and Barbas, respectively (Figure 3.2a). Surprisingly, it was not until our recent report that a method for utilizing α,β–unsaturated acid chlorides **5** or carboxylic acids as dienophiles for organocatalytic asymmetric DA reactions has been successfully established. However, more importantly,

our initial results have unveiled the first example of DA–initiated, stereodivergent organocascade (Figure 3.2b) delivering complex and stereochemically diverse scaffolds found in bioactive compounds with excellent relative and absolute stereocontrol [65].
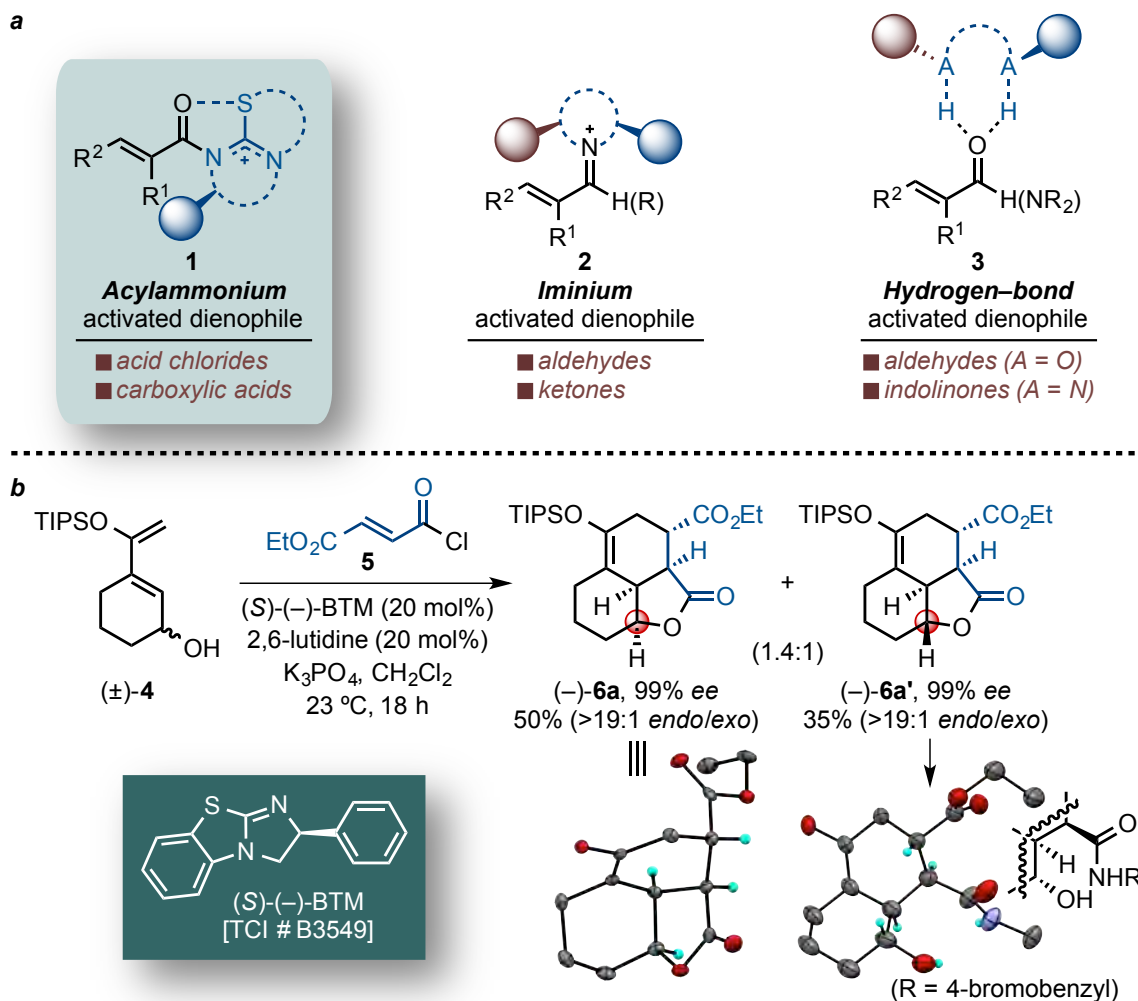
Figure 3.2 (a) Representative activation modes of α,β–unsaturated carbonyl compounds for organocatalytic asymmetric DA reactions. Formation of acylammonium–activated dienophiles **1** from acid chlorides or *in situ* activated carboxylic acids enables organocatalytic LUMO–lowering activation for DA cycloadditions. (b) The seminal example of DA–mediated, stereodivergent resolution of the racemic diene (±)-**4** employing α,β–unsaturated acylammonium salt, generated *in situ* from acid chloride **5** and isothiourea catalyst, (*S*)-(–)-BTM.

With potential applications for diversity–oriented synthesis (DOS), we have implemented a synergistic combination of a chiral isothiourea catalyst capable of exercising high relative and absolute stereocontrol and a Brønsted base impacting *endo*/*exo* selectivities enabling stereodivergent access to the full array of stereoisomeric cycloadducts in our initial findings [65]. The increasing importance of DOS to access structurally complex and diverse small–molecule libraries [77] is premised on its value for drug discovery [78], chemical genetics [79] and identification of small–molecule modulators of challenging biological targets [80]. In particular, synthetic methods that rapidly generate stereochemical complexity [81] are important for drug lead discovery and a recent success for drug development is exemplified by the antimalarial agent, NITD609, currently in Phase IIa clinical trials [82]. Furthermore, natural product–inspired libraries are providing higher success rates in identifying more potent and drug–like molecules [83].

In our ongoing studies to unravel the Lewis base–Brønsted base synergy, we observed certain trends pertaining to diastereocontrol that, based upon the observed temperature–independence, could culminate in a hierarchical set of empirically derived, practical guidelines allowing for both prediction and tenability of diastereoselectivity. Most known asymmetric reactions possess temperature–dependent diastereodifferentiation and thus are performed at low temperatures due to their strategic design to induce sufficient $\Delta\Delta H^{\ddagger}$ by steric repulsion, structural strain, or electronic interaction in the transition states. Conversely, from a synthetic viewpoint, entropy–controlled asymmetric transformations with sufficient $\Delta\Delta S^{\ddagger}$ are preferable due to their

45

independence of the reaction temperature. However, entropy–driven diastereoselective reactions remain particularly scarce. To date, only two reports have demonstrated the principle of entropy–controlled stereoselectivity, which include an intramolecular [2 + 2] cycloaddition of a chiral pentanediol tether [84] and a vinylation of a cyclic chiral nitrone [85]. To our knowledge, entropy–driven diastereodifferentiation in an organocatalyzed transformation have yet to be shown.

Intrigued by this possibility and operational simplicity of our highly asymmetric stereodivergent organocascade, we conducted a thorough study to optimize the reaction conditions and further delineate the substrate scope. Herein, we demonstrate the ability of a single chiral organic small molecule, the isothiourea–based tertiary amine, to catalyze highly enantio– and diastereoselective DA–initiated organocascades. We have found that the function of the catalyst can be modulated to induce diastereodivergent pathways by applying an external stereoelectronic stimulus. By judiciously choosing particular Brønsted bases, we can switch the enforced sense of diastereoinduction, thus potentially allowing access to all possible diastereoisomeric cycloadducts. The present study suggests the potential of the stereoelectronic effects to induce sufficient differential activation entropy and reveal a new aspect for designing asymmetric transformations. While the applicability of this concept has been demonstrated as mentioned above, questions remain as to the exact nature of active catalytic species and the role of Brønsted base in the enantio– and diastereodetermining step of the organocascade. In fact, it has thus far remained unclear whether a species corresponding

to catalyst–Brønsted base amalgam is actually involved in the catalytic process. Here we report the results of experiments and computations that shed light on these questions.

3.2 Substrate Scope of the Stereodivergent DAL

To explore the potential of α,β–unsaturated acylammonium salts as competent dienophiles for the stereodivergent Diels–Alder/lactonization organocascade, we targeted the synthesis of complex, γ–substituted *cis*–fused bicyclic γ–lactones, ubiquitous and privileged structural motifs found in biologically active natural products (Figure 3.3b), potentially accessible in a single operation (**7→8→11**) (Figure 3.3a). Conventional strategies toward complex γ–substituted bicyclic γ–lactones typically require multistep processes involving *exo*–selective diastereoselective intramolecular DA cycloadditions (**7→10→11**) employing optically active dienes [86] including those obtained by enzymatic resolution [87] (**7→9→10**). Toward introducing stereochemical complexity to the described strategy, we utilized racemic dienes bearing a pendant carbinol, *e.g.* (±)-**7** ($R^6 \neq R^7$) to open possibilities for a stereodivergent lactonization. This strategy has the potential to generate up to four new stereocenters through catalyst control independent of the resident stereocenter, and the subsequent lactonization step would deliver diastereomeric polycyclic adducts with distinct topologies that may facilitate separation.
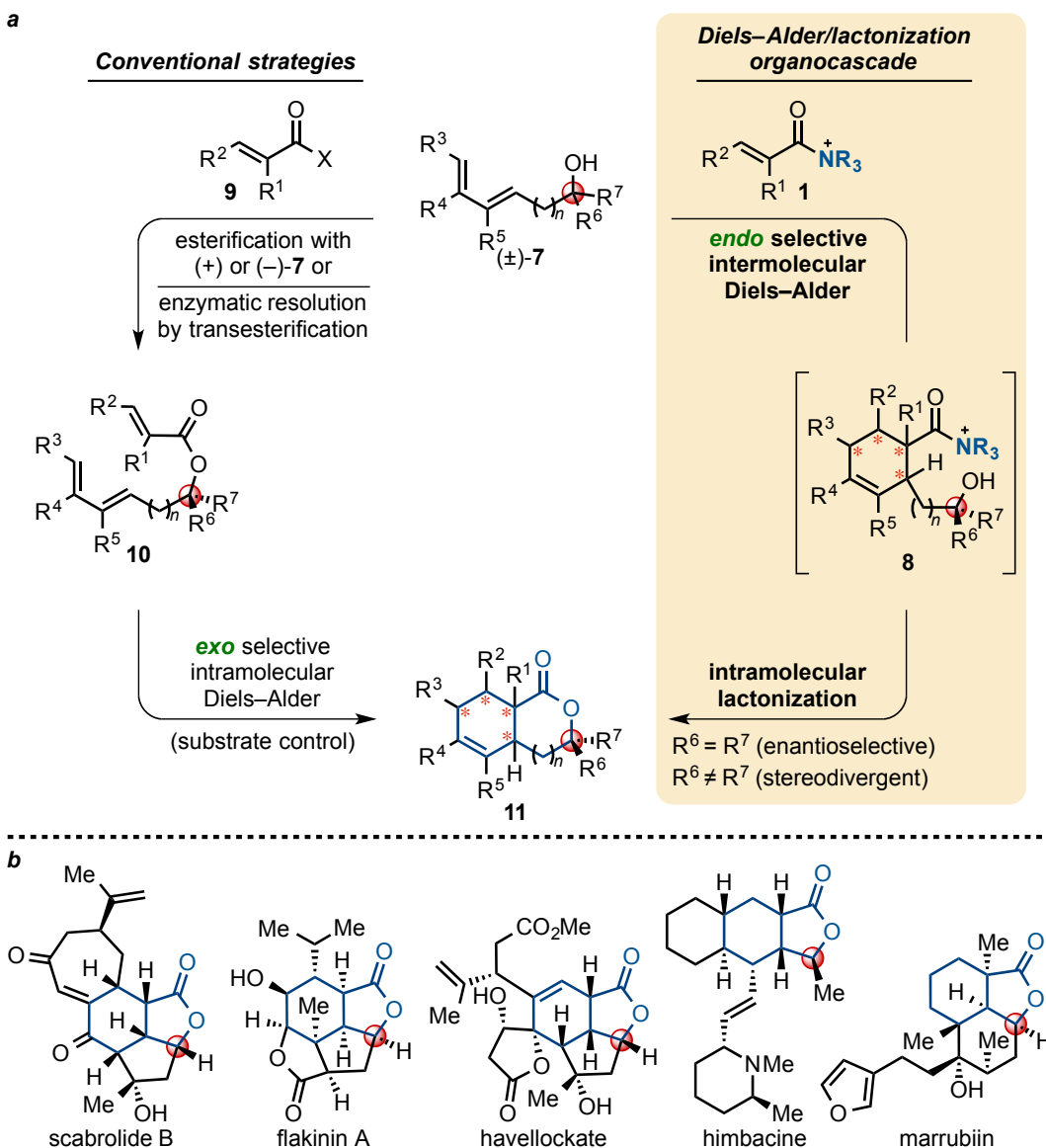
Figure 3.3 (a) Comparison of conventional strategies (**7**→**10**→**11**) toward complex, γ–substituted optically active bicyclic γ–lactones **11** with the described single–operation, Diels–Alder/lactonization (DAL) organocascade (**7**→**8**→**11**). Use of racemic dienes (±)-**7** bearing a pendant carbinol stereocenter (denoted with a red circle) enables a diastereodivergent organocascade that introduces up to four additional stereocenters through catalyst control independent of the resident stereocenter. (b) Selected structures of naturally occurring and biologically active terpenoids containing γ–substituted, *cis*–fused bicyclic γ–lactones.

We initiated our scope survey of the stereodivergent DAL organocascade with the racemic silyloxydiene (±)-**13a** bearing a pendant, secondary benzylic alcohol and ethyl fumaroyl chloride (**12a**) in the presence of (*S*)-(–)-BTM to deliver a readily separable 1.5:1 diastereomeric mixture of bicyclic γ-lactones (–)-**14a** (99% *ee*) and (+)-**14a'** (98% *ee*) in 48% and 31% yield, respectively (Table 3.1). Similarly, diene (±)-**13b** bearing a pendant, tertiary benzylic alcohol afforded cycloadducts (+)-**14b** (41% yield, 99% *ee*) and (+)-**14b'** (23% yield, 99% *ee*) on gram–scale as a separable 1.8:1 diastereomeric mixture bearing four contiguous stereocenters, including a quaternary carbon. In contrast, racemic silyloxydiene (±)-**13c** possessing a (*Z,Z*)–configured diene, a pendant secondary benzylic alcohol, and an *n*–propyl substituent provided *trans*–fused bicyclic γ–lactone (+)-**14c** as a single diastereomer with five contiguous stereocenters in 40% yield (99% *ee*) despite the cis-substituent that typically impedes effective cycloaddition [88]. To the best of our knowledge, there is no report to date of an asymmetric, catalytic DA cycloaddition with a *cis*–substituent diene that occurs at ambient temperature (23 ºC) [89]. We also targeted more complex polycycles through this stereodivergent DAL process by use of the racemic monocyclic diene (±)-**13d** bearing a secondary cyclohexanol. Cycloaddition of this diene with crotonoyl chloride (**12b**) gave the fused, tricyclic 6,6,5–system on gram–scale as separable diastereomers (–)-**14d** and (–)-**14d'** in 35% (99% *ee*) and 24% yield (99% *ee*), respectively. The absolute configuration of crystalline cycloadduct (–)-**6a** was previously determined unambiguously by X–ray analysis while cycloadduct (–)-**6a'** required ring opening of γ-lactone with 4–bromobenzylamine (Figure 3.2b).

49

Table 3.1 Diels–Alder mediated stereodivergent resolution of racemic dienes employing α,β–unsaturated acylammonium salts[a]

entry	diene	acid chloride	cycloadducts % yield (endo:exo, % ee)		
1	(±)-**13a**	**12a**	(−)-**14a** 48 (>19:1, 99)	+ (1.5:1)	(+)-**14a'** 31 (>19:1, 98)
2	(±)-**13b**	**12a**	(+)-**14b** 41 (>19:1, 99) [gram scale]	+ (1.8:1)	(+)-**14b'** 23 (>19:1, 99)
3	(±)-**13c**	**12a**	(+)-**14c** 40 (>19:1, 99)	+ (>19:1)	**14c'** not observed
4	(±)-**13d**	**12b**	(−)-**14d** 35 (>19:1, 99) [gram scale]	+ (1.5:1)	(−)-**14d'** 24 (>19:1, 99)

[a]Unless otherwise specified, all reactions performed with dienes (±)-**13a**–**d** (1.0 equiv.), acid chlorides **12a**,**b** (1.5 equiv.), K$_3$PO$_4$ (3.0 equiv.), 2,6–lutidine (20 mol%), and (S)-(−)-BTM (20 mol%) at 23 °C for 18 h. Yields and diastereomeric ratios are based on isolated, purified cycloadducts. Enantiomeric excess was determined by chiral–phase HPLC (see Supplemental Figure S3).

This structural information in conjunction with 2D NMR analysis enabled assignment of the relative and absolute con-figurations of cycloadducts **14a–d** and **14a'–d'**. In general, lower yields observed in these cases were due to decomposition of dienes and irreversible acylation of the tethered alcohol moiety (*e.g.* (±)-**S10**, see Supplemental p. 216). While more sterically demanding α,β– and β,β–disubstituted acid chlorides and non–oxygenated dienes required extended reaction times, elevated temperatures, or higher catalyst loadings to achieve synthetically useful yields.

3.3   Asymmetric Organocatalytic Diels–Alder Cycloaddition of Furanyl Dienes

Toward expanding the breadth of this strategy, we then explored the utility of achiral furanyl dienes bearing a pendant amine to study the potential for terminal lactamization, and more importantly, to address a long–standing unsolved problem of asymmetric organocatalytic DA cycloaddition of furans (Figure 3.4, **15→16→20**). Cycloadditions of furans are notably reversible due to their intrinsic aromaticity, and hence additional activation techniques, such as Lewis–acid catalysis and high–pressure chemistry, are required to obtain a sufficient amount of the desired adducts. Furthermore, the lability of the cycloadducts, even at relatively low temperatures, as well as the sensitivity to acidic conditions of both furans and cycloadducts, typically necessitate immediate post–modification and preclude the use of ambient conditions and strong Lewis–acids. In fact, only two examples of catalytic asymmetric DA reactions of furans have been effectively (67–94% yield, 97–99% *ee*, 4–7.3:1 *endo/exo*) exemplified by Evans [90] (**15→18→20**) and Corey [91] (**15→19→20**) utilizing chiral

51

bis(oxazoline)Cu(II) and oxazaborolidium Lewis–acid catalysts, respectively. The former method is restricted to the reaction temperature of −78 ºC, due to rapid equilibration at higher temperatures, thus permitting isolation of the kinetic product mixture favoring *endo* cycloadduct, while the latter is limited to 2,2,2–trifluoroethyl acrylate as the only suitable dienophile with practical efficacy.
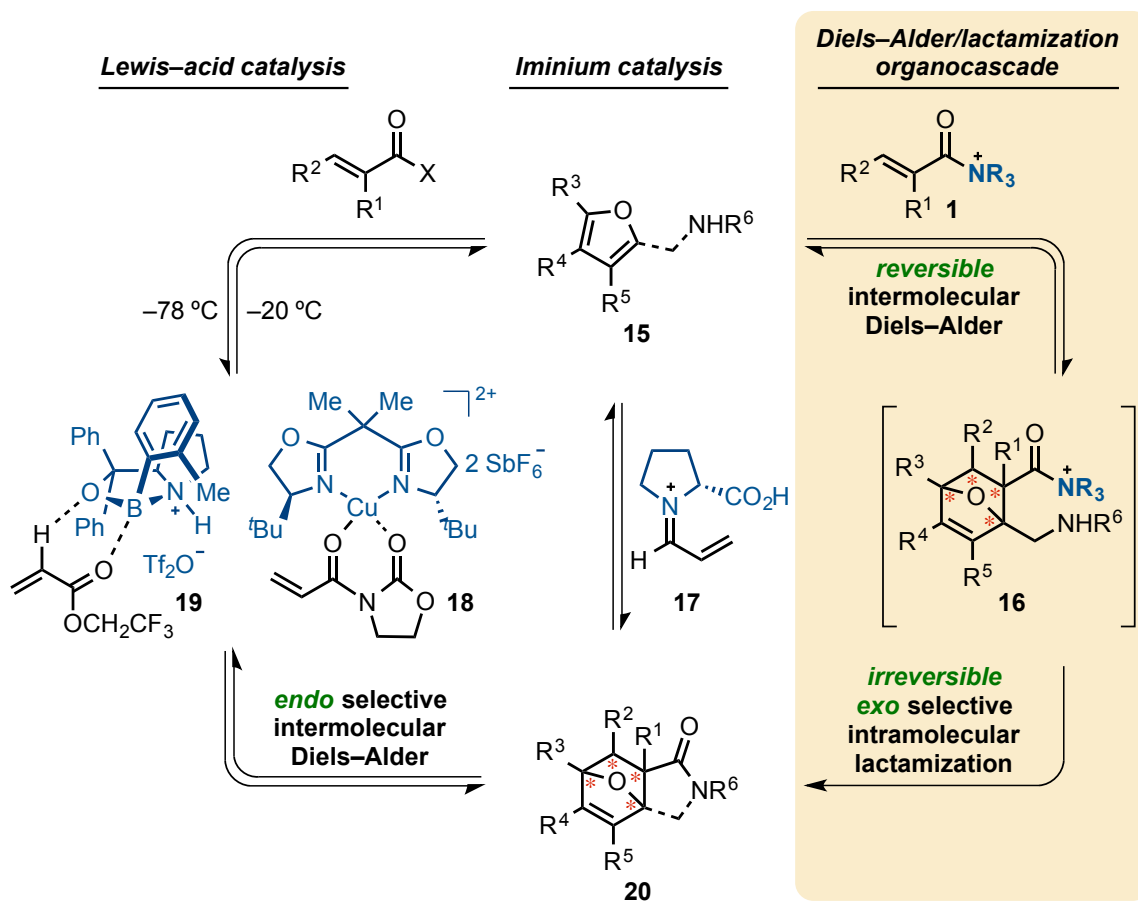
Figure 3.4 Comparison of asymmetric, Lewis–acid catalyzed and previously attempted organocatalytic DA cycloaddition of furans with the described single–operation, Diels–Alder/lactamization (DAL) organocascade.

Recently, Kotsuki [92] attempted the first asymmetric organocatalytic DA reaction of furans catalyzed by 50 mol% *D*–proline (**15**→**17**→**20**) under high–pressure (0.8 GPa), unfortunately however, with insufficient yields (26%) and impractical enantio– (20% *ee*) and diastereoselectivities (1.4:1 *exo/endo*). Low reactivity of furan, poor conversions and the occurrence of side reactions have made this approach problematic. We therefore reasoned that a furan with a pendant, stereoelectronically–tuned amine **15** would initially participate in a reversible intermolecular DA cycloaddition with α,β–unsaturated acylammonium salt **1**, followed by a terminal, irreversible intramolecular lactamization step thus permitting the formation of the thermodynamic *exo* cycloadduct. We initiated our studies of the nucleophile–catalyzed Diels–Alder/lactamization (DAL) organocascade with the furfuryl sulfonamide **21** (Figure 3.5), readily obtained in a single step from inexpensive commercially available materials (see Supplementary). For the initial dienophile precursor, we chose commercially available acryloyl chloride (**22**) in order to impede the anticipated racemic background cycloaddition.
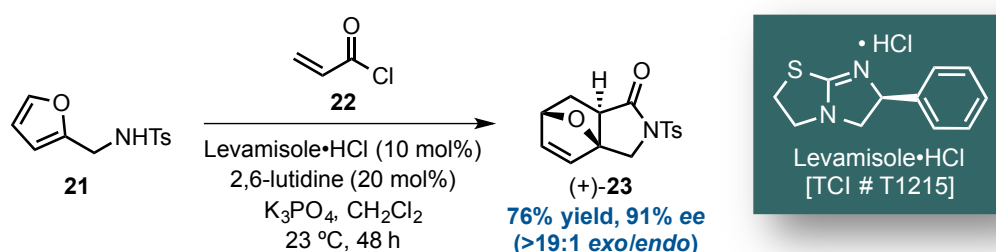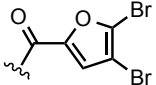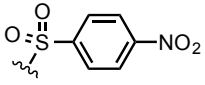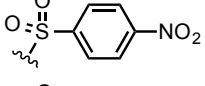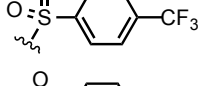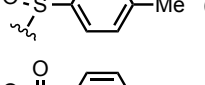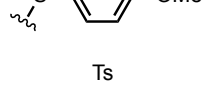
Figure 3.5 The first successful example of highly enatio– and diastereoselective organocatalytic DA cycloaddition of the furanyl diene by means of Diels–Alder/lactamization organocascade.

Our initial reaction conditions involved generation of the α,β–unsaturated acylammonium dienophile in CH_2Cl_2 at ambient temperature (23 ℃) utilizing inexpensive Levamisole hydrochloride (10 mol%) as a nucleophilic promoter with 20 mol% 2,6–lutidine as a shuttle base [93] and potassium phosphate (K_3PO_4, 3.0 equiv.) as stoichiometric insoluble base. To our delight, the reaction generated the *oxa*–bridged *trans*–fused tricyclic γ–lactam **23** in 76% yield and 91% *ee* as a single thermodynamic *exo* diastereomer. Remarkably, this tricyclic γ–lactam was stored at ambient temperatures (23 ℃) for an extended amount of time without racemization. To determine substrate generality and the influence of *N*–substituent groups on enantioselectivity of this process, several dienes **24a–i** with varying electronic and steric properties were evaluated (Table 3.2) under the optimized reaction conditions with highly reactive, doubly–activated ethyl fumaroyl chloride (**12a**). A single *exo* diastereomer was generated in each case, as determined by ^{1}H NMR analysis of the crude reaction mixtures. Predictably, furanyl diene **24a** containing sterically–demanded triphenylmethyl (trityl) group, failed to undergo resultant organocascade (entry 1, Table 3.2) with the acylammonium salt derived from isothiourea (*S*)-(−)-BTM and ethyl fumaroyl chloride (**12a**). Similarly, furanyl dienes **24b–d** possessing *tert*–butyloxycarbonyl (Boc), benzoyl (Bz), and 4,5–dibromofuranoyl groups, respectively, did not afford the corresponding *oxa*–bridged *trans*–fused tricyclic γ–lactams **25b–d** (entries 2–4, Table 3.2), presumably due to delocalization of the nitrogen lone pair onto the oxygen, thus rendering amides **24b–d** much less nucleophilic.

Table 3.2 Optimization of the asymmetric Diels–Alder/lactamization cascade with ethyl fumaroyl chloride[a]

24a–i + 12a → 25a–i (>19:1 *exo/endo*)
(S)-(–)-BTM, **base**, CH₂Cl₂, 23 °C, 48 h
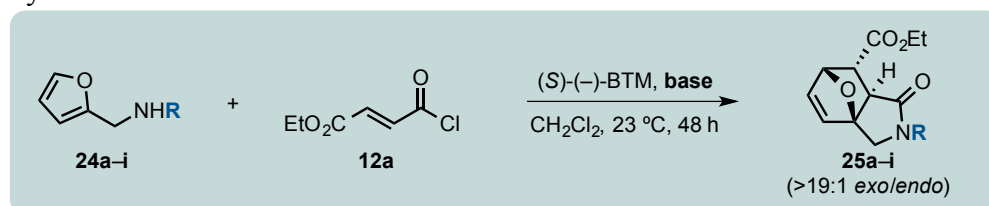
entry	R	catalyst loading (mol%)	base	ee (yield†) %
1	CPh₃	100	2,6-lutidine	*n.r.*
2	Boc	100	2,6-lutidine	*n.r.*
3	Bz	100	2,6-lutidine	*n.r.*
4	(4,5-dibromofuroyl)	100	2,6-lutidine	*n.r.*
5	Bn	100	2,6-lutidine	3 (92)
6	(4-nitrophenylsulfonyl)	0	2,6-lutidine	– (28)
7	(4-nitrophenylsulfonyl)	100	2,6-lutidine	40 (46)
8	(4-CF₃-phenylsulfonyl)	100	2,6-lutidine	51 (40)
9	(4-Me-phenylsulfonyl) (Ts)	100	2,6-lutidine	70 (75)
10	(4-OMe-phenylsulfonyl)	100	2,6-lutidine	75 (82)
11	Ts	20	2,6-lutidine	42 (86)
12	Ts	20	pyridine	83 (88)
13‡	Ts	20	pyridine	92 (85)

[a]Screening studies were performed with dienes **23a–i** (1.0 equiv.), ethyl fumaroyl chloride (**12a**, 1.2 equiv.), (S)-(–)-BTM and base (1.0 equiv.) in CH₂Cl₂ (0.1 M). †All yields refer to isolated, purified yields of cycloadducts. Diastereomeric (*endo/exo*) ratios were determined by ¹H–NMR (500 MHz) analysis of the crude reaction mixture. Enantiomeric excess (*ee*) was determined by chiral–phase HPLC. ‡Acid chloride **12a** was added as a solution in CH₂Cl₂ by syringe pump over 5 h.

Conversely, highly nucleophilic benzylamine **24e** generated the desired cycloadduct **25e** in 92% yield (entry 5, Table 3.2), however with a complete loss of enantioinduction, suggesting the initial *N*–acylation followed by an intramolecular DA cycloaddition as a plausible racemic background pathway. We next screened several *para*–substituted sulfonamides **24f–i** in search for a tunable substituent. As anticipated, in the absence of a nucleophilic promoter, a substantial background DAL proceeds with ethyl fumaroyl chloride (**12a**) to afford a single *exo*–diastereomer of racemic tricyclic γ–lactam (±)-**25f** in 28% yield (entry 6, Table 3.2). The effect of *para*–substituted sulfonamides on enantioselectivity of the described organocascade follows the order: $NO_2 < CF_3 < Me <$ OMe (entries 7–10, Table 3.2). This trend presumably reflects the electron–donor ability of these substituents toward reducing the acidity of corresponding sulfonamides [94] and consequently preventing undesirable *N*–acylation/intramolecular DA pathway. Lowered catalyst loading of 20 mol% (*S*)-(−)-BTM delivered the tricyclic γ-lactam **25h** (entry 11, Table 3.2) with comparable yield (86%) but diminished enantiocontrol (42% *ee*). Efforts to improve enantioinduction through use of a sterically unhindered Brønsted base were successful with pyridine as stoichiometric base provided **25h** in 88% yield (83% *ee*, entry 12, Table 3.2). Extending addition times of the acid chloride **12a** (entry 13, Table 3.2) ensured high enantioselectivity (85% yield, 92% *ee*) presumably by enabling the asymmetric DAL process to compete effectively with the racemic background pathway.

During the course of optimization, we began to realize that a facile cycloreversion reaction between furanyl diene and an isothiourea–bound acylammonium salt could provide a new, straightforward and metal–free catalytic approach toward

enantio– and diastereomerically pure heteropolycyclic scaffolds from their readily accessible achiral counterparts. This presented us with an attractive opportunity to envisage an efficient dynamic kinetic asymmetric transformation (DYKAT) type IV process [95], wherein epimerization of depicted diastereomers E_{RR}, E_{SS}, E_{RS}, and E_{SR} proceeds through reversible destruction of both centers yielding two achiral intermediates C and D (Figure 3.6a). To date, only two case studies of DYKAT type IV have been reported: Córdova's proline–catalyzed one–pot, two–step, polyketide sugar synthesis [96], and Griengl's one-pot, multienzymatic synthesis of 2–amino–1–phenylethanol from glycine and benzaldehyde [97]. Therefore, as depicted in Figure 3.6b, we postulated that a dynamic cycloreversion of the initial kinetic endo intermediate E_{RSRR} (*endo*) to thermodynamically stable *exo* intermediate E_{SRRR} (*exo*) would occur through a retro–Diels–Alder/Diels–Alder (rDA/DA) sequence driven by an intrinsically favorable cycloreversion of furans (E_{RSRR} (*endo*) $\leftrightarrow$ C+D $\leftrightarrow$ E_{SRRR} (*exo*)), followed by a subsequent termination by irreversible spontaneous lactamization (preferentially E_{SRRR} (*exo*) $\rightarrow$ F_{SRRR}). In particular, the isothiourea catalyst could serve dual catalytic role to mediate both the enantioselective forward cycloaddition and the *in situ* cycloreversion of short–lived, diastereomeric acylammonium intermediates. The realization of an efficient DYKAT type IV process with a chiral tertiary amine–catalyzed organocascade is conceptually appealing and adds a new dimension to the repertoire of what remains among the most challenging, yet desirable, goals in catalytic asymmetric synthesis.
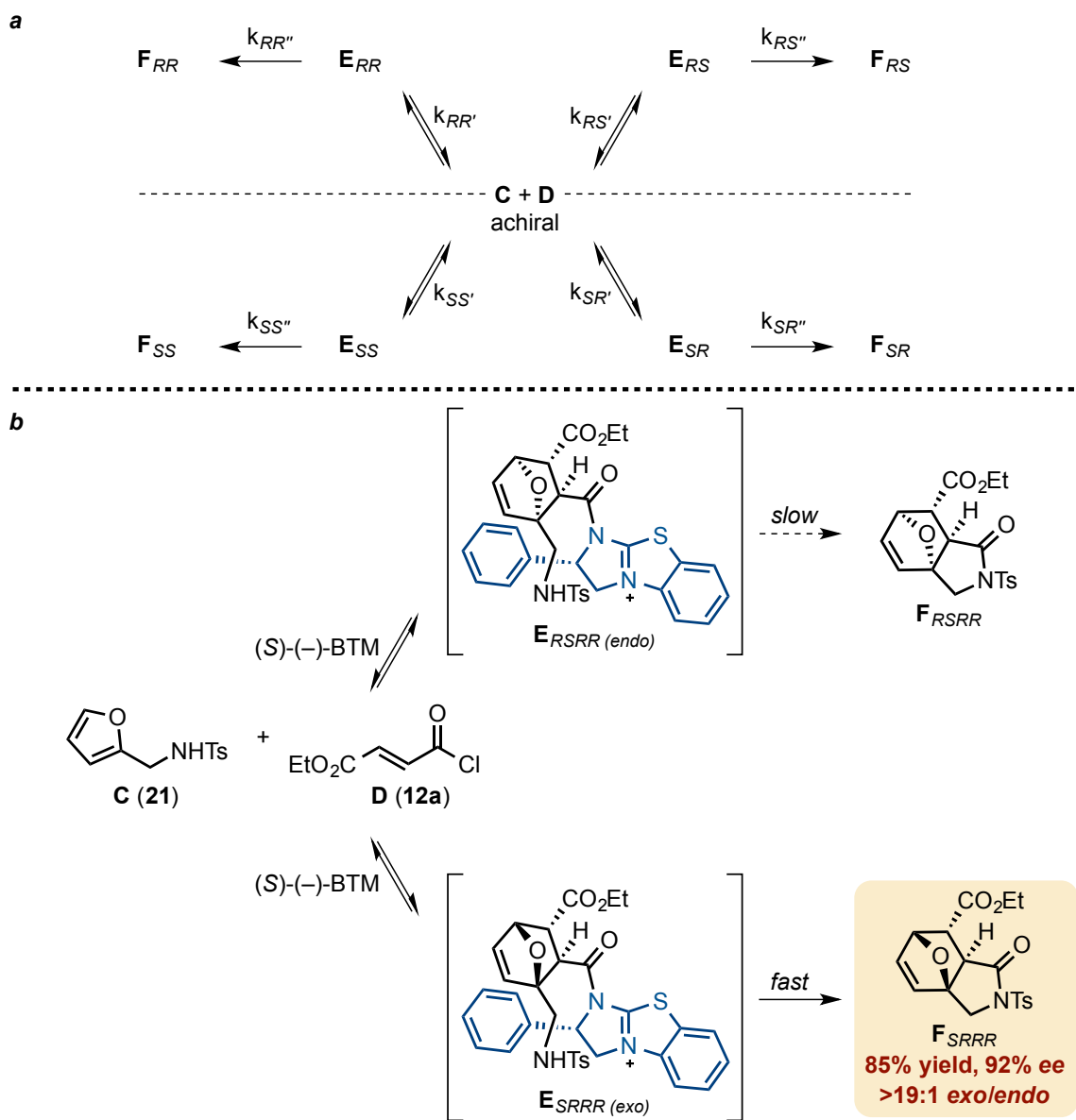
Figure 3.6 (a) DYKAT type IV. E_{RS}/E_{SR} and E_{RR}/E_{SS} are enantiomeric pairs of initial diastereomeric adducts; F_{RS}/F_{SR} and F_{RR}/F_{SS} are enantiomeric pairs of final diastereomeric products; $k_{RR'}$, $k_{RS'}$, $k_{SR'}$, and $k_{SS'}$ are equilibration rates of formation E_{RS}/E_{SR} and E_{RR}/E_{SS}; $k_{RR''}$, $k_{RS''}$, $k_{SR''}$, and $k_{SS''}$ are rates of irreversible formation of F_{RS}/F_{SR} and F_{RR}/F_{SS}. (b) Representative organocatalyzed DYKAT type IV process proceeding through retro–Diels–Alder/Diels–Alder/lactamization cascade sequence.

Furthermore, the striking simplicity, excellent diastereo– and enantioselectivity, and high yield render this approach as a promising protocol for de novo synthesis of heteropolycyclic scaffolds with multiple stereo-centers.

3.4   Synthetic Applications

Synthetic applications towards biologically relevant targets are the ultimate validation for the development of any methodology. By way of demonstration, several case studies were chosen in order to highlight the utility of the DAL strategy (Figure 3.7). First, reduction of tricyclic lactone (–)-**14d** followed by desilylation under thermodynamic conditions, set the desired *trans*–decalin ring system found in bicyclic keto–diol (+)-**26**, a compound previously utilized in racemic form for the synthesis of (+)-dihydrocompactin [98], a potent hypocholesterolemic agent, first isolated by a group at Merck in 1981 [99], and related to the well known statin drugs, lovastatin (Mevacor®) and simvastatin (Zocor®). In another application, acid–catalyzed aromatization of the *oxa*–bridged bicyclo[2.2.1] system followed by *N*–detosylation of the amide (+)-**23** delivered a versatile isoindolinone (**27**, Figure 3.7b) previously employed to access the indoprofen, a nonsteroidal anti–inflammatory drug and cyclooxygenase inhibitor that was recently found to upregulate the survival motor neuron protein [100]. This showcase approach further enables the production of an expensive isoindolinone (**27**, 500 $/g, Sigma–Aldrich #CDS020611) from a cheap commercial furfurylamine (0.15 $/g, Alfa–Aesar #B23975) and offers DAL organocascade as an expedient method for modification of biomass–derived furans to high–value materials.
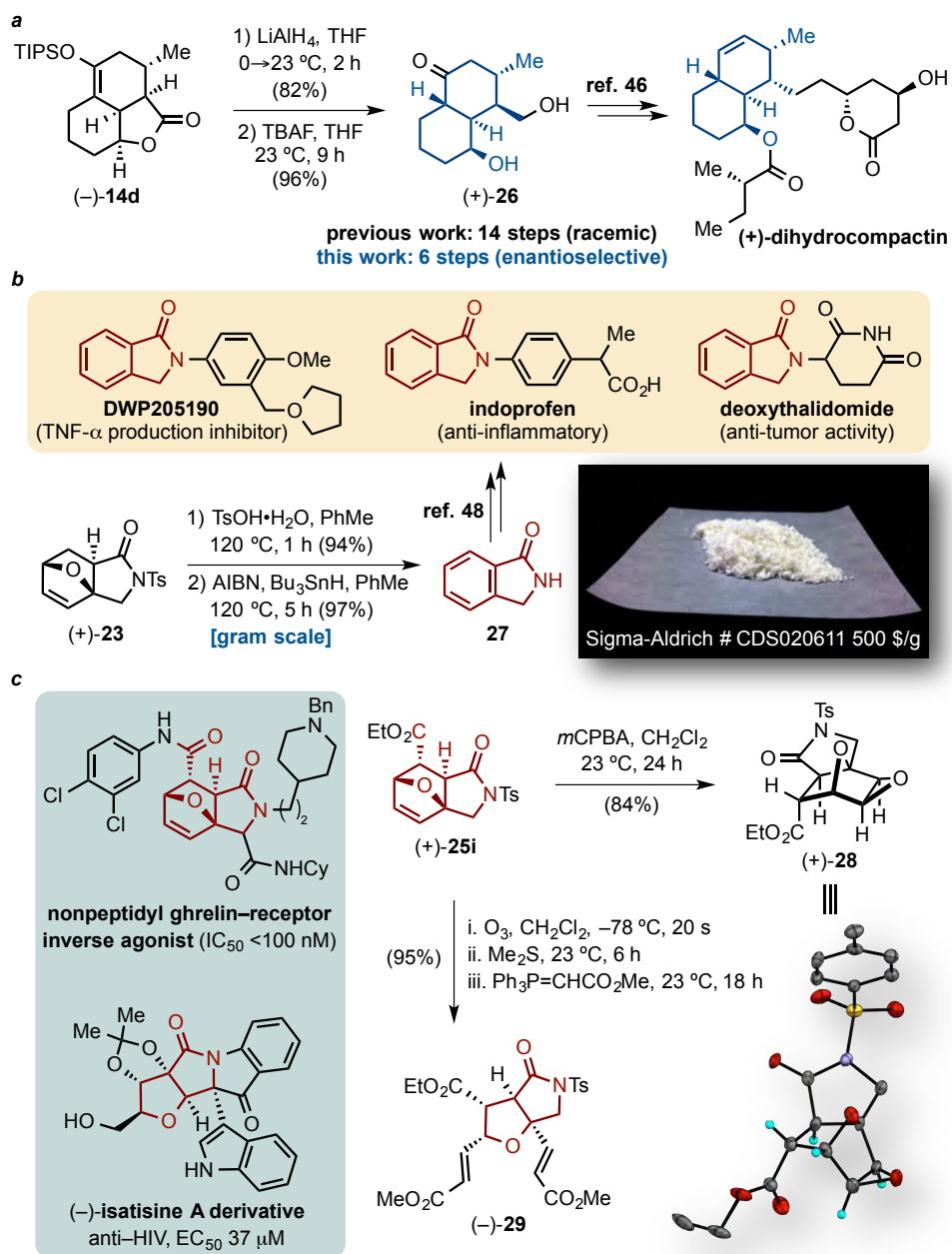
Figure 3.7 (a) Application of the tricyclic γ–lactone (–)-**14d** to a formal synthesis of (+)-dihydrocompactin. (b) Conversion of the tricyclic γ–lactam (+)-**23** to a versatile isoindolinone **27** previously employed to access indoprofen. (c) Epoxidation of the tricyclic γ–lactam (+)-**25i** to a fully substituted cyclohexane bearing four fused rings with six contiguous stereocenters. Transformation of (+)-**25i** to a fully substituted tetrahydrofuran (–)-**30** representing the core structure of the natural product, isatisine A. Inset is a single crystal X–ray structure in ORTEP format (50% probability, see Supplemental Figure S2).

Nonpeptidyl ghrelin–receptor inverse agonists with IC_{50} values of <100 nM were recently disclosed by 7TM Pharma [101] and contain *oxa*–bridged tricyclic γ–lactams as a central core structure reminiscent of optically active (+)-**25i**. The representative racemic compound depicted in Figure 3.7c was subjected to *in vivo* assays to determine its effect on weight loss in rats and was found to result in a ca. 20% weight loss relative to controls. As a further demonstration of this point, (+)-**25i** was readily converted in a single step to a fully substituted tetrahydrofuran (–)-**29** corresponding to the core structure of the natural product, (–)-isatisine A. This was achieved by a tandem ozonolytic cleavage of the olefin followed by *in situ* Wittig olefination with methyl (triphenylphosphoranylidene)acetate. The acetonide derivative of the natural product (–)-isatisine A, shown in Figure 3.7c, is an artifact during the isolation that was found to exhibit cytotoxicity against C8166 with CC_{50} = 302 μM and anti–HIV activity of EC_{50} = 37 μM [102]. Finally, epoxidation of the tricyclic γ–lactam (+)-**25i** furnished a fully substituted cyclohexane bearing four fused rings with six contiguous stereogenic centers as crystalline needles and permitted unambiguous assignment of the absolute configuration of (+)-**25i** by X–ray analysis (see Supplementary Figure S2).

3.5 Effects of Brønsted Base on Acylammonium Salt Formation and Initial Diels–Alder Step

During our previous screening studies, we determined that certain tertiary–amine Brønsted bases exerted a profound effect on *endo*/*exo* selectivity. We concluded that base likely plays a dual role of facilitating deprotonation of the pendant alcohol during

lactonization and ensuring the free–base form of the catalyst, however certain tertiary–amine Brønsted bases can act as Lewis base catalysts leading to racemic product [103]. Thus, we next considered the extent to which a Brønsted base could effectively compete with a chiral catalyst in the formation of corresponding acylammonium salt. Consequently, these achiral acylammonium dienophiles would enable the racemic DAL process to compete effectively with asymmetric pathway. Our quantum chemical calculations on acylammonium salt formation between ethyl fumaroyl chloride (**12a**) and various tertiary–amine Brønsted bases indicate, as shown in Figure 3.8a, that only pyridine and triethylamine (Et$_3$N) with energy barriers of 12.4 and 13.1 kcal/mol, respectively, would plausibly compete with the (*S*)-(−)-BTM catalyst (13.0 kcal/mol). However, both reactions are endergonic, with reverse energy barriers of only 7.1–9.5 kcal/mol, and thus are readily reversible [104]. With these results in hand, we next sought to provide support from experimental screen of selected Brønsted bases employing acid chloride **12a** with (*S*)-(−)-BTM as catalyst (Figure 3.8b) and indeed as expected Et$_3$N, pyridine and even Hünig's base (^{i}Pr$_2$NEt) led to greatly reduced enantioselectivity (60–85% *ee*) compared to 2,6–lutidine (99% *ee*) and 2,6–di–*tert*–butylpyridine (DTBP, 99% *ee*) by enabling the racemic background pathway to compete effectively with the asymmetric DAL process.
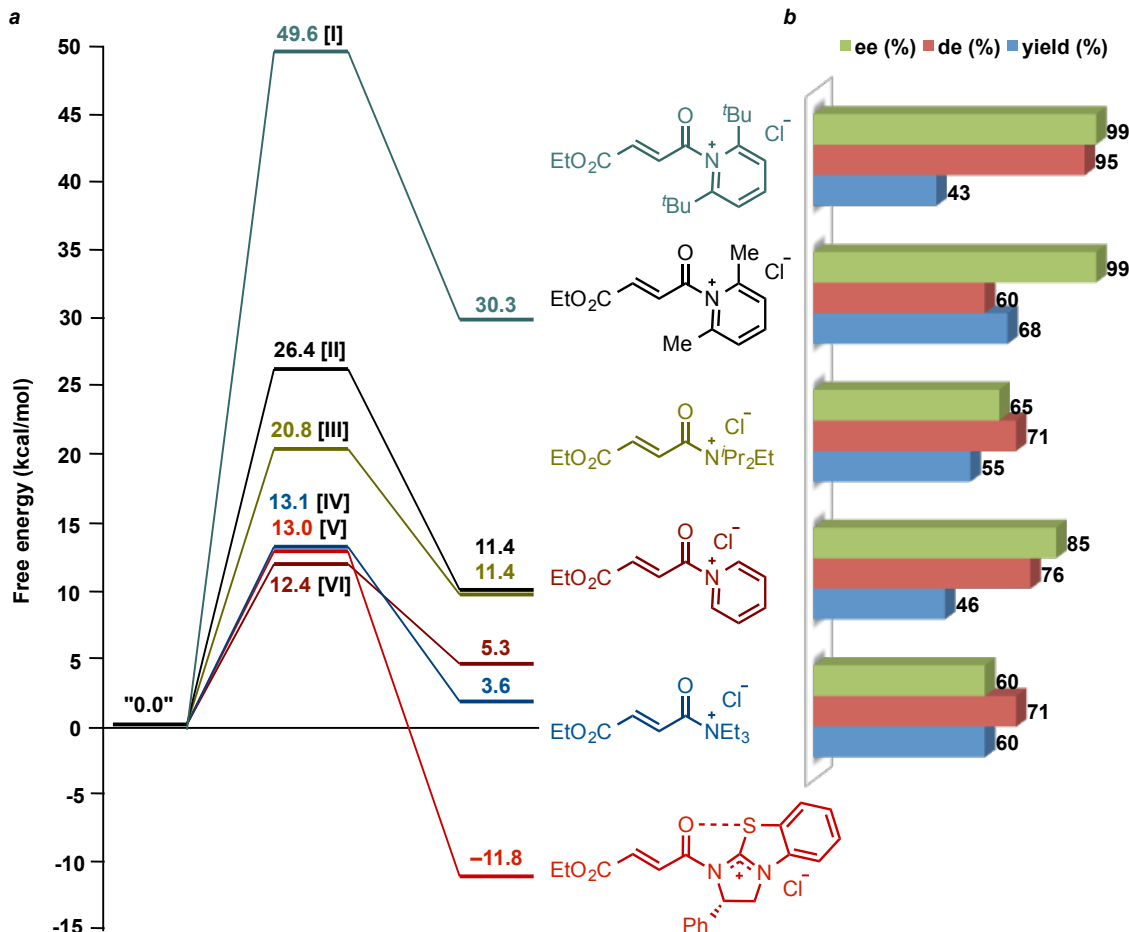
Figure 3.8 (a) Comparison of acylammonium salt formation between (*S*)-(−)-BTM catalyst and various tertiary–amine Brønsted bases. Free energies of transition state structures (TSSs) and products shown in kcal/mol relative to energies of separated reactants were computed using SMD(DCM)–M06–2X/6–31G(d). (b) Base screening studies were performed with acid chloride **12a** (1.2 equiv) and (*S*)-(−)-BTM (20 mol%) in CH₂Cl₂ (0.1 M). All yields refer to isolated, purified yields of cycloadducts. Diastereomeric (*endo*/*exo*) ratios were determined by ¹H NMR (500 MHz) analysis of the crude reaction mixture. Enantiomeric excess was determined by chiral–phase HPLC and is only shown for the major (*endo*) diastereomer (*ee* values for the *exo* diastereomer were similar).

Interestingly, acylammonium salt formations through chloride ion exchange reactions with both (*S*)-(−)-BTM and tertiary–amine Brønsted bases proceeded by an apparent π attack on the carbonyl π bond with no discernible tetrahedral intermediates (Figure 3.9a)

typical of an addition–elimination pathway; instead, these reactions proceeded by a concerted S_N2–type mechanism. Considerable difference between the energies of a carbonyl π bond and a carbon–oxygen σ bond contribute to the reluctance to form a tetrahedral intermediate.[54] Computational results in this study fully corroborated earlier modeling on intermediacy of tetrahedral species [105]. To gain further insights into the extent of LUMO–lowering activation upon acylammonium salt formation, revealed during our previous studies, we postulated that such activation would originate from inductive effects propagated through the σ–framework, which could ultimately be revealed through reduced electron density at the β–carbon [106]. We therefore performed ^1H–^{13}C gHMQC experiment and measured the ^{13}C NMR chemical shifts in CDCl$_3$ at 23°C for the acylammonium salt **30** formed through chloride ion exchange reaction of the acid chloride **12a** with the Lewis base, (*S*)-(−)-BTM (Figure 3.9b). However, no significant change in the chemical shift of the β–carbon of acylammonium **30** (δ 136.7 ppm) was observed compared to the acid chloride **12a** (δ 136.8 ppm). Further investigation into the chemical shift of the carbonyl carbon revealed slight upfield shift in **30** (δ 163.6 ppm) compared to the acid chloride **12a** (δ 164.1 ppm) suggestive of shielding effect from steric impediment at the carbonyl carbon induced by the isothiourea catalyst, (*S*)-(−)-BTM. Thus, isothiourea–catalyzed acylammonium formation may not lead to dramatic LUMO–lowering activation, as previously suggested, but rather a significant decrease in nucleophilic substitution at carbonyl carbon enabling DA–initiated organocascade.
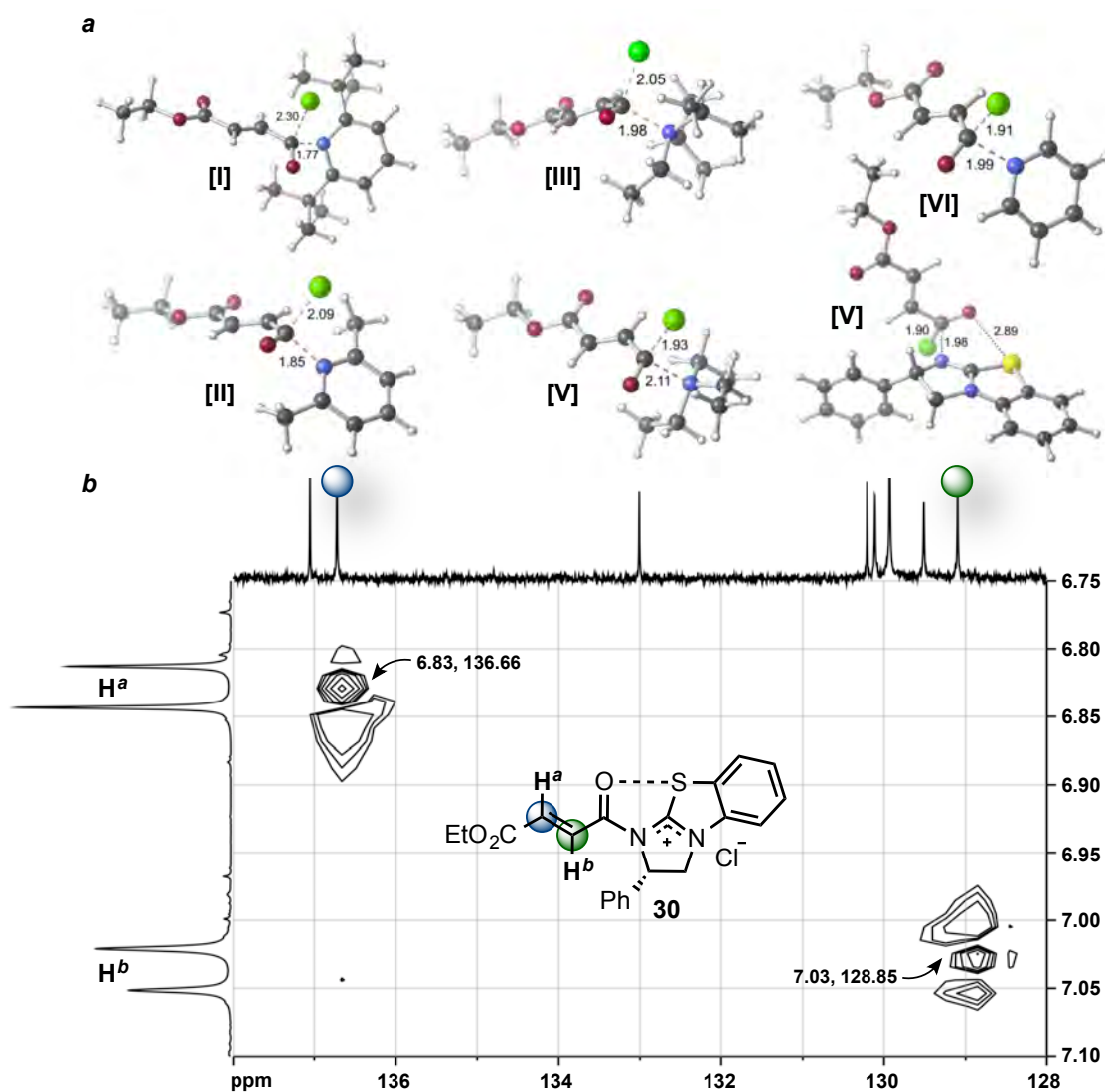
Figure 3.9 (a) Calculated TSSs (I–VI) for the formation of acylammonium salts with various Brønsted bases optimized at the M06–2X/6–31G(d) level with an implicit solvent model [SMD (dichloromethane)]. Selected bond distances are shown (Å). (b) Section of the ^{1}H–^{13}C gHMQC NMR spectrum of the acylammonium salt **30** in CDCl$_3$ formed from a 1:1 mixture of (*S*)-(–)-BTM and ethyl fumaroyl chloride **12a**.

In accordance with aforementioned results, we next sought to calculate and compare the energy barriers for the initial DA step between chiral and achiral activated dienophiles

(Table 3.3). On the basis of these findings, we concluded that only a BTM–bound acylammonium dienophile with an exergonic profile possesses sufficient activation energy barrier to undergo the initial DA cycloaddition. Intriguingly, acylammonium salts derived from DTBP, Et$_3$N and ^{i}Pr$_2$NEt may undergo DA cycloaddition *via* a stepwise mechanism.

Table 3.3 Comparison of free energies for the initial DA cycloaddition between BTM– bound acylammonium dienophile and various Brønsted bases.

a. Energies computed with SMD(DCM)–M06–2X/6–31G(d) and shown in kcal/mol relative to separated reactants.

	BTM		Pyridine		2,6–Lutidine		DTBP		Triethylamine		Hünig's base	
	endo	*exo*	*endo*	*exo*	*endo*	*exo*	*endo*	*exo*	*endo*	*exo*	*endo*	*exo*
TS	10.7	12.0	24.9	25.3	30.0	30.1	53.9, 44.0	50.8	25.1	28.1, 22.3	–	–
MIN	–30.7	–35.7	15.6	–0.34	–	–	40.9, –	59.1	3.3	21.1, –	–	–

b. Energies computed with SMD(DCM)–M06–2X/6–31G(d) and shown in kcal/mol relative to preformed acylammonium and diene

	BTM		Pyridine		2,6–Lutidine		DTBP		Triethylamine		Hünig's base	
	endo	*exo*	*endo*	*exo*	*endo*	*exo*	*endo*	*exo*	*endo*	*exo*	*endo*	*exo*
TS	16.6	17.8	12.5	13.0	18.4	18.6	21.8, 12.0	18.7	17.6	20.6, 14.7	–	–
MIN	–24.9	–29.9	3.2	–12.7	–	–	8.8,	27.1	–4.3	13.5,	–	–

3.6 Effects of Brønsted Base on the Origins of the Diastereoselectivity in the Diels–Alder–Initiated Cascades

Based upon aforementioned computations and experiments suggesting that a Brønsted base cannot compete effectively with a chiral isothiourea catalyst in either the acylammonium formation or the initial Diels–Alder cycloaddition, we sought to compute an explicit Brønsted base model and to elucidate the stereoelectronic effects it triggers on the TSSs implicated in the initial Diels–Alder step. On the basis of previous studies

[107], we envisaged a complex formation through a hydrogen–bond network between tertiary–amines Brønsted base and the alcohol moiety of silyloxydiene. To gain further insights into the extent of hydrogen–bond formation between the Brønsted base and the diene, we postulated that such interaction could be detected by an increased electron density at the carbinol–carbon of diene due to inductive effects propagated through the σ–framework. We therefore performed standard ^{13}C NMR (500 MHz) experiments in CD_2Cl_2 (0.1 M) at 23 ºC and measured the changes in chemical shifts of the silyloxydienyl carbinol–carbon upon immediate mixing with an equimolar amount of a Brønsted base and their spectra were compared to the spectrum of the free diene **31** (Figure 3.10a). ^{13}C NMR spectrum of an equimolar mixture of **31** and DTBP in the absence and presence of DTBP are rather similar (Figure 3.10b) indicating that a complex does not form under these conditions. This is also supported by the virtually unchanged chemical shift (62.56 ppm) of the carbinol–carbon ($\Delta\delta$ = +0.02), relative to free **31** (62.54 ppm). The inability of the nitrogen atom in DTBP to participate in hydrogen–bonding is rationalized as due to steric hindrance [108] induced by adjacent *tert*–butyl substituents and is largely responsible for the very low relative basicity [109]. On the contrary, the corresponding ^{13}C NMR spectrum for an equimolar mixture of **31** and pyridine shows pronounced upfield change in the chemical shift ($\Delta\delta$ = –0.22 ppm) for the carbinol–carbon (Figure 3.10c) signifying formation of a hydrogen–bonded complex.
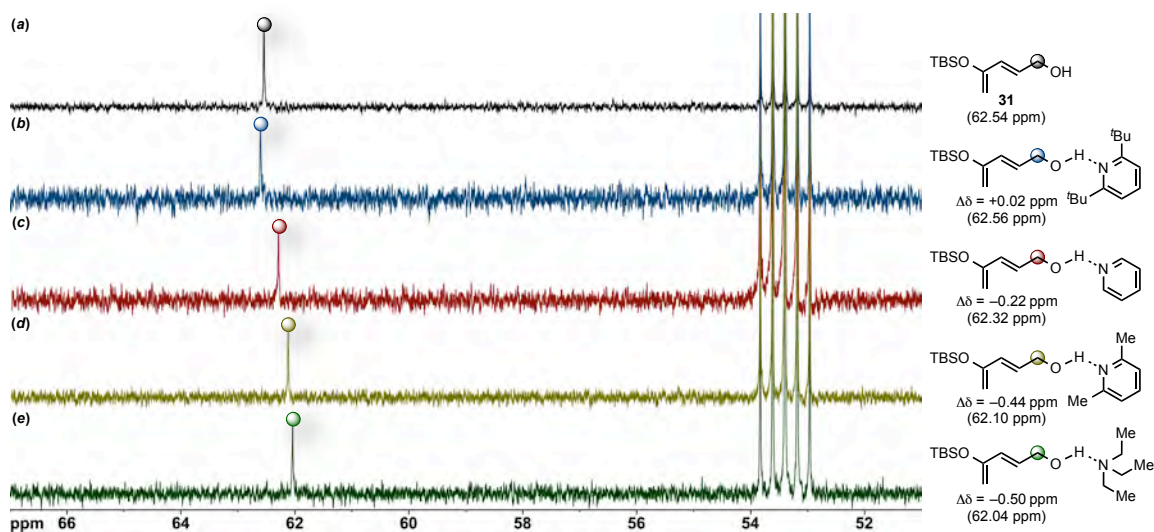
Figure 3.10 Sections of the ^{13}C NMR (500 MHz) spectra in CD$_2$Cl$_2$ at 23 ºC of an equimolar mixture of (a) diene **31** and (b) DTBP, (c) pyridine, (d) 2,6–lutidine, (e) Et$_3$N.

The extent of complexation was particularly evident in the ^{13}C NMR spectrum of **31** and 2,6–lutidine mixture by a profound upfield change in the chemical shift ($\Delta\delta = -0.44$ ppm) of the carbinol–carbon (Figure 3.10d). ^{13}C NMR spectrum of an equimolar mixture of **31** and Et$_3$N (Figure 3.10e) equally indicated complex formation with an upfield chemical shift of 62.04 ppm, relative to free **31** (62.54 ppm). These upfield shifts qualitatively correlate with hydrogen–bond strength and Brønsted basicity, suggestive of the potential bimolecular complexation, for which the pKa values (in DMSO) and $\Delta\delta$ differences follow the order: DTBP (0.9 [110], +0.02) < pyridine (3.4 [111], –0.22) < 2,6–lutidine (4.46 [112], –0.44) < Et$_3$N (9.0 [113], –0.50). On the basis of our spectroscopic studies, both TSSs for the initial DA cycloaddition were probed with

explicit bimolecular hydrogen–bond complex involving silyloxydiene **32** and 2,6–lutidine (Figure 3.11).
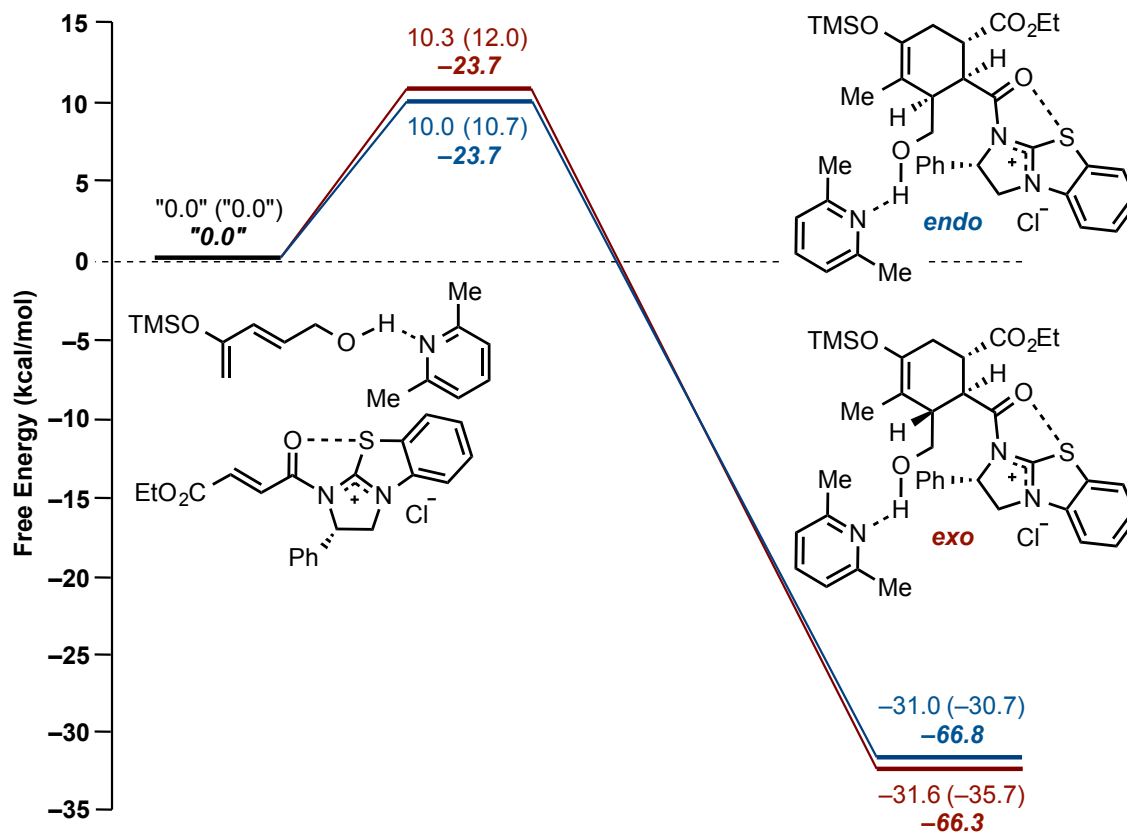
Figure 3.11 Free energies and enthalpies (shown in bold, italic) are in kcal/mol relative to separated reactant species calculated at SMD(DCM)–M06–2X/6–31G(d). An explicit base (2,6–lutidine) was modeled to study stereoelectronic effects on TSSs involved in the initial DA cycloaddition (values inside parentheses represent free energies without explicit base).

Therefore, a manual conformational search, sampling numerous possible orientations of the 2,6–lutidine, generated two lowest energy conformers corresponding to the *endo* and *exo* TSSs (Figure 3.12). Indeed, computational studies indicate that 2,6–lutidine can participate in hydrogen–bonding with the terminal alcohol of the diene and

simultaneously engage in CH–π and π–π stacking interactions with the benzotetramisole moiety of the BTM–bound acylammonium salt.
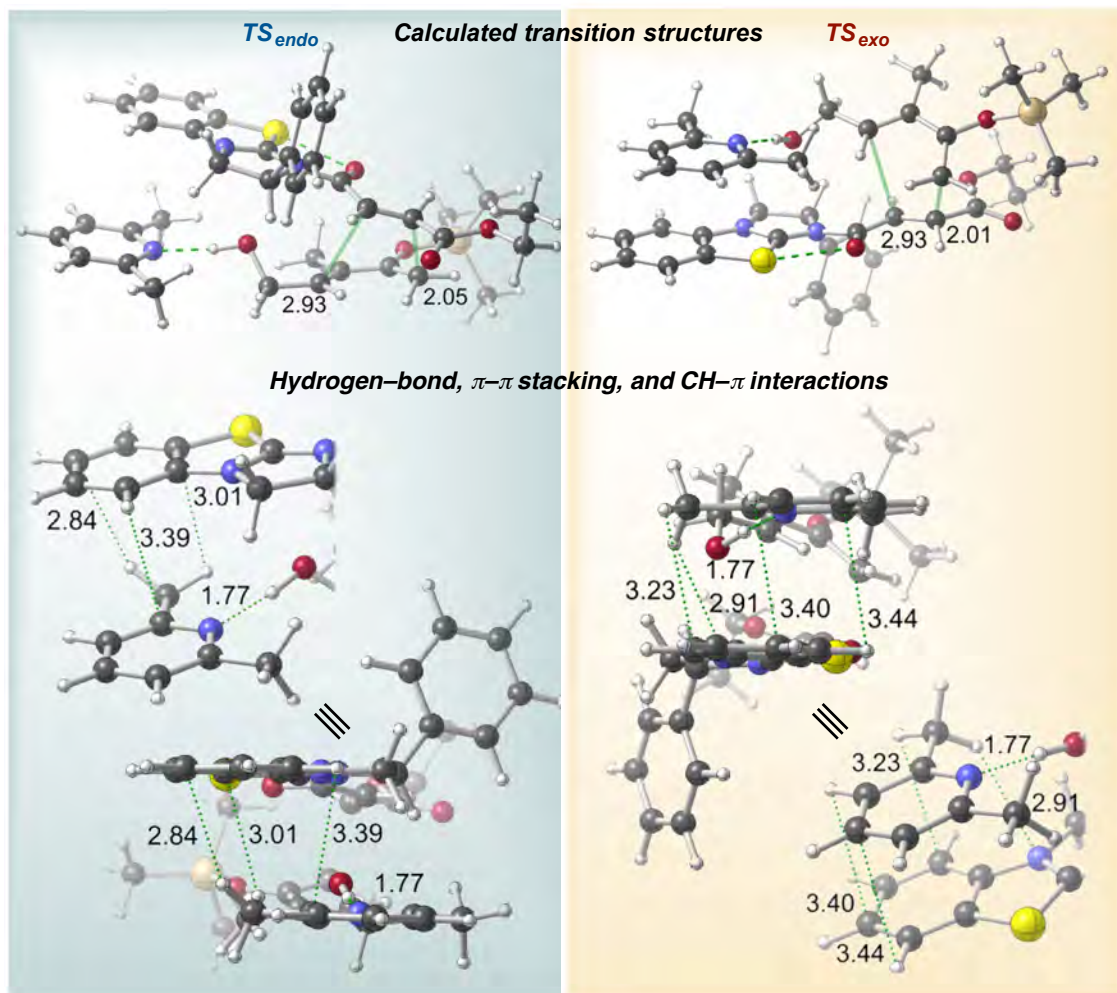
Figure 3.12 Optimized TSSs leading to *endo* and *exo* cycloadducts showing π–π stacking and CH–π interactions between BTM–bound acylammonium salt and hydrogen–bonded Brønsted base–diene complex. Select bond distances are shown (Å).

Remarkably, these interactions selectively lower the energy barrier for the TSS leading to *exo* cycloadduct (12.0→10.3 kcal/mol) [114]. In contrast, the energy barrier for the TSS leading to *endo* cycloadduct is reduced by only 0.7 kcal/mol (10.7→10.0 kcal/mol).

These results do not conflict with our previous findings on the origin of enantioselectivity and bear important implications for catalyst design; however, sticking similarity in energies (0.3 kcal/mol) between TSSs leading to *endo* and *exo* cycloadducts ($\Delta\Delta G_{TSS}$) led us to question the origin of the observed diastereoselectivity (>19:1 *endo*/*exo*) in these reactions.

3.7 Entropy–Controlled Diastereodifferentiation in Diels–Alder–Initiated Cascades

On the basis of these computations, we decided to probe the implications of enthalpy and entropy in diastereodifferentiation. While the predicted diastereoselectivity for the base–complexed DA cycloaddition in Figure 3.11 is larger when entropy is neglected; the opposite was found to be true for the base–free reaction (Figure 3.13a). For the latter, almost no diastereoselectivity is predicted on the basis of enthalpy alone for the asymmetric reaction, irrespective of computational model. However, differences in free energy barriers varied based on the model chemistry. Our confidence in the validity of these results led us to consider the possibility that the diastereoselectivity was not controlled by enthalpy (*i.e.*, predicted $\Delta\Delta H$s are insignificant), but rather by entropy. A point of caution, however, should be expressed regarding the computation of entropy in quantum chemical computations [115] and the accuracy of computing dispersion interactions [116].
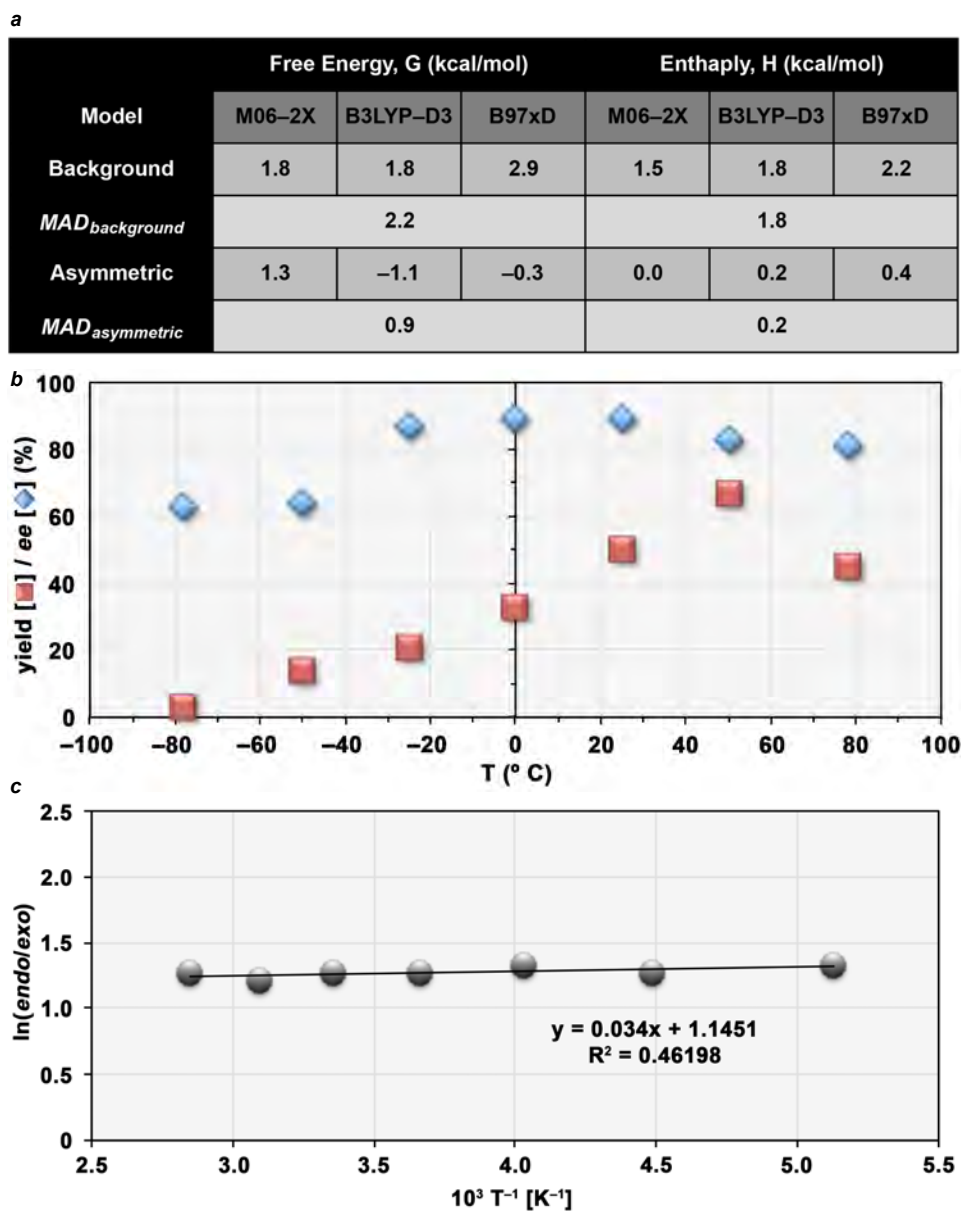
Figure 3.13 (a) Free energies and enthalpies of TSSs from the racemic background and asymmetric DA cycloadditions computed with SMD(DCM)–M06–2X/6–31G(d). Energies shown in kcal/mol relative to separated reactants. (b) Plots of yield and enantiomeric excess as a function of temperature. Enantiomeric excess was determined by chiral–phase HPLC and is only shown for the major (*endo*) diastereomer (*ee* values for the *exo* diastereomer were similar). (c) Eyring plot of ln(*endo/exo*) as a function of $10^3\ T^{-1}$. The abscissa was extended to T→∞ to obtain the y–intercept. Differential activation parameters are $\Delta\Delta H^{\ddagger} = 0.068$ kcal·mol^{-1} and $\Delta\Delta S^{\ddagger} = 2.28$ kcal·mol^{-1}·K^{-1}.

To minimize these uncertainties, we next investigated the potential of DAL organocascades that may have sufficient $\Delta\Delta S^{\ddagger}$, the diastereodifferentiating ability over a wide range of temperatures. Plots of yield and enantiomeric excess as a function of temperature (Figure 3.13b) indicate profound dominance of the background racemic reaction at the extremities of both curves, likely due to inefficient acylammonium formation at temperatures below −20 ºC and adequately competent background reaction above 50 ºC. We next set about a systematic study of the dependence of diastereoselection on temperature in the range from −78 to +80 °C. Reactions were analyzed after 18 h, and the relative *endo*/*exo* ratios and the enantioselectivity were concurrently determined by chiral–phase HPLC of the crude products mixture. The chemical yields were determined after flash chromatography on silica gel. Plot of the ln(*endo*/*exo*) as a function of 10^3 T^{-1} (K^{-1}) are shown in Figure 3.13c. The Eyring treatment of the reaction rates of independent processes that generate diastereomers in asymmetric reaction provides a differential activation enthalpy ($\Delta\Delta H^{\ddagger}$) and entropy ($\Delta\Delta S^{\ddagger}$) as shown in eq 1.

$$\ln\frac{k_R}{k_S} = \frac{-(\Delta H_R^{\ddagger} - \Delta H_S^{\ddagger})}{RT} + \frac{(\Delta S_R^{\ddagger} - \Delta S_S^{\ddagger})}{R} = \frac{-\Delta\Delta H^{\ddagger}}{RT} + \frac{\Delta\Delta S^{\ddagger}}{R} \tag{1}$$

Applying eq 1 to results of Figure 3.13c, we may easily calculate for our reaction that $\Delta\Delta H^{\ddagger}$ = 0.068 kcal·mol^{-1} and $\Delta\Delta S^{\ddagger}$ = 2.28 kcal·mol^{-1}·K^{-1}. The "flat" temperature dependency observed in this temperature range (ΔT = 160 ºC) clearly demonstrates that the reaction is predominantly stereocontrolled by the differential activation entropy, $\Delta\Delta S^{\ddagger}$. In our reaction system, the dominance of entropic factors in the −78→+80 °C

temperature interval suggests that steric interactions between acylammonium salt and the approaching diene along the two dienyl diastereotopic faces do not play a significant role in determining the diastereochemical outcome of the reaction. The effective induction of $\Delta\Delta S^{\ddagger}$ in this case can be explained as follows. Formation of a six–membered cyclohexene ring from intermolecular DA cycloaddition between flexible silyloxydiene and acylammonium salt requires a great loss of entropy, the degree of which largely depends on the conformational property of both substrates. The accompanying large entropy loss would result in enough difference in entropy between the two diastereomeric states from the influence of the chirality on the cycloadducts. This difference is carried over to the transition states to give $\Delta\Delta S^{\ddagger}$.

3.8 Switching Diastereoselection and Achieving the Full Matrix of Possible Stereoisomeric Products

Based upon aforementioned computations suggesting selective stabilization of the *exo* TSS by CH–π and π–π stacking interactions, we reasoned that judicious installation of an electron–withdrawing substituent onto the C7 position of the benzothiazole moiety would enhance interactions to a Brønsted base by withdrawing electron density from the π–cloud of the substituted benzotetramisole ring, reducing the repulsive electrostatic and steric interaction with the non–substituted pyridine ring [117]. Conversely, an electron–donating substituent would donate electron density into the π–system and diminish the π–stacking interaction, thus potentially altering *endo/exo*

74

selectivity. In addition, a closer analysis of the optimized TSSs revealed a potential for an $n{\rightarrow}\pi^*$ interaction between the hydroxyl group and imidazolium cation in both *exo* (3.04 Å) and *endo* (2.79 Å) TSSs (Figure 3.14a). We targeted a highly electron withdrawing nitro group and an electron–donating pyrrolidinyl group, reminiscent of a potent nucleophilic 4–pyrrolidinopyridine (4–PPY) catalyst, as two potential substituents at the C7 position on the benzothiazole moiety due to their synthetic practicality. As expected, the calculated electrostatic potential (ESP) surfaces for proposed catalysts (Figure 3.14b) revealed an enlarged positive ESP region over the imidazole portion in 7–nitrobenzotetramisole, presenting an opportunity to perturb the energy of the TSSs by stabilizing the $n{\rightarrow}\pi^*$ interaction, and thus potentially altering *endo*/*exo* selectivity. The synthesis of these catalysts commenced with nitration of a cheap commercial 2–chlorobenzothiazole (**32**, 0.95 \$/g, AK Scientific # S750) with a mixture of concentrated sulfuric acid and fuming nitric acid to provide **33** [118], which was used directly in the next step without further purification (Figure 3.14c). Employing Smith's recently improved, scalable two–step protocol [119], nitrothiazole **33** was subjected to the reaction with (*R*)-phenylglycinol in neat ethyldiisopropylamine and furnished alcohol **34** without chromatographic isolation.
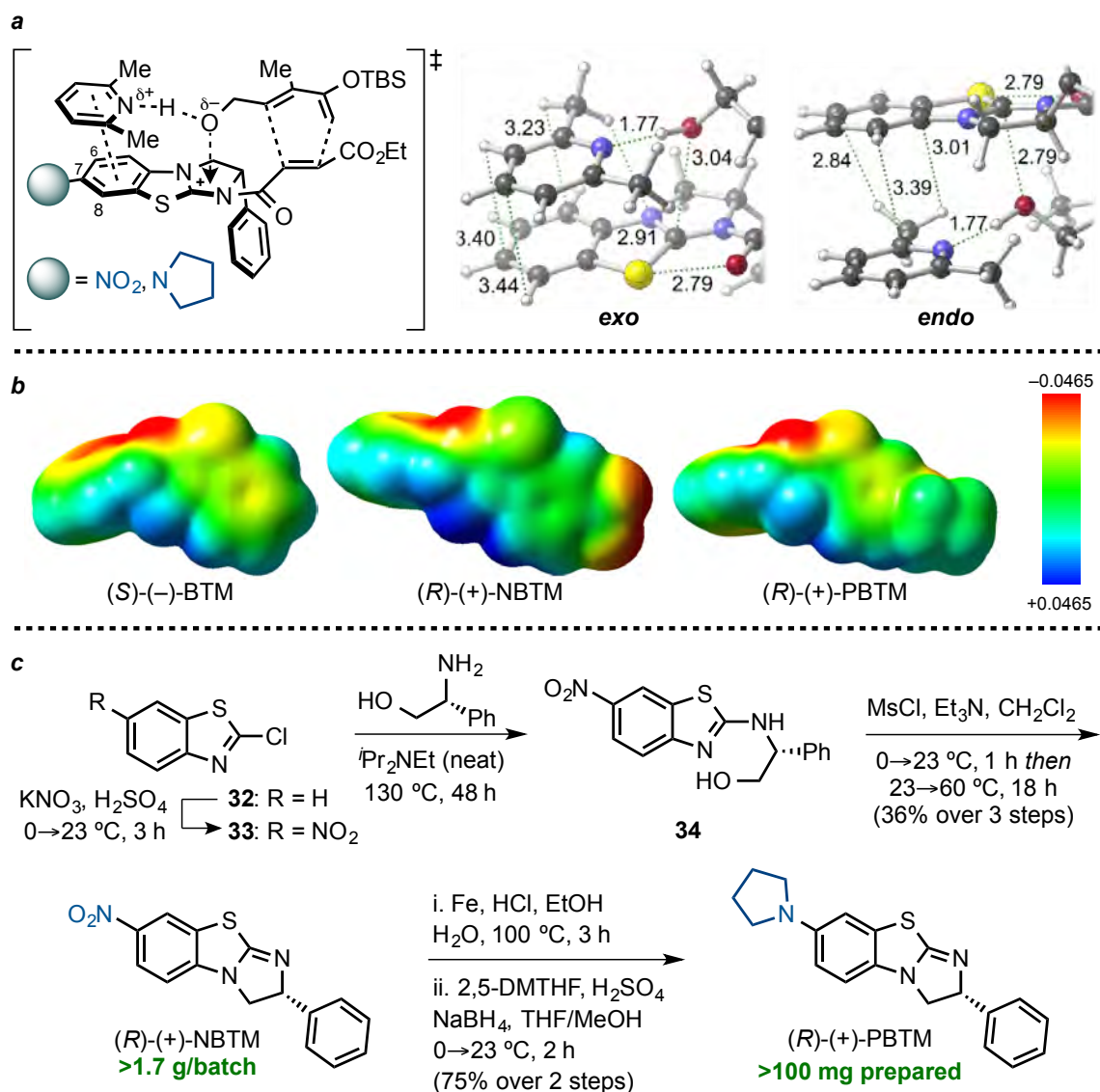
Figure 3.14 (a) Rational catalyst design potentially capable of switching diastereoselection in DAL organocascade, and TSSs depicting potential energy stabilization by $n{\rightarrow}\pi^*$ interaction optimized with SMD(DCM)–M06–2X/6–31G(d) level of theory with an implicit Brønsted base (2,6–lutidine) model. Selected bond distances are shown (Å). (b) Calculated ESP plots for BTM, NBTM and PBTM. (c) Preparative synthesis of electronically tuned NBTM and PBTM catalysts.

Treating **34** with methanesulfonyl chloride and heating a dichloromethane solution of the resultant mesylate at reflux in the presence of triethylamine and methanol overnight provided >1.7 grams of 7–nitrobenzotetramisole, (*R*)-(+)-NBTM, as the sole product in 36% yield over three steps after chromatography. The nitro group was readily reduced with iron powder in ethanol under catalytic quantities of hydrochloric acid to afford the corresponding amine, which then underwent reductive amination with 2,5–dimethoxytetrahydrofuran (DMTHF) and sodium borohydride in presence of catalytic sulfuric acid [120] and formed the desired pyrrolidinylbenzotetramisole, (*R*)-(+)-PBTM in 75% yield over two steps.

Given the ability to access both *endo* and *exo* transition states using particular Brønsted bases, we studied the potential of a fully stereodivergent variant of the DAL with a racemic diene to access all possible stereoisomers of a particular family of cycloadducts. Employing racemic silyloxydiene (±)-**35** bearing a pendant secondary benzylic alcohol, ethyl fumaroyl chloride (**12a**), and (*S*)-(–)-BTM (20 mol%) with 2.0 equiv. of 2,6–lutidine, four chromatographically separable diastereomers (–)-**36** (27% yield, 98% *ee*), (+)-**36'** (22% yield, 99% *ee*), (+)-**36''** (25% yield, 99% *ee*) and (–)-**36'''** (18% yield, 97% *ee*) were produced in 92% combined yield (entry 1, Table 3.4). This reaction could be readily performed on a preparative scale with only 10 mol% (*S*)-(–)-BTM providing 76% combined yield (see Supplementary p. 216). Probing commercial pyridines with electron–withdrawing substituents, such as 2– and 3–bromopyridine, and 2,6–dibromopyridine, was ineffective toward formation of the de-sired cycloadducts presumably due to reduced basicity.

Table 3.4 Rapid access to a fully separable stereoisomeric complement of a given scaffold obtained by base and catalyst permutation for diversity–oriented synthesis.
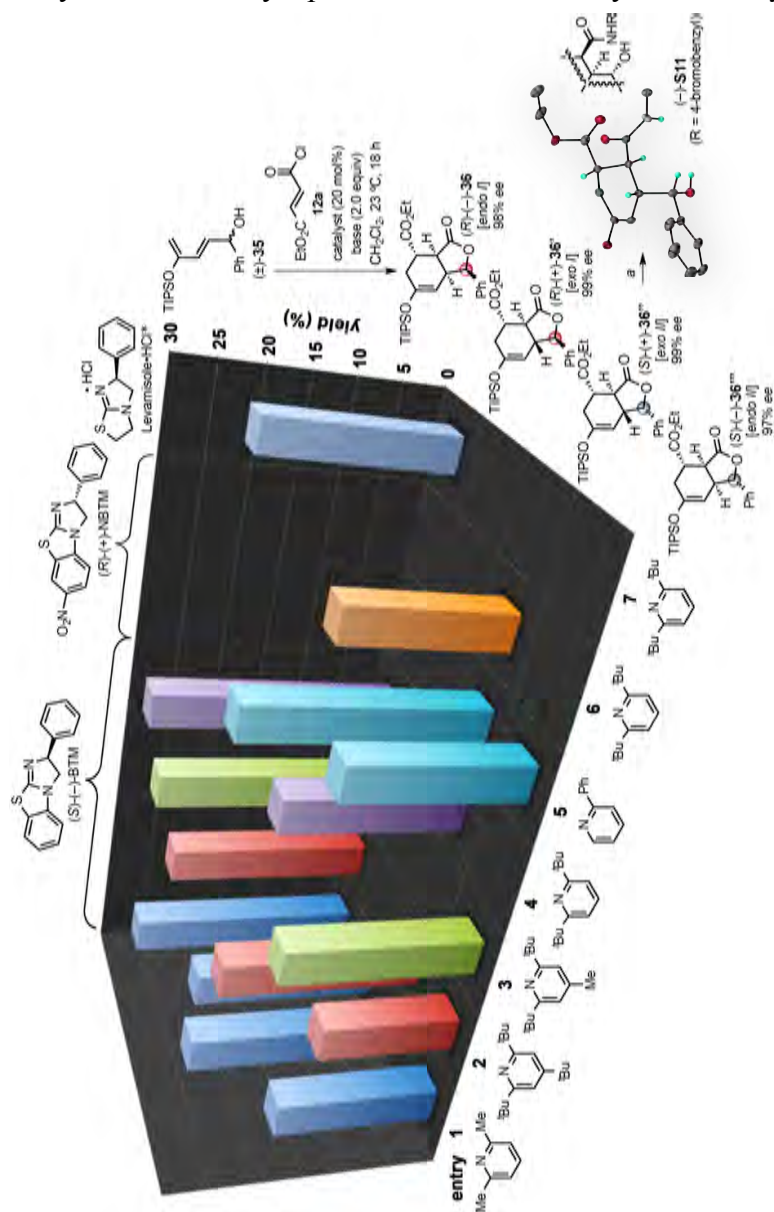
Reactions were performed with diene (±)-**35** (1.0 equiv.), acid chloride **12a** (1.5 equiv.), base (2.0 equiv.) and catalyst (20 mol%) at 23 ℃ for 18 h. Yields and diastereomeric ratios are based on isolated, purified cycloadducts. Enantiomeric excess was determined by chiral–phase HPLC (see Supplemental Figure S3, pp. 267–279). *Employed in free–base form. Inset is a single crystal X–ray structure in ORTEP format (50% probability; TIPS and 4–bromobenzyl groups are removed for clarity, see Supplemental Figure S1). ^{a}4–BrC$_6$H$_4$CH$_2$NH$_2$, THF, 23 ℃, 36 h (46%).

In contrast, pyridines with electron–donating groups, such as 3– and 4–methoxypyridine, caused merely negligible deviations in diastereoselection. To our surprise, 2,4,6–tri–*tert*–butylpyridine (TTBP) selectively suppressed formation of the *exo I* diastereomer, (+)-**36'** (entry 2, Table 3.4), whereas 2,6–di–*tert*–butyl–4–methylpyridine (DTBMP) deterred formation of both *exo I* and *II* diastereomers, (+)-**36'** and (+)-**36''** (entry 3, Table 3.4). In addition, 2,6–di–*tert*–butylpyridine (DTBP) imposed preferential formation of both *endo I* and *exo II* diastereomers, (−)-**36** and (+)-**36''**, in 29% and 20% yields, respectively (entry 4, Table 3.4). Intrigued by these permutations, we next sought to exploit our synthetic, electronically–tuned benzotetramisole–derived catalysts in conjunction with various substituted pyridine bases. Accordingly, highly nucleophilic, electron–rich (*R*)-(+)-PBTM catalyst accelerated the formation of corresponding cycloadducts, likely due to exceedingly rapid formation of the resultant acylammonium salt, however without noticeable deviations in diastereoselection. In contrast, serendipitous permutation of the (*R*)-(+)-NBTM catalyst and 2–phenylpyridine selectively impeded reactivity of the (*R*)-enantiomer of (±)-**35**, consequently resulting in formation of both *exo II* and *endo II*, diastereomers, (+)-**36''** and (−)-**36'''**, in 26% and 19% yields, respectively (entry 5, Table 3.4). To our delight, a single *exo II* diastereomer, (+)-**36''**, was obtained in 18% yield (99% *ee*) by permutation of (*R*)-(+)-NBTM and 2,6–di–*tert*–butylpyridine (entry 6, Table 3.4). In addition, a single *endo I* diastereomer, (−)-**36**, was obtained in 22% yield (99% *ee*) by a combination of 2,6–di–*tert*–butylpyridine with a free–base form of Levamisole·HCl (entry 7, Table 3.4). The relative and absolute configuration of a derivative of (+)-**36''** was confirmed by X–ray analysis (see Supplementary Figure S1)

79

and together with comparative 2D NMR analysis enabled assignment of the relative and absolute configurations of (−)-**36**, (+)-**36'** and (−)-**36'''**. It should be noted that use of (*Z*)-(±)-**35** and the use of catalyst antipodes would theoretically enable access to the remaining diastereomeric and enantiomeric members (16 total) of this family of cycloadducts. Despite uncertainty about their origin, these preliminary results suggest that the judicious choice of a designer catalyst and the Brønsted base could be used in tandem to switch the sense of the diastereoselection in stereodivergent Diels–Alder– initiated organocascades, thereby affording the enantioenriched cycloadducts on demand.

3.9   Conclusions

In conclusion, factors affecting the selectivity of stereodivergent, Diels–Alder– initiated organocascades were investigated systematically with a view to understanding, predicting, and tuning the stereochemical outcome. An evaluation of various experimental and computational parameters were performed in order to derive a more detailed understanding of what renders this process selective. The substrate scope of the stereodivergent organocascade has been extended to tethered secondary and tertiary racemic alcohols leading to the corresponding optically active γ–substituted *cis*– and *trans*–fused bicyclic γ–lactones in good yields with excellent enantiocontrol. The long– standing obstacle was surmounted in the first highly enatio– and diastereoselective organocatalytic DA cycloaddition of furan–tethered achiral sulfonamides, which led to the generation of *oxa*–bridged *trans*–fused tricyclic γ–lactams guided by a rare example

of dynamic kinetic asymmetric transformation (DYKAT) type IV. Computations indicated that benzotetramisole–derived acylammonium formation proceeded by an exergonic, concerted S_N2–type mechanism without discernible tetrahedral intermediate typical of an addition–elimination pathway. Detailed computations in corroboration with spectroscopic studies provided insights into the role of Brønsted base and revealed the formation of a hydrogen–bonded complex that permitted selective lowering of the energy barrier in the exo transition state through $n{\rightarrow}\pi^*$, CH–π and π–π stacking interactions. Synergistic evaluation of computed free energies and enthalpies of TSSs in conjunction with observed temperature independence in the $-78{\rightarrow}+80$ °C interval and experimentally obtained values for $\Delta\Delta H^{\ddagger}$ (0.068 kcal·mol^{-1}) and $\Delta\Delta S^{\ddagger}$ (2.28 kcal·mol^{-1}·K^{-1}) demonstrated that the reaction is predominantly stereocontrolled by the differential activation entropy, $\Delta\Delta S^{\ddagger}$. The combined results described herein have allowed us to put forth the full catalytic cycle. While the described organocascade demonstrates admirable scope, it has clear limitations. The utility of this methodology was show-cased through the formal syntheses of the nonsteroidal anti–inflammatory agent indoprofen and a member of the fungus–derived and widely marketed statin drugs (+)-dihydrocompactin, and the concise approaches to the core structures of the natural product isatisine A and the nonpeptidyl ghrelin–receptor inverse agonist. Lastly, we have documented the possibility of using a single chiral organocatalyst to fully control the stereochemical outcome of the stereodivergent Diels–Alder–initiated organocascade. We found that the judicious combination of Lewis and Brønsted bases can alter the sense of diastereoselection. We are currently undertaking further mechanistic investigations to

fully understand the origins of this tunable diastereoselectivity. On the basis of our current findings, we envisage that programming the function of a catalyst using stereoelectronic stimuli may provide new synthetic opportunities and conceptual perspectives for confronting major challenges associated with the synthesis of all possible stereoisomers of a particular constitutional family of chiral molecules that cannot be addressed by traditional approaches. Further studies to investigate the stereoselectivity principles described in this report and applications toward natural product synthesis are ongoing in our laboratories and will be reported in due course.

SUMMARY

In summary, we have unveiled a new and versatile family of chiral dienophiles, α,β–unsaturated acylammonium salts, that undergo enantioselective and stereodivergent DAL organocascades rapidly generating complex and stereochemically diverse scaffolds. This scalable process proceeds under mild conditions, provides excellent relative and absolute stereocontrol, and utilizes readily prepared dienes, commodity acid chlorides, and commercially available organocatalysts. A prominent feature of the described methodology is the use of a DA reaction to initiate an organocascade; a strategy with limited precedent. The utility of the DAL was demonstrated by conversion of the derived bicyclic lactones to several core structures of natural products constituting formal syntheses in some cases. Computational results suggest kinetic preference for an *endo* TS with enantiocontrol ascribed to stereoelectronic and conformational preferences of the acylammonium salt dienophiles. Further applications and mechanistic investigations are underway to delineate the scope of this methodology.

The factors affecting the selectivity of stereodivergent, Diels–Alder–initiated organocascades were investigated systematically with a view to understanding, predicting, and tuning the stereochemical outcome. An evaluation of various experimental and computational parameters were performed in order to derive a more detailed understanding of what renders this process selective. The substrate scope of the stereodivergent organocascade has been extended to tethered secondary and tertiary racemic alcohols leading to the corresponding optically active γ–substituted *cis–* and

trans–fused bicyclic γ–lactones in good yields with excellent enantiocontrol. The long–standing obstacle was surmounted in the first highly enatio– and diastereoselective organocatalytic DA cycloaddition of furan–tethered achiral sulfonamides, which led to the generation of *oxa*–bridged *trans*–fused tricyclic γ–lactams guided by a rare example of dynamic kinetic asymmetric transformation (DYKAT) type IV. Computations indicated that benzotetramisole–derived acylammonium formation proceeded by an exergonic, concerted S_N2–type mechanism without discernible tetrahedral intermediate typical of an addition–elimination pathway. Detailed computations in corroboration with spectroscopic studies provided insights into the role of Brønsted base and revealed the formation of a hydrogen–bonded complex that permitted selective lowering of the energy barrier in the exo transition state through $n \rightarrow \pi^*$, CH–π and π–π stacking interactions. Synergistic evaluation of computed free energies and enthalpies of TSSs in conjunction with observed temperature independence in the $-78 \rightarrow +80$ °C interval and experimentally obtained values for $\Delta\Delta H^\ddagger$ (0.068 kcal·mol^{-1}) and $\Delta\Delta S^\ddagger$ (2.28 kcal·mol^{-1}·K^{-1}) demonstrated that the reaction is predominantly stereocontrolled by the differential activation entropy, $\Delta\Delta S^\ddagger$. The combined results described herein have allowed us to put forth the full catalytic cycle. While the described organocascade demonstrates admirable scope, it has clear limitations. The utility of this methodology was show-cased through the formal syntheses of the nonsteroidal anti–inflammatory agent indoprofen and a member of the fungus–derived and widely marketed statin drugs (+)-dihydrocompactin, and the concise approaches to the core structures of the natural product isatisine A and the nonpeptidyl ghrelin–receptor inverse agonist. Lastly, we have

documented the possibility of using a single chiral organocatalyst to fully control the stereochemical outcome of the stereodivergent Diels–Alder–initiated organocascade. We found that the judicious combination of Lewis and Brønsted bases can alter the sense of diastereoselection. We are currently undertaking further mechanistic investigations to fully understand the origins of this tunable diastereoselectivity. On the basis of our current findings, we envisage that programming the function of a catalyst using stereoelectronic stimuli may provide new synthetic opportunities and conceptual perspectives for confronting major challenges associated with the synthesis of all possible stereoisomers of a particular constitutional family of chiral molecules that cannot be addressed by traditional approaches. Further studies to investigate the stereoselectivity principles described in this report and applications toward natural product synthesis are ongoing in our laboratories and will be reported in due course.

REFERENCES

[1]   (a) B. Lindstrom and L. J. Pettersson, *Cattech*, 2003, **7**, 130-138; (b) J. Liebig, *Ann. Chem. Pharm.*, 1860, **13**, 246-247; (c) G. Bredig and P. S. Fiske, *Biochem. Z.*, 1912, **46**, 7-23; (d) F. G. Fischer and A. Marschall, *Ber. Dtsch. Chem. Ges.*, 1931, **64**, 2825-2827; (e) R. Kuhn, W. Badstubner and C. Grundmann, *Ber. Dtsch. Chem. Ges.*, 1936, **69**, 98-107; (f) W. Langenbeck, *Angew. Chem.*, 1928, **41**, 740-745; (g) W. Langenbeck, *2nd ed., Springer, Berlin*, 1949; (h) H. Pracejus, *Liebigs Ann. Chem.*, 1960, **634**, 9-22; (i) H. Pracejus, *Liebigs Ann. Chem.*, 1960, **634**, 23-29; (j) U. Eder, G. Sauer and R. Weichert, *Angew. Chem. Int. Ed.*, 1971, **10**, 496-497; (k) Z. G. Hajos and D. R. Parrish, *J. Org. Chem.*, 1974, **39**, 1615-1621.

[2]   (a) T. Ooi, M. Kameda and K. Maruoka, *J. Am. Chem. Soc.*, 1999, **121**, 6519-6520; (b) E. J. Corey and M. J. Grogan, *Org. Lett.*, 1999, **1**, 157-160; (c) M. S. Sigman and E. N. Jacobsen, *J. Am. Chem. Soc.*, 1998, **120**, 5315-5316; (d) J. C. Ruble, H. A. Latham and G. C. Fu, *J. Am. Chem. Soc.*, 1997, **119**, 1492-1493; (e) E. J. Corey, F. Xu and M. C. Noe, *J. Am. Chem. Soc.*, 1997, **119**, 12414-12415; (f) Y. Tu, Z. X. Wang and Y. Shi, *J. Am. Chem. Soc.*, 1996, **118**, 9806-9807; (g) S. E. Denmark, D. M. Coe, N. E. Pratt and B. D. Griedel, *J. Org. Chem.*, 1994, **59**, 6161-6163; (h) M. J. Odonnell, W. D. Bennett and S. D. Wu, *J. Am. Chem. Soc.*, 1989, **111**, 2353-2355; (i) J. I. Oku and S. Inoue, *J. Chem. Soc. Chem. Commun.*, 1981, 229-230; (j) S. Julia, J. Masana and J. C. Vega, *Angew. Chem. Int. Ed.*, 1980, **19**, 929-931.

[3]   B. List, R. A. Lerner and C. F. Barbas, *J. Am. Chem. Soc.*, 2000, **122**, 2395-2396.

[4]   K. A. Ahrendt, C. J. Borths and D. W. C. MacMillan, *J. Am. Chem. Soc.*, 2000, **122**, 4243-4244.

[5]   (a) S. Nakamura, *Org. Biomol. Chem.*, 2014, **12**, 394-405; (b) J. Mlynarski and S. Bas, *Chem. Soc. Rev.*, 2014, **43**, 577-587; (c) J. Mahatthananchai and J. W. Bode, *Acc. Chem. Res.*, 2014, **47**, 696-707; (d) X. Zeng, *Chem. Rev.*, 2013, **113**, 6864-

6900; (e) Y. Wei and M. Shi, *Chem. Rev.*, 2013, **113**, 6659-6690; (f) C. M. R. Volla, I. Atodiresei and M. Rueping, *Chem. Rev.*, 2013, **114**, 2390-2431; (g) S. Shirakawa and K. Maruoka, *Angew. Chem. Int. Ed.*, 2013, **52**, 4312-4348; (h) U. Scheffler and R. Mahrwald, *Chem. Eur. J.*, 2013, **19**, 14346-14396; (i) J. Novacek and M. Waser, *Eur. J. Org. Chem.*, 2013, 637-648; (j) D. J. Nelson and S. P. Nolan, *Chem. Soc. Rev.*, 2013, **42**, 6723-6753; (k) K. Murai and H. Fujioka, *Heterocycles*, 2013, **87**, 763-805; (l) G. Masson, C. Lalli, M. Benohoud and G. Dagousset, *Chem. Soc. Rev.*, 2013, **42**, 902-923; (m) M. Mahlau and B. List, *Angew. Chem. Int. Ed.*, 2013, **52**, 518-533; (n) P. Kumar and N. Dwivedi, *Acc. Chem. Res.*, 2013, **46**, 289-299; (o) X. Jiang and R. Wang, *Chem. Rev.*, 2013, **113**, 5515-5546; (p) Z. Du and Z. Shao, *Chem. Soc. Rev.*, 2013, **42**, 1337-1378; (q) J. Aleman and S. Cabrera, *Chem. Soc. Rev.*, 2013, **42**, 774-793; (r) C.-X. Zhuo, W. Zhang and S.-L. You, *Angew. Chem. Int. Ed.*, 2012, **51**, 12662-12686; (s) C. Zheng and S.-L. You, *Chem. Soc. Rev.*, 2012, **41**, 2498-2518; (t) R. C. Wende and P. R. Schreiner, *Green Chem.*, 2012, **14**, 1821-1849; (u) J. E. Taylor, S. D. Bull and J. M. J. Williams, *Chem. Soc. Rev.*, 2012, **41**, 2109-2121; (v) R. J. Phipps, G. L. Hamilton and F. D. Toste, *Nat. Chem.*, 2012, **4**, 603-614; (w) H. Pellissier, *Adv. Synth. Catal.*, 2012, **354**, 237-294; (x) J. Mlynarski and B. Gut, *Chem. Soc. Rev.*, 2012, **41**, 587-596; (y) P. Melchiorre, *Angew. Chem. Int. Ed.*, 2012, **51**, 9748-9770; (z) C. M. Marson, *Chem. Soc. Rev.*, 2012, **41**, 7712-7722; (aa) J. Mahatthananchai, A. M. Dumas and J. W. Bode, *Angew. Chem. Int. Ed.*, 2012, **51**, 10954-10990; (ab) L.-Q. Lu, J.-R. Chen and W.-J. Xiao, *Acc. Chem. Res.*, 2012, **45**, 1278-1293; (ac) C. C. J. Loh and D. Enders, *Chem. Eur. J.*, 2012, **18**, 10212-10225; (ad) T.-Y. Liu, M. Xie and Y.-C. Chen, *Chem. Soc. Rev.*, 2012, **41**, 4101-4112; (ae) F. Giacalone, M. Gruttadauria, P. Agrigento and R. Noto, *Chem. Soc. Rev.*, 2012, **41**, 2406-2447; (af) C. de Graaff, E. Ruijter and R. V. A. Orru, *Chem. Soc. Rev.*, 2012, **41**, 3969-4009; (ag) R. Dalpozzo, G. Bartoli and G. Bencivenni, *Chem. Soc. Rev.*, 2012, **41**, 7247-7290; (ah) A.-M. Caminade, A. Ouali, M. Keller and J.-P. Majoral, *Chem. Soc. Rev.*, 2012, **41**, 4113-4125; (ai)

J.-F. Briere, S. Oudeyer, V. Dalla and V. Levacher, *Chem. Soc. Rev.*, 2012, **41**, 1696-1707; (aj) J. Yu, F. Shi and L.-Z. Gong, *Acc. Chem. Res.*, 2011, **44**, 1156-1171; (ak) G. Valero, X. Companyo and R. Rios, *Chem. Eur. J.*, 2011, **17**, 2018-2037; (al) S. Schenker, A. Zamfir, M. Freund and S. B. Tsogoeva, *Eur. J. Org. Chem.*, 2011, 2209-2222; (am) M. Rueping, B. J. Nachtsheim, W. Ieawsuwan and I. Atodiresei, *Angew. Chem. Int. Ed.*, 2011, **50**, 6706-6720; (an) M. Rueping, A. Kuenkel and I. Atodiresei, *Chem. Soc. Rev.*, 2011, **40**, 4539-4549; (ao) M. Rueping, J. Dufour and F. R. Schoepke, *Green Chem.*, 2011, **13**, 1084-1105; (ap) S. Piovesana, D. M. S. Schietroma and M. Bella, *Angew. Chem. Int. Ed.*, 2011, **50**, 6216-6232; (aq) S. V. Pansare and E. K. Paul, *Chem. Eur. J.*, 2011, **17**, 8770-8779; (ar) J. M. R. Narayanam and C. R. J. Stephenson, *Chem. Soc. Rev.*, 2011, **40**, 102-113; (as) C. E. Mueller and P. R. Schreiner, *Angew. Chem. Int. Ed.*, 2011, **50**, 6012-6042; (at) A. Moyano and R. Rios, *Chem. Rev.*, 2011, **111**, 4703-4832; (au) M. D. Diaz de Villegas, J. A. Galvez, P. Etayo, R. Badorrey and P. Lopez-Ram-de-Viu, *Chem Soc Rev*, 2011, **40**, 5564-5587; (av) P. H.-Y. Cheong, C. Y. Legault, J. M. Um, N. Celebi-Oelcuem and K. N. Houk, *Chem. Rev.*, 2011, **111**, 5042-5137; (aw) C. A. Busacca, D. R. Fandrick, J. J. Song and C. H. Senanayake, *Adv. Synth. Catal.*, 2011, **353**, 1825-1864; (ax) J. Aleman, A. Parra, H. Jiang and K. A. Jorgensen, *Chem. Eur. J.*, 2011, **17**, 6890-6899; (ay) L. Albrecht, H. Jiang and K. A. Jorgensen, *Angew. Chem. Int. Ed.*, 2011, **50**, 8492-8509; (az) B. Weiner, W. Szymanski, D. B. Janssen, A. J. Minnaard and B. L. Feringa, *Chem. Soc. Rev.*, 2010, **39**, 1656-1691; (ba) Y. Wei and M. Shi, *Acc. Chem. Res.*, 2010, **43**, 1005-1018; (bb) B. M. Trost and C. S. Brindle, *Chem. Soc. Rev.*, 2010, **39**, 1600-1632; (bc) V. Terrasson, R. M. de Figueiredo and J. M. Campagne, *Eur. J. Org. Chem.*, 2010, 2635-2655; (bd) M. Nielsen, C. B. Jacobsen, N. Holub, M. W. Paixao and K. A. Jorgensen, *Angew. Chem. Int. Ed.*, 2010, **49**, 2668-2679; (be) A. Moyano, N. El-Hamdouni and A. Atlamsani, *Chem. Eur. J.*, 2010, **16**, 5260-5273; (bf) E. Marques-Lopez, R. P. Herrera and M. Christmann, *Nat. Prod. Rep.*, 2010, **27**, 1138-1167; (bg) T. E. Kristensen and

T. Hansen, *Eur. J. Org. Chem.*, 2010, 3179-3204; (bh) C. Grondal, M. Jeanty and D. Enders, *Nat. Chem.*, 2010, **2**, 167-178; (bi) G. Bartoli, G. Bencivenni and R. Dalpozzo, *Chem. Soc. Rev.*, 2010, **39**, 4449-4465; (bj) L. Albrecht, A. Albrecht, H. Krawczyk and K. A. Jorgensen, *Chem. Eur. J.*, 2010, **16**, 28-48; (bk) A.-N. R. Alba, X. Companyo and R. Rios, *Chem. Soc. Rev.*, 2010, **39**, 2018-2033.

[6]   A. G. Doyle and E. N. Jacobsen, *Chem. Rev.*, 2007, **107**, 5713-5743.

[7]   (a) G. Lelais, D. W. C. MacMillan, *Aldrichimica Acta*, 2006, **39**, 79-87; (b) A. E rkkila, I. Majander and P. M. Pihko, *Chem. Rev.*, 2007, **107**, 5416-5470.

[8]   (a) B. List, *Acc. Chem. Res.*, 2004, **37**, 548-557; (b) S. Mukherjee, J. W. Yang, S. Hoffmann and B. List, *Chem. Rev.*, 2007, **107**, 5471-5569; (c) P. Kumar and N. Dwivedi, *Acc. Chem. Res.*, 2012, **46**, 289-299; (d) J.-L. Li, T.-Y. Liu and Y.-C. Chen, *Acc. Chem. Res.*, 2012, **45**, 1491-1500.

[9]   (a) Ł. Albrecht, G. Dickmeiss, F. C. Acosta, C. Rodríguez-Escrich, R. L. Davis and K. A. Jørgensen, *J. Am. Chem. Soc.*, 2012, **134**, 2543-2546; (b) D. B. Ramachary and Y. V. Reddy, *Eur. J. Org. Chem.*, 2012, 865-887.

[10]   (a) Ł. Albrecht, F. C. Acosta, A. Fraile, A. Albrecht, J. Christensen and K. A. Jorgensen, *Angew. Chem. Int. Ed.*, 2012, **51**, 9088-9092; (b) X.-F. Xiong, Q. Zhou, J. Gu, L. Dong, T.-Y. Liu and Y.-C. Chen, *Angew. Chem. Int. Ed.*, 2012, **51**, 4401-4404; (c) H. Jiang, D. C. Cruz, Y. Li, V. H. Lauridsen and K. A. Jørgensen, *J. Am. Chem. Soc.*, 2013, **135**, 5200-5207; (d) I. Kumar, P. Ramaraju and N. A. Mir, *Org. Biomol. Chem.*, 2013, **11**, 709-716.

[11]   J. Stiller, P. H. Poulsen, D. Cruz, J. Dourado, R. Davis and K. A. Jorgensen, *Chem. Sci.*, 2014, Advance Article.

[12]   (a) J. L. Methot and W. R. Roush, *Adv. Synth. Catal.*, 2004, **346**, 1035-1050; (b) Y. Wang, J. Pan, Z. Chen, X. Sun and Z. Wang, *Mini Rev. Med. Chem.*, 2013, **13**, 836-844; (c) Y. C. Fan and O. Kwon, *Chem. Commun.*, 2013, **49**, 11588-11619.

[13]   (a) R. P. Wurz, *Chem. Rev.*, 2007, **107**, 5570-5595; (b) A. Enriquez-Garcia and E. P. Kundig, *Chem. Soc. Rev.*, 2012, **41**, 7803-7831; (c) S. France, D. J. Guerin, S. J. Miller and T. Lectka, *Chem. Rev.*, 2003, **103**, 2985-3012.

[14]   G. C. Fu, *Acc. Chem. Res.*, 2004, **37**, 542-547.

[15]   S. A. Shaw, P. Aleman and E. Vedejs, *J. Am. Chem. Soc.*, 2003, **125**, 13368-13369.

[16]   M. Kobayashi and S. Okamoto, *Tetrahedron Lett.*, 2006, **47**, 4347-4350.

[17]   V. B. Birman, E. W. Uffman, H. Jiang, X. Li and C. J. Kilbane, *J. Am. Chem. Soc.*, 2004, **126**, 12226-12227.

[18]   V. B. Birman and X. M. Li, *Org. Lett.*, 2006, **8**, 1351-1354.

[19]   V. B. Birman and X. M. Li, *Org. Lett.*, 2008, **10**, 1115-1118.

[20]   (a) E. Bappert, P. Muller and G. C. Fu, *Chem. Commun.*, 2006, 2604-2606; (b) E. R. T. Robinson, C. Fallan, C. Simal, A. M. Z. Slawin and A. D. Smith, *Chem. Sci.*, 2013, **4**, 2193-2200; (c) S. Vellalath, K. N. Van and D. Romo, *Angew. Chem. Int. Ed.*, 2013, **52**, 13688-13693; (d) G. Liu, M. E. Shirley, K. N. Van, R. L. McFarlin and D. Romo, *Nat. Chem.*, 2013, **5**, 1049-1057; (e) M. E. Abbasov, B. M. Hudson, D. J. Tantillo, and D. Romo, *J. Am. Chem. Soc.*, 2014, **136**, 4492-4495.

[21]   (a) M. J. Gaunt and C. C. C. Johansson, *Chem. Rev.*, 2007, **107**, 5596-5605; (b) C. L. Chandler and B. List, *J. Am. Chem. Soc.*, 2008, **130**, 6737-6739; (c) A. Michrowska and B. List, *Nat. Chem.*, 2009, **1**, 225-228.

[22]   (a) P. S. Tiseni and R. Peters, *Angew. Chem. Int. Ed.*, 2007, **46**, 5325-5328; (b) L. C. Morrill, S. M. Smith, A. M. Z. Slawin and A. D. Smith, *J. Org. Chem.*, 2014, **79**, 1640-1655.

[23]   (a) S. J. Ryan, L. Candish and D. W. Lupton, *Chem. Soc. Rev.*, 2013, **42**, 4906-4917; (b) H. U. Vora, P. Wheeler and T. Rovis, *Adv. Synth. Catal.*, 2012, **354**, 1617-1639; (c) J. Izquierdo, G. E. Hutson, D. T. Cohen and K. A. Scheidt, *Angew. Chem. Int. Ed.*, 2012, **51**, 11686-11698; (d) A. Grossmann and D. Enders, *Angew. Chem. Int. Ed.*, 2012, **51**, 314-325; (e) D. T. Cohen and K. A. Scheidt, *Chem. Sci.*, 2012, **3**, 53-57; (f) X. Bugaut and F. Glorius, *Chem. Soc. Rev.*, 2012, **41**, 3511-3522; (g) A. T. Biju, N. Kuhl and F. Glorius, *Acc. Chem. Res.*, 2011, **44**, 1182-1195; (h) J. L. Moore and T. Rovis, *in Topics in Current*

Chemistry, ed. B. List, Springer, Berlin, vol. 291, 2009, pp. 77–144; (i) V. Nair, S. Vellalath and B. P. Babu, *Chem. Soc. Rev.*, 2008, **37**, 2691–2698; (j) N. Marion, S. Diez-Gonzalez and S. P. Nolan, *Angew. Chem. Int. Ed.*, 2007, **46**, 2988-3000; (k) D. Enders, O. Niemeier and A. Henseler, *Chem. Rev.*, 2007, **107**, 5606-5655; (l) D. Enders and T. Balensiefer, *Acc. Chem. Res.*, 2004, **37**, 534-541.

[24]   T. Kano, R. Sakamoto, M. Akakura and K. Maruoka, *J. Am. Chem. Soc.*, 2012, **134**, 7516-7520.

[25]   B. List, I. Čorić, O. O. Grygorenko, P. S. J. Kaib, I. Komarov, A. Lee, M. Leutzsch, S. Chandra Pan, A. V. Tymtsunik and M. van Gemmeren, *Angew. Chem. Int. Ed.*, 2014, **53**, 282-285.

[26]   (a) B. D. Horning and D. W. C. MacMillan, *J. Am. Chem. Soc.*, 2013, **135**, 6442-6445; (b) S. B. Jones, B. Simmons, A. Mastracchio and D. W. C. MacMillan, *Nature* 2011, **475**, 183-188.

[27]   (a) A. G. Kravina, J. Mahatthananchai and J. W. Bode, *Angew. Chem. Int. Ed.*, 2012, **51**, 9433-9436; (b) K. P. Jang, G. E. Hutson, R. C. Johnston, E. O. McCusker, P. H. Y. Cheong and K. A. Scheidt, *J. Am. Chem. Soc.*, 2013, **136**, 76-79; (c) N. A. White, D. A. DiRocco and T. Rovis, *J. Am. Chem. Soc.*, 2013, **135**, 8504-8507; (d) M. Wang, Z. Huang, J. Xu and Y. R. Chi, *J. Am. Chem. Soc.*, 2014, **136**, 1214-1217.

[28]   Z. Fu, J. Xu, T. Zhu, W. W. Leong and Y. R. Chi, *Nat. Chem.*, 2013, **5**, 835-839.

[29]   (a) M. Wadamoto, E. M. Phillips, T. E. Reynolds and K. A. Scheidt, *J. Am. Chem. Soc.*, 2007, **129**, 10098-10099; (b) E. M. Phillips, J. M. Roberts and K. A. Scheidt, *Org. Lett.*, 2010, **12**, 2830-2833.

[30]   (a) X. Han, F. Zhong, Y. Wang and Y. Lu, *Angew. Chem. Int. Ed.*, 2012, **51**, 767-770; (b) K. Albertshofer, B. Tan and C. F. Barbas, *Org. Lett.*, 2013, **15**, 2958-2961; (c) R. J. Lundgren, A. Wilsily, N. Marion, C. Ma, Y. K. Chung and G. C. Fu, *Angew. Chem. Int. Ed.*, 2013, **52**, 2525-2528; (d) F. Zhong, X. Dou, X. Han, W. Yao, Q. Zhu, Y. Meng and Y. Lu, *Angew. Chem. Int. Ed.*, 2013, **52**, 943-947.

[31]   I. P. Andrews and O. Kwon, *Chem. Sci.*, 2012, **3**, 2510-2514.

[32]   (a) C. A. Leverett, V. C. Purohit, A. G. Johnson, R. L. Davis, D. J. Tantillo and D. Romo, *J. Am. Chem. Soc.*, 2012, **134**, 13348-13356; (b) C. A. Leverett, V. C. Purohit and D. Romo, *Angew. Chem. Int. Ed.*, 2010, **49**, 9479-9483; (c) R. L. Davis, C. A. Leverett, D. Romo and D. J. Tantillo, *J. Org. Chem.*, 2011, **76**, 7167-7174.

[33]   (a) Y. Feng, M. M. Majireck and S. M. Weinreb *J. Org. Chem.*, 2014, **79**, 7-24; (b) Y. Feng, M. M. Majireck and S. M. Weinreb, *Angew. Chem. Int. Ed.,* 2012, **51**, 12846-12849.

[34]   (a) Davies, H. M. L.; Sorensen, E. J. *Chem. Soc. Rev.* **2009**, *38*, 2981. (b) Grondal, C.; Jeanty, M.; Enders, D. *Nat. Chem.* **2010**, *2*, 167. (c) Jones, S. B.; Simmons, B.; Mastracchio, A.; MacMillan, D. W. C. *Nature* **2011**, *475*, 183.

[35]   (a) Nicolaou, K. C.; Snyder, S. A.; Montagnon, T.; Vassilikogiannakis, G. *Angew. Chem. Int. Ed.* **2002**, *41*, 1668. (b) Juhl, M.; Tanner, D. *Chem. Soc. Rev.* **2009**, *38*, 2983.

[36]   (a) Evans, D. A.; Johnson, J. S. In *Comprehensive Asymmetric Catalysis*; Jacobsen, E. N., Pfaltz, A., Yamamoto, H., Eds.; Springer: New York, 1999; Vol. 3, p 1177 and references therein.

[37]   (a) Ahrendt, K. A.; Borths, C. J.; MacMillan, D. W. C. *J. Am. Chem. Soc.* **2000**, *122*, 4243. (b) Northrup, A. B.; MacMillan, D. W. C. *J. Am. Chem. Soc.* **2002**, *124*, 2458.

[38]   (a) Thayumanavan, R.; Dhevalapally, B.; Sakthivel, S.; Tanaka, F.; Barbas, C. F., III. *Tetrahedron Lett.* **2002**, *43*, 3817. (b) Jia, Z.; Jiang, H.; Li, J.; Gschwend, B.; Li, Q.; Yin, X.; Grouleff, J.; Chen, Y.; Jørgensen, K. A. *J. Am. Chem. Soc.* **2011**, *133*, 5053.

[39]   (a) Shen, J.; Nguyen, T. T.; Goh, Y. P.; Ye, W.; Fu, X.; Xu, J.; Tan, C. H. *J. Am. Chem. Soc.* **2006**, *128*, 13692. (b) Wang, Y.; Li, H. M.; Wang, Y. Q.; Liu, Y.; Foxman, B. M.; Deng, L. *J. Am. Chem. Soc.* **2007**, *129*, 6364.

[40]   (a) Huang, Y.; Unni, A. K.; Thadani, A. N.; Rawal, V. H. *Nature* **2003**, *424*, 146. (b) Thadani, A. N.; Stankovic, A. R.; Rawal, V. H. *Proc. Natl. Acad. Sci. U.S.A.* **2004**, *101*, 5846. (c) Tan, B.; Hernández-Torres, G.; Barbas, C. F., III. *J. Am. Chem. Soc.* **2011**, *133*, 12354.

[41]   (a) Bappert, E.; Muller, P.; Fu, G. C. *Chem. Commun.* **2006**, 2604. (b) Robinson, E. R. T.; Fallan, C.; Simal, C.; Slawin, A. M. Z.; Smith, A. D. *Chem. Sci.* **2013**, *4*, 2193. (c) Liu, G.; Shirley, M. E.; Van, K. N.; McFarlin, R. L.; Romo, D. *Nat. Chem.* **2013**, *5*, 1049. (d) Vellalath, S.; Van, K. N.; Romo, D. *Angew. Chem. Int. Ed.* **2013**, *52*, 13688.

[42]   (a) Miller, L. C.; Ndungu, J. M.; Sarpong, R. *Angew. Chem. Int. Ed.* **2009**, *48*, 2398. (b) Miller, L. C.; Sarpong, R. *Chem. Soc. Rev.* **2011**, *40*, 4550 and references therein.

[43]   (a) Danishefsky, S; Kitahara, T. *J. Am. Chem. Soc.* **1974**, *96*, 7807. (b) Danishefsky, S.; Kitahara, T.; Yan, C. F.; Morris, J. *J. Am. Chem. Soc.* **1979**, *101*, 6996. (c) Danishefsky, S. *Acc. Chem. Res.* **1981**, *14*, 400.

[44]   (a) Birman, V. B.; Li, X. M. *Org. Lett.* **2008**, *10*, 1115. (b) Birman, V. B.; Li, X. M. *Org. Lett.* **2006**, *8*, 1351.

[45]   Hafez, A. M.; Taggi, A. E.; Wack, H.; Esterbrook, J.; Lectka, T. *Org. Lett.* **2001**, *3*, 2049.

[46]   (a) Sauer, J. *Angew. Chem. Int. Ed.* **1966**, *5*, 211. (b) Sauer, J. *Angew. Chem. Int. Ed.* **1967**, *6*, 16.

[47]   Takatori, K.; Hasegawa, K.; Narai, S.; Kajiwara, M. *Hetero-cycles* **1996**, *42*, 525.

[48]   (a) Corey, E. J.; Jardine, P. D. S.; Mohri, T. *Tetrahedron Lett.* **1988**, *29*, 6409. (b) Nagashima, S.; Kanematsu, K. *Tetrahedron: Asym.* **1990**, *1*, 743. (c) Calvo, D.; Port, M.; Delpech, B.; Lett, R. *Tetrahedron Lett.* **1996**, *37*, 1023.

[49]   (a) Tischler, M.; Andersen, R. J. *Tetrahedron Lett.* **1989**, *30*, 5717. (b) Okamura, H.; Yamauchi, K.; Miyawaki, K.; Iwagawa, T.; Nakatani, M. *Tetrahedron Lett.* **1997**, *38*, 263. (c) White, J. D.; Takabe, K.; Prisbylla, M. P. *J. Org. Chem.* **1985**, *50*, 5233.

[50]   (a) Birman, V. B.; Li, X. M.; Han, Z. F. *Org. Lett.* **2007**, *9*, 37. (b) Liu, P.; Yang, X.; Birman, V. B.; Houk, K. N. *Org. Lett.* **2012**, *14*, 3288.

[51]   (a) Jones, S. B.; Simmons, B.; MacMillan, D. W. C. *J. Am. Chem. Soc.* **2009**, *131*, 13606. (b) Horning, B. D.; MacMillan, D. W. C. *J. Am. Chem. Soc.* **2013**, *135*, 6442.

[52]   C. S. Schindler and E. N. Jacobsen, *Science*, 2013, **340**, 1052-1053.

[53]   S. K. Branch, M. Eichelbaum, B. Testa and A. Somogyi, *Stereochemical aspects of drug action and disposition*, Springer, Berlin; New York, 2003.

[54]   B. M. Wang, F. H. Wu, Y. Wang, X. F. Liu and L. Deng, *J. Am. Chem. Soc.*, 2007, **129**, 768-769.

[55]   (a) X. X. Yan, Q. Peng, Q. Li, K. Zhang, J. Yao, X. L. Hou and Y. D. Wu, *J. Am. Chem. Soc.*, 2008, **130**, 14362-+; (b) A. Nojiri, N. Kumagai and M. Shibasaki, *J. Am. Chem. Soc.*, 2009, **131**, 3779-3784.

[56]   M. Morgen, S. Bretzke, P. F. Li and D. Menche, *Org. Lett.*, 2010, **12**, 4494-4497.

[57]   M. Luparia, M. T. Oliveira, D. Audisio, F. Frebault, R. Goddard and N. Maulide, *Angew. Chem. Int. Ed.*, 2011, **50**, 12631-12635.

[58]   X. Tian, C. Cassani, Y. K. Liu, A. Moran, A. Urakawa, P. Galzerano, E. Arceo and P. Melchiorre, *J. Am. Chem. Soc.*, 2011, **133**, 17934-17941.

[59]   E. L. McInturff, E. Yamaguchi and M. J. Krische, *J. Am. Chem. Soc.*, 2012, **134**, 20628-20631.

[60]   S. Krautwald, D. Sarlah, M. A. Schafroth and E. M. Carreira, *Science*, 2013, **340**, 1065-1068.

[61]   F. Romanov-Michailidis, M. Pupier, L. Guenee and A. Alexakis, *Chem. Commun.*, 2014, **50**, 13461-13464.

[62]   L. C. Miller and R. Sarpong, *Chem. Soc. Rev.*, 2011, **40**, 4550-4562.

[63]   L. C. Miller, J. M. Ndungu and R. Sarpong, *Angew. Chem. Int. Ed.*, 2009, **48**, 2398-2402.

[64]   M. E. Abbasov and D. Romo, *Nat. Prod. Rep.*, 2014, **31**, 1318-1327.

[65] M. E. Abbasov, B. M. Hudson, D. J. Tantillo and D. Romo, *J. Am. Chem. Soc.*, 2014, **136**, 4492-4495.

[66] E. Bappert, P. Muller and G. C. Fu, *Chem. Commun.*, 2006, 2604-2606.

[67] E. R. T. Robinson, C. Fallan, C. Simal, A. M. Z. Slawin and A. D. Smith, *Chem. Sci.*, 2013, **4**, 2193-2200.

[68] G. Liu, M. E. Shirley, K. N. Van, R. L. McFarlin and D. Romo, *Nat. Chem.*, 2013, **5**, 1049-1057.

[69] S. Vellalath, K. N. Van and D. Romo, *Angew. Chem. Int. Ed.*, 2013, **52**, 13688-13693.

[70] Y. Fukata, K. Asano and S. Matsubara, *J. Am. Chem. Soc.*, 2015, **137**, 5320-5323.

[71] O. Diels and K. Alder, *Liebigs. Ann. Chem.*, 1928, **460**, 98-122.

[72] K. C. Nicolaou, S. A. Snyder, T. Montagnon and G. Vassilikogiannakis, *Angew. Chem. Int. Ed.*, 2002, **41**, 1668-1698.

[73] (a) K. A. Ahrendt, C. J. Borths and D. W. C. MacMillan, *J. Am. Chem. Soc.*, 2000, **122**, 4243-4244; (b) A. B. Northrup and D. W. C. MacMillan, *J. Am. Chem. Soc.*, 2002, **124**, 2458-2460.

[74] (a) R. Thayumanavan, B. Dhevalapally, K. Sakthivel, F. Tanaka and C. F. Barbas, *Tetrahedron Lett*, 2002, **43**, 3817-3820; (b) Z. J. Jia, H. Jiang, J. L. Li, B. Gschwend, Q. Z. Li, X. A. Yin, J. Grouleff, Y. C. Chen and K. A. Jorgensen, *J. Am. Chem. Soc.*, 2011, **133**, 5053-5061.

[75] Y. Wang, H. M. Li, Y. Q. Wang, Y. Liu, B. M. Foxman and L. Deng, *J. Am. Chem. Soc.*, 2007, **129**, 6364-6365.

[76] (a) Y. Huang, A. K. Unni, A. N. Thadani and V. H. Rawal, *Nature*, 2003, **424**, 146-146; (b) B. Tan, G. Hernández-Torres and C. F. Barbas, *J. Am. Chem. Soc.*, 2011, **133**, 12354-12357.

[77] S. L. Schreiber, *Science*, 2000, **287**, 1964-1969.

[78] (a) J. A. Frearson and I. T. Collie, *Drug Discov. Today*, 2009, **14**, 1150-1158; (b) S. Dandapani and L. A. Marcaurelle, *Nat. Chem. Biol.*, 2010, **6**, 861-863; (c) R.

Macarron, M. N. Banks, D. Bojanic, D. J. Burns, D. A. Cirovic, T. Garyantes, D. V. Green, R. P. Hertzberg, W. P. Janzen, J. W. Paslay, U. Schopfer and G. S. Sittampalam, *Nat. Rev. Drug Discov.*, 2011, **10**, 188-195.

[79]   C. J. O'Connor, L. Laraia and D. R. Spring, *Chem. Soc. Rev.*, 2011, **40**, 4332-4345.

[80]   (a) D. S. Tan, *Nat. Chem. Biol.*, 2005, **1**, 74-84; (b) O. C. CJ, H. S. Beckmann and D. R. Spring, *Chem. Soc. Rev.*, 2012, **41**, 4444-4456.

[81]   (a) D. A. Annis, O. Helluin and E. N. Jacobsen, *Angew. Chem. Int. Ed.*, 1998, **37**, 1907-1909; (b) B. A. Harrison, T. M. Gierasch, C. Neilan, G. W. Pasternak and G. L. Verdine, *J. Am. Chem. Soc.*, 2002, **124**, 13352-13353.

[82]   (a) M. Rottmann, C. McNamara, B. K. S. Yeung, M. C. S. Lee, B. Zou, B. Russell, P. Seitz, D. M. Plouffe, N. V. Dharia, J. Tan, S. B. Cohen, K. R. Spencer, G. E. González-Páez, S. B. Lakshminarayana, A. Goh, R. Suwanarusk, T. Jegla, E. K. Schmitt, H.-P. Beck, R. Brun, F. Nosten, L. Renia, V. Dartois, T. H. Keller, D. A. Fidock, E. A. Winzeler and T. T. Diagana, *Science*, 2010, **329**, 1175-1180; (b) S. Dandapani, E. Comer, J. R. Duvall and B. Munoz, *Future Medicinal Chemistry*, 2012, **4**, 2279-2294.

[83]   (a) L.-M. Xu, Y.-F. Liang, Q.-D. Ye, Z. Yang, M. Foley, S. A. Snyder and D.-W. Ma, in *Organic Chemistry – Breakthroughs and Perspectives*, Wiley-VCH Verlag GmbH & Co. KGaA2012, pp. 1-31; (b) J. Clardy and C. Walsh, *Nature*, 2004, **432**, 829-837.

[84]   T. Sugimura, T. Tei, A. Mori, T. Okuyama and A. Tai, *J. Am. Chem. Soc.*, 2000, **122**, 2128-2129.

[85]   M. Lombardo, S. Fabbroni and C. Trombini, *J. Org. Chem.*, 2001, **66**, 1264-1268.

[86]   L. S. M. Wong and M. S. Sherburn, *Org. Lett.*, 2003, **5**, 3603-3606.

[87]   S. Akai, K. Tanimoto and Y. Kita, *Angew. Chem. Int. Ed.*, 2004, **43**, 1407-1410.

[88]   J. Sauer, *Angew. Chem. Int. Ed.*, 1966, **5**, 211.

[89]   W. R. Roush and D. A. Barda, *J. Am. Chem. Soc.*, 1997, **119**, 7402-7403.

[90] (a) D. A. Evans and D. M. Barnes, *Tetrahedron Lett*, 1997, **38**, 57-58; (b) D. A. Evans, D. M. Barnes, J. S. Johnson, R. Lectka, P. von Matt, S. J. Miller, J. A. Murry, R. D. Norcross, E. A. Shaughnessy and K. R. Campos, *J. Am. Chem. Soc.*, 1999, **121**, 7582-7594.

[91] (a) D. H. Ryua, K. H. Kim, J. Y. Sim and E. J. Corey, *Tetrahedron Lett*, 2007, **48**, 5735-5737; (b) D. Liu, E. Canales and E. J. Corey, *J. Am. Chem. Soc.*, 2007, **129**, 1498-1499.

[92] A. Mimoto, K. Nakano, Y. Ichikawa and H. Kotsuki, *Heterocycles*, 2010, **80**, 799-804.

[93] A. M. Hafez, A. E. Taggi, H. Wack, J. Esterbrook and T. Lectka, *Org. Lett.*, 2001, **3**, 2049-2051.

[94] S. Sanli, Y. Altun, N. Sanli, G. Alsancak and J. L. Beltran, *J. Chem. Eng. Data*, 2009, **54**, 3014-3021.

[95] J. Steinreiber, K. Faber and H. Griengl, *Chemistry*, 2008, **14**, 8060-8072.

[96] A. Cordova, I. Ibrahem, J. Casas, H. Sunden, M. Engqvist and E. Reyes, *Chem. Eur. J.*, 2005, **11**, 4772-4784.

[97] J. Steinreiber, M. Schurmann, M. Wolberg, F. van Assema, C. Reisinger, K. Tesko, D. Mink and H. Griengl, *Angew. Chem. Int. Ed.*, 2007, **46**, 1624-1626.

[98] H. Hagiwara, M. Konno, T. Nakano and H. Uda, *J. Chem. Soc. Perk. Trans. 1*, 1994, 2417-2430.

[99] Y. K. Tonylam, V. P. Gullo, R. T. Goegelman, D. Jorn, L. Huang, C. Deriso, R. L. Monaghan and I. Putter, *J. Antibiot.*, 1981, **34**, 614-616.

[100] M. R. Lunn, D. E. Root, A. M. Martino, S. P. Flaherty, B. P. Kelley, D. D. Coovert, A. H. Burghes, N. T. Man, G. E. Morris, J. H. Zhou, E. J. Androphy, C. J. Sumner and B. R. Stockwell, *Chem. Biol.*, 2004, **11**, 1489-1493.

[101] T. Linnanen, O. Rist, M. Grimstrup, T. Frimurer, T. Hoegberg, F. E. Nielsen and L. O. Gerlach, WO08092681, 2008.

[102] J.-F. Liu, Z.-Y. Jiang, R.-R. Wang, Y.-T. Zheng, J.-J. Chen, X.-M. Zhang and Y.-B. Ma, *Org. Lett.*, 2007, **9**, 4127-4129.

[103]   J. Ammer, M. Baidya, S. Kobayashi and H. Mayr, *J. Phys. Org. Chem.*, 2010, **23**, 1029-1035.

[104]   A. J. Wagner and S. D. Rychnovsky, *Org Lett*, 2013, **15**, 5504-5507.

[105]   (a) J. M. Fox, O. Dmitrenko, L. A. Liao and R. D. Bach, *J. Org. Chem.*, 2004, **69**, 7317-7328; (b) M. Adler, S. Adler and G. Boche, *J. Phys. Org. Chem.*, 2005, **18**, 193-209.

[106]   S. Vellalath, K. N. Van and D. Romo, *Tetrahedron Lett.*, 2015, **56**, 3647-3652.

[107]   B. Saikia, I. Suryanarayana, B. K. Saikia and I. Haque, *Spectrochim. Acta. A*, 1991, **47**, 791-798.

[108]   D. Farcasiu, M. Lezcano and A. Vinslava, *New. J. Chem.*, 2000, **24**, 199-201.

[109]   E. M. Arnett and B. Chawla, *J. Am. Chem. Soc.*, 1979, **101**, 7141-7146.

[110]   R. L. Benoit, M. Frechette and D. Lefebvre, *Can. J. Chem.*, 1988, **66**, 1159-1162.

[111]   F. G. Bordwell, *Acc. Chem. Res.*, 1988, **21**, 456-463.

[112]   I. M. Kolthoff, Chantoon.Mk and S. Bhowmik, *J. Am. Chem. Soc.*, 1968, **90**, 23.

[113]   (a) J. H. Aasheim, H. Fliegl, E. Uggerud, T. Bonge-Hansen and O. Eisenstein, *New. J. Chem.*, 2014, **38**, 5975-5982; (b) S. E. Wheeler and J. W. G. Bloom, *J. Phys. Chem. A*, 2014, **118**, 6133-6147.

[114]   R. E. Plata and D. A. Singleton, *J. Am. Chem. Soc.*, 2015, **137**, 3811-3826.

[115]   J. P. Wagner and P. R. Schreiner, *Angewandte Chemie International Edition*, 2015, DOI: 10.1002/anie.201503476.

[116]   M. J. Frisch et al. *Gaussian 09, Revision D.01, Gaussian, Inc., Wallingford CT*, 2009.

[117]   (a) Y. Zhao and D. G. Truhlar, *Acc. Chem. Res.*, 2008, **41**, 157-167; (b) Y. Zhao and D. Truhlar, *Theor. Chem. Acc.*, 2008, **120**, 215-241.

[118]   (a) S. E. Wheeler, *J. Am. Chem. Soc.*, 2011, **133**, 10262-10274; (b) S. E. Wheeler, *Acc. Chem. Res.*, 2013, **46**, 1029-1038.

[119]   J. Qi, M. S. Han, Y. C. Chang and C. H. Tung, *Bioconjugate Chem.*, 2011, **22**, 1758-1762.

[120]   D. S. B. Daniels, S. R. Smith, T. Lebl, P. Shapland and A. D. Smith, *Synthesis*, 2015, **47**, 34-41.

APPENDIX A
SUPPORTING INFORMATION

General Procedures

All non-aqueous reactions were performed under a nitrogen atmosphere in oven-dried glassware. Dichloromethane (CH_2Cl_2), tetrahydrofuran (THF), diethyl ether (Et_2O), acetonitrile (CH_3CN) and toluene (PhMe) were dried by passing through activated alumina (solvent purification system). Diisopropylethylamine ($EtN(^iPr)_2$) and triethylamine (Et_3N) were distilled from calcium hydride prior to use. Other solvents and reagents were used as received from commercially available sources. Deuterated solvents were purchased from Cambridge Isotopes and used as received. ^{1}H NMR spectra were measured at 500 MHz and referenced relative to residual chloroform (7.26 ppm) or benzene (7.16 ppm) and were reported in parts per million. Coupling constants (*J*) were reported in Hertz (Hz), with multiplicity reported following usual convention: s, singlet; d, doublet; t, triplet; q, quartet; dd, doublet of doublets; dt, doublet of triplets; dq, doublet of quartets; qd, quartet of doublets; td, triplet of doublets; tt, triplet of triplets; ddd, doublet of doublet of doublets; ddt, doublet of doublet of triplets; ddq, doublet of doublet of quartets; dddd, doublet of doublet of doublet of doublets; ddddt, doublet of doublet of doublet of triplets; ddquint, doublet of doublet of quintets; m, multiplet, br s, broad singlet. ^{13}C NMR spectra were measured at 125 MHz and referenced relative to residual chloroform (77.23 ppm) or benzene (128.06 ppm) and were reported in parts per million (ppm). Flash column chromatography was performed with 60Å Silica Gel (230-400 mesh) as stationary phase on an automated flash chromatography system (EtOAc/hexanes as eluent unless indicated otherwise). High-resolution mass spectra (ESI) were obtained through the Laboratory for Biological Mass Spectrometry (Texas A&M University). Thin Layer Chromatography (TLC) was performed using glass-backed silica gel F254 (Silicycle, 250 μm thickness). Visualization of developed plates was performed by fluorescence quenching or by treating with Seebach's[1] staining solution. *Fourier* Transform Infrared (FTIR) spectra

were recorded as thin films on NaCl plates. Optical rotations were recorded on a polarimeter at 589 nm employing a 25 mm cell. High Performance Liquid Chromatography (HPLC) was performed on a chromatographic system using various chiral columns (25 cm) as noted. X-ray diffraction was obtained by the X-ray Diffraction Laboratory at Texas A&M University. (R)-(–)-HBTM,[2] TMSQD[3] and BzQN[4] were synthesized according to literature procedures. (S)-(–)-BTM and (R)-(+)-BTM were purchased from TCI chemicals and used as received. (DHQ)₂PHAL, (S)-(–)-Tetramisole and (–)-Tröger's base were purchased from Sigma-Aldrich and used as received. (R)-(+)-PPY* was purchased from Strem chemicals and used as received. All unsaturated acid chlorides were purchased from Sigma-Aldrich and used as received without further purification.

Abbreviation List

DBU	=	1,8-diazabicyclo[5.4.0]undec-7-ene
EtN(^{i}Pr)$_2$	=	*N,N*-diisopropylethylamine
Et$_3$N	=	triethylamine
DTBP	=	2,6-di-*tert*-butylpyridine
DIBAl-H	=	diisobutylaluminum hydride
TIPSOTf	=	triisopropylsilyl trifluoromethanesulfonate
TBHP	=	*tert*-butyl hydroperoxide
Rh$_2$(cap)$_4$	=	dirhodium tetracaprolactamate
TsCl	=	4-toluenesulfonyl chloride
TASF	=	tris(dimethylamino)sulfonium difluorotrimethylsilicate
(R)-(–)-HBTM	=	(R)-(–)-homobenzotetramisole
(S)-(–)-BTM	=	(S)-(–)-benzotetramisole
TMSQD	=	*O*-trimethylsilyl quinidine
BzQN	=	*O*-benzoyl quinine
(DHQ)₂PHAL	=	Hydroquinine 1,4-phthalazinediyl diether
(R)-(+)-PPY*	=	(R)-4-pyrrolidinopyrindinyl(pentamethylcyclopentadienyl)iron

CHAPTER II

Preparation of S3, S4, S7, S8, S11, S12, S14, S15, S17, S18, 2a-f, and (±)-2g:
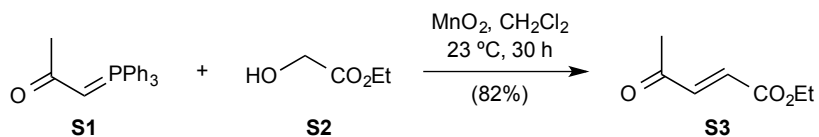
(*E*)-ethyl 4-oxopent-2-enoate (S3): (*E*)-ethyl 4-oxopent-2-enoate **S3** was prepared by a modified reported procedure.[5] To a solution of 1-(triphenylphosphoranylidene)-2-propanone **S1** (21.0 g, 65.9 mmol, 1.0 equiv.) and ethyl glycolate **S2** (7.5 mL, 79.2 mmol, 1.2 equiv.) in anhydrous CH_2Cl_2 (220 mL) was added MnO_2 (57.5 g, 661.3 mmol, 10.0 equiv.) and vigorously stirred at ambient temperature (23 °C) for 30 h. The mixture was filtered through a short pad of celite and the filtrate was concentrated using rotary evaporation. The residue was then diluted with cold Et_2O (100 mL), filtered through a plug of celite and washed with additional Et_2O (50 mL). The filtrate was concentrated by rotary evaporation and purified by an automated flash chromatography system (5 → 20% EtOAc/hexanes) providing 7.68 g (82% yield) of ketoester **S3** as a pale yellow liquid: TLC (EtOAc:hexanes, 1:9 *v/v*): $R_f = 0.38$; ^{1}H NMR (500 MHz, CDCl$_3$): δ 6.99 (d, $J = 16.1$ Hz, 1H), 6.62 (dd, $J = 16.1$, 0.4 Hz, 1H), 4.24 (qd, $J = 7.1$, 0.4 Hz, 2H), 2.34 (s, 3H), 1.30 (td, $J = 7.1$, 0.5 Hz, 3H); ^{13}C NMR (125 MHz; CDCl$_3$): δ 197.7, 165.5, 140.0, 131.7, 61.5, 28.2, 14.2; IR (thin film): 2985, 1726, 1703, 1687 cm^{-1}; HRMS (ESI+) *m/z* calcd for $C_7H_{10}LiO_3$ [M+Li]$^+$: 149.0790, found: 149.0784.
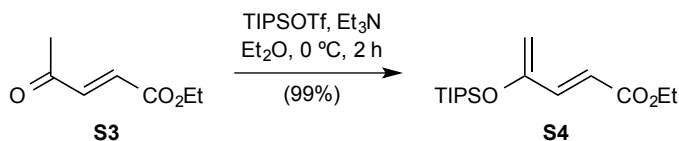

(*E*)-ethyl 4-(((triisopropylsilyl)oxy)penta-2,4-dienoate (S4): To a solution of ketoester **S3** (2.25 g, 15.8 mmol, 1.0 equiv.) in anhydrous Et_2O (32 mL) at 0 °C was added Et_3N (4.4 mL, 31.6 mmol, 2.0 equiv.) dropwise. After stirring for 10 min, TIPSOTf (5.1 mL,

18.9 mmol, 1.2 equiv.) was added over a period of 30 min. The reaction was stirred for 2 h at 0 ºC then quenched with a saturated aqueous solution of $NaHCO_3$ (30 mL). The aqueous layer was extracted with Et_2O (2 × 50 mL) and the combined organic extracts were then washed with brine (50 mL). The organic layer was then dried over anhydrous $MgSO_4$, filtered, and concentrated by rotary evaporation. The residue was purified by an automated flash chromatography system (0.5 → 10% EtOAc/hexanes) providing 4.70 g (99% yield) of diene **S4** as a clear colorless liquid: TLC (EtOAc:hexanes, 1:9 *v/v*): R_f = 0.73; ^{1}H NMR (500 MHz, CDCl$_3$): δ 7.07 (d, *J* = 15.2 Hz, 1H), 6.18 (d, *J* = 15.2 Hz, 1H), 4.62 (dd, J = 1.3, 0.5 Hz, 1H), 4.61 (dd, J = 1.2, 0.6 Hz, 1H), 4.21 (q, *J* = 7.1 Hz, 2H), 1.30 (t, *J* = 7.1 Hz, 3H), 1.28–1.20 (m, 3H), 1.10 (d, *J* = 7.3 Hz, 18H); ^{13}C NMR (125 MHz; CDCl$_3$): δ 167.3, 154.0, 142.6, 119.2, 101.8, 60.6, 18.1 (6), 14.4, 12.9 (3); IR (thin film): 2946, 2869, 1719, 1638, 1593 cm^{-1}; HRMS (ESI+) *m/z* calcd for $C_{16}H_{31}O_3Si$ [M+H]$^+$: 299.2037, found: 299.2054.
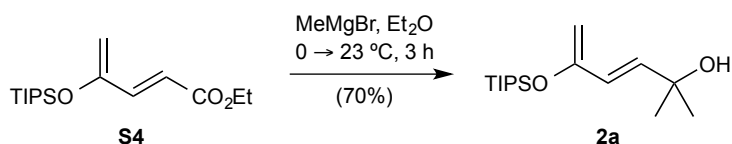
(*E*)-2-methyl-5-((triisopropylsilyl)oxy)hexa-3,5-dien-2-ol (2a): To a solution of diene **S4** (5.20 g, 17.4 mmol, 1.0 equiv.) in anhydrous Et_2O (60 mL) at 0 ºC was added MeMgBr (3.0 M solution in Et_2O, 13.4 mL, 40.2 mmol, 2.3 equiv.) was added over a period of 1 h. The reaction was stirred for 2 h at 23 ºC then quenched with a saturated aqueous solution of NH_4Cl (30 mL). The aqueous layer was extracted with Et_2O (2 × 50 mL) and the combined organic extracts were then washed with brine (30 mL). The organic layer was then dried over anhydrous $MgSO_4$, filtered, and concentrated by rotary evaporation. The residue was purified by an automated flash chromatography system (0.5 → 15% EtOAc/hexanes) providing 3.47 g (70% yield) of silyloxydiene alcohol **2a** as a clear colorless oil: TLC (EtOAc:hexanes, 1:9 *v/v*): R_f = 0.35; ^{1}H NMR (500 MHz; CDCl$_3$): δ 6.18 (d, *J* = 15.4 Hz, 1H), 6.05 (d, *J* = 15.4 Hz, 1H), 4.31 (s, 1H), 4.28 (s, 1H), 1.34 (s, 6H), 1.26–1.21 (m, 3H), 1.10 (d, *J* = 7.3 Hz, 18H); ^{13}C NMR (125 MHz;

CDCl$_3$): δ 155.1, 138.2, 124.8, 95.2, 70.8, 29.9 (2), 18.2 (6), 12.9 (3); IR (thin film): 3374, 2945, 2868, 1591 cm^{-1}; HRMS (ESI+) *m/z* calcd for C$_{16}$H$_{33}$O$_2$Si [M+H]$^+$: 285.2250, found: 285.2242.
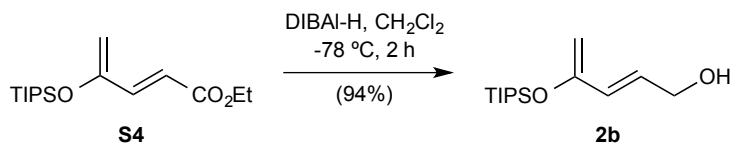

(*E*)-4-((triisopropylsilyl)oxy)penta-2,4-dien-1-ol (2b): To a solution of diene **S4** (4.70 g, 15.7 mmol, 1.0 equiv.) in anhydrous CH$_2$Cl$_2$ (120 mL) at -78 °C was added DIBAl-H (1.0 M solution in CH$_2$Cl$_2$, 47.0 mL, 3.0 equiv.) dropwise. The reaction was stirred for 2 h then carefully quenched in sequence with H$_2$O (1.9 mL), 15% aqueous NaOH (1.9 mL), and H$_2$O (4.7 mL). The dry ice/acetone bath was removed and the mixture was allowed to warm up to ambient temperature (23 °C) on its own accord. Subsequently, anhydrous MgSO$_4$ was added and the reaction mixture was vigorously stirred for 30 min, filtered through a pad of celite and concentrated by rotary evaporation. The residue was purified by an automated flash chromatography (5 → 20% EtOAc/hexanes) providing 3.78 g (94% yield) of silyloxydiene alcohol **2b** as a pale yellow oil: TLC (EtOAc:hexanes, 1:9 *v/v*): R$_f$ = 0.32; ^{1}H NMR (500 MHz, CDCl$_3$): δ 6.19 (dt, *J* = 15.2, 5.4 Hz, 1H), 6.09 (dt, *J* = 15.2, 1.4 Hz, 1H), 4.31 (d, *J* = 0.5 Hz, 1H), 4.27 (d, *J* = 0.4 Hz, 1H), 4.24 (d, *J* = 5.2 Hz, 2H), 1.27–1.20 (m, 3H), 1.10 (d, *J* = 7.3 Hz, 18H); ^{13}C NMR (125 MHz; CDCl$_3$): δ 154.8, 129.2, 129.0, 95.1, 63.1, 18.2 (6), 12.9 (3); IR (thin film): 3318, 2945, 2868, 1662, 1591 cm^{-1}; HRMS (ESI+) *m/z* calcd for C$_{14}$H$_{29}$O$_2$Si [M+H]$^+$: 257.1937, found: 257.1926.
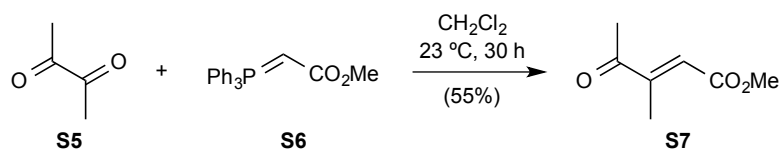
Methyl (*E*)-3-methyl-4-oxopent-2-enoate (S7): To a solution of 2,3-butanedione **S5** (2.6 mL, 30.0 mmol, 1.0 equiv.) in anhydrous CH$_2$Cl$_2$ (150 mL) was added methyl

(triphenylphosphoranylidene)acetate **S6** (10.0 g, 30.0 mmol, 1.0 equiv.) and stirred at ambient temperature (23 ºC) for 30 h. The mixture was filtered through a short pad of celite and the filtrate was concentrated using rotary evaporation. The residue was then diluted with cold Et$_2$O (80 mL), filtered through a plug of celite and washed with additional Et$_2$O (40 mL). The filtrate was concentrated by rotary evaporation and purified by an automated flash chromatography system (5 → 20% EtOAc/hexanes) providing 2.34 g (55% yield) of ketoester **S7** as a clear colorless oil: TLC (EtOAc:hexanes, 1:9 *v/v*): R$_f$ = 0.45; ^{1}H NMR (500 MHz, CDCl$_3$): δ 6.56 (q, *J* = 1.5 Hz, 1H), 3.77 (s, 3H), 2.36 (s, 3H), 2.19 (d, *J* = 1.5 Hz, 3H); ^{13}C NMR (125 MHz; CDCl$_3$): δ 199.9, 166.7, 150.9, 126.1, 51.9, 26.3, 13.2; IR (thin film): 2955,1728, 1687, 1642 cm^{-1}; HRMS (ESI+) *m/z* calcd for C$_7$H$_{10}$LiO$_3$ [M+Li]$^+$: 149.0790, found: 149.0797.
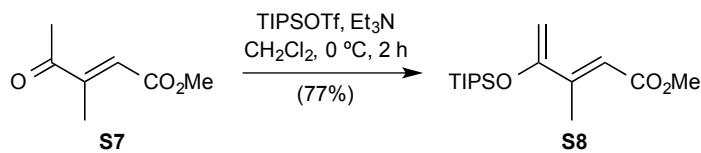
Methyl (*E*)-3-methyl-4-((triisopropylsilyl)oxy)penta-2,4-dienoate (S8): To a solution of ketoester **S7** (2.34 g, 16.5 mmol, 1.0 equiv.) in anhydrous CH$_2$Cl$_2$ (60 mL) at 0 ºC was added Et$_3$N (5.7 mL, 41.2 mmol, 2.5 equiv.) dropwise. After stirring for 10 min, TIPSOTf (5.3 mL, 19.8 mmol, 1.2 equiv.) was added over a period of 30 min. The reaction was stirred for 2 h at 0 ºC then quenched with a saturated aqueous solution of NaHCO$_3$ (30 mL). The aqueous layer was extracted with Et$_2$O (2 × 50 mL) and the combined organic extracts were then washed with brine (50 mL). The organic layer was then dried over anhydrous MgSO$_4$, filtered, and concentrated by rotary evaporation. The residue was purified by an automated flash chromatography system (0.5 → 10% EtOAc/hexanes) providing 3.79 g (77% yield) of diene **S8** as a yellow oil: TLC (EtOAc:hexanes, 1:9 *v/v*): R$_f$ = 0.76; ^{1}H NMR (500 MHz, CDCl$_3$): δ 6.39 (d, *J* = 0.6 Hz, 1H), 4.80 (d, *J* = 1.9 Hz, 1H), 4.56 (d, *J* = 1.9 Hz, 1H), 3.71 (s, 3H), 2.28 (d, *J* = 1.2 Hz, 3H), 1.28-1.20 (m, 3H), 1.10 (d, *J* = 7.3 Hz, 18H). ^{13}C NMR (125 MHz; CDCl$_3$): δ 168.1, 156.6, 149.8, 115.8, 96.2, 51.2, 18.2 (6), 14.6, 12.9 (3); IR (thin film): 2947, 2869, 1722,

1629, 1597 cm^{-1}; HRMS (ESI+) *m/z* calcd for C$_{16}$H$_{31}$O$_3$Si [M+H]$^+$: 299.2042, found: 299.2029.
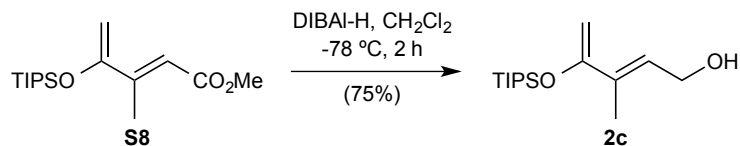

(*E*)-3-methyl-4-((triisopropylsilyl)oxy)penta-2,4-dien-1-ol (2c): To a solution of diene **S8** (7.5 g, 25.1 mmol, 1.0 equiv.) in anhydrous CH$_2$Cl$_2$ (180 mL) at -78 °C was added DIBAl-H (1.0 M solution in CH$_2$Cl$_2$, 72.0 mL, 3.0 equiv.) dropwise. The reaction was stirred for 2 h at -78 °C then carefully quenched in sequence with H$_2$O (2.9 mL), 15% aqueous NaOH (2.9 mL), and H$_2$O (7.2 mL). The dry ice/acetone bath was removed and the mixture was allowed to warm up to ambient temperature (23 °C) on its own accord. Subsequently, anhydrous MgSO$_4$ was added and the reaction mixture was vigorously stirred for 30 min, filtered through a pad of celite and concentrated by rotary evaporation. The residue was purified by an automated flash chromatography (5 → 20% EtOAc/hexanes) providing 4.88 g (75% yield) of silyloxydiene alcohol **2c** as a clear colorless oil: TLC (EtOAc:hexanes, 1:9 *v/v*): R$_f$ = 0.30; ^{1}H NMR (500 MHz, C$_6$D$_6$): δ 6.44 (tt, *J* = 6.48, 0.55 Hz, 1H), 4.45 (d, *J* = 1.2 Hz, 1H), 4.36 (d, *J* = 0.9 Hz, 1H), 4.06 (d, *J* = 6.3 Hz, 2H), 1.62 (d, *J* = 0.9 Hz, 3H), 1.23-1.18 (m, 3H), 1.14 (d, *J* = 6.2 Hz, 18H); ^{13}C NMR (125 MHz; C$_6$D$_6$): δ 157.7, 132.6, 128.1, 91.1, 59.8, 18.4 (6), 13.5, 13.2 (3); IR (thin film): 3320, 2945, 2868, 1593 cm^{-1}; HRMS (ESI+) *m/z* calcd for C$_{15}$H$_{31}$O$_2$Si [M+H]$^+$: 271.2093, found: 271.2092.
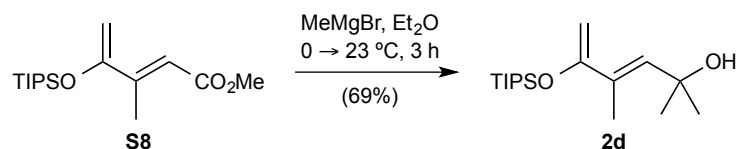
(*E*)-2,4-dimethyl-5-((triisopropylsilyl)oxy)hexa-3,5-dien-2-ol (2d): To a solution of diene **S8** (1.0 g, 3.2 mmol, 1.0 equiv.) in anhydrous Et$_2$O (10 mL) at 0 °C was added MeMgBr (3.0 M solution in Et$_2$O, 2.5 mL, 7.4 mmol, 2.3 equiv.) over a period of 1 h.

The reaction was stirred for 2 h at 23 ºC then quenched with a saturated aqueous solution of NH$_4$Cl (5 mL). The aqueous layer was extracted with Et$_2$O (2 × 10 mL) and the combined organic extracts were then washed with brine (5 mL). The organic layer was then dried over anhydrous MgSO$_4$, filtered, and concentrated by rotary evaporation. The residue was purified by an automated flash chromatography system (0.5 → 15% EtOAc/hexanes) providing 0.65 g (69% yield) of silyloxydiene alcohol **2d** as a clear colorless oil: TLC (EtOAc:hexanes, 1:9 *v/v*): R$_f$ = 0.48; ^{1}H-NMR (500 MHz; CDCl$_3$): δ 6.25 (s, 1H), 4.47 (s, 1H), 4.29 (s, 1H), 2.02 (s, 3H), 1.40 (s, 6H), 1.27-1.20 (m, 3H), 1.09 (d, *J* = 7.5 Hz, 18H).; ^{13}C NMR (125 MHz; CDCl$_3$): δ 158.0, 134.6, 132.8, 91.2, 71.2, 31.4 (2), 18.2 (6), 14.0, 12.9 (3); IR (thin film): 3406, 2945, 2868, 1664, 1593 cm^{-1}; HRMS (ESI+) *m/z* calcd for C$_{17}$H$_{35}$O$_2$Si [M+H]$^+$: 299.2406, found: 299.2420.
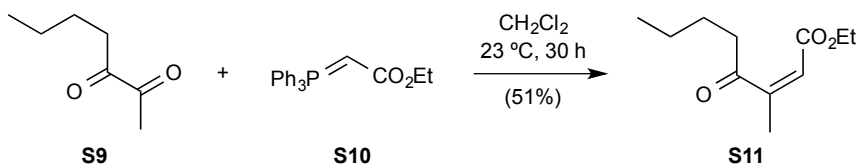
Ethyl (*Z*)-3-methyl-4-oxooct-2-enoate (S11): To a solution of 2,3-heptanedione **S9** (16.8 mL, 120.0 mmol, 1.2 equiv.) in anhydrous CH$_2$Cl$_2$ (250 mL) was added ethyl (triphenylphosphoranylidene)acetate **S10** (35.0 g, 100.0 mmol, 1.0 equiv.) and stir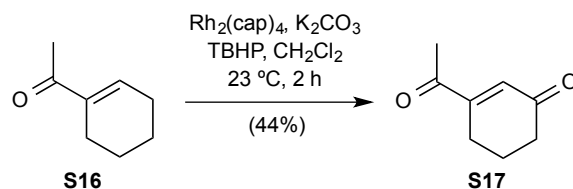red at ambient temperature (23 °C) for 30 h. The mixture was filtered through a short pad of celite and the filtrate was concentrated using rotary evaporation. The residue was then diluted with cold Et$_2$O (200 mL), filtered through a plug of celite and washed with additional Et$_2$O (50 mL). The filtrate was concentrated by rotary evaporation and purified by an automated flash chromatography system (5 → 15% EtOAc/hexanes) providing 10.15 g (51% yield) of ketoester **S11** as a pale yellow oil: TLC (EtOAc:hexanes, 1:9 *v/v*): R$_f$ = 0.59; ^{1}H NMR (500 MHz, CDCl$_3$): δ 6.52 (q, *J* = 1.5 Hz, 1H), 4.22 (q, *J* = 7.1 Hz, 2H), 2.68 (t, *J* = 7.4 Hz, 2H), 2.20 (d, *J* = 1.5 Hz, 3H), 1.62-1.56 (m, 2H), 1.36-1.28 (m, 2H), 1.30 (t, *J* = 7.1 Hz, 3H), 0.90 (t, *J* = 7.4 Hz, 3H); ^{13}C NMR (125 MHz; CDCl$_3$): δ 202.6, 166.4, 150.8, 125.3, 60.8, 38.1, 26.4, 22.4, 14.3,

14.0, 13.5; IR (thin film): 2961, 2936, 1725, 1687 cm^{-1}; HRMS (ESI+) *m/z* calcd for C$_{11}$H$_{18}$LiO$_3$ [M+Li]$^+$: 205.1416, found: 205.1424.
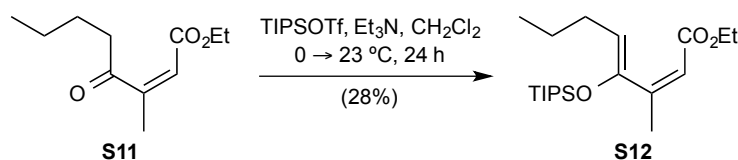
Ethyl (2*Z*,4*Z*)-3-methyl-4-((triisopropylsilyl)oxy)octa-2,4-dienoate (S12): To a solution of ketoester **S11** (3.51 g, 17.7 mmol, 1.0 equiv.) in anhydrous CH$_2$Cl$_2$ (60 mL) at 0 °C was added Et$_3$N (3.7 mL, 26.6 mmol, 1.5 equiv.) dropwise. After stirring for 10 min, TIPSOTf (5.7 mL, 21.2 mmol, 1.2 equiv.) was added over a period of 30 min. The reaction was stirred for 2 h at 0 °C. The mixture was then allowed to warm up to ambient temperature (23 °C) on its own accord and stirred for 22 h. The reaction was quenched with a saturated aqueous solution of NaHCO$_3$ (30 mL). The aqueous layer was extracted with Et$_2$O (2 × 50 mL) and the combined organic extracts were then washed with brine (50 mL). The organic layer was then dried over anhydrous MgSO$_4$, filtered, and concentrated by rotary evaporation. The residue was purified by an automated flash chromatography system (5 → 25% CH$_2$Cl$_2$/hexanes) providing 1.75 g (28% yield) of diene **S12** as a pale yellow oil: TLC (CH$_2$Cl$_2$:hexanes, 1:4 *v/v*): R$_f$ = 0.41; ^{1}H NMR (500 MHz, CDCl$_3$): δ 6.11 (d, *J* = 0.5 Hz, 1H), 5.18 (t, *J* = 7.2 Hz, 1H), 4.16 (q, *J* = 7.1 Hz, 2H), 2.27 (d, *J* = 0.8 Hz, 3H), 2.15 (q, *J* = 7.4 Hz, 2H), 1.40 (q, *J* = 7.5 Hz, 2H), 1.27 (t, *J* = 7.1 Hz, 3H), 1.21-1.14 (m, 3H), 1.09 (d, *J* = 1.9 Hz, 18H), 0.92 (t, *J* = 7.3 Hz, 3H). ^{13}C NMR (125 MHz; CDCl$_3$): δ 167.7, 152.1, 151.3, 115.8, 114.8, 59.7, 28.7, 22.7, 18.1 (6), 15.4, 14.5, 14.1, 13.9 (3); IR (thin film): 2960, 2869, 1716, 1623 cm^{-1}; HRMS (MALDI+) *m/z* calcd for C$_{20}$H$_{39}$O$_3$Si [M+H]$^+$: 355.2668, found: 355.2644.
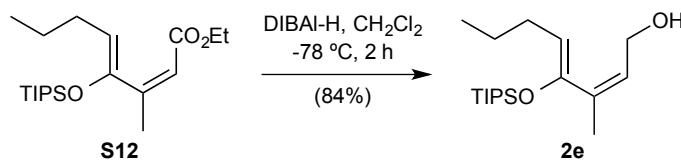
(2Z,4Z)-3-methyl-4-((triisopropylsilyl)oxy)octa-2,4-dien-1-ol (2e): To a solution of diene **S12** (1.1 g, 3.1 mmol, 1.0 equiv.) in anhydrous CH_2Cl_2 (25 mL) at -78 ºC was added DIBAl-H (1.0 M solution in CH_2Cl_2, 9.3 mL, 3.0 equiv.) dropwise. The reaction was stirred for 2 h at -78 ºC then carefully quenched in sequence with H_2O (0.37 mL), 15% aqueous NaOH (0.37 mL), and H_2O (0.93 mL). The dry ice/acetone bath was removed and the mixture was allowed to warm up to ambient temperature (23 ºC) on its own accord. Subsequently, anhydrous $MgSO_4$ was added and the reaction mixture was vigorously stirred for 30 min, filtered through a pad of celite and concentrated by rotary evaporation. The residue was purified by an automated flash chromatography (5 → 20% EtOAc/hexanes) providing 0.80 g (84% yield) of silyloxydiene alcohol **2e** as a clear colorless oil: TLC (EtOAc:hexanes, 1:9 v/v): R_f = 0.36; ^{1}H NMR (500 MHz, CDCl$_3$): δ 5.95 (td, J = 6.8, 0.8 Hz, 1H), 4.84 (t, J = 7.1 Hz, 1H), 4.26 (d, J = 6.8 Hz, 2H), 2.11 (q, J = 7.4 Hz, 2H), 1.79 (d, J = 1.1 Hz, 3H), 1.38 (dq, J = 14.9, 7.4 Hz, 2H), 1.21-1.16 (m, 3H), 1.10 (d, J = 6.8 Hz, 18H), 0.91 (t, J = 7.4 Hz, 3H); ^{13}C NMR (125 MHz; CDCl$_3$): δ 151.3, 135.8, 124.5, 110.9, 59.9, 28.4, 23.0, 18.2 (6), 14.3, 14.2, 14.0 (3); IR (thin film): 3332, 2959, 2868, 1626 cm^{-1}; HRMS (ESI+) m/z calcd for $C_{18}H_{37}O_2Si$ [M+H]$^+$: 313.2563, found: 313.2571.
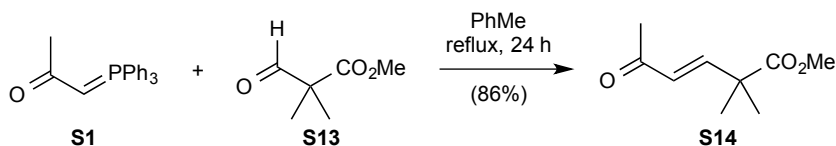
Methyl (E)-2,2-dimethyl-5-oxohex-3-enoate (S14): To a solution of 1-(triphenyl-phosphoranylidene)-2-propanone **S1** (4.32 g, 13.6 mmol, 1.3 equiv.) in anhydrous PhMe (35 mL) was added methyl 2,2-dimethyl-3-oxopropanoate **S13** (1.36 g, 10.5 mmol, 1.0 equiv.), which was freshly prepared from methyl 2,2-dimethyl-3-hydroxypropionate[6] and used immediately without purification, and the mixture was refluxed (115-120 ºC)

for 24 h. The mixture was filtered through a short pad of celite and the filtrate was concentrated using rotary evaporation. The residue was then diluted with cold Et$_2$O (25 mL), filtered through a plug of celite and washed with additional Et$_2$O (10 mL). The filtrate was concentrated by rotary evaporation and purified by an automated flash chromatography system (5 → 20% EtOAc/hexanes) providing 1.52 g (86% yield) of ketoester **S14** as a clear colorless oil: TLC (EtOAc:hexanes, 1:9 *v/v*): R$_f$ = 0.26; ^{1}H NMR (500 MHz, CDCl$_3$): δ 6.92 (d, *J* = 16.3 Hz, 1H), 6.05 (d, *J* = 16.3 Hz, 1H), 3.68 (s, 3H), 2.25 (s, 3H), 1.34 (s, 6H); ^{13}C NMR (125 MHz; CDCl$_3$): δ 198.7, 175.4, 150.4, 128.8, 52.6, 44.8, 27.3, 24.6 (2); IR (thin film): 2983, 2954, 1734, 1702, 1681, 1626 cm^{-1}; HRMS (ESI+) *m/z* calcd for C$_9$H$_{14}$LiO$_3$ [M+Li]$^+$: 177.1103, found: 177.1108.
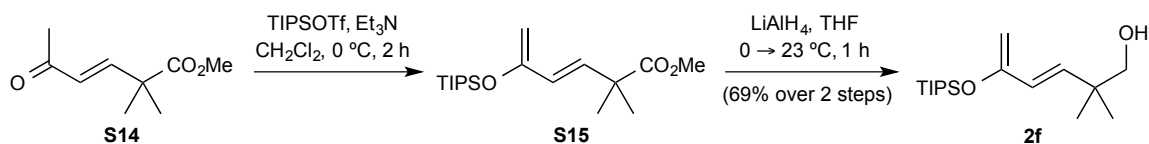
(*E*)-2,2-dimethyl-5-((triisopropylsilyl)oxy)hexa-3,5-dien-1-ol (2f): To a solution of ketoester **S14** (1.52 g, 8.9 mmol, 1.0 equiv.) in anhydrous CH$_2$Cl$_2$ (45 mL) at 0 ºC was added Et$_3$N (1.5 mL, 10.7 mmol, 1.2 equiv.) dropwise. After stirring for 10 min, TIPSOTf (2.6 mL, 9.6 mmol, 1.1 equiv.) was added over a period of 30 min. The reaction was stirred for 2 h at 0 ºC then quenched with a saturated aqueous solution of NaHCO$_3$ (20 mL). The aqueous layer was extracted with Et$_2$O (2 × 50 mL) and the combined organic extracts were then washed with brine (50 mL). The organic layer was then dried over anhydrous MgSO$_4$, filtered, and concentrated by rotary evaporation to afford crude diene **S15** as a pale yellow oil. The crude material was of sufficient purity to be carried on directly to the next step (Note: purification of this compound led to extensive loss of material on SiO$_2$).

To a solution of crude diene **S15** in anhydrous THF (64 mL) at 0 ºC was added LiAlH$_4$ (2.0 M solution in THF, 4.5 mL, 1.1 equiv.) dropwise. The reaction was stirred for 30 min at 0 ºC then allowed to warm up to ambient temperature (23 ºC) and stirred for 30 min. The reaction was then cooled to 0 ºC and carefully quenched in sequence

with 0.36 mL H_2O, 0.36 mL 15% aqueous NaOH, and 0.90 mL H_2O. The ice bath was removed and the mixture was allowed to warm up to ambient temperature (23 ºC) on its own accord. Subsequently, anhydrous $MgSO_4$ was added and the reaction mixture was vigorously stirred for 30 min, filtered through a pad of celite and concentrated by rotary evaporation. The residue was purified by an automated flash chromatography (5 → 20% EtOAc/hexanes) providing 1.83 g (69% yield over 2 steps) of silyloxydiene alcohol **2f** as a clear colorless oil: TLC (EtOAc:hexanes, 1:9 v/v): R_f = 0.29; ^{1}H NMR (500 MHz, CDCl$_3$): δ 6.00 (d, J = 15.6 Hz, 1H), 5.89 (dd, J = 15.6, 0.8 Hz, 1H), 4.29 (s, 1H), 4.25 (s, 1H), 3.35 (s, 2H), 1.27-1.19 (m, 3H), 1.10 (d, J = 7.3 Hz, 18H), 1.05 (s, 6H); ^{13}C NMR (125 MHz; CDCl$_3$): δ 155.2, 137.5, 127.0, 94.5, 71.7, 38.4, 23.9 (2), 18.2 (6), 12.9 (3); IR (thin film): 3377, 2948, 2870, 1593 cm^{-1}; HRMS (ESI+) m/z calcd for $C_{17}H_{35}O_2Si$ [M+H]$^+$: 299.2406, found: 299.2413.

3-acetylcyclohex-2-en-1-one (S17): 3-acetylcyclohex-2-en-1-one **S17** was prepared by a modified reported procedure.[7] To a solution of 1-acetyl-1-cyclohexene **S16** (5.2 mL, 40.3 mmol, 1.0 equiv.) in anhydrous CH_2Cl_2 (150 mL) was added in sequence K_2CO_3 (2.78 g, 20.2 mmol, 0.5 equiv.), Rh$_2$(cap)$_4$ (42 mg, 0.064 mmol, 0.0016 equiv.) and TBHP (5.0-6.0 M solution in decane, 40.0 mL, 201.5 mmol, 5.0 equiv.). The reaction mixture was exposed to air and vigorously stirred at ambient temperature (23 ºC) for 2 h. The mixture was filtered through a short pad of SiO_2 and the filtrate was concentrated using rotary evaporation. Purification by an automated flash chromatography system (5 → 20% EtOAc/hexanes) afforded 2.42 g (44% yield) of diketone **S17** as a yellow oil: TLC (EtOAc:hexanes, 1:9 v/v): R_f = 0.20; ^{1}H NMR (500 MHz, CDCl$_3$): δ 6.55 (t, J = 1.7 Hz, 1H), 2.49 (td, J = 6.0, 1.7 Hz, 2H), 2.44 (t, J = 6.8 Hz, 2H), 2.38 (s, 3H), 2.01 (dt, J = 13.1, 6.4 Hz, 2H); ^{13}C NMR (125 MHz; CDCl$_3$): δ 201.5, 200.2, 154.7, 132.5, 38.0,

26.2, 23.4, 22.0; IR (thin film): 2955, 1681 cm^{-1}; HRMS (ESI+) *m/z* calcd for C$_8$H$_{10}$LiO$_2$ [M+Li]$^+$: 145.0841, found: 145.0838.
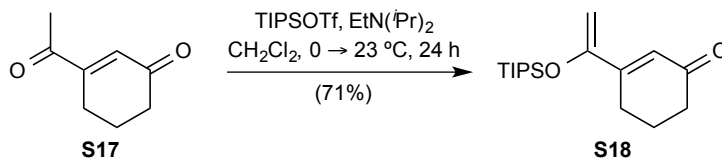
3-(1-((triisopropylsilyl)oxy)vinyl)cyclohex-2-en-1-one (S18): To a solution of diketone **S17** (3.28 g, 23.7 mmol, 1.0 equiv.) in anhydrous CH$_2$Cl$_2$ (100 mL) at 0 ºC was added EtN(^{i}Pr)$_2$ (9.1 mL, 52.2 mmol, 2.2 equiv.) dropwise. After stirring for 10 min, TIPSOTf (7.7 mL, 28.5 mmol, 1.2 equiv.) was added over a period of 30 min. The reaction was stirred for 2 h at 0 ºC. The mixture was then allowed to warm up to ambient temperature (23 ºC) on its own accord and stirred for 22 h. The reaction was quenched with a saturated aqueous solution of NaHCO$_3$ (50 mL). The aqueous layer was extracted with Et$_2$O (2 × 50 mL) and the combined organic extracts were then washed with brine (50 mL). The organic layer was then dried over anhydrous MgSO$_4$, filtered, and concentrated by rotary evaporation. The residue was purified by an automated flash chromatography system (5 → 15% EtOAc/hexanes) providing 4.94 g (71% yield) of diene **S18** as a yellow oil: TLC (EtOAc:hexanes, 1:9 *v/v*): R$_f$ = 0.49; ^{1}H NMR (500 MHz, CDCl$_3$): δ 6.44 (s, 1H), 4.83 (dd, *J* = 2.1, 0.5 Hz, 1H), 4.61 (dd, *J* = 2.1, 0.5 Hz, 1H), 2.48 (td, *J* = 6.1, 1.3 Hz, 2H), 2.40 (t, *J* = 6.7 Hz, 2H), 2.06-2.01 (m, 2H), 1.28-1.23 (m, 3H), 1.09 (d, *J* = 7.3 Hz, 18H); ^{13}C NMR (125 MHz; CDCl$_3$): δ 200.9, 155.2, 155.1, 124.6, 96.9, 37.7, 25.6, 22.7, 18.2 (6), 12.9 (3); IR (thin film): 2945, 2867, 1669 cm^{-1}; HRMS (ESI+) *m/z* calcd for C$_{17}$H$_{31}$O$_2$Si [M+H]$^+$: 295.2093, found: 295.2116.
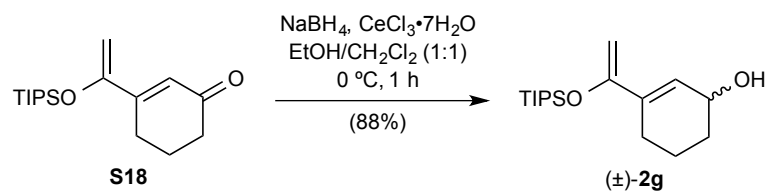
3-(1-((triisopropylsilyl)oxy)vinyl)cyclohex-2-en-1-ol ((±)-2g): To a solution of diene **S18** (3.11 g, 10.6 mmol, 1.0 equiv.) in absolute EtOH (105 mL) and anhydrous CH$_2$Cl$_2$ (105 mL) at 0 ℃ was added CeCl$_3$•7H$_2$O (4.33 g, 11.6 mmol, 1.1 equiv.) in one portion. After stirring for 20 min, NaBH$_4$ (1.0 g, 26.4 mmol, 2.5 equiv.) was added portionwise over a period of 30 min. The reaction was stirred for 30 min at 0 ℃ then quenched with a saturated aqueous solution of NaHCO$_3$ (20 mL). The aqueous layer was extracted with CH$_2$Cl$_2$ (2 × 80 mL) and the combined organic extracts were then washed with brine (20 mL). The organic layer was then dried over anhydrous MgSO$_4$, filtered, and concentrated by rotary evaporation. The residue was purified by an automated flash chromatography system (5 → 15% EtOAc/hexanes) providing 2.75 g (88% yield) of silyloxydiene alcohol (±)-**2g** as a clear colorless oil: TLC (EtOAc:hexanes, 1:9 *v/v*): R$_f$ = 0.46; ^{1}H NMR (500 MHz, CDCl$_3$): δ 6.30-6.30 (m, 1H), 4.41 (dt, *J* = 1.6, 0.5 Hz, 1H), 4.33-4.30 (m, 1H), 4.28 (d, *J* = 1.6 Hz, 1H), 2.22-2.15 (m, 1H), 2.13-2.07 (m, 1H), 1.91-1.86 (m, 1H), 1.83-1.76 (m, 1H), 1.65-1.51 (m, 2H), 1.28-1.20 (m, 3H), 1.10 (d, *J* = 6.7 Hz, 18H); ^{13}C NMR (125 MHz; CDCl$_3$): δ 156.2, 136.3, 126.8, 91.1, 66.5, 31.9, 25.1, 19.5, 18.3 (6), 13.0 (3); IR (thin film): 3333, 2943, 2867, 1662, 1593 cm^{-1}; HRMS (ESI+) *m/z* calcd for C$_{17}$H$_{33}$O$_2$Si [M+H]$^+$: 297.2250, found: 297.2264.

DAL optimization studies (Tables S1-S3):

NOTE: The relative and absolute configuration of *trans*-fused bicyclic γ-lactone (+)-**3c'** was unambiguously assigned by X-ray analysis using anomalous dispersion (see **Figure S3**). Based on this structure, detailed 2D NMR analysis, and computational studies (see **Figure S6**) which predict the *endo* transition state as the lowest energy pathway, we

propose the relative and absolute configurations of bicyclic γ-lactones **3a** and **3a'** as shown in **Table 1a**.

Catalyst screening studies for the enantioselective DAL process (Table S1): Into a dried, 2-mL clear-glass vial (12 × 32 mm) equipped with a magnetic stir bar was added silyloxydiene alcohol **2a** (28 mg, 0.10 mmol, 1.0 equiv.), *catalyst* (0.020 mmol, 20 mol%), 2,6-lutidine (35 mL, 0.30 mmol, 3.0 equiv.) and anhydrous CH_2Cl_2 (1.0 mL, to make final concentration of silyloxydiene alcohol 0.1 M) at ambient temperature (23 ºC). With vigorous stirring, ethyl fumaroyl chloride **1a** (16 mL, 0.12 mmol, 1.2 equiv.) was added dropwise. After stirring for 18 h at ambient temperature (23 ºC), the reaction mixture was concentrated by rotary evaporation and purified by an automated flash chromatography (5 → 20% EtOAc/hexanes) to afford an inseparable 1.5:1 mixture of endo/exo diastereomers (as judged by ^{1}H NMR) of bicyclic γ-lactones **3a** and **3a'** as a clear colorless oil: TLC (EtOAc:hexanes, 1:9 *v/v*): R_f = 0.47. (HPLC data is provided for the 1.5:1 mixture of endo/exo diastereomers) Enantiomeric excess was determined by chiral HPLC analysis in comparison with authentic racemic material using a Chiralcel OD-H column: hexanes:^{i}PrOH = 95:05, flow rate 0.5 mL/min, λ = 210 nm: t_{major} = 10.3 min, t_{minor} = 10.9 min; t_{minor} = 12.7 min, t_{major} = 19.4 min. Absolute stereochemistry was assigned by analogy to bicyclic γ-lactone (+)-**3c'**. (NMR data is provided for the 1.5:1 mixture of *endo/exo* diastereomers) ^{1}H NMR (500 MHz; CDCl$_3$): δ 4.78 (s, 1.0H), 4.67 (dd, *J* = 3.3, 2.3 Hz, 1.5H), 4.22-4.06 (m, 5.1H), 3.45 (dd, J = 7.6, 2.3 Hz, 1.5H), 3.25-3.22 (m, 2.4H), 2.96-2.93 (m, 1.6H), 2.90-2.85 (m, 0.9H), 2.43 (d, *J* = 16.8 Hz, 1.5H), 2.34 (ddt, *J* = 17.4, 6.5, 2.5 Hz, 1.5H), 2.17-2.08 (m, 2.9H), 1.43 (s, 3.1H), 1.42 (s, 3.3H), 1.32 (s, 4.6H), 1.29 (s, 4.4H), 1.24-1.19 (m, 7.4H), 1.13-1.07 (m, 7.7H), 1.03-1.00 (m, 45.3H). ^{13}C NMR (125 MHz; CDCl$_3$): δ 176.4, 174.2, 172.9, 172.1, 152.8, 150.9, 101.2, 99.3, 86.2, 84.7, 61.17, 61.16, 46.9, 42.7, 41.5, 40.3, 38.3, 30.5, 30.1, 28.0, 27.6, 27.5, 24.3, 21.0, 17.9 (12), 14.16, 14.08, 12.57 (3), 12.48 (3); IR (thin film): 2945, 2868, 1778, 1769, 1739, 1732, 1666, 1645 cm^{-1}; HRMS (ESI+) *m/z* calcd for $C_{22}H_{39}O_5Si$ [M+H]$^+$: 411.2567, found: 411.2576.

Table S1. Catalyst screening studies for the enantioselective DAL process.
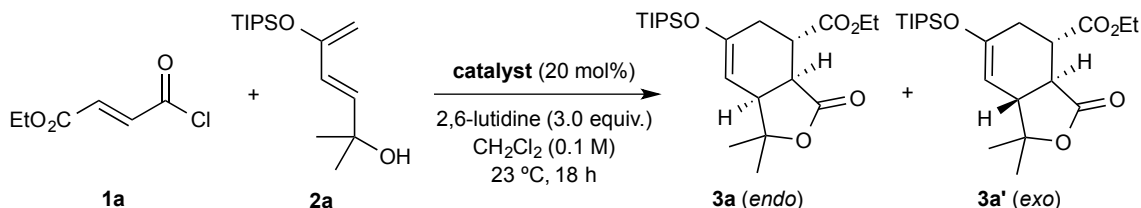
entry	catalyst (20 mol%)	temperature (°C)	dr (endo/exo)[¶]	% ee (endo)[§,‡]	yield (%)[Ø]
1	–	23	1.2 : 1	0	21
2	A	23	1.5 : 1	2	40
3	B	23	1.5 : 1	4	31
4	C	23	1.5 : 1	7	34
5	D	23	1.5 : 1	10	52
6	E	23	1.5 : 1	11	35
7	F	23	1.5 : 1	82	56
8	G	23	1.5 : 1	90	64
9[†]	G	23	1.5 : 1	95	60
10	H	23	1.5 : 1	92	63
11[†]	H	23	1.5 : 1	99	58
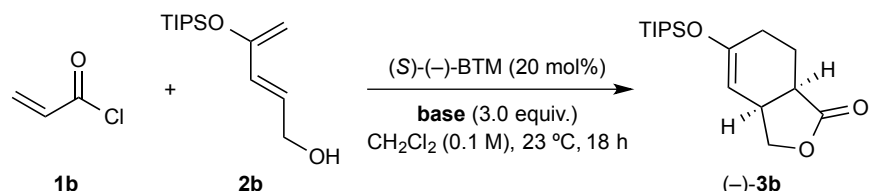
[¶] Determined by ^{1}H NMR analysis of the crude reaction mixture. [§] Determined by chiral HPLC analysis. [‡] Enantiomeric excess of the major **3a** (endo) diastereomer. [Ø] Isolated yield of the 1.5:1 diastereomeric mixture. [†] Ethyl fumaroyl chloride **1a** in CH$_2$Cl$_2$ (0.3 mL) was added over a period of 5 h by syringe pump addition.
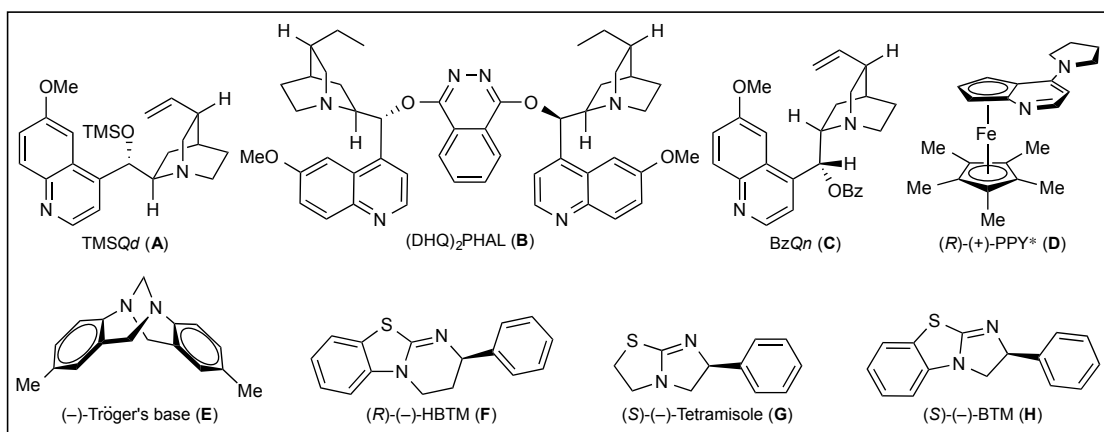
Base screening studies for the enantioselective DAL process (Table S2): Into a dried, 2-mL clear-glass vial (12 × 32 mm) equipped with a magnetic stir bar was added silyloxydiene alcohol **2b** (26 mg, 0.10 mmol, 1.0 equiv.), (S)-(−)-BTM (5.0 mg, 0.020 mmol, 20 mol%), *base* (0.30 mmol, 3.0 equiv.) and anhydrous CH$_2$Cl$_2$ (1.0 mL, to make final concentration of silyloxydiene alcohol 0.1 M) at ambient temperature (23 °C). With vigorous stirring, acryloyl chloride **1b** (10 mL, 0.12 mmol, 1.2 equiv.) was added

dropwise. After stirring for 18 h at ambient temperature (23 ºC), the reaction mixture was filtered through a short pad of celite and the filtrate was concentrated using rotary evaporation. The crude mixture was analyzed by ^{1}H NMR (500 MHz) and purified by an automated flash chromatography (5 → 20% EtOAc/hexanes) to afford bicyclic γ-lactone (–)-**3b**. All spectral data matched that reported henceforth.

Table S2. Base screening studies for the enantioselective DAL process.

entry	base	dr (endo/exo)[¶]	ee (%)[§,‡]	conversion (%)[†,¶]
1	–	n.d.	n.d.	<5
2	K$_2$CO$_3$	n.d.	n.d.	<5
3	Et$_3$N	2.4 : 1	60	>95 (60)
4	EtN(^{i}Pr)$_2$	2.4 : 1	65	>95 (55)
5	DBU	2.1 : 1	11	>95 (30)
6	pyridine	3.2 : 1	85	>95 (46)
7	2,6-lutidine	1 : 1	99	>95 (68)
8	2,6-di-*tert*-butylpyridine	>19 : 1	99	>95 (43)
9	K$_3$PO$_4$/2,6-lutidine (20 mol%)	>19 : 1	99	>95 (64)
10	2-phenylbenzimidazole	1.7 : 1	84	>95
11	2-phenylquinoline	12 : 1	96	>95
12	benzo[*h*]quinoline	2.8 : 1	96	>95
13	acridine	2.8 : 1	99	>95
14	1,10-phenanthroline	4.4 : 1	97	>95
15	8-(tosylamino)quinoline	6.5 : 1	96	>95
16	2,6-diphenylpyridine	n.d.	n.d.	<5

[¶]Determined by ^{1}H NMR analysis of the crude reaction mixture. [§] Determined by chiral HPLC analysis. [‡] Enantiomeric excess of the major (–)-**3b** (*endo*) diastereomer. [†] Yields in parentheses refer to isolated yields. *n.d.* = not determined.

2,6-di-*tert*-butylpyridine   2,6-diphenylpyridine   2-phenylbenzimidazole   2-phenylquinoline

benzo[*h*]quinoline   acridine   1,10-phenanthroline   8-(tosylamino)quinoline
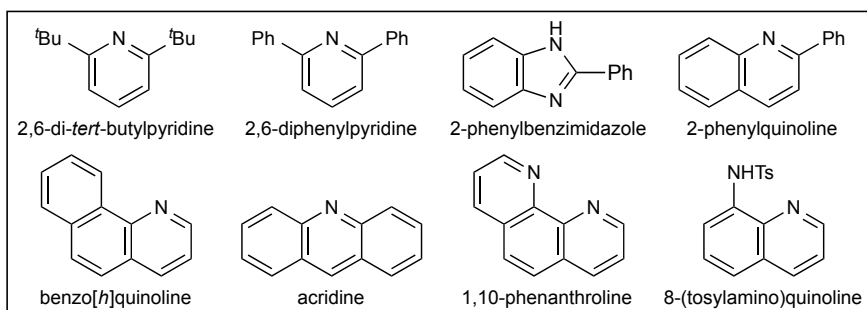
Solvent screening studies for the enantioselective DAL process (Table S3): Into a dried, 2-mL clear-glass vial (12 × 32 mm) equipped with a magnetic stir bar was added silyloxydiene alcohol **2b** (26 mg, 0.10 mmol, 1.0 equiv.), (*S*)-(–)-BTM (5.0 mg, 0.020 mmol, 20 mol%), 2,6-di-*tert*-butylpyridine (0.30 mmol, 3.0 equiv.) and anhydrous *solvent* (1.0 mL, to make final concentration of silyloxydiene alcohol 0.1 M) at ambient temperature (23 ºC). With vigorous stirring, acryloyl chloride **1b** (10 mL, 0.12 mmol, 1.2 equiv.) was added dropwise. After stirring for 18 h at ambient temperature (23 ºC), the reaction mixture was filtered through a short pad of celite and the filtrate was concentrated using rotary evaporation. The crude mixture of bicyclic γ-lactone (–)-**3b** was analyzed by ^{1}H NMR (500 MHz) and chiral HPLC. All spectral data matched that reported henceforth.

Table S3. Solvent screening studies for the enantioselective DAL process.
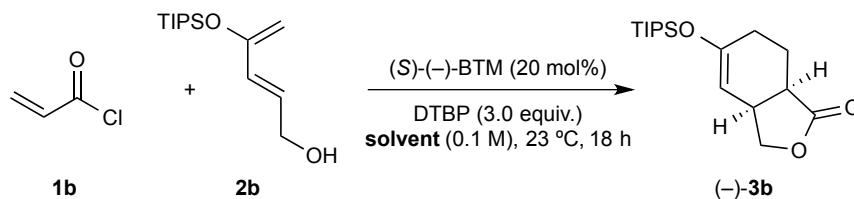
entry	solvent	relative polarity[¶]	*dr* (*endo/exo*)[Ø]	*ee* (%)[‡,§]
1	PhMe[†,€]	0.099	8.3 : 1	92
2	PhH[†,€]	0.111	11.7 : 1	92
3	Et$_2$O[†,€]	0.117	2.8 : 1	48
4	1,4-dioxane[†]	0.164	*n.d.*	*n.d.*
5	THF[†]	0.207	*n.d.*	*n.d.*
6	EtOAc[†]	0.228	*n.d.*	*n.d.*
7	DME[†,€]	0.231	>19 : 1	78
8	CHCl$_3$	0.259	>19 : 1	97
9	CH$_2$Cl$_2$	0.309	>19 : 1	99
10	DCE	0.327	>19 : 1	93
11	acetone[†]	0.355	*n.d.*	*n.d.*
12	DMF	0.386	3.7 : 1	36
13	DMSO[Δ]	0.444	*n.d.*	*n.d.*
14	MeCN	0.460	2.1 : 1	67

[¶] The values for relative polarity are normalized from measurements of solvent shifts of absorption spectra and were extracted from Christian Reichardt, Solvents and Solvent Effects in Organic Chemistry, Wiley-VCH Publishers, 3rd ed., 2003. [Ø] Determined by ^{1}H NMR analysis of the crude reaction mixture. [‡] Determined by chiral HPLC analysis. [§] Enantiomeric excess of the major (–)-**3b** (*endo*) diastereomer. [†] Instantaneous formation of precipirate (insoluble acylammonium salt) upon addition of acid chloride. [€] Reaction mixture became homogeneous over a period of 18 h. [Δ] Instantaneous exothermic reaction upon addition of acid chloride. *n.d.* = not determined.

Representative procedure for the enantioselective DAL process as described for bicyclic γ-lactone (–)-3b:

NOTE: The relative and absolute configuration of *trans*-fused bicyclic γ-lactone (+)-**3c'** was unambiguously assigned by X-ray analysis using anomalous dispersion (see **Figure S3**). Based on this structure, detailed 2D NMR analysis, and computational studies (see **Figure S6**) which predict the *endo* transition state as the lowest energy pathway, we propose the relative and absolute configurations of bicyclic lactones **3b–j** as shown in **Figure 2.1**.
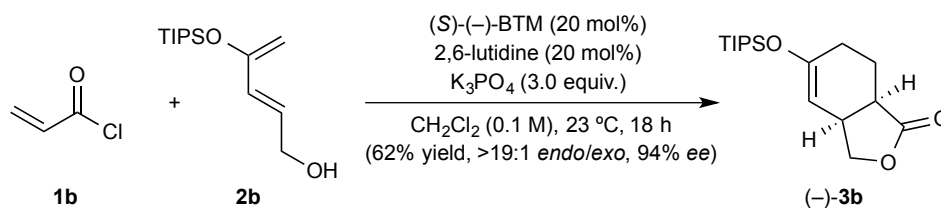
(3a*S*,7a*R*)-5-((triisopropylsilyl)oxy)-3a,6,7,7a-tetrahydroisobenzofuran-1(3*H*)-on ((–)-3b): To an oven-dried, 25-mL round-bottomed flask equipped with a magnetic stir bar was added silyloxydiene alcohol **2b** (144 mg, 0.56 mmol, 1.0 equiv.), (*S*)-(–)-BTM (28 mg, 0.11 mmol, 20 mol%), 2,6-lutidine (13 mL, 0.11 mmol, 20 mol%), K$_3$PO$_4$ (0.36 g, 1.68 mmol, 3.0 equiv.) and anhydrous CH$_2$Cl$_2$ (4.0 mL, to make final concentration of silyloxydiene alcohol 0.1 M) at ambient temperature (23 ºC). With vigorous stirring, acryloyl chloride **1b** (68 mL, 0.84 mmol, 1.5 equiv.) in CH$_2$Cl$_2$ (1.6 mL) was added over a period of 5 h by syringe pump addition. After stirring for an additional 13 h, the reaction mixture was filtered through a pad of celite and concentrated by rotary evaporation. Purification by an automated flash chromatography (5 → 20% EtOAc/hexanes) afforded a single diastereomer (as judged by ^{1}H NMR) of bicyclic γ-lactone (–)-**3b** (107 mg, 62% yield, 94% *ee*) as a clear colorless oil: TLC (EtOAc:hexanes, 1:9 *v/v*): R$_f$ = 0.34; $[\alpha]_D^{17.7}$ = –52.31 (*c* = 1.30, CHCl$_3$). Enantiomeric excess was determined by chiral HPLC analysis in comparison with authentic racemic material using a Chiralcel OD-H column: hexanes:^{i}PrOH = 98:02, flow rate 0.5 mL/min,

λ = 210 nm: t_{major} = 15.9 min, t_{minor} = 17.9 min; 94% *ee*. Absolute stereochemistry was assigned by analogy to bicyclic γ-lactone (+)-**3c'**. ^{1}H NMR (500 MHz; CDCl$_3$): δ 4.77-4.77 (m, 1H), 4.33 (dd, *J* = 8.8, 5.9 Hz, 1H), 3.99 (dd, *J* = 8.8, 2.0 Hz, 1H), 3.17-3.13 (m, 1H), 2.75 (dt, *J* = 7.6, 4.0 Hz, 1H), 2.22-2.14 (m, 2H), 2.03-1.97 (m, 1H), 1.87-1.80 (m, 1H), 1.15-1.11 (m, 3H), 1.06 (dd, *J* = 7.1, 2.9 Hz, 18H); ^{13}C NMR (125 MHz; CDCl$_3$): δ 178.6, 153.8, 102.2, 73.2, 37.7, 35.6, 26.2, 20.7, 18.0 (6), 12.7 (3); IR (thin film): 2944, 2867, 1775, 1665 cm^{-1}; HRMS (ESI+) *m/z* calcd for C$_{17}$H$_{30}$LiO$_3$Si [M+Li]$^+$: 317.2124, found: 317. 2119.
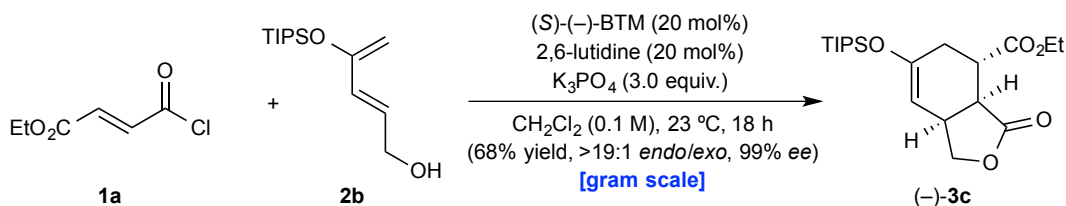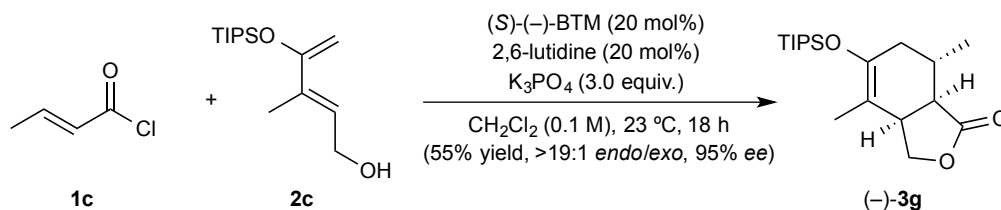

Ethyl (3a*S*,4*S*,7a*S*)-3-oxo-6-((triisopropylsilyl)oxy)-1,3,3a,4,5,7a-hexahydroiso-benzofuran-4-carboxylate ((−)-3c): Prepared according to the representative procedure using silyloxydiene alcohol **2b** (1.44 g, 5.6 mmol, 1.0 equiv.), (*S*)-(−)-BTM (283 mg, 1.1 mmol, 20 mol%), 2,6-lutidine (0.13 mL, 1.1 mmol, 20 mol%), K$_3$PO$_4$ (3.6 g, 16.8 mmol, 3.0 equiv.) in anhydrous CH$_2$Cl$_2$ (40 mL, to make final concentration of silyloxydiene alcohol 0.1 M) and ethyl fumaroyl chloride **1a** (0.97 mL, 7.3 mmol, dissolved in 16 mL CH$_2$Cl$_2$, 1.3 equiv.) at ambient temperature (23 °C). Upon completion (as judged by TLC), the reaction mixture was purified by an automated flash chromatography (5 → 20% EtOAc/hexanes) to afford a single diastereomer (as judged by ^{1}H NMR) of bicyclic γ-lactone (−)-**3c** (1.46 g, 68% yield, 99% *ee*) and ester **S19** (0.41 g, 19% yield) shown below.

(−)-**3c**: clear colorless oil; TLC (EtOAc:hexanes, 1:9 *v/v*): R$_f$ = 0.49; $[\alpha]_D^{22.1}$ = −81.33 (*c* = 3.00, CHCl$_3$). Enantiomeric excess was determined by chiral HPLC analysis in comparison with authentic racemic material using a Chiralcel OD-H column: hexanes:^{i}PrOH = 95:05, flow rate 0.5 mL/min, λ = 210 nm: t_{minor} = 15.4 min, t_{major} =

18.1 min; 99% *ee*. Absolute stereochemistry was assigned by analogy to bicyclic γ-lactone (+)-**3c'**. ^{1}H NMR (500 MHz; CDCl$_3$): δ 4.73 (t, *J* = 2.5 Hz, 1H), 4.37 (dd, *J* = 8.8, 5.6 Hz, 1H), 4.22-4.09 (m, 2H), 4.03 (d, *J* = 8.8 Hz, 1H), 3.30-3.26 (m, 2H), 3.20 (dd, *J* = 7.3, 2.3 Hz, 1H), 2.49 (dd, *J* = 17.7, 1.4 Hz, 1H), 2.39 (ddt, *J* = 17.7, 6.9, 2.4 Hz, 1H), 1.25 (t, *J* = 7.1 Hz, 3H), 1.16-1.09 (m, 3H), 1.04 (d, *J* = 6.4 Hz, 18H); ^{13}C NMR (125 MHz; CDCl$_3$): δ 177.2, 172.9, 151.3, 101.7, 73.3, 61.3, 39.4, 37.8, 34.1, 27.9, 17.9 (6), 14.1, 12.6 (3); IR (thin film): 2945, 2867, 1773, 1732, 1668 cm^{-1}; HRMS (ESI+) *m/z* calcd for C$_{20}$H$_{34}$NaO$_5$Si [M+Na]$^+$: 405.2068, found: 405.2088.
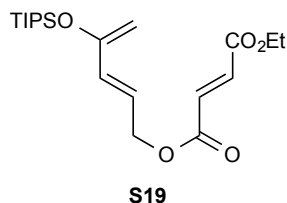
Ethyl ((E)-4-((triisopropylsilyl)oxy)penta-2,4-dien-1-yl) fuma-rate (S19): pale yellow oil; TLC (EtOAc:hexanes, 1:9 v/v): R$_f$ = 0.78. ^{1}H NMR (500 MHz; CDCl$_3$): δ 6.92-6.80 (m, 2H), 6.16-6.08 (m, 2H), 4.77 (d, *J* = 4.8 Hz, 2H), 4.37 (s, 1H), 4.32 (s, 1H), 4.26 (q, *J* = 7.1 Hz, 2H), 1.32 (t, *J* = 7.1 Hz, 3H), 1.27-1.20 (m, 3H), 1.10 (d, *J* = 7.3 Hz, 18H); ^{13}C NMR (125 MHz; CDCl$_3$): δ 165.1, 164.8, 154.3, 134.1, 133.5, 132.3, 123.1, 96.3, 65.1, 61.5, 18.2 (6), 14.3, 12.9 (3); IR (thin film): 2946, 2869, 1727, 1594 cm^{-1}; HRMS (ESI+) *m/z* calcd for C$_{20}$H$_{34}$LiO$_5$Si [M+Li]$^+$: 389.2336, found: 389.2332.

Use of a lower catalyst loading for the DAL (10 mol%) as described for bicyclic g-lactone (–)-3c: This reaction was performed according to the procedure described above for (–)-**3c** with the exception that a lower catalyst loading (10 vs. 20 mol%), a lower "shuttle" base loading (10 vs. 20 mol%) and a longer addition time (10 vs. 5 h) were employed. Silyloxydiene alcohol **2b** (100 mg, 0.39 mmol, 1.0 equiv.), (*S*)-(–)-BTM (10 mg, 0.039 mmol, 10 mol%), 2,6-lutidine (4.5 mL, 0.039 mmol, 10 mol%), K$_3$PO$_4$ (248 mg, 1.2 mmol, 3.0 equiv.) in anhydrous CH$_2$Cl$_2$ (3.0 mL, to make final concentration of silyloxydiene alcohol 0.1 M) and ethyl fumaroyl chloride **1a** (68 mL, 0.51 mmol, dissolved in 0.9 mL CH$_2$Cl$_2$, 1.3 equiv.). The solution of ethyl fumaroyl chloride **1a** was added by syringe pump over 10 h and the reaction was allowed to stir for 8 h at ambient

temperature (23 ℃). Upon completion (as judged by TLC), the reaction mixture was purified by an automated flash chromatography (5 → 20% EtOAc/hexanes) to afford a single diastereomer (as judged by ^{1}H NMR) of bicyclic γ-lactone (–)-**3c** (59 mg, 40% yield, 98% *ee*) and ester **S19** (34 mg, 23% yield). Enantiomeric excess was determined by chiral HPLC analysis in comparison with authentic racemic material using a Chiralcel OD-H column: hexanes:^{i}PrOH = 95:05, flow rate 0.5 mL/min, λ = 210 nm: t_{minor} = 15.3 min, t_{major} = 18.2 min; 98% *ee*. All spectral data matched that reported above.
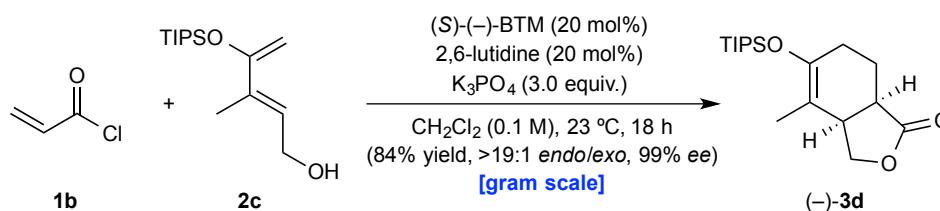
(3a*R*,7a*R*)-4-methyl-5-((triisopropylsilyl)oxy)-3a,6,7,7a-tetrahydroisobenzofuran-1(3*H*)-one ((–)-3d): Prepared according to the representative procedure using silyloxydiene alcohol **2c** (4.0 g, 14.8 mmol, 1.0 equiv.), (*S*)-(–)-BTM (747 mg, 2.9 mmol, 20 mol%), 2,6-lutidine (0.34 mL, 2.9 mmol, 20 mol%), K$_3$PO$_4$ (9.4 g, 44.4 mmol, 3.0 equiv.) in anhydrous CH$_2$Cl$_2$ (130 mL, to make final concentration of silyloxydiene alcohol 0.1 M) and acryloyl chloride **1b** (1.8 mL, 22.2 mmol, dissolved in 18 mL CH$_2$Cl$_2$, 1.5 equiv.) at ambient temperature (23 ℃). Upon completion (as judged by TLC), the reaction mixture was purified by an automated flash chromatography (5 → 20% EtOAc/hexanes) to afford a single diastereomer (as judged by ^{1}H NMR) of bicyclic γ-lactone (–)-**3d** (4.03 g, 84% yield, 99% *ee*) as a clear colorless oil: TLC (EtOAc:hexanes, 1:9 *v/v*): R$_f$ = 0.37; $[\alpha]_D^{20.3}$ = –87.50 (*c* = 1.60, CHCl$_3$). Enantiomeric excess was determined by chiral HPLC analysis in comparison with authentic racemic material using a Chiralcel AS-H column: hexanes:^{i}PrOH = 99:01, flow rate 1.0 mL/min, λ = 210 nm: t_{major} = 10.3 min, t_{minor} = 11.5 min; 99% *ee*. Absolute stereochemistry was assigned by analogy to bicyclic γ-lactone (+)-**3c'**. ^{1}H NMR (500 MHz; CDCl$_3$): δ 4.32 (dd, *J* = 9.0, 6.5 Hz, 1H), 4.14 (dd, *J* = 9.0, 3.1 Hz, 1H), 3.04-3.01 (m, 1H), 2.77 (dt, *J* =

7.7, 5.0 Hz, 1H), 2.24-2.17 (m, 1H), 2.13-2.08 (m, 1H), 2.07-2.01 (m, 1H), 1.86-1.79 (m, 1H), 1.66 (s, 3H), 1.14-1.09 (m, 3H), 1.06 (dd, J = 6.6, 2.1 Hz, 18H); ^{13}C NMR (125 MHz; CDCl$_3$): δ 178.9, 146.8, 107.7, 71.2, 40.6, 38.5, 27.0, 21.2, 18.1 (6), 14.2, 13.3 (3); IR (thin film): 2944, 2867, 1775, 1677 cm^{-1}; HRMS (ESI+) m/z calcd for C$_{18}$H$_{32}$NaO$_3$Si [M+Na]$^+$: 347.2018, found: 347.2024.
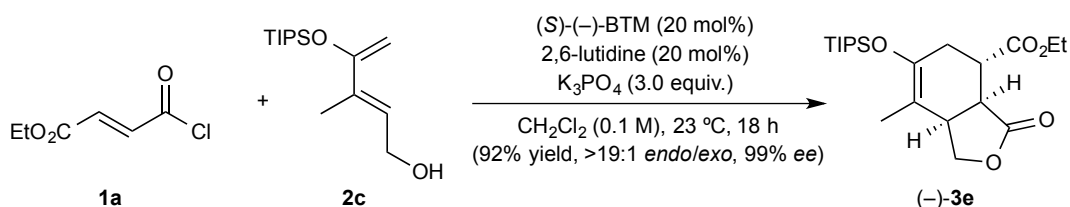
Ethyl (3aS,4S,7aR)-7-methyl-3-oxo-6-((triisopropylsilyl)oxy)-1,3,3a,4,5,7a-hexa-hydroisobenzofuran-4-carboxylate ((–)-3e): Prepared according to the representative procedure using silyloxydiene alcohol **2c** (50 mg, 0.19 mmol, 1.0 equiv.), (S)-(–)-BTM (9.3 mg, 0.037 mmol, 20 mol%), 2,6-lutidine (4.3 mL, 0.037 mmol, 20 mol%), K$_3$PO$_4$ (98 mg, 0.46 mmol, 3.0 equiv.) in anhydrous CH$_2$Cl$_2$ (1.0 mL, to make final concentration of silyloxydiene alcohol 0.1 M) and ethyl fumaroyl chloride **1a** (37 mL, 0.28 mmol, dissolved in 0.9 mL CH$_2$Cl$_2$, 1.5 equiv.) at ambient temperature (23 °C). Upon completion (as judged by TLC), the reaction mixture was purified by an automated flash chromatography (5 → 20% EtOAc/hexanes) to afford a single diastereomer (as judged by ^{1}H NMR) of bicyclic γ-lactone (–)-**3e** (67 mg, 92% yield, 99% *ee*) as a clear colorless oil: TLC (EtOAc:hexanes, 1:4 *v/v*): R$_f$ = 0.62; $[\alpha]_D^{20.2}$ = – 78.86 (*c* = 3.50, CHCl$_3$). Enantiomeric excess was determined by chiral HPLC analysis in comparison with authentic racemic material using a Chiralcel OD-H column: hexanes:^{i}PrOH = 98:02, flow rate 0.4 mL/min, λ = 210 nm: t$_{major}$ = 20.0 min, t$_{minor}$ = 21.3 min; 99% *ee*. Absolute stereochemistry was assigned by analogy to bicyclic γ-lactone (+)-**3c'**. ^{1}H NMR (500 MHz; CDCl$_3$): δ 4.33 (dd, J = 9.1, 6.0 Hz, 1H), 4.23-4.20 (m, 1H), 4.20-4.08 (m, 2H), 3.24 (ddd, J = 7.5, 3.2, 1.2 Hz, 1H), 3.22-3.20 (m, 1H), 3.19-3.16 (m, 1H), 2.51 (ddq, J = 17.1, 2.4, 1.2 Hz, 1H), 2.43 (ddquint, J = 17.1, 6.5, 2.3

Hz, 1H), 1.63 (t, J = 0.9 Hz, 3H), 1.25 (t, J = 7.1 Hz, 3H), 1.16-1.10 (m, 3H), 1.05 (dd, J = 6.9, 3.3 Hz, 18H); ^{13}C NMR (125 MHz; CDCl$_3$): δ 177.5, 172.8, 144.2, 107.4, 71.0, 61.3, 40.0, 39.2, 38.0, 28.5, 18.0 (6), 14.1, 13.9, 13.2 (3); IR (thin film): 2945, 2868, 1777, 1732, 1679 cm^{-1}; HRMS (ESI+) m/z calcd for C$_{21}$H$_{37}$O$_5$Si [M+H]$^+$: 397.2410, found: 397.2432.
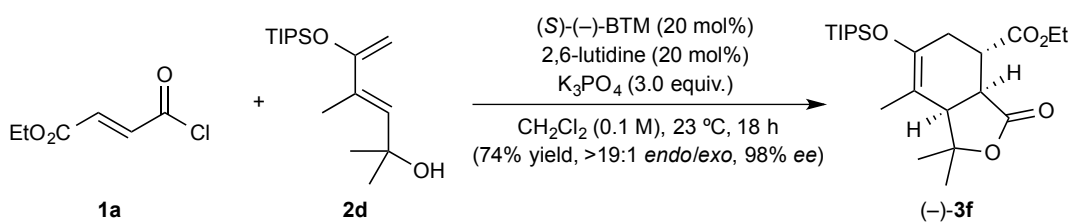
Ethyl (3aS,4S,7aR)-1,1,7-trimethyl-3-oxo-6-((triisopropylsilyl)oxy)-1,3,3a,4,5,7a-hexahydroisobenzofuran-4-carboxylate ((–)-3f): Prepared according to the representative procedure using silyloxydiene alcohol **2d** (30 mg, 0.10 mmol, 1.0 equiv.), (S)-(–)-BTM (5.0 mg, 0.020 mmol, 20 mol%), 2,6-lutidine (2.3 mL, 0.020 mmol, 20 mol%), K$_3$PO$_4$ (64 mg, 0.30 mmol, 3.0 equiv.) in anhydrous CH$_2$Cl$_2$ (0.7 mL, to make final concentration of silyloxydiene alcohol 0.1 M) and ethyl fumaroyl chloride **1a** (20 mL, 0.15 mmol, dissolved in 0.3 mL CH$_2$Cl$_2$, 1.5 equiv.) at ambient temperature (23 ºC). Upon completion (as judged by TLC), the reaction mixture was purified by an automated flash chromatography (5 → 20% EtOAc/hexanes) to afford a single diastereomer (as judged by ^{1}H NMR) of bicyclic γ-lactone (–)-**3f** (25 mg, 74% yield, 98% *ee*) as a clear colorless oil: TLC (EtOAc:hexanes, 1:9 *v/v*): R$_f$ = 0.35; $[\alpha]_D^{18.4}$ = – 25.60 (c = 2.50, CHCl$_3$). Enantiomeric excess was determined by chiral HPLC analysis in comparison with authentic racemic material using a Chiralcel OD-H column: hexanes:^{i}PrOH = 95:05, flow rate 0.5 mL/min, λ = 210 nm: t$_{major}$ = 11.6 min, t$_{minor}$ = 13.6 min; 98% *ee*. Absolute stereochemistry was assigned by analogy to bicyclic γ-lactone (+)-**3c'**. ^{1}H NMR (500 MHz; CDCl$_3$): δ 4.17 (q, J = 7.1 Hz, 2H), 3.37 (ddd, J = 9.1, 6.3, 0.9 Hz, 1H), 3.10 (q, J = 5.9 Hz, 1H), 2.92 (d, J = 9.5 Hz, 1H), 2.50 (ddd, J = 16.4, 5.6, 1.2 Hz, 1H), 2.30 (ddt, J = 16.4, 5.4, 1.8 Hz, 1H), 1.65 (s, 3H), 1.52 (s, 3H),

1.34 (s, 3H), 1.25 (t, J = 7.1 Hz, 3H), 1.15-1.10 (m, 3H), 1.08 (d, J = 6.8 Hz, 18H); ^{13}C NMR (125 MHz; CDCl$_3$): δ 176.5, 172.9, 145.5, 107.1, 87.5, 61.3, 49.3, 42.0, 40.5, 30.4, 30.3, 25.3, 18.1 (6), 17.0, 14.3, 13.3 (3); IR (thin film): 2945, 2868, 1768, 1735, 1671 cm^{-1}; HRMS (ESI+) m/z calcd for C$_{23}$H$_{41}$O$_5$Si [M+H]$^+$: 425.2723, found: 425.2705.
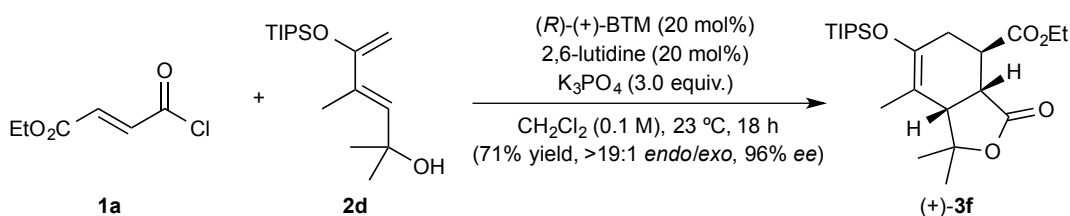
Ethyl (3aR,4R,7aS)-1,1,7-trimethyl-3-oxo-6-((triisopropylsilyl)oxy)-1,3,3a,4,5,7a-hexahydroisobenzofuran-4-carboxylate ((+)-3f): Prepared according to the representative procedure using siloxydiene alcohol **2d** (554 mg, 1.86 mmol, 1.0 equiv.), (R)-(+)-BTM (94 mg, 0.37 mmol, 20 mol%), 2,6-lutidine (43 mL, 0.37 mmol, 20 mol%), K$_3$PO$_4$ (1.20 g, 5.57 mmol, 3.0 equiv.) in anhydrous CH$_2$Cl$_2$ (13 mL, to make final concentration of siloxydiene alcohol 0.1 M) and ethyl fumaroyl chloride **1a** (0.37 mL, 2.78 mmol, dissolved in 5.5 mL CH$_2$Cl$_2$, 1.5 equiv.) at ambient temperature (23 °C). Upon completion (as judged by TLC), the reaction mixture was purified by an automated flash chromatography (5 → 20% EtOAc/hexanes) to afford a single diastereomer (as judged by ^{1}H NMR) of bicyclic γ-lactone (+)-**3f** (558 mg, 71% yield, 96% ee) as a clear colorless oil: $[\alpha]_D^{19.0}$ = +27.83 (c = 2.30, CHCl$_3$). Enantiomeric excess was determined by chiral HPLC analysis in comparison with authentic racemic material using a Chiralcel OD-H column: hexanes:^{i}PrOH = 95:05, flow rate 0.5 mL/min, λ = 210 nm: t_{minor} = 11.4 min, t_{major} = 13.5 min; 96% ee. Absolute stereochemistry was assigned by analogy to bicyclic γ-lactone (+)-**3c'**. All spectral data matched that reported above.

(3a*R*,7*S*,7a*R*)-4,7-dimethyl-5-((triisopropylsilyl)oxy)-3a,6,7,7a-tetrahydroisobenzo-furan-1(3*H*)-one ((–)-3g): Prepared according to the representative procedure using siloxydiene alcohol **2c** (287 mg, 1.06 mmol, 1.0 equiv.), (*S*)-(–)-BTM (53 mg, 0.21 mmol, 20 mol%), 2,6-lutidine (25 mL, 0.21 mmol, 20 mol%), K$_3$PO$_4$ (675 mg, 3.18 mmol, 3.0 equiv.) in anhydrous CH$_2$Cl$_2$ (7.5 mL, to make final concentration of siloxydiene alcohol 0.1 M) and crotonoyl chloride **1c** (0.15 mL, 1.6 mmol, dissolved in 2.5 mL CH$_2$Cl$_2$, 1.5 equiv.) at ambient temperature (23 ºC). Upon completion (as judged by TLC), the reaction mixture was purified by an automated flash chromatography (5 → 20% EtOAc/hexanes) to afford a single diastereomer (as judged by ^{1}H NMR) of bicyclic γ-lactone (–)-**3g** (197 mg, 55% yield, 95% *ee*) as a clear colorless oil: TLC (EtOAc:hexanes, 1:9 *v/v*): R$_f$ = 0.43; $[\alpha]_D^{20.5}$ = –64.57 (*c* = 7.00, CHCl$_3$). Enantiomeric excess was determined by chiral HPLC analysis in comparison with authentic racemic material using a Chiralcel OD-H column: hexanes:^{i}PrOH = 98:02, flow rate 0.5 mL/min, λ = 210 nm: t$_{minor}$ = 16.0 min, t$_{major}$ = 17.0 min; 95% *ee*. Absolute stereochemistry was assigned by analogy to bicyclic γ-lactone (+)-**3c'**. ^{1}H NMR (500 MHz; CDCl$_3$): δ 4.33 (dd, *J* = 8.8, 6.7 Hz, 1H), 4.09 (dd, *J* = 8.8, 4.7 Hz, 1H), 2.99 (q, *J* = 5.8 Hz, 1H), 2.39 (t, *J* = 6.8 Hz, 1H), 2.33-2.30 (m, 1H), 2.29-2.27 (m, 1H), 1.85-1.80 (m, 1H), 1.63 (s, 3H), 1.13-1.09 (m, 6H), 1.05 (dd, *J* = 6.7, 2.3 Hz, 18H); ^{13}C NMR (125 MHz; CDCl$_3$): δ 178.3, 144.9, 106.4, 71.5, 44.6, 39.8, 35.2, 26.9, 19.2, 18.1 (6), 13.9, 13.2 (3); IR (thin film): 2945, 2868, 1772, 1678 cm^{-1}; HRMS (ESI+) *m/z* calcd for C$_{19}$H$_{35}$O$_3$Si [M+H]$^+$: 339.2355, found: 339.2382.
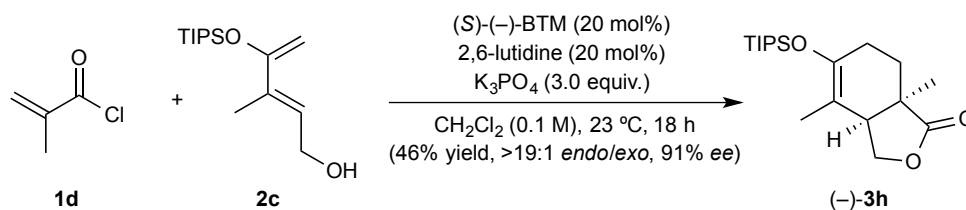
(3a*S*,7a*R*)-4,7a-dimethyl-5-((triisopropylsilyl)oxy)-3a,6,7,7a-tetrahydroisobenzo-furan-1(3*H*)-one ((–)-3h): Prepared by a modified representative procedure. To an oven-dried, 50-mL round-bottomed flask equipped with a magnetic stir bar was added (*S*)-(–)-BTM (87 mg, 0.34 mmol, 20 mol%), 2,6-lutidine (40 mL, 0.34 mmol, 20 mol%), K_3PO_4 (1.10 g, 5.16 mmol, 3.0 equiv.) and anhydrous CH_2Cl_2 (10 mL, to make final concentration of silyloxydiene alcohol 0.07 M) at ambient temperature (23 °C). With vigorous stirring, silyloxydiene alcohol **2c** (464 mg, 1.72 mmol, 1.0 equiv.) in CH_2Cl_2 (3.5 mL) and methacryloyl chloride **1d** (0.25 mL, 2.58 mmol, 1.5 equiv.) in CH_2Cl_2 (3.5 mL) were simultaneously added over a period of 8 h using two separate syringe pumps. After stirring for an additional 10 h, the reaction mixture was filtered through a pad of celite and concentrated by rotary evaporation. Purification by an automated flash chromatography (5 → 20% EtOAc/hexanes) afforded a single diastereomer (as judged by ¹H NMR) of bicyclic γ-lactone (–)-**3h** (266 mg, 46% yield, 91% *ee*) as a clear colorless oil: TLC (EtOAc:hexanes, 1:9 *v/v*): R_f = 0.45; $[\alpha]_D^{20.4}$ = –60.00 (*c* = 0.40, CHCl₃). Enantiomeric excess was determined by chiral HPLC analysis in comparison with authentic racemic material using a Chiralcel AS-H column: hexanes:*i*PrOH = 98:02, flow rate 0.5 mL/min, λ = 210 nm: t_{major} = 11.8 min, t_{minor} = 14.0 min; 91% *ee*. Absolute stereochemistry was assigned by analogy to bicyclic γ-lactone (+)-**3c'**. ¹H NMR (500 MHz; CDCl₃): δ 4.45 (dd, *J* = 8.9, 7.3 Hz, 1H), 3.97 (dd, *J* = 8.9, 6.2 Hz, 1H), 2.63 (t, *J* = 6.7 Hz, 1H), 2.17-2.13 (m, 2H), 1.94 (ddd, *J* = 13.2, 7.3, 5.9 Hz, 1H), 1.64 (s, 3H), 1.63-1.59 (m, 1H), 1.25 (s, 3H), 1.15-1.11 (m, 3H), 1.08 (d, *J* = 6.3 Hz, 18H); ¹³C NMR (125 MHz; CDCl₃): δ 181.7, 145.6, 107.7, 70.6, 47.8, 41.1, 28.6, 26.7, 21.5, 18.1 (6), 17.8, 13.3 (3); IR (thin film): 2944, 2867, 1776, 1680 cm⁻¹; HRMS (ESI+) *m/z* calcd for $C_{19}H_{34}NaO_3Si$ [M+Na]⁺: 361.2175, found: 361.2181.
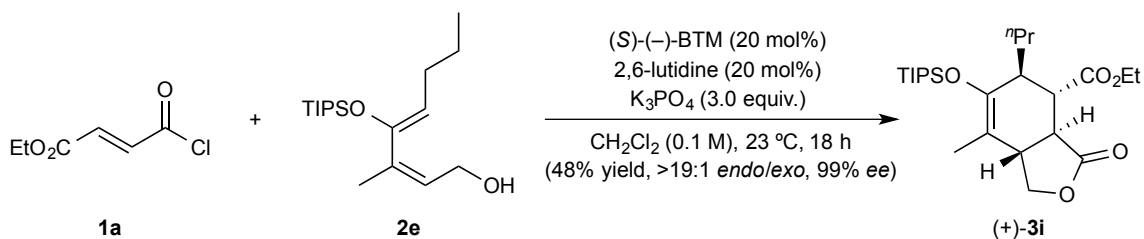
Ethyl (3aS,4S,5S,7aS)-7-methyl-3-oxo-5-propyl-6-((triisopropylsilyl)oxy)-1,3,3a,4,5,7a-hexahydroisobenzofuran-4-carboxylate ((+)-3i): Prepared according to the representative procedure using siloxydiene alcohol **2e** (740 mg, 2.37 mmol, 1.0 equiv.), (S)-(−)-BTM (120 mg, 0.47 mmol, 20 mol%), 2,6-lutidine (55 mL, 0.47 mmol, 20 mol%), K$_3$PO$_4$ (1.50 g, 7.11 mmol, 3.0 equiv.) in anhydrous CH$_2$Cl$_2$ (17 mL, to make final concentration of siloxydiene alcohol 0.1 M) and ethyl fumaroyl chloride **1a** (0.47 mL, 3.56 mmol, dissolved in 6.0 mL CH$_2$Cl$_2$, 1.5 equiv.) at ambient temperature (23 °C). Upon completion (as judged by TLC), the reaction mixture was purified by an automated flash chromatography (5 → 20% EtOAc/hexanes) to afford a single diastereomer (as judged by ^{1}H NMR) of bicyclic γ-lactone (+)-**3i** (496 mg, 48% yield, 99% *ee*) as a clear colorless oil: TLC (EtOAc:hexanes, 1:9 *v/v*): R$_f$ = 0.44; $[\alpha]_D^{19.0}$ = +61.33 (*c* = 1.50, CHCl$_3$). Enantiomeric excess was determined by chiral HPLC analysis in comparison with authentic racemic material using a Chiralcel AD-H column: hexanes:^{i}PrOH = 95:05, flow rate 0.5 mL/min, λ = 210 nm: t$_{major}$ = 11.4 min, t$_{minor}$ = 12.7 min; 99% *ee*. The relative stereochemistry of bicyclic γ-lactone (+)-**3i** was assigned based on detailed 2D NMR analysis following g-lactone ring opening with 4-bromobenzylamine as described for amide (−)-**S20** (page S29). Absolute stereochemistry was assigned by analogy to bicyclic g-lactone (+)-**3c'**. ^{1}H NMR (500 MHz; CDCl$_3$): δ 4.39 (dd, *J* = 7.9, 6.1 Hz, 1H), 4.29-4.17 (m, 2H), 3.90 (dd, *J* = 10.9, 8.0 Hz, 1H), 2.85 (dd, *J* = 11.5, 6.3 Hz, 1H), 2.80-2.74 (m, 1H), 2.69 (dd, *J* = 13.6, 11.5 Hz, 1H), 2.53 (t, *J* = 6.2 Hz, 1H), 1.65-1.57 (m, 5H), 1.31 (t, *J* = 7.2 Hz, 3H), 1.28-1.25 (m, 1H), 1.19-1.13 (m, 4H), 1.10 (d, *J* = 5.7 Hz, 18H), 0.84 (t, *J* = 7.2 Hz, 3H); ^{13}C NMR (125 MHz; CDCl$_3$): δ 174.6, 170.9, 148.2, 109.0, 70.6, 61.1, 44.0, 43.9, 43.6, 41.2, 32.9, 22.0, 18.2

(6), 14.8, 14.2, 13.8, 13.1 (3); IR (thin film): 2946, 2869, 1794, 1736, 1658 cm^{-1}; HRMS (ESI+) *m/z* calcd for C$_{24}$H$_{43}$O$_5$Si [M+H]$^+$: 439.2880, found: 439.2882.

Use of a lower catalyst loading for the DAL (5 mol%) as described for bicyclic g-lactone (+)-3i: This reaction was performed according to the procedure described above for (+)-**3i** with the exception that a lower catalyst loading (5 vs. 20 mol%), a lower "shuttle" base loading (5 vs. 20 mol%) and a longer addition time (15 vs. 5 h) were employed. Silyloxydiene alcohol **2e** (31 mg, 0.10 mmol, 1.0 equiv.), (*S*)-(–)-BTM (1.3 mg, 0.0050 mmol, 5 mol%), 2,6-lutidine (0.6 mL, 0.0050 mmol, 5 mol%), K$_3$PO$_4$ (64 mg, 0.30 mmol, 3.0 equiv.) in anhydrous CH$_2$Cl$_2$ (0.7 mL, to make final concentration of silyloxydiene alcohol 0.1 M) and ethyl fumaroyl chloride **1a** (20 mL, 0.15 mmol, dissolved in 0.3 mL CH$_2$Cl$_2$, 1.5 equiv.). The solution of ethyl fumaroyl chloride **1a** was added by syringe pump over 15 h and the reaction was allowed to stir for 3 h at ambient temperature (23 ºC). Upon completion (as judged by TLC), the reaction mixture was purified by an automated flash chromatography (5 → 20% EtOAc/hexanes) to afford a single diastereomer (as judged by ^{1}H NMR) of bicyclic γ-lactone (+)-**3i** (16 mg, 37% yield, 97% *ee*) as a clear colorless oil. Enantiomeric excess was determined by chiral HPLC analysis in comparison with authentic racemic material using a Chiralcel AD-H column: hexanes:^{i}PrOH = 95:05, flow rate 0.5 mL/min, λ = 210 nm: t$_{major}$ = 11.4 min, t$_{minor}$ = 12.8 min; 97% *ee*. All spectral data matched that reported above.
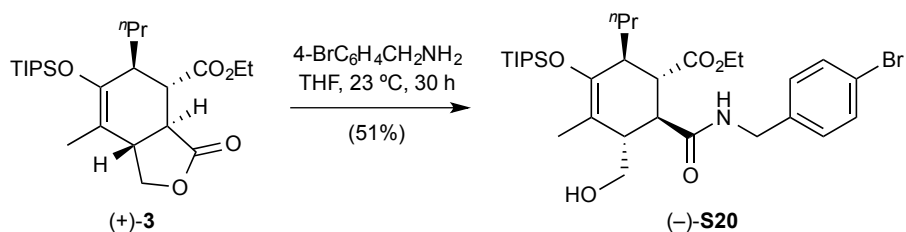
Ethyl (1*S*,2*S*,5*S*,6*S*)-6-((4-bromobenzyl)carbamoyl)-5-(hydroxymethyl)-4-methyl-2-propyl-3-((triisopropylsilyl)oxy)cyclohex-3-ene-1-carboxylate ((–)-S20): Into an oven-dried, 10-mL round-bottomed flask containing a solution of bicyclic γ-lactone (+)-**3i** (120 mg, 0.27 mmol, 1.0 equiv.) in THF (2.7 mL, to make final concentration of

bicyclic g-lactone 0.1 M), was added dropwise 4-bromobenzylamine (0.14 mL, 1.1 mmol, 4.0 equiv.). The reaction was allowed to stir at ambient temperature (23 ºC) for 30 h. Upon completion (as judged by TLC), the reaction was concentrated by rotary evaporation and purified by an automated flash chromatography system (20 → 50% EtOAc/hexanes) to afford amide (–)-**S20** (86 mg, 51% yield) as a pale yellow solid: m.p. 126-130 ºC; TLC (EtOAc:hexanes, 1:2 *v/v*): R_f = 0.55; $[\alpha]_D^{18.1}$ = –14.10 (*c* = 8.60, CHCl$_3$). ^{1}H NMR (500 MHz; CDCl$_3$): δ 7.42 (d, *J* = 8.4 Hz, 2H), 7.18 (d, *J* = 8.2 Hz, 2H), 6.70 (t, *J* = 5.8 Hz, 1H), 4.43 (dd, *J* = 15.0, 6.1 Hz, 1H), 4.31 (dd, *J* = 15.0, 5.6 Hz, 1H), 4.10-4.00 (m, 2H), 3.70 (dd, *J* = 11.1, 4.6 Hz, 1H), 3.63 (dd, *J* = 11.2, 2.5 Hz, 1H), 3.15 (dd, *J* = 12.4, 4.5 Hz, 1H), 2.98 (dd, *J* = 12.3, 8.6 Hz, 1H), 2.49-2.45 (m, 2H), 1.60 (s, 3H), 1.44-1.37 (m, 2H), 1.27-1.13 (m, 8H), 1.11 (t, *J* = 6.3 Hz, 18H), 0.81 (t, *J* = 7.2 Hz, 3H); ^{13}C NMR (125 MHz; CDCl$_3$): δ 175.4, 173.7, 150.8, 137.7, 131.7 (2), 129.6 (2), 121.2, 107.3, 62.6, 60.6, 45.7, 44.9, 43.1, 42.0, 40.9, 34.2, 21.6, 18.2 (6), 14.9, 14.1, 14.0, 13.6 (3); IR (thin film): 3424, 3288, 2945, 2868, 1731, 1676, 1632, 1556 cm^{-1}; HRMS (ESI+) *m/z* calcd for C$_{31}$H$_{51}$BrNO$_5$Si [M+H]$^+$: 624.2720, found: 624.2693.
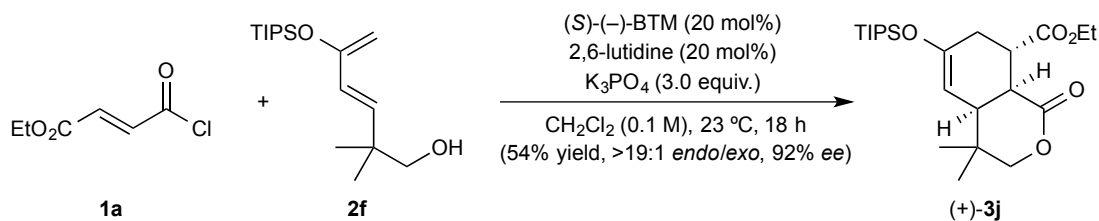
Ethyl (4a*S*,8*S*,8a*S*)-4,4-dimethyl-1-oxo-6-((triisopropylsilyl)oxy)-3,4,4a,7,8,8a-hexahydro-1*H*-isochromene-8-carboxylate ((+)-3j): Prepared according to the representative procedure using silyloxydiene alcohol **2f** (30 mg, 0.10 mmol, 1.0 equiv.), (*S*)-(–)-BTM (5.0 mg, 0.020 mmol, 20 mol%), 2,6-lutidine (2.3 mL, 0.020 mmol, 20 mol%), K$_3$PO$_4$ (64 mg, 0.30 mmol, 3.0 equiv.) in anhydrous CH$_2$Cl$_2$ (0.7 mL, to make final concentration of silyloxydiene alcohol 0.1 M) and ethyl fumaroyl chloride **1a** (20 mL, 0.15 mmol, dissolved in 0.3 mL CH$_2$Cl$_2$, 1.5 equiv.) at ambient temperature (23 ºC). Upon completion (as judged by TLC), the reaction mixture was purified by an

automated flash chromatography (5 → 20% EtOAc/hexanes) to afford a single diastereomer (as judged by ^{1}H NMR) of bicyclic δ-lactone (+)-**3j** (23 mg, 54% yield, 92% *ee*) as a clear colorless oil: TLC (EtOAc:hexanes, 1:9 *v/v*): R_f = 0.35; $[\alpha]_D^{18.6}$ = +21.05 (*c* = 0.57, CHCl$_3$). Enantiomeric excess was determined by chiral HPLC analysis in comparison with authentic racemic material using a Chiralcel OD-H column: hexanes:^{i}PrOH = 95:05, flow rate 0.5 mL/min, λ = 210 nm: t_{minor} = 10.7 min, t_{major} = 12.5 min; 92% *ee*. Absolute stereochemistry was assigned by analogy to bicyclic γ-lactone (+)-**3c'**. ^{1}H NMR (500 MHz; CDCl$_3$): δ 4.79-4.78 (m, 1H), 4.17-4.04 (m, 2H), 3.94 (d, *J* = 10.9 Hz, 1H), 3.80 (dd, *J* = 10.9, 1.5 Hz, 1H), 3.49 (dt, *J* = 4.8, 2.4 Hz, 1H), 3.32 (dd, *J* = 7.1, 3.1 Hz, 1H), 2.49-2.44 (m, 2H), 2.31 (ddt, *J* = 17.5, 6.2, 3.0 Hz, 1H), 1.21 (t, *J* = 7.1 Hz, 3H), 1.14 (s, 3H), 1.12-1.07 (m, 3H), 1.02 (d, *J* = 6.7 Hz, 18H), 0.90 (s, 3H); ^{13}C NMR (125 MHz; CDCl$_3$): δ 172.9, 172.2, 152.2, 100.4, 75.8, 61.0, 40.1, 39.4, 38.4, 33.2, 27.7, 24.3, 22.6, 18.0 (6), 14.2, 12.6 (3); IR (thin film): 2945, 2868, 1730, 1661 cm^{-1}; HRMS (ESI+) *m/z* calcd for C$_{23}$H$_{41}$O$_5$Si [M+H]$^+$: 425.2723, found: 425.2725.

Representative procedure for the stereodivergent DAL process as described for bicyclic γ-lactones (–)-3k and (+)-3k':
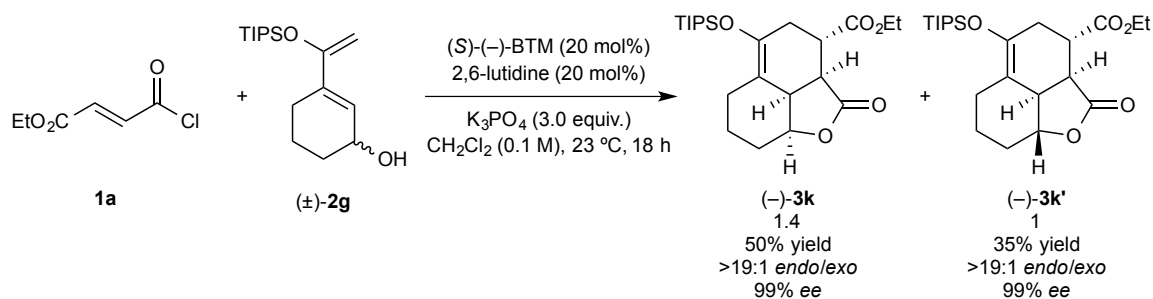
Ethyl (2a*S*,2a^1*R*,3*S*,8a*S*)-2-oxo-5-((triisopropylsilyl)oxy)-2a,2a^1,3,4,6,7,8,8a-octahydro-2*H*-naphtho[1,8-*bc*]furan-3-carboxylate ((–)-3k) and ethyl (2a*S*,2a^1*R*,3*S*, 8a*R*)-2-oxo-5-((triisopropylsilyl)oxy)-2a,2a^1,3,4,6,7,8,8a-octahydro-2*H*-naphtho[1,8 - *bc*]furan-3-carboxylate ((–)-3k'): Prepared according to the representative procedure

using siloxydiene alcohol (±)-**2g** (250 mg, 0.84 mmol, 1.0 equiv.), (*S*)-(−)-BTM (43 mg, 0.17 mmol, 20 mol%), 2,6-lutidine (20 mL, 0.17 mmol, 20 mol%), K_3PO_4 (535 mg, 2.52 mmol, 3.0 equiv.) in anhydrous CH_2Cl_2 (6.5 mL, to make final concentration of siloxydiene alcohol 0.1 M) and ethyl fumaroyl chloride **1a** (0.17 mL, 1.26 mmol, dissolved in 1.9 mL CH_2Cl_2, 1.5 equiv.) at ambient temperature (23 ºC). Upon completion (as judged by TLC), the reaction mixture was purified by an automated flash chromatography (5 → 20% EtOAc/hexanes) to afford a single *endo* diastereomer (as judged by ^{1}H NMR) of bicyclic γ-lactone (−)-**3k** (179 mg, 50% yield, 99% *ee*) and a single *endo* diastereomer (as judged by ^{1}H NMR) of bicyclic γ-lactone (−)-**3k'** (124 mg, 35% yield, 99% *ee*).

(−)-**3k**: colorless solid; m.p. 58-61 ºC (recrystallized from hexanes); TLC (EtOAc:hexanes, 1:9 *v/v*): R_f = 0.30; $[\alpha]_D^{19.2}$ = −31.30 (*c* = 2.30, CHCl₃). Enantiomeric excess was determined by chiral HPLC analysis in comparison with authentic racemic material using a Chiralcel AS-H column: hexanes:[i]PrOH = 97:03, flow rate 0.5 mL/min, λ = 210 nm: t_{major} = 21.1 min, t_{minor} = 28.6 min; 99% *ee*. Absolute stereochemistry was assigned based on X-ray analysis using anomalous dispersion (see **Figure S1**). ^{1}H NMR (500 MHz; CDCl₃): δ 4.56 (q, *J* = 3.3 Hz, 1H), 4.18-4.05 (m, 2H), 3.23-3.19 (m, 2H), 3.03-3.01 (m, 1H), 2.92-2.89 (m, 1H), 2.52-2.50 (m, 2H), 2.15-2.12 (m, 1H), 1.71-1.64 (m, 1H), 1.58-1.54 (m, 1H), 1.48-1.35 (m, 2H), 1.23 (t, *J* = 7.1 Hz, 3H), 1.14-1.08 (m, 3H), 1.03 (d, *J* = 6.6 Hz, 18H); ^{13}C NMR (125 MHz; CDCl₃): δ 177.6, 173.2, 142.9, 109.6, 79.5, 61.3, 43.0, 38.4, 36.6, 27.9, 27.6, 24.4, 20.7, 18.0 (6), 14.2, 13.3 (3); IR (thin film): 2944, 2867, 1778, 1733, 1677 cm^{-1}; HRMS (ESI+) *m/z* calcd for $C_{23}H_{39}O_5Si$ [M+H]⁺: 423.2567, found: 423.2558.

(−)-**3k'**: clear colorless oil; TLC (EtOAc:hexanes, 1:9 *v/v*): R_f = 0.42; $[\alpha]_D^{19.0}$ = −13.33 (*c* = 0.60, CHCl₃). Enantiomeric excess was determined by chiral HPLC analysis in comparison with authentic racemic material using a Chiralcel OD-H column: hexanes:[i]PrOH = 95:05, flow rate 0.5 mL/min, λ = 210 nm: t_{minor} = 17.4 min, t_{major} = 25.7 min; 99% *ee*. Absolute stereochemistry was assigned by derivatization as described

below. ^{1}H NMR (500 MHz; CDCl$_3$): δ 4.27-4.15 (m, 2H), 3.86 (td, J = 11.2, 3.4 Hz, 1H), 2.93-2.86 (m, 2H), 2.75 (ddd, J = 14.0, 5.1, 1.5 Hz, 1H), 2.56-2.50 (m, 1H), 2.47 (dd, J = 11.0, 6.8 Hz, 1H), 2.26 (dq, J = 11.4, 3.5 Hz, 1H), 2.18 (dd, J = 15.6, 3.2 Hz, 1H), 1.98-1.93 (m, 1H), 1.74-1.69 (m, 1H), 1.65 (td, J = 12.0, 4.0 Hz, 1H), 1.49-1.39 (m, 1H), 1.27 (t, J = 7.1 Hz, 3H), 1.12-1.08 (m, 3H), 1.06 (d, J = 4.5 Hz, 18H); ^{13}C NMR (125 MHz; CDCl$_3$): δ 175.7, 172.6, 140.0, 110.9, 83.9, 61.4, 47.7, 40.9, 38.8, 33.2, 30.4, 24.8, 24.5, 18.0 (6), 14.2, 13.1 (3); IR (thin film): 2945, 2868, 1787, 1737, 1697 cm^{-1}; HRMS (ESI+) m/z calcd for C$_{23}$H$_{39}$O$_5$Si [M+H]$^+$: 423.2567, found: 423.2571.
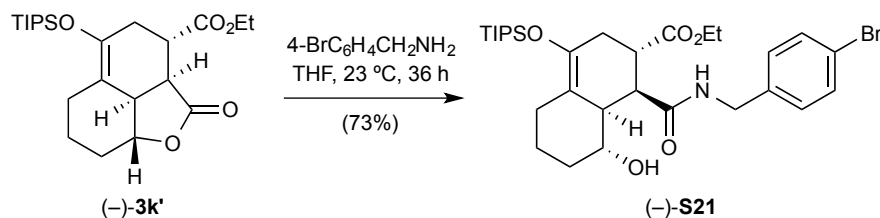
Ethyl (1S,2S,8R,8aR)-1-((4-bromobenzyl)carbamoyl)-8-hydroxy-4-((triisopropyl-silyl)oxy)-1,2,3,5,6,7,8,8a-octahydronaphthalene-2-carboxylate ((–)-S21): Into an oven-dried, 5-mL round-bottomed flask containing a solution of tricyclic γ-lactone (–)-**3k'** (57 mg, 0.14 mmol, 1.0 equiv.) in THF (1.4 mL, to make final concentration of tricyclic g-lactone 0.1 M), was added dropwise 4-bromobenzylamine (68 mL, 0.54 mmol, 4.0 equiv.). The reaction was allowed to stir at ambient temperature (23 ºC) for 36 h. Upon completion (as judged by TLC), the reaction was concentrated by rotary evaporation and purified by an automated flash chromatography system (20 → 50% EtOAc/hexanes) to afford bicyclic amide (–)-**S21** (60.1 mg, 73% yield) as a white solid: m.p. 143-147 ºC (recrystallized from Et$_2$O); TLC (EtOAc:hexanes, 1:2 v/v): R$_f$ = 0.40; $[\alpha]_D^{18.5}$ = –42.00 (c = 6.00, CHCl$_3$). Absolute stereochemistry was assigned based on X-ray analysis using anomalous dispersion (see **Figure S2**). ^{1}H NMR (500 MHz; CDCl$_3$): δ 7.42 (d, J = 8.2 Hz, 2H), 7.18 (d, J = 8.2 Hz, 2H), 6.44 (t, J = 5.7 Hz, 1H), 4.51 (dd, J = 15.0, 6.3 Hz, 1H), 4.23 (dd, J = 15.0, 5.2 Hz, 1H), 4.12 (q, J = 7.1 Hz, 2H), 3.67 (td, J

132

= 9.9, 4.4 Hz, 1H), 3.53 (br s, 1H), 3.13 (td, J = 11.0, 5.7 Hz, 1H), 2.85 (d, J = 12.8 Hz, 1H), 2.71 (dd, J = 11.1, 5.4 Hz, 1H), 2.41 (dd, J = 16.3, 5.7 Hz, 1H), 2.34 (dd, J = 9.6, 5.3 Hz, 1H), 2.26-2.21 (m, 1H), 2.02-1.98 (m, 1H), 1.73-1.69 (m, 1H), 1.42-1.31 (m, 2H), 1.29-1.25 (m, 1H), 1.22 (t, J = 7.1 Hz, 3H), 1.12-1.08 (m, 3H), 1.05 (d, J = 4.3 Hz, 18H); ^{13}C NMR (125 MHz; CDCl$_3$): δ 177.0, 174.9, 140.6, 137.2, 131.7 (2), 129.7 (2), 121.4, 115.3, 71.3, 61.0, 48.5, 45.6, 43.3, 39.4, 35.6, 33.5, 27.2, 24.9, 18.1 (6), 14.2, 13.2 (3); IR (thin film): 3286, 2942, 2867, 1732, 1714, 1680, 1644, 1557 cm^{-1}; HRMS (ESI+) m/z calcd for C$_{30}$H$_{47}$BrNO$_5$Si [M+H]$^{+}$: 608.2407, found: 608.2386.
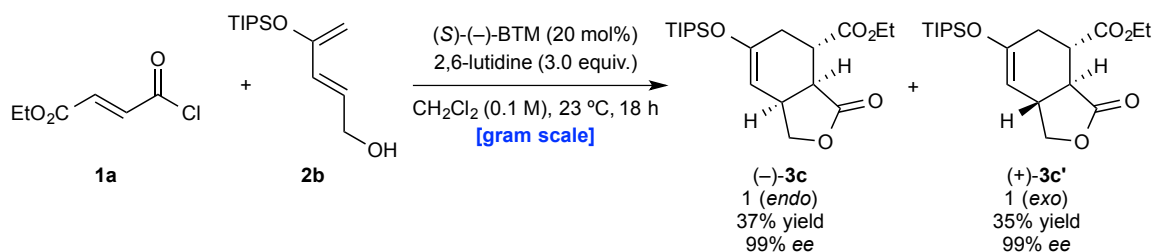
Ethyl (3a*S*,4*S*,7a*S*)-3-oxo-6-((triisopropylsilyl)oxy)-1,3,3a,4,5,7a-hexahydroiso-benzofuran-4-carboxylate ((–)-3c) and ethyl (3a*S*,4*S*,7a*R*)-3-oxo-6-((triisopropyl-silyl)oxy)-1,3,3a,4,5,7a-hexahydroisobenzofuran-4-carboxylate ((+)-3c'): To an oven-dried, 250-mL round-bottomed flask equipped with a magnetic stir bar was added siloxydiene alcohol **2b** (2.12 g, 8.22 mmol, 1.0 equiv.), (*S*)-(–)-BTM (416 mg, 1.64 mmol, 20 mol%), 2,6-lutidine (2.9 mL, 24.6 mmol, 3.0 equiv.) and anhydrous CH$_2$Cl$_2$ (70 mL, to make final concentration of siloxydiene alcohol 0.1 M) at ambient temperature (23 ºC). With vigorous stirring, ethyl fumaroyl chloride **1a** (1.31 mL, 9.86 mmol, 1.5 equiv.) in CH$_2$Cl$_2$ (12 mL) was added over a period of 5 h by syringe pump addition. After stirring for an additional 13 h, the reaction mixture was filtered through a short pad of SiO$_2$ and the filtrate was concentrated by rotary evaporation. Purification by an automated flash chromatography (5 → 20% EtOAc/hexanes) afforded bicyclic γ-lactones (–)-**3c** (1.16 g, 37% yield, 99% *ee*) and (+)-**3c'** (1.10 g, 35% yield, 99% *ee*). (–)-**3c**: All spectral data matched that reported above.

(+)-**3c'**: colorless solid; m.p. 62.1-64.7 °C (recrystallized from CH$_2$Cl$_2$); TLC (EtOAc:hexanes, 1:4 *v/v*): R$_f$ = 0.58; $[\alpha]_D^{21.8}$ = +66.67 (*c* = 3.00, CHCl$_3$). Enantiomeric excess was determined by chiral HPLC analysis in comparison with authentic racemic material using a Chiralcel OD-H column: hexanes:^{i}PrOH = 95:05, flow rate 0.5 mL/min, λ = 210 nm: t$_{minor}$ = 22.1 min, t$_{major}$ = 26.1 min; 99% *ee*. Absolute stereochemistry was assigned based on X-ray analysis using anomalous dispersion (see **Figure S3**). ^{1}H NMR (500 MHz; CDCl$_3$): δ 4.92 (d, *J* = 1.3 Hz, 1H), 4.40 (dd, *J* = 8.0, 6.6 Hz, 1H), 4.28-4.20 (m, 2H), 3.84 (dd, *J* = 11.3, 8.0 Hz, 1H), 2.93 (ddddt, *J* = 13.2, 11.5, 6.6, 3.3, 1.7 Hz, 1H), 2.81 (ddd, *J* = 11.6, 10.6, 7.1 Hz, 1H), 2.58 (dd, *J* = 13.3, 11.7 Hz, 1H), 2.52 (dddd, *J* = 17.6, 7.1, 2.0, 1.2 Hz, 1H), 2.44 (dddd, *J* = 17.7, 10.5, 3.3, 1.9 Hz, 1H), 1.30 (t, *J* = 7.1 Hz, 3H), 1.19-1.12 (m, 3H), 1.06 (d, *J* = 6.9 Hz, 18H); ^{13}C NMR (125 MHz; CDCl$_3$): δ 173.9, 172.9, 152.8, 99.5, 71.5, 61.4, 45.1, 40.1, 39.5, 34.4, 18.0 (6), 14.2, 12.6 (3); IR (thin film): 2945, 2868, 1792, 1737, 1650 cm^{-1}; HRMS (ESI+) *m/z* calcd for C$_{20}$H$_{34}$LiO$_5$Si [M+Li]$^+$: 389.2336, found: 389.2334.

Use of TsCl for *in situ* activation of carboxylic acid (1e) for the stereodivergent DAL process as described for bicyclic γ-lactones (–)-3c and (+)-3c':
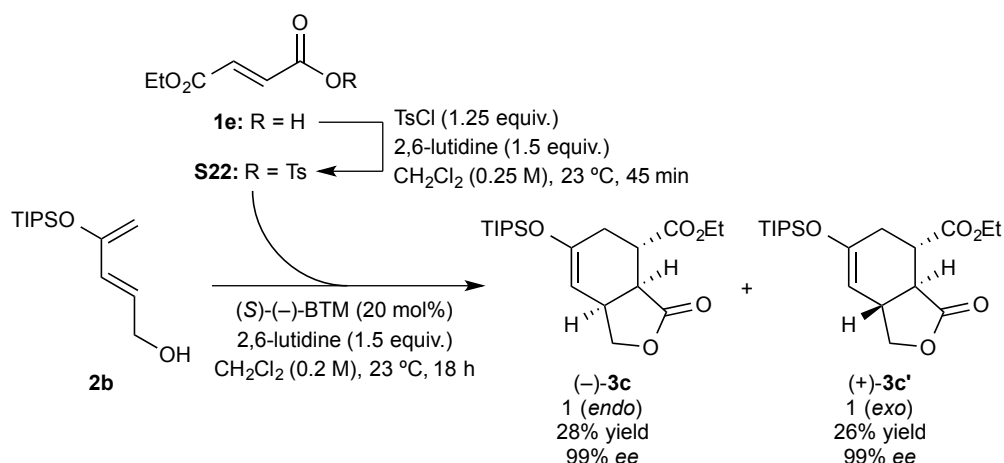
To a solution of *mono*-ethyl fumarate **1e** (18.7 mg, 0.13 mmol, 1.3 equiv.) and TsCl (23.8 mg, 0.125 mmol, 1.25 equiv.) in anhydrous CH$_2$Cl$_2$ (0.5 mL, to make final

concentration of mixed tosyl anhydride **S22** 0.25 M) was added 2,6-lutidine (18 mL, 0.15 mmol, 1.5 equiv.). The mixture was stirred for 45 min at ambient temperature (23 ºC) and then drawn into the syringe. The solution of **S22** was then transferred *via* syringe pump into a second flask containing silyloxydiene alcohol **2b** (25.6 mg, 0.10 mmol, 1.0 equiv.), (*S*)-(–)-BTM (5.0 mg, 0.020 mmol, 20 mol%), 2,6-lutidine (18 mL, 0.15 mmol, 1.5 equiv) and anhydrous CH_2Cl_2 (0.5 mL) over 5 h. The reaction was stirred for an additional 13 h at ambient temperature (23 ºC), concentrated by rotary evaporation, and then directly purified by an automated flash chromatography (5 → 20% EtOAc/hexanes) to afford bicyclic g-lactones (–)-**3c** (10.8 mg, 28% yield, 99% *ee*) and (+)-**3c'** (10.2 mg, 26% yield, 99% *ee*). All spectral data matched that reported above.

Synthetic applications of bicyclic g-lactones (–)-3d and (–)-3h:

(–)-**3d**   (–)-**4**
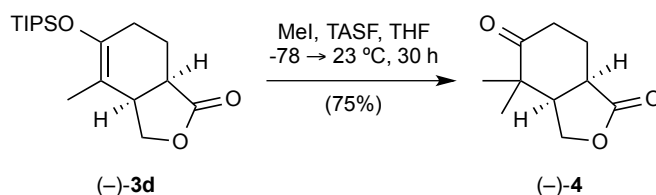
(3a*R*,7a*R*)-4,4-dimethyltetrahydroisobenzofuran-1,5(3*H*,4*H*)-dione ((–)-4): Into an oven-dried, 5-mL round-bottomed flask containing a solution of bicyclic γ-lactone (–)-**3d** (50 mg, 0.17 mmol, 1.0 equiv.) and MeI (0.11 mL, 1.77 mmol, 10.0 equiv.) in THF (0.20 mL, to make final concentration of bicyclic g-lactone 0.9 M), was added TASF (73 mg, 0.26 mmol, 1.5 equiv.) in one portion at -78 ºC. The dry ice/acetone bath was removed and the mixture was allowed to warm up to ambient temperature (23 ºC) on its own accord and the reaction was allowed to stir for 30 h. Upon completion (as judged by TLC), the mixture was filtered through a short pad of celite, concentrated by rotary evaporation and purified by an automated flash chromatography system (20 → 50% EtOAc/hexanes) to afford α,α-dimethyl ketone (–)-**4** (24 mg, 75% yield) as a clear colorless oil: TLC (EtOAc:hexanes, 1:1 *v/v*): R_f = 0.31; $[\alpha]_D^{19.0}$ = –10.67 (*c* = 0.75, $CHCl_3$). ^{1}H NMR (500 MHz; $CDCl_3$): δ 4.37 (dd, *J* = 9.7, 7.7 Hz, 1H), 4.04 (dd, *J* = 9.7,

7.9 Hz, 1H), 2.99 (q, J = 7.9 Hz, 1H), 2.81 (q, J = 7.9 Hz, 1H), 2.61-2.54 (m, 1H), 2.42-2.32 (m, 2H), 2.18-2.10 (m, 1H), 1.24 (s, 3H), 1.05 (s, 3H); ^{13}C NMR (125 MHz; CDCl$_3$): δ 213.1, 178.5, 68.8, 47.2, 44.9, 37.0, 35.8, 26.5, 23.4, 21.2; IR (thin film): 2971, 1771, 1710 cm^{-1}; HRMS (ESI+) m/z calcd for C$_{10}$H$_{15}$O$_3$ [M+H]$^+$: 183.1021, found: 183.1027.
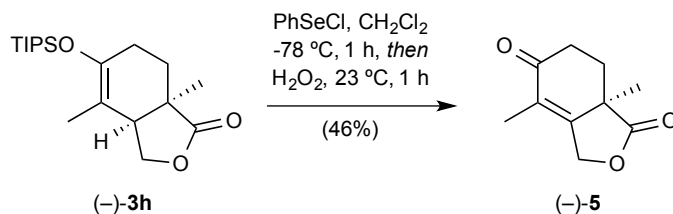
(R)-4,7a-dimethyl-7,7a-dihydroisobenzofuran-1,5(3H,6H)-dione ((–)-5): Into an oven-dried, 25-mL round-bottomed flask containing a solution of bicyclic g-lactone (–)-**3h** (130 mg, 0.38 mmol, 1.0 equiv.) in CH$_2$Cl$_2$ (4.7 mL, to make initial concentration of bicyclic g-lactone 0.08 M), was added PhSeCl (88 mg, 0.46 mmol, 1.2 equiv.) in CH$_2$Cl$_2$ (3.0 mL, to make final concentration of bicyclic g-lactone 0.05 M) dropwise at -78 ℃. After stirring for 15 min, H$_2$O$_2$ (35% wt. % in H$_2$O, 52 mL, 3.8 mmol, 10.0 equiv.) was added dropwise. The dry ice/acetone bath was removed and the mixture was allowed to warm up to ambient temperature (23 ℃) on its own accord over 45 min. Upon completion (as judged by TLC), the mixture was filtered through a short pad of celite, concentrated by rotary evaporation and purified by an automated flash chromatography system (10 → 40% EtOAc/hexanes) to afford enone γ-lactone (–)-**5** (31 mg, 46% yield) as a white crystalline semisolid: TLC (EtOAc:hexanes, 1:2 v/v): R$_f$ = 0.29; $[\alpha]_D^{18.9}$ = – 11.11 (c = 0.36, CHCl$_3$). ^{1}H NMR (500 MHz; CDCl$_3$): δ 4.99 (q, J = 1.1 Hz, 2H), 2.66-2.53 (m, 2H), 2.22 (ddd, J = 13.3, 5.2, 2.2 Hz, 1H), 2.09 (td, J = 13.4, 6.0 Hz, 1H), 1.74 (t, J = 1.1 Hz, 3H), 1.51 (s, 3H); ^{13}C NMR (125 MHz; CDCl$_3$): δ 196.7, 178.4, 154.7, 129.0, 67.4, 41.5, 32.6, 29.7, 21.4, 10.9; IR (thin film): 2924, 1778, 1668 cm^{-1}; HRMS (ESI+) m/z calcd for C$_{10}$H$_{11}$O$_3$ [M–H]$^+$: 179.0708, found: 179.0711.

Single crystal X-ray structures and selected crystallographic data for compounds (–)-3k, (–)-S21 and (+)-3c' (Figures S1-S3):

Figure S1. Single crystal X-ray structure (ORTEP) of tricyclic γ-lactone (–)-3k. The crystals were grown from a concentrated solution of tricyclic γ-lactone (–)-**3k** in hexanes (2.0 mL), using a slow evaporation method (probability ellipsoids are shown at the 50% level). X-ray crystallographic data have been deposited in the Cambridge Crystallographic Data Centre database (http://www.ccdc.cam.ac.uk/) under accession code CCDC 972245.

Alert level B:
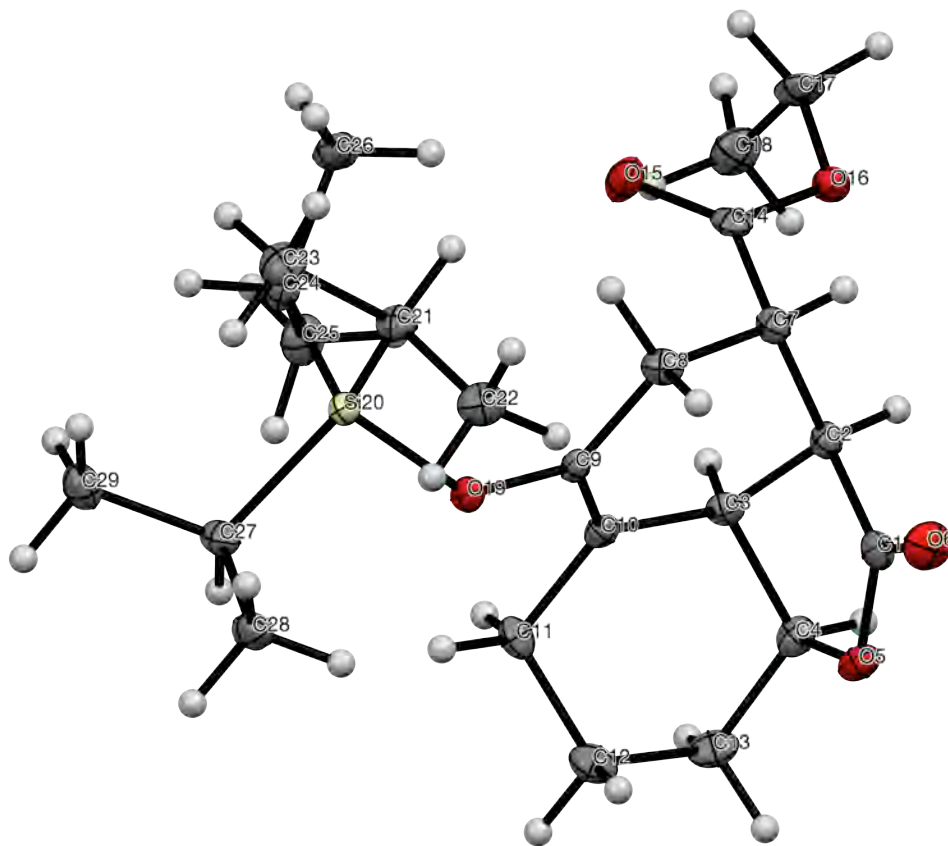
THETM01_ALERT_3_B The value of sine(theta_max)/wavelength is less than 0.575. Calculated sin(theta_max)/wavelength = 0.5614. Author Response: Data was collected on a Bruker GADDS instrument with Cu-source and MWPC (multiwire proportional

137

counter) detector. Under these experimental conditions the maximum angle that can be collected is 120 degrees two-theta.

Table 1. Crystal data and structure refinement for DRB_MA_130730_G_B2.

Crystal Parameters	Crystal Data	
Identification code	b2	
Empirical formula	$C_{23} H_{38} O_5 Si$	
Formula weight	422.62	
Temperature	110(2) K	
Wavelength	1.54178 Å	
Crystal system	Orthorhombic	
Space group	P2(1)2(1)2(1)	
Unit cell dimensions	a = 8.6924(6) Å	a = 90º
	b = 8.9976(6) Å	b = 90º
	c = 29.0972(18) Å	g = 90º
Volume	2275.7(3) Å^3	
Z	4	
Density (calculated)	1.234 Mg/m^3	
Absorption coefficient	1.157 mm^{-1}	
F(000)	920	
Crystal size	0.13 × 0.07 × 0.03 mm^3	
Theta range for data collection	3.04 to 59.95º	
Index ranges	$-9 \le h \le 9, -9 \le k \le 10, -32 \le l \le 31$	
Reflections collected	18633	
Independent reflections	3357 [R(int) = 0.0615]	
Completeness to theta = 59.95º	99.8%	
Absorption correction	Semi-empirical from equivalents	

Max. and min. transmission	0.9661 and 0.8641
Refinement method	Full-matrix least-squares on F^2
Data / restraints / parameters	3357 / 0 / 269
Goodness-of-fit on F^2	1.044
Final R indices [I>2sigma(I)]	$R_1 = 0.0299$, $wR_2 = 0.0708$
R indices (all data)	$R_1 = 0.0322$, $wR_2 = 0.0715$
Absolute structure parameter	0.00(2)
Largest diff. peak and hole	0.167 and -0.240 e.Å^{-3}

Table 2. Atomic coordinates (× 10^4) and equivalent isotropic displacement parameters (Å^2 × 10^3) for DRB_MA_130730_G_B2. U(eq) is defined as one third of the trace of the orthogonalized U^{ij} tensor.

Atom	x	y	z	U(eq)
Si(20)	4673(1)	4355(1)	5769(1)	12(1)
O(16)	9567(2)	-615(2)	6467(1)	17(1)
O(19)	5729(1)	4434(2)	6248(1)	14(1)
O(5)	9365(2)	4100(1)	7441(1)	18(1)
O(15)	7446(2)	105(2)	6084(1)	24(1)
O(6)	10899(2)	4472(2)	6835(1)	25(1)
C(14)	8607(2)	404(2)	6285(1)	15(1)
C(1)	9985(2)	3702(2)	7033(1)	17(1)
C(10)	6605(2)	3117(2)	6893(1)	13(1)
C(7)	9199(2)	1964(2)	6372(1)	14(1)
C(9)	6780(2)	3508(2)	6454(1)	12(1)
C(27)	3109(2)	5732(2)	5901(1)	16(1)
C(2)	9344(2)	2199(2)	6891(1)	14(1)
C(22)	7020(3)	6156(2)	5350(1)	21(1)
C(3)	7806(2)	2194(2)	7141(1)	13(1)

C(4)	8292(2)	2929(2)	7595(1)	17(1)
C(29)	1694(2)	5606(2)	5586(1)	22(1)
C(8)	8143(2)	3128(2)	6158(1)	15(1)
C(11)	5281(2)	3646(2)	7186(1)	17(1)
C(25)	3485(3)	1700(2)	6151(1)	23(1)
C(18)	7855(3)	-2535(2)	6774(1)	27(1)
C(17)	9061(3)	-2154(2)	6424(1)	21(1)
C(21)	5919(2)	4863(2)	5261(1)	16(1)
C(12)	5896(2)	4514(2)	7598(1)	22(1)
C(26)	4707(3)	1402(2)	5368(1)	23(1)
C(24)	3803(2)	2455(2)	5686(1)	18(1)
C(28)	3667(3)	7343(2)	5916(1)	21(1)
C(13)	7021(3)	3593(2)	7878(1)	22(1)
C(23)	4979(3)	5129(3)	4820(1)	24(1)

Figure S2. Single crystal X-ray structure (ORTEP) of bicyclic amide (–)-S21. The crystals were grown from a concentrated solution of bicyclic amide (–)-**S21** in Et$_2$O (2.0 mL), using a slow evaporation method (probability ellipsoids are shown at the 50% level). X-ray crystallographic data have been deposited in the Cambridge Crystallographic Data Centre database (http://www.ccdc.cam.ac.uk/) under accession code CCDC 972248.
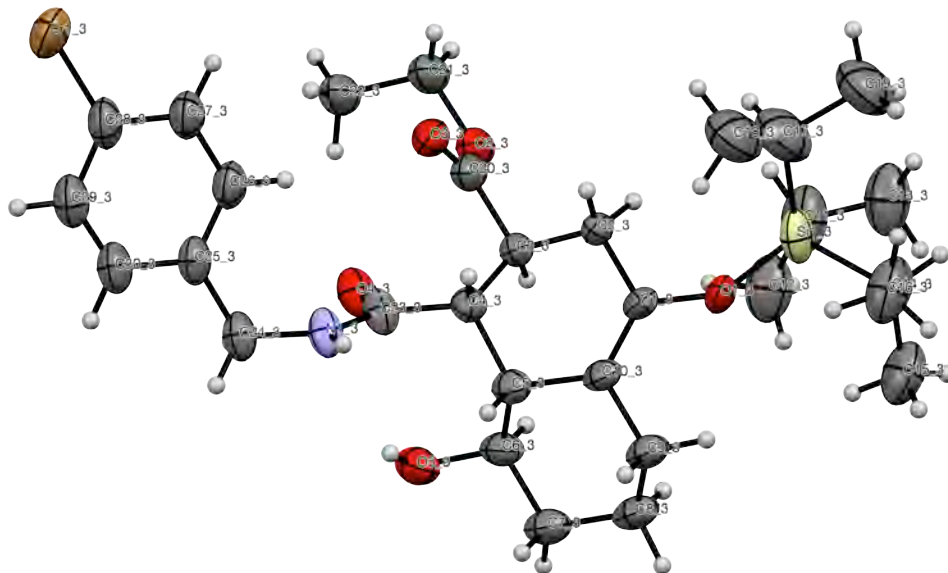
Alert level B:

Crystal system given = triclinic. PLAT019_ALERT_1_B Check _diffrn_measured_ fraction_theta_full/_max = 0.927. Author Response: Physical limitations of the GADDS X-ray diffractometer and triclinic system.

PLAT220_ALERT_2_B Large Non-Solvent C Ueq(max)/Ueq(min) … 4.4 Ratio. Author Response: Possible disorder in the terminal groups. The disorder was not modeled.

PLAT242_ALERT_2_B Low Ueq as Compared to Neighbors for … Si1_4 Check. Author Response: Possible disorder in the Si terminal groups. The disorder was not modeled.

PLAT341_ALERT_3_B Low Bond Precision on C-C Bonds … 0.0194 Ang. <u>Author</u> <u>Response</u>: Diffuse scattering due to disorder lowers the precision of the C-C bond length determination.

Table 1. Crystal data and structure refinement for DR89.

Crystal Parameters	Crystal Data	
Identification code	dr89	
Empirical formula	C_{30} H_{46} Br N O_5 Si	
Formula weight	608.68	
Temperature	110(2) K	
Crystal system	Triclinic	
Space group	P1	
Unit cell dimensions	a = 13.4034(9) Å	a = 89.539(5)°
	b = 13.4037(9) Å	b = 89.620(5)°
	c = 17.8225(13) Å	g = 87.393(5)°
Volume	3198.4(4) Å^3	
Z	4	
Density (calculated)	1.264 Mg/m^3	
Absorption coefficient	2.400 mm^{-1}	
F(000)	1288.0	
Crystal size	0.11 × 0.1 × 0.01 mm^3	
Radiation	CuK a (l = 1.54178)	
Theta range for data collection	4.958 to 128.74°	
Index ranges	−15 ≤ h ≤ 15, −15 ≤ k ≤ 15, −20 ≤ l ≤ 20	
Reflections collected	55755	
Independent reflections	18937 [R(int) = 0.0831]	
Data / restraints / parameters	18937 / 2631 / 1372	

Goodness-of-fit on F^2		1.089		
Final R indices [I>2sigma(I)]		$R_1 = 0.0896$, $wR_2 = 0.2171$		
R indices (all data)		$R_1 = 0.1063$, $wR_2 = 0.2373$		
Largest diff. peak and hole		0.84 and -0.73 e.Å^{-3}		

Table 2. Fractional atomic coordinates ($\times$ 10^4) and equivalent isotropic displacement parameters ($\text{Å}^2 \times 10^3$) for DR89. U(eq) is defined as one third of the trace of the orthogonalized U^{ij} tensor.

Atom	x	y	z	U(eq)
Br1_3	10682(3)	15286(3)	10137.5(16)	81.8(9)
Si1_3	9768(4)	14978(4)	2986(3)	56.5(14)
O1_3	9221(7)	14314(6)	3624(4)	43(2)
O2_3	8532(9)	17264(7)	5792(6)	56(2)
O3_3	9470(9)	16079(9)	6369(7)	56(3)
O4_3	7289(8)	15692(8)	6721(6)	52(3)
O5_3	6011(8)	14206(10)	5963(6)	54(3)
N1_3	7793(10)	14158(8)	7106(5)	47(2)
C1_3	8766(10)	14473(9)	4301(6)	38(2)
C2_3	9095(10)	15341(10)	4752(6)	40(2)
C3_3	8383(9)	15607(8)	5397(6)	40(2)
C4_3	8190(8)	14644(8)	5820(5)	39(2)
C5_3	7630(7)	13926(8)	5334(6)	42(2)
C6_3	6489(7)	14178(10)	5245(7)	49(2)
C7_3	6045(9)	13404(12)	4750(8)	55(3)
C8_3	6539(9)	13318(12)	4003(8)	53(3)
C9_3	7673(9)	13055(10)	4074(7)	48(3)
C10_3	8092(8)	13839(8)	4559(6)	40(2)

143

C11_3	9086(12)	16206(10)	2802(8)	86(5)
C12_3	7970(13)	16218(17)	2957(14)	88(5)
C13_3	9268(18)	16626(16)	2046(11)	90(5)
C14_3	9813(13)	14210(11)	2111(7)	75(4)
C15_3	8822(14)	13897(16)	1847(12)	82(5)
C16_3	10498(16)	13237(14)	2269(11)	76(5)
C17_3	11044(10)	15212(12)	3317(9)	101(5)
C18_3	11520(14)	14410(20)	3861(14)	99(6)
C19_3	11774(13)	15440(20)	2663(13)	106(6)
C20_3	8853(10)	16338(9)	5910(7)	52(2)
C21_3	8929(13)	18013(11)	6287(9)	62(3)
C22_3	8415(16)	17993(17)	7043(9)	66(4)
C23_3	7695(10)	14872(8)	6569(6)	45(2)
C24_3	7414(9)	14304(12)	7852(6)	49(3)
C25_3	8225(10)	14564(13)	8400(6)	51(3)
C26_3	9024(11)	15094(13)	8193(7)	55(3)
C27_3	9749(12)	15362(14)	8706(6)	57(3)
C28_3	9645(11)	15075(15)	9459(7)	60(3)
C29_3	8875(12)	14467(16)	9660(7)	64(3)
C30_3	8190(11)	14213(14)	9146(7)	59(3)

Figure S3. Single crystal X-ray structure (ORTEP) of bicyclic γ-lactone (+)-3c'. The crystals were grown from a concentrated solution of bicyclic γ-lactone (+)-**3c'** in CH$_2$Cl$_2$ (2.0 mL), using a slow evaporation method (probability ellipsoids are shown at the 50% level). X-ray crystallographic data have been deposited in the Cambridge Crystallographic Data Centre database (http://www.ccdc.cam.ac.uk/) under accession code CCDC 972247.

Alert level B:
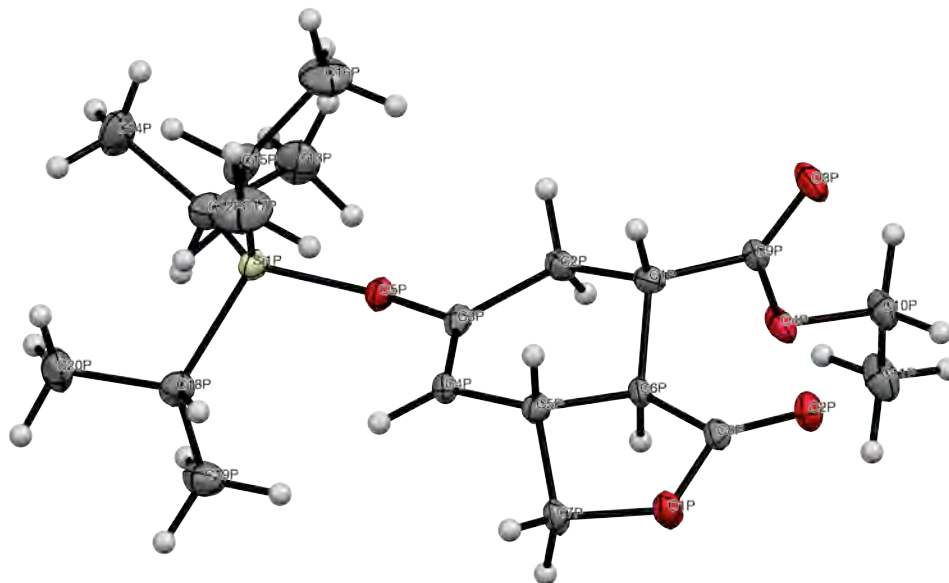
THETM01_ALERT_3_B The value of sine(theta_max)/wavelength is less than 0.575. Calculated sin(theta_max)/wavelength = 0.5617. <u>Author Response</u>: Data was collected on a Bruker GADDS instrument with Cu-source and MWPC (multiwire proportional counter) detector. Under these experimental conditions the maximum angle that can be collected is 120 degrees two-theta.

Table 1. Crystal data and structure refinement for DRB_MA_130306_G_904F2.

Crystal Parameters	Crystal Data	
Identification code	drb	
Empirical formula	$C_{20} H_{34} O_5 Si$	
Formula weight	382.56	
Temperature	110(2) K	
Wavelength	1.54178 Å	
Crystal system	Monoclinic	
Space group	P2(1)	
Unit cell dimensions	a = 16.6474(7) Å	a = 90º
	b = 34.4793(14) Å	b = 95.850(2)º
	c = 19.1312(8) Å	g = 90º
Volume	10923.9(8) Å^3	
Z	20	
Density (calculated)	1.163 Mg/m^3	
Absorption coefficient	1.155 mm^{-1}	
F(000)	4160	
Crystal size	0.28 × 0.06 × 0.05 mm^3	
Theta range for data collection	2.32 to 60.00º	
Index ranges	$-18 \le h \le 18, -37 \le k \le 35, -21 \le l \le 21$	
Reflections collected	225412	
Independent reflections	31523 [R(int) = 0.0593]	
Completeness to theta = 60.00º	99.3%	
Absorption correction	Semi-empirical from equivalents	
Max. and min. transmission	0.9445 and 0.7380	
Refinement method	Full-matrix least-squares on F^2	
Data / restraints / parameters	31523 / 1 / 2412	

Goodness-of-fit on F^2		1.069
Final R indices [I>2sigma(I)]		$R_1 = 0.0551$, $wR_2 = 0.1469$
R indices (all data)		$R_1 = 0.0610$, $wR_2 = 0.1564$
Absolute structure (Hooft / Flack) parameter		-0.006(7) / 0.013(14)
Extinction coefficient		0.00031(2)
Largest diff. peak and hole		0.720 and -0.591 e.Å^{-3}

Table 2. Atomic coordinates ($\times 10^4$) and equivalent isotropic displacement parameters ($\text{Å}^2 \times 10^3$) for DRB_MA_130306_G_904F2. U(eq) is defined as one third of the trace of the orthogonalized U^{ij} tensor.

Atom	x	y	z	U(eq)
Si(1P)	6042(1)	7578(1)	6596(1)	16(1)
O(1P)	7243(1)	7429(1)	10228(1)	22(1)
O(2P)	8590(1)	7377(1)	10271(1)	25(1)
O(3P)	9775(1)	7420(1)	8850(1)	31(1)
O(4P)	9083(1)	6861(1)	8811(1)	23(1)
O(5P)	6727(1)	7326(1)	7110(1)	18(1)
C(1P)	8323(2)	7436(1)	8634(2)	17(1)
C(2P)	7926(2)	7322(1)	7896(2)	19(1)
C(3P)	7020(2)	7388(1)	7795(2)	16(1)
C(4P)	6558(2)	7482(1)	8303(2)	15(1)
C(5P)	6959(2)	7552(1)	9028(2)	16(1)
C(6P)	7734(2)	7319(1)	9152(2)	16(1)
C(7P)	6557(2)	7434(1)	9677(2)	19(1)
C(8P)	7942(2)	7376(1)	9925(2)	17(1)
C(9P)	9146(2)	7246(1)	8778(2)	17(1)

|				
C(10P)	9836(2)	6646(1)	8958(2)	22(1)
C(11P)	9644(2)	6225(1)	8786(2)	29(1)
C(12P)	6146(2)	7366(1)	5698(2)	24(1)
C(13P)	6983(2)	7195(1)	5615(2)	33(1)
C(14P)	5908(2)	7651(1)	5103(2)	33(1)
C(15P)	6291(2)	8109(1)	6643(2)	25(1)
C(16P)	7199(2)	8182(1)	6627(2)	36(1)
C(17P)	5966(2)	8328(1)	7261(2)	43(1)
C(18P)	4999(2)	7481(1)	6854(2)	20(1)
C(19P)	4865(2)	7044(1)	6963(2)	28(1)
C(20P)	4340(2)	7644(1)	6315(2)	30(1)
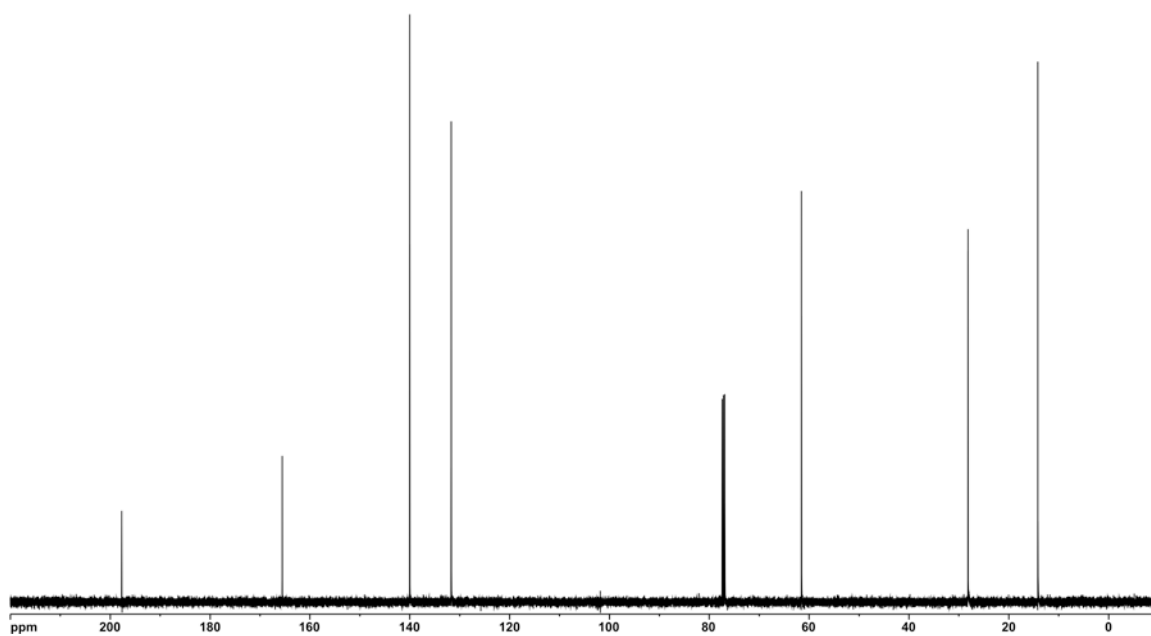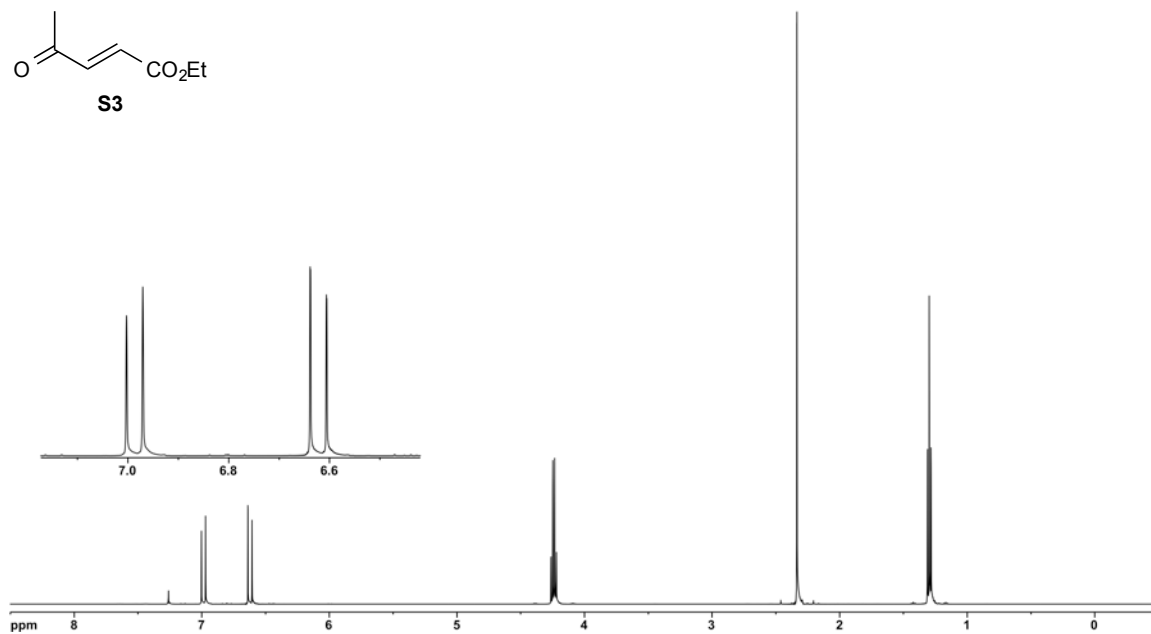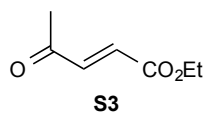
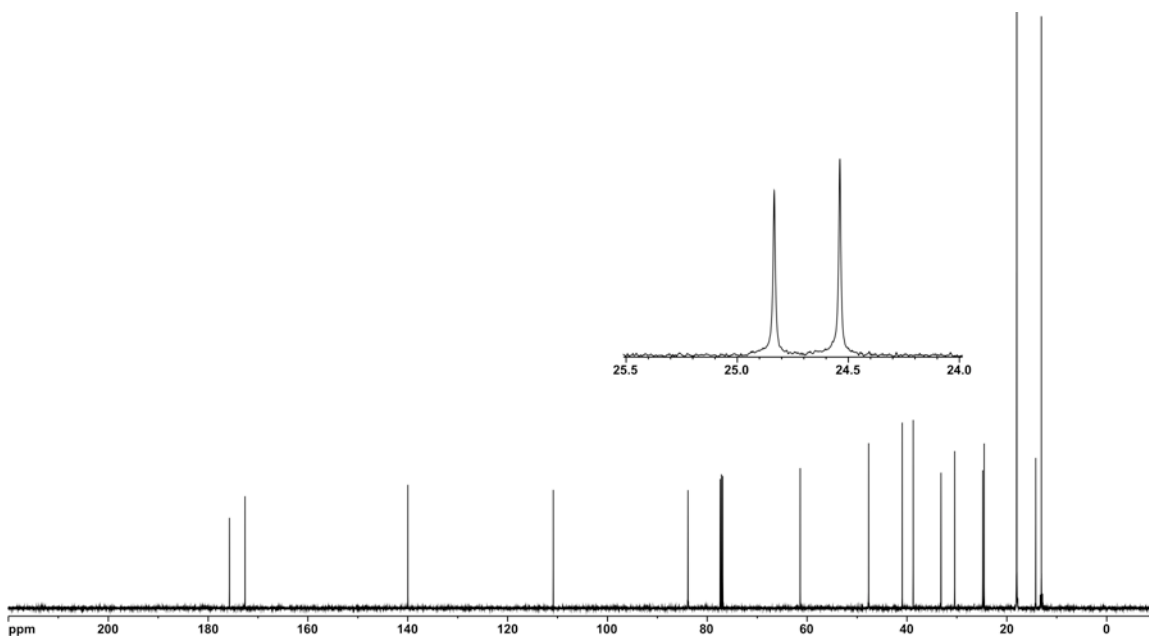^{1}H (500 MHz) and ^{13}C NMR (125 MHz) spectra of ketoester **S3** in CDCl$_3$
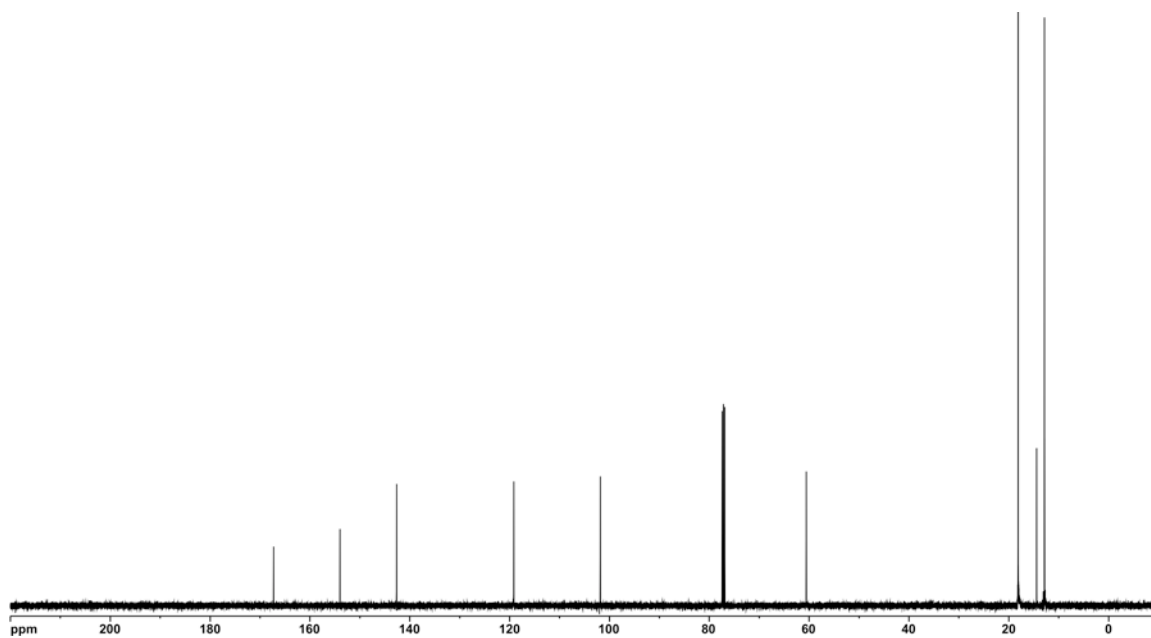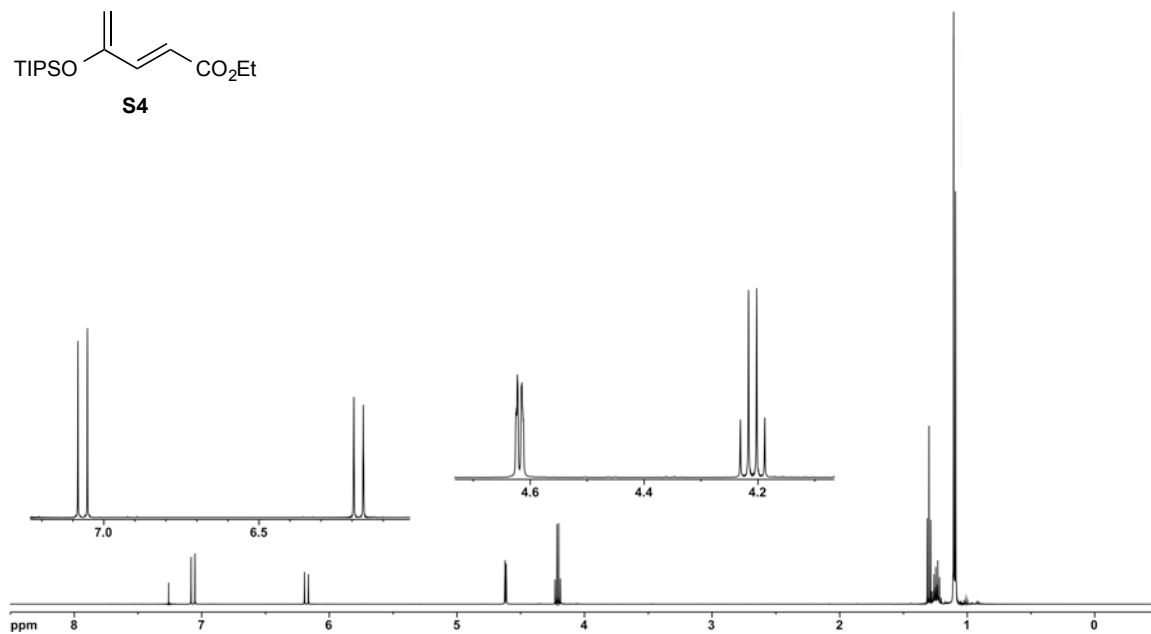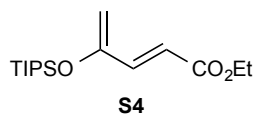
^{1}H (500 MHz) and ^{13}C NMR (125 MHz) spectra of diene **S4** in CDCl$_3$
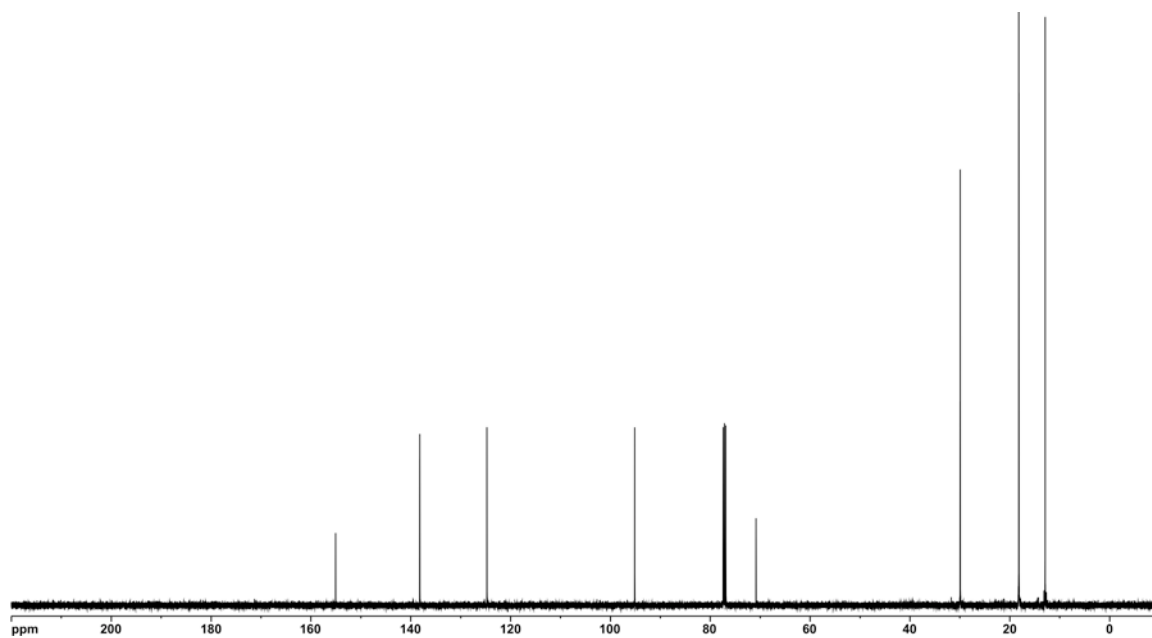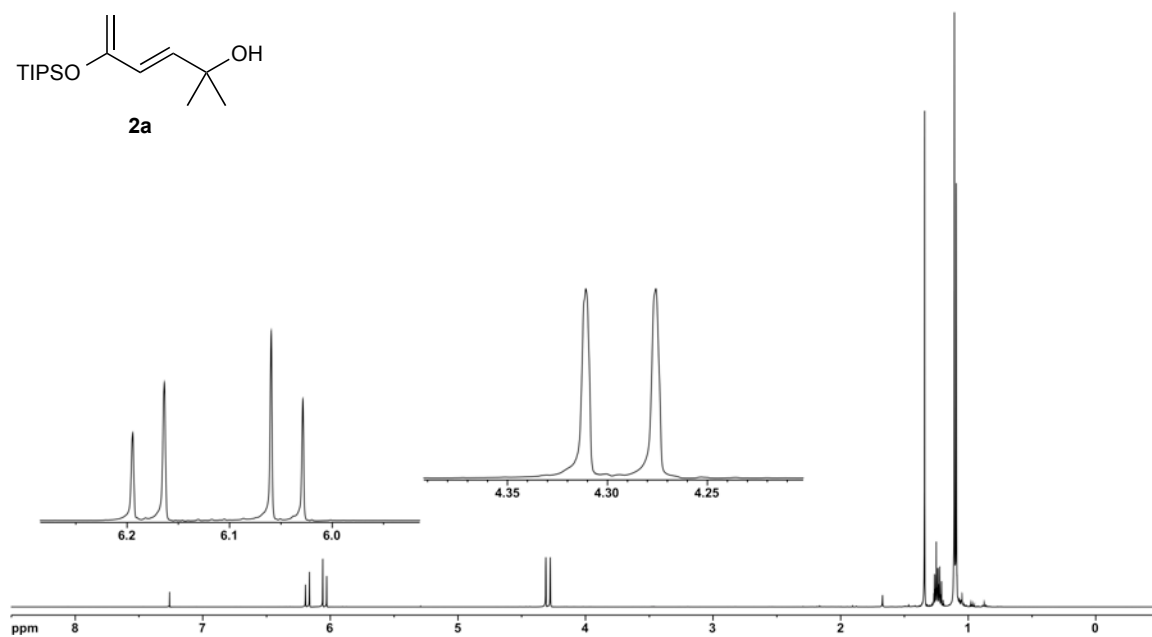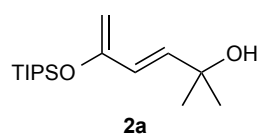
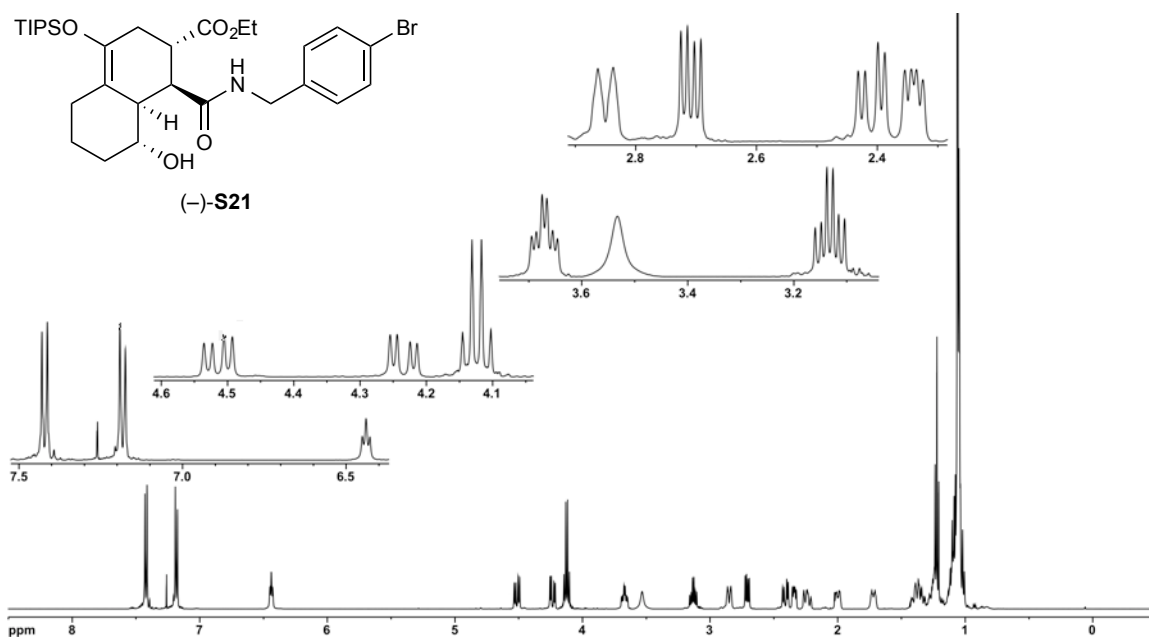^{1}H (500 MHz) and ^{13}C NMR (125 MHz) spectra of silyloxydiene alcohol **2a** in CDCl$_3$
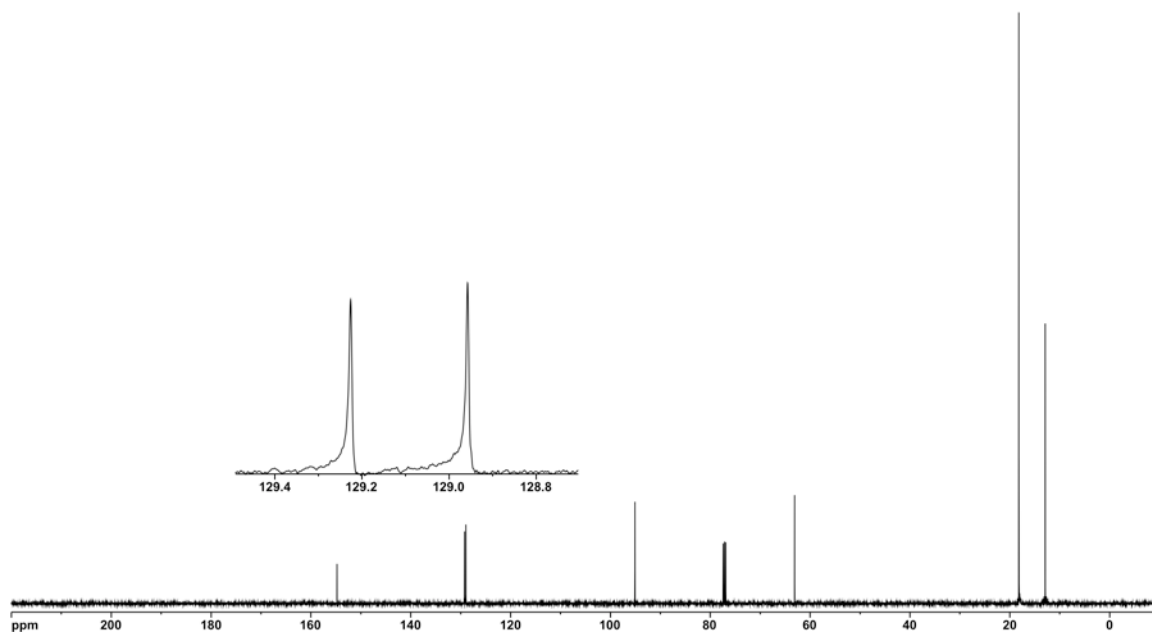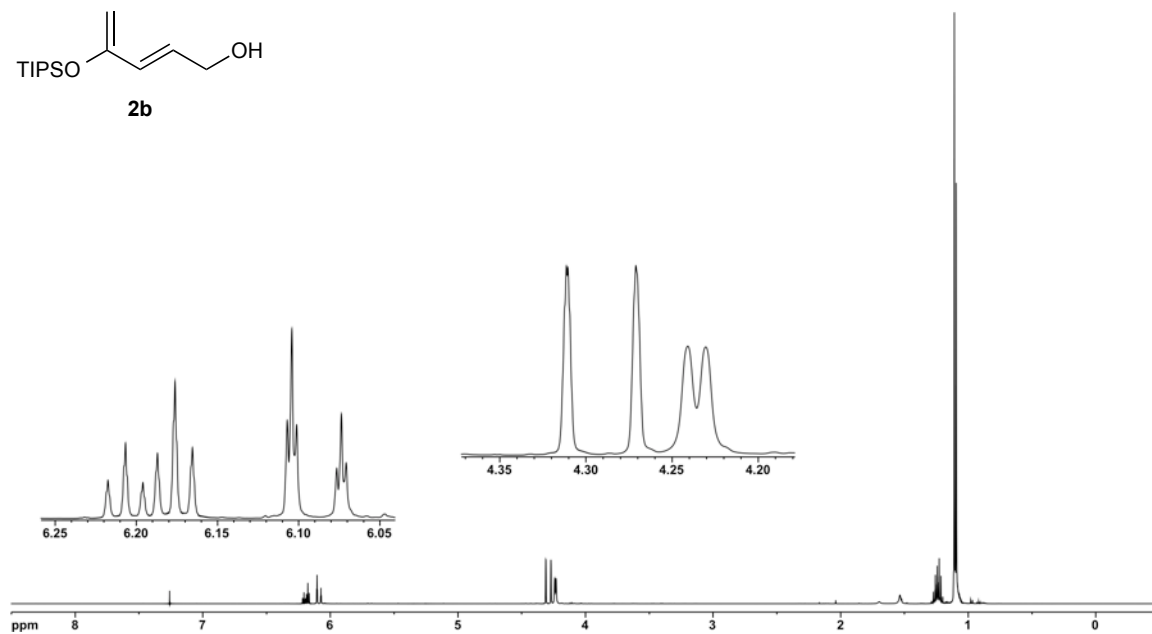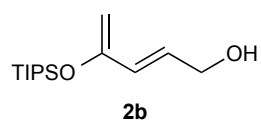
^{1}H (500 MHz) and ^{13}C NMR (125 MHz) spectra of silyloxydiene alcohol **2b** in CDCl$_3$
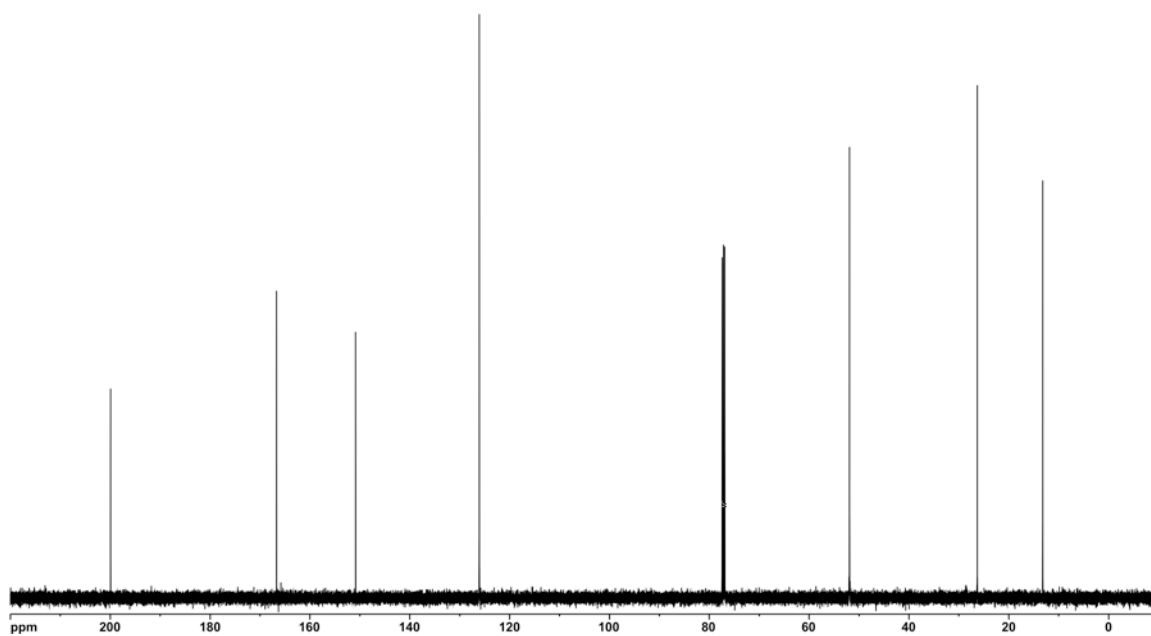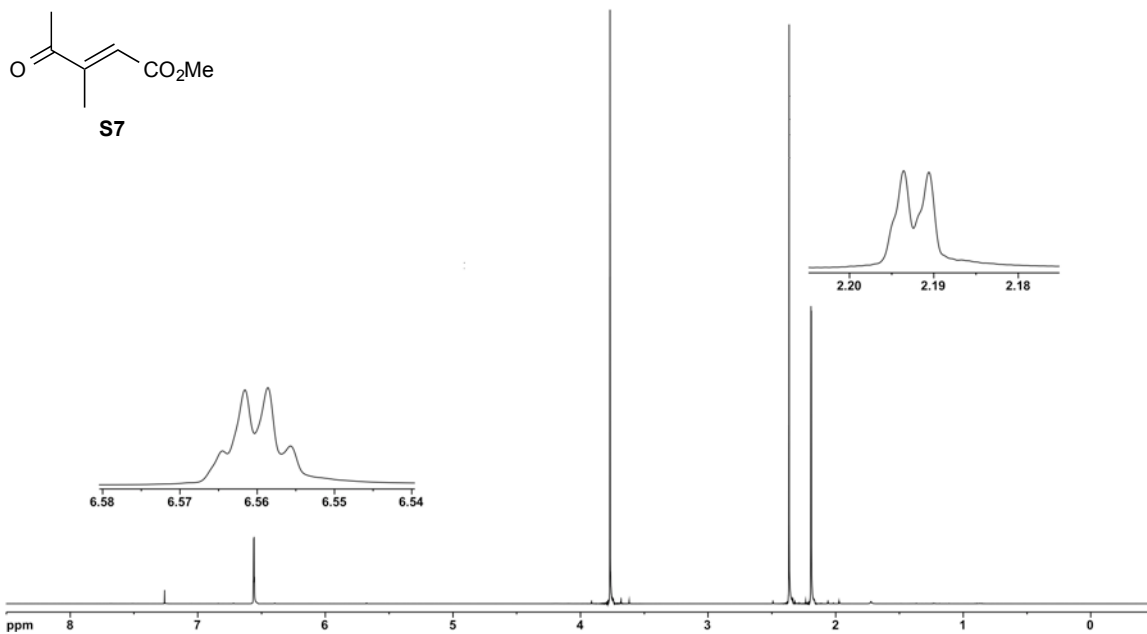
^{1}H (500 MHz) and ^{13}C NMR (125 MHz) spectra of ketoester **S7** in CDCl$_3$
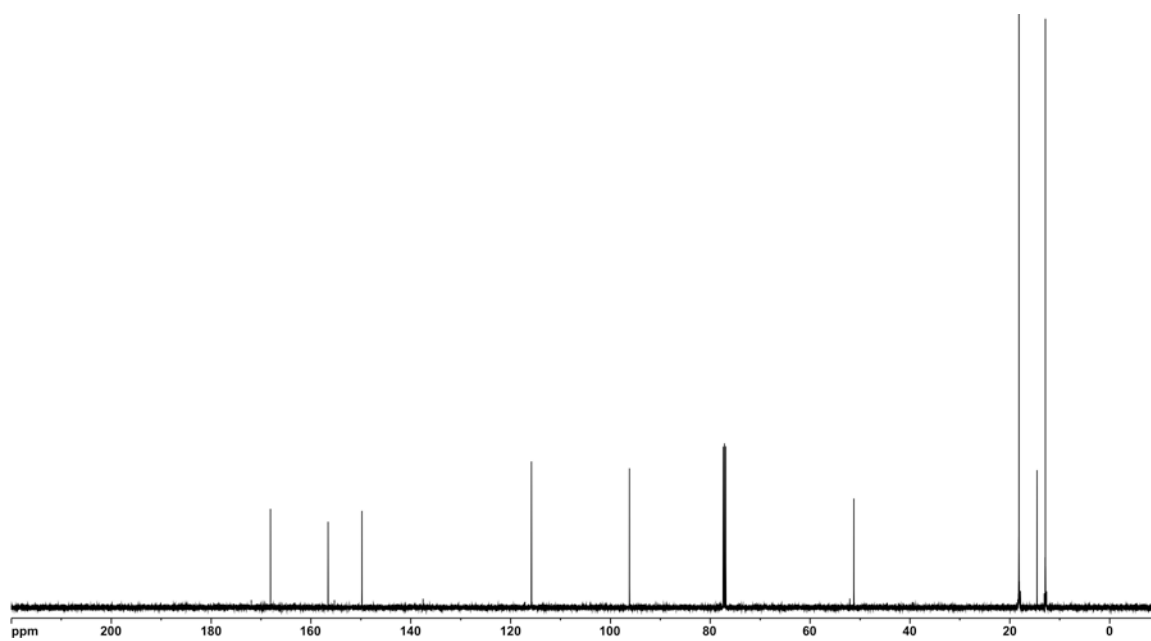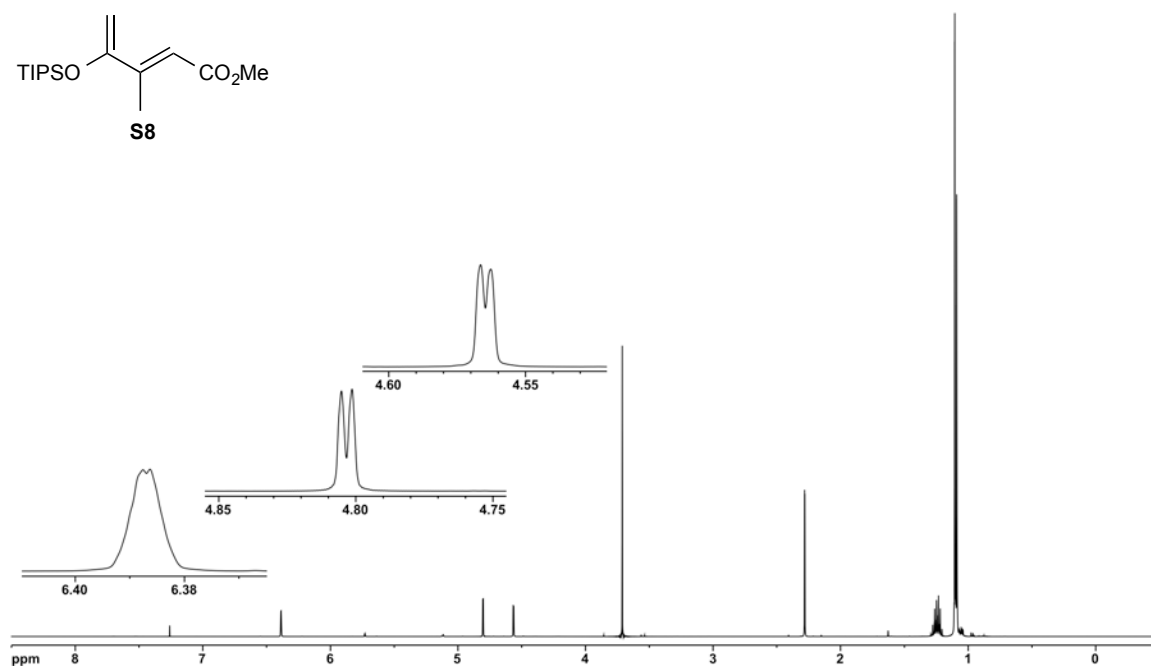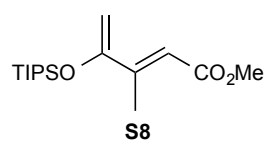
^{1}H (500 MHz) and ^{13}C NMR (125 MHz) spectra of diene **S8** in CDCl$_3$
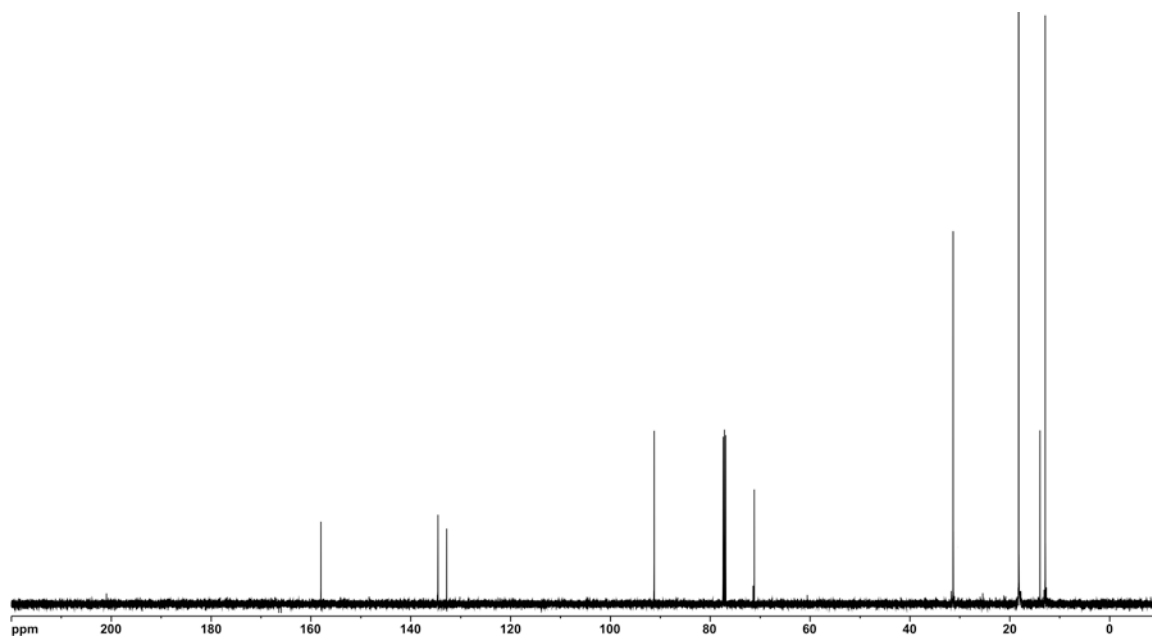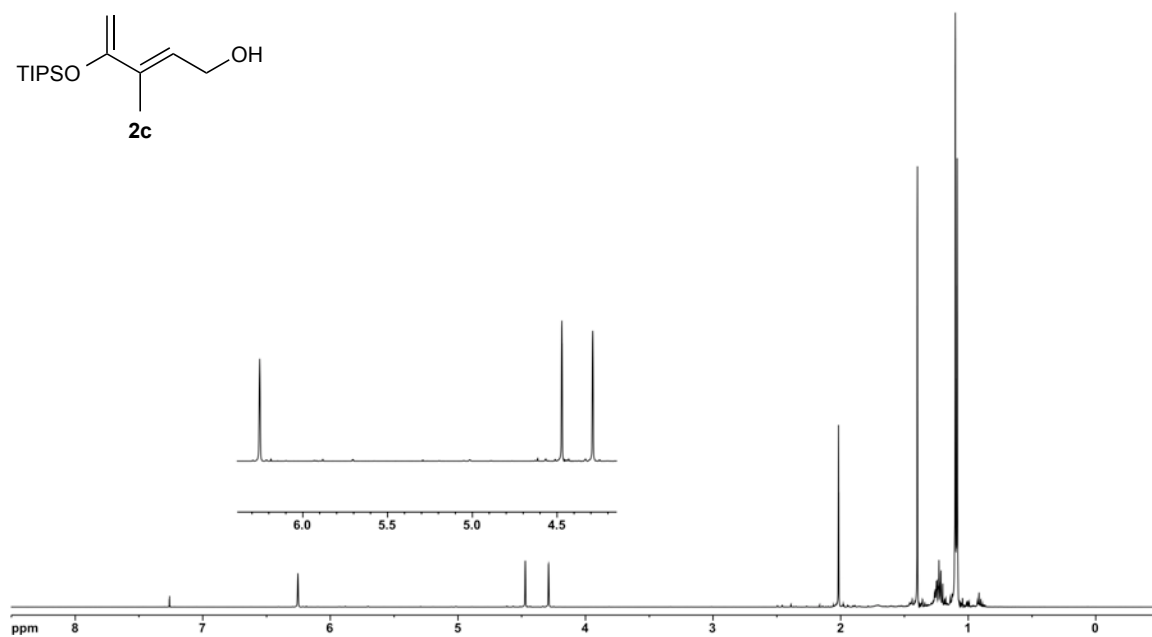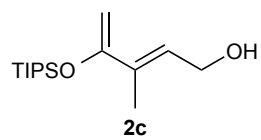
^{1}H (500 MHz) and ^{13}C NMR (125 MHz) spectra of silyloxydiene alcohol **2c** in CDCl$_3$

155
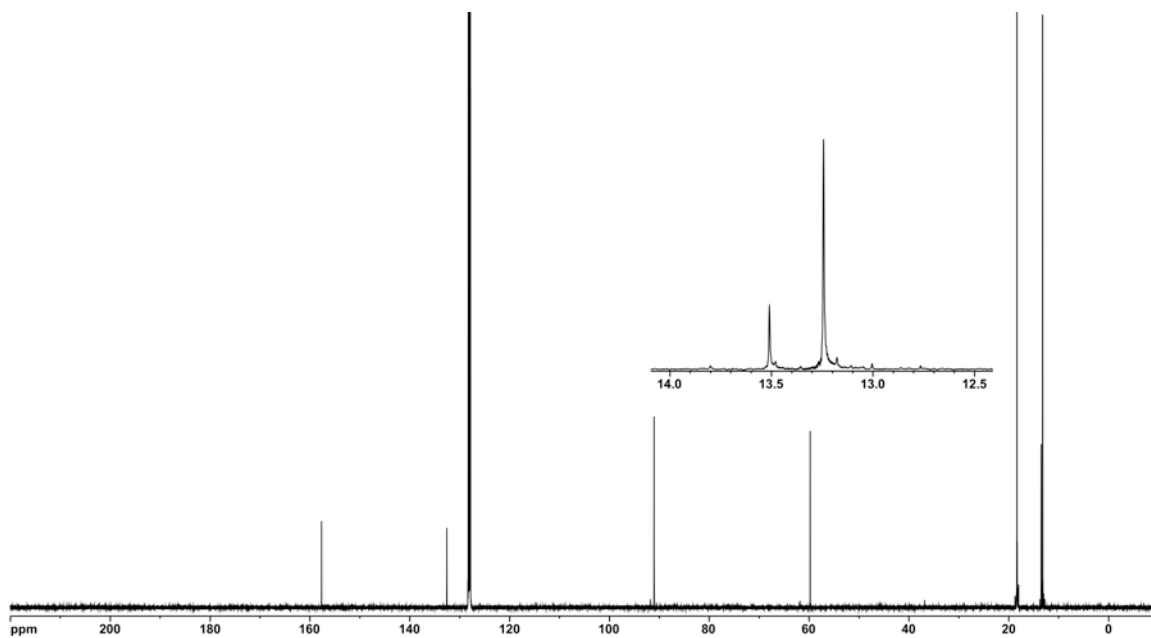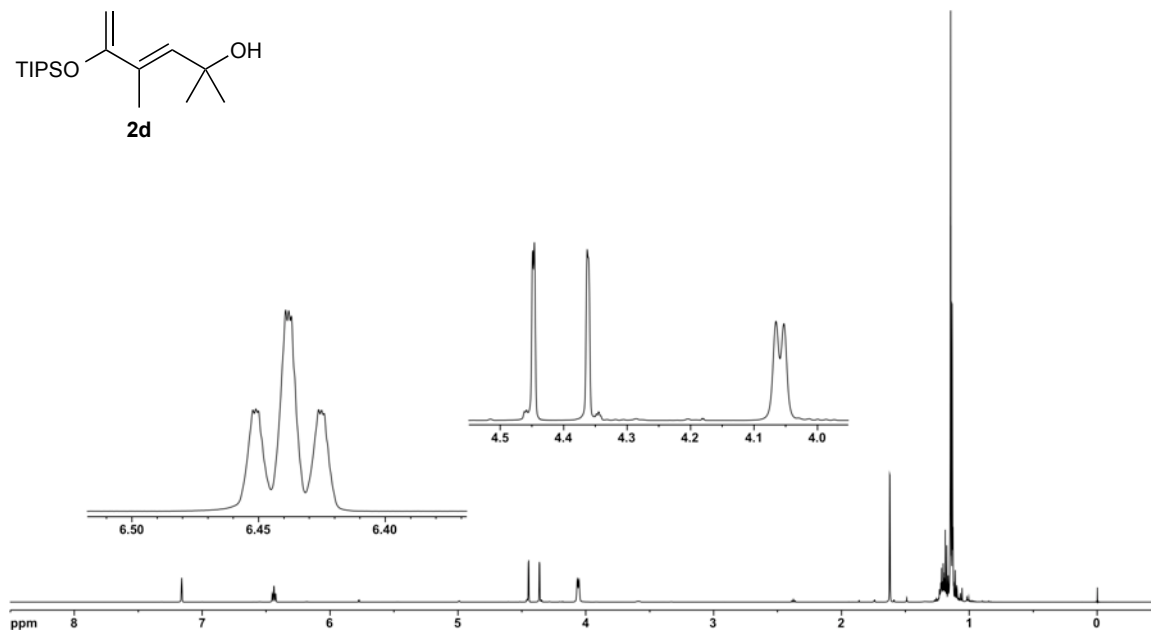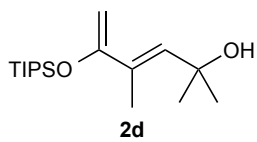
^{1}H (500 MHz) and ^{13}C NMR (125 MHz) spectra of silyloxydiene alcohol **2d** in C_6D_6
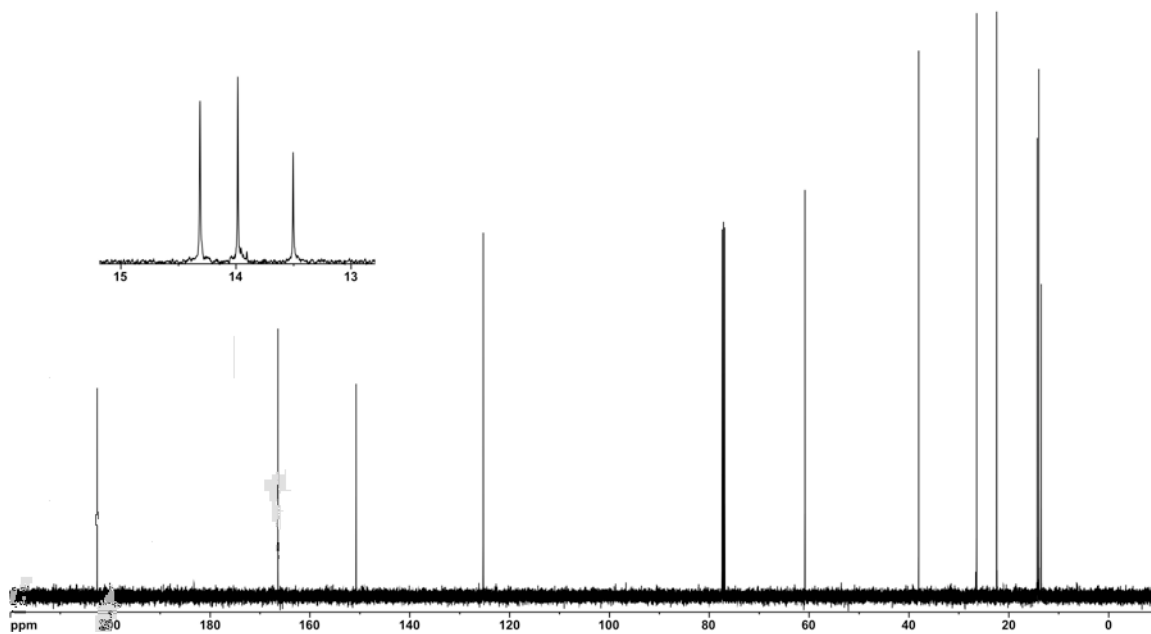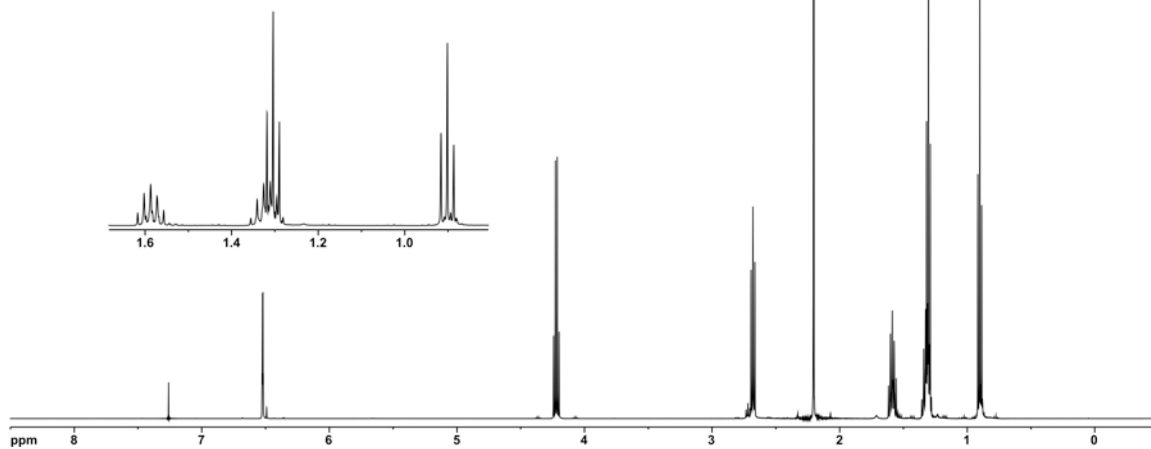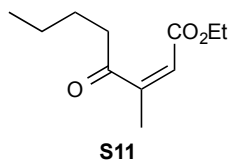
^{1}H (500 MHz) and ^{13}C NMR (125 MHz) spectra of ketoester **S11** in CDCl$_3$
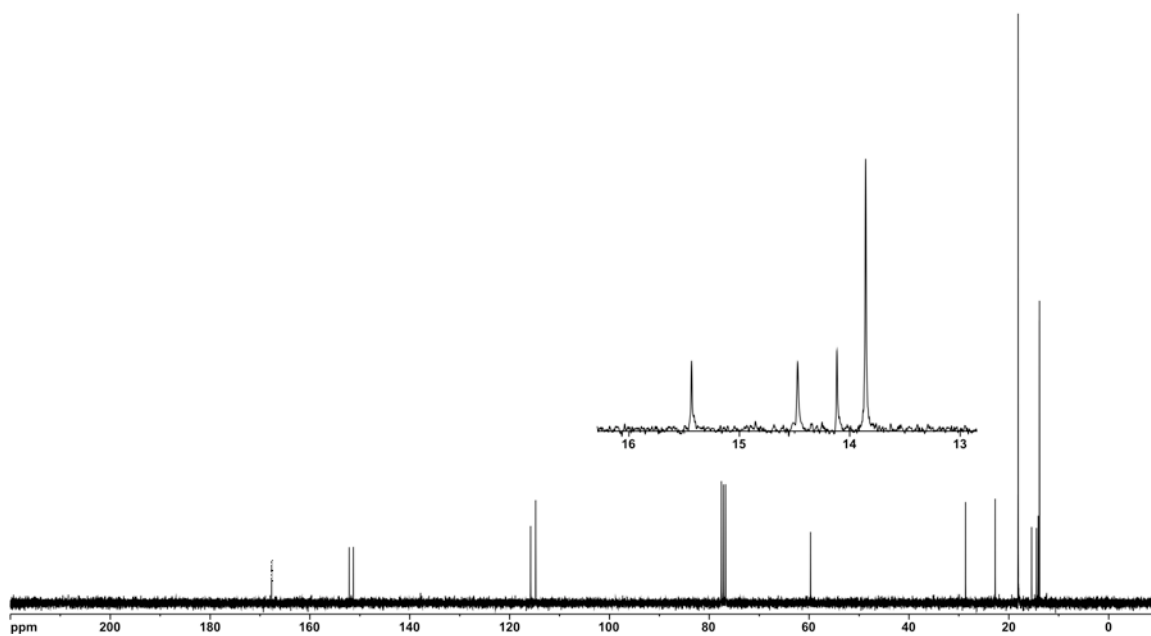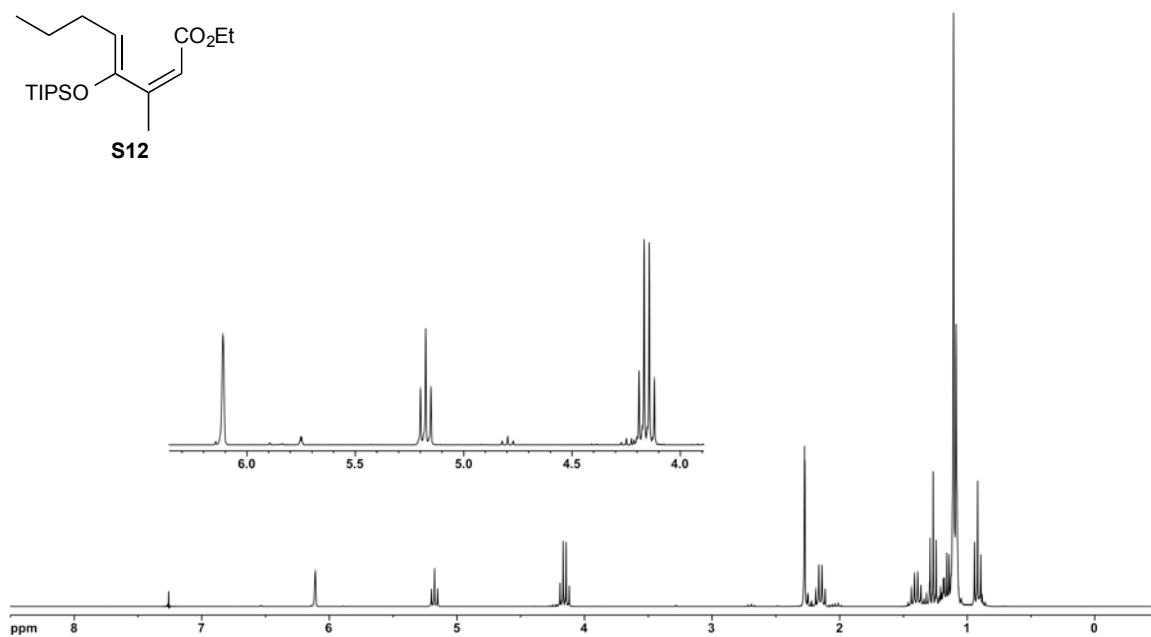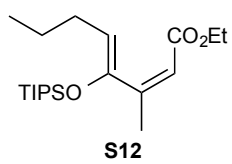
^{1}H (500 MHz) and ^{13}C NMR (125 MHz) spectra of diene **S12** in CDCl$_3$
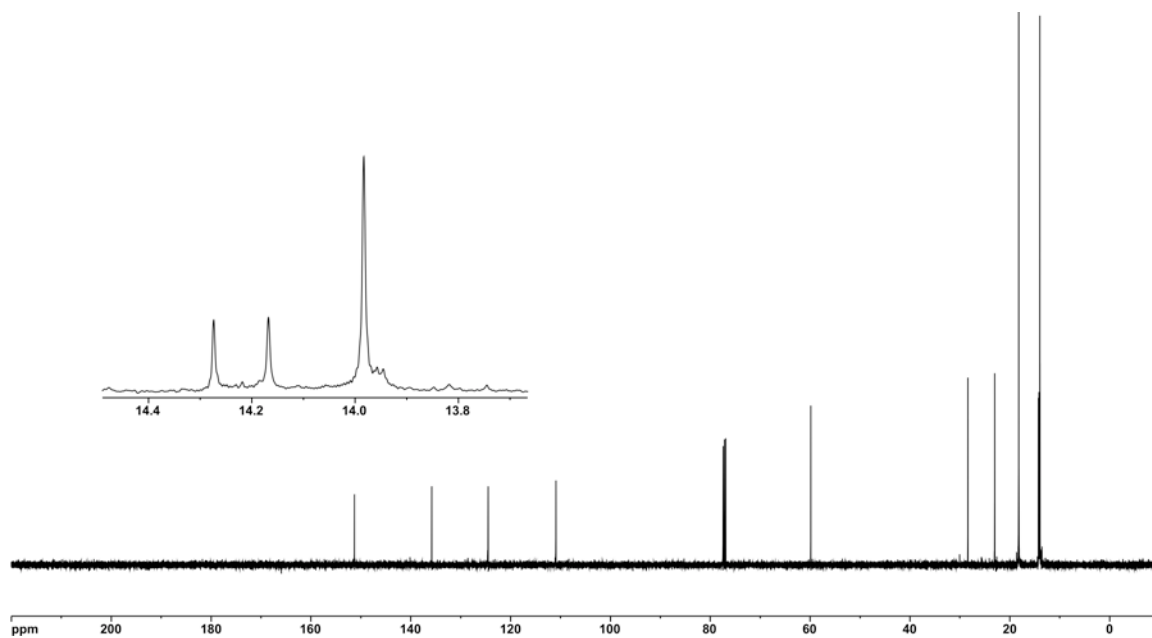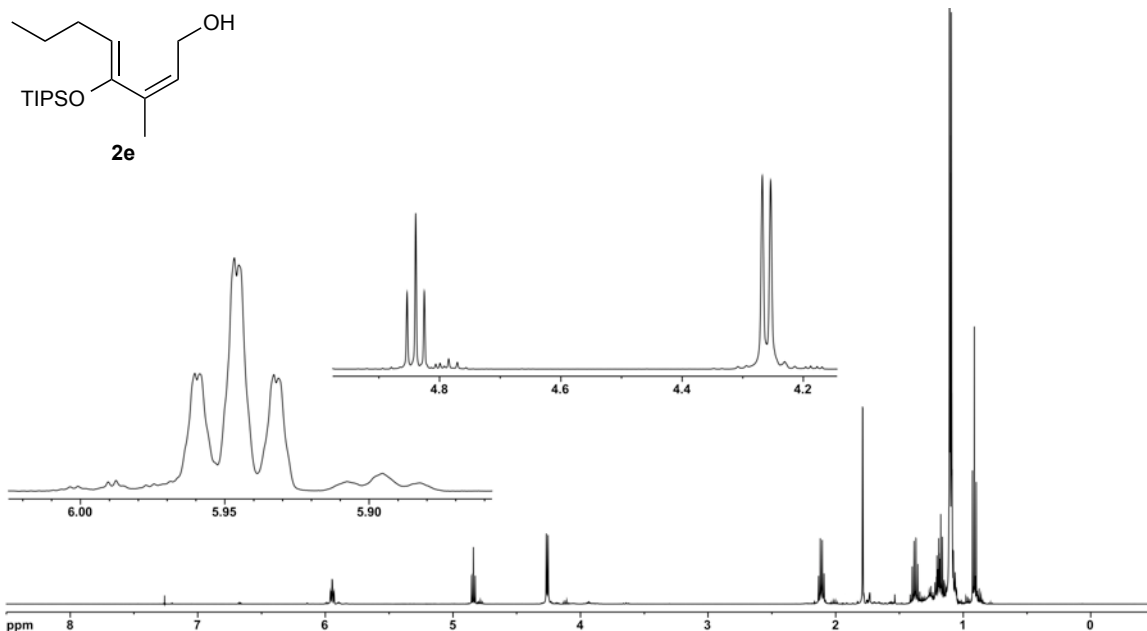
^{1}H (500 MHz) and ^{13}C NMR (125 MHz) spectra of silyloxydiene alcohol **2e** in CDCl$_3$
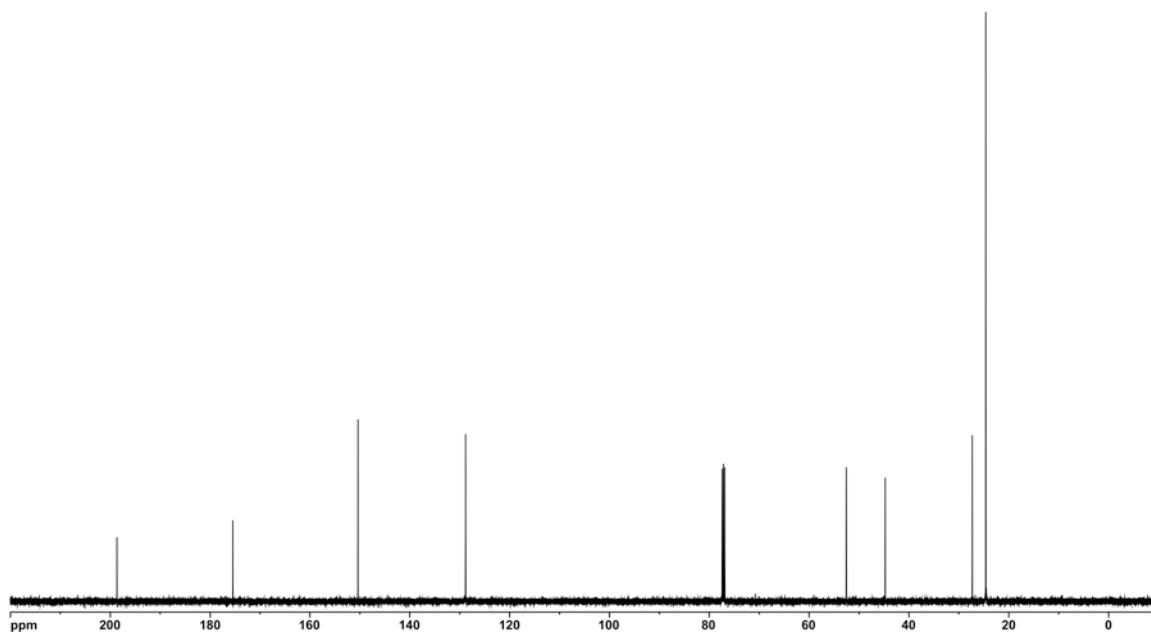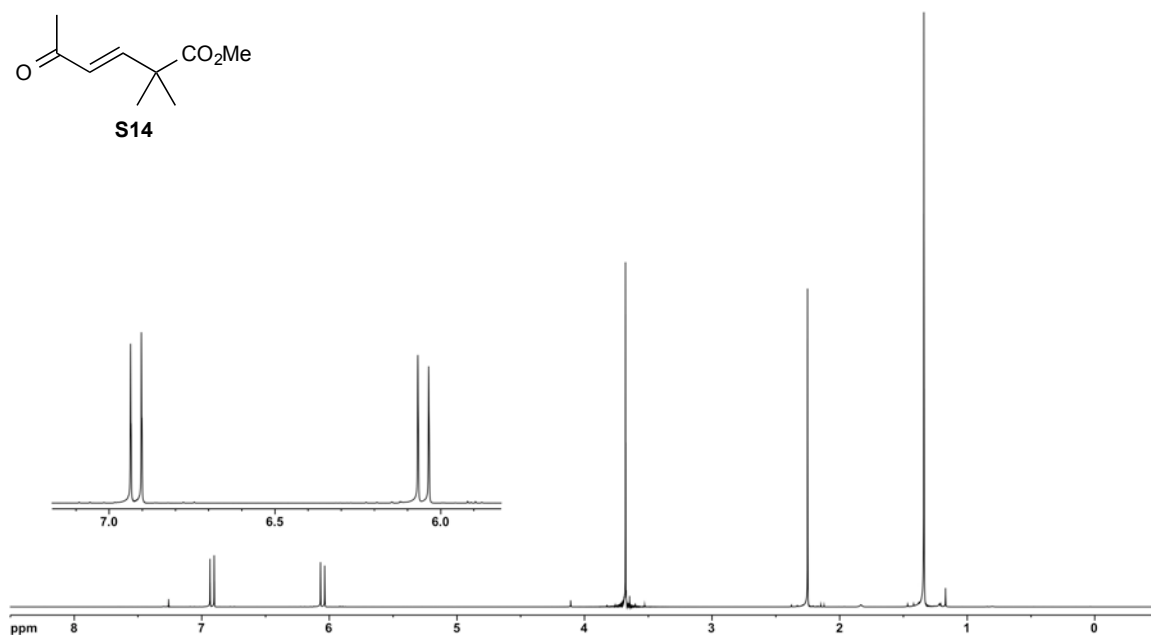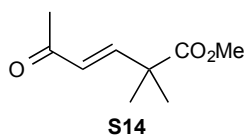
^{1}H (500 MHz) and ^{13}C NMR (125 MHz) spectra of ketoester **S14** in CDCl$_3$
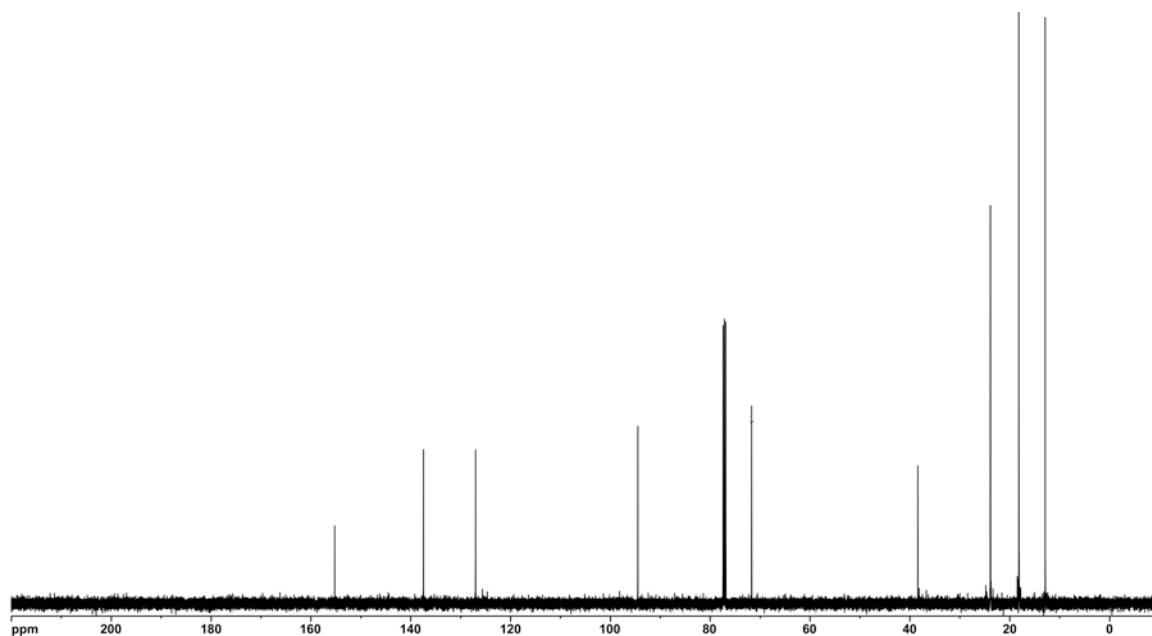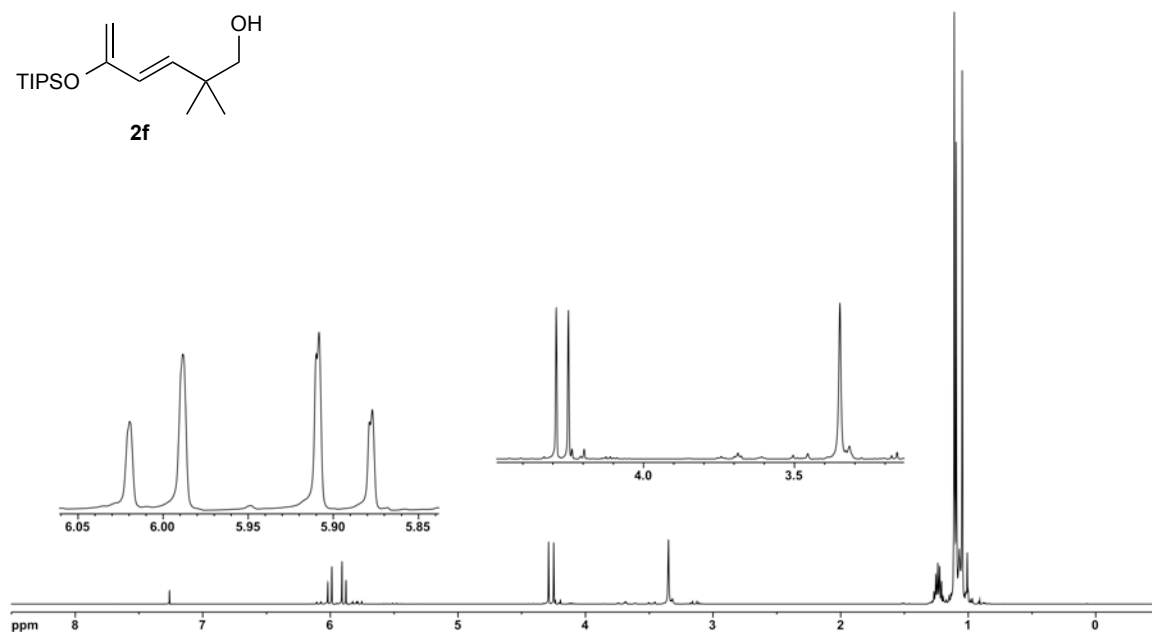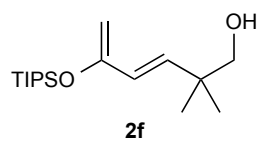
^{1}H (500 MHz) and ^{13}C NMR (125 MHz) spectra of silyloxydiene alcohol **2f** in CDCl$_3$
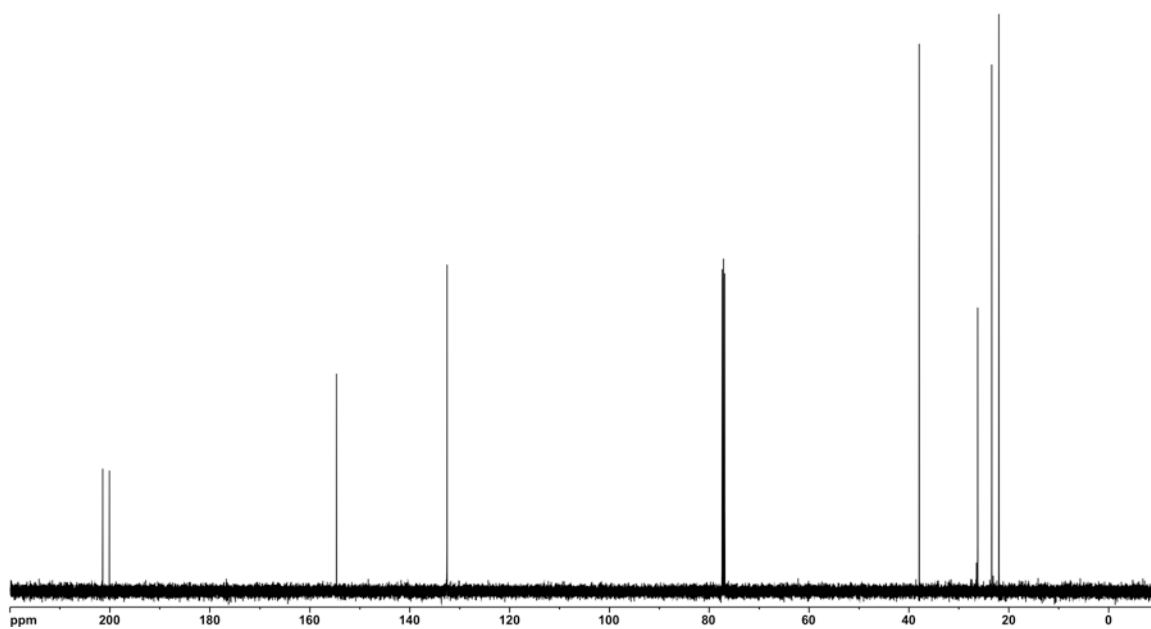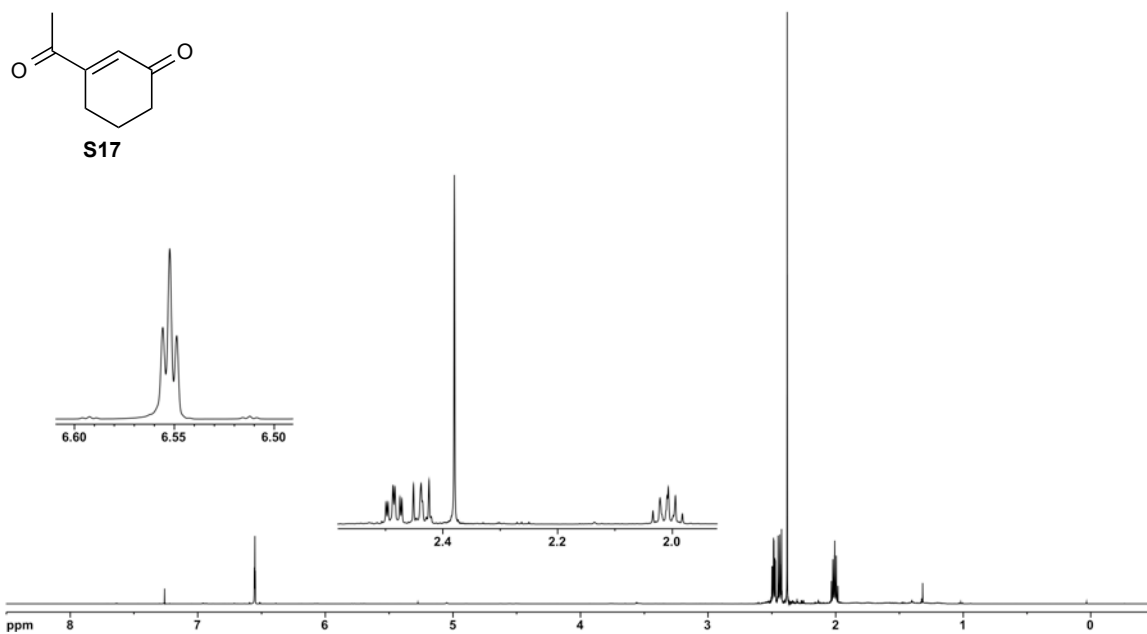
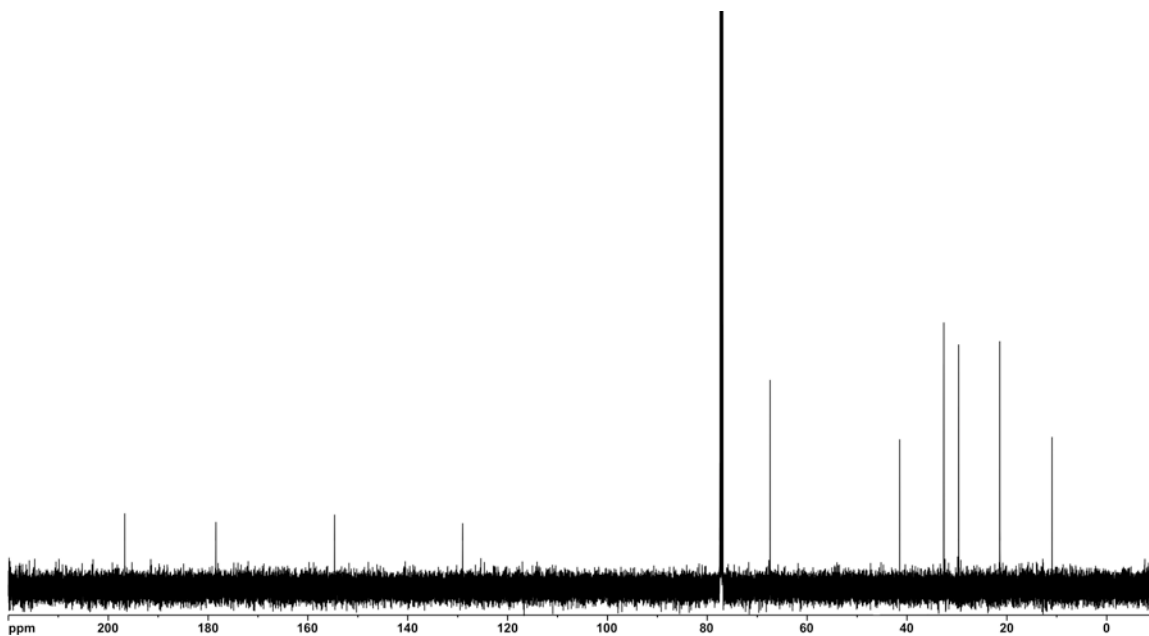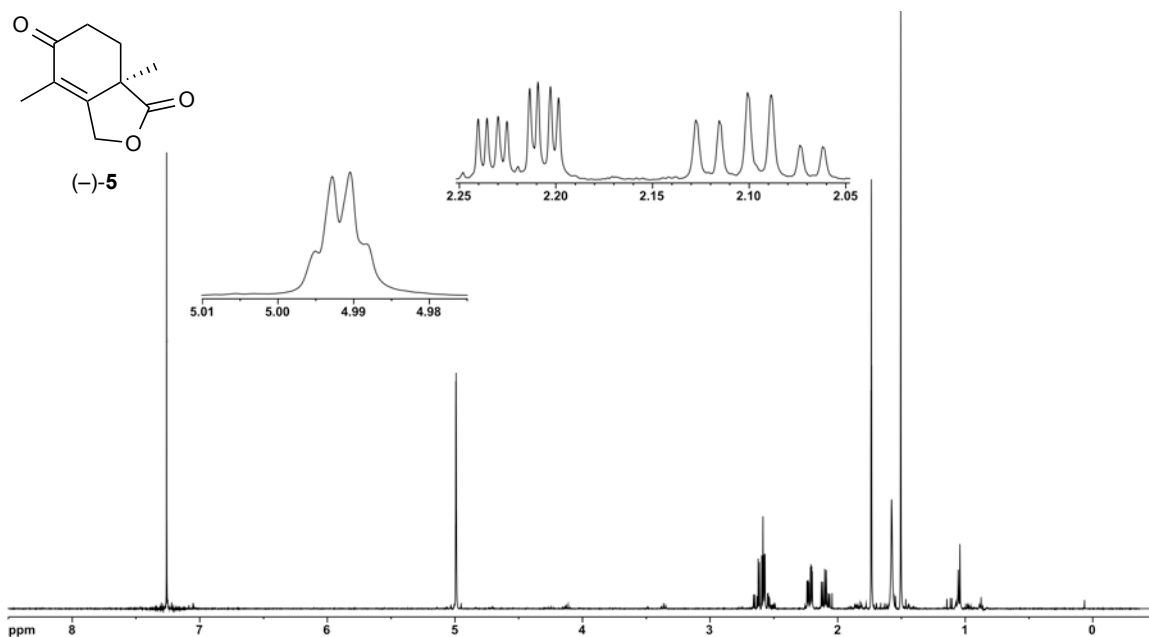^{1}H (500 MHz) and ^{13}C NMR (125 MHz) spectra of diketone **S17** in CDCl$_3$
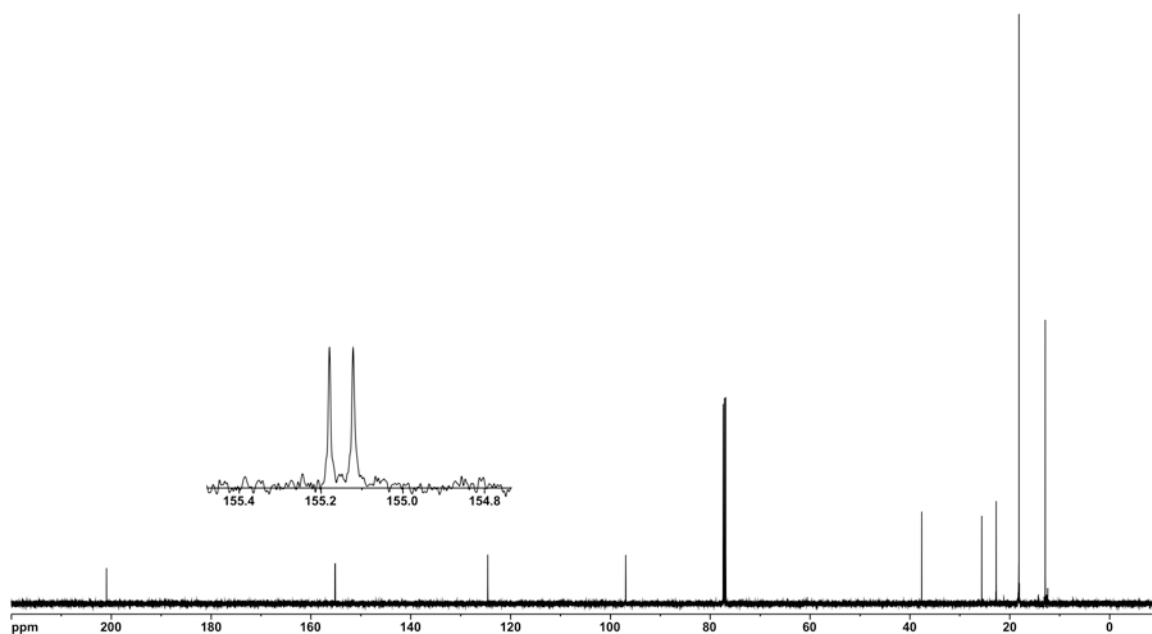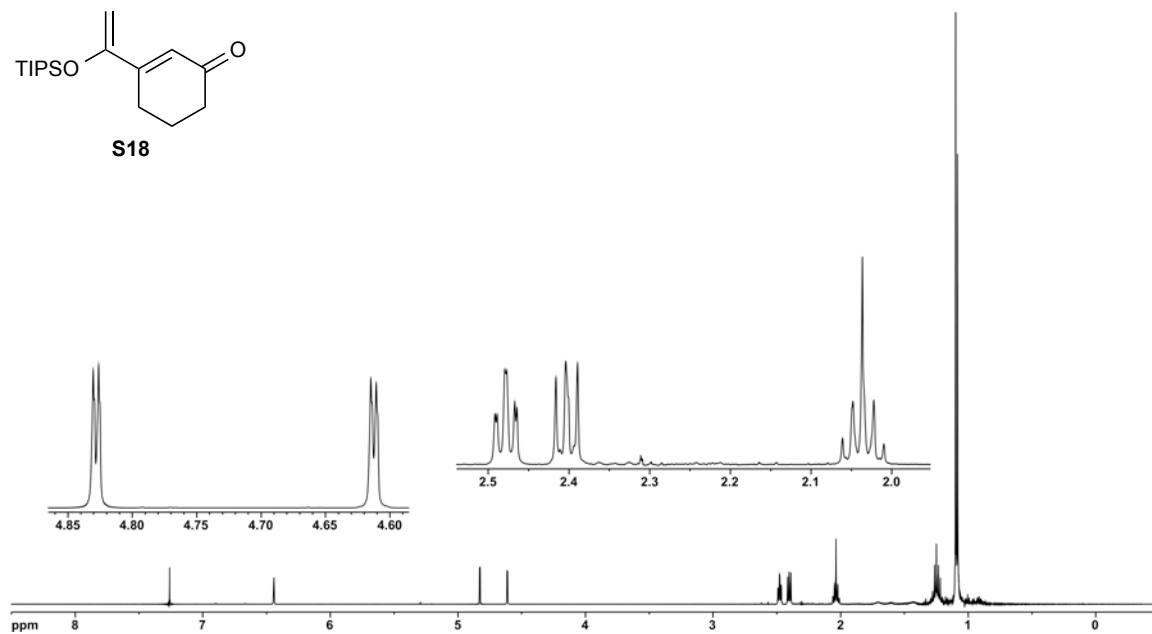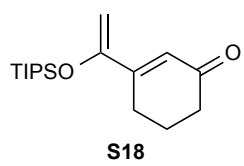
^{1}H (500 MHz) and ^{13}C NMR (125 MHz) spectra of diene **S18** in CDCl$_3$
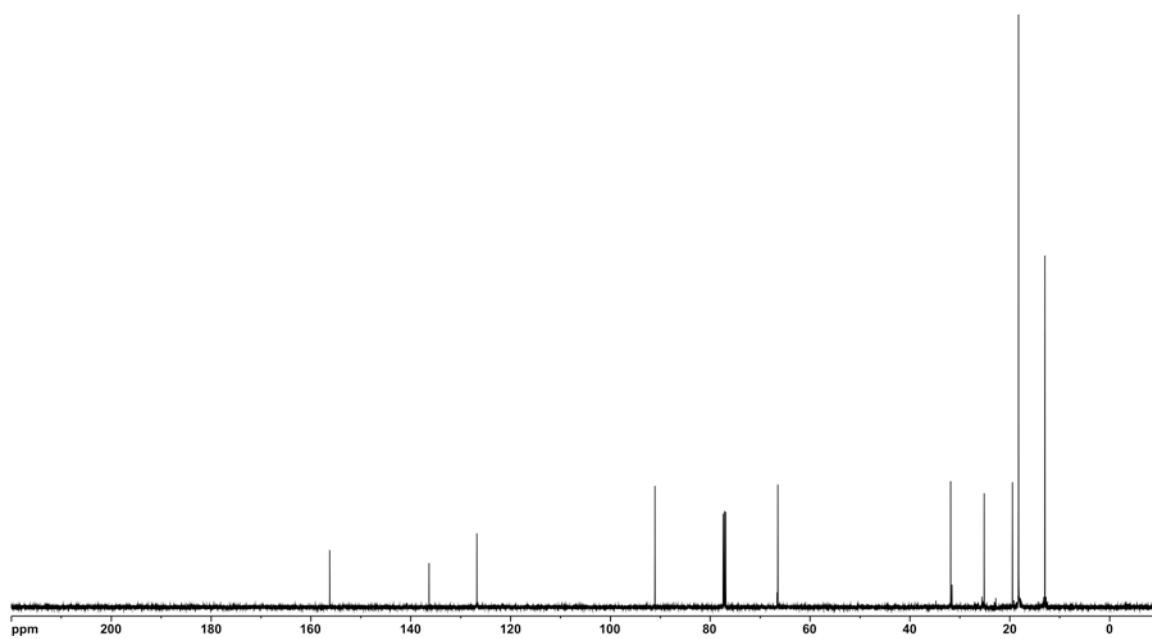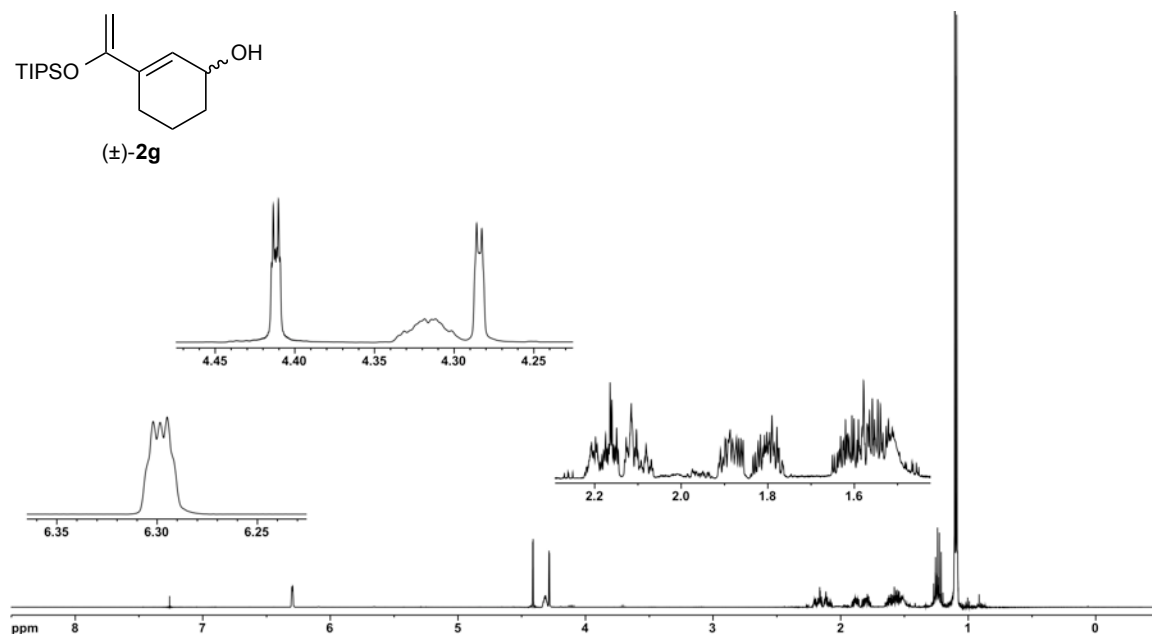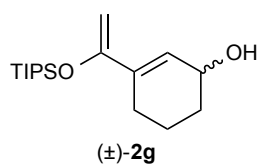
^{1}H (500 MHz) and ^{13}C NMR (125 MHz) spectra of silyloxydiene alcohol (±)-**2g** in CDCl$_3$
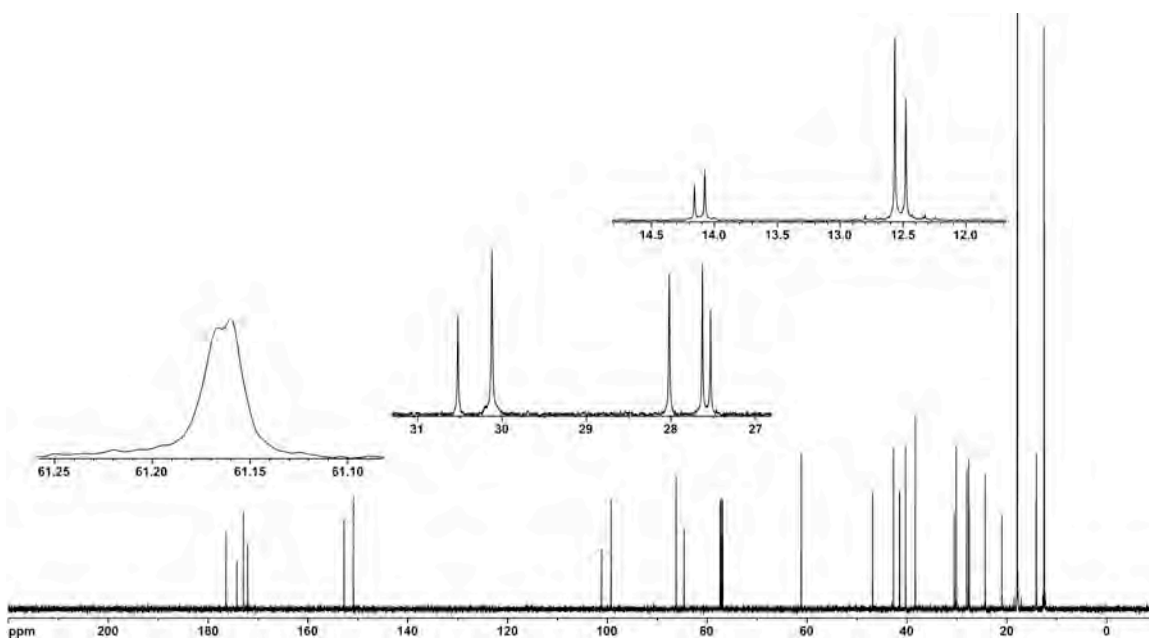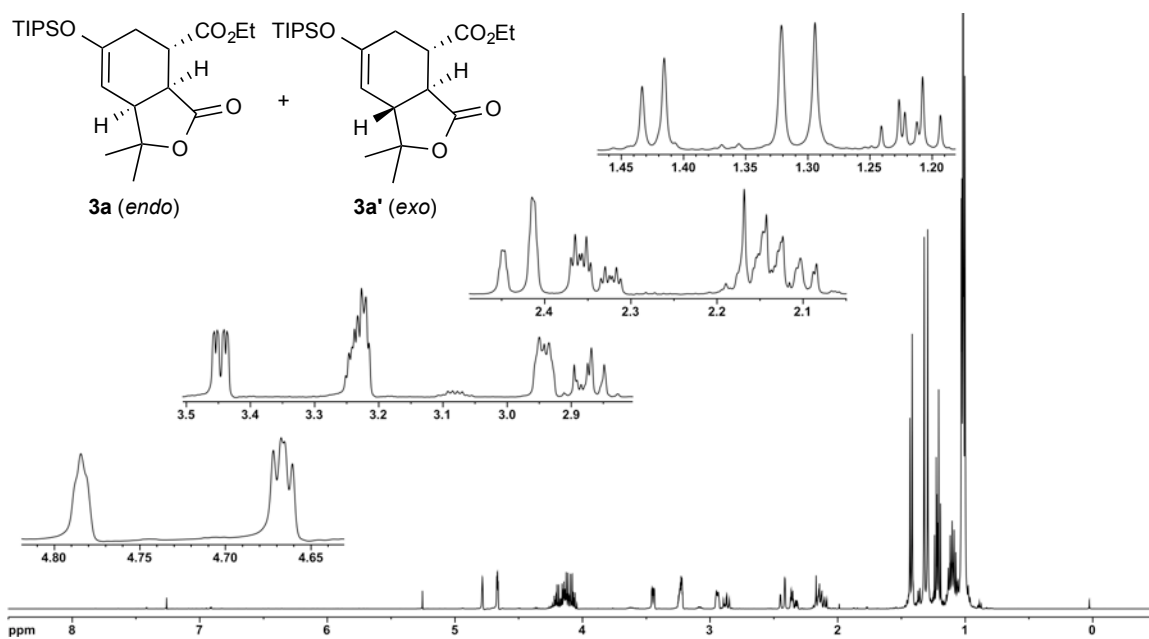
^{1}H (500 MHz) and ^{13}C NMR (125 MHz) spectra of bicyclic γ-lactones **3a** and **3a'**

(1.5:1 mixture of *endo/exo* diastereomers) in CDCl$_3$
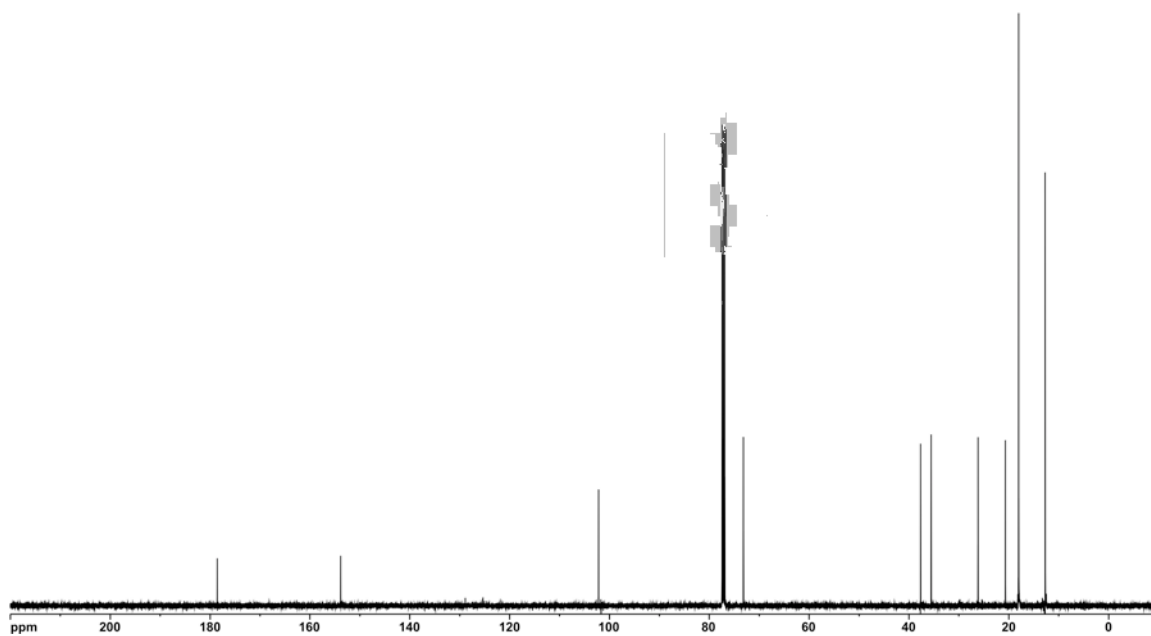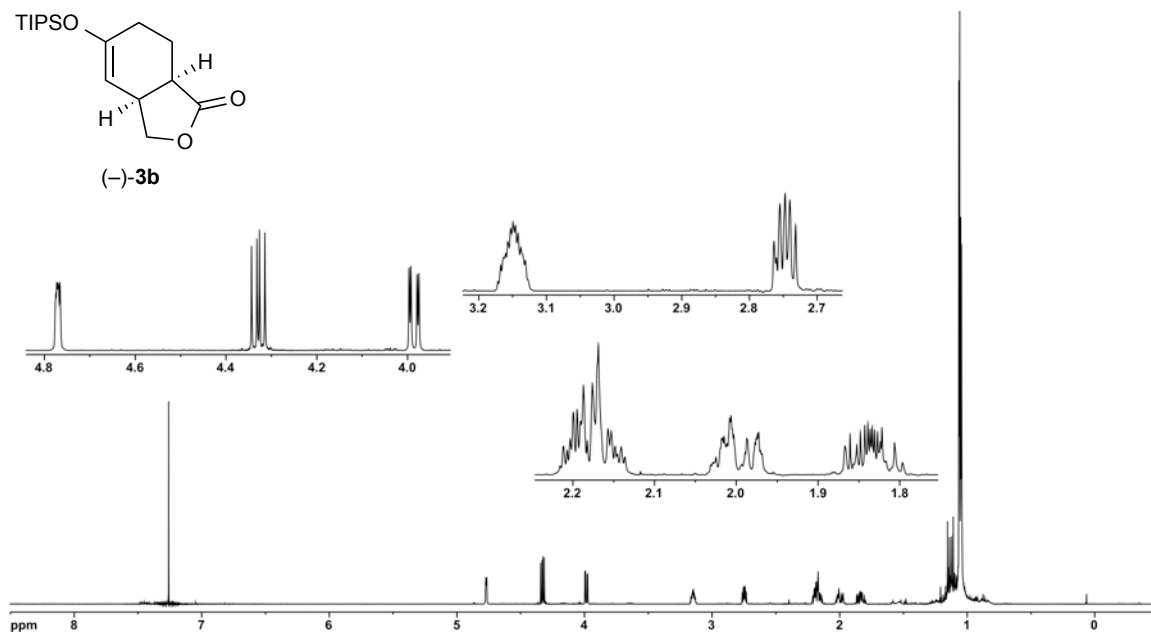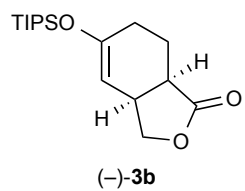
^{1}H (500 MHz) and ^{13}C NMR (125 MHz) spectra of bicyclic γ-lactone (–)-**3b** in CDCl$_3$
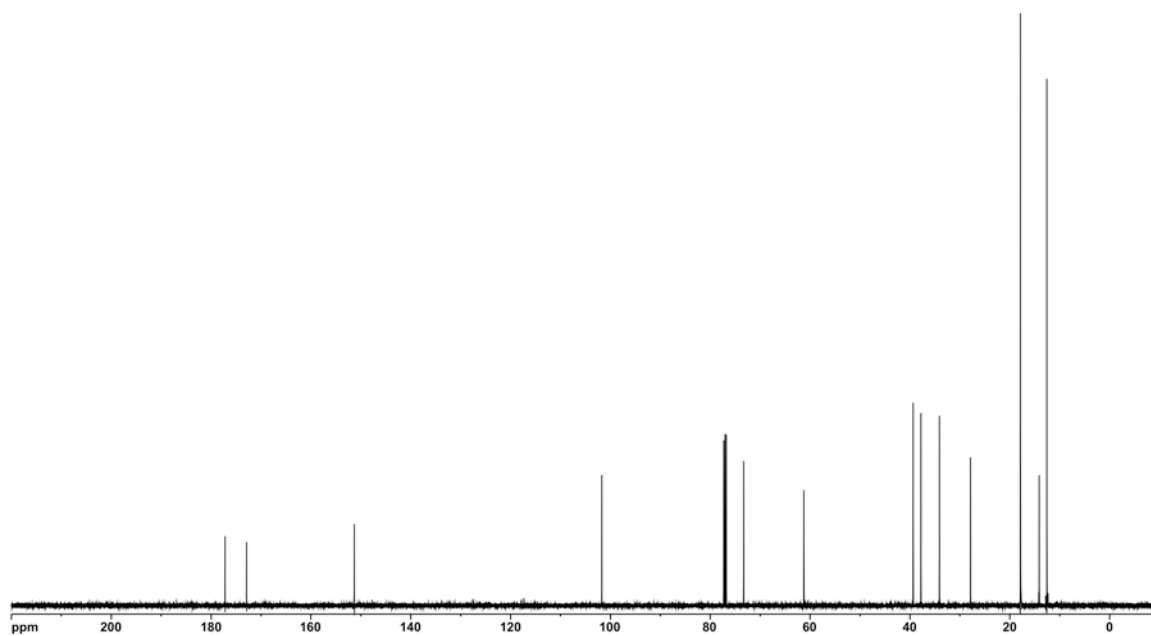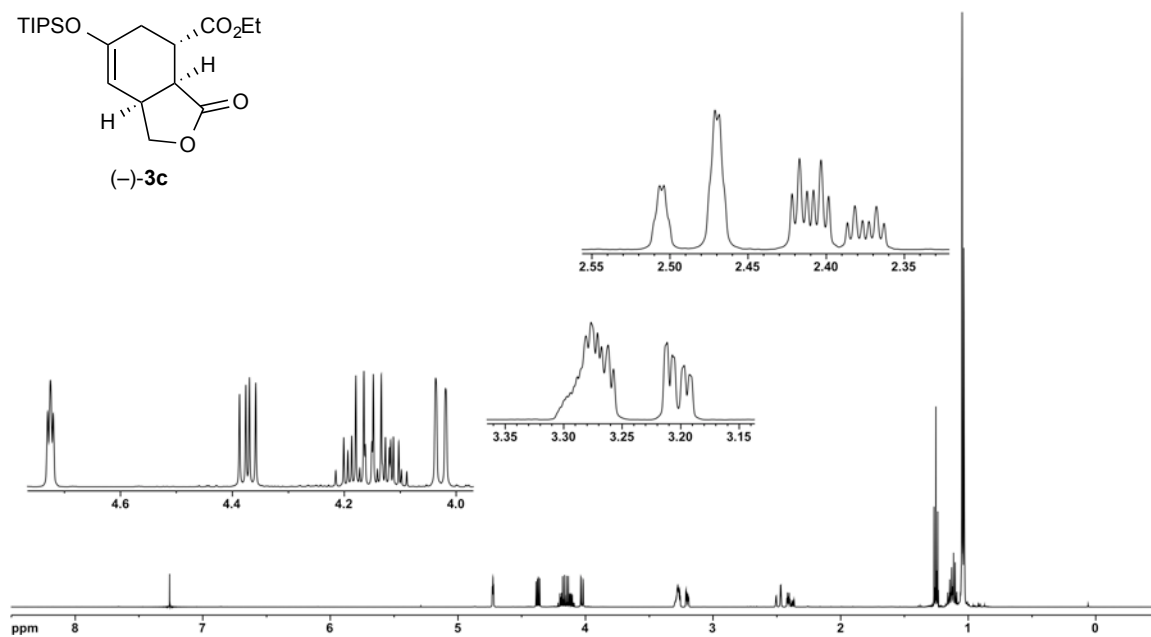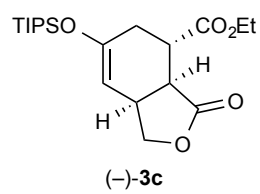
^{1}H (500 MHz) and ^{13}C NMR (125 MHz) spectra of bicyclic γ-lactone (–)-**3c** in CDCl$_3$
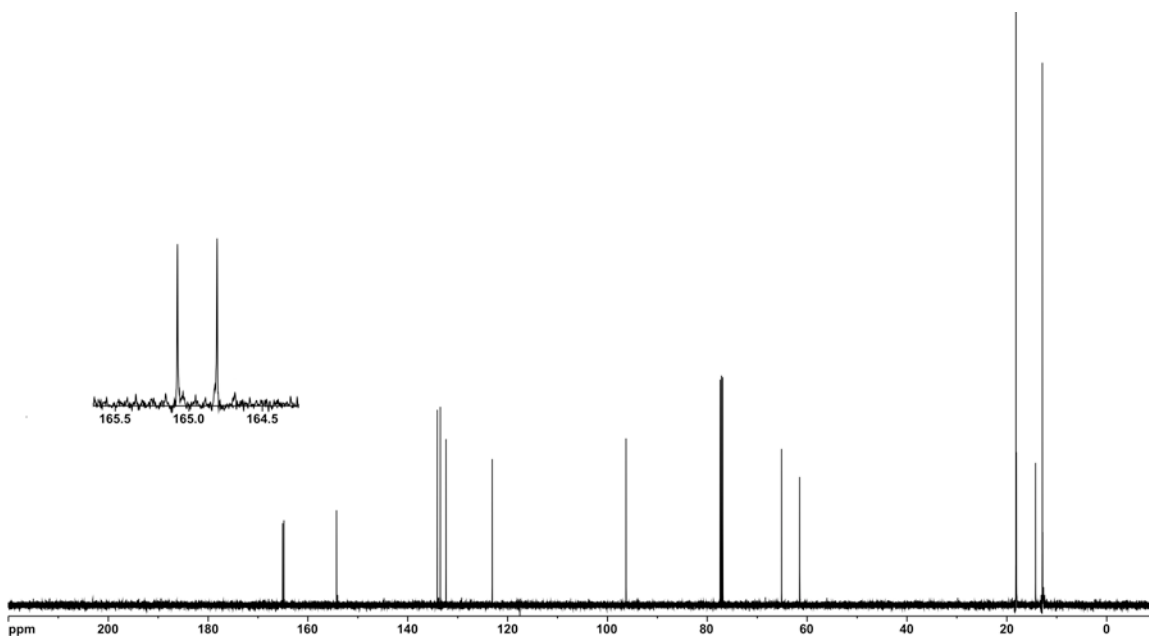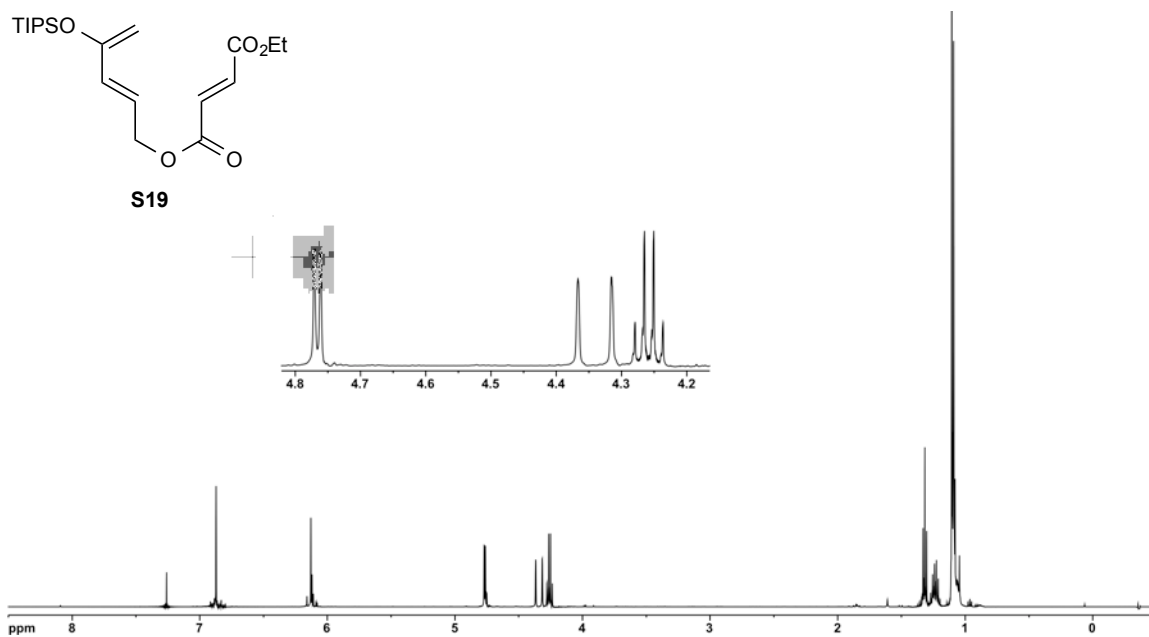
^{1}H (500 MHz) and ^{13}C NMR (125 MHz) spectra of ester **S19** in CDCl$_3$
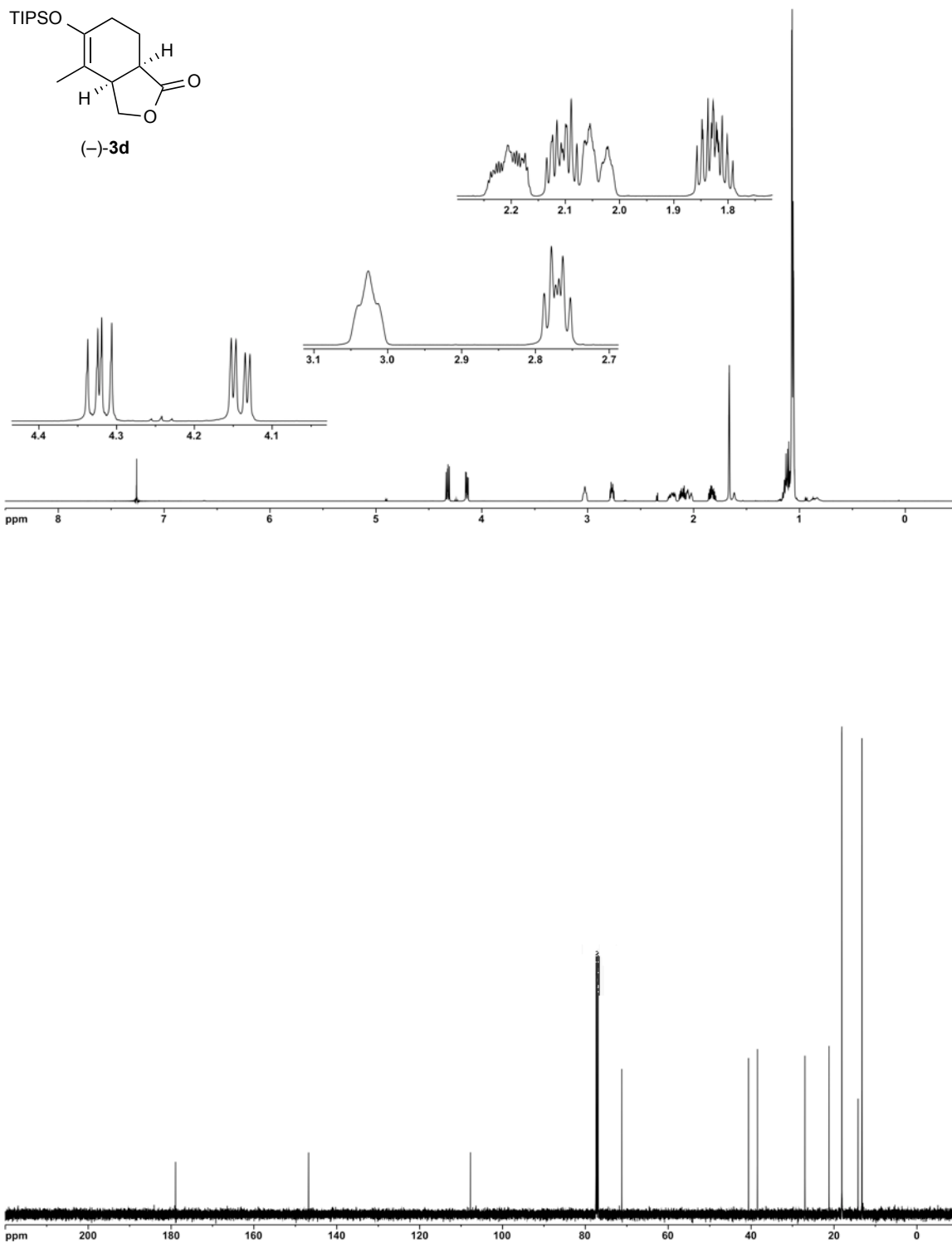
^{1}H (500 MHz) and ^{13}C NMR (125 MHz) spectra of bicyclic γ-lactone (–)-**3d** in CDCl$_3$
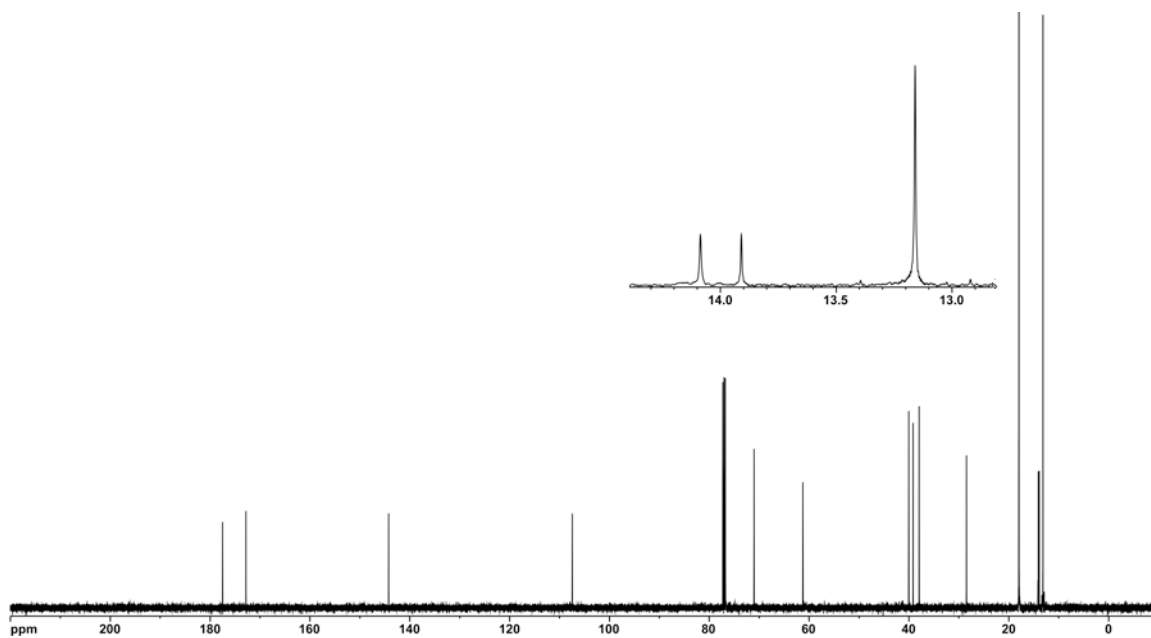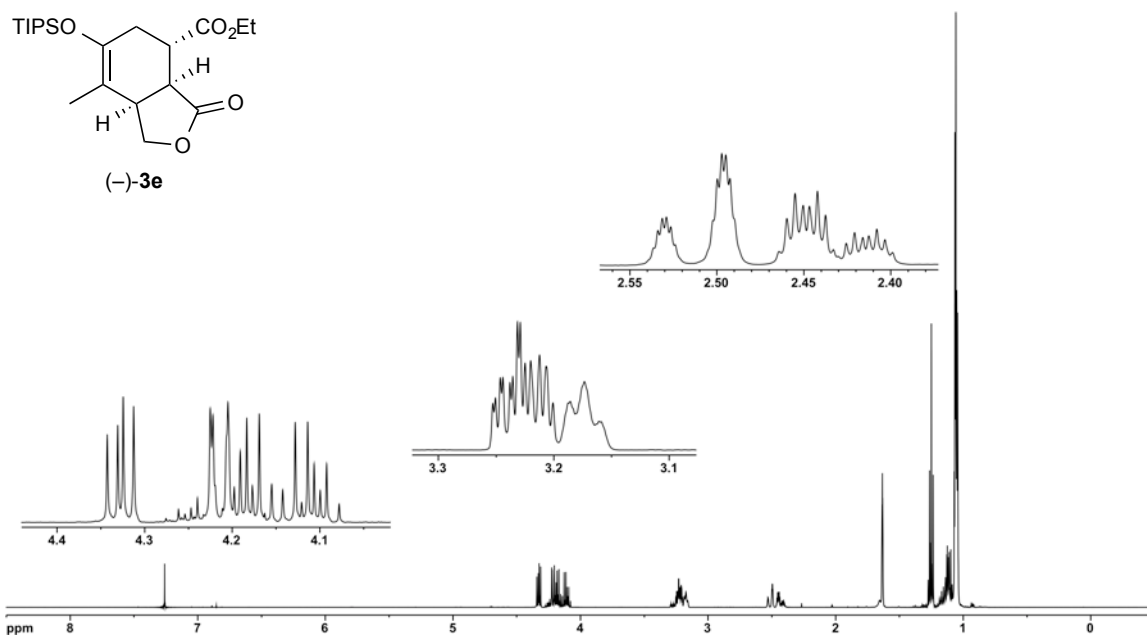
^{1}H (500 MHz) and ^{13}C NMR (125 MHz) spectra of bicyclic γ-lactone (–)-**3e** in CDCl₃
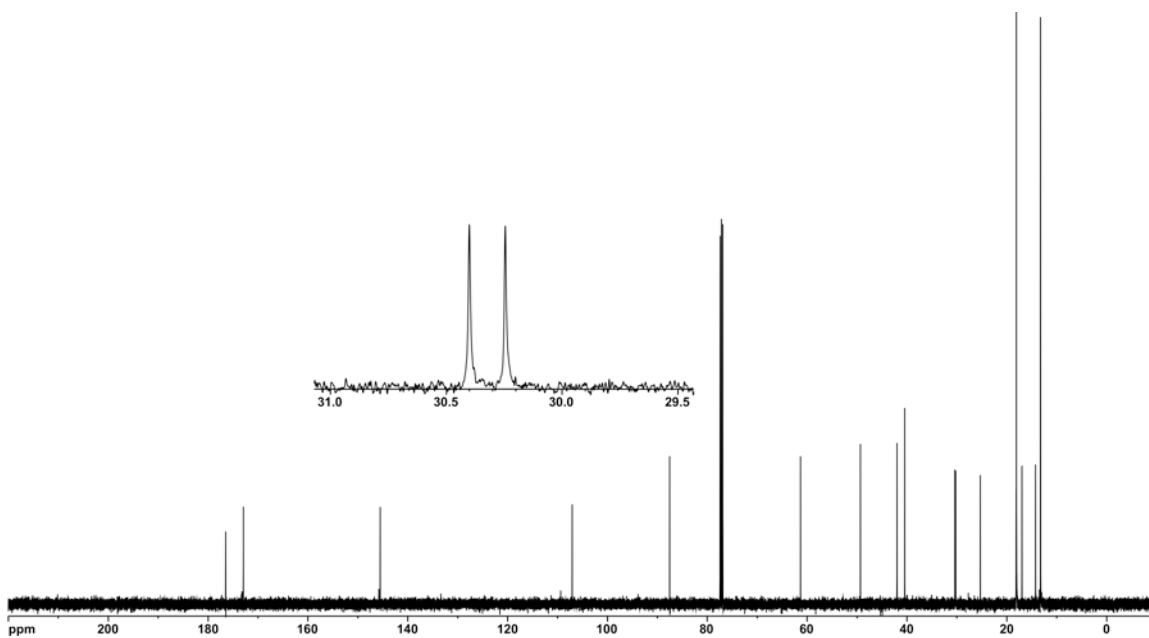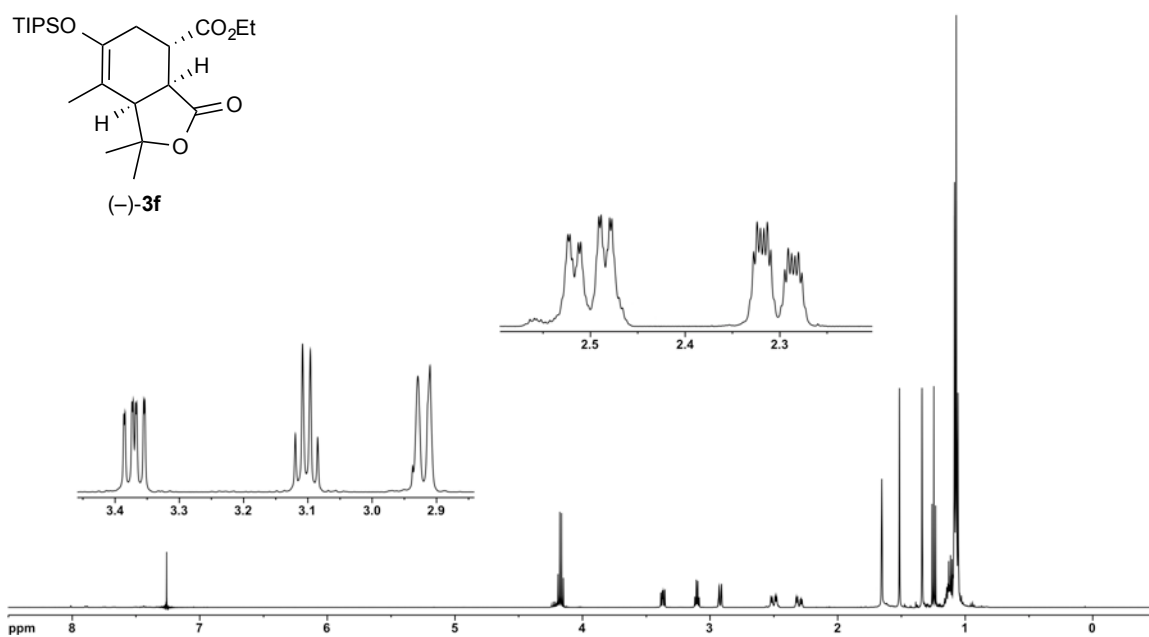
^{1}H (500 MHz) and ^{13}C NMR (125 MHz) spectra of bicyclic γ-lactone (–)-**3f** in CDCl$_3$

TIPSO

(−)-**3g**
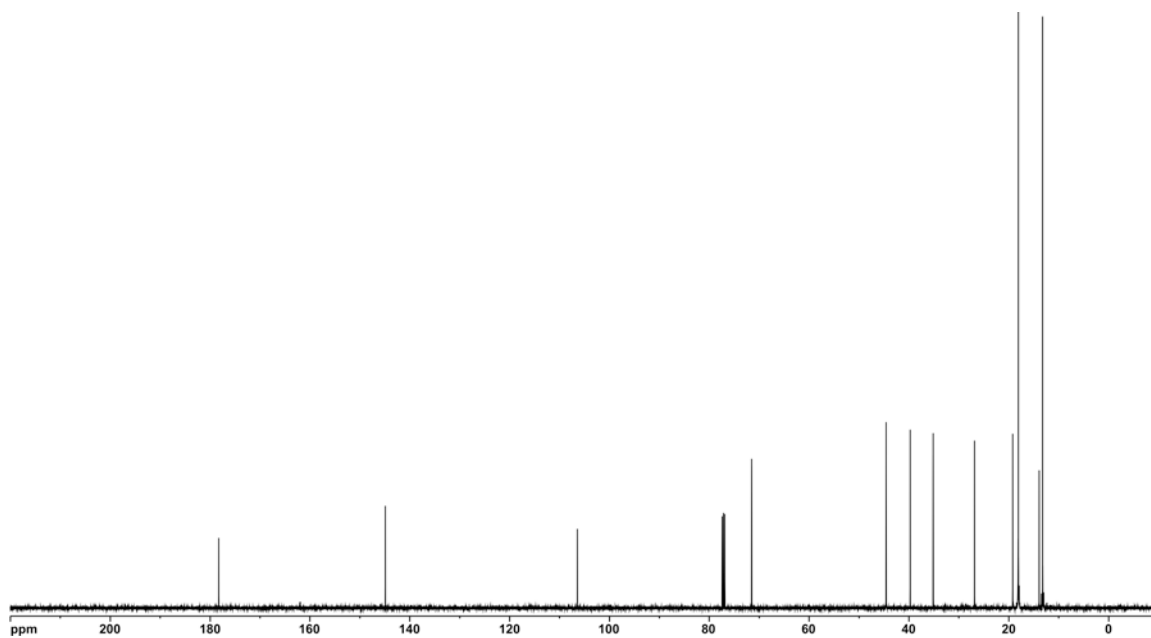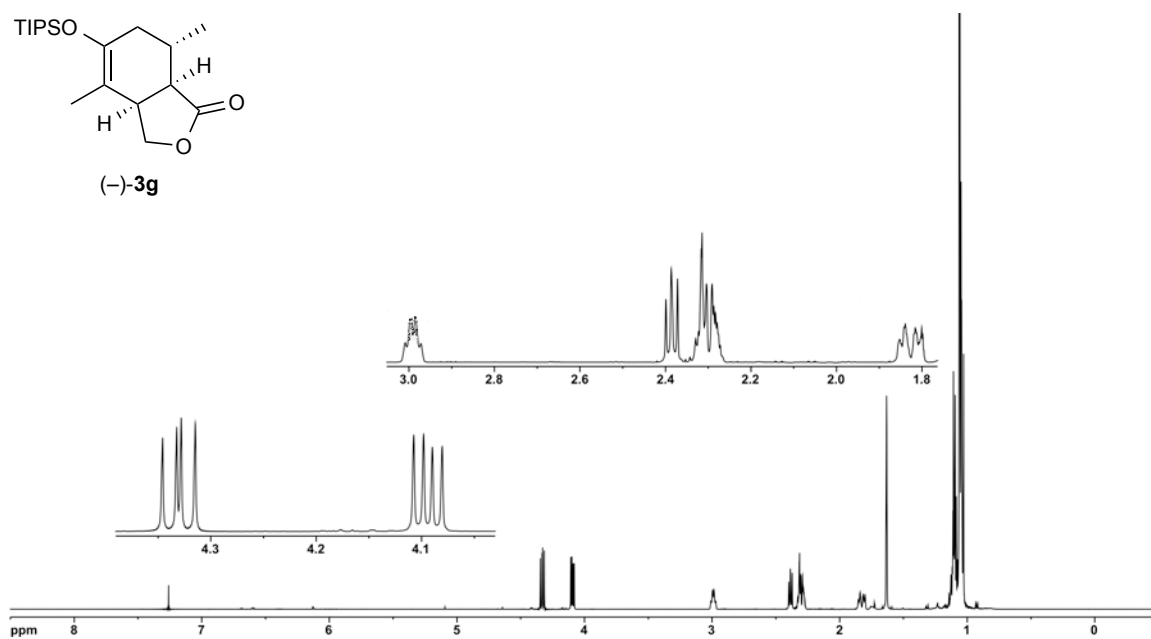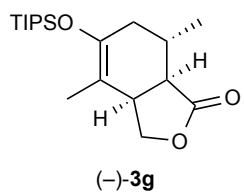
^{1}H (500 MHz) and ^{13}C NMR (125 MHz) spectra of bicyclic γ-lactone (−)-**3g** in CDCl$_3$
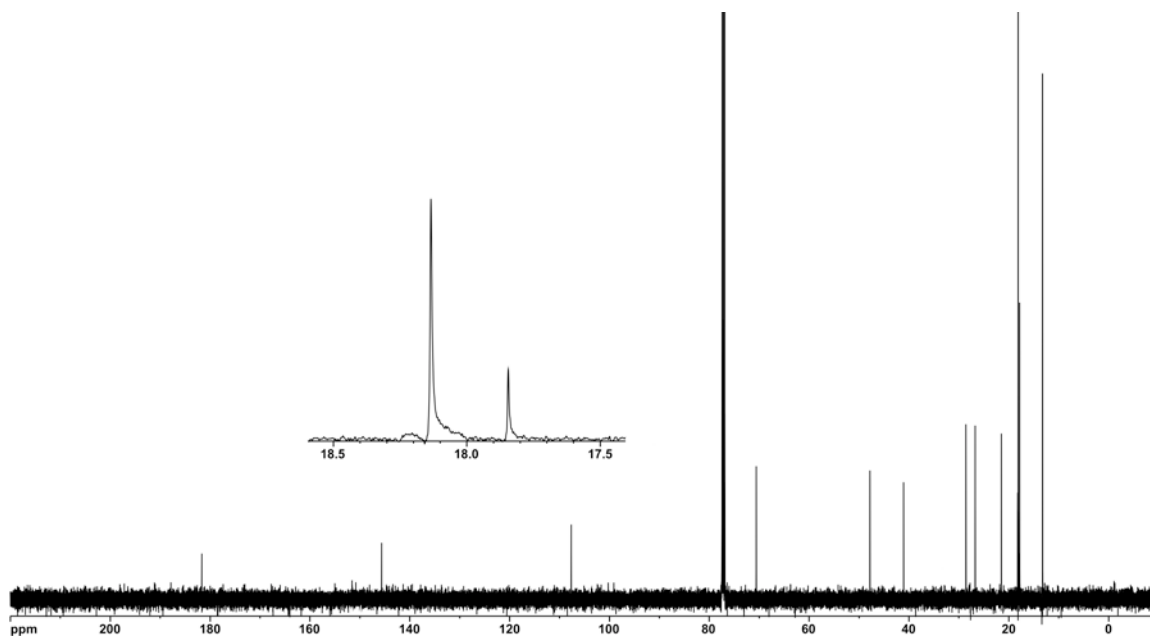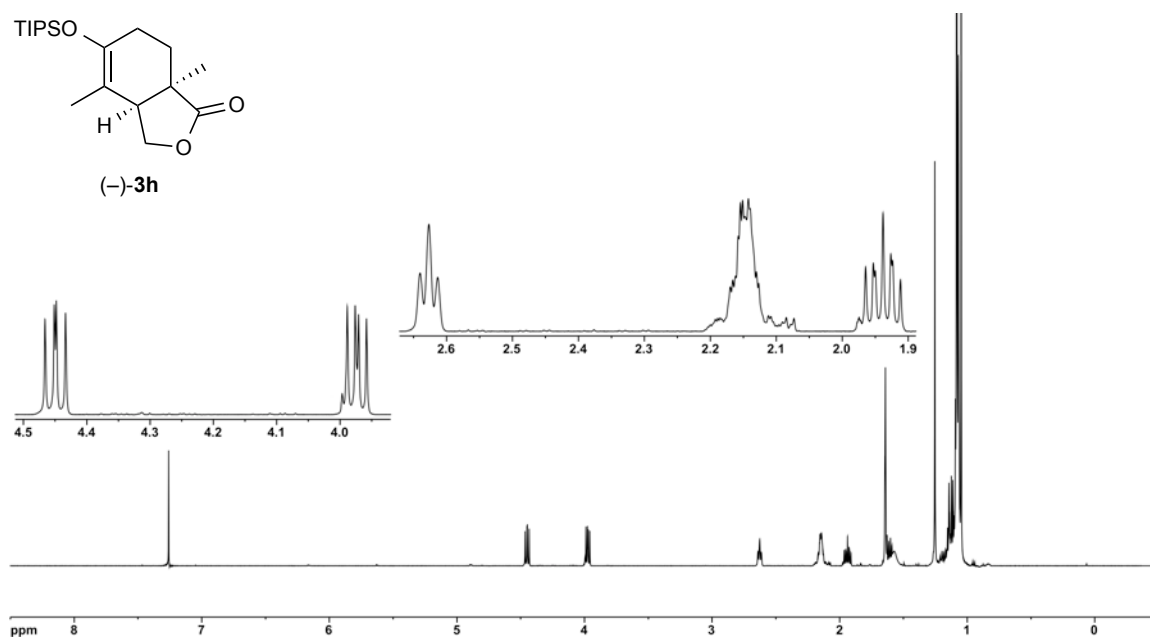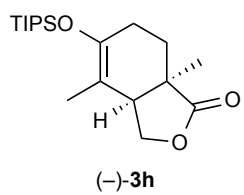
^{1}H (500 MHz) and ^{13}C NMR (125 MHz) spectra of bicyclic γ-lactone (–)-**3h** in CDCl$_3$
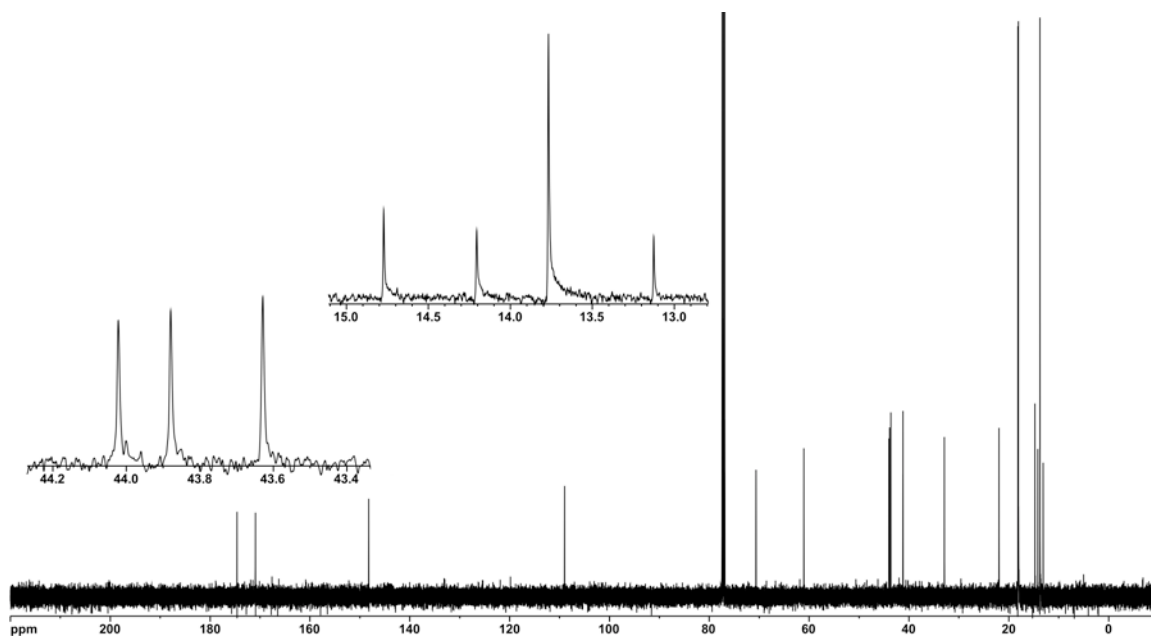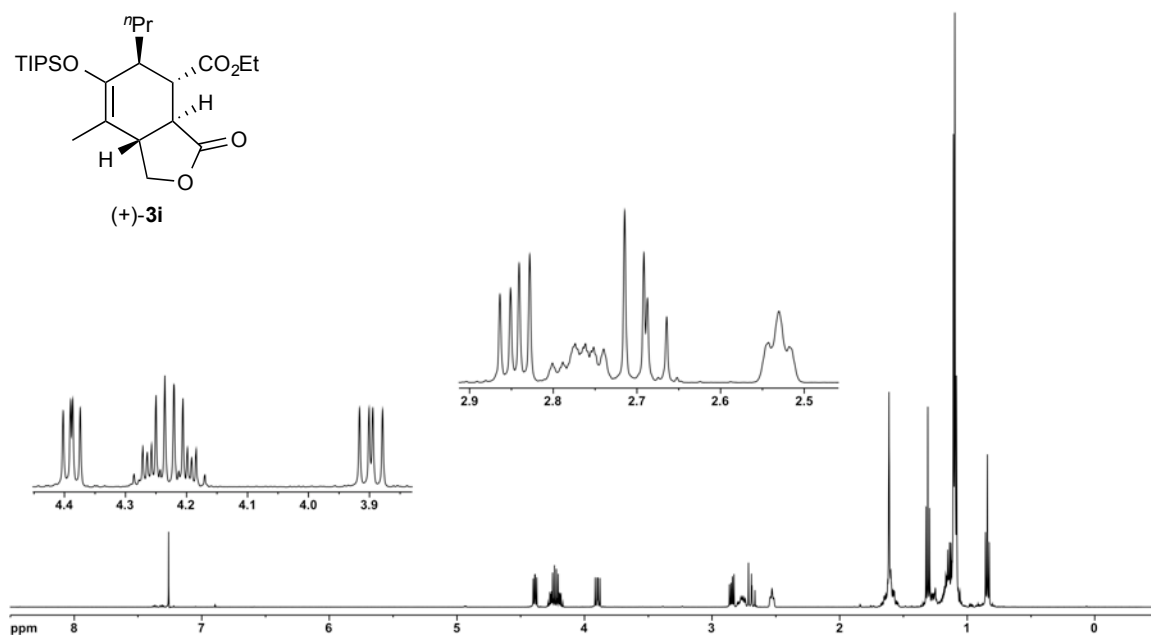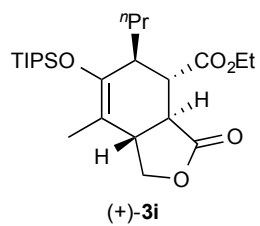
^{1}H (500 MHz) and ^{13}C NMR (125 MHz) spectra of bicyclic γ-lactone (+)-**3i** in CDCl₃
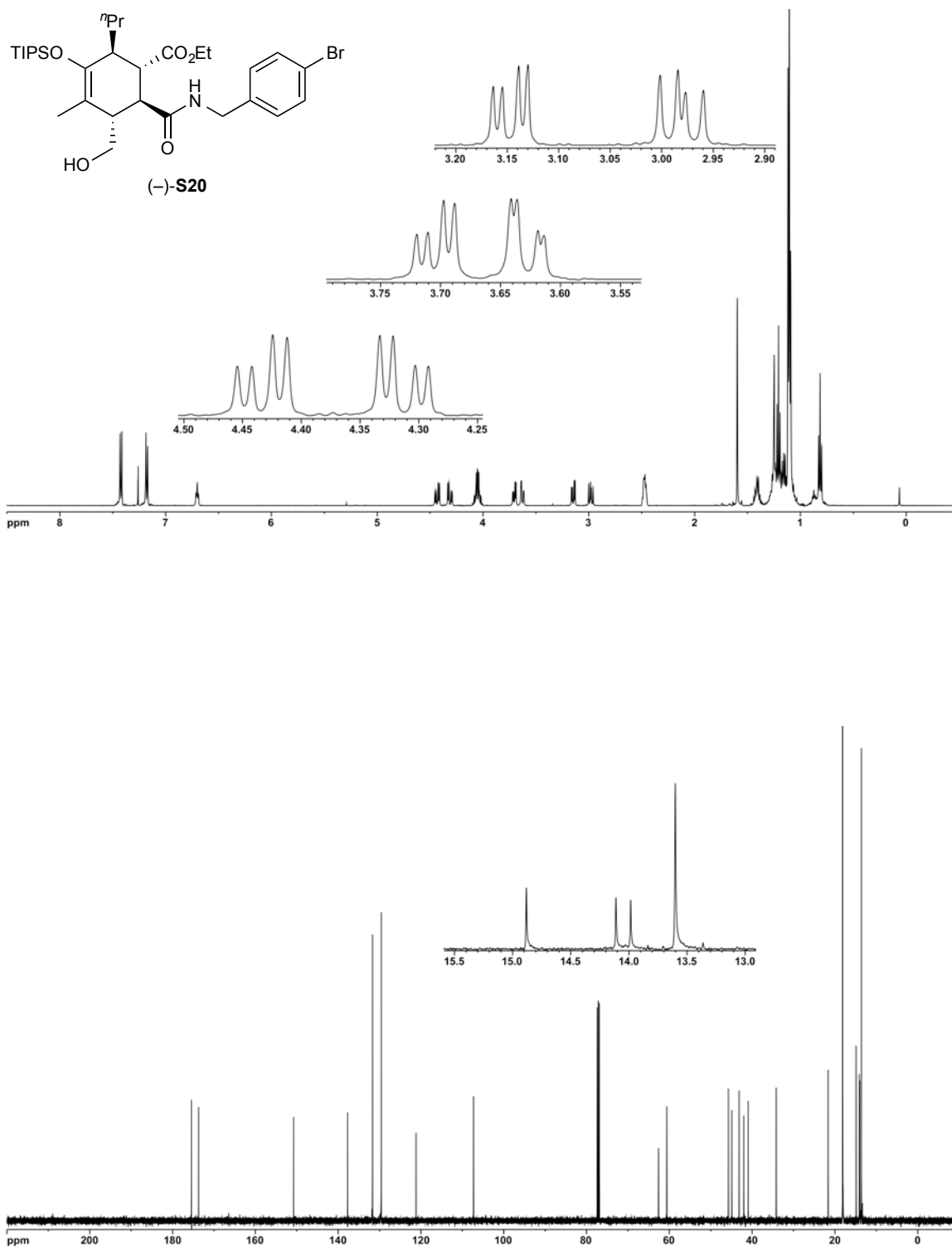
^{1}H (500 MHz) and ^{13}C NMR (125 MHz) spectra of amide (−)-**S20** in CDCl$_3$
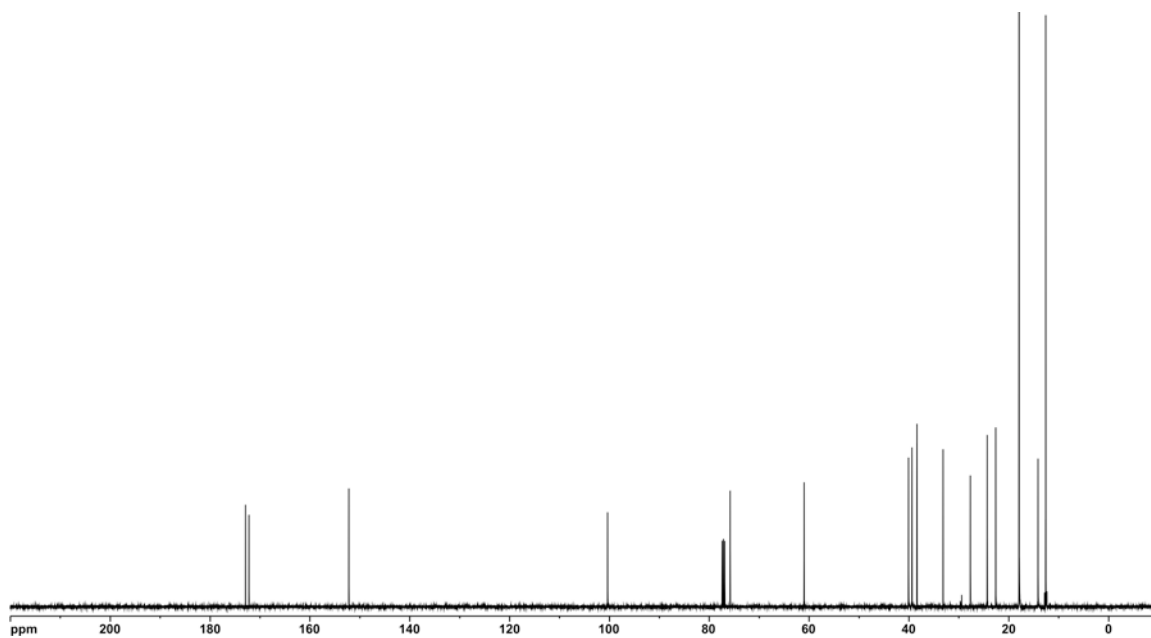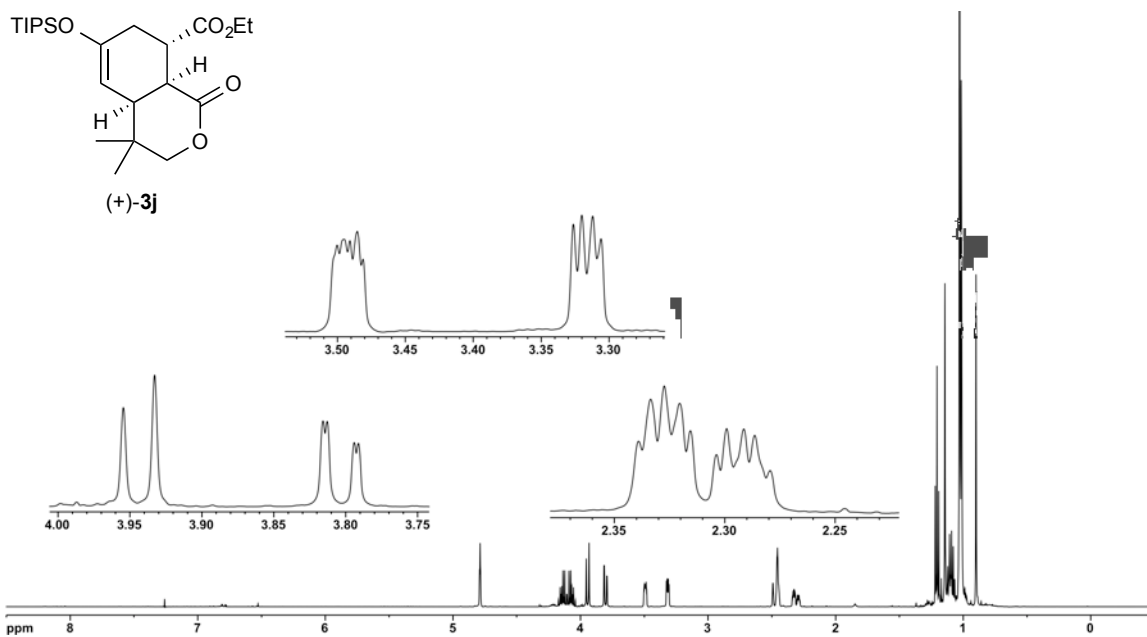
^{1}H (500 MHz) and ^{13}C NMR (125 MHz) spectra of bicyclic δ-lactone (+)-**3j** in CDCl$_3$

^1H (500 MHz) and ^{13}C NMR (125 MHz) spectra of tricyclic γ-lactone (−)-**3k** in CDCl$_3$

177
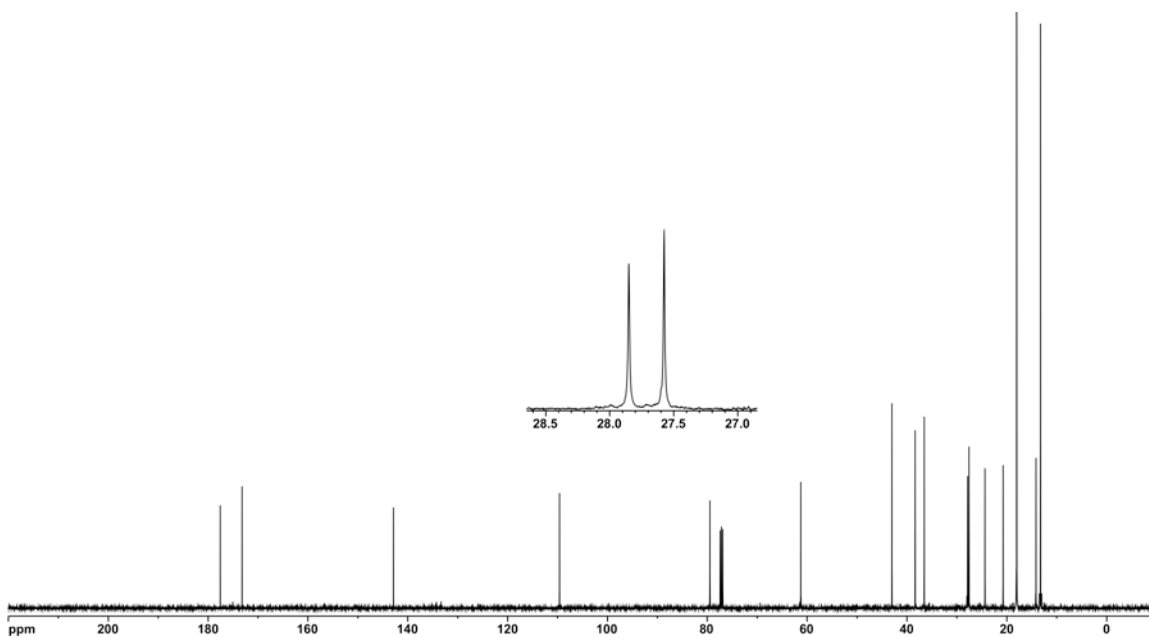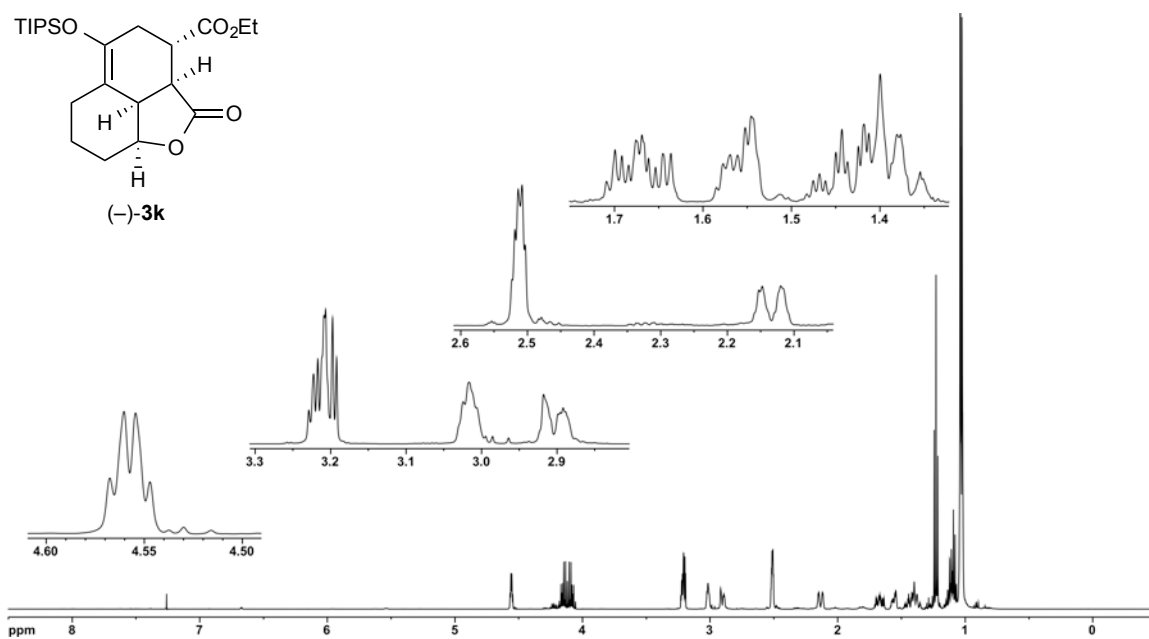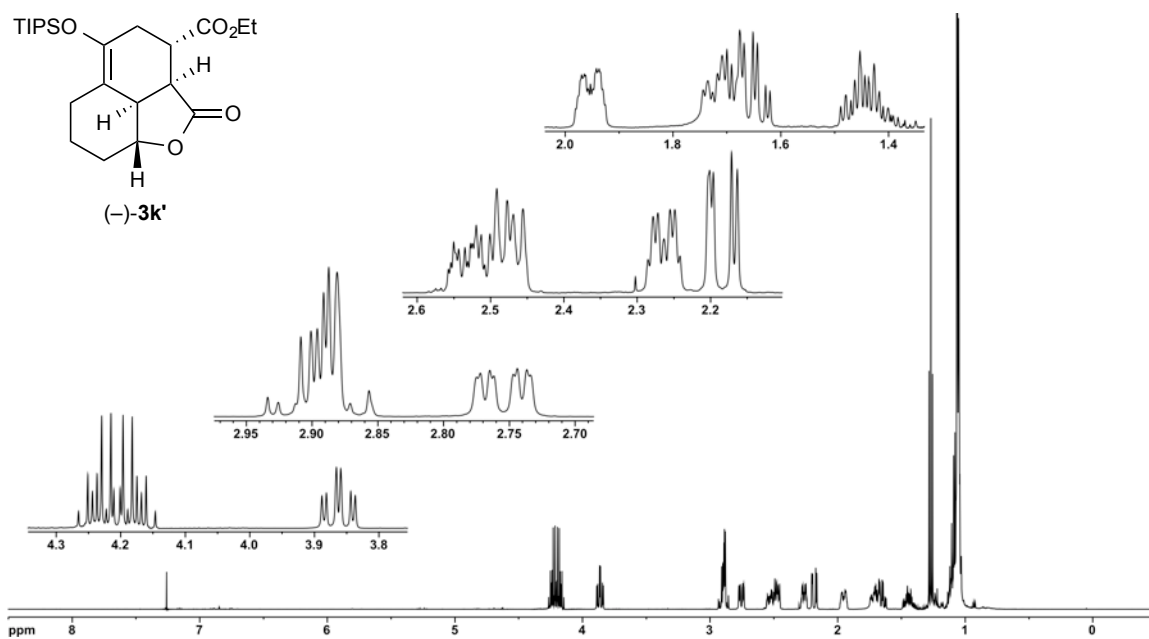
^{1}H (500 MHz) and ^{13}C NMR (125 MHz) spectra of tricyclic γ-lactone (−)-**3k'** in CDCl$_3$
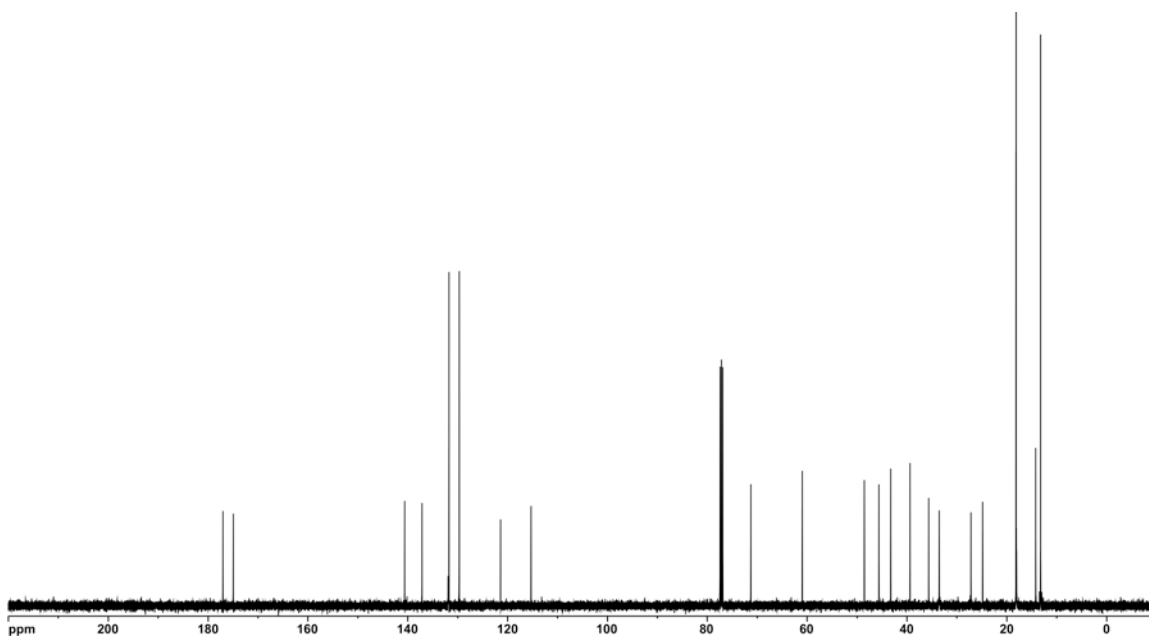
^{1}H (500 MHz) and ^{13}C NMR (125 MHz) spectra of bicyclic amide (–)-**S21** in CDCl$_3$
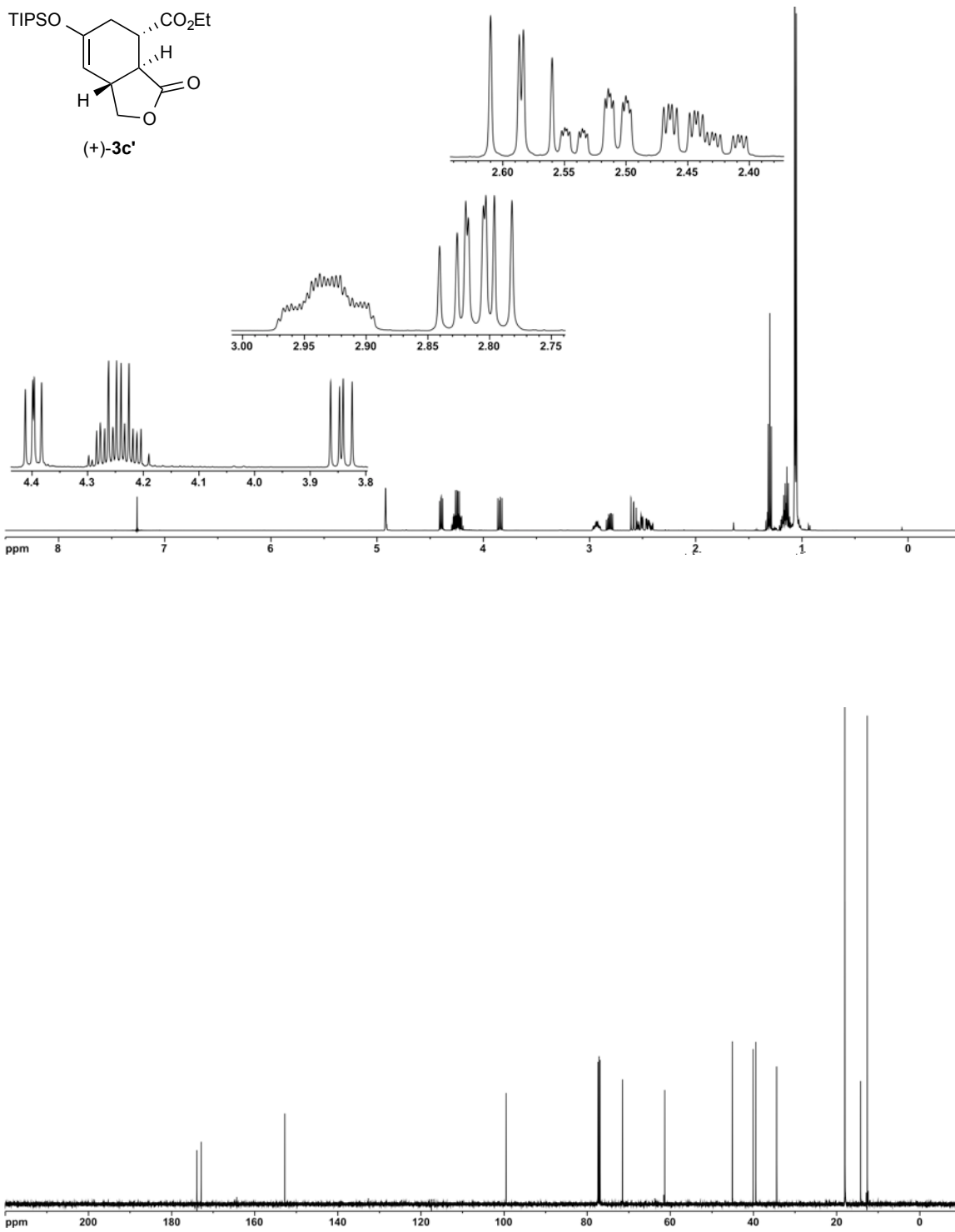
TIPSO, CO₂Et

(+)-3c'

^{1}H (500 MHz) and ^{13}C NMR (125 MHz) spectra of bicyclic γ-lactone (+)-**3c'** in CDCl₃
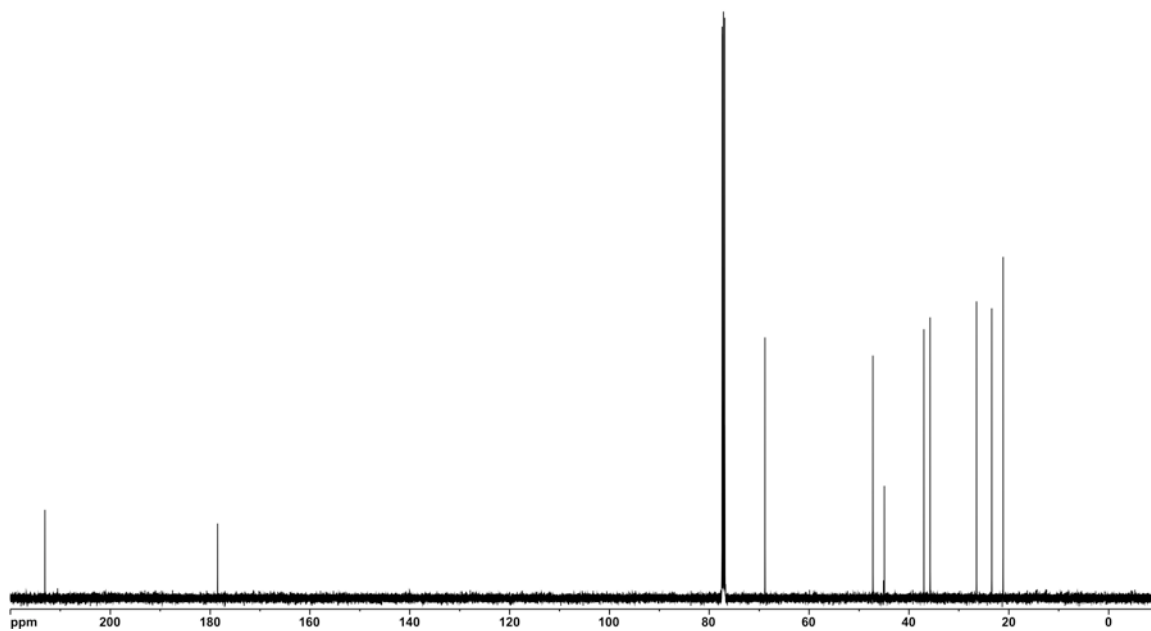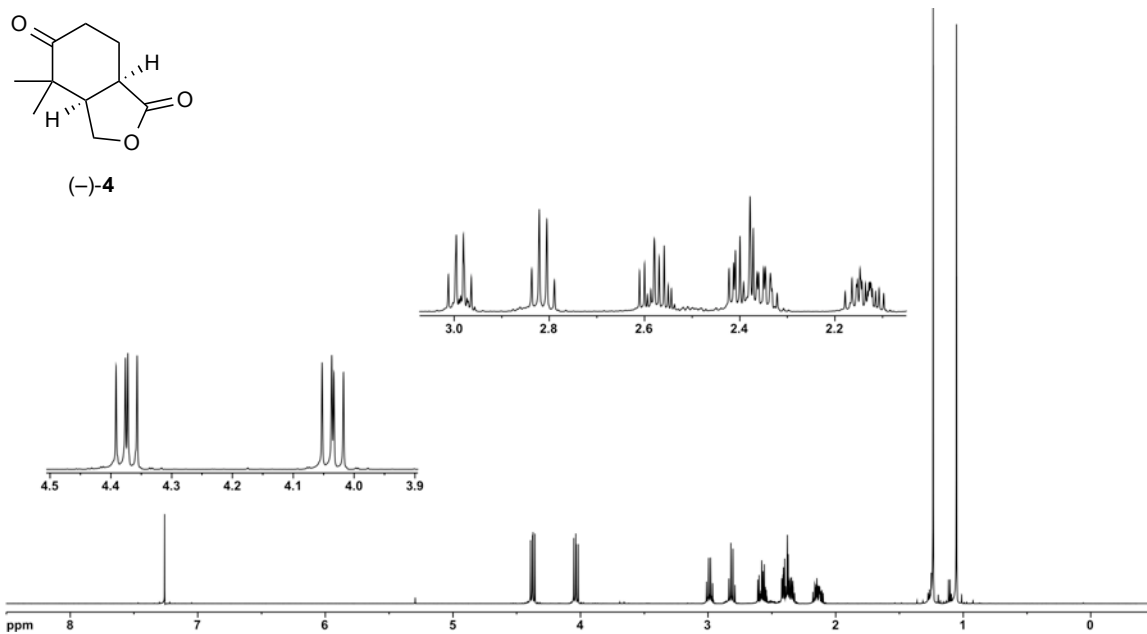
^{1}H (500 MHz) and ^{13}C NMR (125 MHz) spectra of α,α-dimethyl ketone (–)-**4** in CDCl$_3$

^{1}H (500 MHz) and ^{13}C NMR (125 MHz) spectra of enone γ-lactone (–)-**5** in CDCl$_3$

Figure S12. Chiral HPLC determination of enantiomeric excess of bicyclic γ-lactones 3a and 3a':

Chiral HPLC analysis of bicyclic γ-lactone 3a and 3a': Chiralcel OD-H column: hexanes:^{i}PrOH = 95:05, flow rate 0.5 mL/min, λ = 210 nm: t_{major} = 10.3 min, t_{minor} = 10.9 min; 99% *ee*; t_{minor} = 12.7 min, t_{major} = 19.4 min; 99% *ee*.

Table S1, entry 11:
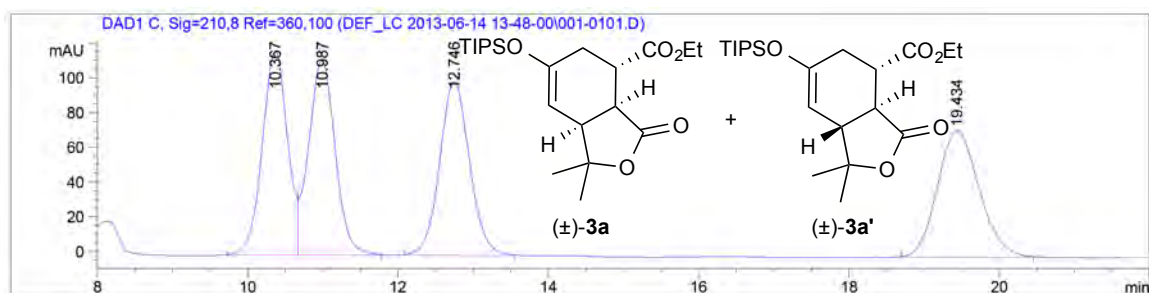
Signal 3: DAD1 C, Sig=210,8 Ref=360,100

Peak #	RetTime [min]	Type	Width [min]	Area [mAU*s]	Height [mAU]	Area %
1	10.367	BV	0.3620	2754.59033	117.28511	24.8423
2	10.987	VB	0.3772	2763.33936	112.26688	24.9212
3	12.746	BB	0.4276	2769.97803	99.87013	24.9811
4	19.434	BB	0.5993	2800.39136	72.71989	25.2554

Totals : 1.10883e4 402.14201
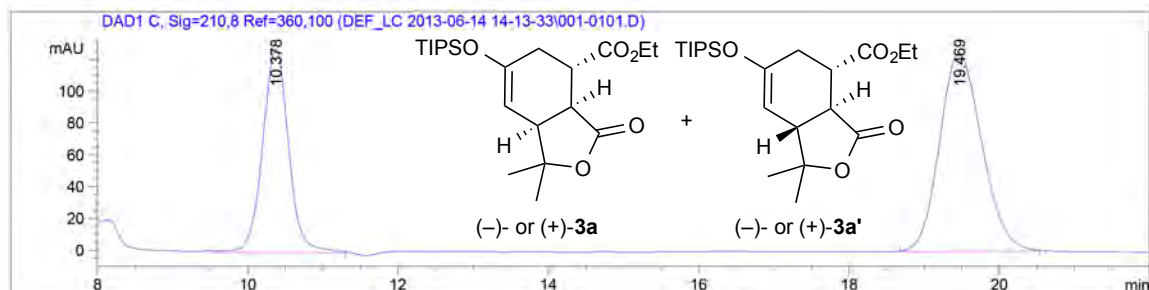
Signal 3: DAD1 C, Sig=210,8 Ref=360,100

Peak #	RetTime [min]	Type	Width [min]	Area [mAU*s]	Height [mAU]	Area %
1	10.378	MM	0.4019	3085.39746	127.96414	38.8161
2	19.469	BB	0.6070	4863.35352	124.70683	61.1839

Totals : 7948.75098 252.67097

Figure S13. Chiral HPLC determinations of enantiomeric excess of bicyclic lactones 3b-j:

Determination of enantiomeric excess of bicyclic γ-lactone (–)-3b:

Chiral HPLC analysis of bicyclic γ-lactone (–)-3b: Chiralcel OD-H column: hexanes:^{i}PrOH = 98:02, flow rate 0.5 mL/min, λ = 210 nm: t_{major} = 15.9 min, t_{minor} = 17.9 min; 94% *ee*.
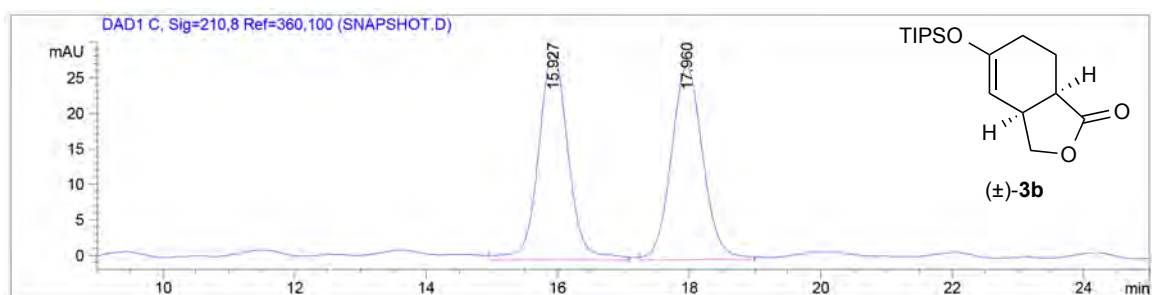

```
Signal 3: DAD1 C, Sig=210,8 Ref=360,100

Peak RetTime Type  Width      Area      Height     Area
  #   [min]        [min]    [mAU*s]      [mAU]       %
----|-------|----|-------|-----------|-----------|--------|
  1  15.927 VB    0.4815  914.27545   29.18653   50.2026
  2  17.960 BB    0.5175  906.89441   27.16312   49.7974

Totals :                 1821.16986   56.34965
```
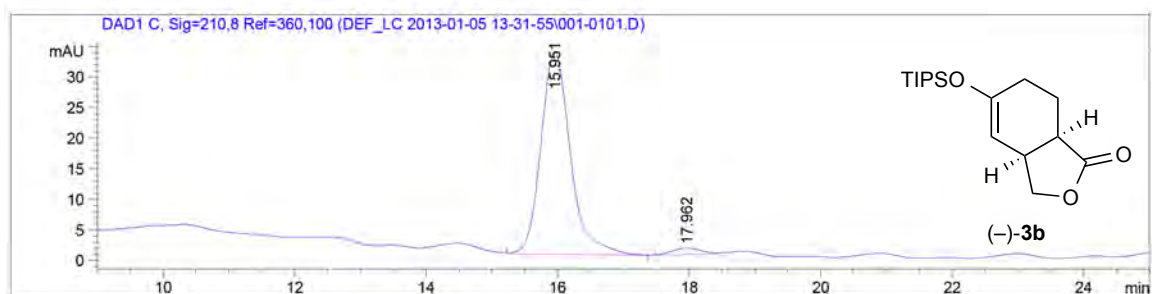


```
Signal 3: DAD1 C, Sig=210,8 Ref=360,100

Peak RetTime Type  Width      Area      Height     Area
  #   [min]        [min]    [mAU*s]      [mAU]       %
----|-------|----|-------|-----------|-----------|--------|
  1  15.951 MM    0.5203 1032.26636   33.06614   97.0640
  2  17.962 MM    0.5113   31.22353    1.01772    2.9360

Totals :                 1063.48989   34.08386
```

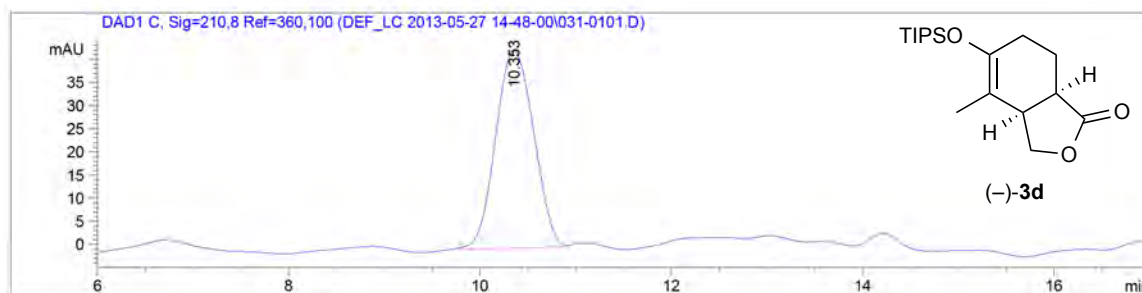**Determination of enantiomeric excess of bicyclic γ-lactone (–)-3c:**

Chiral HPLC analysis of bicyclic γ-lactone (–)-3c: Chiralcel OD-H column: hexanes:^{i}PrOH = 95:05, flow rate 0.5 mL/min, λ = 210 nm: t_{minor} = 15.4 min, t_{major} = 18.1 min; 99% *ee* (using 20 mol% (*S*)-(–)-BTM), 98% *ee* (using 10 mol% (*S*)-(–)-BTM).
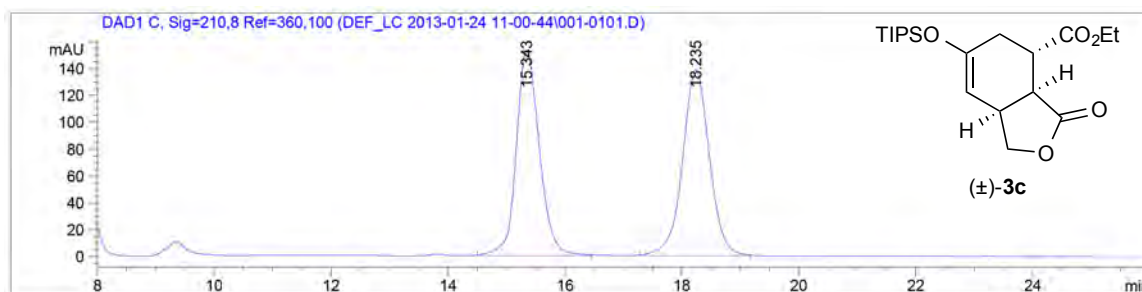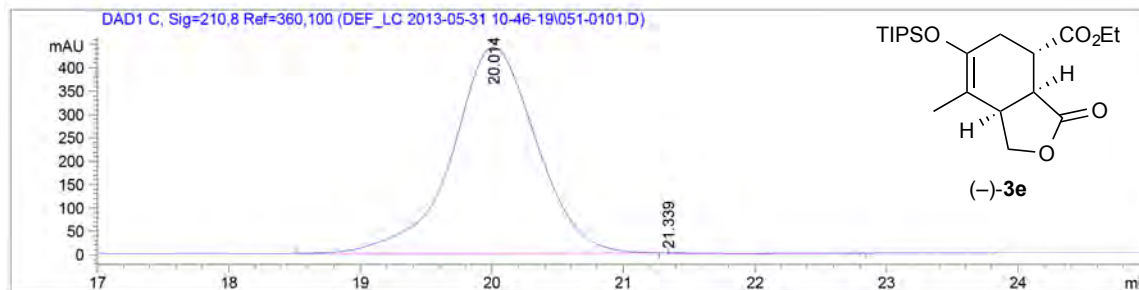

Signal 3: DAD1 C, Sig=210,8 Ref=360,100

Peak #	RetTime [min]	Type	Width [min]	Area [mAU*s]	Height [mAU]	Area %
1	15.343	MM	0.4858	4449.61182	152.66600	50.1120
2	18.235	BB	0.4896	4429.72021	138.32141	49.8880

Totals :   8879.33203 290.98741

Using 20 mol% (*S*)-(–)-BTM:
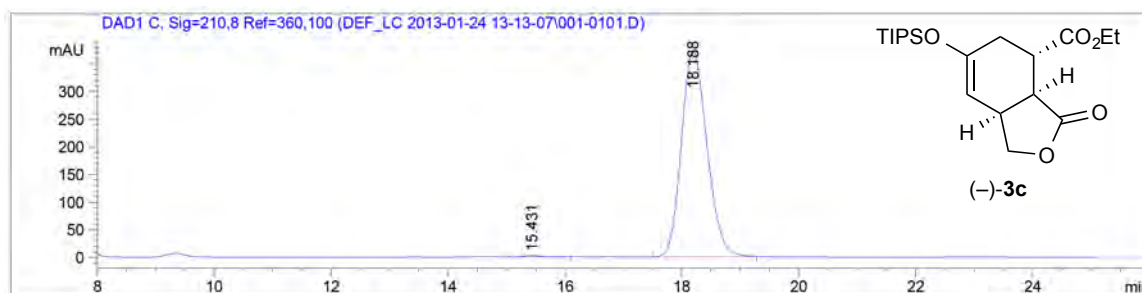
Signal 3: DAD1 C, Sig=210,8 Ref=360,100

Peak #	RetTime [min]	Type	Width [min]	Area [mAU*s]	Height [mAU]	Area %
1	15.431	BB	0.3303	52.56739	2.53123	0.4602
2	18.188	BB	0.4743	1.13713e4	372.35049	99.5398

Totals :   1.14239e4 374.88173

Using 10 mol% (*S*)-(–)-BTM:
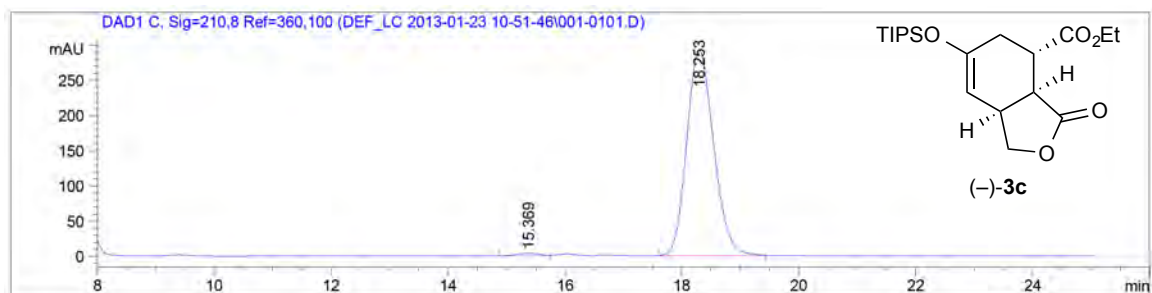
Signal 3: DAD1 C, Sig=210,8 Ref=360,100

```
Peak RetTime Type  Width     Area       Height      Area
 #   [min]          [min]   [mAU*s]     [mAU]         %
----|-------|----|-------|----------|-----------|--------|
  1  15.369  BV   0.4333    99.30708    3.37506   1.0494
  2  18.253  BB   0.4961  9363.54004  292.00168  98.9506

Totals :                  9462.84712  295.37674
```

Determination of enantiomeric excess of bicyclic γ-lactone (–)-3d:

Chiral HPLC analysis of bicyclic γ-lactone (–)-3d: Chiralcel AS-H column: hexanes:*i*PrOH = 99:01, flow rate 1.0 mL/min, λ = 210 nm: t_{major} = 10.3 min, t_{minor} = 11.5 min; 99% *ee*.
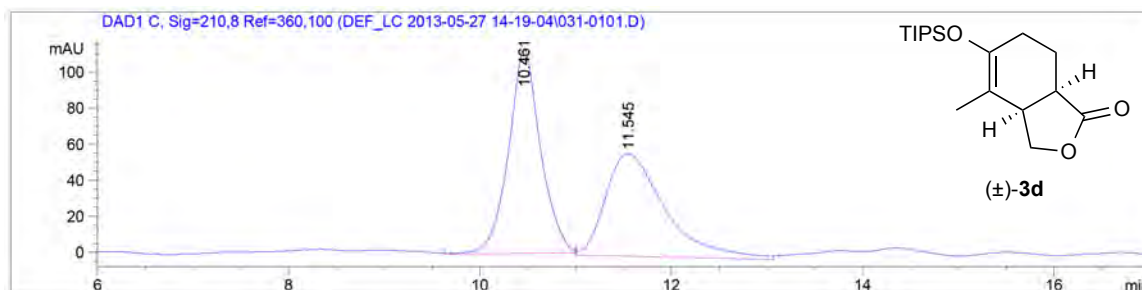
Signal 3: DAD1 C, Sig=210,8 Ref=360,100

Peak #	RetTime [min]	Type	Width [min]	Area [mAU*s]	Height [mAU]	Area %
1	10.461	MM	0.3872	2622.94019	112.89551	51.7560
2	11.545	MM	0.7187	2444.95142	56.69883	48.2440

Totals : 5067.89160 169.59433

Signal 3: DAD1 C, Sig=210,8 Ref=360,100

Peak #	RetTime [min]	Type	Width [min]	Area [mAU*s]	Height [mAU]	Area %
1	10.353	BV	0.4441	1179.79602	42.73602	100.0000

Totals : 1179.79602 42.73602

187

Determination of enantiomeric excess of bicyclic γ-lactone (–)-3e:

**Chiral HPLC analysis of bicyclic γ-lactone (–)-3e:** Chiralcel OD-H column: hexanes:^{i}PrOH = 98:02, flow rate 0.4 mL/min, λ = 210 nm: t_{major} = 20.0 min, t_{minor} = 21.3 min; 99% *ee*.
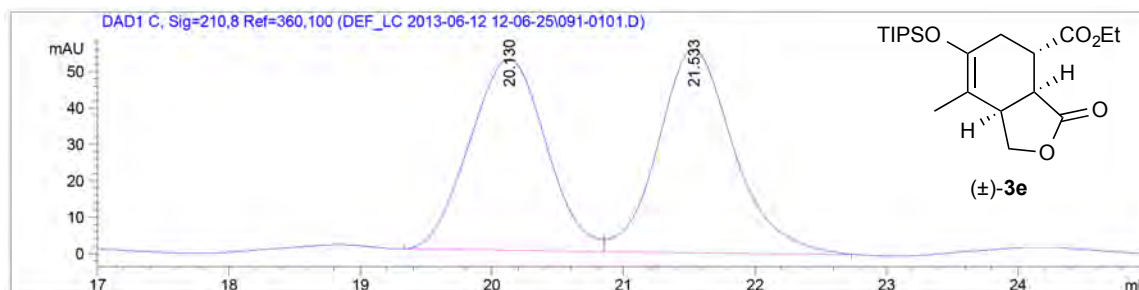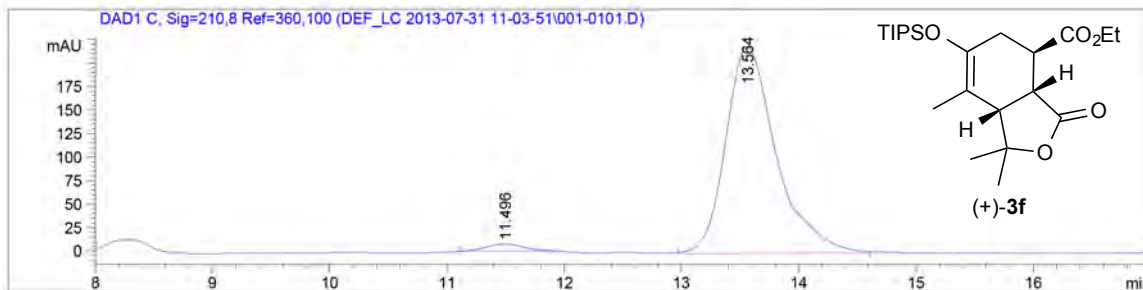

Signal 3: DAD1 C, Sig=210,8 Ref=360,100

Peak #	RetTime [min]	Type	Width [min]	Area [mAU*s]	Height [mAU]	Area %
1	20.130	BV	0.6185	2121.67554	52.60606	48.6533
2	21.533	VB	0.6094	2239.12891	55.88930	51.3467

Totals :   4360.80444 108.49536

Signal 3: DAD1 C, Sig=210,8 Ref=360,100

Peak #	RetTime [min]	Type	Width [min]	Area [mAU*s]	Height [mAU]	Area %
1	20.014	BB	0.6478	1.96563e4	441.19595	99.8988
2	21.339	MM	0.1555	19.91752	1.55744	0.1012

Totals :   1.96762e4 442.75339

Determination of enantiomeric excess of bicyclic γ-lactone (–)-3f:

Chiral HPLC analysis of bicyclic γ-lactone (–)-3f: Chiralcel OD-H column: hexanes:^{i}PrOH = 95:05, flow rate 0.5 mL/min, λ = 210 nm: t_{major} = 11.6 min, t_{minor} = 13.6 min; 98% *ee*.


```
Signal 3: DAD1 C, Sig=210,8 Ref=360,100

Peak RetTime Type  Width      Area        Height     Area
  #   [min]        [min]    [mAU*s]      [mAU]        %
----|-------|----|-------|----------|-----------|--------|
  1  11.609  BB   0.3884 3964.71484  156.04489  50.1639
  2  13.645  BV   0.4256 3938.81152  142.89645  49.8361

Totals :                 7903.52637  298.94135
```
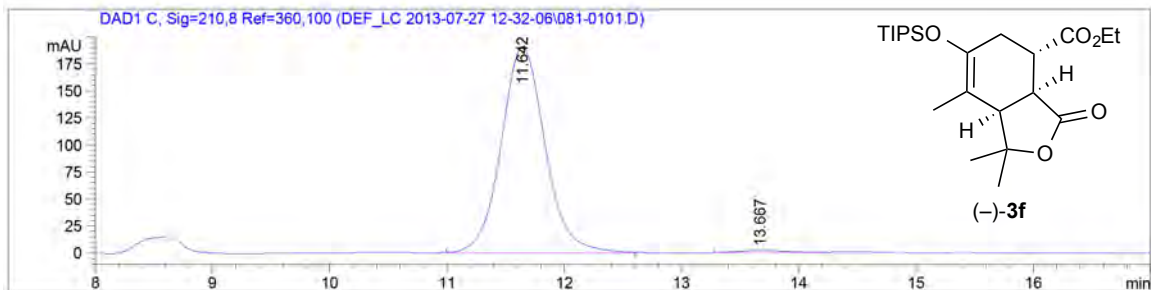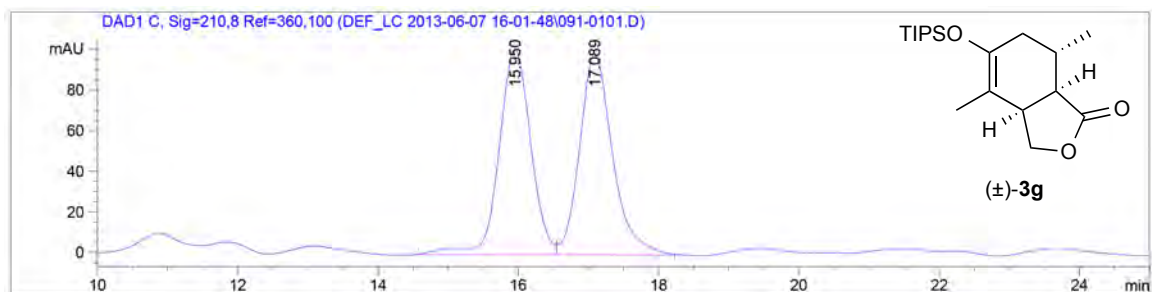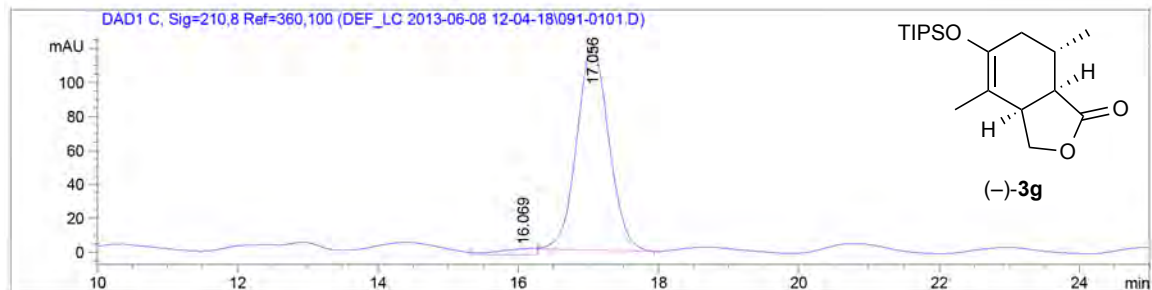


```
Signal 3: DAD1 C, Sig=210,8 Ref=360,100

Peak RetTime Type  Width      Area        Height     Area
  #   [min]        [min]    [mAU*s]      [mAU]        %
----|-------|----|-------|----------|-----------|--------|
  1  11.642  BB   0.3965 4945.87793  190.72485  99.0991
  2  13.667  BB   0.2957   44.95997    1.87553   0.9009

Totals :                 4990.83790  192.60038
```

Determination of enantiomeric excess of bicyclic γ-lactone (+)-3f:

Chiral HPLC analysis of bicyclic γ-lactone (+)-3f: Chiralcel OD-H column: hexanes:^{i}PrOH = 95:05, flow rate 0.5 mL/min, λ = 210 nm: t_{minor} = 11.4 min, t_{major} = 13.5 min; 96% *ee*.


```
Signal 3: DAD1 C, Sig=210,8 Ref=360,100

Peak RetTime Type  Width     Area       Height     Area
 #   [min]        [min]    [mAU*s]     [mAU]       %
----|-------|----|-------|-----------|-----------|--------|
  1  11.609 BB   0.3884 3964.71484  156.04489   50.1639
  2  13.645 BV   0.4256 3938.81152  142.89645   49.8361

Totals :                7903.52637  298.94135
```



```
Signal 3: DAD1 C, Sig=210,8 Ref=360,100

Peak RetTime Type  Width     Area       Height     Area
 #   [min]        [min]    [mAU*s]     [mAU]       %
----|-------|----|-------|-----------|-----------|--------|
  1  11.496 MM   0.3682  165.08434    7.47177    2.1938
  2  13.564 MM   0.5582 7359.91846  219.76448   97.8062

Totals :                7525.00279  227.23625
```

Determination of enantiomeric excess of bicyclic γ-lactone (–)-3g:

**Chiral HPLC analysis of bicyclic γ-lactone (–)-3g:** Chiralcel OD-H column: hexanes:^{i}PrOH = 98:02, flow rate 0.5 mL/min, λ = 210 nm: t_{minor} = 16.0 min, t_{major} = 17.0 min; 95% *ee*.

Signal 3: DAD1 C, Sig=210,8 Ref=360,100

```
Peak RetTime Type  Width     Area        Height      Area
 #   [min]        [min]    [mAU*s]      [mAU]         %
----|-------|----|-------|----------|----------|--------|
 1  15.950 BV    0.4880 3186.13794  101.00188  49.7150
 2  17.089 VB    0.5011 3222.66260   98.14114  50.2850

Totals :               6408.80054  199.14302
```


Signal 3: DAD1 C, Sig=210,8 Ref=360,100

```
Peak RetTime Type  Width     Area        Height      Area
 #   [min]        [min]    [mAU*s]      [mAU]         %
----|-------|----|-------|----------|----------|--------|
 1  16.069 MM    0.6625   87.59249    2.20367   2.2516
 2  17.056 BB    0.4934 3802.59204  119.45309  97.7484

Totals :               3890.18453  121.65676
```

Determination of enantiomeric excess of bicyclic γ-lactone (–)-3h:

Chiral HPLC analysis of bicyclic γ-lactone (–)-3h: Chiralcel AS-H column: hexanes:^{i}PrOH = 98:02, flow rate 0.5 mL/min, λ = 210 nm: t_{major} = 11.8 min, t_{minor} = 14.0 min; 91% *ee*.
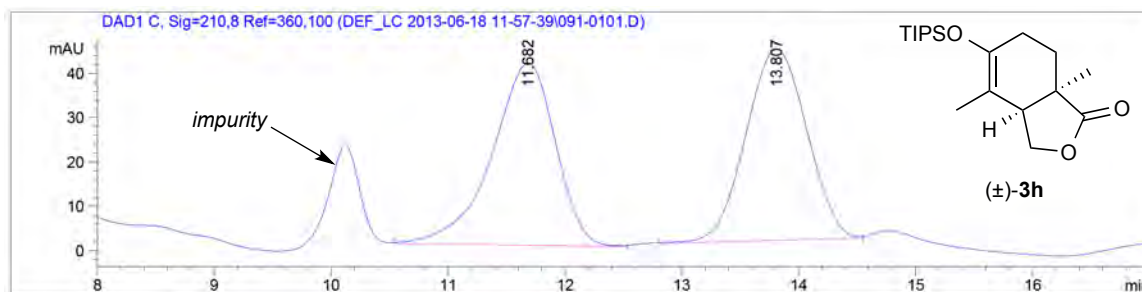

```
Signal 3: DAD1 C, Sig=210,8 Ref=360,100

Peak RetTime Type  Width     Area      Height     Area
  #   [min]        [min]    [mAU*s]    [mAU]        %
----|-------|----|-------|----------|----------|--------|
  1  11.682 MM   0.6297 1554.04358   41.13143   49.8886
  2  13.807 MM   0.6046 1560.98486   43.03236   50.1114

Totals :                3115.02844   84.16378
```
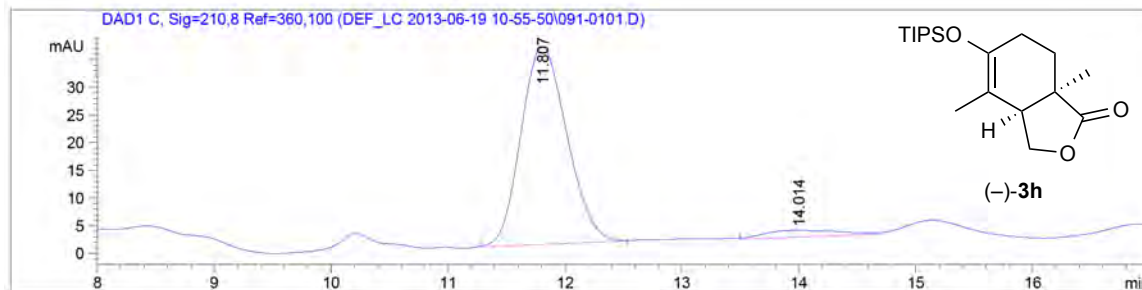


```
Signal 3: DAD1 C, Sig=210,8 Ref=360,100

Peak RetTime Type  Width     Area      Height     Area
  #   [min]        [min]    [mAU*s]    [mAU]        %
----|-------|----|-------|----------|----------|--------|
  1  11.807 BB   0.5004 9266.48242  290.29224   95.5840
  2  14.014 BB   0.7472  428.11127    9.54867    4.4160

Totals :                9694.59369  299.84090
```

Determination of enantiomeric excess of bicyclic γ-lactone (+)-3i:

**Chiral HPLC analysis of bicyclic γ-lactone (+)-3i:** Chiralcel AD-H column: hexanes:^{i}PrOH = 95:05, flow rate 0.5 mL/min, λ = 210 nm: t_{major} = 11.4 min, t_{minor} = 12.8 min; 99% *ee* (using 20 mol% (*S*)-(–)-BTM), 97% *ee* (using 5 mol% (*S*)-(–)-BTM).
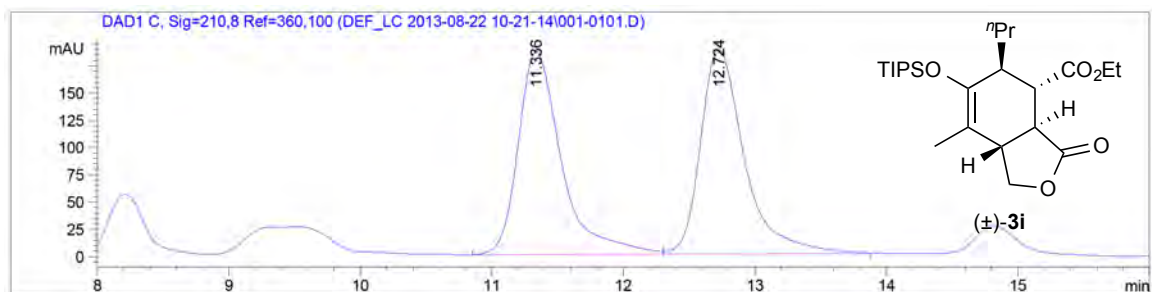
Signal 3: DAD1 C, Sig=210,8 Ref=360,100

```
Peak RetTime Type  Width     Area       Height      Area
  #   [min]        [min]    [mAU*s]     [mAU]        %
----|-------|----|-------|-----------|-----------|--------|
  1  11.336 BV   0.3475 4267.38916  186.10463   49.4355
  2  12.724 VB   0.3557 4364.84277  187.40324   50.5645

Totals :               8632.23193   373.50787
```

Using 20 mol% (*S*)-(–)-BTM:
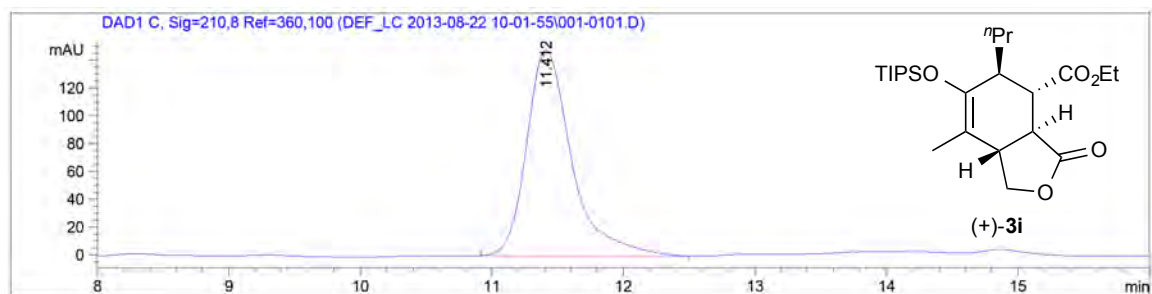
Signal 3: DAD1 C, Sig=210,8 Ref=360,100

```
Peak RetTime Type  Width     Area       Height      Area
  #   [min]        [min]    [mAU*s]     [mAU]        %
----|-------|----|-------|-----------|-----------|--------|
  1  11.412 BB   0.3652 3537.73755  147.84750 100.0000

Totals :               3537.73755   147.84750
```

Using 5 mol% (*S*)-(–)-BTM:
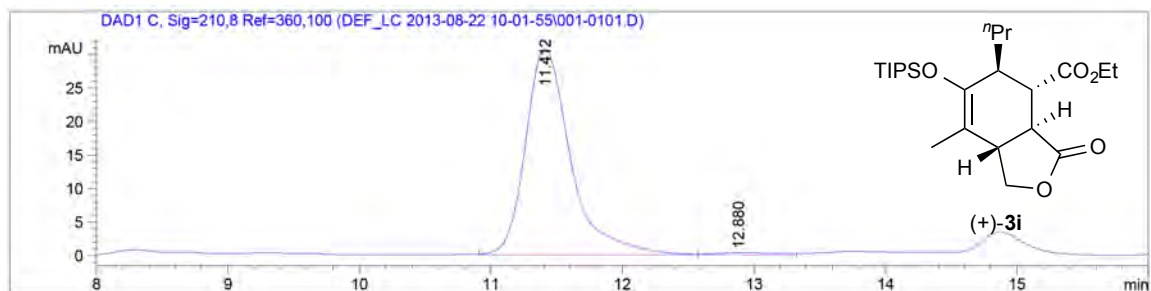
Signal 3: DAD1 C, Sig=210,8 Ref=360,100

```
Peak  RetTime Type  Width     Area       Height     Area
  #    [min]        [min]    [mAU*s]     [mAU]        %
----|-------|----|-------|----------|----------|--------|
  1   11.412 BV    0.3628  733.42120   30.69212  98.4827
  2   12.880 VB    0.3948   11.29927 3.44362e-1   1.5173

Totals :                   744.72048   31.03648
```

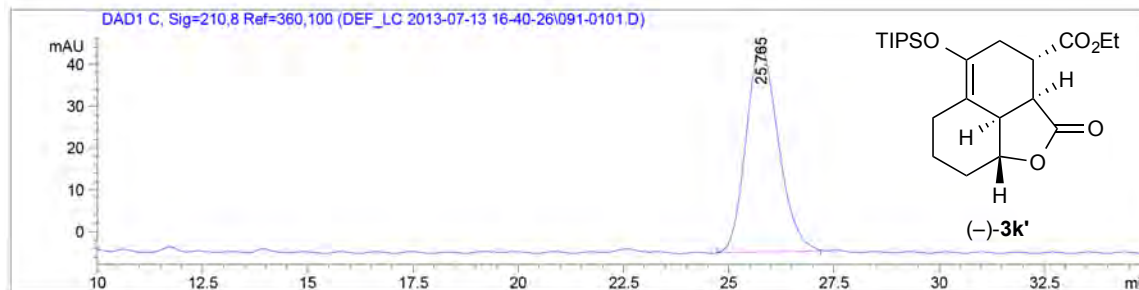**Determination of enantiomeric excess of bicyclic δ-lactone (+)-3j:**

Chiral HPLC analysis of bicyclic δ-lactone (+)-3j: Chiralcel OD-H column: hexanes:^{i}PrOH = 95:05, flow rate 0.5 mL/min, λ = 210 nm: t_{minor} = 10.7 min, t_{major} = 12.5 min; 92% *ee*.
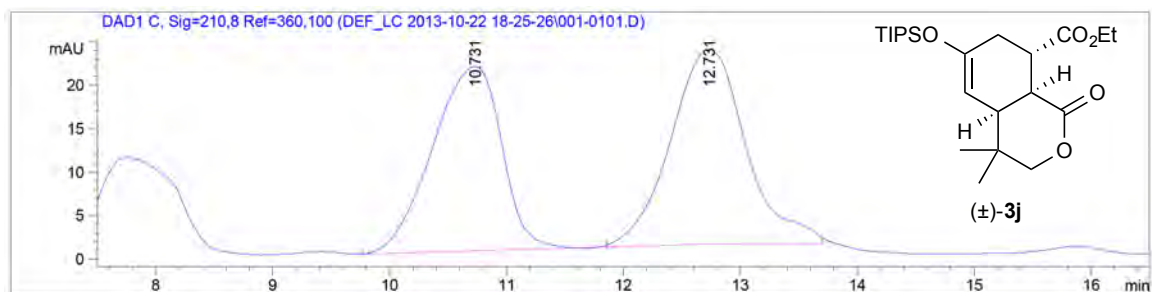
Signal 3: DAD1 C, Sig=210,8 Ref=360,100

```
Peak RetTime Type  Width     Area       Height     Area
 #    [min]        [min]    [mAU*s]     [mAU]        %
----|-------|----|-------|----------|----------|--------|
  1  10.731 BB   0.6469  868.67236   21.16243  48.0105
  2  12.731 BV   0.6094  940.66602   22.33294  51.9895

Totals :                1809.33838   43.49536
```
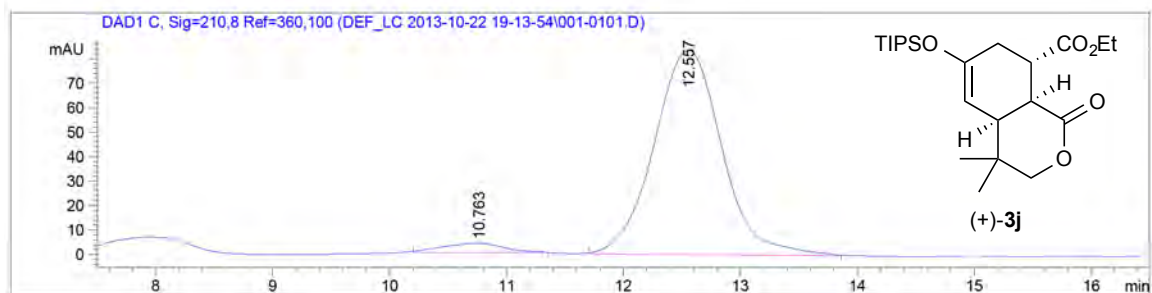

Signal 3: DAD1 C, Sig=210,8 Ref=360,100

```
Peak RetTime Type  Width     Area       Height     Area
 #    [min]        [min]    [mAU*s]     [mAU]        %
----|-------|----|-------|----------|----------|--------|
  1  10.763 MM   0.5989  131.20264    3.65145   3.7611
  2  12.557 BB   0.6211 3357.17163   83.48924  96.2389

Totals :                3488.37427   87.14069
```

195

Figure S14. Chiral HPLC determinations of enantiomeric excess of lactones 3k, 3k' and 3c':

**Determination of enantiomeric excess of tricyclic γ-lactone (–)-3k:**

Chiral HPLC analysis of tricyclic γ-lactone (–)-3k: Chiralcel AS-H column: hexanes:^{i}PrOH = 97:03, flow rate 0.5 mL/min, λ = 210 nm: t_{major} = 21.1 min, t_{minor} = 28.6 min; 99% *ee*.
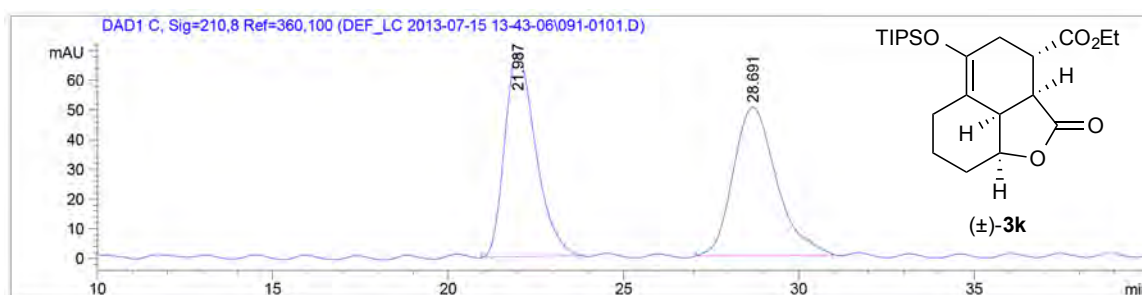

```
Signal 3: DAD1 C, Sig=210,8 Ref=360,100

Peak RetTime Type  Width     Area       Height     Area
 #   [min]        [min]     [mAU*s]     [mAU]        %
----|-------|----|-------|-----------|-----------|--------|
  1  21.987 BB   0.9366 4223.71094   68.57260   49.4877
  2  28.691 BB   1.2717 4311.16748   50.10910   50.5123

Totals :                8534.87842  118.68170
```
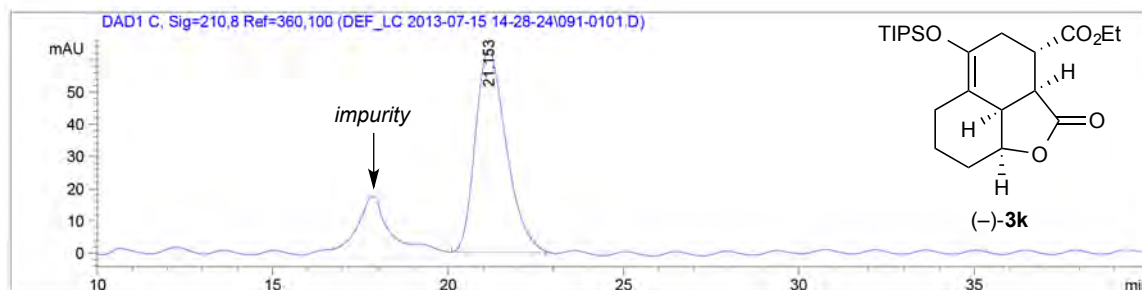


```
Signal 3: DAD1 C, Sig=210,8 Ref=360,100

Peak RetTime Type  Width     Area       Height      Area
 #   [min]        [min]     [mAU*s]     [mAU]         %
----|-------|----|-------|-----------|-----------|--------|
  1  21.153 BB   0.9376 3851.73779   62.79996  100.0000

Totals :                3851.73779   62.79996
```

196

Determination of enantiomeric excess of tricyclic γ-lactone (–)-3k':

Chiral HPLC analysis of tricyclic γ-lactone (–)-3k': Chiralcel OD-H column: hexanes:^{i}PrOH = 95:05, flow rate 0.5 mL/min, λ = 210 nm: t_{minor} = 17.4 min, t_{major} = 25.7 min; 99% *ee*.
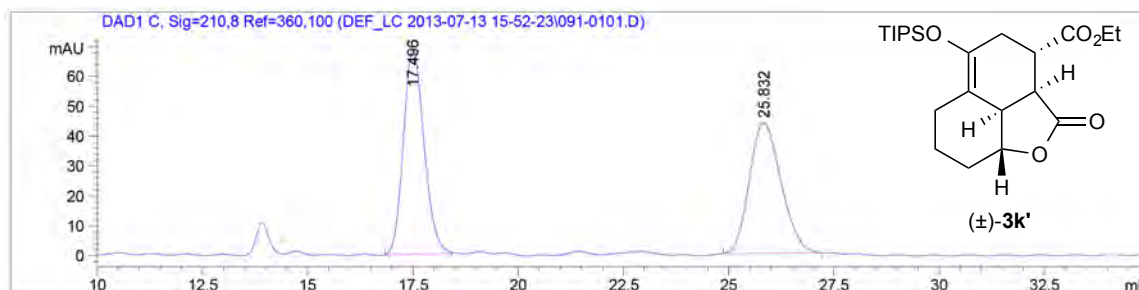
Signal 3: DAD1 C, Sig=210,8 Ref=360,100

```
Peak RetTime Type  Width      Area       Height      Area
 #   [min]        [min]     [mAU*s]     [mAU]        %
----|-------|----|-------|-----------|----------|---------|
  1  17.496 BB    0.5305 2341.91187   68.56427   50.6538
  2  25.832 BB    0.8102 2281.45386   43.76495   49.3462

Totals :                 4623.36572  112.32922
```


Signal 3: DAD1 C, Sig=210,8 Ref=360,100

```
Peak RetTime Type  Width      Area       Height      Area
 #   [min]        [min]     [mAU*s]     [mAU]         %
----|-------|----|-------|-----------|----------|---------|
  1  25.765 BB    0.8166 2615.85327   48.86073 100.0000

Totals :                 2615.85327   48.86073
```

Determination of enantiomeric excess of bicyclic γ-lactone (+)-3c':

Chiral HPLC analysis of bicyclic γ-lactone (+)-3c': Chiralcel OD-H column: hexanes:^{i}PrOH = 95:05, flow rate 0.5 mL/min, λ = 210 nm: t_{minor} = 22.1 min, t_{major} = 26.1 min; 99% *ee*.
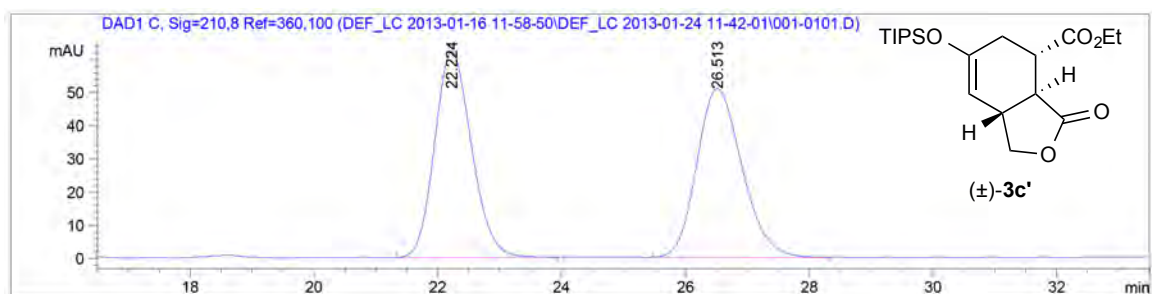

```
Signal 3: DAD1 C, Sig=210,8 Ref=360,100

Peak RetTime Type  Width     Area        Height      Area
 #   [min]        [min]    [mAU*s]      [mAU]         %
----|-------|----|-------|----------|----------|--------|
  1  22.224 BB    0.6433 2574.76782    62.15416  49.9667
  2  26.513 BB    0.7918 2578.20190    50.82896  50.0333

Totals :                 5152.96973   112.98312
```
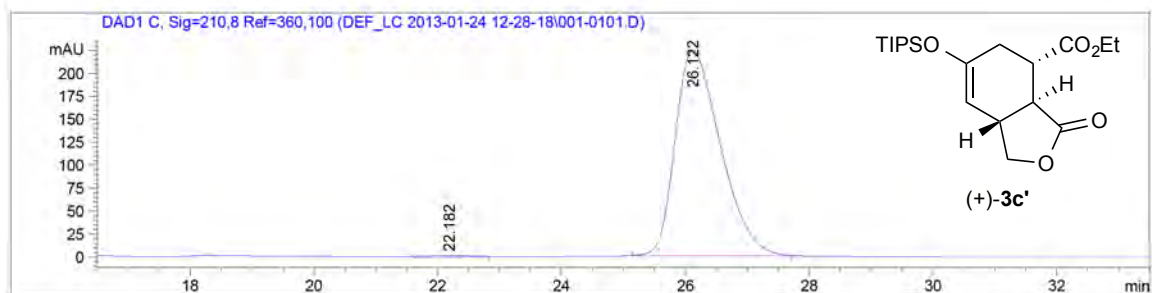


```
Signal 3: DAD1 C, Sig=210,8 Ref=360,100

Peak RetTime Type  Width     Area        Height      Area
 #   [min]        [min]    [mAU*s]      [mAU]         %
----|-------|----|-------|----------|----------|--------|
  1  22.182 MM    0.8519   85.42705    1.67124   0.7437
  2  26.122 BB    0.7879 1.14013e4   223.98254  99.2563

Totals :                 1.14867e4   225.65378
```

Supporting Information References (CHAPTER II):

[1]   Seebach, D., Imwinkelried, R. & Stucky, G. Optically-active alcohols from 1,3-dioxan-4-ones – a practical version of enantioselective synthesis with nucleophilic-substitution at acetal centers. *Helv. Chim. Acta.* **70**, 448-464 (1987).

[2]   Birman, V. B. & Li, X. M. Homobenzotetramisole: An effective catalyst for kinetic resolution of aryl-cycloalkanols. *Org. Lett.* **10**, 1115-1118 (2008).

[3]   Calter, M. A. Catalytic, asymmetric dimerization of methylketene. *J. Org. Chem.* **61**, 8006-8007 (1996).

[4]   Pracejus, H. & Matje, H. Zusammenhänge zwischen dem räumlichen Bau einiger alkaloidartiger Katalysatoren und ihren stereospezifischen Wirkungen bei asymmetrischen Estersynthesen. *J. Prakt. Chem.* **24**, 195-205 (1964).

[5]   Runcie, K. A. & Taylor, R. J. K. The *in situ* oxidation-Wittig reaction of a-hydroxyketones. *Chem. Commun.* 974-975 (2002).

[6]   Ng, S. S. & Jamison, T. F. Simple alkenes as substitutes for organometallic reagents: Nickel-catalyzed, intermolecular coupling of aldehydes, silyl triflates, and alpha olefins. *J. Am. Chem. Soc.* **127**, 14194-14195 (2005).

[7]   Yu, J. Q. & Corey, E. J. A mild, catalytic, and highly selective method for the oxidation of α,β-enones to 1,4-enediones. *J. Am. Chem. Soc.* **125**, 3232-3233 (2003).

CHAPTER III

Preparation of S3, S4, S5, S8, S9, (±)-13a, (±)-13b and (±)-13c:
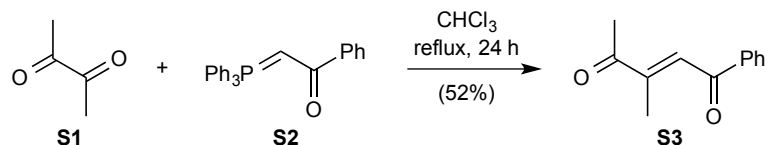
(***E***)-**3-methyl-1-phenylpent-2-ene-1,4-dione (S3):** To a solution of 2,3-butanedione **S1** (2.0 mL, 23.2 mmol, 1.0 equiv.) in anhydrous CHCl$_3$ (77 mL) was added (benzoylmethylene)triphenylphosphorane **S2** (8.84 g, 23.2 mmol, 1.0 equiv.) and refluxed (65-70 °C) for 24 h. The mixture was filtered through a short pad of celite and the filtrate was concentrated using rotary evaporation. The residue was then diluted with cold Et$_2$O (50 mL), filtered through a plug of celite and washed with additional Et$_2$O (25 mL). The filtrate was concentrated by rotary evaporation and purified by an automated flash chromatography system (5 → 15% EtOAc/hexanes) providing 2.24 g (52% yield) of diketone **S3** as a yellow oil: TLC (EtOAc:hexanes, 1:9 *v/v*): R$_f$ = 0.42; ^{1}H NMR (500 MHz, CDCl$_3$): δ 7.95-7.93 (m, 2H), 7.62-7.58 (m, 1H), 7.51-7.48 (m, 2H), 7.44-7.42 (m, 1H), 2.47 (s, 3H), 2.07 (d, *J* = 1.4 Hz, 3H); ^{13}C NMR (125 MHz; CDCl$_3$): δ 200.1, 193.3, 147.0, 137.3, 133.9, 131.8, 129.0 (2), 128.7 (2), 26.4, 14.0; IR (thin film): 1681, 1668, 1597 cm^{-1}; HRMS (ESI+) *m/z* calcd for C$_{12}$H$_{12}$LiO$_2$ [M+Li]$^+$: 195.0997, found: 195.0988.
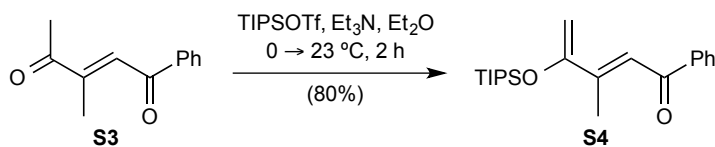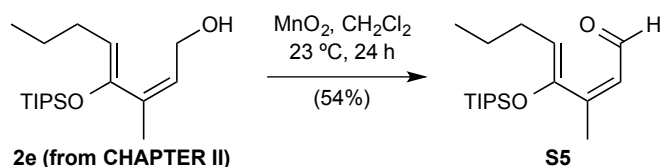

(***E***)-**3-methyl-1-phenyl-4-((triisopropylsilyl)oxy)penta-2,4-dien-1-one** **(S4):** To a solution of diketone **S3** (2.24 g, 11.9 mmol, 1.0 equiv.) in anhydrous Et$_2$O (40 mL) at 0 °C was added Et$_3$N (2.5 mL, 17.9 mmol, 1.5 equiv.) dropwise. After stirring for 10 min, TIPSOTf (3.8 mL, 14.3 mmol, 1.2 equiv.) was added over a period of 30 min. The

reaction was stirred for 30 min at 0 ºC then allowed to warm up to ambient temperature (23 ºC) and stirred for 1 h. The reaction mixture was then quenched with a saturated aqueous solution of NaHCO$_3$ (20 mL). The aqueous layer was extracted with Et$_2$O (2 x 50 mL) and the combined organic extracts were then washed with brine (50 mL). The organic layer was then dried over anhydrous MgSO$_4$, filtered, and concentrated by rotary evaporation. The residue was purified by an automated flash chromatography system (0.5 → 10% EtOAc/hexanes) providing 3.28 g (80% yield) of diene **S4** as a yellow oil: TLC (EtOAc:hexanes, 1:9 *v/v*): R$_f$ = 0.87; ^{1}H NMR (500 MHz, CDCl$_3$): δ 7.97-7.94 (m, 2H), 7.54 (tt, *J* = 7.4, 1.7 Hz, 1H), 7.48-7.44 (m, 3H), 4.90 (d, *J* = 2.0 Hz, 1H), 4.66 (d, *J* = 1.9 Hz, 1H), 2.28 (d, *J* = 1.1 Hz, 3H), 1.33-1.26 (m, 3H), 1.14 (d, *J* = 7.3 Hz, 18H); ^{13}C NMR (125 MHz; CDCl$_3$): δ 193.1, 156.9, 148.3, 139.4, 132.7, 128.6 (2), 128.4 (2), 121.0, 96.8, 18.2 (6), 15.3, 12.9 (3); IR (thin film): 2946, 2869, 1660, 1594 cm^{-1}; HRMS (ESI+) *m/z* calcd for C$_{21}$H$_{33}$O$_2$Si [M+H]$^+$: 345.2250, found: 345.2255.
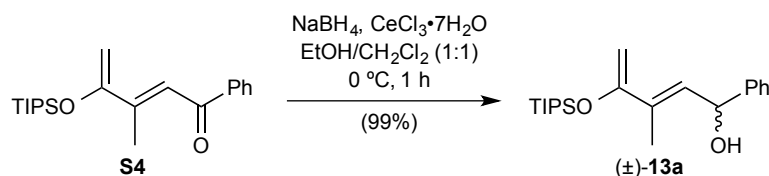
(*E*)-3-methyl-1-phenyl-4-((triisopropylsilyl)oxy)penta-2,4-dien-1-ol ((±)-13a): To a solution of diene **S4** (100 mg, 0.29 mmol, 1.0 equiv.) in absolute EtOH (1.9 mL) and anhydrous CH$_2$Cl$_2$ (1.9 mL) at 0 ºC was added CeCl$_3$•7H$_2$O (120 mg, 0.32 mmol, 1.1 equiv.) in one portion. After stirring for 15 min, NaBH$_4$ (27 mg, 0.73 mmol, 2.5 equiv.) was added portionwise over a period of 1 min. The reaction was stirred for 45 min at 0 ºC then quenched with a saturated aqueous solution of NaHCO$_3$ (2.0 mL). The aqueous layer was extracted with CH$_2$Cl$_2$ (2 x 5.0 mL) and the combined organic extracts were then washed with brine (2.0 mL). The organic layer was then dried over anhydrous MgSO$_4$, filtered, and concentrated by rotary evaporation. The residue was purified by an automated flash chromatography system (5 → 20% EtOAc/hexanes) providing 101 mg (99% yield) of silyloxydiene alcohol (±)-**13a** as a pale yellow oil: TLC (EtOAc:hexanes, 1:9 *v/v*): R$_f$ = 0.42; ^{1}H NMR (500 MHz, CDCl$_3$): δ 7.42-7.27 (m, 5H), 6.35 (d, *J* = 8.8

Hz, 1H), 5.58 (d, J = 8.8 Hz, 1H), 4.52 (d, J = 1.4 Hz, 1H), 4.38 (s, 1H), 1.93 (d, J = 1.1 Hz, 3H), 1.26-1.21 (m, 3H), 1.10 (dd, J = 7.4, 2.2 Hz, 18H); ^{13}C NMR (125 MHz; CDCl$_3$): δ 157.1, 143.6, 133.0, 129.8, 128.6 (2), 127.6, 126.3 (2), 92.1, 71.2, 18.2 (6), 14.0, 12.9 (3); IR (thin film): 3384, 2945, 2867, 1595 cm^{-1}; HRMS (ESI+) m/z calcd for C$_{21}$H$_{34}$O$_2$Si [M+H]$^+$: 347.2406, found: 347.2390.
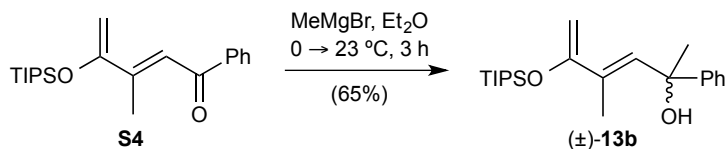
(*E*)-4-methyl-2-phenyl-5-((triisopropylsilyl)oxy)hexa-3,5-dien-2-ol ((±)-13b): To a solution of diene **S4** (3.28 g, 9.5 mmol, 1.0 equiv.) in anhydrous Et$_2$O (50 mL) at 0 ºC was added MeMgBr (3.0 M solution in Et$_2$O, 4.8 mL, 14.4 mmol, 1.5 equiv.) over a period of 1 h. The reaction was stirred for 2 h at 23 ºC then quenched with a saturated aqueous solution of NH$_4$Cl (25 mL). The aqueous layer was extracted with Et$_2$O (2 x 30 mL) and the combined organic extracts were then washed with brine (25 mL). The organic layer was then dried over anhydrous MgSO$_4$, filtered, and concentrated by rotary evaporation. The residue was purified by an automated flash chromatography system (5 → 15% EtOAc/hexanes) providing 2.22 g (65% yield) of silyloxydiene alcohol (±)-**13b** as a clear colorless oil: TLC (EtOAc:hexanes, 1:9 *v/v*): R$_f$ = 0.58; ^{1}H-NMR (500 MHz; CDCl$_3$): δ 7.47-7.45 (m, 2H), 7.33-7.30 (m, 2H), 7.24-7.20 (m, 1H), 6.65 (s, 1H), 4.46 (d, J = 1.5 Hz, 1H), 4.32 (d, J = 0.5 Hz, 1H), 1.67 (s, 3H), 1.64 (d, J = 0.7 Hz, 3H), 1.28-1.22 (m, 3H), 1.12 (dd, J = 7.4, 0.8 Hz, 18H).; ^{13}C NMR (125 MHz; CDCl$_3$): δ 157.6, 148.6, 135.0, 134.7, 128.2 (2), 126.6, 125.2 (2), 91.8, 74.2, 34.1, 18.3 (6), 14.6, 12.9 (3); IR (thin film): 3454, 2945, 2867, 1594 cm^{-1}; HRMS (ESI+) m/z calcd for C$_{22}$H$_{37}$O$_2$Si [M+H]$^+$: 361.2563, found: 361.2549.

(2Z,4Z)-3-methyl-4-((triisopropylsilyl)oxy)octa-2,4-dienal (S5): To a solution of silyloxydiene alcohol **2e** (0.96 g, 3.1 mmol, 1.0 equiv.) in anhydrous CH_2Cl_2 (20 mL) was added MnO_2 (5.34 g, 61.4 mmol, 20.0 equiv.) and vigorously stirred at ambient temperature (23 °C) for 24 h. The mixture was filtered through a short pad of celite and the filtrate was concentrated using rotary evaporation. Purification by an automated flash chromatography system (5 → 15% EtOAc/hexanes) afforded 0.38 g (54% yield) of aldehyde **S5** as a pale yellow oil: TLC (EtOAc:hexanes, 1:9 *v/v*): R_f = 0.49; ^{1}H NMR (500 MHz, CDCl$_3$): δ 10.11 (d, J = 8.1 Hz, 1H), 6.29 (dd, J = 8.1, 0.4 Hz, 1H), 5.37 (t, J = 7.3 Hz, 1H), 2.26 (d, J = 1.0 Hz, 3H), 2.19 (q, J = 7.4 Hz, 2H), 1.43 (sext, J = 7.4 Hz, 2H), 1.22-1.16 (m, 3H), 1.09 (d, J = 7.0 Hz, 18H), 0.93 (t, J = 7.4 Hz, 3H); ^{13}C NMR (125 MHz; CDCl$_3$): δ 192.0, 154.3, 150.8, 124.9, 118.2, 28.9, 22.6, 18.1 (6), 14.3, 14.1, 14.0 (3); IR (thin film): 2960, 2869, 1668, 1618 cm^{-1}; HRMS (ESI+) *m/z* calcd for C$_{18}$H$_{35}$O$_2$Si [M+H]$^+$: 311.2406, found: 311.2403.
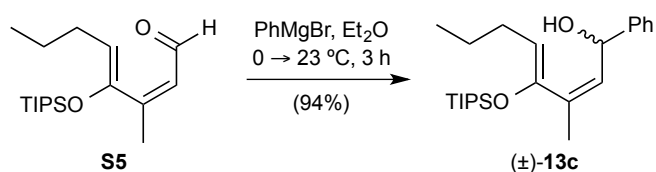
(2Z,4Z)-3-methyl-1-phenyl-4-((triisopropylsilyl)oxy)octa-2,4-dien-1-ol ((±)-13c): To a solution of aldehyde **S5** (0.38 g, 1.2 mmol, 1.0 equiv.) in anhydrous Et$_2$O (8.0 mL) at 0 °C was added PhMgBr (3.0 M solution in Et$_2$O, 0.53 mL, 1.6 mmol, 1.3 equiv.) over a period of 1 h. The reaction was stirred for 2 h at 23 °C then quenched with a saturated aqueous solution of NH$_4$Cl (4 mL). The aqueous layer was extracted with Et$_2$O (2 x 10 mL) and the combined organic extracts were then washed with brine (5 mL). The organic layer was then dried over anhydrous MgSO$_4$, filtered, and concentrated by rotary evaporation. The residue was purified by an automated flash chromatography system (5

→ 20% EtOAc/hexanes) providing 0.44 g (94% yield) of silyloxydiene alcohol (±)-**13c** as a pale yellow oil: TLC (EtOAc:hexanes, 1:9 *v/v*): R_f = 0.42; ^{1}H NMR (500 MHz; CDCl$_3$): δ 7.42-7.25 (m, 5H), 5.98 (dd, *J* = 8.9, 0.4 Hz, 1H), 5.57 (d, *J* = 8.9 Hz, 1H), 4.90 (t, *J* = 7.1 Hz, 1H), 2.19-2.07 (m, 2H), 1.95 (t, *J* = 0.5 Hz, 3H), 1.40 (dt, *J* = 14.9, 7.4 Hz, 2H), 1.15-1.04 (m, 21H), 0.94 (t, *J* = 7.4 Hz, 3H); ^{13}C NMR (125 MHz; CDCl$_3$): δ 151.2, 143.8, 134.8, 128.5 (2), 128.1, 127.5, 126.0 (2), 111.4, 71.3, 28.5, 23.0, 18.1 (6), 14.7, 14.2, 13.9 (3); IR (thin film): 3356, 2946, 2867 cm^{-1}; HRMS (ESI+) *m/z* calcd for C$_{24}$H$_{39}$OSi [M–OH]$^+$: 371.2765, found: 371.2715.
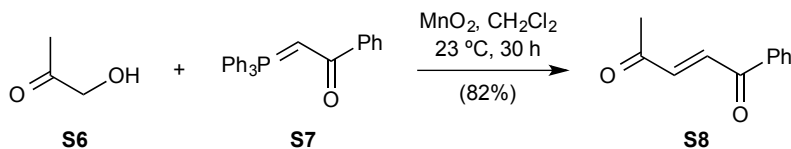
(*E*)-1-phenylpent-2-ene-1,4-dione (S8): To a solution of hydroxyacetone **S6** (2.4 mL, 34.2 mmol, 1.3 equiv.) and (benzoylmethylene)triphenylphosphorane **S7** (10.0 g, 26.3 mmol, 1.0 equiv.) in anhydrous CH$_2$Cl$_2$ (90 mL) was added MnO$_2$ (23.0 g, 262.9 mmol, 10.0 equiv.) and vigorously stirred at ambient temperature (23 ºC) for 30 h. The mixture was filtered through a short pad of celite and the filtrate was concentrated using rotary evaporation. The residue was then diluted with cold Et$_2$O (100 mL), filtered through a plug of celite and washed with additional Et$_2$O (50 mL). The filtrate was concentrated by rotary evaporation and purified by an automated flash chromatography system (5 → 25% EtOAc/hexanes) providing 3.76 g (82% yield) of diketone **S8** as a yellow solid: m.p. = 42-47 ºC; TLC (EtOAc:hexanes, 1:9 *v/v*): R_f = 0.28; ^{1}H NMR (500 MHz, CDCl$_3$): δ 7.98-7.96 (m, 2H), 7.68 (d, *J* = 15.8 Hz, 1H), 7.63-7.59 (m, 1H), 7.51-7.48 (m, 2H), 7.06 (d, *J* = 15.7 Hz, 1H), 2.42 (s, 3H); ^{13}C NMR (125 MHz; CDCl$_3$): δ 198.0, 190.4, 138.5, 136.7, 134.02, 133.97, 128.98 (2), 128.90 (2), 29.1; IR (thin film): 1668, 1614 cm^{-1}; HRMS (ESI+) *m/z* calcd for C$_{11}$H$_{10}$LiO$_2$ [M+Li]$^+$: 181.0841, found: 181.0833.
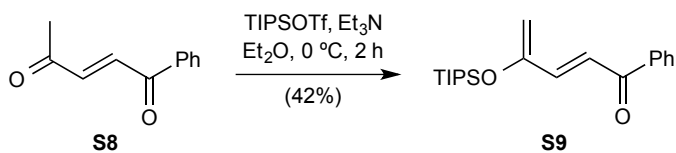
(*E*)-1-phenyl-4-((triisopropylsilyl)oxy)penta-2,4-dien-1-one (S9): To a solution of diketone **S8** (4.77 g, 27.4 mmol, 1.0 equiv.) in anhydrous Et$_2$O (91 mL) at 0 °C was added Et$_3$N (5.7 mL, 40.9 mmol, 1.5 equiv.) dropwise. After stirring for 10 min, TIPSOTf (8.8 mL, 32.7 mmol, 1.2 equiv.) was added over a period of 30 min. The reaction was stirred for 2 h at 0 °C then quenched with a saturated aqueous solution of NaHCO$_3$ (45 mL). The aqueous layer was extracted with Et$_2$O (2 x 50 mL) and the combined organic extracts were then washed with brine (50 mL). The organic layer was then dried over anhydrous MgSO$_4$, filtered, and concentrated by rotary evaporation. The residue was purified by an automated flash chromatography system (0.5 → 10% EtOAc/hexanes) providing 3.76 g (42% yield) of diene **S9** as an orange oil: TLC (EtOAc:hexanes, 1:9 *v/v*): R$_f$ = 0.79; ^{1}H NMR (500 MHz, CDCl$_3$): δ 7.96-7.95 (m, 2H), 7.59-7.55 (m, 1H), 7.50-7.47 (m, 2H), 7.35 (dd, *J* = 14.9, 0.3 Hz, 1H), 7.21 (d, *J* = 14.9 Hz, 1H), 4.75 (s, 2H), 1.33-1.27 (m, 3H), 1.15 (d, *J* = 7.3 Hz, 18H); ^{13}C NMR (125 MHz; CDCl$_3$): δ 190.8, 154.5, 142.5, 138.3, 132.9, 128.8 (2), 128.6 (2), 122.6, 103.4, 18.2 (6), 12.9 (3); IR (thin film): 2946, 2868, 1667, 1607, 1590 cm^{-1}; HRMS (ESI+) *m/z* calcd for C$_{20}$H$_{31}$O$_2$Si [M+H]$^+$: 331.2093, found: 331.2178.
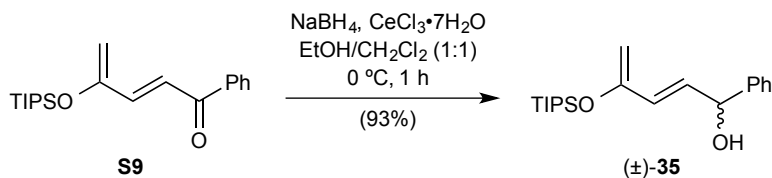
(*E*)-1-phenyl-4-((triisopropylsilyl)oxy)penta-2,4-dien-1-ol ((±)-35): To a solution of diene **S9** (3.67 g, 11.1 mmol, 1.0 equiv.) in absolute EtOH (74 mL) and anhydrous CH$_2$Cl$_2$ (74 mL) at 0 °C was added CeCl$_3$•7H$_2$O (4.34 g, 11.7 mmol, 1.1 equiv.) in one portion. After stirring for 20 min, NaBH$_4$ (1.1 g, 27.8 mmol, 2.5 equiv.) was added portionwise over a period of 30 min. The reaction was stirred for 30 min at 0 °C then quenched with a saturated aqueous solution of NaHCO$_3$ (30 mL). The aqueous layer was

extracted with CH_2Cl_2 (2 x 100 mL) and washed with brine (30 mL). The organic layer was then dried over anhydrous $MgSO_4$, filtered, and concentrated by rotary evaporation. The residue was purified by an automated flash chromatography system (5 → 20% EtOAc/hexanes) providing 3.43 g (93% yield) of silyloxydiene alcohol (±)-**35** as a yellow oil: TLC (EtOAc:hexanes, 1:9 *v/v*): R_f = 0.37; ^{1}H NMR (500 MHz, $CDCl_3$): δ 7.41-7.28 (m, 5H), 6.28 (ddd, *J* = 15.2, 6.1, 0.4 Hz, 1H), 6.17 (dd, *J* = 15.2, 1.1 Hz, 1H), 5.31 (d, *J* = 6.1 Hz, 1H), 4.37 (s, 1H), 4.33 (s, 1H), 1.27-1.22 (m, 3H), 1.11 (d, *J* = 7.4 Hz, 18H); ^{13}C NMR (125 MHz; $CDCl_3$): δ 154.8, 142.9, 132.1, 128.7, 128.6 (2), 127.8, 126.6 (2), 95.7, 74.4, 18.2 (6), 12.9 (3); IR (thin film): 3356, 2945, 2868, 1592 cm^{-1}; HRMS (ESI+) *m/z* calcd for $C_{20}H_{33}O_2Si$ $[M+H]^+$: 333.2250, found: 333.2245.

**Representative procedure for the stereodivergent DAL process as described for bicyclic γ-lactones (–)-14a and (+)-14a':**
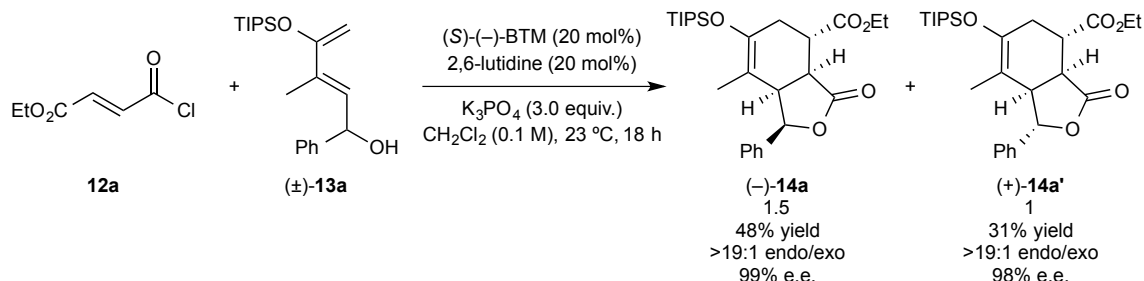
Ethyl (1R,3aS,4S,7aR)-7-methyl-3-oxo-1-phenyl-6-((triisopropylsilyl)oxy)-1,3,3a,4, 5,7a-hexahydroisobenzofuran-4-carboxylate ((–)-14a) and ethyl (1S,3aS,4S,7aR)-7-methyl-3-oxo-1-phenyl-6-((triisopropylsilyl)oxy)-1,3,3a,4,5,7a-hexahydroiso-bezofuran-4-carboxylate ((+)-14a'): To an oven-dried, 5-mL round-bottomed flask equipped with a magnetic stir bar was added silyloxydiene alcohol (±)-**13a** (34 mg, 0.10 mmol, 1.0 equiv.), (S)-(–)-BTM (5.0 mg, 0.020 mmol, 20 mol%), 2,6-lutidine (2.3 mL, 0.020 mmol, 20 mol%), K_3PO_4 (64.0 mg, 0.30 mmol, 3.0 equiv.) and anhydrous CH_2Cl_2 (0.7 mL, to make final concentration of silyloxydiene alcohol 0.1 M) at ambient temperature (23 ºC). With vigorous stirring, ethyl fumaroyl chloride **12a** (20 mL, 0.15 mmol, 1.5 equiv.) in CH_2Cl_2 (0.3 mL) was added over a period of 5 h by syringe pump addition. After stirring for an additional 13 h, the reaction mixture was filtered through a pad of celite and concentrated by rotary evaporation. Purification by an automated flash chromatography (5 → 20% EtOAc/hexanes) afforded a single *endo* diastereomer (as judged by ^{1}H NMR) of bicyclic γ-lactone (–)-**14a** (20 mg, 48% yield, 99% e.e.) and a single *endo* diastereomer (as judged by ^{1}H NMR) of bicyclic γ-lactone (+)-**14a'** (13 mg, 31% yield, 98% e.e.).

(–)-**14a**: clear colorless oil; TLC (EtOAc:hexanes, 1:9 *v/v*): R_f = 0.53; $[\alpha]_D^{18.5}$ = –22.86 (*c* = 1.40, CHCl$_3$). Enantiomeric excess was determined by chiral HPLC analysis in comparison with authentic racemic material using a Chiralcel OD-H column: hexanes:^{i}PrOH = 95:05, flow rate 0.5 mL/min, λ = 210 nm: t_{major} = 11.4 min, t_{minor} =

13.4 min; 99% e.e. Absolute stereochemistry was assigned by analogy to tricyclic γ-lactone (–)-**3k**. ^{1}H NMR (500 MHz; CDCl$_3$): δ 7.42-7.39 (m, 2H), 7.35-7.30 (m, 3H), 5.39 (s, 1H), 4.17-4.04 (m, 2H), 3.29 (ddd, J = 7.7, 3.3, 0.9 Hz, 1H), 3.26 (dd, J = 6.1, 3.2 Hz, 1H), 3.19 (d, J = 7.5 Hz, 1H), 2.57-2.53 (m, 1H), 2.49 (ddt, J = 17.1, 6.0, 2.3 Hz, 1H), 1.80 (s, 3H), 1.21 (t, J = 7.1 Hz, 3H), 1.17-1.12 (m, 3H), 1.09 (dd, J = 6.8, 2.1 Hz, 18H); ^{13}C NMR (125 MHz; CDCl$_3$): δ 177.7, 172.8, 144.4, 139.7, 129.0 (2), 128.3, 124.9 (2), 108.0, 83.6, 61.4, 47.6, 38.5, 38.3, 28.8, 18.1 (6), 14.5, 14.2, 13.3 (3); IR (thin film): 2944, 2867, 1780, 1732, 1676 cm^{-1}; HRMS (ESI+) m/z calcd for C$_{27}$H$_{41}$O$_5$Si [M+H]$^+$: 473.2723, found: 473.2734.

(+)-**14a'**: clear colorless oil; TLC (EtOAc:hexanes, 1:9 v/v): R$_f$ = 0.50; $[\alpha]_D^{18.8}$ = +30.38 (c = 0.80, CHCl$_3$). Enantiomeric excess was determined by chiral HPLC analysis in comparison with authentic racemic material using a Chiralcel AS-H column: hexanes:^{i}PrOH = 95:05, flow rate 0.5 mL/min, λ = 210 nm: t$_{major}$ = 16.9 min, t$_{minor}$ = 19.4 min; 98% e.e. Absolute stereochemistry was assigned by analogy to bicyclic amide (–)-**S21**. ^{1}H NMR (500 MHz; CDCl$_3$): δ 7.41-7.38 (m, 5H), 5.07 (d, J = 10.2 Hz, 1H), 4.35-4.22 (m, 2H), 3.08-3.04 (m, 1H), 2.96 (d, J = 11.5 Hz, 1H), 2.93-2.88 (m, 1H), 2.56-2.52 (m, 2H), 1.35-1.32 (m, 6H), 1.13-1.08 (m, 3H), 1.06 (dd, J = 6.7, 2.4 Hz, 18H); ^{13}C NMR (125 MHz; CDCl$_3$): δ 173.3, 172.9, 144.8, 137.0, 129.6, 128.8 (2), 128.1 (2), 109.8, 85.4, 61.4, 50.0, 46.5, 39.9, 34.7, 18.1 (6), 14.3, 13.33, 13.27 (3); IR (thin film): 2946, 2869, 1790, 1738, 1663 cm^{-1}; HRMS (ESI+) m/z calcd for C$_{27}$H$_{41}$O$_5$Si [M+H]$^+$: 473.2723, found: 473.2735.
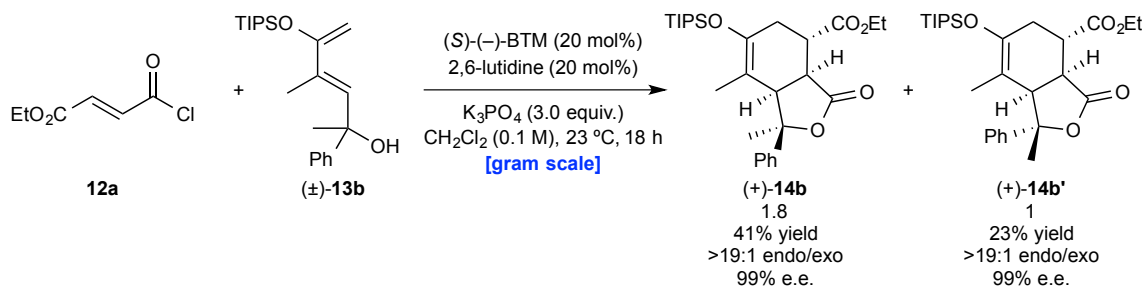
Ethyl (1*R*,3a*S*,4*S*,7a*R*)-1,7-dimethyl-3-oxo-1-phenyl-6-((triisopropylsilyl)oxy)-1,3,3a,4,5,7a-hexahydroisobenzofuran-4-carboxylate ((+)-14b) and ethyl (1*S*,3a*S*,4*S*,7a*R*)-1,7-dimethyl-3-oxo-1-phenyl-6-((triisopropylsilyl)oxy)-1,3,3a,4,5,7a-hexahydroisobenzofuran-4-carboxylate ((+)-14b'): Prepared according to the representative procedure using silyloxydiene alcohol (±)-**13b** (2.03 g, 5.63 mmol, 1.0 equiv.), (*S*)-(−)-BTM (284 mg, 1.13 mmol, 20 mol%), 2,6-lutidine (0.13 mL, 1.13 mmol, 20 mol%), K₃PO₄ (3.59 g, 16.89 mmol, 3.0 equiv.) in anhydrous CH₂Cl₂ (56 mL, to make initial concentration of silyloxydiene alcohol 0.1 M) and ethyl fumaroyl chloride **12a** (1.13 mL, 8.44 mmol, dissolved in 24 mL CH₂Cl₂, 1.5 equiv.) at ambient temperature (23 ºC). Upon completion (as judged by TLC), the reaction mixture was purified by an automated flash chromatography (5 → 20% EtOAc/hexanes) to afford a single *endo* diastereomer (as judged by ¹H NMR) of bicyclic γ-lactone (+)-**14b** (1.09 g, 41% yield, 99% e.e.) and a single *endo* diastereomer (as judged by ¹H NMR) of bicyclic γ-lactone (+)-**14b'** (0.62 g, 23% yield, 99% e.e.).

(+)-**14b**: clear colorless oil; TLC (EtOAc:hexanes, 1:9 *v/v*): R_f = 0.54; $[\alpha]_D^{20.1}$ = +30.30 (*c* = 3.30, CHCl₃). Enantiomeric excess was determined by chiral HPLC analysis in comparison with authentic racemic material using a Chiralcel OD-H column: hexanes:*i*PrOH = 95:05, flow rate 0.5 mL/min, λ = 210 nm: t_{major} = 12.0 min, t_{minor} = 16.1 min; 99% e.e. Absolute stereochemistry was assigned by analogy to tricyclic γ-lactone (−)-**3k**. ¹H NMR (500 MHz; CDCl₃): δ 7.33-7.28 (m, 5H), 4.21-4.11 (m, 2H), 3.59 (ddd, *J* = 8.3, 4.4, 1.3 Hz, 1H), 3.21 (d, *J* = 8.3 Hz, 1H), 3.18 (dd, *J* = 9.7, 4.2 Hz, 1H), 2.53-2.49 (m, 1H), 2.38 (ddt, *J* = 16.5, 5.6, 2.1 Hz, 1H), 1.93 (s, 3H), 1.25 (t, *J* = 7.1 Hz, 3H), 1.08-1.04 (m, 3H), 1.02 (dd, *J* = 5.7, 3.7 Hz, 18H), 0.87 (s, 3H); ¹³C NMR

(125 MHz; CDCl$_3$): δ 177.1, 172.8, 145.6, 141.2, 128.1 (2), 127.9, 126.2 (2), 107.4, 89.3, 61.3, 52.5, 42.4, 39.5, 29.5, 28.1, 18.1 (6), 16.4, 14.2, 13.2 (3); IR (thin film): 2945, 2867, 1770, 1732, 1666 cm^{-1}; HRMS (ESI+) m/z calcd for C$_{28}$H$_{43}$O$_5$Si [M+H]$^+$: 487.2880, found: 487.2862.

(+)-**14b'**: clear colorless oil; TLC (EtOAc:hexanes, 1:9 v/v): R$_f$ = 0.65; $[\alpha]_D^{19.7}$ = +51.85 (c = 2.70, CHCl$_3$). Enantiomeric excess was determined by chiral HPLC analysis in comparison with authentic racemic material using a Chiralcel AD-H column: hexanes:^{i}PrOH = 95:05, flow rate 0.8 mL/min, λ = 210 nm: t$_{major}$ = 6.5 min, t$_{minor}$ = 7.9 min; 99% e.e. Absolute stereochemistry was assigned by analogy to bicyclic amide (−)-**S21**. ^{1}H NMR (500 MHz; CDCl$_3$): δ 7.43-7.41 (m, 2H), 7.34-7.29 (m, 3H), 4.30-4.15 (m, 2H), 3.02 (dt, J = 13.5, 1.4 Hz, 1H), 2.85 (t, J = 12.5 Hz, 1H), 2.77 (td, J = 10.9, 6.5 Hz, 1H), 2.49-2.36 (m, 2H), 1.92 (s, 3H), 1.88 (s, 3H), 1.29 (t, J = 7.1 Hz, 3H), 1.11-1.07 (m, 3H), 1.05 (d, J = 6.7 Hz, 18H); ^{13}C NMR (125 MHz; CDCl$_3$): δ 173.6, 173.1, 145.8, 139.9, 128.6 (2), 128.2, 126.2 (2), 109.4, 88.6, 61.3, 54.7, 44.3, 39.9, 35.0, 30.1, 18.1 (6), 14.26, 14.21, 13.2(3); IR (thin film): 2945, 2868, 1786, 1737, 1652 cm^{-1}; HRMS (ESI+) m/z calcd for C$_{28}$H$_{43}$O$_5$Si [M+H]$^+$: 487.2880, found: 487.2891.
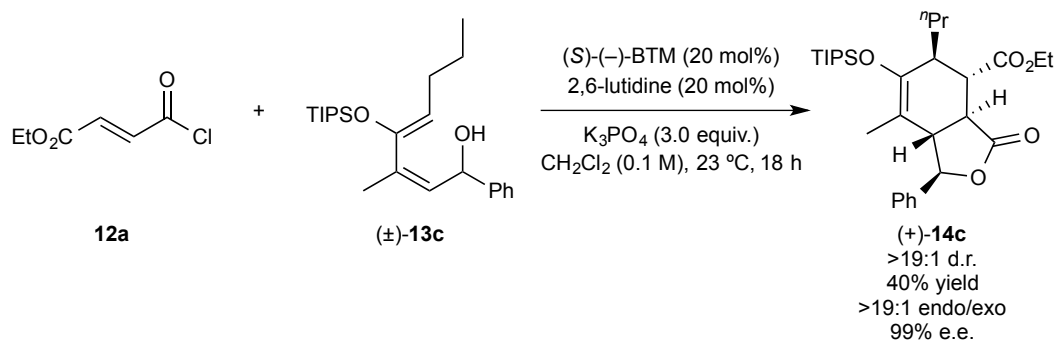
Ethyl (1R,3aS,4S,5S,7aS)-7-methyl-3-oxo-1-phenyl-5-propyl-6-((triisopropylsilyl)-oxy)-1,3,3a,4,5,7a-hexahydroisobenzofuran-4-carboxylate ((+)-14c): Prepared according to the representative procedure using silyloxydiene alcohol (±)-**13c** (39 mg, 0.10 mmol, 1.0 equiv.), (S)-(−)-BTM (5.0 mg, 0.020 mmol, 20 mol%), 2,6-lutidine (2.3 mL, 0.020 mmol, 20 mol%), K$_3$PO$_4$ (64 mg, 0.30 mmol, 3.0 equiv.) in anhydrous

CH₂Cl₂ (0.7 mL, to make final concentration of silyloxydiene alcohol 0.1 M) and ethyl fumaroyl chloride **12a** (20 mL, 0.15 mmol, dissolved in 0.3 mL CH₂Cl₂, 1.5 equiv.) at ambient temperature (23 ºC). Upon completion (as judged by TLC), the reaction mixture was purified by an automated flash chromatography (5 → 20% EtOAc/hexanes) to afford a single *endo* diastereomer (as judged by ¹H NMR) of bicyclic γ-lactone (+)-**14c** (20 mg, 40% yield, 99% e.e.) as a clear colorless oil: TLC (EtOAc:hexanes, 1:9 *v/v*): R$_f$ = 0.42; $[\alpha]_D^{20.1}$ = +41.03 (*c* = 0.39, CHCl₃). Enantiomeric excess was determined by chiral HPLC analysis in comparison with authentic racemic material using a Chiralpak IA column: hexanes:^{i}PrOH = 95:05, flow rate 0.5 mL/min, λ = 210 nm: t$_{major}$ = 28.9 min, t$_{minor}$ = 43.7 min; 99% e.e. Absolute stereochemistry was assigned by analogy to tricyclic γ-lactone (–)-**3k**. ¹H NMR (500 MHz; CDCl₃): δ 7.41-7.38 (m, 5H), 5.06 (d, *J* = 10.1 Hz, 1H), 4.32-4.19 (m, 2H), 3.03 (dd, *J* = 13.3, 11.7 Hz, 1H), 2.95 (dd, *J* = 11.6, 6.2 Hz, 1H), 2.91 (dd, *J* = 12.2, 10.9 Hz, 1H), 2.53 (t, *J* = 6.3 Hz, 1H), 1.73-1.60 (m, 2H), 1.33 (t, *J* = 7.2 Hz, 3H), 1.27 (s, 3H), 1.24-1.16 (m, 2H), 1.11-1.08 (m, 3H), 1.06 (d, *J* = 6.4 Hz, 18H), 0.87 (t, *J* = 7.2 Hz, 3H); ¹³C NMR (125 MHz; CDCl₃): δ 173.5, 170.9, 148.5, 137.2, 129.5, 128.8 (2), 128.1 (2), 109.5, 85.1, 61.1, 50.7, 43.8, 43.4, 42.8, 33.0, 22.1, 18.2 (6), 14.8, 14.25, 14.24, 13.8 (3); IR (thin film): 2948, 2870, 1793, 1737, 1653 cm⁻¹; HRMS (ESI+) *m/z* calcd for C₃₀H₄₇O₅Si [M+H]⁺: 515.3193, found: 515.3211.
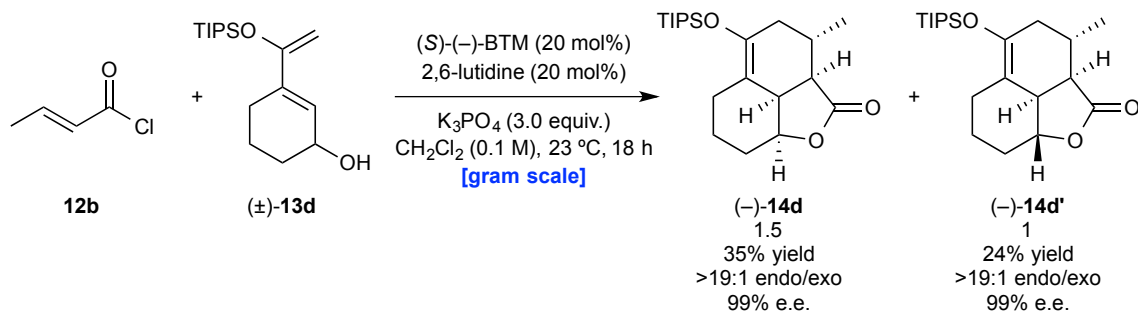
(2a*R*,2a¹*R*,3*S*,8a*S*)-3-methyl-5-((triisopropylsilyl)oxy)-2a,2a¹,3,4,6,7,8,8a-octahydro -2*H*-naphtho[1,8-*bc*]furan-2-one ((–)-14d) and (2a*R*,2a¹*R*,3*S*,8a*R*)-3-methyl-5-((triisopropylsilyl)oxy)-2a,2a¹,3,4,6,7,8,8a-octahydro-2*H*-naphtho[1,8-*bc*]furan-2-one ((–)-14d'): Prepared by a modified representative procedure. To an oven-dried, 250-

mL round-bottomed flask equipped with a magnetic stir bar was added silyloxydiene alcohol (±)-**13d** (2.73 g, 9.21 mmol, 1.0 equiv.), (*S*)-(–)-BTM (465 mg, 1.84 mmol, 20 mol%), 2,6-lutidine (0.21 mL, 1.84 mmol, 20 mol%), K$_3$PO$_4$ (5.87 g, 27.63 mmol, 3.0 equiv.) and anhydrous CH$_2$Cl$_2$ (80 mL, to make final concentration of silyloxydiene alcohol 0.1 M) at ambient temperature (23 °C). With vigorous stirring, crotonoyl chloride **12b** (1.32 mL, 13.82 mmol, 1.5 equiv.) in CH$_2$Cl$_2$ (12 mL) was added over a period of ~5 min. After stirring for 18 h, the reaction mixture was filtered through a pad of celite and concentrated by rotary evaporation. Purification by an automated flash chromatography (5 → 20% EtOAc/hexanes) afforded a single *endo* diastereomer (as judged by ^{1}H NMR) of tricyclic γ-lactone (–)-**14d** (1.17 g, 35% yield, 99% e.e.) and a single *endo* diastereomer (as judged by ^{1}H NMR) of tricyclic γ-lactone (–)-**14d'** (0.80 g, 24% yield, 99% e.e.).

(–)-**14d**: clear colorless oil; TLC (EtOAc:hexanes, 1:9 *v/v*): R$_f$ = 0.34; $[\alpha]_D^{19.2}$ = –62.86 (*c* = 3.50, CHCl$_3$). Enantiomeric excess was determined by chiral HPLC analysis in comparison with authentic racemic material using a Chiralcel OD-H column: hexanes:^{i}PrOH = 95:05, flow rate 0.5 mL/min, λ = 210 nm: t$_{minor}$ = 11.1 min, t$_{major}$ = 12.1 min; 99% e.e. Absolute stereochemistry was assigned by analogy to tricyclic γ-lactone (–)-**3k**. ^{1}H NMR (500 MHz; CDCl$_3$): δ 4.49 (q, *J* = 3.3 Hz, 1H), 2.96-2.93 (m, 1H), 2.88 (d, *J* = 2.2 Hz, 1H), 2.57-2.51 (m, 2H), 2.50-2.44 (m, 1H), 2.19-2.15 (m, 1H), 1.74 (d, *J* = 17.2 Hz, 1H), 1.71-1.65 (m, 1H), 1.61-1.56 (m, 1H), 1.49 (tt, *J* = 12.6, 3.3 Hz, 1H), 1.42 (td, *J* = 12.4, 2.2 Hz, 1H), 1.13-1.07 (m, 6H), 1.05 (d, *J* = 5.9 Hz, 18H); ^{13}C NMR (125 MHz; CDCl$_3$): δ 178.5, 143.6, 108.6, 79.4, 47.6, 37.6, 33.2, 27.8, 25.0, 24.4, 21.0, 20.3, 18.1 (6), 13.4 (3); IR (thin film): 2943, 2867, 1778, 1675 cm^{-1}; HRMS (ESI+) *m/z* calcd for C$_{21}$H$_{37}$O$_3$Si [M+H]$^+$: 365.2512, found: 365.2510.

(–)-**14d'**: clear colorless oil; TLC (EtOAc:hexanes, 1:9 *v/v*): R$_f$ = 0.49; $[\alpha]_D^{19.6}$ = –12.50 (*c* = 1.60, CHCl$_3$). Enantiomeric excess was determined by chiral HPLC analysis in comparison with authentic racemic material using a Chiralpak IA column: hexanes:^{i}PrOH = 95:05, flow rate 0.5 mL/min, λ = 230 nm: t$_{minor}$ = 14.1 min, t$_{major}$ =

17.2 min; 99% e.e. Absolute stereochemistry was assigned by analogy to bicyclic amide (–)-**S21**. ^{1}H NMR (500 MHz; CDCl$_3$): δ 3.90 (td, J = 11.2, 3.4 Hz, 1H), 2.76 (ddd, J = 13.9, 5.1, 1.6 Hz, 1H), 2.40 (dd, J = 10.7, 7.8 Hz, 1H), 2.27-2.19 (m, 2H), 2.17-2.10 (m, 1H), 2.09-2.02 (m, 2H), 1.97-1.91 (m, 1H), 1.73-1.61 (m, 2H), 1.49-1.41 (m, 1H), 1.17 (d, J = 6.1 Hz, 3H), 1.14-1.10 (m, 3H), 1.08 (d, J = 5.6 Hz, 18H); ^{13}C NMR (125 MHz; CDCl$_3$): δ 177.8, 141.3, 110.9, 84.5, 48.8, 45.7, 38.9, 30.7, 28.1, 24.9, 24.8, 18.9, 18.1 (6), 13.2 (3); IR (thin film): 2944, 2867, 1766, 1737, 1697 cm^{-1}; HRMS (ESI+) m/z calcd for C$_{21}$H$_{37}$O$_3$Si [M+H]$^+$: 365.2512, found: 365.2497.
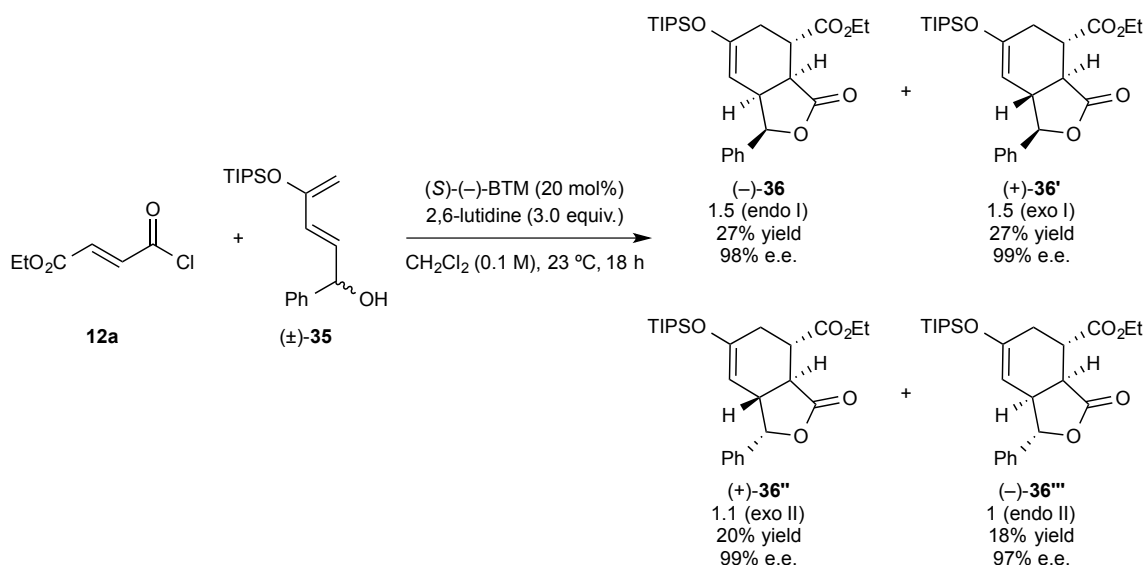
Ethyl (1R,3aS,4S,7aS)-3-oxo-1-phenyl-6-((triisopropylsilyl)oxy)-1,3,3a,4,5,7a-hexa-hydroisobenzofuran-4-carboxylate ((–)-36), ethyl (1R,3aS,4S,7aR)-3-oxo-1-phenyl-6-((triisopropylsilyl)oxy)-1,3,3a,4,5,7a-hexahydroisobenzofuran-4-carboxylate ((+)-36'), ethyl (1S,3aS,4S,7aR)-3-oxo-1-phenyl-6-((triisopropylsilyl)oxy)-1,3,3a, 4,5,7a-hexahydroisobenzofuran-4-carboxylate ((+)-36'') and ethyl (1S,3aS,4S, 7aS)-3-oxo-1-phenyl-6-((triisopropylsilyl)oxy)-1,3,3a,4,5,7a-hexahydro-isobenzo-furan-4-carboxylate ((–)-36'''): Prepared according to the representative procedure using silyloxydiene alcohol (±)-**35** (33 mg, 0.10 mmol, 1.0 equiv.), (S)-(–)-BTM (5.0 mg, 0.020 mmol, 20 mol%), 2,6-lutidine (35 mL, 0.30 mmol, 3.0 equiv.) in anhydrous CH$_2$Cl$_2$ (0.7 mL, to make final concentration of silyloxydiene alcohol 0.1 M) and ethyl

fumaroyl chloride **12a** (20 mL, 0.15 mmol, dissolved in 0.3 mL CH₂Cl₂, 1.5 equiv.) at ambient temperature (23 ℃). Upon completion (as judged by TLC), the reaction mixture was purified by an automated flash chromatography (5 → 20% EtOAc/hexanes) to afford bicyclic γ-lactones (–)-**36** (12.1 mg, 27% yield, 98% e.e.), (+)-**36'** (12.0 mg, 27% yield, 99% e.e.), (+)-**36''** (9.0 mg, 20% yield, 99% e.e.) and (–)-**36'''** (8.3 mg, 18% yield, 97% e.e.).

(–)-**36:** clear colorless oil; TLC (EtOAc:hexanes, 1:9 v/v): R_f = 0.49; $[\alpha]_D^{21.0}$ = –16.40 (c = 10.00, CHCl₃). Enantiomeric excess was determined by chiral HPLC analysis in comparison with authentic racemic material using a Chiralcel OD-H column: hexanes:^{i}PrOH = 95:05, flow rate 0.5 mL/min, λ = 210 nm: t_{major} = 11.3 min, t_{minor} = 13.6 min; 98% e.e. Absolute stereochemistry was assigned by analogy to amide (–)-**S11**. ^{1}H NMR (500 MHz; CDCl₃): δ 7.40-7.37 (m, 2H), 7.34-7.29 (m, 3H), 5.20 (d, J = 2.2 Hz, 1H), 4.92 (dd, J = 2.9, 1.8 Hz, 1H), 4.18-4.07 (m, 2H), 3.28-3.24 (m, 2H), 3.20 (dd, J = 7.6, 4.1 Hz, 1H), 2.51 (ddq, J = 17.6, 2.6, 0.8 Hz, 1H), 2.44 (ddt, J = 17.6, 6.5, 2.1 Hz, 1H), 1.22 (t, J = 7.1 Hz, 3H), 1.19-1.14 (m, 3H), 1.07 (dd, J = 7.2, 1.7 Hz, 18H); ^{13}C NMR (125 MHz; CDCl₃): δ 177.1, 172.8, 151.4, 138.8, 128.9 (2), 128.4, 125.0 (2), 101.6, 85.9, 61.4, 42.6, 38.3, 38.1, 28.8, 18.0 (6), 14.2, 12.4 (3); IR (thin film): 2944, 2867, 1779, 1732, 1667 cm^{-1}; HRMS (ESI+) m/z calcd for C₂₆H₃₉O₅Si [M+H]$^+$: 459.2567, found: 459.2589.

(+)-**36':** clear colorless oil; TLC (EtOAc:hexanes, 1:9 v/v): R_f = 0.43; $[\alpha]_D^{20.2}$ = +35.20 (c = 10.00, CHCl₃). Enantiomeric excess was determined by chiral HPLC analysis in comparison with authentic racemic material using a Chiralcel OD-H column: hexanes:^{i}PrOH = 95:05, flow rate 0.5 mL/min, λ = 210 nm: t_{major} = 22.8 min, t_{minor} = 34.0 min; 99% e.e. Absolute stereochemistry was assigned by analogy to amide (–)-**S11**. ^{1}H NMR (500 MHz; CDCl₃): δ 7.43-7.33 (m, 5H), 4.96 (d, J = 9.7 Hz, 1H), 4.88 (d, J = 1.4 Hz, 1H), 4.33-4.22 (m, 2H), 2.90-2.86 (m, 2H), 2.85-2.78 (m, 1H), 2.56-2.44 (m, 2H), 1.33 (t, J = 7.1 Hz, 3H), 1.15-1.08 (m, 3H), 1.05 (t, J = 6.6 Hz, 18H); 13C NMR (125 MHz; CDCl₃): δ 173.1, 172.8, 153.0, 136.5, 129.1, 129.0 (2), 126.1 (2), 98.7, 84.8,

61.4, 48.2, 46.6, 39.4, 34.4, 18.0 (6), 14.2, 12.6 (3); IR (thin film): 2945, 2868, 1790, 1738, 1650 cm^{-1}; HRMS (ESI+) *m/z* calcd for C$_{26}$H$_{39}$O$_5$Si [M+H]$^+$: 459.2567, found: 459.2544.

(+)-**36''**: clear colorless oil; TLC (EtOAc:hexanes, 1:9 *v/v*): R$_f$ = 0.38; $[\alpha]_D^{21.2}$ = +30.80 (*c* = 10.00, CHCl$_3$). Enantiomeric excess was determined by chiral HPLC analysis in comparison with authentic racemic material using a Chiralcel OD-H column: hexanes:^{i}PrOH = 95:05, flow rate 0.5 mL/min, λ = 210 nm: t$_{minor}$ = 21.7 min, t$_{major}$ = 37.0 min; 99% e.e. Absolute stereochemistry was assigned by derivatization as described on page S216. ^{1}H NMR (500 MHz; CDCl$_3$): δ 7.37-7.30 (m, 3H), 7.19-7.17 (m, 2H), 5.64 (d, *J* = 7.4 Hz, 1H), 4.84 (d, *J* = 1.2 Hz, 1H), 4.31-4.18 (m, 2H), 3.35 (dddt, *J* = 13.5, 7.6, 3.6, 1.9 Hz, 1H), 2.83 (ddd, *J* = 11.6, 10.4, 6.9 Hz, 1H), 2.73 (dd, *J* = 13.6, 11.6 Hz, 1H), 2.43 (dddd, *J* = 17.7, 6.9, 2.0, 1.1 Hz, 1H), 2.22 (dddd, *J* = 17.6, 10.4, 3.5, 1.9 Hz, 1H), 1.31 (t, *J* = 7.1 Hz, 3H), 1.05-1.02 (m, 3H), 0.94-0.84 (m, 18H); ^{13}C NMR (125 MHz; CDCl$_3$): δ 174.2, 173.0, 151.8, 134.9, 128.5 (2), 128.3, 125.5 (2), 100.0, 81.3, 61.3, 43.7, 40.6, 39.5, 34.1, 17.9 (6), 14.2, 12.3 (3); IR (thin film): 2945, 2867, 1790, 1738, 1650 cm^{-1}; HRMS (ESI+) *m/z* calcd for C$_{26}$H$_{39}$O$_5$Si [M+H]$^+$: 459.2567, found: 459.2584.

(−)-**36'''**: clear colorless oil; TLC (EtOAc:hexanes, 1:9 *v/v*): R$_f$ = 0.31; $[\alpha]_D^{21.1}$ = −15.20 (*c* = 10.00, CHCl$_3$). Enantiomeric excess was determined by chiral HPLC analysis in comparison with authentic racemic material using a Chiralcel AS-H column: hexanes:^{i}PrOH = 95:05, flow rate 0.5 mL/min, λ = 210 nm: t$_{major}$ = 15.5 min, t$_{minor}$ = 28.2 min; 97% e.e. Absolute stereochemistry was assigned by analogy to amide (−)-**S11**. ^{1}H NMR (500 MHz; CDCl$_3$): δ 7.37-7.32 (m, 2H), 7.29-7.26 (m, 1H), 7.25-7.23 (m, 2H), 5.63 (d, *J* = 5.2 Hz, 1H), 4.19-4.11 (m, 2H), 3.99-3.99 (m, 1H), 3.59-3.55 (m, 1H), 3.49 (dd, *J* = 6.8, 2.6 Hz, 1H), 3.34 (dt, *J* = 5.4, 2.8 Hz, 1H), 2.48-2.46 (m, 2H), 1.25 (t, *J* = 7.1 Hz, 3H), 0.90-0.82 (m, 21H); ^{13}C NMR (125 MHz; CDCl$_3$): δ 176.8, 173.0, 151.4, 135.7, 128.5 (2), 127.9, 125.3 (2), 97.8, 82.9, 61.3, 41.9, 40.0, 37.8, 27.9, 17.8

(6), 14.2, 12.2 (3); IR (thin film): 2945, 2867, 1778, 1731, 1665 cm^{-1}; HRMS (ESI+) *m/z* calcd for C$_{26}$H$_{39}$O$_5$Si [M+H]$^+$: 459.2567, found: 459.2592.

Use of a lower catalyst loading for the DAL (10 mol%) as described for bicyclic γ-lactones (−)-36, (+)-36', (+)-36'' and (−)-36''' on gram scale: This reaction was performed according to the procedure described above for (−)-**36**, (+)-**36'**, (+)-**36''** and (−)-**36'''** with the exception that a lower catalyst loading (10 vs. 20 mol%), and a longer addition time (10 vs. 5 h) were employed. Silyloxydiene alcohol (±)-**35** (3.30 g, 9.92 mmol, 1.0 equiv.), (*S*)-(−)-BTM (250 mg, 0.99 mmol, 10 mol%), 2,6-lutidine (3.47 mL, 29.7 mmol, 3.0 equiv.) in anhydrous CH$_2$Cl$_2$ (80 mL, to make final concentration of silyloxydiene alcohol 0.1 M) and ethyl fumaroyl chloride **12a** (2.0 mL, 14.8 mmol, dissolved in 15 mL CH$_2$Cl$_2$, 1.5 equiv.) at ambient temperature (23 ºC). The solution of ethyl fumaroyl chloride **12a** was added by syringe pump over 10 h and the reaction was allowed to stir for 8 h at ambient temperature (23 ºC). Upon completion (as judged by TLC), the reaction mixture was purified by an automated flash chromatography (5 → 20% EtOAc/hexanes) to afford bicyclic γ-lactones (−)-**36** (0.80 g, 18% yield, 98% e.e.), (+)-**36'** (0.74 g, 16% yield, 99% e.e.), (+)-**36''** (0.69 g, 15% yield, 99% e.e.), (−)-**36'''** (0.68 g, 15% yield, 97% e.e.) and ester (±)-**S10** (0.54 g, 12% yield). All spectral data matched that reported above.
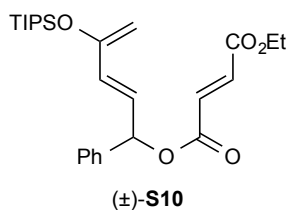
Ethyl ((*E*)-1-phenyl-4-((triisopropylsilyl)oxy)penta-2,4-dien-1-yl) fumarate ((±)-S10): pale yellow oil; TLC (EtOAc:hexanes, 1:9 *v/v*): R$_f$ = 0.77; $[\alpha]_D^{21.1}$ = 0.00 (*c* = 3.00, CHCl$_3$). ^{1}H NMR (500 MHz; CDCl$_3$): δ 7.37-7.36 (m, 3H), 7.32-7.29 (m, 2H), 7.15 (dd, *J* = 15.9, 10.9 Hz, 1H), 6.94-6.85 (m, 2H), 6.48 (d, *J* = 15.9 Hz, 1H), 5.68 (d, *J* = 10.9 Hz, 1H), 4.68 (s, 2H), 4.27 (q, *J* = 7.1 Hz, 2H), 1.33 (t, *J* = 7.1 Hz, 3H), 1.27-1.20 (m, 3H), 1.14 (d, *J* = 7.2 Hz, 18H); ^{13}C NMR (125 MHz; CDCl$_3$): δ 165.0, 164.7, 146.6, 138.0, 134.5, 133.1, 130.4, 128.8 (2), 127.3, 126.3 (2), 122.7, 113.5,

67.1, 61.6, 18.1 (6), 14.2, 13.3 (3); IR (thin film): 2944, 2867, 1727, 1645 cm^{-1}; HRMS (ESI+) m/z calcd for C$_{26}$H$_{39}$O$_5$Si [M+H]$^+$: 459.2567, found: 459.2582.
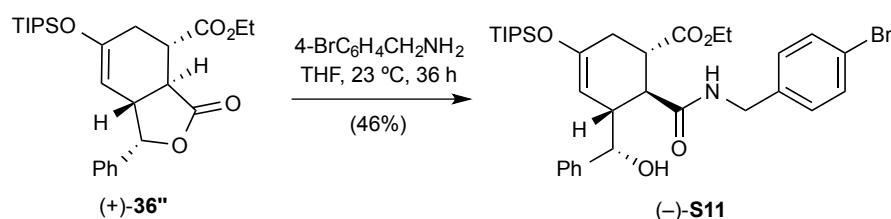
Ethyl (1S,5R,6S)-6-((4-bromobenzyl)carbamoyl)-5-((S)-hydroxy(phenyl)methyl)-3-((triisopropylsilyl)oxy)cyclohex-3-ene-1-carboxylate ((–)-S11): Into an oven-dried, 5-mL round-bottomed flask containing a solution of bicyclic γ-lactone **(+)-36''** (50 mg, 0.11 mmol, 1.0 equiv.) in THF (1.1 mL, to make final concentration of bicyclic g-lactone 0.1 M), was added dropwise 4-bromobenzylamine (70 mL, 0.55 mmol, 5.0 equiv.). The reaction was allowed to stir at ambient temperature (23 ºC) for 36 h. Upon completion (as judged by TLC), the reaction was concentrated by rotary evaporation and purified by an automated flash chromatography system (20 → 50% EtOAc/hexanes) to afford amide (–)-S11 (32 mg, 46% yield) as a white solid: m.p. 151-155 ºC (recrystallized from Et$_2$O); TLC (EtOAc:hexanes, 1:2 v/v): R$_f$ = 0.49; $[\alpha]_D^{20.4}$ = -13.95 (c = 0.86, CHCl$_3$). Absolute stereochemistry was assigned based on X-ray analysis using anomalous dispersion (see **Figure S1**). ^{1}H NMR (500 MHz; CDCl$_3$): δ 7.42 (d, J = 8.3 Hz, 2H), 7.37-7.34 (m, 2H), 7.29-7.24 (m, 3H), 7.19 (d, J = 8.3 Hz, 2H), 6.73 (t, J = 6.0 Hz, 1H), 4.82 (d, J = 4.6 Hz, 1H), 4.51 (dd, J = 14.9, 6.5 Hz, 1H), 4.42 (s, 1H), 4.30 (dd, J = 15.0, 5.5 Hz, 1H), 4.09-3.97 (m, 2H), 3.10-3.06 (m, 2H), 2.83 (dd, J = 11.6, 10.4 Hz, 1H), 2.41-2.24 (m, 2H), 1.22 (t, J = 7.1 Hz, 3H), 1.07-1.03 (m, 3H), 0.99 (dd, J = 14.2, 6.1 Hz, 18H); ^{13}C NMR (125 MHz; CDCl$_3$): δ 174.7, 173.8, 151.9, 142.4, 137.6, 131.8 (2), 129.7 (2), 128.3 (2), 127.2, 125.3 (2), 121.3, 98.5, 73.0, 61.1, 45.9, 45.5, 43.2, 43.1, 32.9, 18.0 (6), 14.2, 12.5 (3); IR (thin film): 3316, 2925, 2866, 1728, 1673, 1645 cm^{-1}; HRMS (ESI+) m/z calcd for C$_{33}$H$_{47}$BrNO$_5$Si [M+H]$^+$: 644.2407, found: 644.2384.

Representative procedure for the Diels-Alder/lactamization process as described for tricyclic γ-lactam (+)-23:
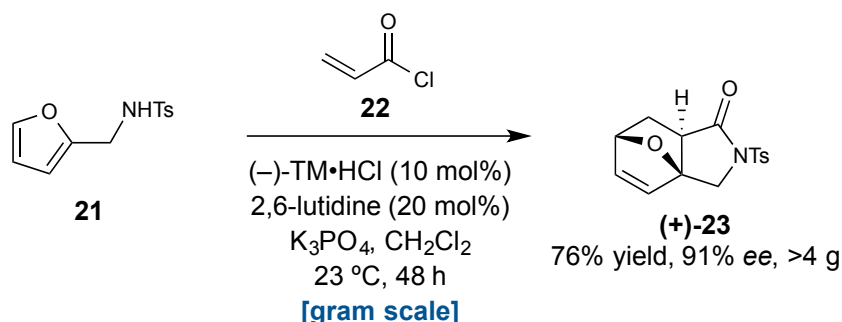
(3aS,6S,7aR)-2-tosyl-2,3,7,7a-tetrahydro-3a,6-epoxyisoindol-1(6H)-one ((+)-23): To an oven-dried, 25-mL round-bottomed flask equipped with a magnetic stir bar was added furanyldiene sulfonamide **21**[1] (4.60 g, 18.3 mmol, 1.0 equiv.), (−)-Levamisole·HCl (442 mg, 1.83 mmol, 10 mol%), 2,6-lutidine (0.43 mL, 3.66 mmol, 20 mol%), K$_3$PO$_4$ (9.7 g, 45.8 mmol, 2.5 equiv.) and anhydrous CH$_2$Cl$_2$ (185 mL, to make final concentration of silyloxydiene alcohol 0.1 M) at ambient temperature (23 ºC). With vigorous stirring, acryloyl chloride **22** (1.8 mL, 21.9 mmol, 1.2 equiv.) in CH$_2$Cl$_2$ (1.2 mL) was added over a period of 5 min. After stirring for an additional 18 h, the reaction mixture was filtered through a pad of celite and concentrated by rotary evaporation. Purification by an automated flash chromatography (10 → 80% EtOAc/hexanes) afforded a single diastereomer (as judged by ^{1}H NMR) of tricyclic γ-lactam (+)-**23** (4.24 g, 76% yield, 91% ee) as a white solid: TLC (EtOAc:hexanes, 1:1 v/v): R$_f$ = 0.44; $[\alpha]_D^{20.0}$ = +5.88 (c = 3.40, CHCl$_3$). Enantiomeric excess was determined by chiral HPLC analysis in comparison with authentic racemic material using a Chiralcel AS-H column: hexanes:^{i}PrOH = 40:60, flow rate 1.0 mL/min, λ = 230 nm: t$_{minor}$ = 12.1 min, t$_{major}$ = 14.8 min; 91% ee. Absolute stereochemistry was assigned by analogy to epoxide (+)-**28**. ^{1}H NMR (500 MHz; CDCl$_3$): δ 7.90 (d, J = 8.3 Hz, 2H), 7.32 (d, J = 8.5 Hz, 2H), 6.41 (dd, J = 5.8, 1.6 Hz, 1H), 6.38 (d, J = 5.8 Hz, 1H), 4.98 (dd, J = 4.5, 1.5 Hz, 1H), 4.45 (d, J = 12.0 Hz, 1H), 4.32 (d, J = 12.0 Hz, 1H), 2.55 (dd, J = 8.7, 3.2 Hz, 1H), 2.42 (s, 3H), 2.09 (dt, J = 11.9, 3.9 Hz, 1H), 1.55 (dd, J = 12.0, 8.7 Hz, 1H); ^{13}C NMR (125 MHz;

CDCl$_3$): δ 172.6, 145.1, 138.0, 135.2, 132.3, 129.7 (2), 128.0 (2), 87.8, 78.9, 49.9, 48.3, 28.9, 21.7; IR (thin film): 2956, 1741 cm^{-1}; HRMS (ESI+) *m/z* calcd for C$_{15}$H$_{16}$NO$_4$S [M+H]$^+$: 306.0800, found: 306.0811.
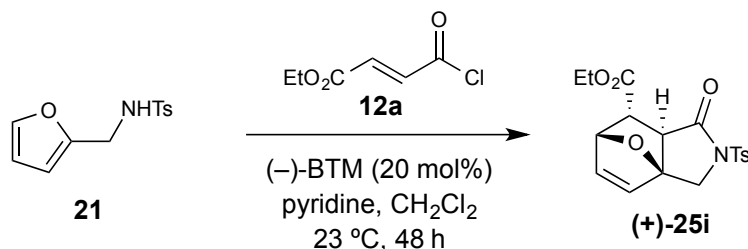
Ethyl (3a*S*,6*R*,7*R*,7a*R*)-1-oxo-2-tosyl-1,2,3,6,7,7a-hexahydro-3a,6-epoxyisoindole-7-carboxylate ((+)-25i): Prepared according to the representative procedure using furanyldiene sulfonamide **21** (360 mg, 1.43 mmol, 1.0 equiv.), (*S*)-(−)-BTM (72 mg, 0.143 mmol, 20 mol%), pyridine (0.13 mL, 1.57 mmol, 1.1 equiv.) in anhydrous CH$_2$Cl$_2$ (1.45 mL, to make initial concentration of furanyldiene sulfonamide 0.1 M) and ethyl fumaroyl chloride **12a** (0.23 mL, 1.72 mmol, dissolved in 0.7 mL CH$_2$Cl$_2$, 1.2 equiv.) at ambient temperature (23 ºC). Upon completion (as judged by TLC), the reaction mixture was purified by an automated flash chromatography (10 → 80% EtOAc/hexanes) to afford a single *endo* diastereomer (as judged by ^{1}H NMR) of tricyclic γ-lactam (+)-**25i** (460 mg, 85% yield, 92% e.e.) as an off-white solid: TLC (EtOAc:hexanes, 1:1 *v/v*): R$_f$ = 0.62; $[\alpha]_D^{19.9}$ = +72.63 (*c* = 3.80, CHCl$_3$). Enantiomeric excess was determined by chiral HPLC analysis in comparison with authentic racemic material using a Chiralcel AD-H column: hexanes:^{i}PrOH = 60:40, flow rate 0.5 mL/min, λ = 230 nm: t$_{minor}$ = 27.2 min, t$_{major}$ = 30.9 min; 94% *ee*. Absolute stereochemistry was assigned by analogy to epoxide (+)-**28**. ^{1}H NMR (500 MHz; CDCl$_3$): δ 7.91 (d, J = 8.4 Hz, 2H), 7.33 (d, J = 8.0 Hz, 2H), 6.53 (d, J = 5.8 Hz, 1H), 6.34 (dd, J = 5.8, 1.6 Hz, 1H), 5.18 (dd, J = 4.9, 1.5 Hz, 1H), 4.45 (d, J = 12.2 Hz, 1H), 4.31 (d, J = 12.2 Hz, 1H), 4.09 (q, J = 7.1 Hz, 2H), 3.36 (dd, J = 4.8, 3.4 Hz, 1H), 3.03 (d, J = 3.3 Hz, 1H), 2.44 (s, 3H), 1.22 (t, J = 7.1 Hz, 3H); ^{13}C NMR (125 MHz; CDCl$_3$): δ 171.1, 169.6, 145.3, 135.8, 134.9, 134.31, 134.30, 129.7 (2), 128.1 (2), 89.1, 80.2, 61.4, 52.1, 49.8, 47.6, 21.7, 14.1; IR (thin film): 2983, 1734 cm^{-1}; HRMS (ESI+) *m/z* calcd for C$_{18}$H$_{20}$NO$_6$S [M+H]$^+$: 378.1011, found: 378.1018.

Synthetic applications of γ-lactone (−)-14d, γ-lactams (+)-23 and (+)-25:

(−)-**14d**   **S12**   (+)-**26**
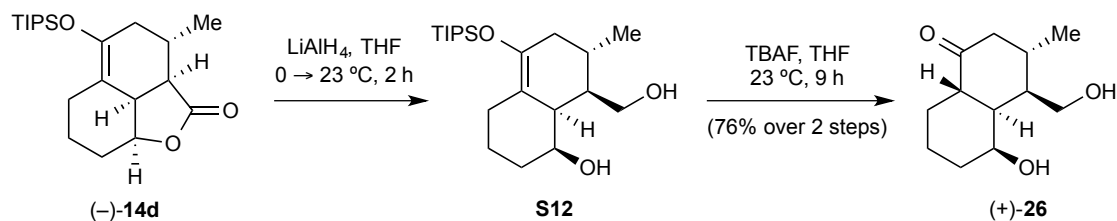
(3*S*,4*R*,4a*R*,5*S*,8a*S*)-5-hydroxy-4-(hydroxymethyl)-3-methyloctahydronaphthalen-1(2*H*)-one ((+)-26): Into an oven-dried, 10-mL round-bottomed flask containing a solution of tricyclic γ-lactone (−)-**14d** (50 mg, 0.14 mmol, 1.0 equiv.) in anhydrous THF (2.7 mL, to make initial concentration of tricyclic γ-lactone 0.05 M) was added LiAlH$_4$ (2.0 M solution in THF, 0.21 mL, 0.42 mmol, 3.0 equiv.) dropwise at 0 ºC. After stirring for 20 min, the ice bath was removed and the mixture was allowed to warm up to ambient temperature (23 ºC) on its own accord over 40 min. Upon completion (as judged by TLC), the reaction mixture was cooled to 0 ºC and carefully quenched in sequence with 17 mL H$_2$O, 17 mL 15% aqueous NaOH, and 42 mL H$_2$O. The ice bath was removed and the mixture was allowed to warm up to ambient temperature (23 ºC) on its own accord. Subsequently, anhydrous MgSO$_4$ was added and the reaction mixture was vigorously stirred for 30 min, filtered through a pad of celite and concentrated by rotary evaporation to afford crude diol **S12** as a clear colorless oil. The crude material was of sufficient purity to be carried on directly to the next step.

To a solution of crude diol **S12** in anhydrous THF (2.8 mL, to make final concentration of crude diol 0.05 M) at 0 ºC was added TBAF (1.0 M solution in THF, 0.70 mL, 0.69 mmol, 5.0 equiv.) dropwise. The reaction was stirred for 10 min at 0 ºC then allowed to warm up to ambient temperature (23 ºC) and stirred for 9 h. The reaction mixture was quenched with a saturated aqueous solution of NH$_4$Cl (2.0 mL). The aqueous layer was extracted with Et$_2$O (2 x 5.0 mL) and washed with brine (2.0 mL). The organic layer was then dried over anhydrous MgSO$_4$, filtered, and concentrated by rotary evaporation. The residue was purified by an automated flash chromatography system (20 → 80% EtOAc/hexanes) providing 22 mg (76% yield over 2 steps) of ketone

(+)-**26** as a clear colorless oil: TLC (EtOAc:hexanes, 3:1 *v/v*): R_f = 0.36; $[\alpha]_D^{19.7}$ = +17.50

(*c* = 0.16, CHCl$_3$). ^{1}H NMR (500 MHz; CDCl$_3$): δ 4.17 (dd, *J* = 11.2, 8.8 Hz, 1H), 4.13

(s, 1H), 3.71 (dd, *J* = 11.3, 2.1 Hz, 1H), 2.71 (td, *J* = 12.0, 3.5 Hz, 1H), 2.41 (dd, *J* =

14.2, 5.7 Hz, 1H), 2.26-2.21 (m, 1H), 2.10-2.08 (m, 1H), 2.06-2.05 (m, 1H), 1.90 (dd, *J*

= 12.8, 4.0 Hz, 1H), 1.84-1.79 (m, 1H), 1.73-1.66 (m, 1H), 1.61-1.55 (m, 1H), 1.47 (tdd,

J = 13.6, 4.1, 2.1 Hz, 1H), 1.29-1.20 (m, 2H), 0.97 (d, *J* = 7.1 Hz, 3H); ^{13}C NMR (125

MHz; CDCl$_3$): δ 213.4, 69.3, 64.9, 46.6, 44.7, 44.4, 43.9, 35.6, 33.8, 25.9, 20.5, 18.9; IR

(thin film): 3332, 2934, 1703 cm^{-1}; HRMS (ESI+) *m/z* calcd for $C_{12}H_{20}LiO_3$ [M+Li]$^+$:

219.1572, found: 219.1582.
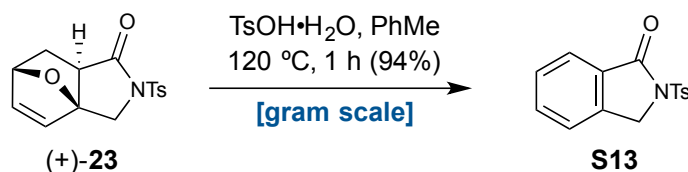
2-Tosylisoindolin-1-one (S13): To a dried pressure tube with *p*-toluenesulfonic acid

monohydrate (6.20 g, 32.8 mmol, 5.0 equiv.) was added an anhydrous toluene (90 mL,

to make initial concentration of (+)-**23** 0.07 M) solution of compound (+)-**23** (2.0 g, 6.55

mmol, 1.0 equiv.). The resulting mixture was purged with Ar for 5 min, then heated at

120 °C for 1 h. The reaction mixture was quenched with a saturated aqueous solution of

NaHCO$_3$ (50 mL). The aqueous layer was extracted with Et$_2$O (2 x 50 mL) and washed

with brine (10 mL). The organic layer was then dried over anhydrous MgSO$_4$, filtered,

and concentrated by rotary evaporation. The residue was purified by an automated flash

chromatography system (5 → 50% EtOAc/hexanes) providing 1.77 g (94% yield) of

lactam **S13** as a white solid: TLC (EtOAc:hexanes, 1:1 *v/v*): R_f = 0.70. ^{1}H NMR (500

MHz; CDCl$_3$): δ 8.05 (d, J = 8.4 Hz, 2H), 7.83 (d, J = 8.4 Hz, 1H), 7.66 (td, J = 7.5, 1.1

Hz, 1H), 7.51 (dd, J = 7.1, 0.5 Hz, 2H), 7.36 (dd, J = 8.1, 0.5 Hz, 2H), 4.94 (s, 2H), 2.44

(s, 3H); ^{13}C NMR (125 MHz; CDCl$_3$): δ 166.1, 145.3, 141.0, 135.4, 133.9, 130.2, 129.8

(2), 128.8, 128.2 (2), 125.1, 123.4, 49.9, 21.7; IR (thin film): 1726, 1171, 1088 cm^{-1};

HRMS (ESI+) *m/z* calcd for $C_{15}H_{14}NO_3S$ [M+H]$^+$: 288.0694, found: 288.0705.
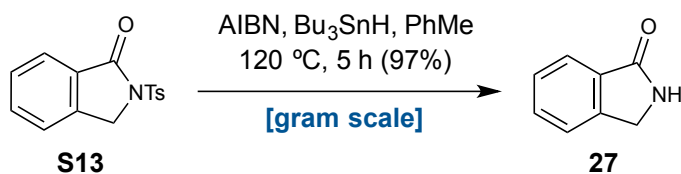
Isoindolin-1-one (27): To a refluxing solution of compound **S13** (2.52 g, 8.78 mmol, 1.0 equiv.) and Bu₃SnH (11.8 mL, 43.9 mmol, 5.0 equiv.) in degassed toluene (300 mL, to make initial concentration of **S13** 0.03 M) was added in three portions AIBN (720 mg, 4.4 mmol, 0.5 equiv.) every 1 h. The reaction mixture was refluxed for another 2 h. The solvent was then evaporated under vacuum, and the crude residue was purified by an automated flash chromatography system (0.1 → 10% MeOH/EtOAc) providing 1.13 g (97% yield) of isoindolinone **27** as a white solid: TLC (MeOH:EtOAc, 1:9 *v/v*): R_f = 0.60. ^{1}H NMR (500 MHz; CDCl₃): δ 8.35 (br s, 1H), 7.87 (d, *J* = 7.4 Hz, 1H), 7.57 (td, *J* = 7.4, 1.0 Hz, 1H), 7.48 (d, *J* = 6.4 Hz, 2H), 4.48 (s, 2H); ^{13}C NMR (125 MHz; CDCl₃): δ 172.4, 143.7, 132.3, 131.7, 127.9, 123.6, 123.2, 45.9; IR (thin film): 3215, 1682 cm^{-1}; HRMS (ESI+) *m/z* calcd for C₈H₈NO [M+H]$^+$: 134.0606, found: 134.0608.
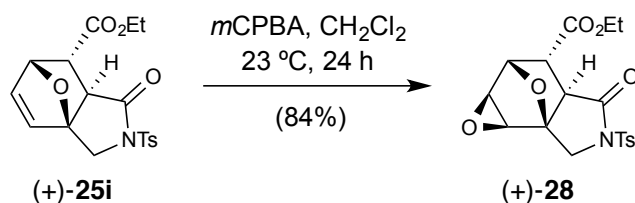
Ethyl (1aS,2S,3R,3aR,6aS,6bS)-4-oxo-5-tosyloctahydro-2,6a-epoxyoxireno[2,3-e]isoindole-3-carboxylate ((+)-28): Under ice cooling (0 ºC), (+)-**25i** (70 mg, 0.19 mmol, 1.0 equiv.) was dissolved in CH₂Cl₂ (2.0 mL, to make initial concentration of (+)-**25i** 0.1 M). After stirring for 10 min, a solution of *m*CPBA (70–75%, 182 mg, 0.74 mmol, 4.0 equiv.) in CH₂Cl₂ (2.0 mL) was slowly added. The solution was stirred for 24 h at 23 ºC. The reaction mixture was purified by an automated flash chromatography system (20 → 80% EtOAc/hexanes) providing 61 mg (76% yield) of epoxide (+)-**28** as a clear colorless oil: TLC (EtOAc:hexanes, 1:1 *v/v*): R_f = 0.44; $[\alpha]_D^{19.7}$ = +43.81 (*c* = 0.21, CHCl₃). Absolute stereochemistry was assigned based on X-ray analysis using

anomalous dispersion (see **Figure S2**). ^{1}H NMR (500 MHz; CDCl$_3$): δ 7.89 (d, J = 8.1 Hz, 2H), 7.33 (d, J = 8.3 Hz, 2H), 4.70 (d, J = 5.2 Hz, 1H), 4.35 (d, J = 12.4 Hz, 1H), 4.28 (d, J = 12.3 Hz, 1H), 4.19 (q, J = 7.1 Hz, 2H), 3.56 (dd, J = 3.2, 0.8 Hz, 1H), 3.43 (dd, J = 3.3, 0.7 Hz, 1H), 3.33 (t, J = 4.4 Hz, 1H), 3.26 (d, J = 3.8 Hz, 1H), 2.44 (s, 3H), 1.28 (td, J = 7.1, 0.9 Hz, 3H); ^{13}C NMR (125 MHz; CDCl$_3$): δ 170.4, 168.7, 145.5, 134.7, 129.8 (2), 128.1 (2), 84.9, 76.3, 62.0, 52.5, 51.0, 48.6, 48.31, 48.19, 21.7, 14.2; IR (thin film): 2984, 1734, 1171 cm^{-1}; HRMS (ESI+) m/z calcd for C$_{18}$H$_{20}$NO$_7$S [M+H]$^+$: 394.0960, found: 394.0972.
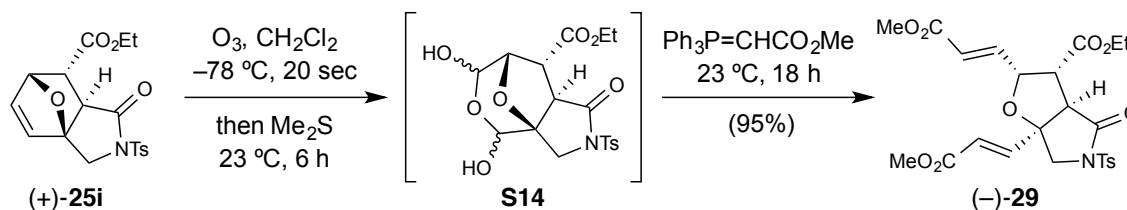
Dimethyl 3,3'-((2R,3R,3aR,6aS)-3-(ethoxycarbonyl)-4-oxo-5-tosylhexahydro-6aH-furo[2,3-c]pyrrole-2,6a-diyl)(2E,2'E)-diacrylate ((–)-29): A solution of tricyclic γ-lactam (+)-**25i** (200 mg, 0.53 mmol, 1.0 equiv.) was dissolved in CH$_2$Cl$_2$ (10.0 mL, to make initial concentration of (+)-**25i** 0.05 M) and cooled to −78 °C. Ozone was bubbled through the reaction solution until a blue color persisted. Excess ozone was removed by blowing N$_2$ gas into the solution with stirring for 10 min. Dimethylsulfide (0.70 mL, 10.6 mmol, 20.0 equiv.) was added by syringe and the reaction was slowly warmed to ambient temperature (23 °C) over 6 h at which time TLC indicated the reaction was complete. ^{1}H NMR analysis from an aliquot of the crude reaction mixture indicated the formation of **S14** intermediate. To a resultant crude mixture of **S14** was added at once methyl (triphenylphosphoranylidene)acetate (445 mg, 1.33 mmol, 2.5 equiv.). The solution was stirred for 18 h at 23 °C. The reaction mixture was purified by an automated flash chromatography system (5 → 50% EtOAc/hexanes) providing 262 mg (95% yield) of lactam (–)-**29** as a clear colorless oil: TLC (EtOAc:hexanes, 1:1 v/v): R$_f$ = 0.66; $[\alpha]_D^{20.1}$ = −36.87 (c = 1.15, CHCl$_3$). ^{1}H NMR (500 MHz; CDCl$_3$): δ 7.91 (d, J = 8.4 Hz, 2H), 7.37 (d, J = 8.4 Hz, 2H), 7.01 (d, J = 15.5 Hz, 1H), 6.86 (dd, J = 15.6, 4.9 Hz, 1H),

6.16 (d, J = 15.5 Hz, 1H), 6.06 (dd, J = 15.6, 1.7 Hz, 1H), 4.57 (ddd, J = 6.5, 4.9, 1.7 Hz, 1H), 4.16-3.97 (m, 5H), 3.75 (s, 3H), 3.75 (s, 3H), 3.52-3.45 (m, 1H), 2.46 (s, 3H), 1.14 (t, J = 7.1 Hz, 3H). ^{13}C NMR (125 MHz; CDCl$_3$): δ 170.7, 168.4, 166.08, 165.89, 146.0, 145.7, 145.4, 141.5, 134.3, 130.0 (2), 128.1 (2), 122.0, 121.7, 83.8, 80.2, 61.7, 56.8, 56.1, 52.1, 51.8, 21.8, 13.9; IR (thin film): 2985, 2954, 1728, 1665, 1597 cm^{-1}; HRMS (ESI+) *m/z* calcd for C$_{24}$H$_{28}$NO$_{10}$S [M+H]$^+$: 522.1434, found: 522.1433.
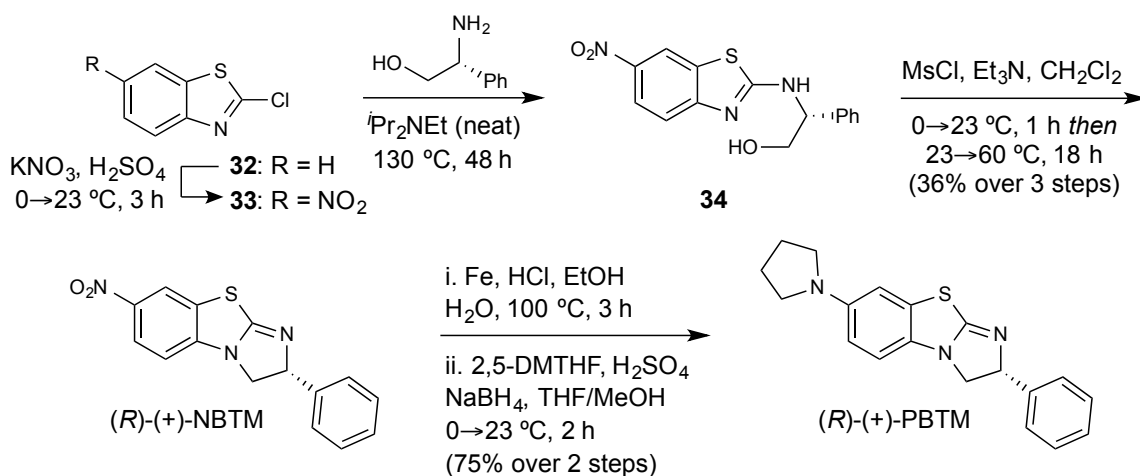
(R)-7-nitro-2-phenyl-2,3-dihydrobenzo[*d*]imidazo[2,1-*b*]thiazole ((R)-(+)-NBTM): 2-Chlorobenzothiazole (4.00 g, 24.0 mmol, 1.0 equiv) was added dropwise to a concentrated H$_2$SO$_4$ (35 mL) in ice water bath (0 ºC). Potassium nitrate (2.63 g, 26.0 mmol, 1.1 equiv) was then added at once. The resulting mixture was stirred at 0 ºC for 1 h and then at room temperature (23 ºC) for 2 h. The solution was subsequently poured onto ice. The precipitate was obtained by filtration and washed several times with ice cold water to obtain **33**[2] with >95% purity as determined by ^{1}H NMR, which was used in the next step without further purification.

A 100 mL pressure tube containing a stirrer bar was charged with (R)-(–)-2-phenylglycinol (2.60 g, 19.0 mmol, 1.2 equiv), crude **33** (~3.40 g, 15.8 mmol, 1.0 equiv) and ^{i}Pr$_2$NEt (55.0 mL, to make initial concentration of **33** 0.3 M). The resulting yellow suspension was stirred vigorously and heated to reflux at 130 °C, at which point the suspended solid had dissolved to leave a yellow solution. After 48 h at 130 ºC, the

orange reaction mixture was allowed to cool to room temperature (23 ºC). Once cooled, the crude reaction mixture was diluted with EtOAc/PhMe/CH$_2$Cl$_2$ (1:1:1, 150 mL) and quenched with 2N HCl (50 mL) under vigorous stirring. The aqueous layer was extracted with CH$_2$Cl$_2$ (2 x 50 mL) and washed with brine (40 mL). The organic layer was then dried over anhydrous MgSO$_4$, filtered, concentrated by rotary evaporation to deliver **34** that was used immediately without purification.

To a crude alcohol **34** (~5.00 g, 15.8 mmol, 1.0 equiv) dissolved in CH$_2$Cl$_2$ (100 mL, to make initial concentration of **34** 0.15 M) was added dropwise Et$_3$N (6.6 ml, 47.4 mmol, 3.0 equiv) and MsCl (1.8 ml, 23.7 mmol, 1.5 equiv) at 0 ºC. The reaction mixture was stirred at 0°C for 1 h. MeOH (1.3 ml, 23.7 mmol, 1.5 equiv) was added *via* syringe and the mixture was stirred at room temperature for 30 minutes, then Et$_3$N (22.0 ml, 158 mmol, 10 equiv) was added. The reaction mixture was refluxed at 60 °C for 18 h, cooled to room temperature, washed with brine, then dried over MgSO$_4$, filtered, and evaporated. The residue was purified by an automated flash chromatography system (10 → 90% EtOAc/hexanes) providing 2.52 g (36% yield over 3 steps) of (*R*)-(+)-NBTM as a pale orange solid: TLC (EtOAc:hexanes, 1:1 *v/v*): R$_f$ = 0.30. $[\alpha]_D^{19.1}$ = +88.42 (*c* = 0.38, CHCl$_3$). ^{1}H NMR (500 MHz; CDCl$_3$): δ 8.21 (dd, J = 2.1, 0.7 Hz, 1H), 8.15 (ddd, J = 8.7, 2.2, 0.9 Hz, 1H), 7.41-7.31 (m, 5H), 6.68 (dd, J = 8.7, 0.6 Hz, 1H), 5.77 (dd, J = 10.1, 7.8 Hz, 1H), 4.36 (td, J = 9.8, 0.7 Hz, 1H), 3.80 (ddd, J = 9.3, 7.8, 0.8 Hz, 1H); ^{13}C NMR (125 MHz; CDCl$_3$): δ 165.1, 142.0, 141.7, 128.9 (2), 128.4, 128.0, 126.4 (2), 124.1, 119.1, 107.05, 107.04, 76.1, 52.0; IR (thin film): 1614, 1593, 1516 cm^{-1}; HRMS (ESI+) *m/z* calcd for C$_{15}$H$_{12}$N$_3$O$_2$S [M+H]$^+$: 298.0650, found: 298.0652.

(*R*)-2-phenyl-7-(pyrrolidin-1-yl)-2,3-dihydrobenzo[*d*]imidazo[2,1-*b*]thiazole ((*R*)-(+)-PBTM): A suspension of Fe (280 mg, 5.0 mmol, 10 equiv) in EtOH (5.0 mL, to make initial concentration of (*R*)-(+)-NBTM 0.1 M) and H$_2$O (1.5 mL) was mixed with HCl (0.2 mL) at room temperature (23 ºC). (*R*)-(+)-NBTM (150 mg, 0.5 mmol, 1.0 equiv) was added to the suspension and refluxed at 100 ºC for 3 h. The resulting mixture was extracted with CH$_2$Cl$_2$ (2 x 20 mL) and washed with brine. The solvent was

removed under reduced pressure and the crude was used in the next step without further purification.

A THF (1.0 mL) solution of 2,5-dimethoxytetrahydrofuran (0.10 mL, 0.59 mmol, 1.3 equiv) and 2.5M H_2SO_4 (0.50 mL, 1.13 mmol, 2.5 equiv) was added dropwise (*ca.* 20 min) to an open vessel containing a solution of the crude amine (~120 mg, 0.45 mmol, 1.0 equiv) in MeOH/THF (3.0 mL, 1:1) and $NaBH_4$ (70 mg, 1.8 mmol, 4.0 equiv) was added under vigorous stirring at 0 ºC. The mixture was then allowed to warm up to room temperature (23 ºC) and stirred for 2 h. Then it was diluted with an aqueous $NaHCO_3$ solution (10 mL), extracted with CH_2Cl_2 (3 × 30 mL), washed with brine, then dried over $MgSO_4$, filtered, and evaporated. The residue was purified by an automated flash chromatography system (10 → 90% EtOAc/hexanes) providing 121 mg (75% yield over 2 steps) of (*R*)-(+)-PBTM as a pale orange solid: TLC (EtOAc:hexanes, 1:1 *v/v*): R_f = 0.45. $[\alpha]_D^{16.2}$ = +97.96 (*c* = 0.49, $CHCl_3$). ^1H NMR (500 MHz; $CDCl_3$): δ 7.41-7.35 (m, 4H), 7.30-7.27 (m, 1H), 6.60-6.58 (m, 2H), 6.41 (dd, J = 8.5, 2.3 Hz, 1H), 5.62 (t, J = 9.3 Hz, 1H), 4.22 (t, J = 9.3 Hz, 1H), 3.66 (t, J = 8.5 Hz, 1H), 3.24 (t, J = 6.5 Hz, 4H), 2.03-2.01 (m, 4H); ^{13}C NMR (125 MHz; $CDCl_3$): δ 167.5, 144.3, 143.3, 128.81, 128.63 (2), 127.8, 127.4, 126.6 (2), 109.8, 109.4, 106.7, 75.1, 53.4, 48.2 (2), 25.4 (2); IR (thin film): 2923, 2850, 1594, 1565 cm^{-1}; HRMS (ESI+) *m/z* calcd for $C_{19}H_{20}N_3S$ [M+H]$^+$: 322.1378, found: 322.1386.

Figure S1. Single crystal X-ray structure (ORTEP) of amide (–)-**S11.** The crystals were grown from a concentrated solution of amide (–)-**S11** in Et$_2$O (2.0 mL), using a slow evaporation method (probability ellipsoids are shown at the 50% level). X-ray crystallographic data have been deposited in the Cambridge Crystallographic Data Centre database (http://www.ccdc.cam.ac.uk/) under accession code CCDC 972246.
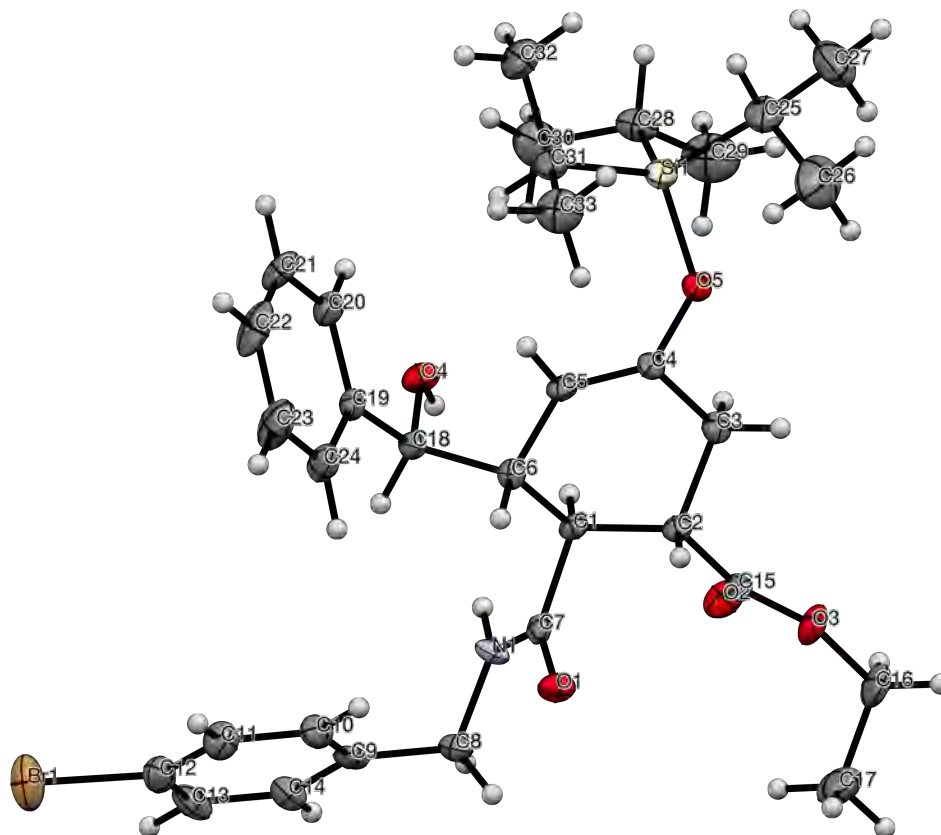
Alert level B:

Crystal system given = orthorhombic

PLAT019_ALERT_1_B Check _diffrn_measured_fraction_theta_full/_max … 0.890.

<u>Author Response</u>: Data was collected on a Bruker GADDS instrument with Cu-source and MWPC (multiwire proportional counter) detector. Under these experimental conditions the maximum angle that can be collected is 120 degrees two-theta.

Table 1. Crystal data and structure refinement for DRB_MA_131001_G_1075C.

Crystal Parameters	Crystal Data
Identification code	1075c
Empirical formula	$C_{33} H_{46} Br N O_5 Si$
Formula weight	644.71
Temperature	110.15 K
Wavelength	1.54178 Å
Crystal system	Orthorhombic
Space group	P 21 21 21
Unit cell dimensions	a = 9.0910(3) Å $\quad$ a = 90º
	b = 18.1061(7) Å $\quad$ b = 90º
	c = 20.6924(7) Å $\quad$ g = 90º
Volume	3406.0(2) Å^3
Z	4
Density (calculated)	1.257 Mg/m^3
Absorption coefficient	2.285 mm^{-1}
F(000)	1360
Crystal size	0.23 x 0.01 x 0.01 mm^3
Theta range for data collection	3.243 to 62.561º
Index ranges	$-10 \leq h \leq 9, -20 \leq k \leq 20, -22 \leq l \leq 23$
Reflections collected	34574
Independent reflections	5224 [R(int) = 0.0645]
Completeness to theta = 67.679º	86.9%
Absorption correction	Semi-empirical from equivalents
Max. and min. transmission	0.7522 and 0.6042
Refinement method	Full-matrix least-squares on F^2
Data / restraints / parameters	5224 / 0 / 378

Goodness-of-fit on F^2		1.126		
Final R indices [I>2sigma(I)]		$R_1 = 0.0328$, $wR_2 = 0.0707$		
R indices (all data)		$R_1 = 0.0423$, $wR_2 = 0.0774$		
Absolute structure parameter		-0.005(8)		
Extinction coefficient		N/A		
Largest diff. peak and hole		0.319 and -0.512 e.Å^{-3}		

Table 2. Atomic coordinates (x 10^4) and equivalent isotropic displacement parameters (Å^2 x 10^3) for DRB_MA_131001_G_1075C. U(eq) is defined as one third of the trace of the orthogonalized U^{ij} tensor.

Atom	x	y	z	U(eq)
Br(1)	2728(1)	4280(1)	8166(1)	44(1)
Si(1)	3297(1)	-1217(1)	4487(1)	22(1)
O(1)	1441(3)	2784(2)	4768(1)	21(1)
O(2)	4103(3)	2482(2)	3520(2)	28(1)
O(3)	1952(3)	2162(2)	3052(1)	28(1)
O(4)	4949(3)	1042(2)	5764(1)	22(1)
O(5)	2642(3)	-439(1)	4168(1)	22(1)
N(1)	3780(4)	3040(2)	5064(2)	18(1)
C(1)	3183(4)	1797(2)	4697(2)	15(1)
C(2)	2520(4)	1584(2)	4038(2)	17(1)
C(3)	3025(4)	811(2)	3845(2)	19(1)
C(4)	2728(5)	280(2)	4383(2)	18(1)
C(5)	2498(5)	489(2)	4985(2)	19(1)
C(6)	2589(4)	1271(2)	5224(2)	16(1)
C(7)	2740(5)	2585(2)	4851(2)	17(1)
C(8)	3504(5)	3817(2)	5227(2)	21(1)

C(9)	3297(4)	3935(2)	5944(2)	21(1)
C(10)	2274(5)	3523(2)	6290(2)	24(1)
C(11)	2083(5)	3633(2)	6946(2)	28(1)
C(12)	2938(5)	4152(2)	7260(2)	28(1)
C(13)	3945(5)	4578(2)	6928(2)	29(1)
C(14)	4122(5)	4467(2)	6267(2)	23(1)
C(15)	2976(5)	2129(2)	3519(2)	20(1)
C(16)	2231(6)	2687(3)	2533(2)	36(1)
C(17)	1646(6)	3434(3)	2714(3)	43(1)
C(18)	3502(4)	1306(2)	5860(2)	18(1)
C(19)	2751(4)	847(2)	6376(2)	19(1)
C(20)	3374(5)	194(2)	6595(2)	26(1)
C(21)	2599(5)	-255(3)	7025(2)	32(1)
C(22)	1229(5)	-45(3)	7241(2)	42(1)
C(23)	627(5)	615(3)	7036(2)	41(1)
C(24)	1383(5)	1063(3)	6611(2)	30(1)
C(25)	2632(6)	-1946(2)	3902(2)	34(1)
C(26)	1200(7)	-1727(3)	3572(3)	57(2)
C(27)	3760(7)	-2181(3)	3392(3)	53(2)
C(28)	5352(5)	-1166(3)	4542(2)	31(1)
C(29)	6061(6)	-795(3)	3948(3)	52(2)
C(30)	5946(6)	-799(3)	5157(3)	46(1)
C(31)	2506(5)	-1392(2)	5311(2)	27(1)
C(32)	3065(6)	-2124(3)	5592(2)	38(1)
C(33)	821(5)	-1363(3)	5330(3)	38(1)

Figure S2. Single crystal X-ray structure (ORTEP) of epoxide (+)-28. The crystals were grown from a concentrated solution of epoxide (+)-**28** in CH_2Cl_2 (4.0 mL), using a slow evaporation method (probability ellipsoids are shown at the 50% level). X-ray crystallographic data have been deposited in the Cambridge Crystallographic Data Centre database (http://www.ccdc.cam.ac.uk/) under *pending* accession code.

Alert level B:
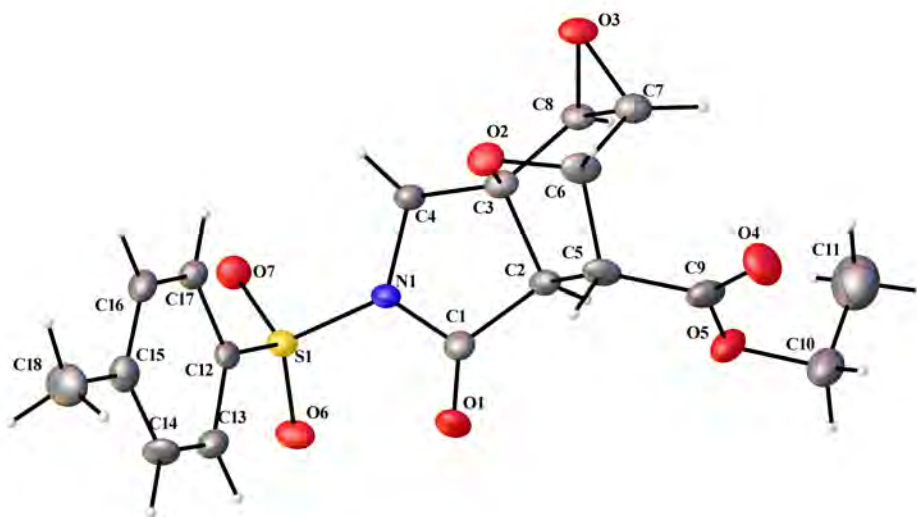
THETM01_ALERT_3_B The value of sine(theta_max)/wavelength is less than 0.575. Calculated sin(theta_max)/wavelength = 0.5679.

Author Response: Data was collected on a Bruker GADDS instrument with Cu-source and MWPC (multiwire proportional counter) detector. Under these experimental conditions the maximum angle that can be collected is 120 degrees two-theta.

PLAT019_ALERT_1_B _diffrn_measured_fraction_theta_full/_max < 1.0 0.857 Report

Author Response: Data was collected on a Bruker GADDS instrument with Cu-source and MWPC (multiwire proportional counter) detector which has geometrical restrictions.

Table 1. Crystal data and structure refinement for DRB_MA_150407_G_EpoN.

Crystal Parameters	Crystal Data
Identification code	epon
Empirical formula	$C_{18} H_{19} N O_7 S$
Formula weight	393.40
Temperature	110.15 K
Wavelength	1.54178 Å
Crystal system	Monoclinic
Space group	P 1 21 1
Unit cell dimensions	$a = 12.8722(5)$ Å $\quad a = 90º$
	$b = 6.6204(2)$ Å $\quad b = 92.069(2)º$
	$c = 20.7083(8)$ Å $\quad g = 90º$
Volume	$1763.59(11)$ Å^3
Z	4
Density (calculated)	1.482 Mg/m^3
Absorption coefficient	2.019 mm^{-1}
F(000)	824
Crystal size	0.54 x 0.02 x 0.02 mm^3
Theta range for data collection	2.135 to 61.119º
Index ranges	$-14 \leq h \leq 14, -7 \leq k \leq 6, -23 \leq l \leq 23$
Reflections collected	31880
Independent reflections	5106 [R(int) = 0.0431]
Completeness to theta = 67.679º	83.0%
Absorption correction	Semi-empirical from equivalents
Max. and min. transmission	0.7519 and 0.5733
Refinement method	Full-matrix least-squares on F^2
Data / restraints / parameters	5106 / 166 / 515

Goodness-of-fit on F^2			1.116	
Final R indices [I>2sigma(I)]			$R_1 = 0.0370$, $wR_2 = 0.0966$	
R indices (all data)			$R_1 = 0.0428$, $wR_2 = 0.1092$	
Absolute structure parameter			0.02(2)	
Extinction coefficient			0.0099(8)	
Largest diff. peak and hole			0.742 and -0.456 e.Å^{-3}	

Table 2. Atomic coordinates (x 10^4) and equivalent isotropic displacement parameters (Å^2 x 10^3) for DRB_MA_150407_G_EpoN. U(eq) is defined as one third of the trace of the orthogonalized Uij tensor.

Atom	x	y	z	U(eq)
S(1)	9919(1)	-663(2)	6245(1)	17(1)
O(1)	8844(3)	2066(5)	5252(2)	27(1)
O(2)	6770(2)	-2054(5)	5451(2)	23(1)
O(3)	6245(2)	-5170(5)	4845(2)	24(1)
O(4)	5750(3)	680(6)	3656(2)	37(1)
O(6)	10712(2)	522(5)	5974(2)	23(1)
O(7)	10157(2)	-2589(5)	6528(2)	24(1)
N(1)	9024(3)	-1169(6)	5674(2)	18(1)
C(1)	8648(3)	266(8)	5232(2)	19(1)
C(2)	7955(3)	-843(7)	4741(2)	17(1)
C(3)	7664(3)	-2765(7)	5114(2)	18(1)
C(4)	8564(3)	-3222(7)	5582(2)	19(1)
C(5)	6885(3)	125(7)	4581(2)	22(1)
C(6)	6159(3)	-1452(7)	4890(2)	22(1)
C(7)	6177(3)	-3332(8)	4472(2)	23(1)
C(8)	7187(3)	-4270(7)	4633(2)	19(1)

C(9)	6624(4)	503(8)	3871(3)	28(1)
O(5A)	7471(9)	1390(30)	3636(7)	34(1)
C(10A)	7267(18)	1920(40)	2962(9)	40(2)
C(11A)	7270(30)	-110(60)	2637(13)	60(2)
O(5)	7476(3)	508(11)	3503(2)	34(1)
C(10)	7346(7)	737(16)	2806(4)	40(2)
C(11)	7232(8)	-1480(20)	2582(4)	60(2)
C(12)	9299(3)	823(7)	6820(2)	17(1)
C(13)	9574(3)	2847(7)	6887(2)	22(1)
C(14)	9155(4)	3937(7)	7384(2)	22(1)
C(15)	8471(4)	3071(8)	7812(2)	24(1)
C(16)	8189(3)	1077(8)	7717(2)	22(1)
C(17)	8604(3)	-81(7)	7226(2)	19(1)
C(18)	8050(4)	4274(10)	8356(2)	37(1)
S(1M)	4581(1)	9471(2)	8775(1)	22(1)
O(1M)	5708(3)	12675(5)	9647(2)	26(1)
O(2M)	7897(2)	9359(5)	9212(1)	22(1)
O(3M)	8924(2)	6465(5)	9692(2)	28(1)
O(4M)	8133(3)	10524(6)	11252(2)	39(1)
O(6M)	3872(2)	10870(6)	9034(2)	30(1)
O(7M)	4286(3)	7413(5)	8670(2)	31(1)
N(1M)	5611(3)	9356(6)	9278(2)	19(1)
C(1M)	6011(3)	10941(8)	9658(2)	19(1)
C(2M)	6895(3)	10075(7)	10078(2)	19(1)
C(3M)	7243(3)	8302(7)	9652(2)	16(1)
C(4M)	6275(3)	7525(7)	9310(2)	21(1)
C(5M)	7885(4)	11407(7)	10125(2)	21(1)
C(6M)	8619(3)	10173(7)	9690(2)	22(1)
C(7M)	8957(3)	8301(8)	10070(2)	25(1)

C(8M)	8019(3)	7005(7)	10045(2)	19(1)
C(9M)	8319(3)	11647(8)	10813(2)	24(1)
O(5M)	8960(30)	13180(40)	10853(11)	36(1)
C(10M)	9379(15)	13580(20)	11503(10)	42(2)
C(11M)	8725(10)	15020(20)	11827(5)	55(2)
O(5N)	8940(50)	13210(70)	10864(19)	36(1)
C(10N)	9470(30)	13780(40)	11471(19)	42(2)
C(11N)	9097(19)	15730(40)	11677(10)	55(2)
C(12M)	5077(3)	10437(7)	8060(2)	20(1)
C(13M)	5293(4)	12493(8)	8005(2)	24(1)
C(14M)	5719(4)	13197(8)	7449(2)	25(1)
C(15M)	5926(3)	11908(8)	6931(2)	24(1)
C(16M)	5681(3)	9894(8)	6989(2)	25(1)
C(17M)	5258(3)	9117(8)	7550(2)	24(1)
C(18M)	6436(4)	12727(9)	6343(2)	30(1)
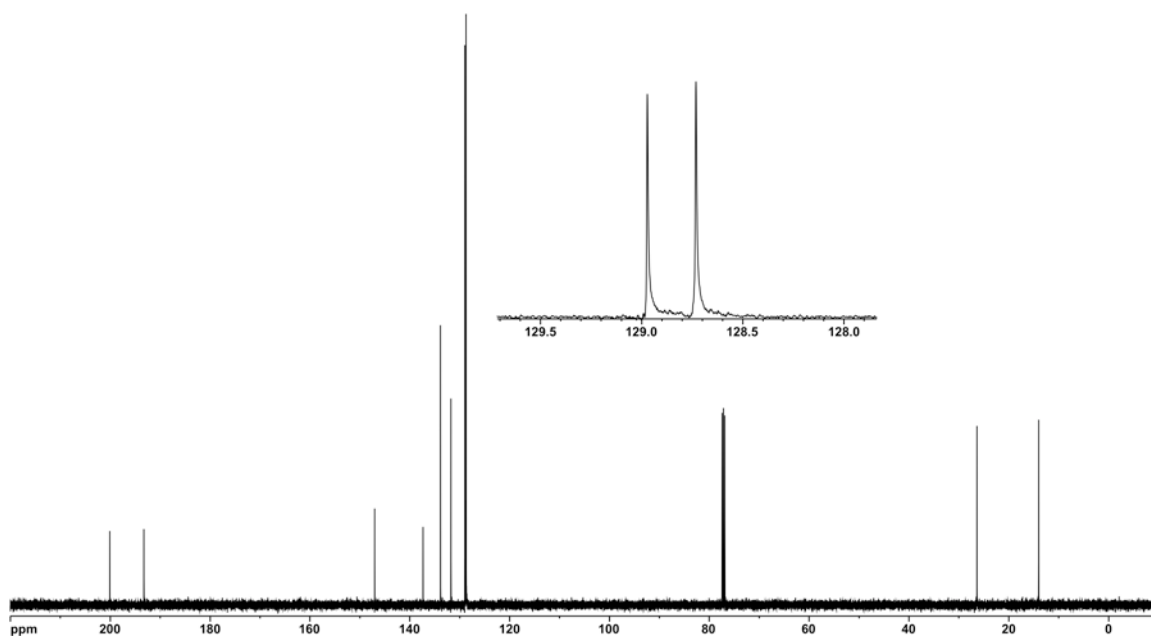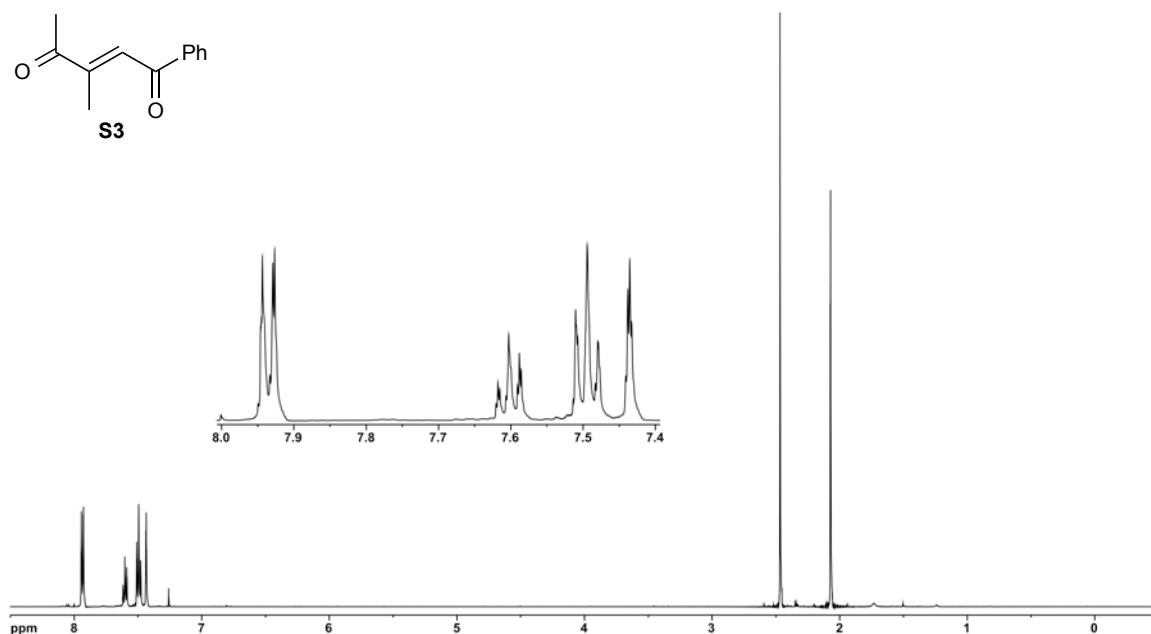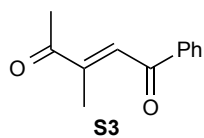
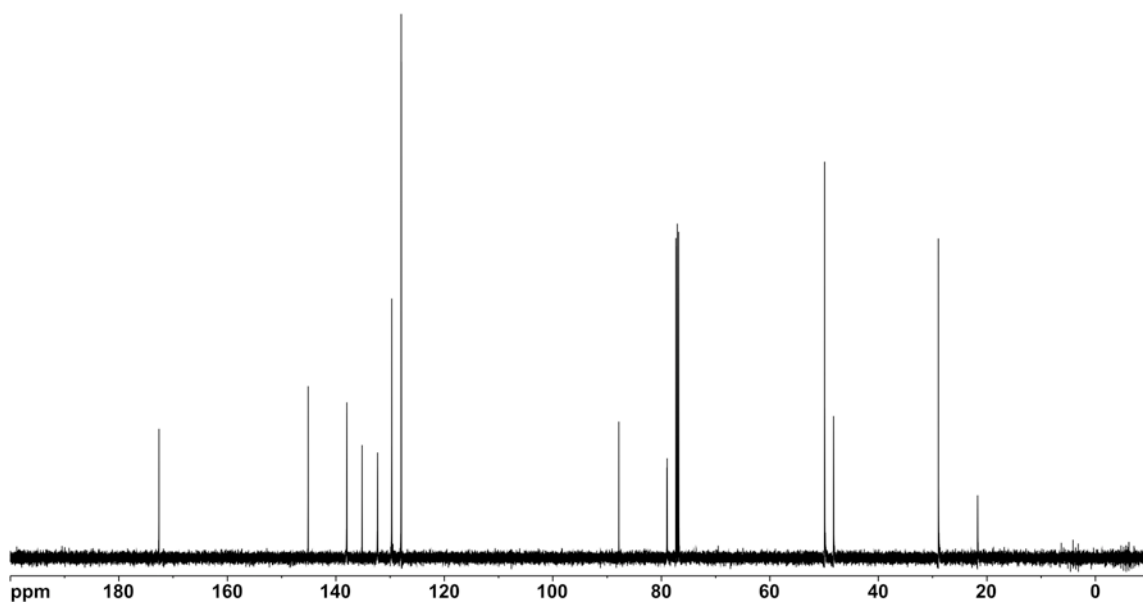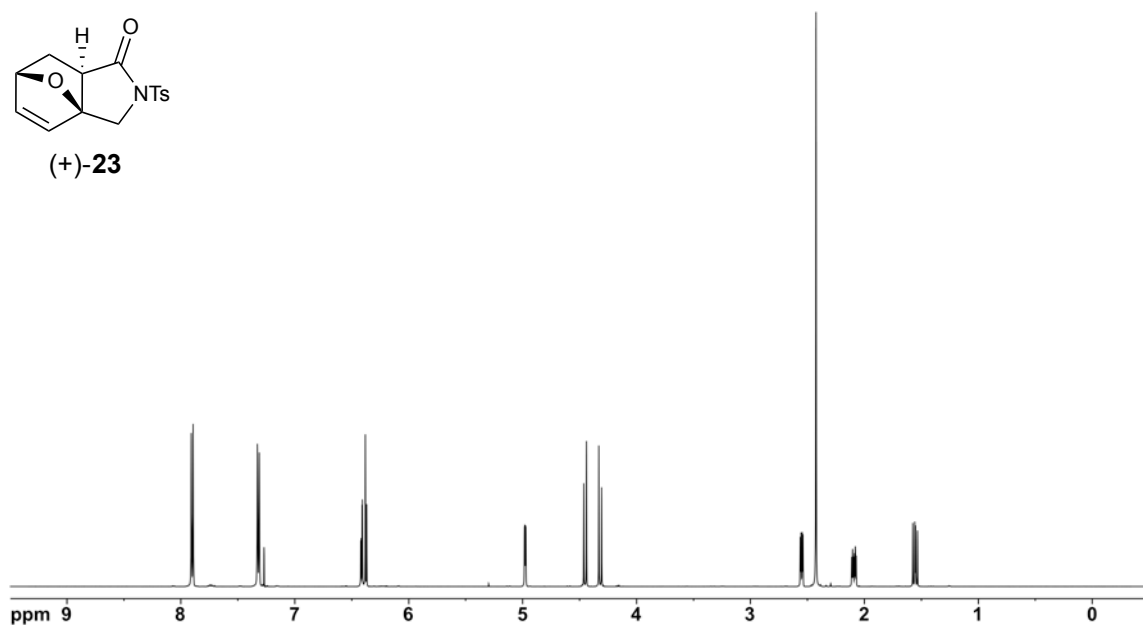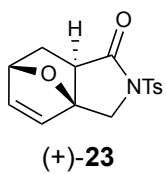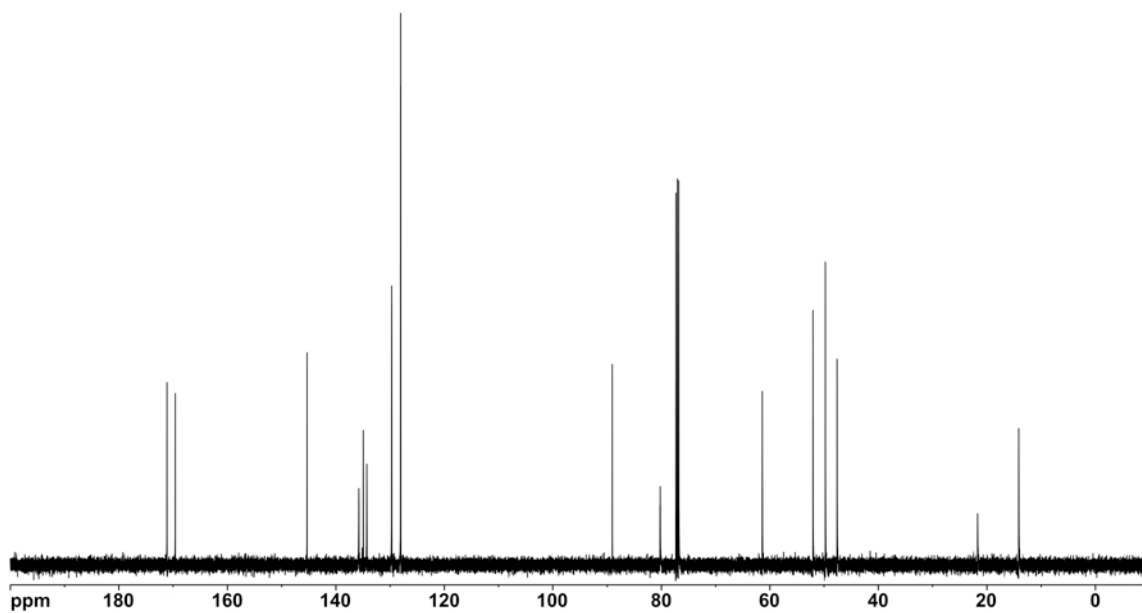^{1}H (500 MHz) and ^{13}C NMR (125 MHz) spectra of diketone **S3** in CDCl$_3$
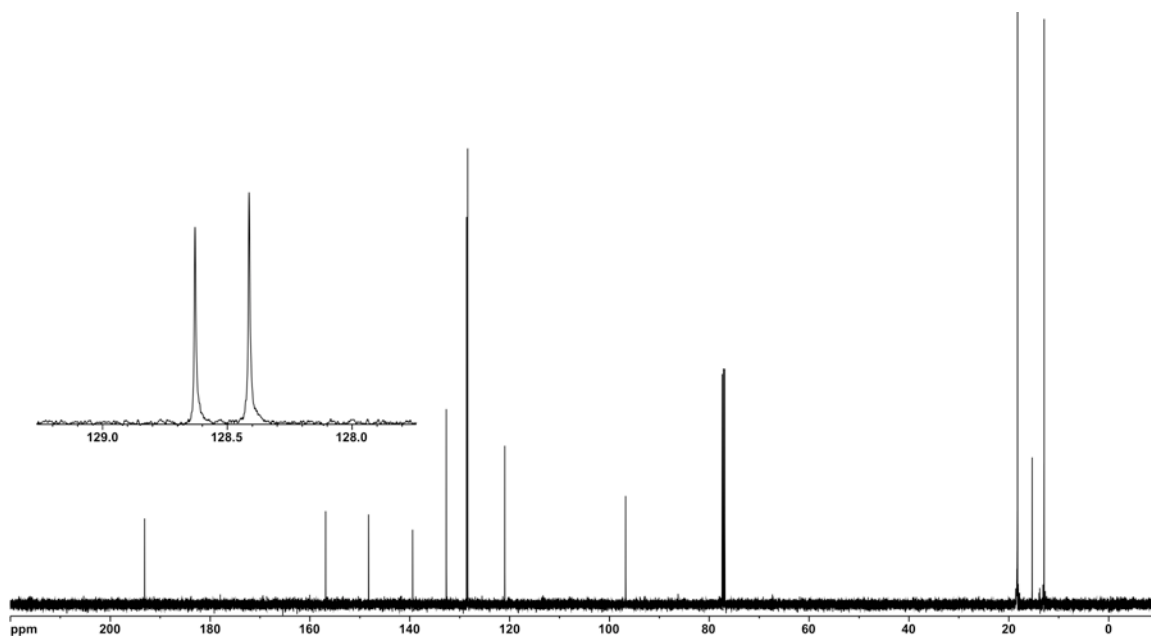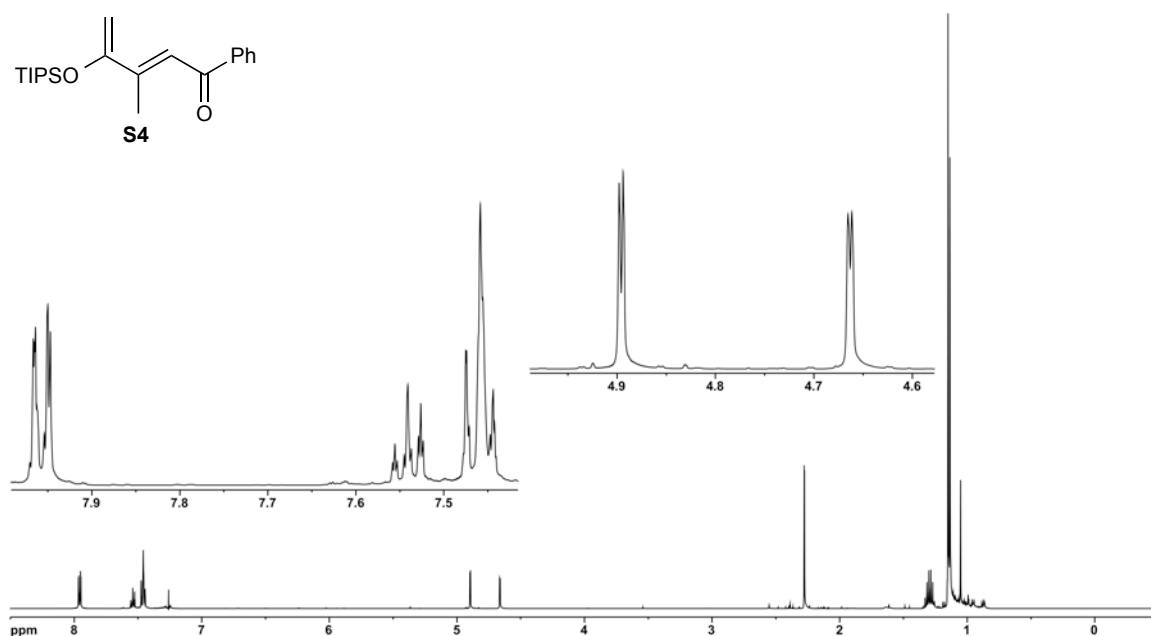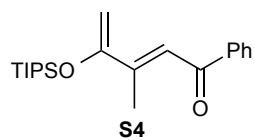
236

^{1}H (500 MHz) and ^{13}C NMR (125 MHz) spectra of diene **S4** in CDCl$_3$
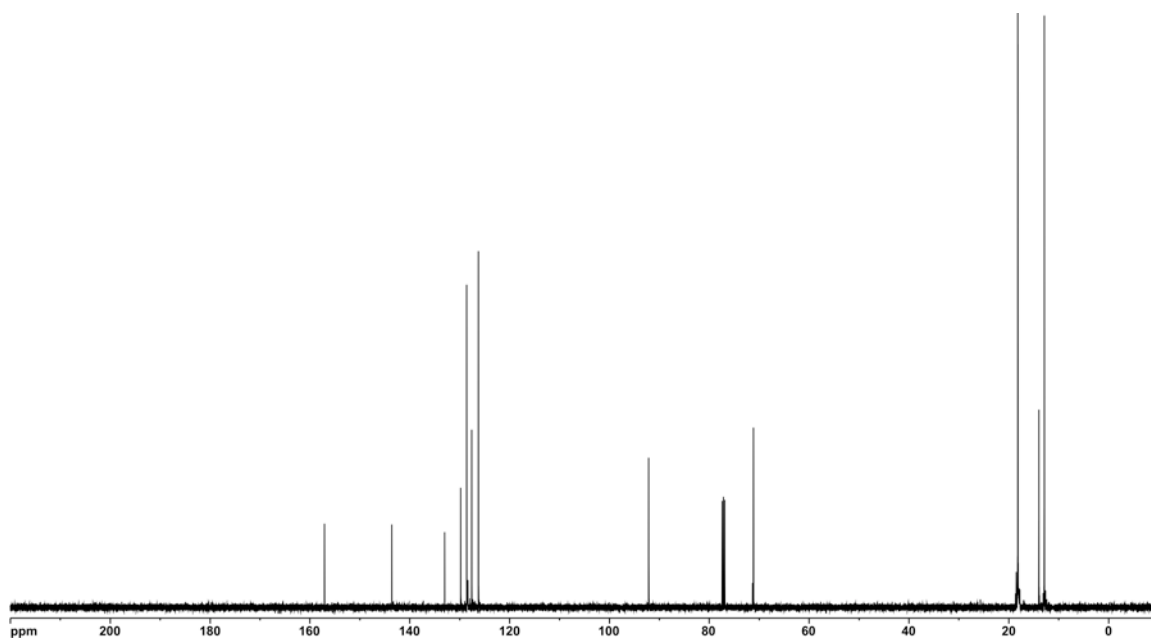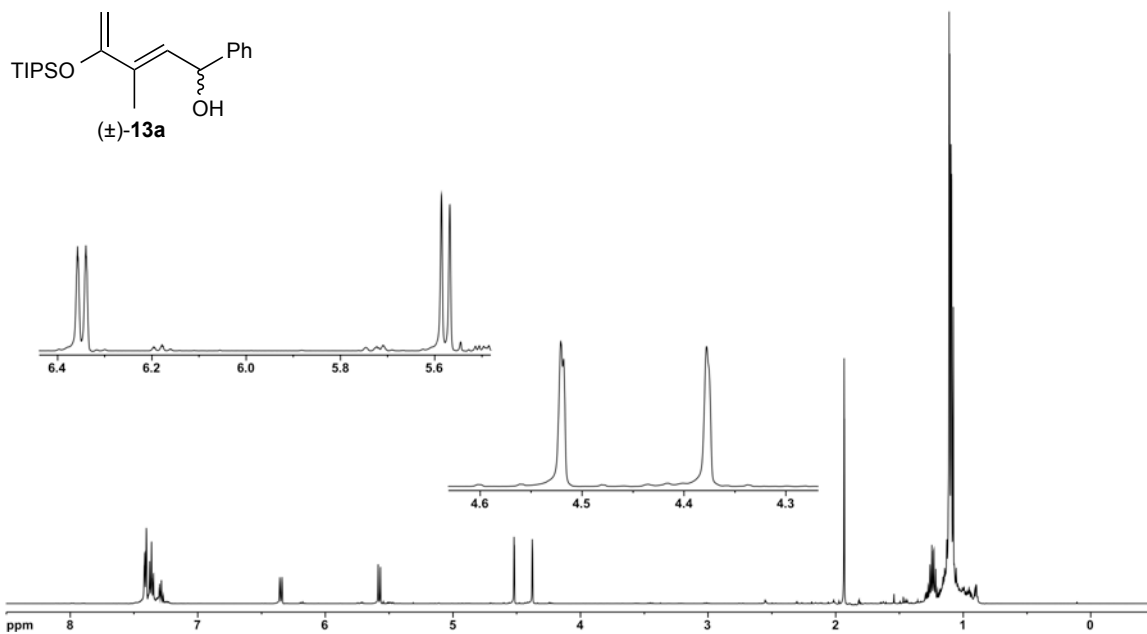
^{1}H (500 MHz) and ^{13}C NMR (125 MHz) spectra of silyloxydiene alcohol (±)-**13a** in CDCl$_3$
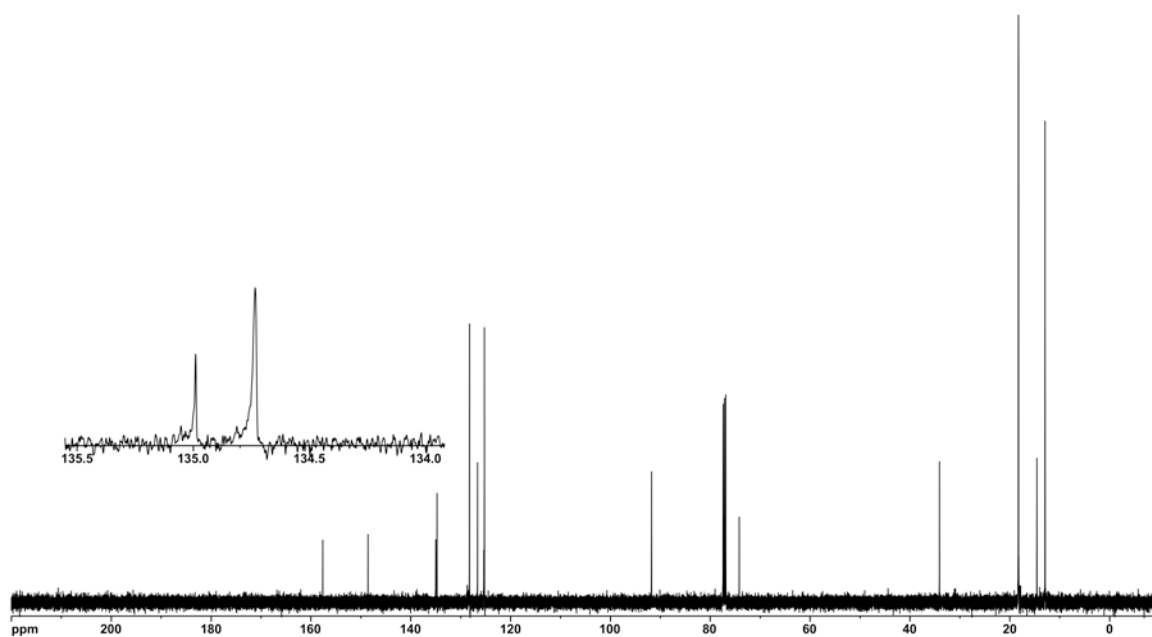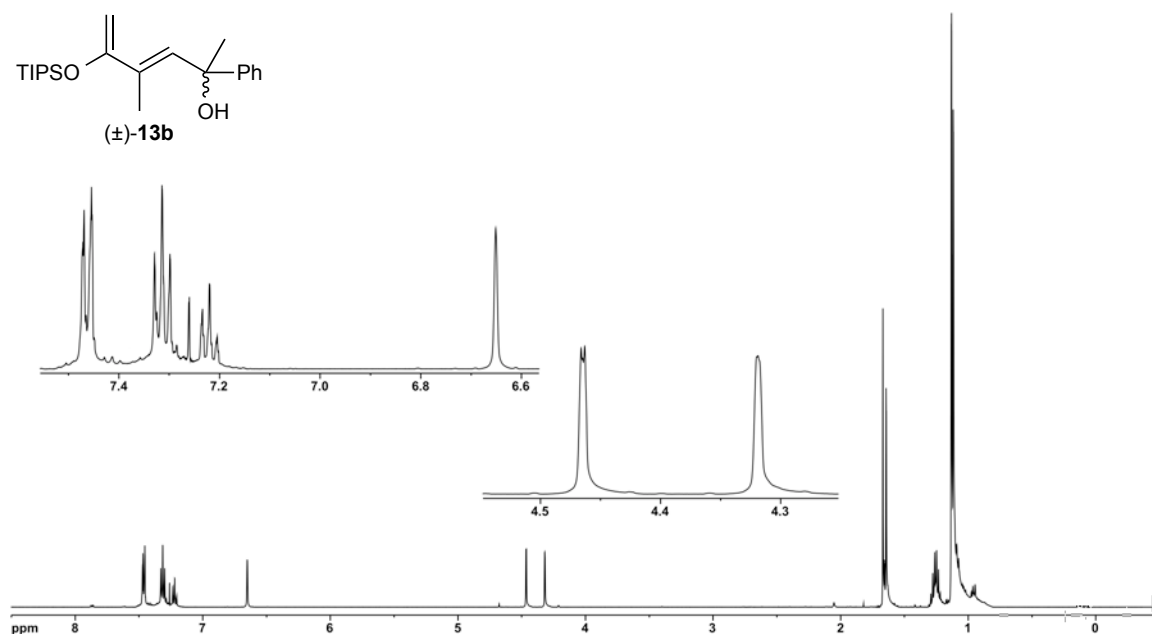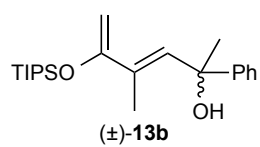
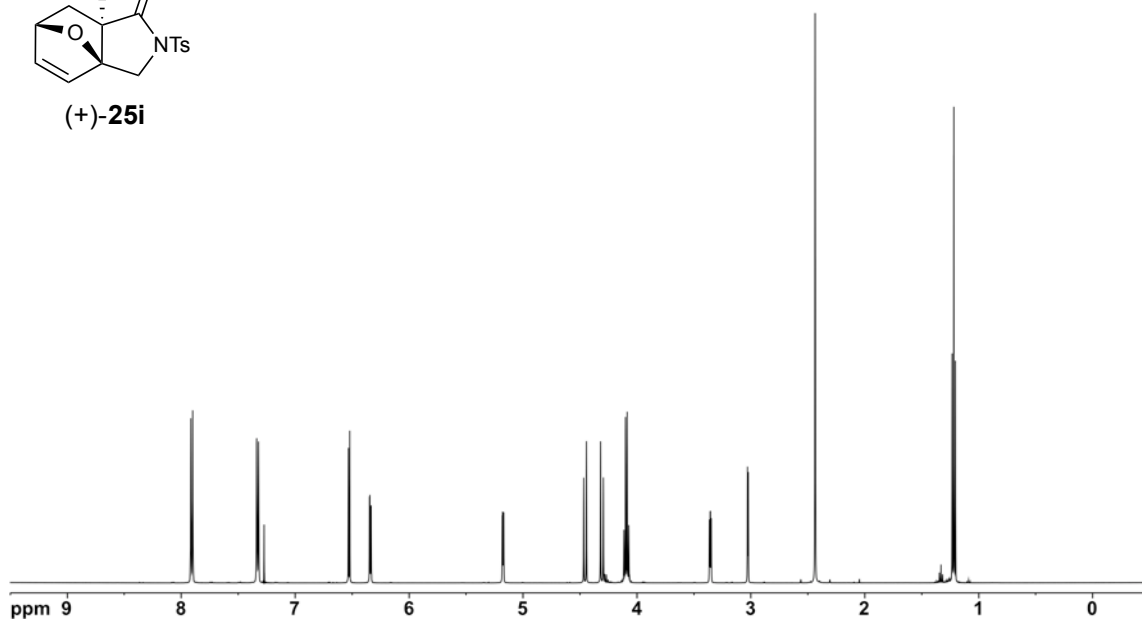^{1}H (500 MHz) and ^{13}C NMR (125 MHz) spectra of silyloxydiene alcohol (±)-**13b** in CDCl$_3$
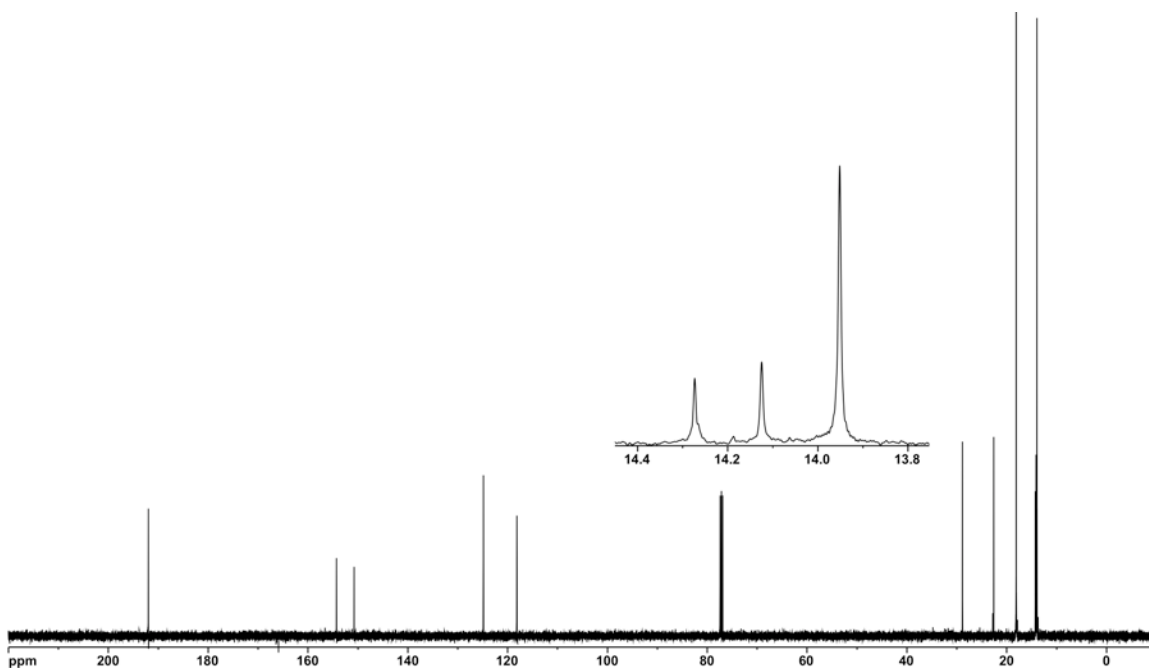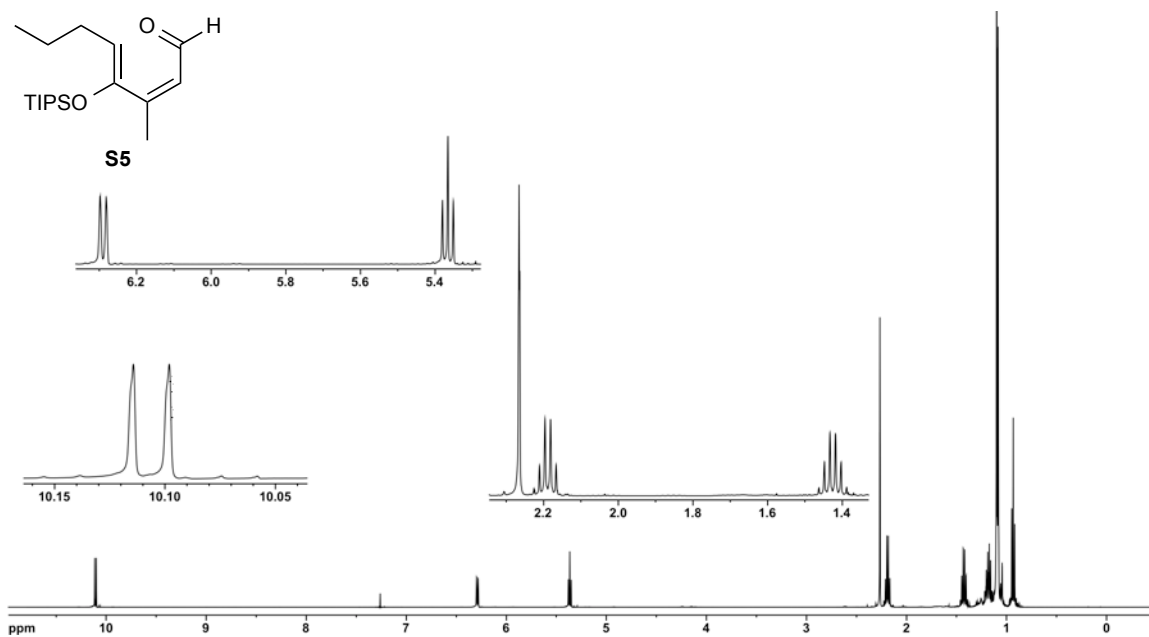
^{1}H (500 MHz) and ^{13}C NMR (125 MHz) spectra of aldehyde **S5** in CDCl$_3$
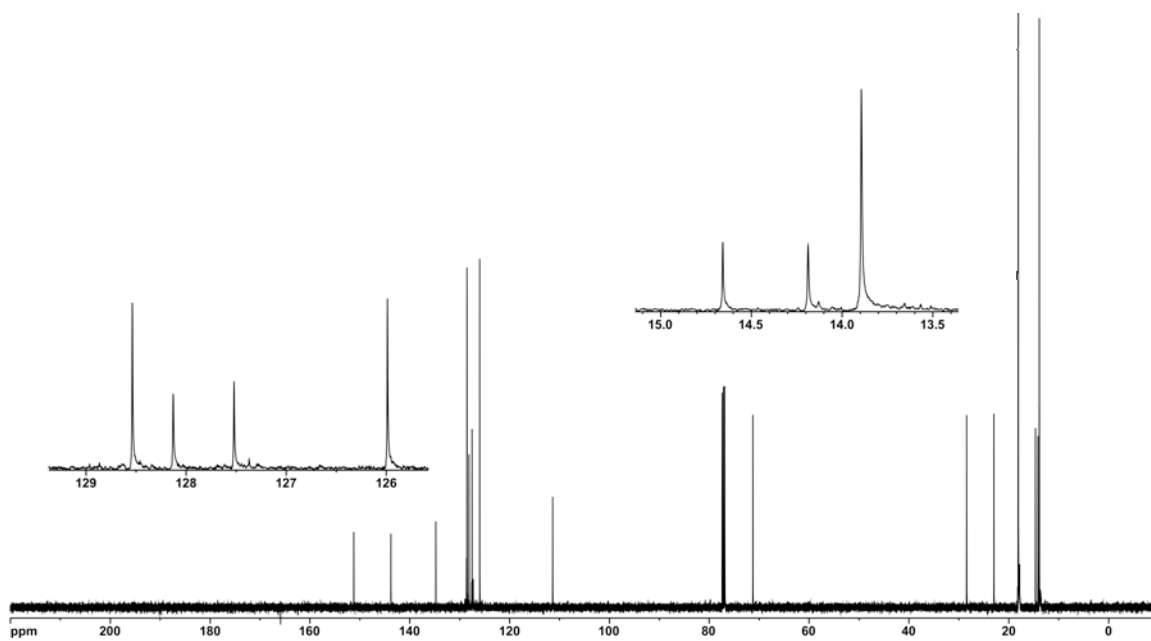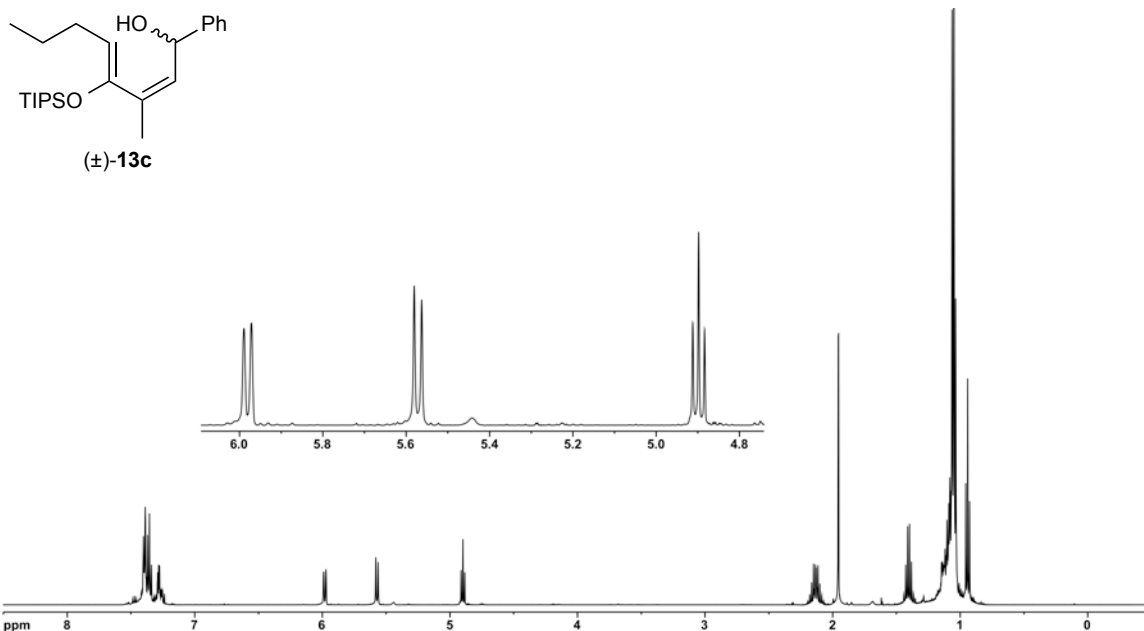
¹H (500 MHz) and ¹³C NMR (125 MHz) spectra of silyloxydiene alcohol (±)-**13c** in CDCl₃
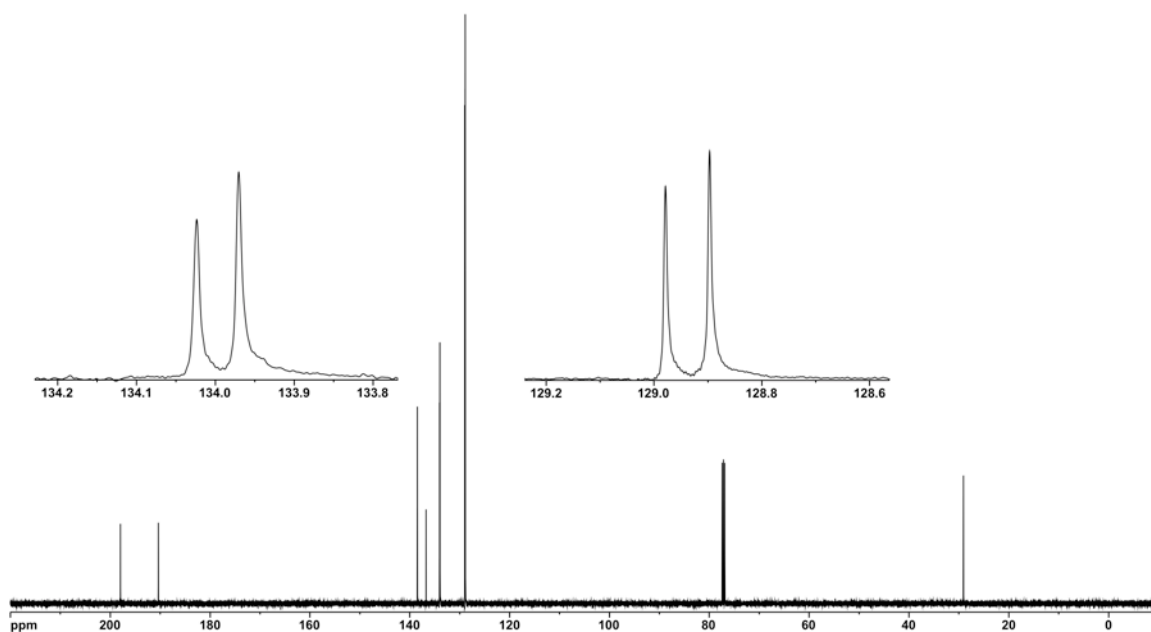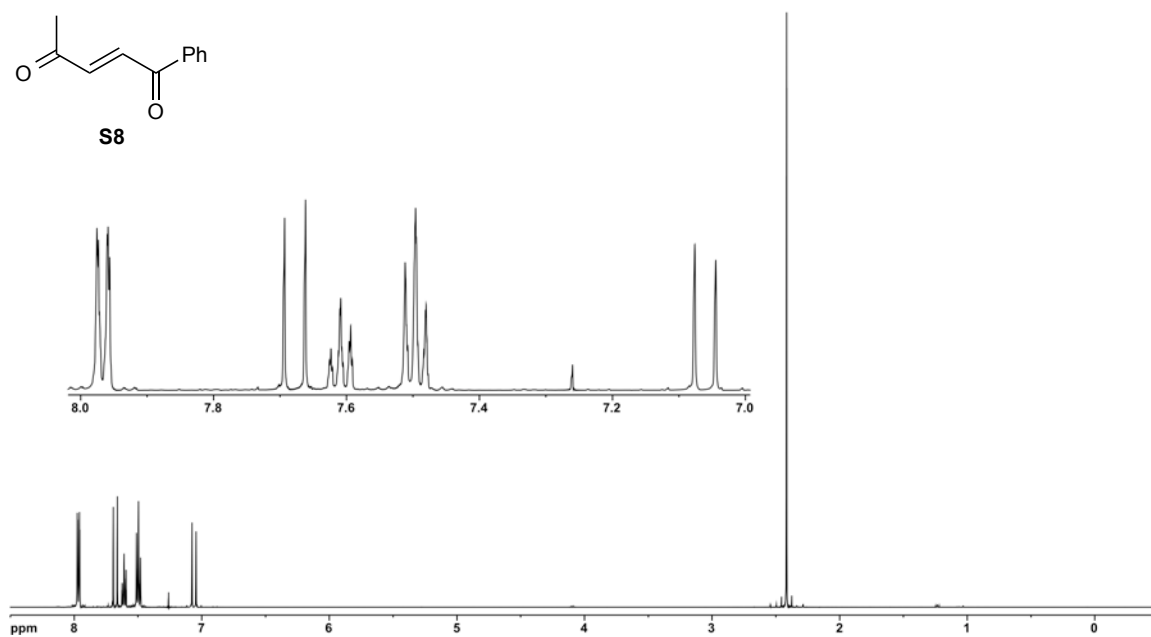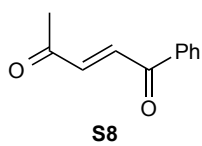
^{1}H (500 MHz) and ^{13}C NMR (125 MHz) spectra of diketone **S8** in CDCl$_3$
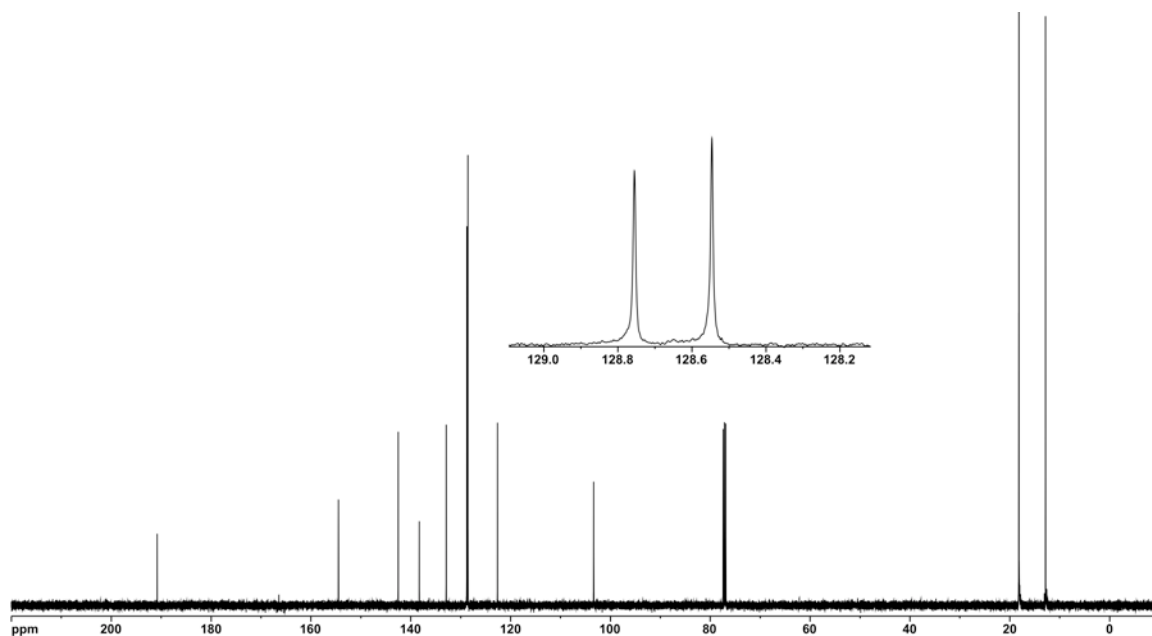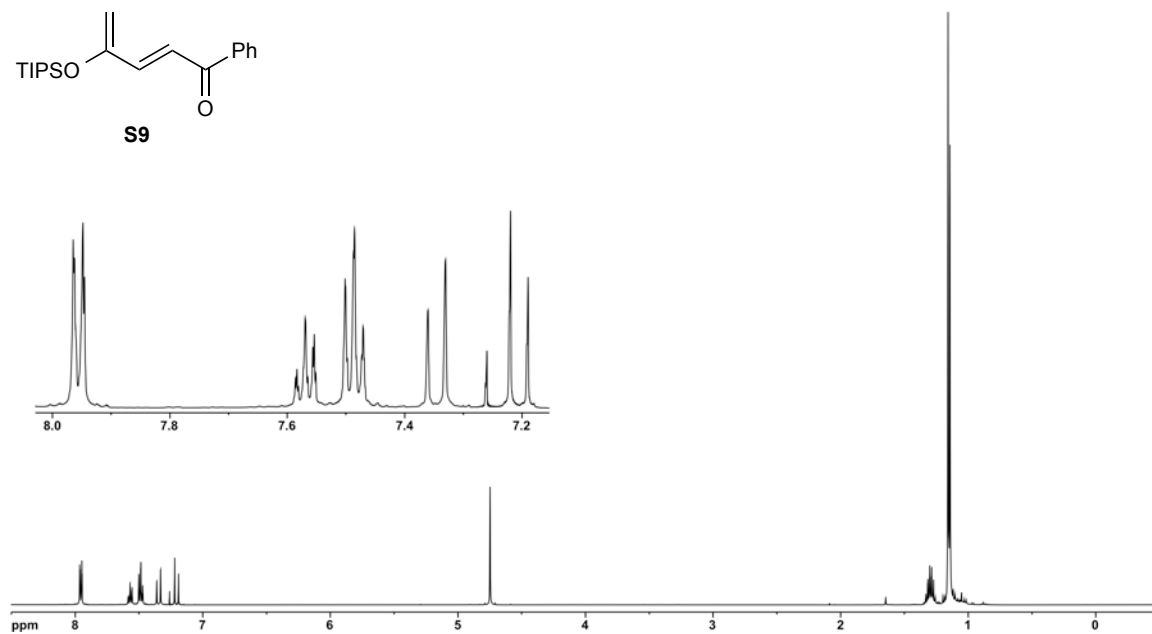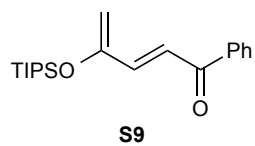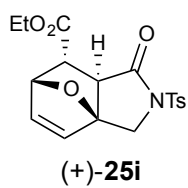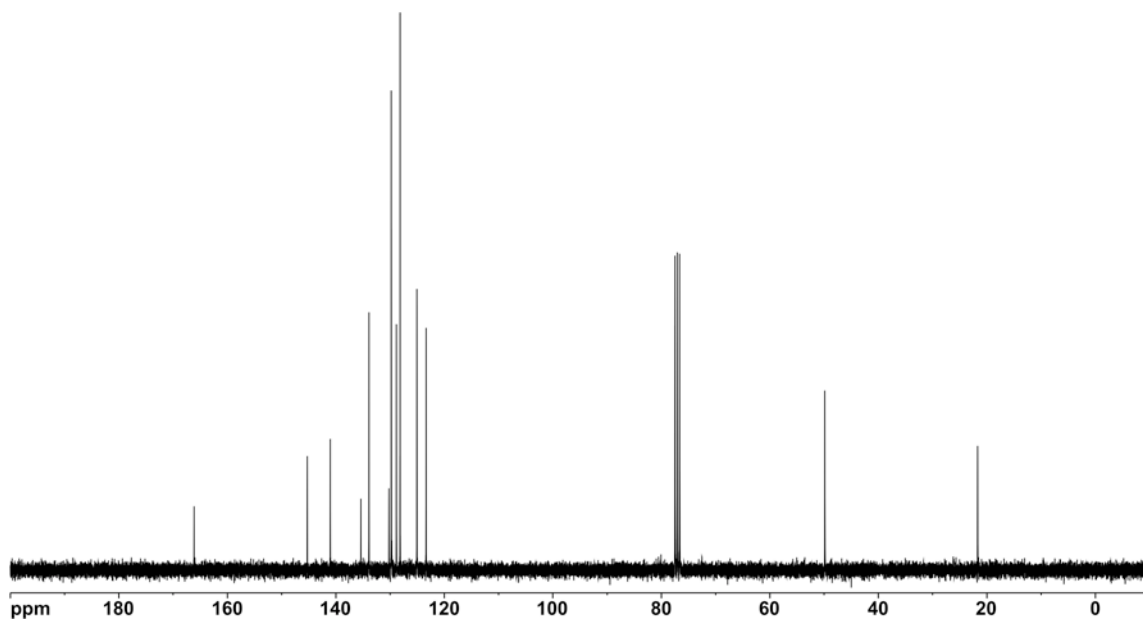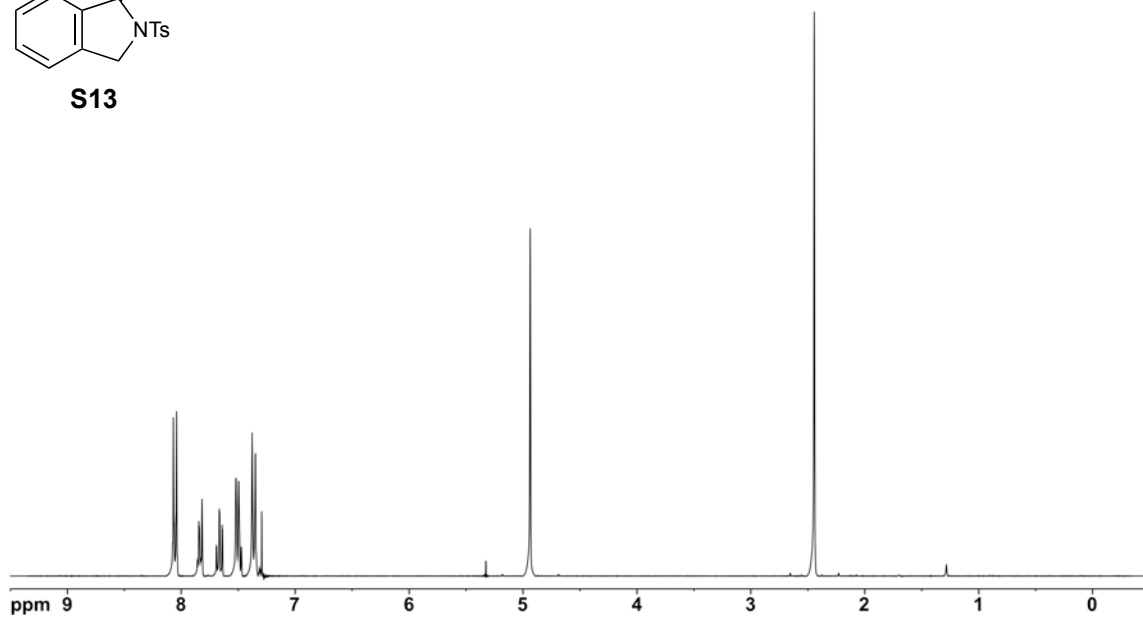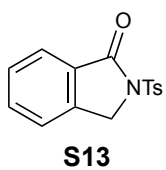
^{1}H (500 MHz) and ^{13}C NMR (125 MHz) spectra of diene **S9** in CDCl$_3$

(±)-**35**
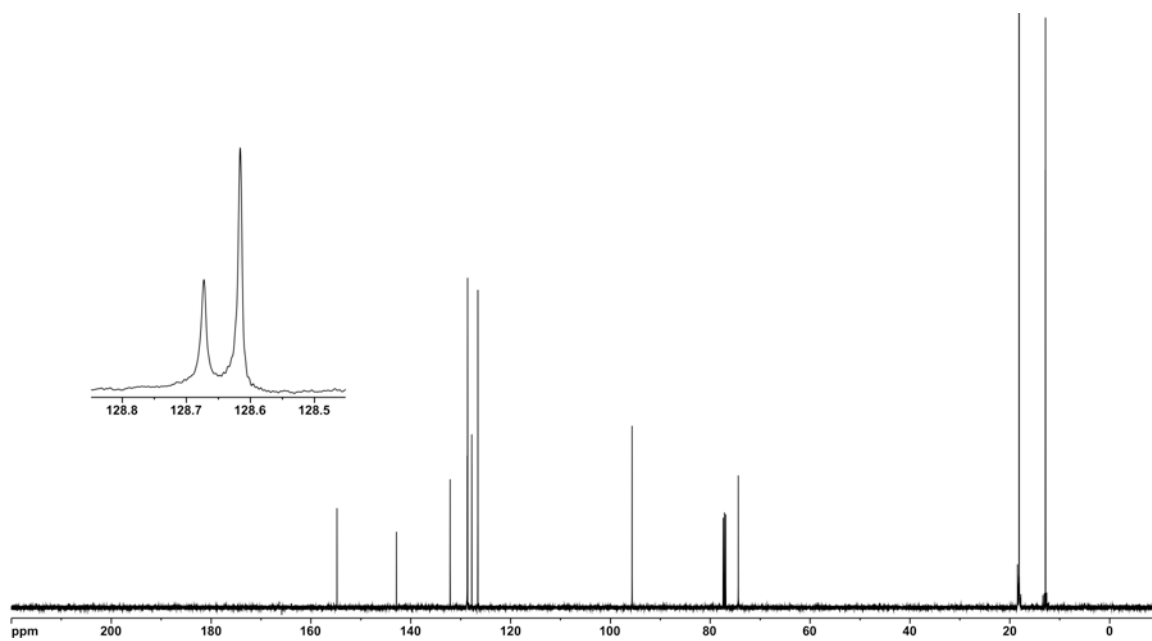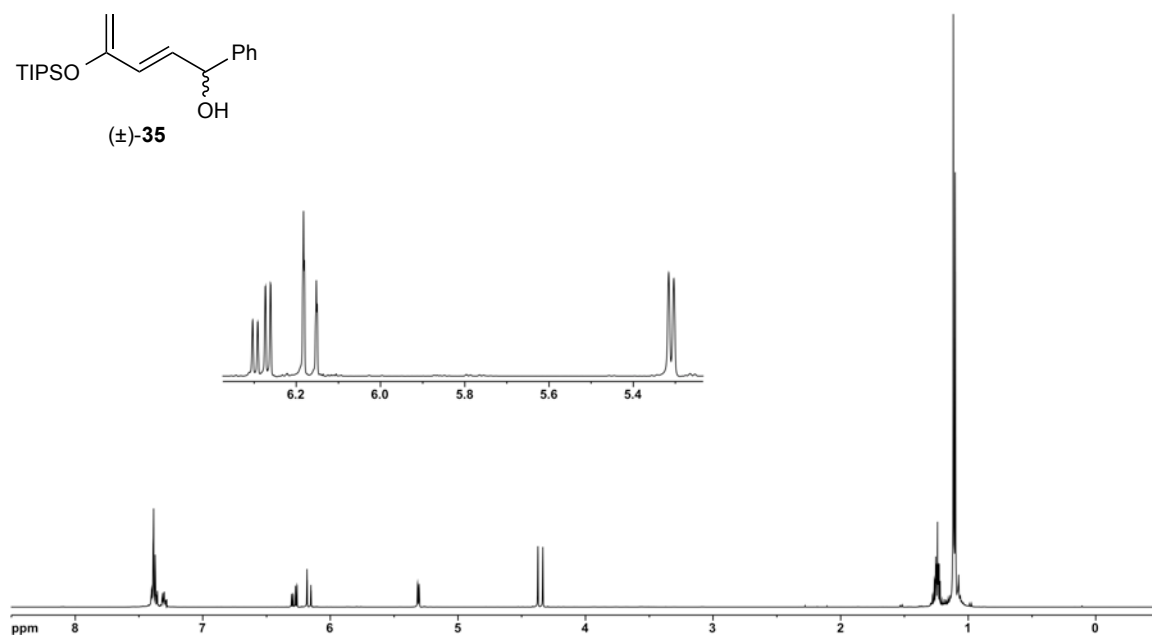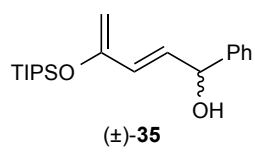
^{1}H (500 MHz) and ^{13}C NMR (125 MHz) spectra of silyloxydiene alcohol (±)-**35** in CDCl$_3$
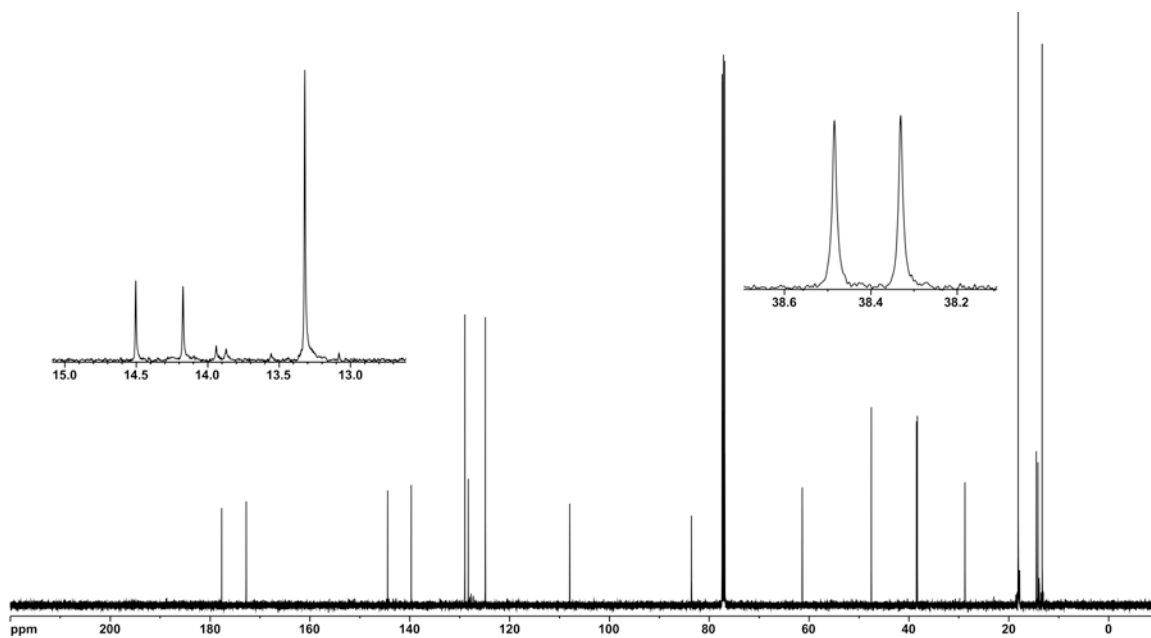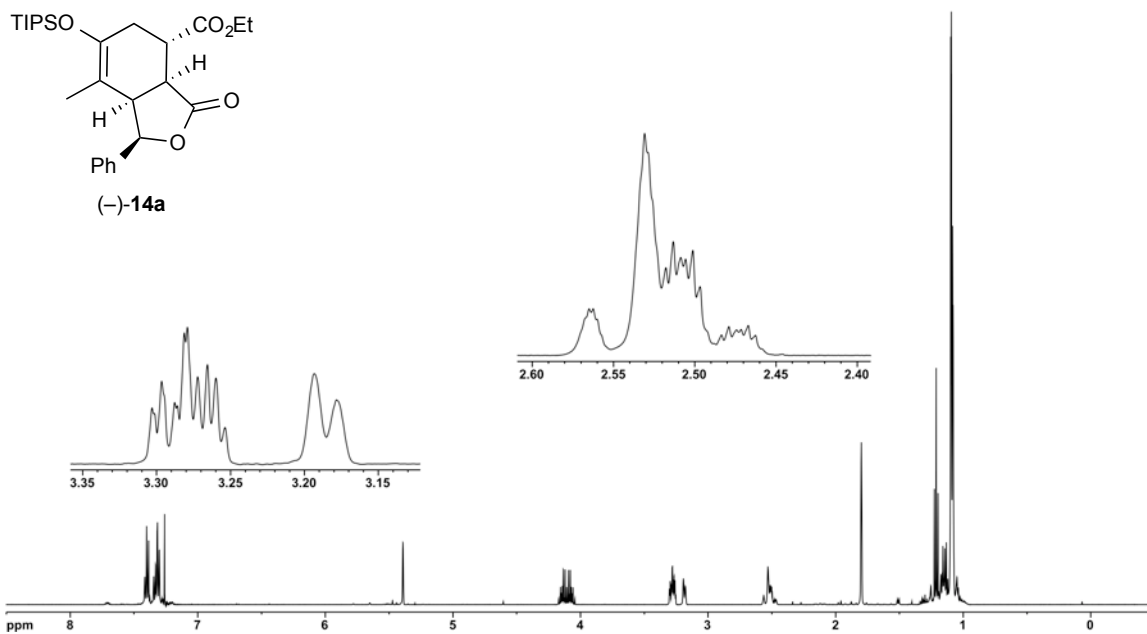
^{1}H (500 MHz) and ^{13}C NMR (125 MHz) spectra of bicyclic γ-lactone (–)-**14a** in CDCl$_3$
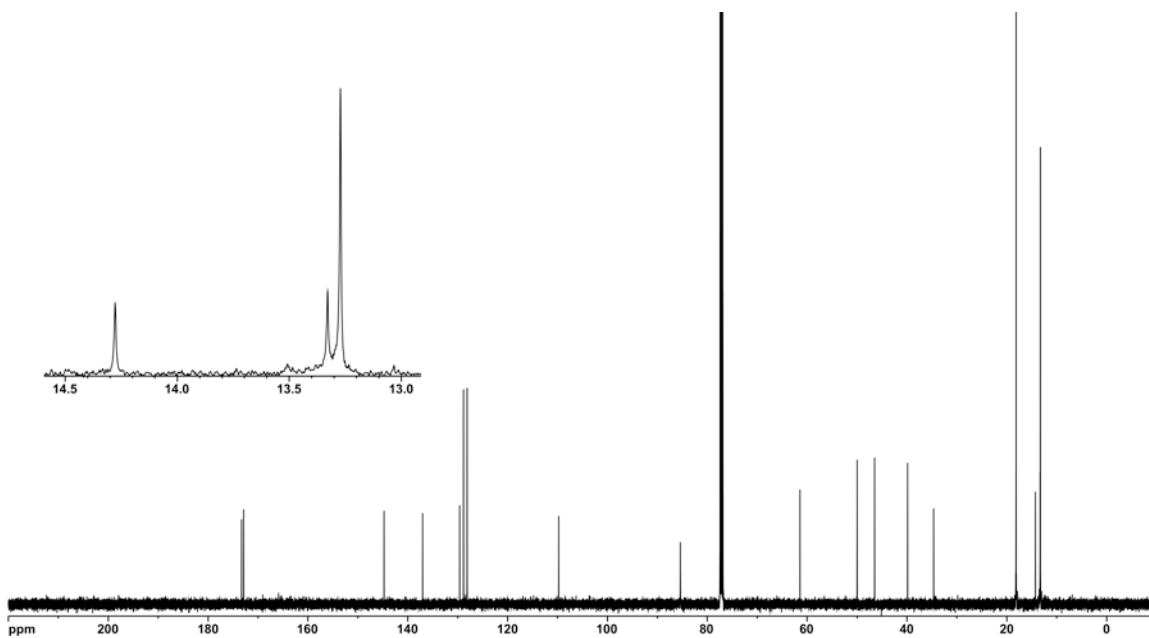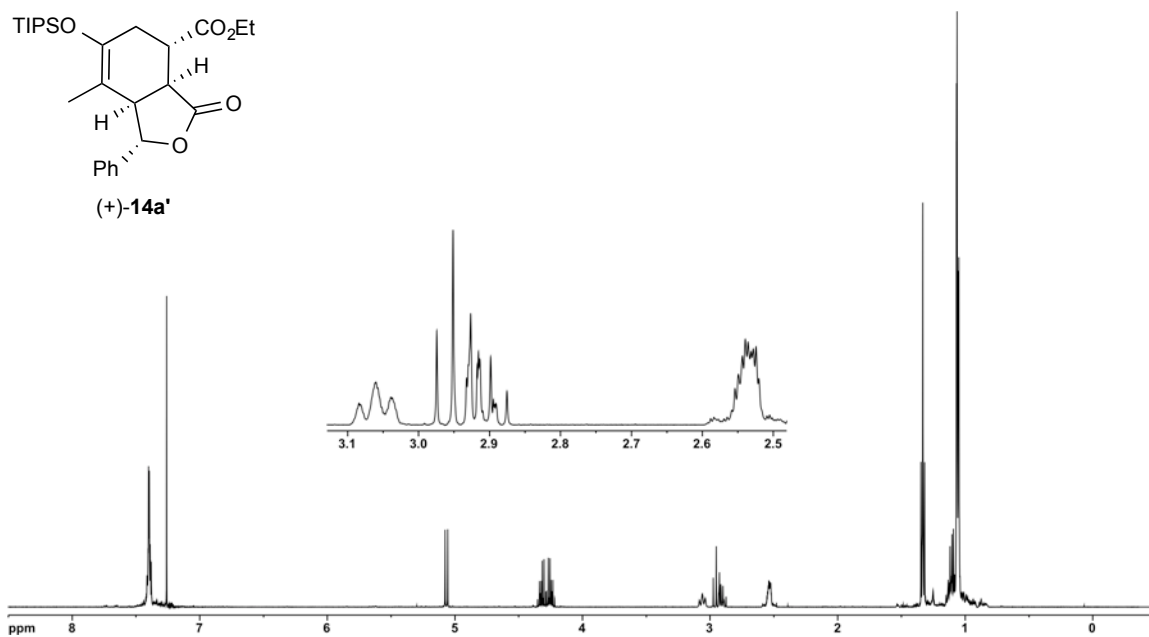
^1H (500 MHz) and ^{13}C NMR (125 MHz) spectra of bicyclic γ-lactone (+)-**14a'** in CDCl$_3$
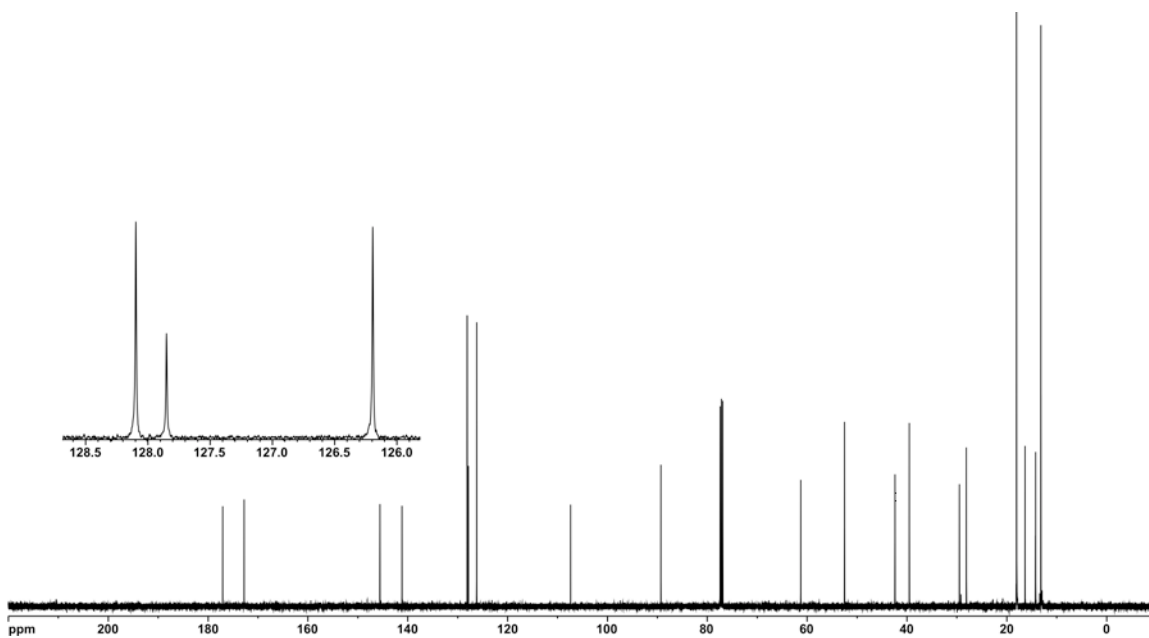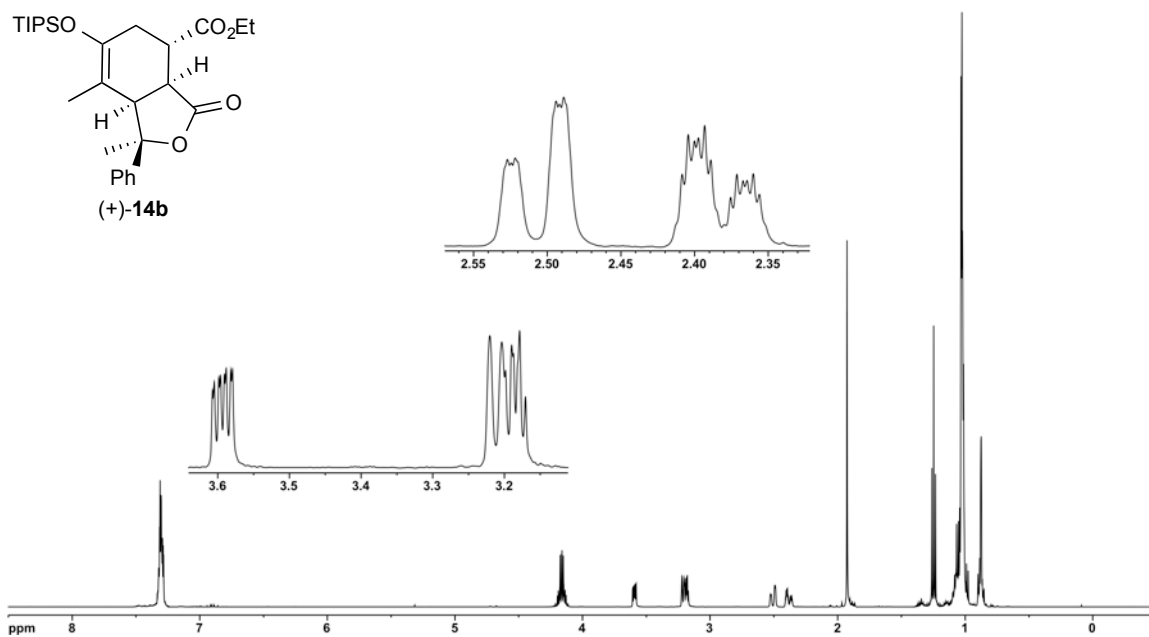
^{1}H (500 MHz) and ^{13}C NMR (125 MHz) spectra of bicyclic γ-lactone (+)-**14b** in CDCl$_3$
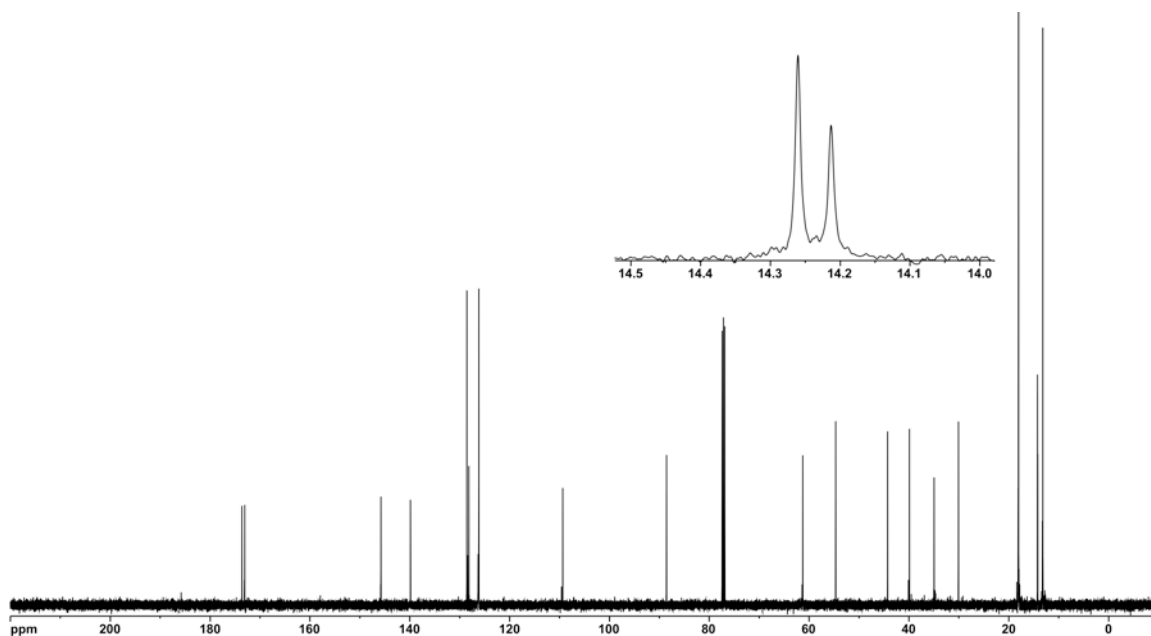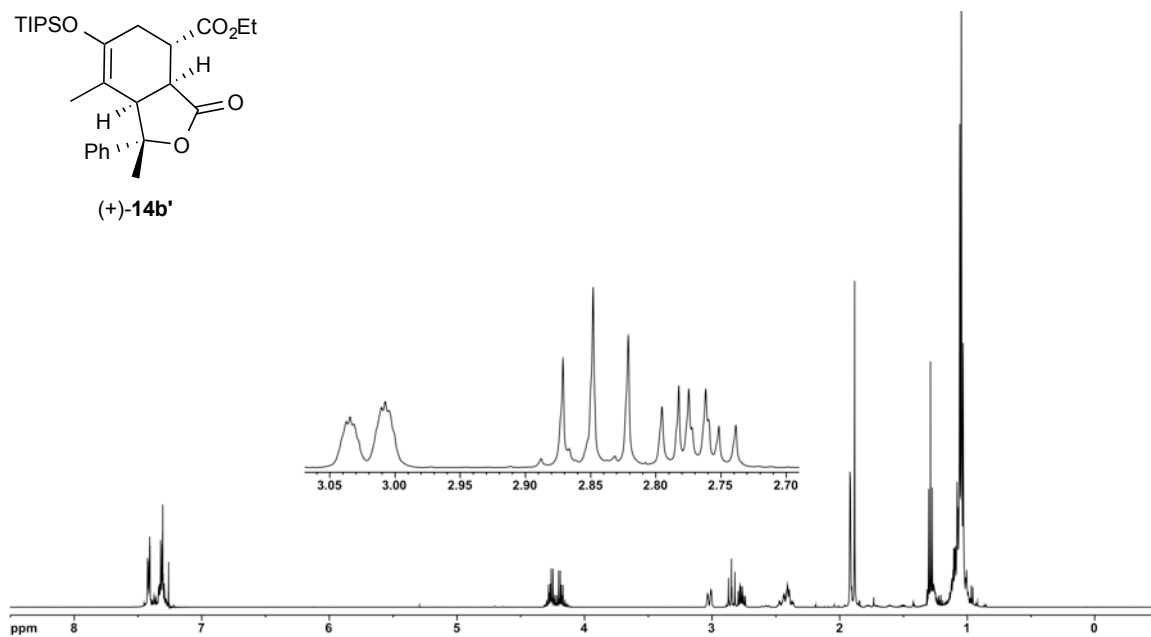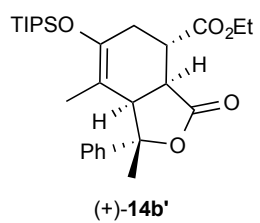
^{1}H (500 MHz) and ^{13}C NMR (125 MHz) spectra of bicyclic γ-lactone (+)-**14b'** in CDCl$_3$
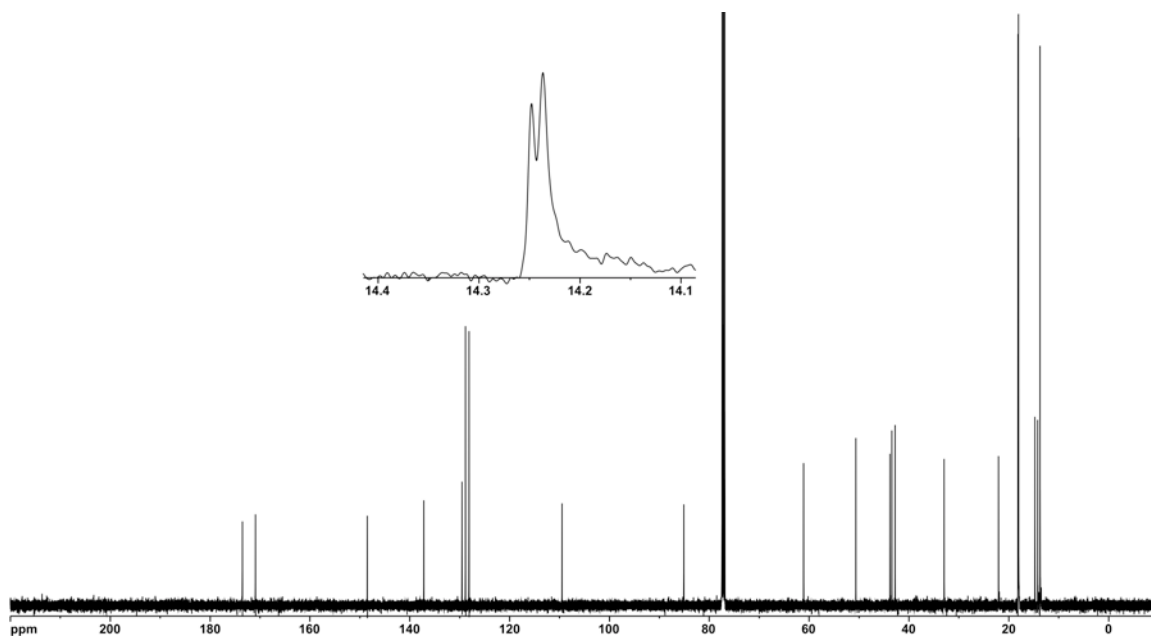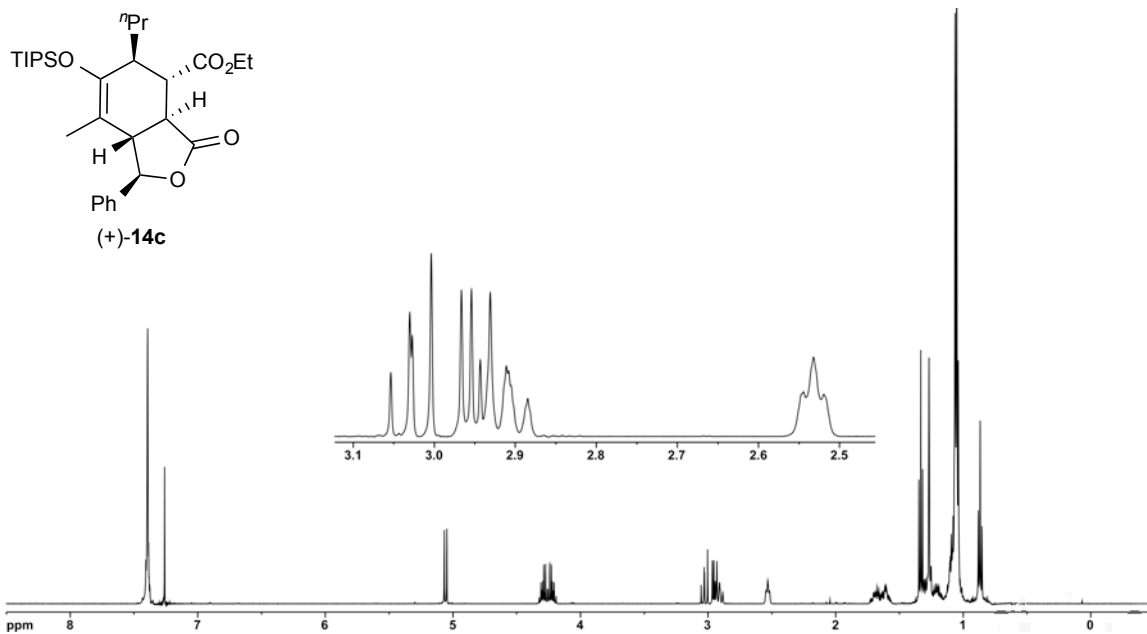
^{1}H (500 MHz) and ^{13}C NMR (125 MHz) spectra of bicyclic γ-lactone (+)-**14c** in CDCl$_3$

^{1}H (500 MHz) and ^{13}C NMR (125 MHz) spectra of tricyclic γ-lactone (–)-**14d** in CDCl$_3$

^{1}H (500 MHz) and ^{13}C NMR (125 MHz) spectra of tricyclic γ-lactone (–)-**14d'** in CDCl$_3$

^{1}H (500 MHz) and ^{13}C NMR (125 MHz) spectra of bicyclic γ-lactone (–)-**36** in CDCl$_3$

^{1}H (500 MHz) and ^{13}C NMR (125 MHz) spectra of bicyclic γ-lactone (+)-**36'** in CDCl$_3$

253
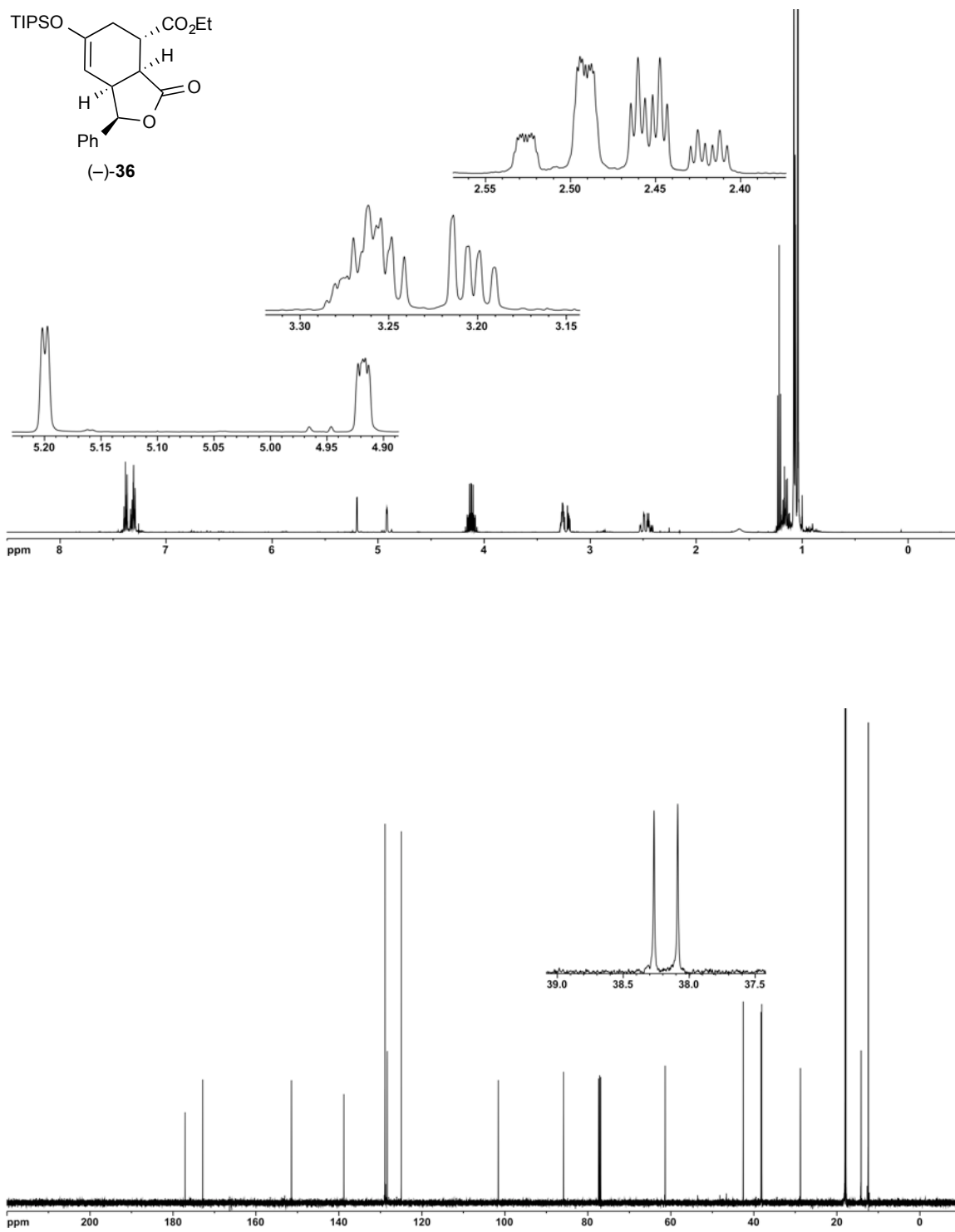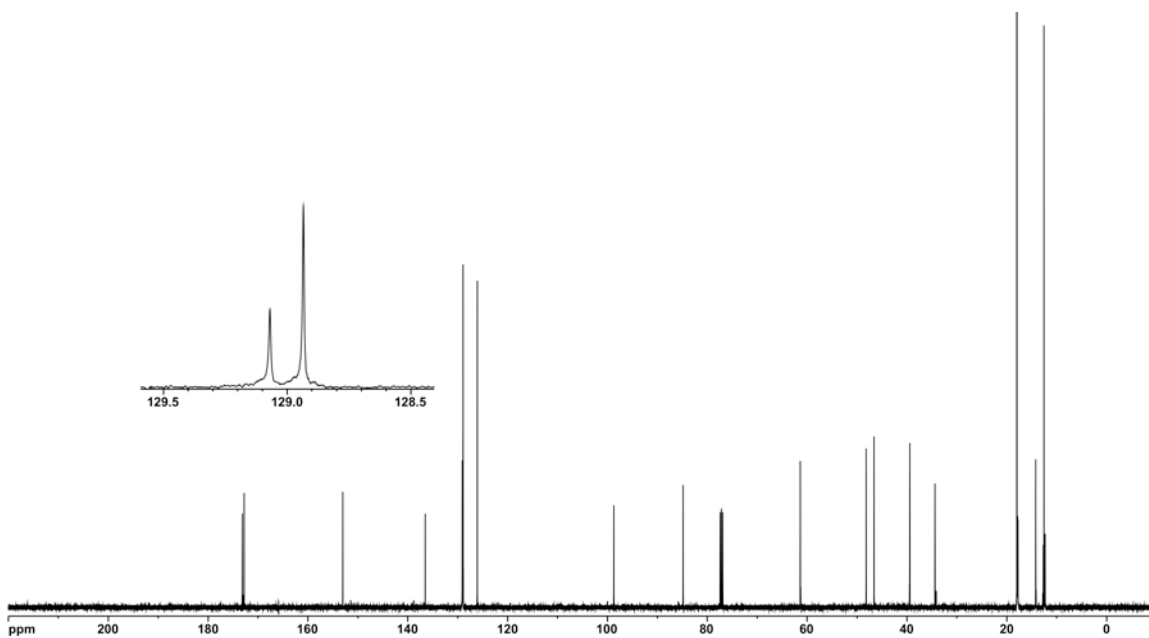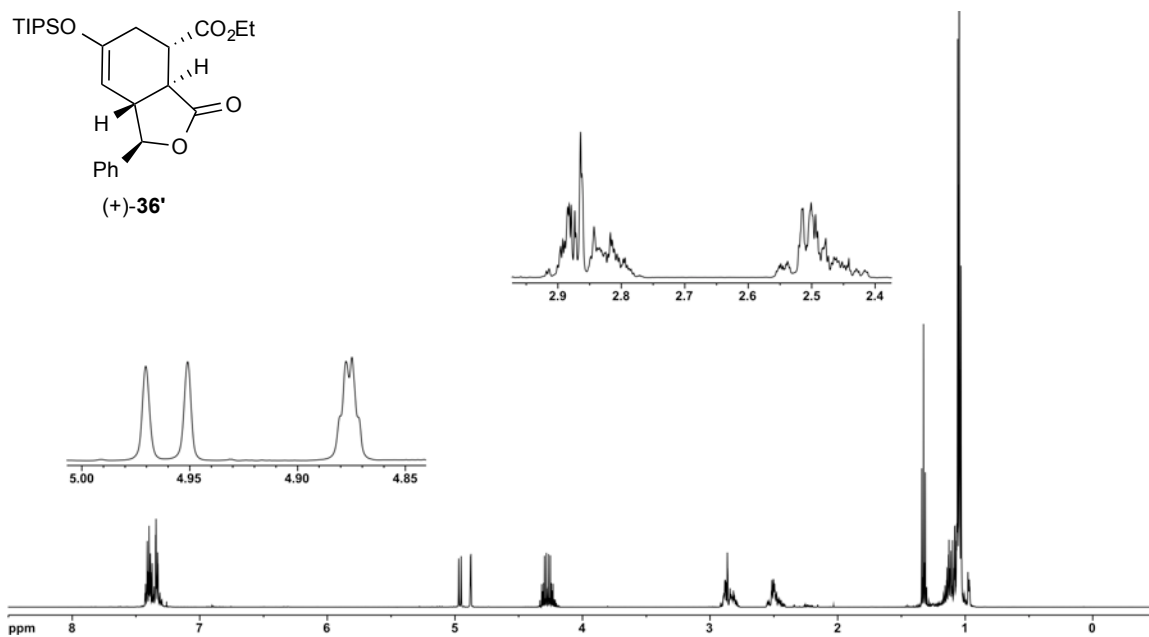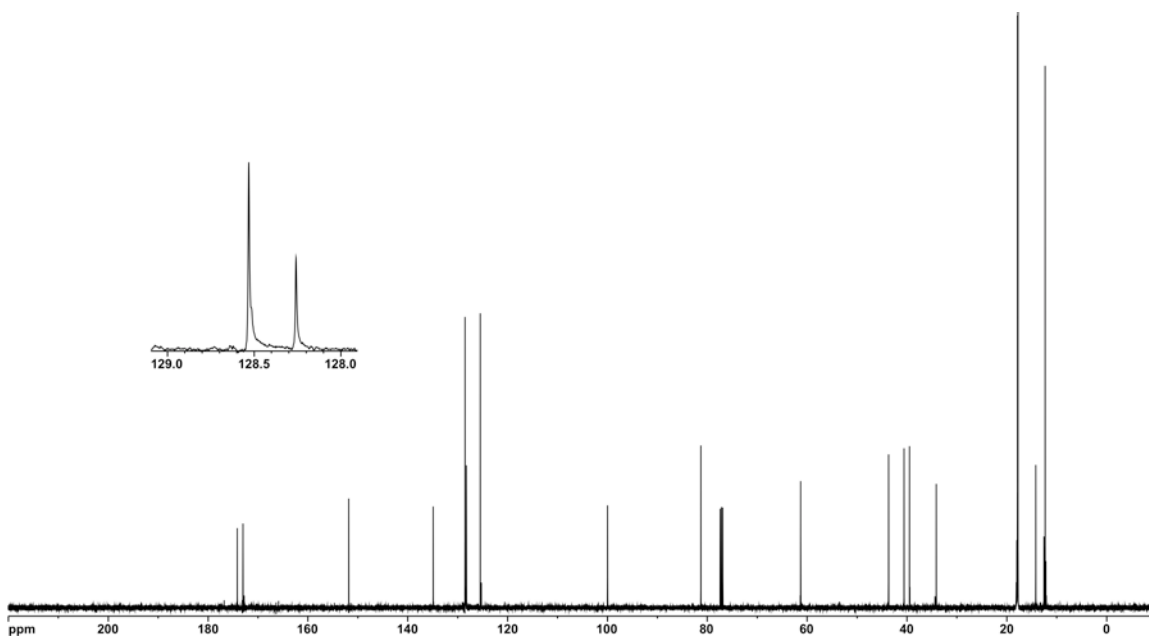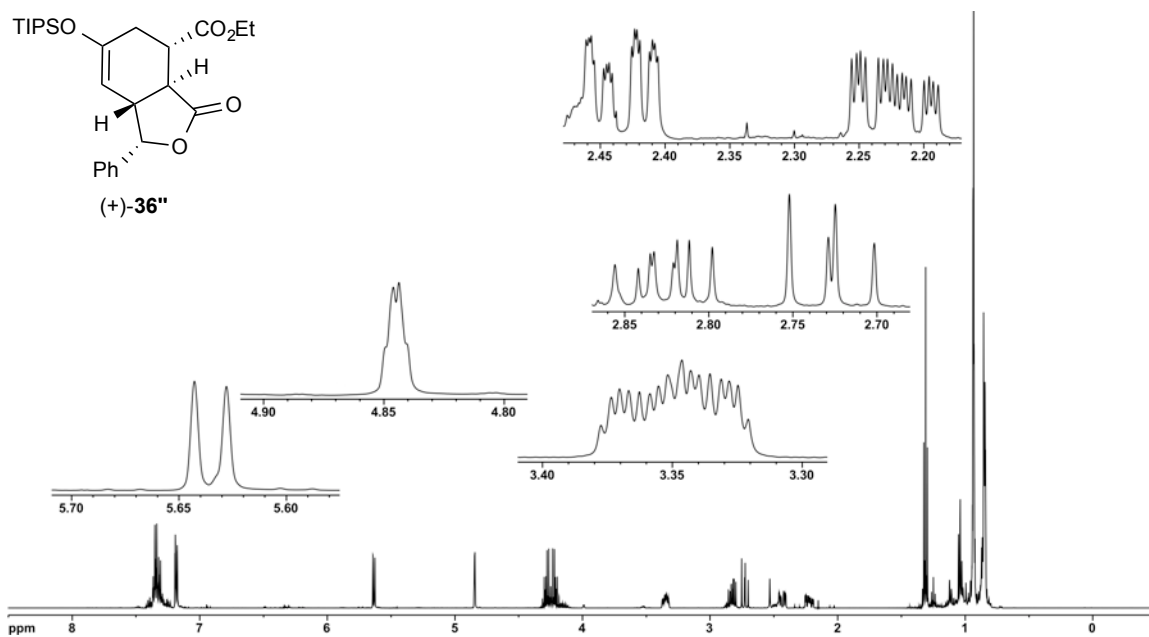
^{1}H (500 MHz) and ^{13}C NMR (125 MHz) spectra of bicyclic γ-lactone (+)-**36''** in CDCl$_3$

^{1}H (500 MHz) and ^{13}C NMR (125 MHz) spectra of bicyclic γ-lactone (–)-**36'''** in CDCl$_3$

^{1}H (500 MHz) and ^{13}C NMR (125 MHz) spectra of ester (±)-**S31** in CDCl$_3$
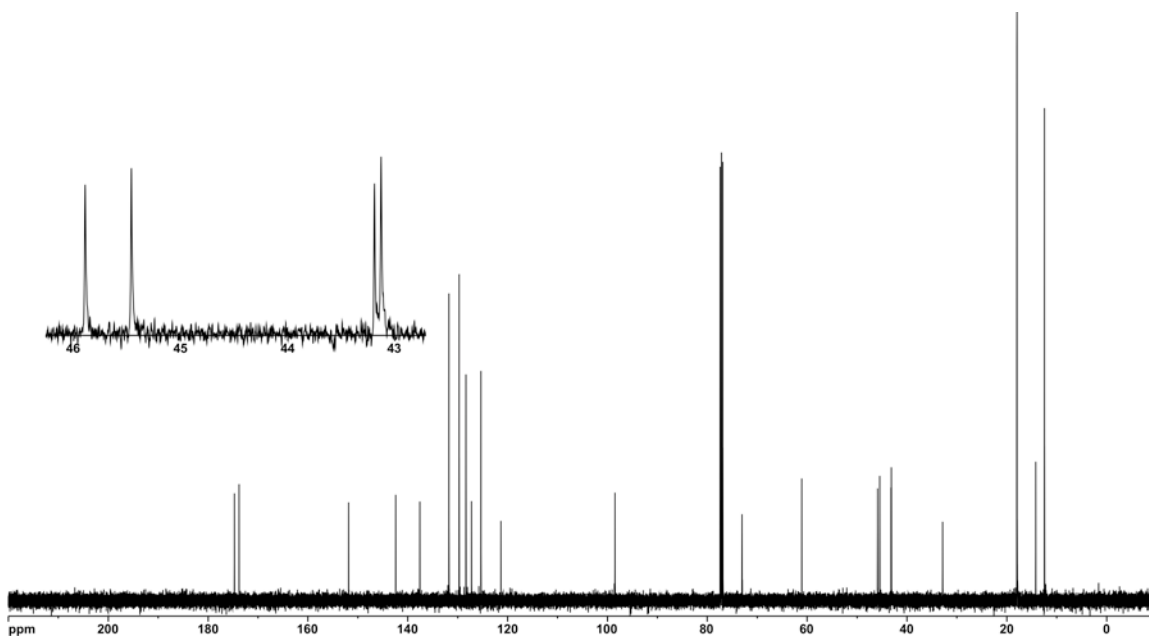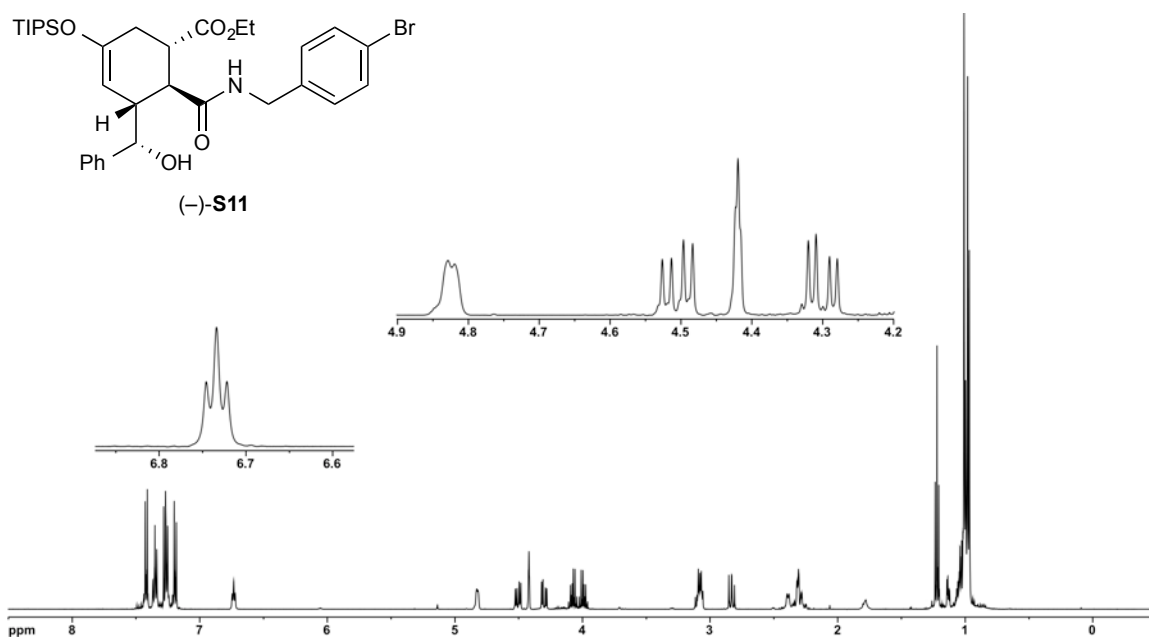
^{1}H (500 MHz) and ^{13}C NMR (125 MHz) spectra of amide (–)-**S11** in CDCl$_3$
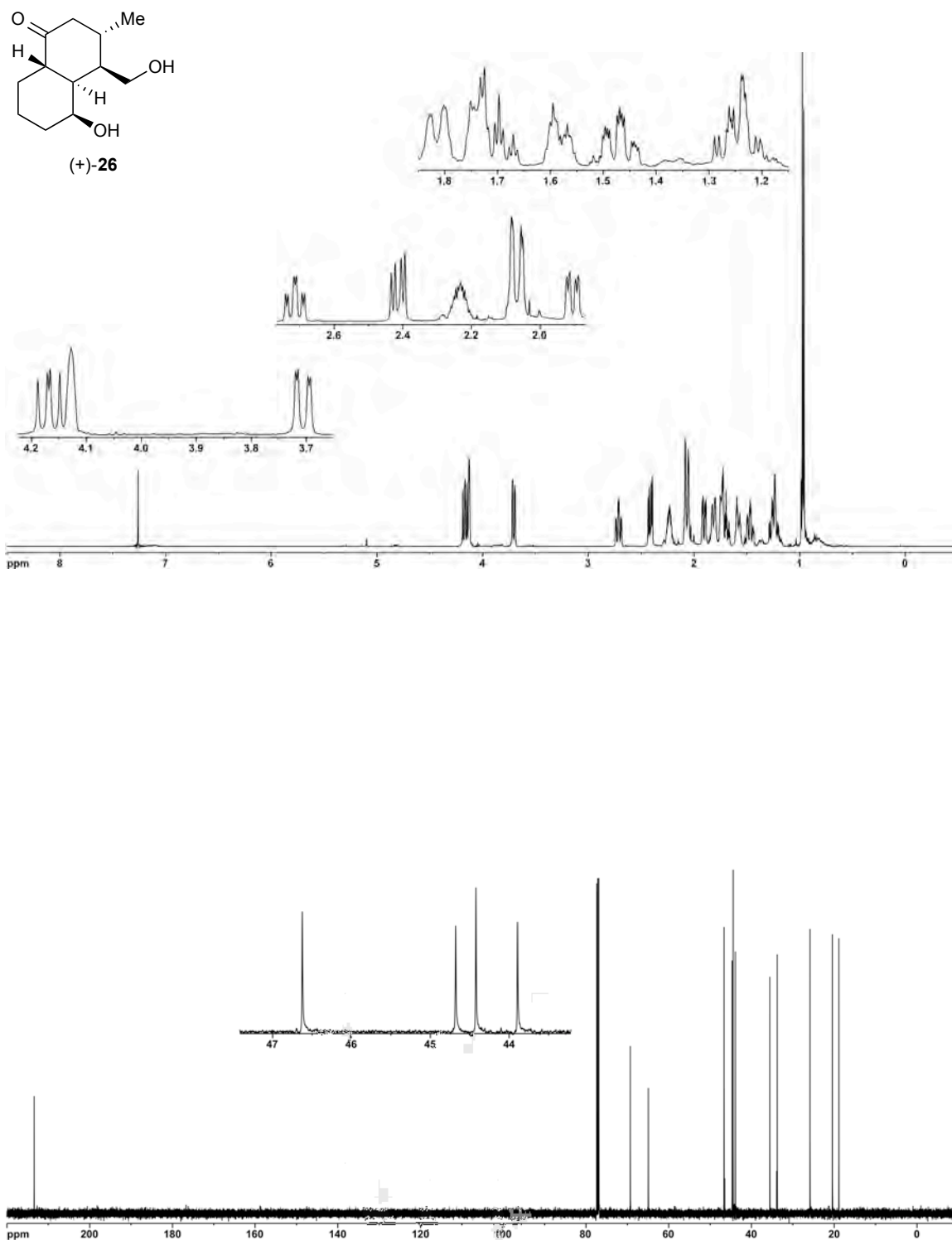
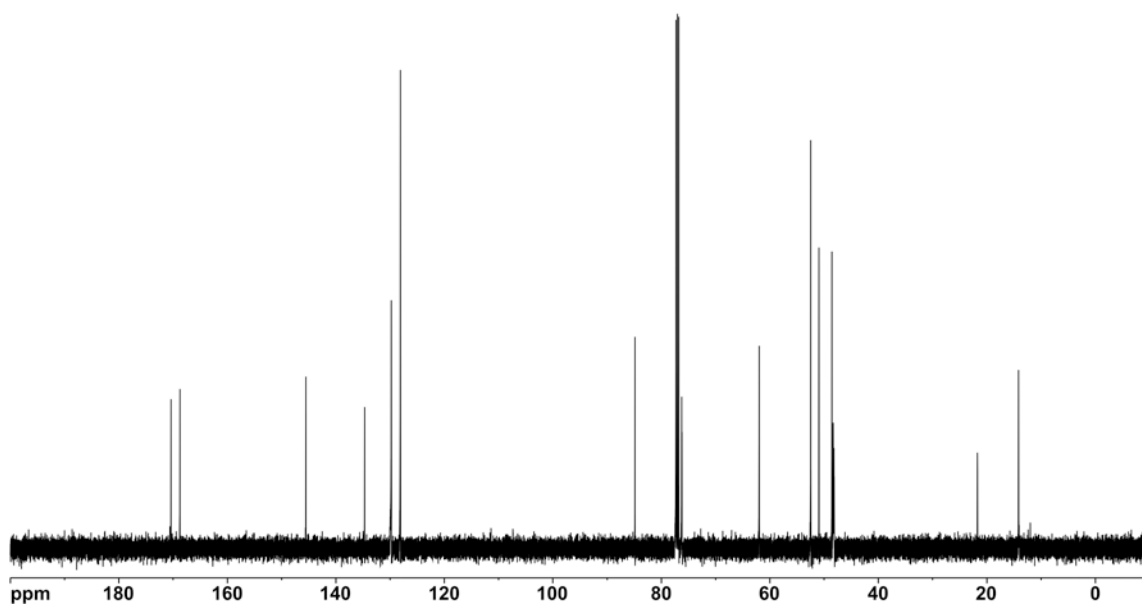^{1}H (500 MHz) and ^{13}C NMR (125 MHz) spectra of ketone (+)-**26** in CDCl$_3$

258

(+)-**23**

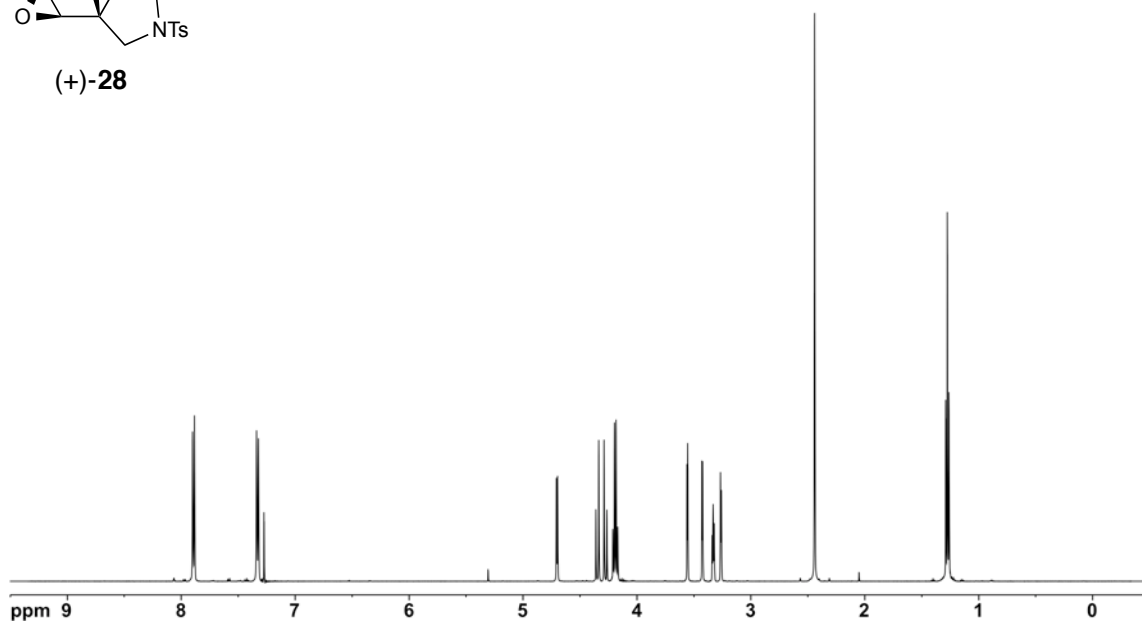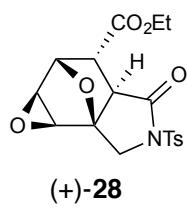^{1}H (500 MHz) and ^{13}C NMR (125 MHz) spectra of lactam (+)-**23** in CDCl$_3$

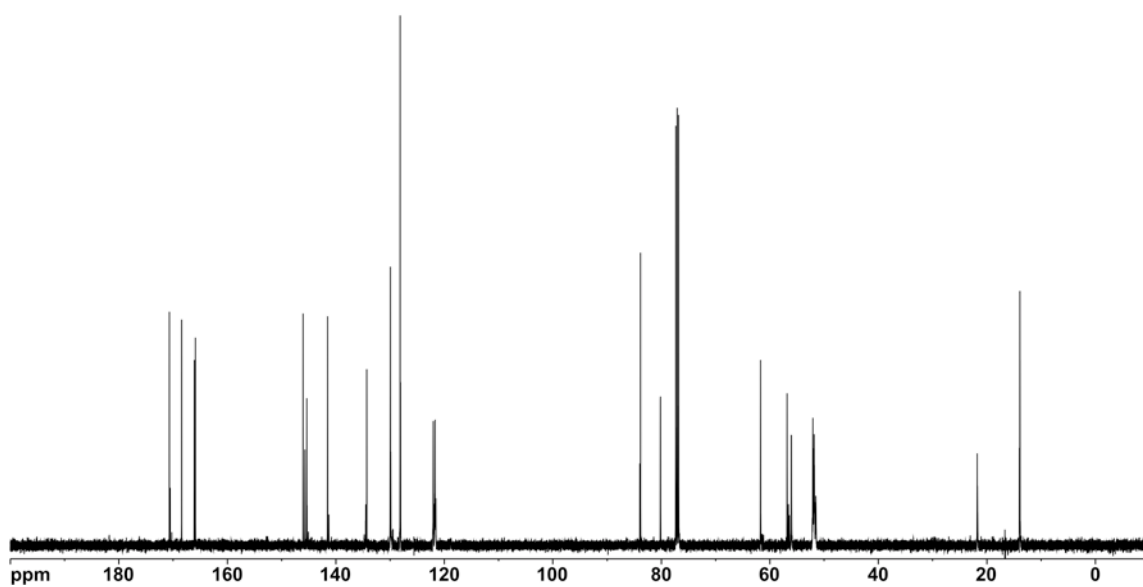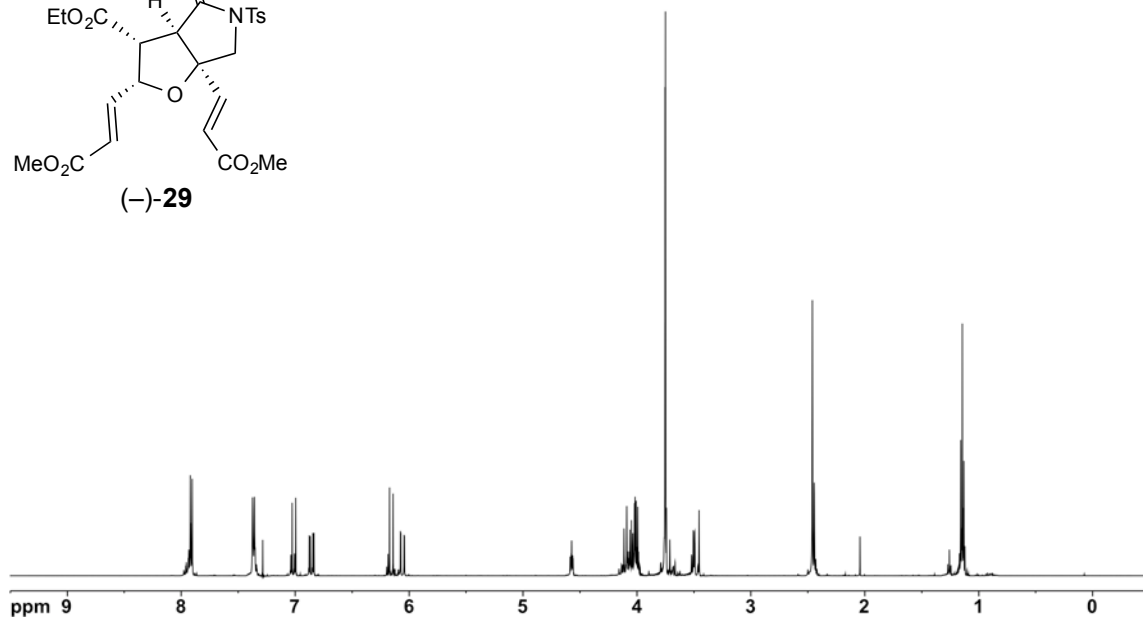^{1}H (500 MHz) and ^{13}C NMR (125 MHz) spectra of lactam (+)-**25i** in CDCl$_3$
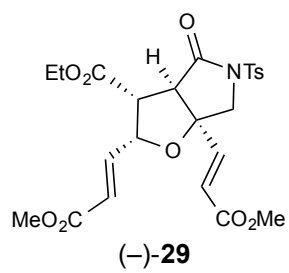
S13

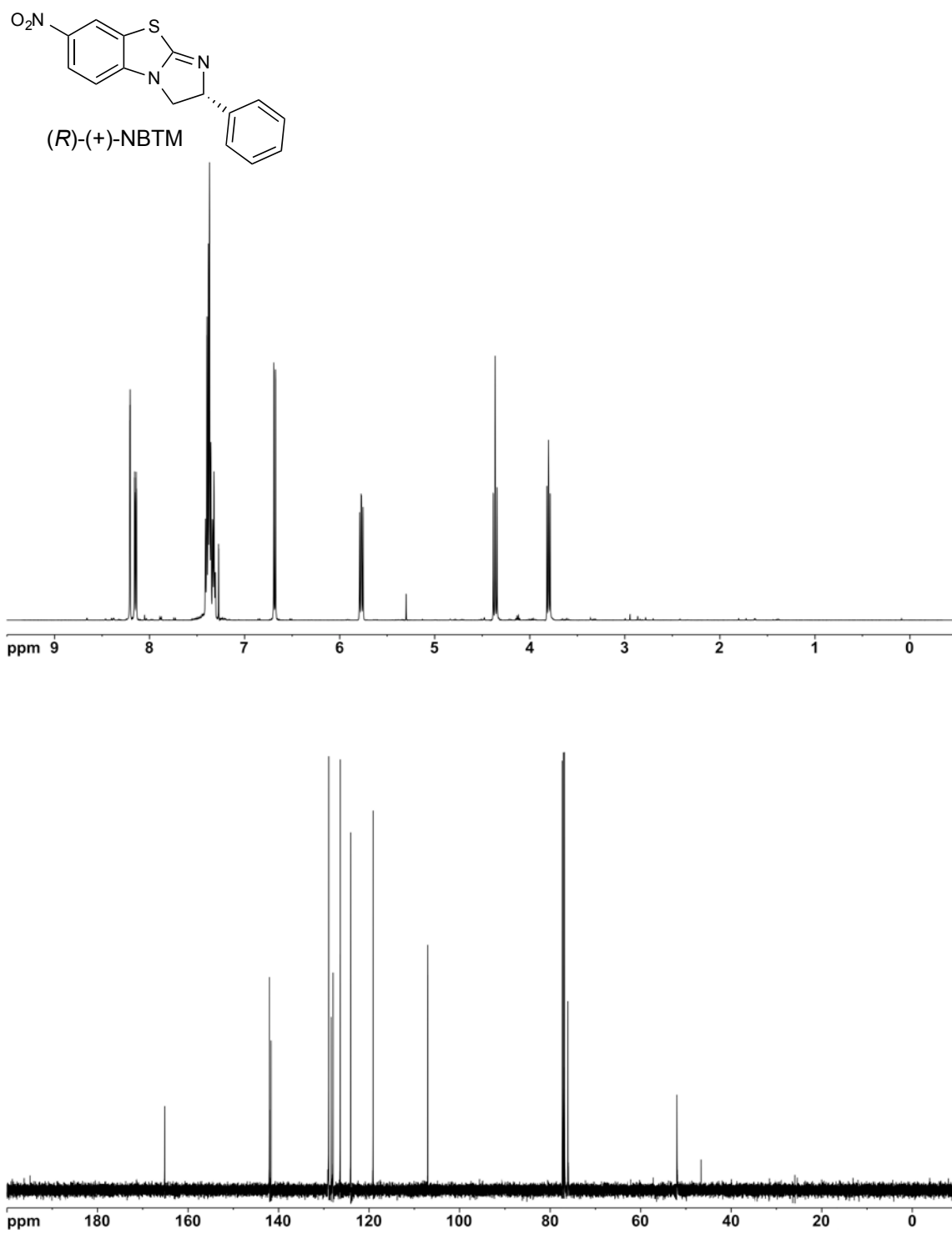^{1}H (500 MHz) and ^{13}C NMR (125 MHz) spectra of lactam **S13** in CDCl$_3$
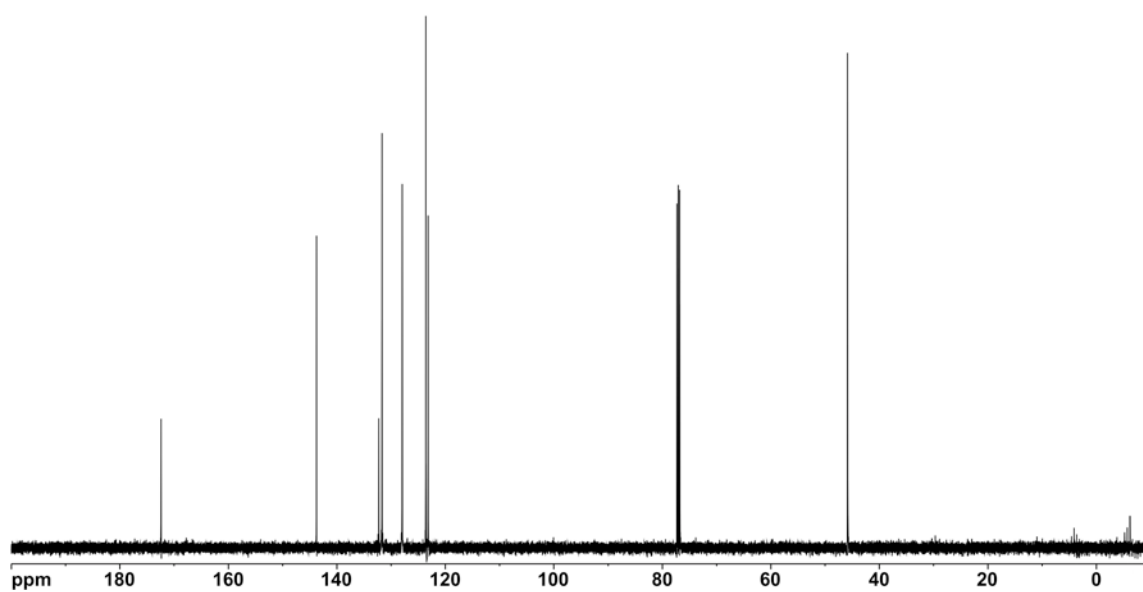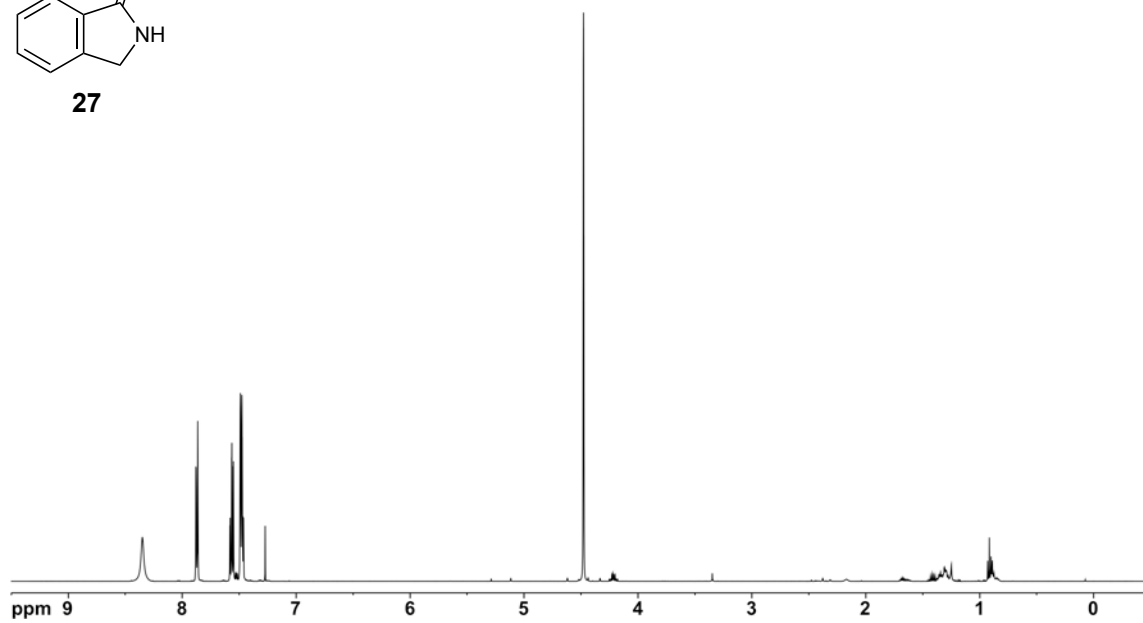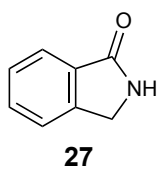
^{1}H (500 MHz) and ^{13}C NMR (125 MHz) spectra of isoindolinone **27** in CDCl$_3$
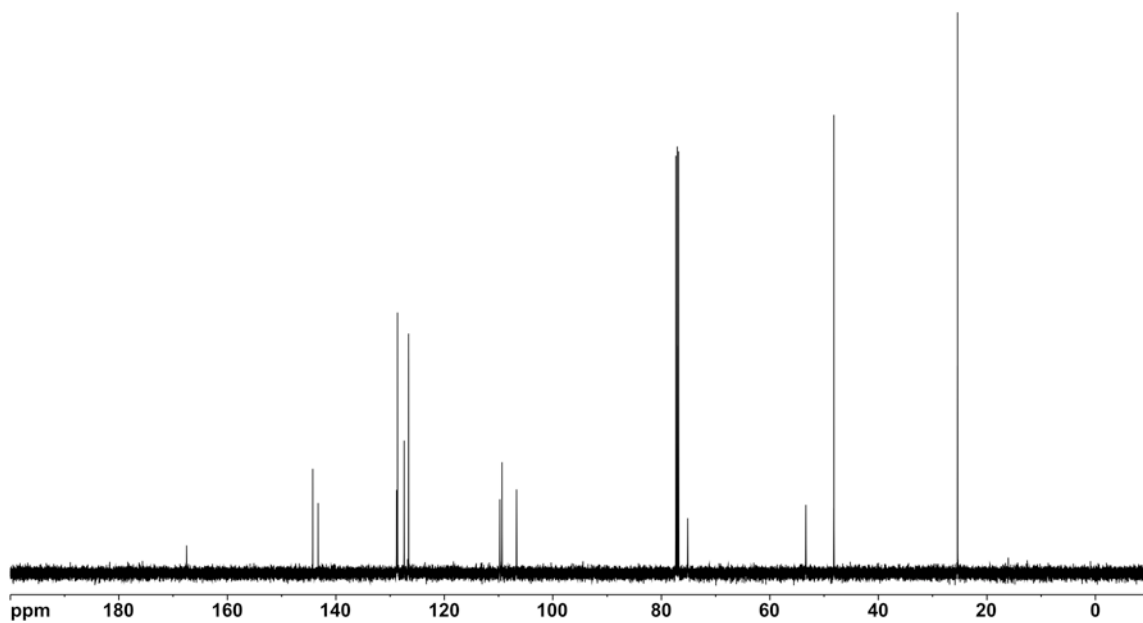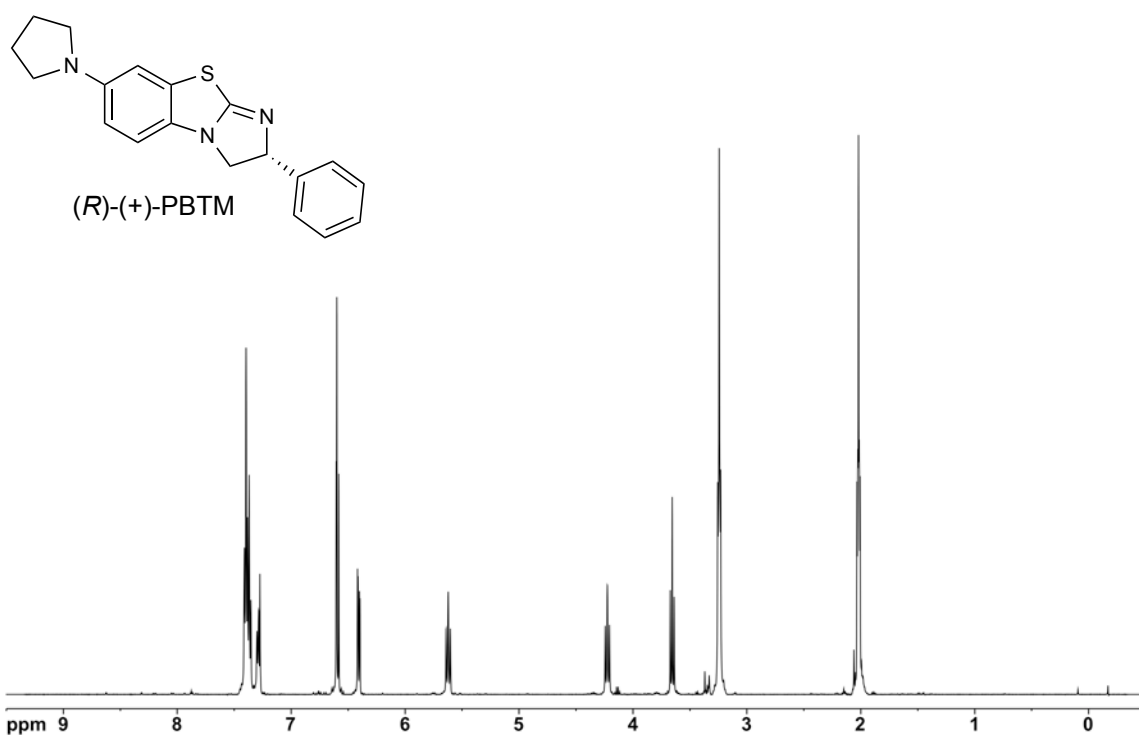
^{1}H (500 MHz) and ^{13}C NMR (125 MHz) spectra of epoxide (+)-**28** in CDCl$_3$

^{1}H (500 MHz) and ^{13}C NMR (125 MHz) spectra of lactam (–)-**29** in CDCl$_3$

^{1}H (500 MHz) and ^{13}C NMR (125 MHz) spectra of (*R*)-(+)-NBTM in CDCl$_3$

^{1}H (500 MHz) and ^{13}C NMR (125 MHz) spectra of (*R*)-(+)-PBTM in CDCl$_3$

Figure S3. Chiral HPLC determinations of enantiomeric excess of lactones 14a-d and 14a'-d':

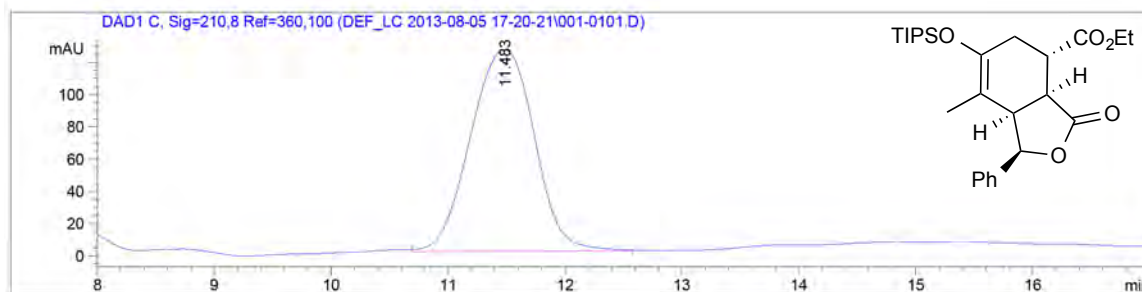**Determination of enantiomeric excess of bicyclic γ-lactone (–)-14a:**

Chiral HPLC analysis of bicyclic γ-lactone (–)-14a: Chiralcel OD-H column: hexanes:^{i}PrOH = 95:05, flow rate 0.5 mL/min, λ = 210 nm: t_{major} = 11.4 min, t_{minor} = 13.4 min; 99% e.e.
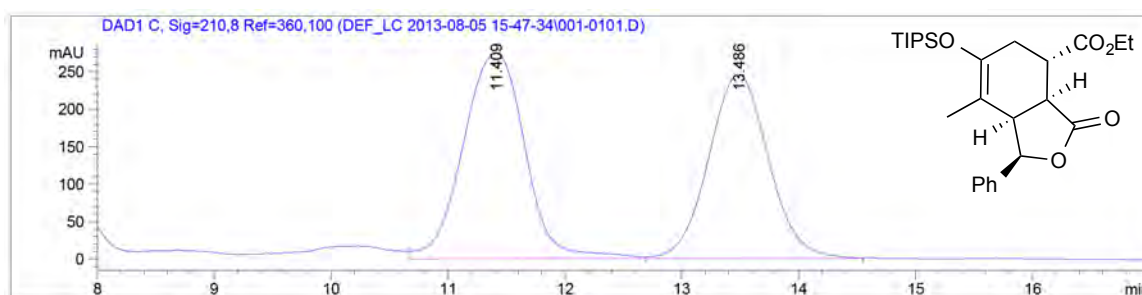
Signal 3: DAD1 C, Sig=210,8 Ref=360,100

```
Peak RetTime Type  Width     Area       Height     Area
 #    [min]        [min]     [mAU*s]     [mAU]        %
----|--------|----|-------|----------|----------|--------|
  1  11.409 VB    0.5858 1.00989e4   274.13562  53.6631
  2  13.486 BB    0.5504 8720.16016  245.47592  46.3369

Totals :                1.88191e4   519.61154
```


Signal 3: DAD1 C, Sig=210,8 Ref=360,100

```
Peak RetTime Type  Width     Area       Height      Area
 #    [min]        [min]     [mAU*s]     [mAU]         %
----|--------|----|-------|----------|----------|--------|
  1  11.483 BB    0.6047 4723.80225  125.05634 100.0000

Totals :                4723.80225  125.05634
```

Determination of enantiomeric excess of bicyclic γ-lactone (+)-14a':

Chiral HPLC analysis of bicyclic γ-lactone (+)-14a': Chiralcel AS-H column: hexanes:^{i}PrOH = 95:05, flow rate 0.5 mL/min, λ = 210 nm: t_{major} = 16.9 min, t_{minor} = 19.4 min; 98% e.e.
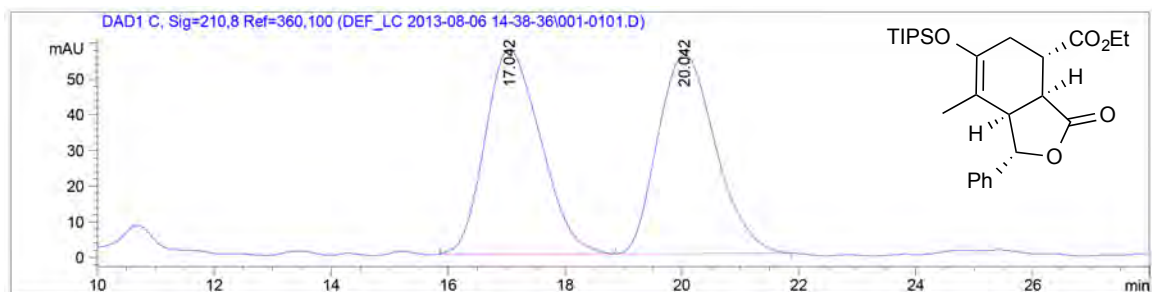
Signal 3: DAD1 C, Sig=210,8 Ref=360,100

Peak #	RetTime [min]	Type	Width [min]	Area [mAU*s]	Height [mAU]	Area %
1	17.042	BB	0.9989	3786.13672	57.29754	49.6845
2	20.042	BB	1.0521	3834.22778	55.77229	50.3155

Totals : 7620.36450 113.06982
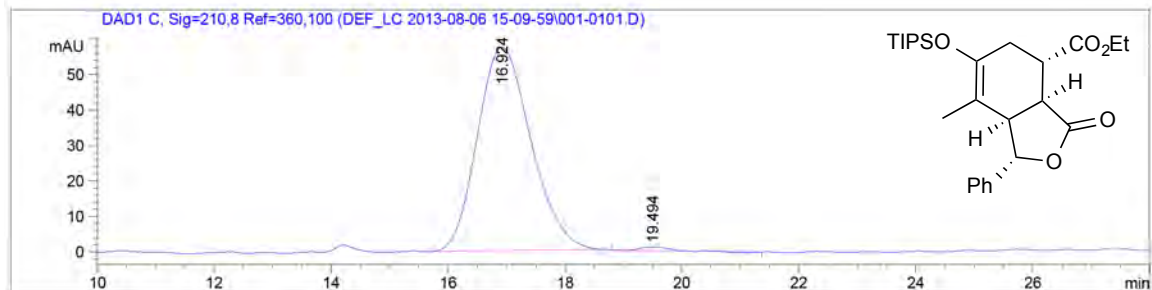

Signal 3: DAD1 C, Sig=210,8 Ref=360,100

Peak #	RetTime [min]	Type	Width [min]	Area [mAU*s]	Height [mAU]	Area %
1	16.924	BB	0.9644	3652.71582	57.39919	98.9651
2	19.494	MM	0.5868	38.19721	1.08484	1.0349

Totals : 3690.91303 58.48403

Determination of enantiomeric excess of bicyclic γ-lactone (+)-14b:

Chiral HPLC analysis of bicyclic γ-lactone (+)-14b: Chiralcel OD-H column: hexanes:^{i}PrOH = 95:05, flow rate 0.5 mL/min, λ = 210 nm: t_{major} = 12.0 min, t_{minor} = 16.1 min; 99% e.e.
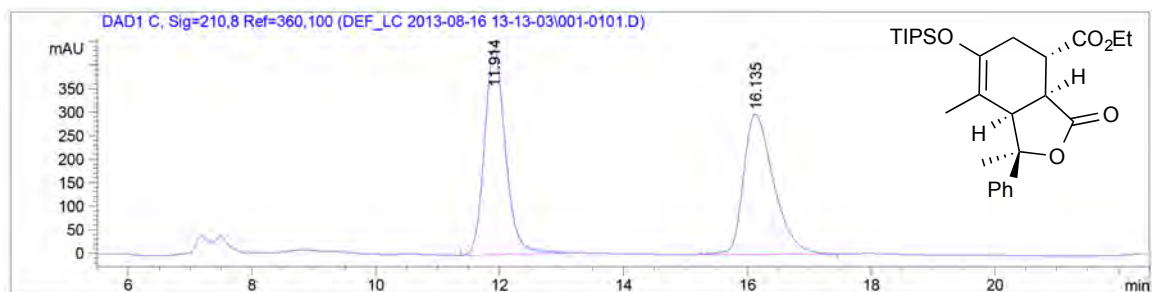

```
Signal 3: DAD1 C, Sig=210,8 Ref=360,100

Peak RetTime Type  Width     Area       Height      Area
 #    [min]        [min]    [mAU*s]      [mAU]        %
----|-------|----|-------|-----------|-----------|--------|
  1  11.914 BB   0.3629 1.02704e4   435.91010  50.5007
  2  16.135 BB   0.5138 1.00668e4   298.20029  49.4993

Totals :                2.03372e4   734.11038
```



```
Signal 3: DAD1 C, Sig=210,8 Ref=360,100

Peak RetTime Type  Width     Area       Height      Area
 #    [min]        [min]    [mAU*s]      [mAU]        %
----|-------|----|-------|-----------|-----------|--------|
  1  12.044 BB   0.3434 3834.70825  173.81255 100.0000

Totals :                3834.70825  173.81255
```

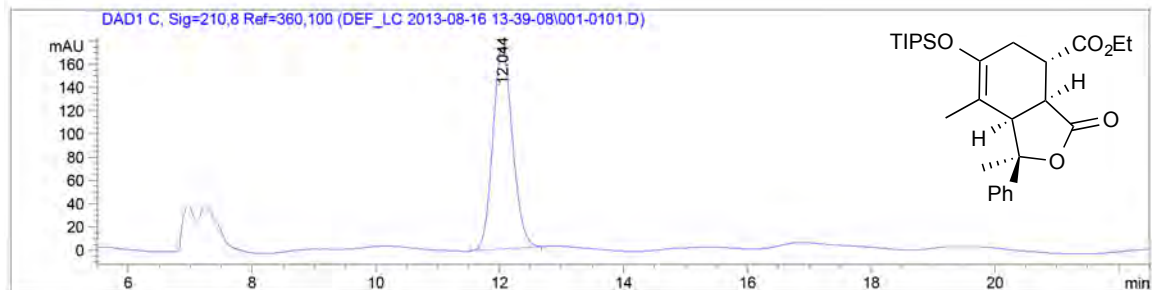**Determination of enantiomeric excess of bicyclic γ-lactone (+)-14b':**

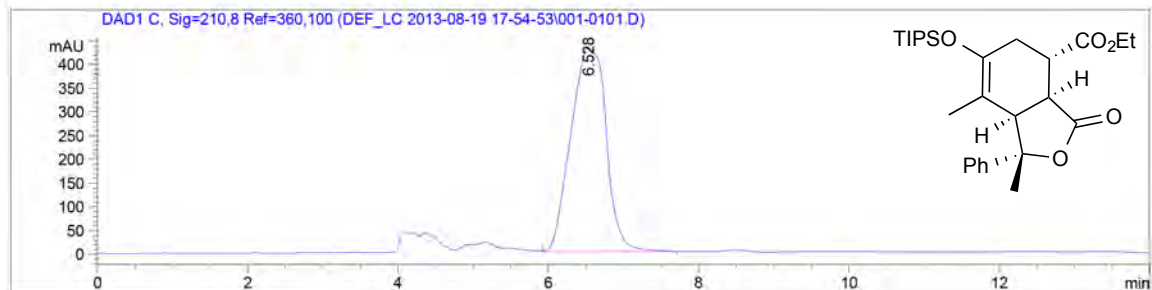**Chiral HPLC analysis of bicyclic γ-lactone (+)-14b':** Chiralcel AD-H column: hexanes:*i*PrOH = 95:05, flow rate 0.8 mL/min, λ = 210 nm: t_{major} = 6.5 min, t_{minor} = 7.9 min; 99% e.e.
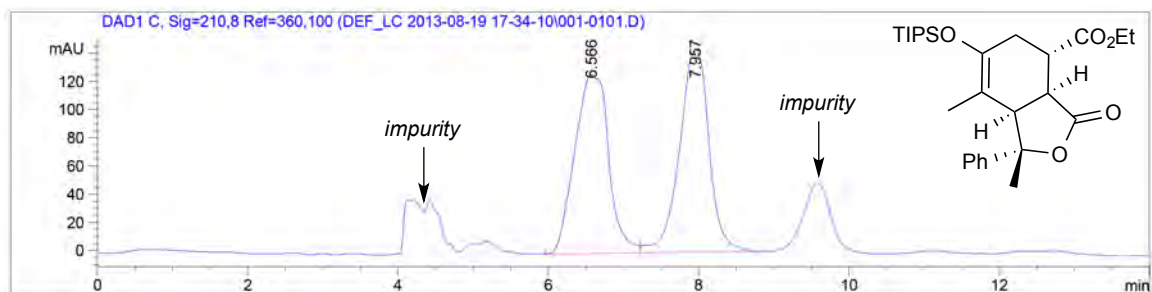

```
Signal 3: DAD1 C, Sig=210,8 Ref=360,100

Peak RetTime Type  Width     Area       Height     Area
 #   [min]        [min]   [mAU*s]     [mAU]       %
----|-------|----|-------|----------|----------|--------|
  1   6.566 BV    0.4437 3982.09033  127.05120  50.2380
  2   7.957 VB    0.4200 3944.36377  143.80565  49.7620

Totals :                 7926.45410  270.85685
```



```
Signal 3: DAD1 C, Sig=210,8 Ref=360,100

Peak RetTime Type  Width     Area       Height     Area
 #   [min]        [min]   [mAU*s]     [mAU]       %
----|-------|----|-------|----------|----------|--------|
  1   6.528 BB    0.4637 1.41129e4   431.31570 100.0000

Totals :                 1.41129e4   431.31570
```

270

Determination of enantiomeric excess of bicyclic γ-lactone (+)-14c:

Chiral HPLC analysis of bicyclic γ-lactone (+)-14c: Chiralpak IA column: hexanes:^{i}PrOH = 95:05, flow rate 0.5 mL/min, λ = 210 nm: t_{major} = 28.9 min, t_{minor} = 43.7 min; 99% e.e.
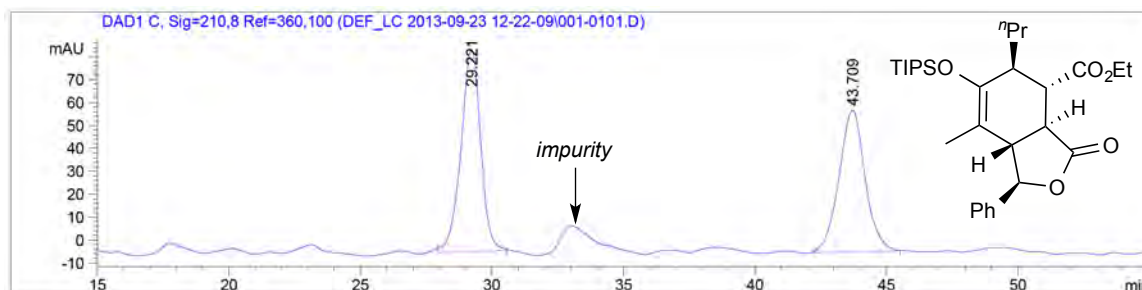
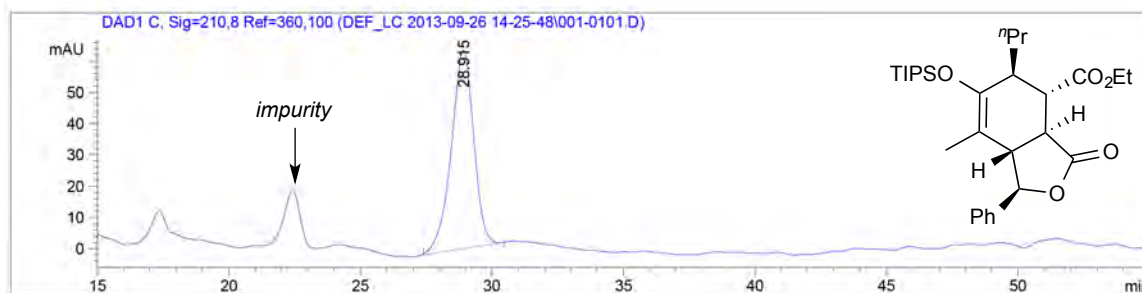Signal 3: DAD1 C, Sig=210,8 Ref=360,100

```
Peak RetTime Type  Width     Area       Height     Area
 #    [min]        [min]    [mAU*s]      [mAU]       %
----|-------|----|-------|----------|----------|--------|
  1  29.221 BB   0.6228 4598.02588  88.11724  51.9386
  2  43.709 BB   0.9143 4254.78027  61.71974  48.0614

Totals :                8852.80615 149.83698
```


Signal 3: DAD1 C, Sig=210,8 Ref=360,100

```
Peak RetTime Type  Width     Area       Height     Area
 #    [min]        [min]    [mAU*s]      [mAU]       %
----|-------|----|-------|----------|----------|--------|
  1  28.915 BB   0.8574 3764.60156  63.51937 100.0000

Totals :                3764.60156  63.51937
```

Determination of enantiomeric excess of tricyclic γ-lactone (–)-14c:

Chiral HPLC analysis of tricyclic γ-lactone (–)-14c: Chiralcel OD-H column: hexanes:^{i}PrOH = 95:05, flow rate 0.5 mL/min, λ = 210 nm: t_{minor} = 11.1 min, t_{major} = 12.1 min; 99% e.e.
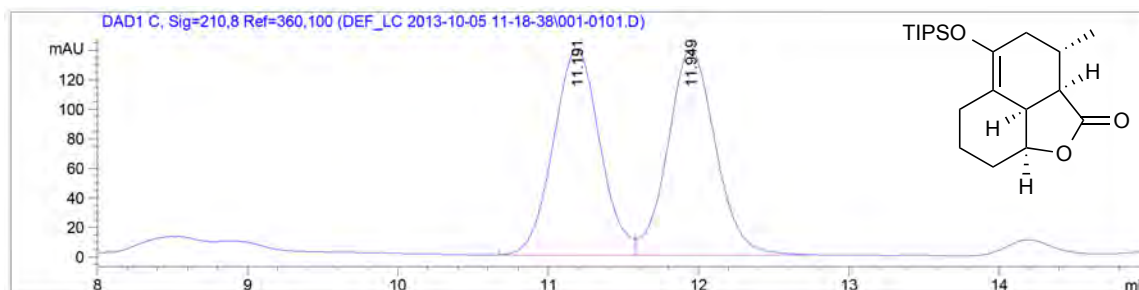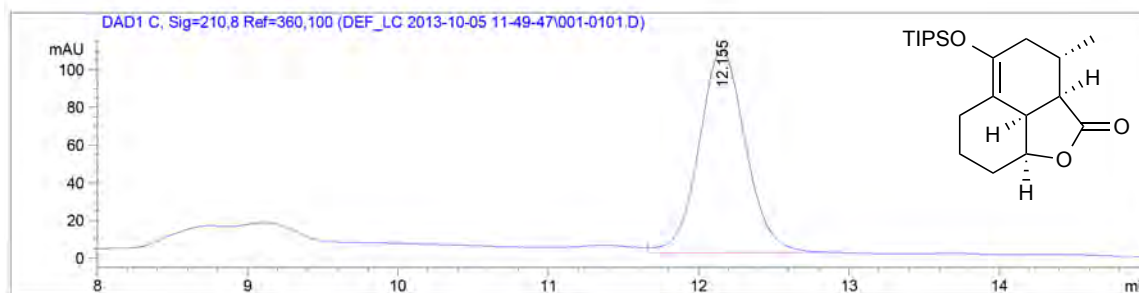

Signal 3: DAD1 C, Sig=210,8 Ref=360,100

```
Peak RetTime Type  Width     Area        Height      Area
 #   [min]        [min]    [mAU*s]      [mAU]        %
----|-------|----|-------|-----------|----------|--------|
  1  11.191 BV   0.3332 2997.38525  139.20857  49.5180
  2  11.949 VB   0.3369 3055.73779  138.77129  50.4820

Totals :                 6053.12305  277.97986
```


Signal 3: DAD1 C, Sig=210,8 Ref=360,100

```
Peak RetTime Type  Width     Area        Height      Area
 #   [min]        [min]    [mAU*s]      [mAU]        %
----|-------|----|-------|-----------|----------|--------|
  1  12.155 VB   0.3300 2325.51343  107.66201 100.0000

Totals :                 2325.51343  107.66201
```

Determination of enantiomeric excess of tricyclic γ-lactone (–)-14d':

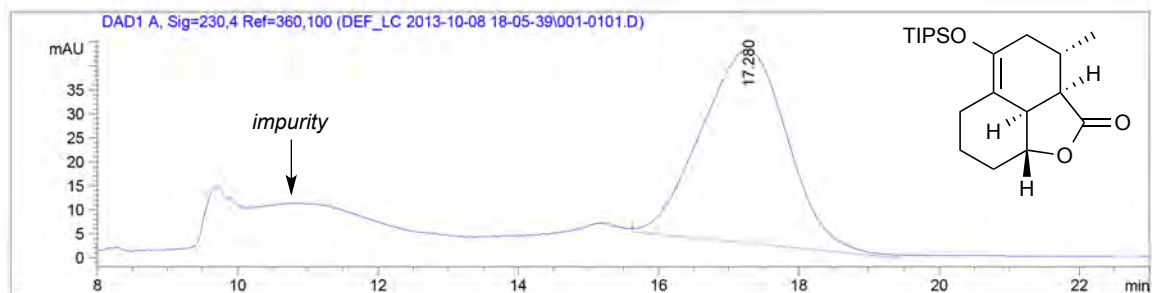**Chiral HPLC analysis of tricyclic γ-lactone (–)-14d':** Chiralpak IA column: hexanes:^{i}PrOH = 95:05, flow rate 0.5 mL/min, λ = 230 nm: t_{minor} = 14.1 min, t_{major} = 17.2 min; 99% e.e.
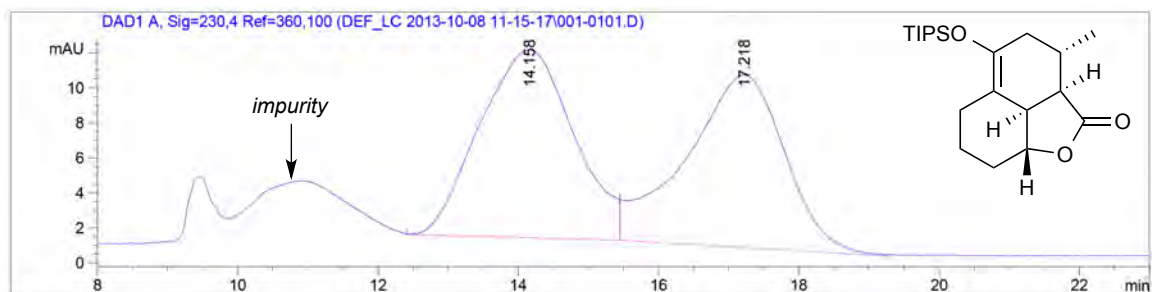

```
Signal 1: DAD1 A, Sig=230,4 Ref=360,100

Peak RetTime Type  Width     Area       Height     Area
 #   [min]        [min]    [mAU*s]     [mAU]        %
----|-------|----|-------|----------|----------|--------|
  1  14.158 MM   1.5510  999.61298   10.74140  51.0243
  2  17.218 MM   1.6256  959.47900    9.83724  48.9757

Totals :                1959.09198   20.57864
```



```
Signal 1: DAD1 A, Sig=230,4 Ref=360,100

Peak RetTime Type  Width     Area       Height     Area
 #   [min]        [min]    [mAU*s]     [mAU]        %
----|-------|----|-------|----------|----------|--------|
  1  17.280 MM   1.4246  3447.87793  40.33750 100.0000

Totals :                3455.97684   41.11370
```

Determination of enantiomeric excess of bicyclic γ-lactone (–)-36:

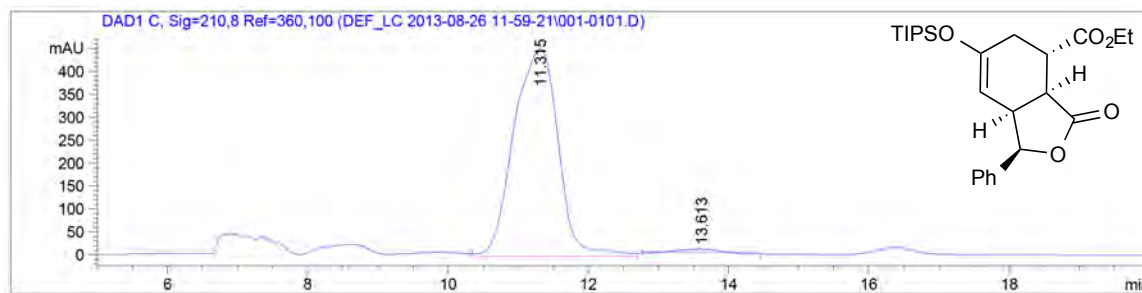**Chiral HPLC analysis of bicyclic γ-lactone (–)-36:** Chiralcel OD-H column: hexanes:^{i}PrOH = 95:05, flow rate 0.5 mL/min, λ = 210 nm: t_{major} = 11.3 min, t_{minor} = 13.6 min; 98% e.e. using 2,6-lutidine (3.0 equiv.).
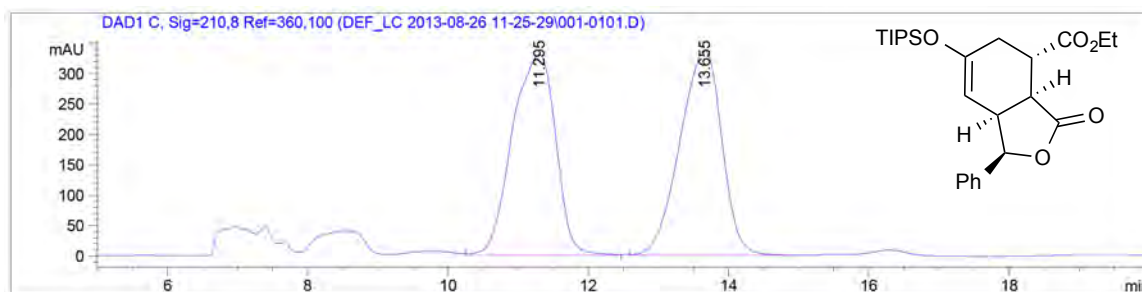
Signal 3: DAD1 C, Sig=210,8 Ref=360,100

```
Peak RetTime Type  Width     Area        Height     Area
 #   [min]        [min]     [mAU*s]     [mAU]      %
----|-------|----|-------|-----------|-----------|--------|
 1  11.295 VB    0.6265 1.42095e4   329.90613  50.4425
 2  13.655 BB    0.6656 1.39602e4   336.77118  49.5575

Totals :                2.81697e4   666.67731
```
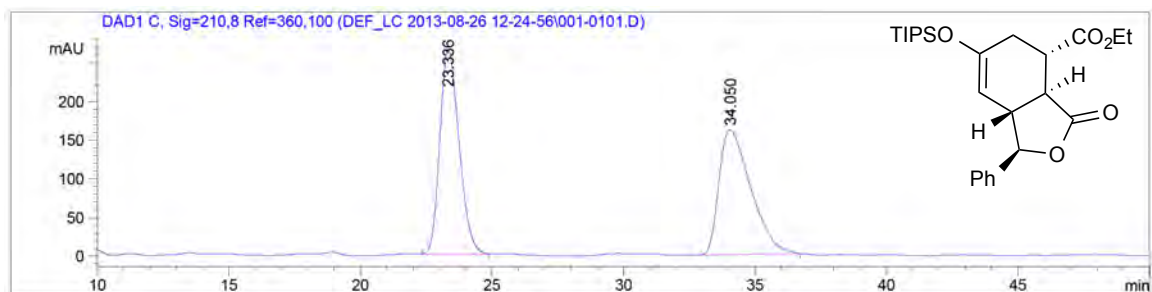

Signal 3: DAD1 C, Sig=210,8 Ref=360,100

```
Peak RetTime Type  Width     Area        Height     Area
 #   [min]        [min]     [mAU*s]     [mAU]      %
----|-------|----|-------|-----------|-----------|--------|
 1  11.315 MM    0.7342 1.99413e4   452.69849  98.9250
 2  13.613 MM    0.5690 216.69820    6.34695   1.0750

Totals :                2.01580e4   459.04544
```

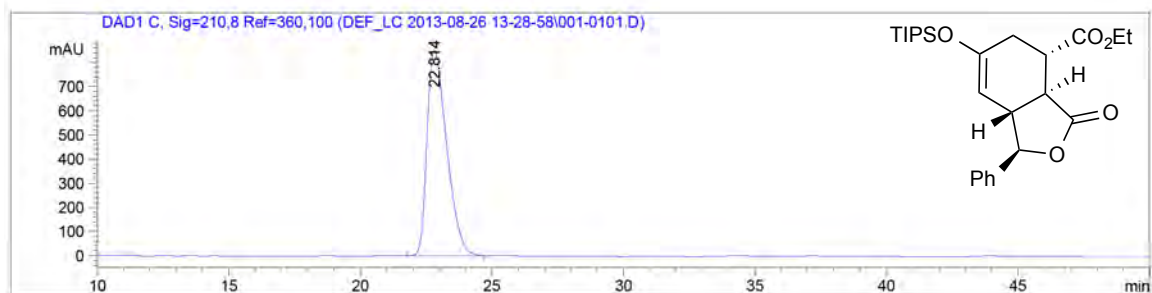**Determination of enantiomeric excess of bicyclic γ-lactone (+)-36':**

Chiral HPLC analysis of bicyclic γ-lactone (+)-36': Chiralcel OD-H column: hexanes:^{i}PrOH = 95:05, flow rate 0.5 mL/min, λ = 210 nm: t_{major} = 22.8 min, t_{minor} = 34.0 min; 99% e.e.

Signal 3: DAD1 C, Sig=210,8 Ref=360,100

```
Peak RetTime Type  Width      Area       Height     Area
 #   [min]        [min]   [mAU*s]      [mAU]        %
----|-------|----|-------|----------|----------|--------|
  1  23.336 BB   0.8007 1.34848e4   264.52606  49.8611
  2  34.050 BB   1.2792 1.35599e4   160.89601  50.1389

Totals :               2.70446e4   425.42207
```
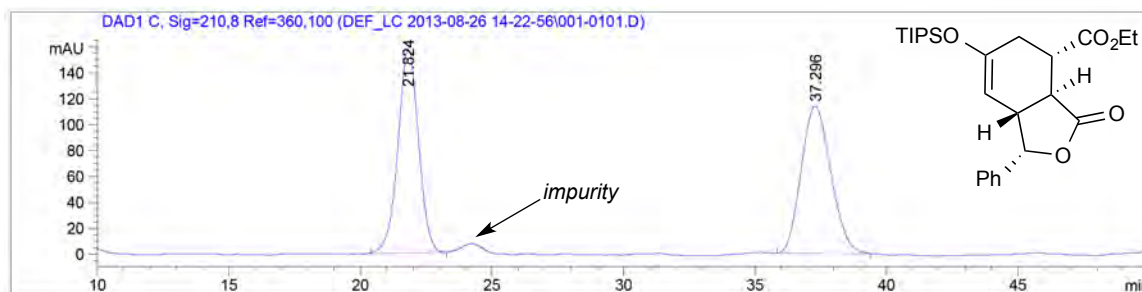

Signal 3: DAD1 C, Sig=210,8 Ref=360,100

```
Peak RetTime Type  Width      Area       Height      Area
 #   [min]        [min]   [mAU*s]      [mAU]         %
----|-------|----|-------|----------|----------|--------|
  1  22.814 BB   0.8057 4.43888e4   852.21271 100.0000

Totals :               4.43888e4   852.21271
```

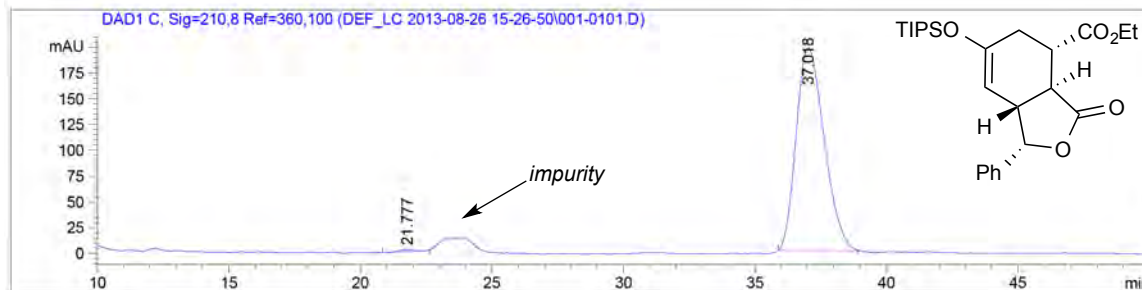**Determination of enantiomeric excess of bicyclic γ-lactone (+)-36'':**

Chiral HPLC analysis of bicyclic γ-lactone (+)-36'': Chiralcel OD-H column: hexanes:^{i}PrOH = 95:05, flow rate 0.5 mL/min, λ = 210 nm: t_{minor} = 21.7 min, t_{major} = 37.0 min; 99% e.e.

Signal 3: DAD1 C, Sig=210,8 Ref=360,100

```
Peak RetTime Type  Width      Area       Height     Area
 #   [min]        [min]    [mAU*s]     [mAU]       %
----|-------|----|-------|----------|----------|--------|
  1  21.824 BB   0.8517 8578.78125  156.95447   49.0045
  2  37.296 BB   1.1605 8927.34082  113.63794   50.9955

Totals :               1.75061e4    270.59241
```
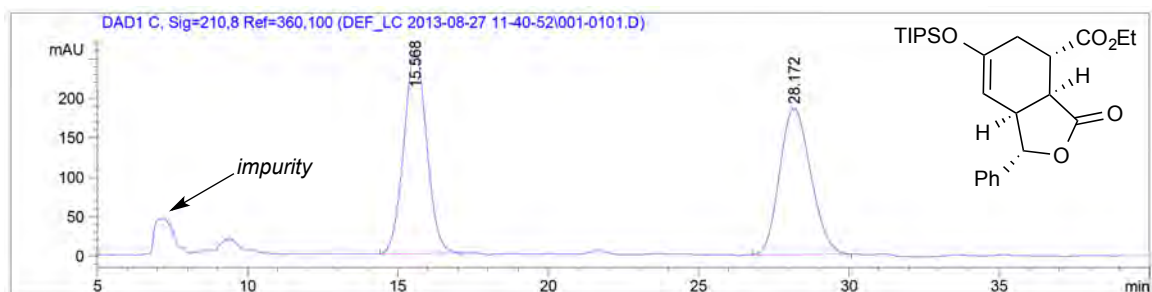

Signal 3: DAD1 C, Sig=210,8 Ref=360,100

```
Peak RetTime Type  Width      Area       Height     Area
 #   [min]        [min]    [mAU*s]     [mAU]       %
----|-------|----|-------|----------|----------|--------|
  1  21.777 MM   0.6535    7.68978 1.96131e-1   0.4870
  2  37.018 BB   1.0976 1571.21863  21.17800   99.5130

Totals :               1578.90841   21.37413
```

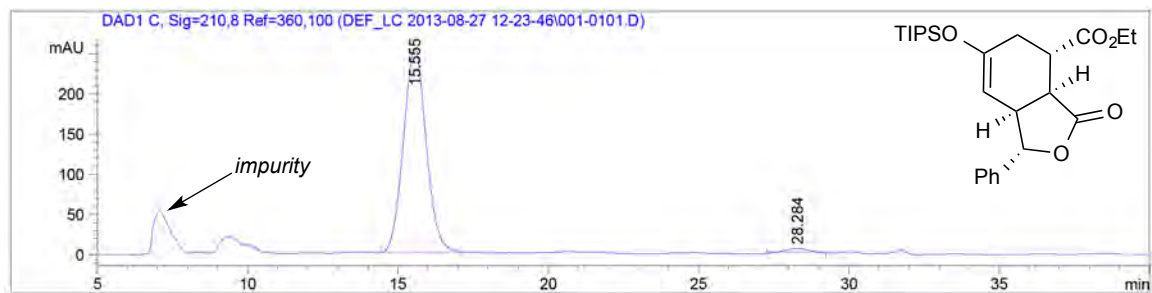**Determination of enantiomeric excess of bicyclic γ-lactone (–)-36''':**

Chiral HPLC analysis of bicyclic γ-lactone (–)-36''': Chiralcel AS-H column: hexanes:^{i}PrOH = 95:05, flow rate 0.5 mL/min, λ = 210 nm: t_{major} = 15.5 min, t_{minor} = 28.2 min; 97% e.e. using 2,6-lutidine (3.0 equiv.).


```
Signal 3: DAD1 C, Sig=210,8 Ref=360,100

Peak RetTime Type  Width     Area      Height     Area
 #   [min]        [min]   [mAU*s]     [mAU]       %
----|-------|----|-------|----------|----------|--------|
  1  15.568 BB   0.8089 1.35702e4   257.45016  50.4264
  2  28.172 BB   1.1175 1.33407e4   185.39282  49.5736

Totals :                 2.69109e4   442.84299
```



```
Signal 3: DAD1 C, Sig=210,8 Ref=360,100

Peak RetTime Type  Width     Area      Height     Area
 #   [min]        [min]   [mAU*s]     [mAU]       %
----|-------|----|-------|----------|----------|--------|
  1  15.555 BB   0.8209 1.33634e4   253.56432  98.3984
  2  28.284 MM   0.8160  217.51129    4.44277   1.6016

Totals :                 1.35809e4   258.00708
```
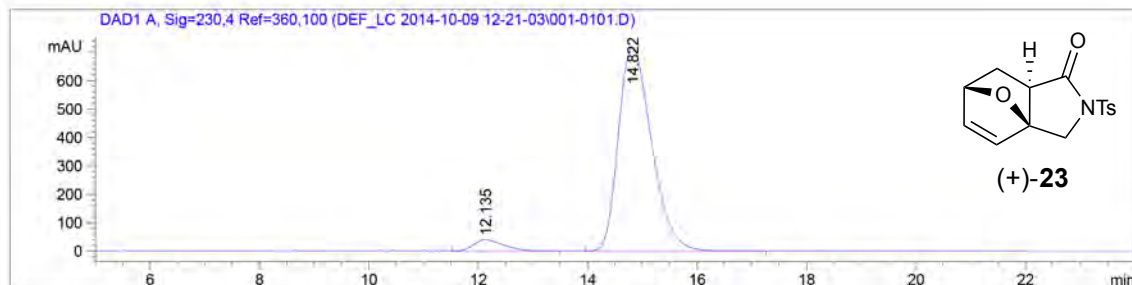
Determination of enantiomeric excess of tricyclic γ-lactam (+)-23:

Chiral HPLC analysis of tricyclic γ-lactam (+)-23: Chiralcel AS-H column: hexanes:^{i}PrOH = 40:60, flow rate 1.0 mL/min, λ = 230 nm: t_{minor} = 12.1 min, t_{major} = 14.8 min; 91% *ee*.
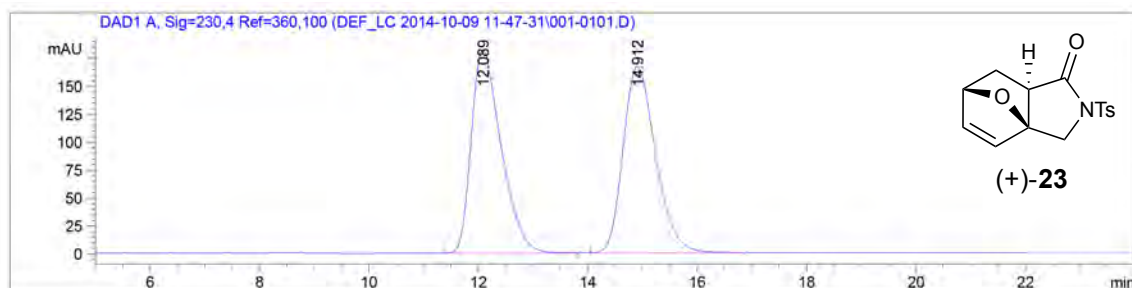
Signal 1: DAD1 A, Sig=230,4 Ref=360,100

Peak #	RetTime [min]	Type	Width [min]	Area [mAU*s]	Height [mAU]	Area %
1	12.089	VB	0.5743	6905.38037	182.16231	50.0142
2	14.912	BB	0.6347	6901.46826	166.79213	49.9858

Signal 1: DAD1 A, Sig=230,4 Ref=360,100

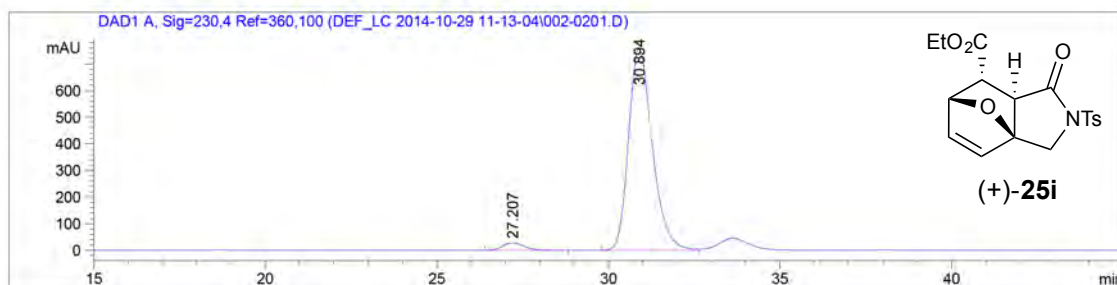| Peak #	RetTime [min]	Type	Width [min]	Area [mAU*s]	Height [mAU]	Area %
1	12.135	VB	0.5555	1479.92871	40.01673	4.6714
2	14.822	BB	0.6515	3.02009e4	716.84735	95.3286

Determination of enantiomeric excess of tricyclic γ-lactam (+)-25i:

Chiral HPLC analysis of tricyclic γ-lactam (+)-25i: Chiralcel AD-H column: hexanes:^{i}PrOH = 60:40, flow rate 0.5 mL/min, λ = 230 nm: t_{minor} = 27.2 min, t_{major} = 30.9 min; 94% *ee*.
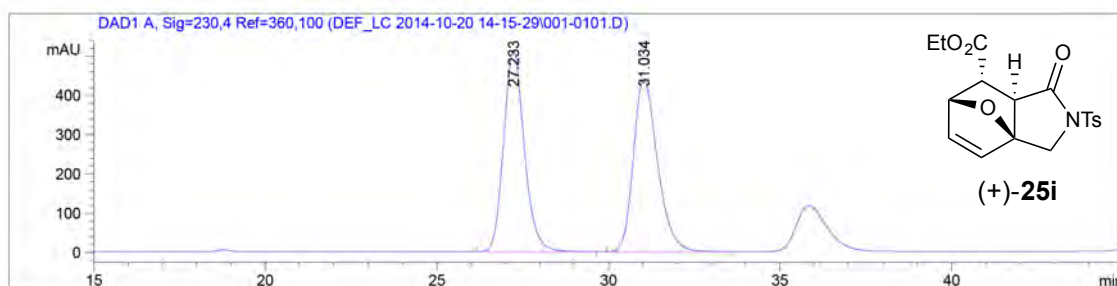
Signal 1: DAD1 A, Sig=230,4 Ref=360,100

Peak #	RetTime [min]	Type	Width [min]	Area [mAU*s]	Height [mAU]	Area %
1	27.233	BB	0.6407	2.14784e4	512.79865	49.9649
2	31.034	BB	0.7523	2.15086e4	441.53778	50.0351

Signal 1: DAD1 A, Sig=230,4 Ref=360,100

Peak #	RetTime [min]	Type	Width [min]	Area [mAU*s]	Height [mAU]	Area %
1	27.207	BB	0.6536	1205.83008	28.50200	3.2022
2	30.894	BV	0.7379	3.64501e4	756.85626	96.7978

Supporting Information References (CHAPTER III):

[1]   Kamal, A.; Reddy, J. S.; Bharathi, E. V.; Dastagiri, D. *Tetrahedron Lett.* **2008**, *49*, 348.

[2]   Qi, J.; Han, M. S.; Chang, Y. C.; Tung, C. H. *Bioconjugate Chem.* **2011**, *22*, 1758.